Practical Aspects of Computational River Hydraulics

J.A. Cunge, F.M. Holly, Jr

Société Grenobloise d'Etudes et d'Applications Hydrauliques, SOGREAH, Grenoble

A. Verwey

International Institute for Hydraulic and Environmental Engineering, Delft

Pitman Advanced Publishing Program

Boston · London · Melbourne

PITMAN PUBLISHING LIMITED
39 Parker Street, London WC2B 5PB

PITMAN PUBLISHING INC
1020 Plain Street, Marshfield, Massachusetts 02050

Associated Companies
Pitman Publishing Pty Ltd, Melbourne
Pitman Publishing New Zealand Ltd, Wellington
Copp Clark Pitman, Toronto

Library of Congress Cataloging in Publication Data
Cunge, J A
Practical aspects of computational river hydraulics
(Monographs and surveys in water resources engineering; 3)
Bibliography: p.
Includes index.
1. Rivers–Mathematical models. 2. Stream measurements–Mathematical models. 3. Channels (Hydraulic engineering)–Mathematical models.
I. Holly, Forrest M., joint author. II. Verwey, Adri, joint author.
III. Title. IV. Series.
TC175.C86 627'.125 79-25810

ISBN 0 273 08442 9

Text in IBM Press Roman by Composer Typesetting, Bath
Printed and bound in Great Britain
at The Pitman Press, Bath

Dans notre monde relatif, toute certitude est mensonge.
H. Poincaré

Contents

Acknowledgements
List of symbols

1 Introduction 1

2 Mathematical formulation of physical processes 7
2.1 Equations of one-dimensional unsteady open channel flow 7
Basic hypotheses 7
Integral relations 9
Differential form of the de St Venant equations 13
Supplementary terms and coefficients 18
2.2 Characteristics – boundary and initial conditions 24
Boundary data requirements 29
2.3 Discontinuous solutions – bores 37
2.4 Simplified channel flow equations 44
Effect of neglecting the inertia terms 45
Effect of neglecting the inertia terms and the $\partial h/\partial x$ term 46
Steady flow equations 48
2.5 Representation of special flow conditions 48
Localized inapplicability of the channel flow equations 49
Quasi two-dimensional flow 50

3 Solution techniques and their evaluation 53
3.1 Discretization and solution of flow relationships 53
Numerical solution by the method of characteristics 54
Numerical solution by the method of finite differences 59
Some finite difference schemes 62
Discretization of boundary conditions 72
Discretization of the quasi-two-dimensional flow equations 75
3.2 Linear analysis of the validity of discretization 77
Convergence and approximation error 77
Numerical stability 80
Amplitude and phase portraits 86
3.3 Discretization of non-linear terms and coefficients 92

Verwey's variant of the Preissmann scheme 96
Abbott–Ionescu scheme 97
Comments 98
3.4 Algorithmic aspects of modelling systems 103
Iterative matrix methods 105
Double sweep methods 106
3.5 Computational principles of steep front simulation 121
Shock fitting method 122
Pseudoviscosity method 124
Through methods 126
3.6 Representation of topographic and hydraulic data 128

4 Flow simulation in natural rivers 132
4.1 Introductory remarks 132
4.2 Choice of equations for channel flow 135
4.3 One-dimensional and two-dimensional modelling 138
4.4 Topological discretization 143
4.5 Hydraulic discretization 159
4.6 Some computational problems in river and flood plain flow simulation 175
Small depths 175
Weir oscillations 178
Flooded weir linearization 180
Steady flow calculations 181
4.7 Concluding remarks 184

5 Model calibration and data needs 185
5.1 Model calibration 185
Steady flow 186
Unsteady flow 193
Example: calibration of the Senegal Valley model 208
Example: calibration of the upper Rhône model 216
Accuracy of calibration 222
5.2 Data needs 225
General remarks 225
Topographic data 228
Hydraulic data 230

6 Modelling of flow regulation in irrigation canals and power cascades 233
6.1 Flow control in irrigation and water supply canals 233
6.2 Surges in power canals 242
6.3 Flow and energy production control in power cascades on canalized rivers 253
6.4 Computational and modelling considerations 260
Modelling of discontinuous fronts 260

Modelling of transitions and control structures 263
Example of gate simulation 265

7 **Movable bed models 271**
7.1 The role of movable bed mathematical models in engineering practice 271
7.2 Basic hypotheses and formulation of equations 273
7.3 Boundary conditions in movable bed modelling 278
7.4 Data requirements 280
7.5 Mathematical analysis of the equations 281
Full unsteady flow equations 281
Simplified system of unsteady flow equations 282
7.6 Numerical solutions 287
Full system of three equations 287
Simplified system of two equations 291
7.7 Models of alluvial channel resistance 295
Physical aspects 295
Energy line gradient formulation 298
Solid transport formulation 298
Examples of application 299
7.8 Criteria involved in choosing a modelling method 307
Factors linked to the physical phenomena simulated 308
Factors linked to numerical methods 309

8 **Transport of pollutants 312**
8.1 Introduction 312
8.2 The dispersion process 313
8.3 One-dimensional dispersion modelling 318
8.4 Evaluation of the longitudinal mixing coefficient 319
8.5 Numerical solution of the one-dimensional convection equation 320
8.6 Numerical solution of the one-dimensional diffusion equation 331
8.7 Example of one-dimensional dispersion modelling – the Vienne river 333
8.8 Two-dimensional dispersion modelling 336
8.9 Example: simulation of two-dimensional dispersion in the Missouri river from a continuous source 340
8.10 Example: simulation of one-dimensional dispersion in Clinch river 343
8.11 Estimating the transverse distribution of longitudinal velocity 346
8.12 Conclusions 349

9 **Special applications 350**
9.1 Flood forecasting and prediction 350
Strategy for implementation of forecasting models 354
Particular calibration and sensitivity study problems 356

9.2 Simulation of dam break waves 357
Physical description of the phenomenon and governing equations 357
Computational problems 360
9.3 Unsteady flow modelling in storm drain networks 365
Pressurized flow 366
Backflow from junctions 368
Backwater effects 368
Small depths 368
Looped networks 369
Hydraulic works 370

10 Costs, benefits and quality 372
10.1 Cost/benefit and cost/quality ratios 372
10.2 Factors affecting the cost of a mathematical model 374
Algorithm and software development 374
Preliminary study 375
Adaptation of existing software to the project's particular features 376
Construction of the model 377
Supplementary surveys and measurements 378
Model calibration 378
Model exploitation and interpretation of results 379
Transfer of models 380
10.3 Quality of a model 380
Differential equations 382
Finite difference operator 383
Solution algorithm and treatment of special features 383
Data input and output 384
Simulation of observed situations 384
10.4 Modeller–user relationship 384
10.5 Examples of cost of mathematical models 385
Upper Nile basin 385
Mekong River Delta 386

11 Transfer of mathematical models 391
11.1 Introduction 391
11.2 Modeller–user relationship 392
11.3 Computer and operating system problems 396
11.4 Trained personnel problems 397
11.5 Examples of transfer operations 399
The transfer of the Mekong Delta mathematical model from Grenoble to Bangkok 399
The transfer of the Senegal River model from Grenoble to Dakar 403

References 407
Index 417

Acknowledgements

The first two authors have acquired most of their experience at the Consulting Engineering firm SOGREAH (Société Grenobloise d'Etudes et d'Applications Hydrauliques). They wish to express their appreciation to SOGREAH for permission to use internal reports and notes, for help in obtaining client's authorisations to use study material, and for material support in preparing the manuscript, especially the final typing.

The first applications of mathematical modelling techniques to river engineering problems in the 1960's were made possible by Dr Alexandre Preissmann, member of SOGREAH's Board of Experts. The first two authors consider it a great privilege to be able to work with the man whose pioneering work launched the present day widespread use of mathematical models. His constant help, guidance and, above all, his criticism have always been a source of encouragement for which we wish to express our profound gratitude.

The third author has greatly appreciated the stimulation of Professor ir. L. J. Mostertman, director of the International Institute for Hydraulic and Environmental Engineering in Delft, who has always made possible the necessary contacts in this field. The third author is also very much indebted to Dr M. B. Abbott. Working with him at the International Institute in Delft represents not only a professional contact but also a personal and stimulating friendship. The author's accumulation of professional experience was made possible by these two colleagues, starting in 1970 through collaboration with the Versuchsanstalt für Wasserbau of the Technische Hochschule München on the development of a mathematical model for a stretch of the river Danube. After completion of this study came the opportunity to develop the hydrodynamic part of the modelling system 'System 11 Siva' at the Computational Hydraulics Centre of the Danish Hydraulic Institute. Here the third author has very much appreciated the useful comments of his colleagues Gaele Rodenhuis, Asger Kej, Peter Hinstrup, and Jens Aage Bertelsen during the construction of the system and its application to real problems. Last, but not least, thanks are given to the co-authors for the considerable amount of additional work they did in Grenoble in integrating the third author's contribution into this work.

Additional thanks must be given to Mr Bill Eichert of the U.S. Army Corps of Engineers, Hydrologic Engineering Center, and to Drs Carl Nordin and Robert Baltzer of the U.S. Geological Survey, for having supplied information on current mathematical modelling activity in their respective organizations.

Finally, we must acknowledge the invaluable contribution of Joyce Holly, who typed the early drafts and did considerable proofreading.

List of symbols

All symbols are defined where they first appear in the text. The following list includes only those symbols which retain the same physical or mathematical significance throughout a chapter or the entire book.

(L = length; M = mass; F = force; T = time)

A	cross-sectional flow area perpendicular to the flow direction (L^2)
A_s	surface area of flood plain cell (L^2)
A_{st}	cross-sectional area available for storage (L^2)
a	gate opening (L)
b	width of cross section at free surface elevation (L)
b_c	channel width (L)
b_{st}	storage width (L)
b_v	valley width (L)
C	Chezy coefficient in empirical roughness laws ($L^{1/2}T^{-1}$); concentration (ML^{-3})
C_a	cross-sectional average concentration (ML^{-3})
Cr	Courant number
c	wave celerity (LT^{-1})
c_p	flood peak celerity (LT^{-1})
d_{50}	median bed material diameter (L)
F_f	bed friction force acting on control volume (F)
F_g	gravitational force acting on control volume (F)
$F_{p1}, F'_{p1}, F''_{p1}, F_{p2}$	pressure forces acting on control volume (F)
Fr	Froude number
G	sediment volumetric discharge (L^3T^{-1})

g	acceleration due to gravity (LT^{-2})
H	depth of rectangular subsection of a composite channel (L); steady flow depth (L)
H_m	depth amplitude of individual component of Fourier series solution (L)
ΔH	head loss (L)
h	water depth (L)
h^*, h_*	superelevations of wave crests and troughs compared to undisturbed free surface level (L)
Im	denotes imaginary part of a complex number
I_1, I_2	cross-sectional moment integrals (L^3 and L^2)
i	constant $\sqrt{-1}$
i	computational point index
J	particular computational point index
J_+, J_-	Riemann invariants (LT^{-1})
j	computational point index; computational cell index
K	channel conveyance factor (L^3T^{-1})
K_n	artificial (numerical) diffusion coefficient (L^2T^{-1})
K_x	longitudinal dispersion coefficient (L^2T^{-1})
k	wave number (L^{-1})
k_{Str}	Strickler coefficient in empirical roughness laws ($L^{1/3}T^{-1}$)
L	downstream limit of computational domain, $x = L$ (L); distance from source beyond which one dimensional dispersion occurs (L); differential operator
L_h	difference operator
l	characteristic length in pseudoviscosity definition (L); distance between the centres of two adjacent flood plain cells (L); turbulent mixing length (L)
M	number of computational points per wavelength
M_f	net momentum flux into control volume (FT)
ΔM	net increase in momentum contained in control volume (FT)
m	index of individual Fourier solution components
n	Manning coefficient in empirical roughness laws ($L^{-1/3}T$); time step index
n_v	flooded area roughness coefficient ($L^{-1/3}T$)

P	wetted perimeter(L); direct inflow into a computational cell (L^3T^{-1})
Q	volumetric water discharge ($L^3\ T^{-1}$)
q	continuous lateral inflow per unit length (L^2T^{-1}); pseudoviscosity coefficient (L^3T^{-2}); discharge per unit width of channel (L^2T^{-1})
R	hydraulic radius A/P (L)
Re	denotes real part of a complex number
R_1	amplification factor of numerical solution compared to exact solution, per time step
R_2	numerical dispersion factor of numerical solution compared to exact solution, per time step
S_f	energy line slope in the x-direction (friction slope)
S_{fs}	free surface slope
S_0	bed slope in the x-direction
T	propagation time (T); wave period (T)
T_f	flood forecasting interval (T)
T_u	flood forecast updating interval (T)
t	time (T)
Δt	time between two computational intervals (T)
U	steady flow velocity (LT^{-1}); cross-sectional average velocity (LT^{-1})
U_m	velocity amplitude of individual component of Fourier series solution (LT^{-1})
U_p	flow velocity at flood peak (LT^{-1})
u	water velocity in x-direction (LT^{-1})
u_*	bed shear (or friction) velocity (LT^{-1})
V	volume of water in flood-plain cell (L^3)
V_0	volume of tracer injected into a river (L^3)
v	discontinuous front propagation velocity (LT^{-1}); velocity in y-direction (LT^{-1})
W_+, W_-	characteristic velocities (LT^{-1})
w	velocity in z-direction (LT^{-1})
x	longitudinal space co-ordinate in horizontal plane (L)
Δx	distance between two computational points in x-direction (L)

y	vertical space co-ordinate above datum (L); water surface elevation (L)
y_b	bed elevation (L)
y_{cb}	elevation at which overbank flooding begins (L)
y_w	weir crest elevation
Z	steady flow bed level (L)
z	transverse space coordinate in horizontal plane (perpendicular to flow direction) (L); river bed level in Chapter 7 (L)
β	non-uniform velocity distribution coefficient
Δ	initial state error
δ	numerical solution damping factor for one wave period
ϵ	empirical mixing coefficient (L^2T^{-1})
ϵ_m	molecular diffusivity (L^2T^{-1})
$\tilde{\epsilon}$	turbulent diffusivity (L^2T^{-1})
η	distance of cross section centroid from water surface (L)
θ	weighting coefficient in finite difference approximations of functions and their space derivatives
κ	von Karman's constant
λ	wavelength (L)
ν	wave frequency (T^{-1})
ξ	point in space from which a trajectory originates (L)
O	order of approximation
π	constant 3.14159...
ρ	water mass density (ML^{-3})
σ	width of cross section (L)
τ_0	tangential wall or bed shear stress (FL^{-2})
Φ	combined resistance and bed slope terms (L^3T^{-2})
φ	discharge coefficient
φ_m	solution damping factor
ψ	weighting coefficient in finite difference approximations of functions and their time derivatives

1 Introduction

Mathematical modelling of flow in rivers is rapidly becoming an accepted engineering tool, whose evolution can be compared to that of reduced scale modelling. Scale models came into use as design and verification tools when the complexity and scope of large structures began to present problems which could not be solved using traditional hydraulic methods, but could be accurately and productively modelled at a reduced scale. The use of scale models and interpretation of their results provided important feedback into the development of theory (similarity, statistics, turbulence, wave motion, sediment movement) as well as experimental science (measuring equipment, laboratory technique, etc.).

The theoretical foundations of physical scale models were laid down by 19th century precursors such as Froude; what was new in the 1930s and 1940s was the general application of scale models to open channel engineering problems. The early role of models as illustrative examples evolved into a role of providing quantitative, reliable results on which design decisions could be based. But as engineering projects became larger and economy considerations were more and more often integrated into overall planning, scale models reached a natural limit to the scope of their application. It is not sufficient merely to be able to produce a satisfactory design of a given structure or to predict flow conditions in its immediate vicinity; the structure's interaction with the overall development plan of a river basin or region must be considered, from both hydraulic and economic points of view. For example, a sophisticated and well-designed sand-trap structure on an irrigation canal will be useless if the canal system cannot deliver sufficient water and with a high enough velocity. Even though scale distortion and engineering experience can be used to extend the scope of scale models, there is some point at which new techniques must be used to obtain simulations which are reliable and economic. These new techniques are those of mathematical modelling.

Mathematical modelling in rivers is the simulation of flow conditions based on the formulation and solution of mathematical relationships expressing known hydraulic principles. The technique finds its origin in the 19th century work of de St Venant and Boussinesq, who formulated the unsteady flow equations, and in the work of Massau, who in 1889 published some early attempts to solve

those equations. Important theoretical concepts were established in the first half of this century, but the first engineering applications of these principles to natural river conditions awaited the development of electronic computers; in 1952–1953 Isaacson, Stoker and Troesch (1954) constructed and ran a mathematical model of portions of the Ohio and Mississippi rivers. Following that pioneering effort the use of mathematical modelling in rivers developed at first quite slowly, then began to accelerate; today (1980) we seem to be in an exponential growth phase, in which everyone is trying to build models. Even when there may appear to be no need for a model in the planning and design of some projects, contracts invariably call for a mathematical modelling effort.

Mathematical modelling in rivers is much more than the use of computers and computer programs to simulate hydraulics. The engineer who works with data processing techniques develops a particular analytical and experimental attitude, a formalization of intuition and thought, an extension and concretization of the thinking process. Most hydraulic engineers have at least once in their career met a hydraulics expert, an engineer of great experience who applies his unformalized engineering intuition to solve a problem. Such an expert can say, 'if you do it that way, the dyke will collapse, but if you do it this way, the dyke will hold'. He is almost always right, even though he may not be able to explain, or formalize, his reasoning process, which is thus inaccessible to anyone else. If his reasoning process were formalized and analysed, it could well serve as the basis of a conceptual mathematical model available to everyone.

This formalization of intuitive hydraulic reasoning is an important aspect of current river modelling development. Faced with the need to come up with answers to design and planning problems as quickly and as economically as possible, engineers have developed a great number of programs and models, formalizing engineering intuition to as great an extent as possible and profiting from modern rapid computing techniques. Generalizations of this experience have led to the development between 1972 and 1976 of what we call *modelling systems*. Such systems comprise all the programmed procedures (software) necessary to construct and operate models of a river with its tributaries, inundated plains, and existing and future structures including dykes, dams, canals, etc. The engineer using such a system could concern himself only with the physical aspect of the problem, just as does the user of a scale model. But in order to be able to interpret model results correctly, he must know something of the hypotheses, limitations, and structure of the modelling system – just as the scale model user must appreciate the limitations of similarity laws. In other words, conceptual modelling must be complemented by what is referred to as *computational hydraulics*, which is the second important area of mathematical modelling development.

Computational hydraulics was born out of the conclusion that the new possibilities offered by computers dictated a new formulation of hydraulic concepts in which our previous knowledge would be only a component. Through interaction among classical hydraulics, modelling experience, and research, basic concepts have been reviewed and revised so that a new body of knowledge has

evolved which provides formal, mathematical support and guidance for the various techniques used in modelling systems. It is impossible to develop a modelling system without using computational hydraulics concepts (just as it is impossible to do so without using classical hydraulics, calculus, numerical analysis, programming, data processing concepts, etc.). Thus there has been a constant interaction between modelling system development and computational hydraulics.

The authors are concerned about two attitudes which seem to be developing in mathematical modelling of rivers. The first one is the black-box syndrome, often symbolized by statements in the press such as '. . . the data were fed into the computer (the black box) and the results which came out were . . .'. The black-box approach, in which one seeks to construct a model which responds to input in the same way as a physical system, is the only possible one when the physical system is poorly understood – in cybernetics, for example. But in river hydraulics we do have a good knowledge of the basic physical processes, and models should be built with this knowledge as a foundation. The black-box use of river modelling systems with little or no awareness of their limitations and constraints, is, in our view, irresponsible.

The second attitude which concerns us is the desire to become immersed in computational techniques to the exclusion of practical considerations. The use of esoteric language and the unwillingness to explain practical details and the relationships between theoretical results (often coming from numerical analysis and gas dynamics) and their practical applications, again opens the door to irresponsibility and even charlatanism. Both of these attitudes inhibit technical progress in river mathematical modelling. It is of course much easier to believe in the fairy's magic wand than to be told that the quality of model results is a direct function of the modeller's efforts to understand the problem – the long way to Tipperary never was, and never will be, very popular. The unwillingness to take the long road can have immediate practical consequences, as can already be seen in the attitudes of some serious organizations. Having suffered the abuse of 'models' which produce either false results or no results at all, these organizations have become understandably discouraged and tend to treat anyone talking about river mathematical modelling as a quack doctor.

We have tried in this book to address ourselves to those who wish to know what are the weak as well as the strong points of mathematical modelling; what can be checked, what can be simulated, and at what price. As consultants ourselves, we realize that we are giving our clients a stick to beat us with. We have tried to dismantle various aspects of river modelling in order to point out strengths and weaknesses and clarify the technical language employed. Without doing so, how can we explain the concept of convergence of a finite difference method to a water resource specialist in a language he can understand? And without the notion of convergence, how can we show him that close reproduction of recorded hydrographs is not sufficient proof of the reliability of a model, that another model may be more reliable even though its reproduction of observed events is not quite as good? How can we explain to an applied mathematician or

systems analyst the relative importance of physical factors represented in the various terms of the flow equations? How can we justify seemingly arbitrary decisions as to the neglect or not of inertial forces, or the use of weir-type or fluvial-type exchange laws? How can we explain to the technical advisor of a sponsoring organization what he should expect of a mathematical model, or how one should be chosen, or how the quality of results depends on the price? These are the kinds of questions we have considered, and although we may not have been able to provide satisfying answers to all of them, we hope that our efforts will have at least convinced the various parties involved in modelling that only through honest understanding can modelling evolve into a mature engineering tool.

In planning this book we were faced with the problem of deciding what kind of reader we wanted to address. One possibility would have been to write for the modelling system developer, staying in the realm of computational hydraulics, numerical methods, solution algorithms, etc. Another possibility would have been to write for the modelling system user, limiting our attention to model schematization, calibration, interpretation of results, examples. But it soon became apparent that we would have to try to reach both kinds of readers. Consider first the modelling of flood propagation in large river systems. Although correct and economical numerical methods must of course be used, the quality of model results depends to a large extent on the skill with which the modeller schematizes the system, i.e. on the 'art' he applies to the emplacement of computational points, flood plain storage cells, selection of boundary conditions, calibration of bed roughness coefficients, and so on. If on the other hand we consider flow in artificial canals subject to rapid flow variations due to turbine and gate manoeuvres, we realize that there is very little skill needed in representing the physical system in discrete model form. In this case it is the numerical method which demands the modeller's close attention, since rapidly varying phenomena cannot be correctly modelled with any off-the-shelf, hastily chosen scheme. And to the preoccupations of the two types of potential readers concerned with these modelling problems, i.e. the developer and the user, we must add those of a third party: the *buyer*, that is to say the organization who pays for model development and use and thus has an interest in appreciating the problems faced in all aspects of modelling.

The structure of this book reflects our attempt to reach these three types of readers. In Chapter 2 we develop the basic integral flow relations from a control volume point of view, then try to show to what extent the normally used differential equations can be considered as equivalent to the true momentum conservation expressed by the integral relations. We introduce the method of characteristics to help in explaining boundary and initial condition requirements as well as the development of flow discontinuities. Then we consider some of the simplified forms of the flow equations and their physical significance, and finally we describe a method of simulating two-dimensional flow on inundated plains. In Chapter 3 we deal with the practical problems involved in numerical solution of the flow relations. Our concern is with the degree to which various methods

approximate momentum conservation in a control volume, and with the practical implications and limitations of formal error, convergence, and stability analyses as applied to typical schemes. We try to show that any proposed method must be judged not only on the basis of its behaviour when applied to simplified linear equations, but also on the way it treats internal and external boundary conditions, non-linear coefficients, and so on. We then outline some solution algorithms which can be used for branched and looped channel and flood plain flow networks.

In Chapters 4 and 5 we discuss the practical problems involved in constructing, calibrating, and exploiting models of natural river systems. Our main preoccupation is the model representation of physical features, and the sensitivity of model quality to this representation. In Chapter 6 we treat the special problems involved in modelling of flow subject to artificial regulation: irrigation systems, derivation canals, and cascade hydroelectric projects.

In Chapters 7 and 8 we describe practical problems involved in the modelling of long-term river bed evolution due to sediment transport, and in the simulation of pollutant transport and dispersion in rivers. Although these topics do not directly fall under the heading of unsteady flow modelling, they are becoming more and more often included with, even becoming the object of, river flow modelling. The practical problems arising in the modelling of both sediment and pollution transport are closely related to those of river flow modelling. In Chapter 9 we briefly consider the modelling problems involved in flood forecasting and prediction, dam break wave calculation, and drainage network simulation. Finally, we throw all caution to the wind and discuss cost/quality and model transfer in Chapters 10 and 11.

The reader may be surprised to find that we have not described any single modelling system in its entirety. At the present time (1980) we are still in the early stages of development and application of modelling systems, and it would appear useless to describe details which are usually available in other publications and which may become obsolete in a few years' time. We have however tried to describe the general principles of modelling systems, giving particular attention to their industrial development involving the joint efforts of hydraulic engineers, applied mathematicians, and data processing specialists. The authors have been personally involved in the development and application of several current systems: SOGREAH's CARIMA system for the simulation of unsteady flow in multiply connected networks of rivers, canals, and inundated areas; the Danish Hydraulic Institute's SIVA System 21 for unsteady flow in multiply connected river and canal networks; SOGREAH's CAREDAS system for unsteady free-surface and pressurized flow in multiply connected drainage networks. We have drawn largely on our own experiences using these systems for examples and illustrations, we hope without displaying any religious fervour for our own methods to the exclusion of others.

We assume that the reader has a basic knowledge of hydraulics and mathematics. We derive certain unsteady flow relationships only when it is necessary to interpret some aspects which are not readily found elsewhere. While

frequently referring the reader to the literature, we have still tried to maintain the self-contained character of the book, which we hope can be read and understood by itself.

2 Mathematical formulation of physical processes

2.1 EQUATIONS OF ONE-DIMENSIONAL UNSTEADY OPEN CHANNEL FLOW

Basic hypotheses

The fundamental notions and hypotheses used in the mathematical modelling of rivers are formalized in the equations of unsteady open channel flow. These equations are simple models of extremely complex phenomena: they incorporate only the most important real-life flow influences, discarding those which are thought to be of secondary importance in view of the purpose of modelling. When dealing with a set of equations, the modeller must be aware of the physical phenomena which they do and do not incorporate. Once the equations are established, their subsequent mathematical and numerical treatment (transformation, solution, study of properties, etc.) does not change their built-in physical restrictions.

For the sake of clarity, we distinguish between channel flow and flood plain flow. Flood plain flow is usually much more complex and more difficult to describe completely than channel flow; paradoxically, however, its mathematical representation in models is much simpler. Most often the role of flooded plains in flood propagation is to provide storage volume with slow exchange of water from one part of the plain to another. The simulation scale of the whole river is usually such that a global, coarse flood plain schematization may be adopted, a representation which is in the end simpler than that used for the channel, as we shall see in Section 2.5. Clearly, this is not the case when the local details of flooded plain flow are to be represented with high accuracy, but then a physical, reduced scale model is called for.

Throughout this book channel flow is assumed to be strictly one-dimensional, even though truly one-dimensional flow does not exist in nature. One of our major concerns in this chapter is to define what is called a 'one-dimensional situation' and to consider to what extent natural river flow can be modelled as such without violating the basic concepts of the one-dimensional flow equations. We begin with a reminder of the de St Venant hypotheses which we consider to be valid throughout this section and, in general, throughout the book except when

some corrective factors which depart from the hypotheses are introduced. The de St Venant (1871) equations for unsteady flow are based upon the following series of assumptions:

(i) The flow is one-dimensional i.e. the velocity is uniform over the cross section and the water level across the section is horizontal.

(ii) The streamline curvature is small and vertical accelerations are negligible, hence the pressure is hydrostatic.

(iii) The effects of boundary friction and turbulence can be accounted for through resistance laws analogous to those used for steady state flow.

(iv) The average channel bed slope is small so that the cosine of the angle it makes with the horizontal may be replaced by unity.

We note that the cross sections of the channel conveying such a flow are of arbitrary shape and may vary along the channel axis, although the variation is limited by the condition of small streamline curvature.

One-dimensional unsteady flow in channels, assuming that the density is constant, can be described by two dependent variables; for example the water stage y and the discharge Q at any given river cross section. These dependent variables define the state of the fluid motion along the water course and in time, i.e. as a function of two independent variables (x for space and t for time). Depending on the nature of the problem one could define other pairs of dependent variables, for example, velocity and depth, as we shall show later on. The equations will of course be different for different pairs of variables, but the physical assumptions will be the same.

Since two dependent variables are sufficient to describe one-dimensional flow, we need only two equations, each of which must represent a physical law. However, we can formulate three physical laws in such flow: conservation of mass, momentum and energy. It may be shown that:

When the flow variables are not continuous (hydraulic jump, bore), two representations are possible: conservation of mass and momentum, or conservation of mass and energy. The two representations are not equivalent, and only one of them is correct.

When the flow variables are continuous, either of the two representations may be used, and they are equivalent.

This question of choice of conservation laws is extremely important from a theoretical as well as a practical point of view, and is dealt with in great detail in the first volume of the present series of books (Abbott, 1979).

Since the mass–momentum couple of conservation laws is applicable to both discontinuous and continuous situations while the mass–energy couple is not, as described by Abbott, we shall base our derivations on mass–momentum conservation.

Integral relations

Let us consider the control volume in the (x, t) plane between cross sections $x = x_1$ and $x = x_2$, and between times $t = t_1$ and $t = t_2$ shown in Fig. 2.1. In the same figure is depicted the cartesian co-ordinate system which will be used throughout the book. We shall establish equations of conservation of mass and momentum for the control volume assuming that all the de St Venant hypotheses are valid. In doing so we shall closely follow Liggett (1975), extending his unit-width analysis to a generalized section. The flow is assumed to be nearly horizontal, i.e. the angle α between the channel bed and the x-axis is sufficiently small so that $\cos \alpha = 1$. Based on these hypotheses, the basic equations can be formulated by using the principles of conservation of mass and momentum within a control volume.

The net inflow of mass into the volume is defined by the time integral of the difference between the mass flowrates entering $(\rho uA)_{x_1}$ and leaving $(\rho uA)_{x_2}$, the control volume:

$$\int_{t_1}^{t_2} [(\rho uA)_{x_1} - (\rho uA)_{x_2}] \, dt \tag{2.1}$$

This net inflow must be equal to the change of storage in the reach during the time interval:

$$\int_{x_1}^{x_2} [(\rho A)_{t_2} - (\rho A)_{t_1}] \, dx \tag{2.2}$$

where ρ = water density; $u = u(x, t)$ = uniform cross-sectional velocity;

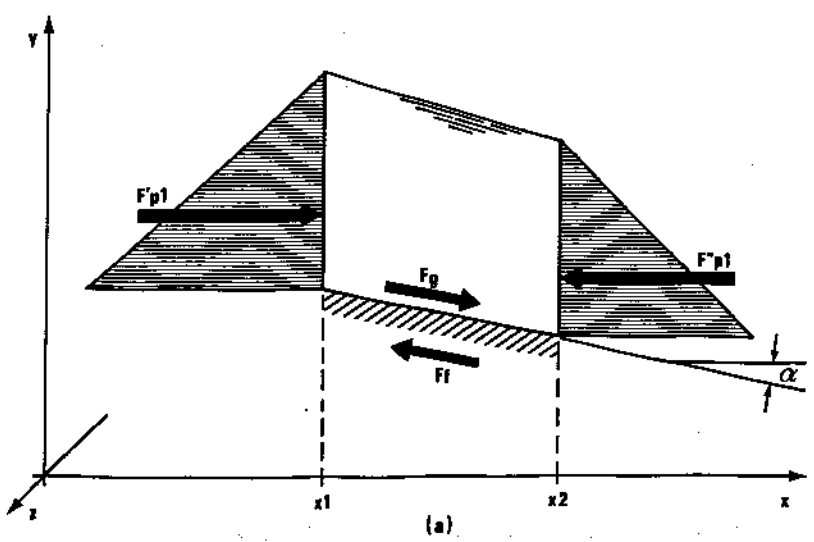

Fig. 2.1. Definition sketch for derivation of unsteady flow equations:
(a) Control volume, section view;

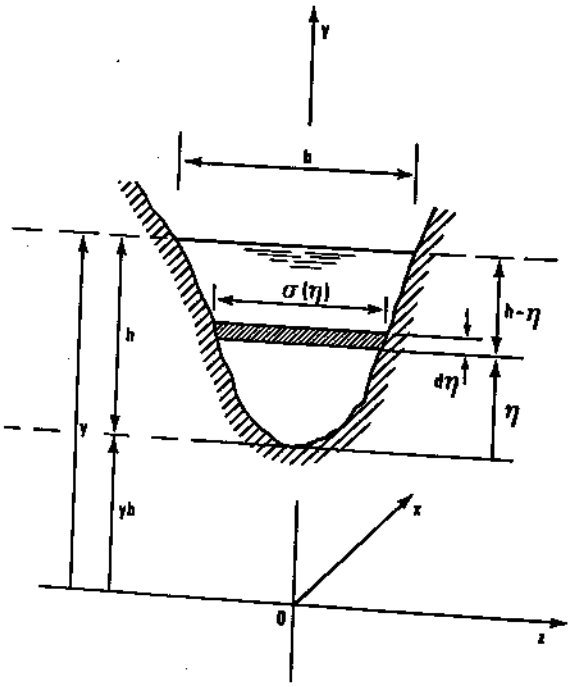

(b)

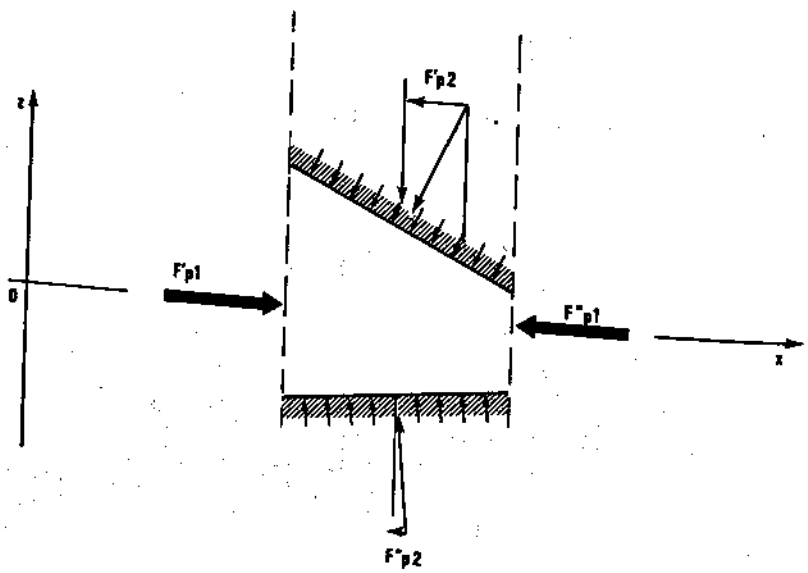

(c)

Fig. 2.1. cont'd (b) cross-section; (c) pressure forces, plan view

$A = A(x, t)$ = wetted cross-sectional area. Consequently the mass continuity integral relation for constant density is

$$\int_{x_1}^{x_2} [(A)_{t_2} - (A)_{t_1}] \, dx + \int_{t_1}^{t_2} [(Q)_{x_2} - (Q)_{x_1}] \, dt = 0 \tag{2.3}$$

where $Q = uA$.

The conservation of momentum in the x-direction requires that the change of momentum in the control volume between times t_1 and t_2 be equal to the sum of the net inflow of momentum into the control volume and the integral of the external forces acting on it over the same time interval. Momentum is the product of mass and velocity, and momentum flux through the flow section is the product of the mass flow rate and velocity, or

$$\text{momentum flux} = \rho uA \times u = \rho u^2 A \tag{2.4}$$

The net momentum flux into the control volume (momentum entering through section $x = x_1$ minus the momentum leaving through the section $x = x_2$) is

$$(\rho u^2 A)_{x_1} - (\rho u^2 A)_{x_2}$$

and the net momentum inflow between t_1 and t_2 is

$$M_f = \int_{t_1}^{t_2} [(\rho u^2 A)_{x_1} - (\rho u^2 A)_{x_2}] \, dt \tag{2.5}$$

The momentum contained in the control volume at any instant is

$$\int_{x_1}^{x_2} \rho uA \, dx$$

and the net increase from t_1 to t_2 is

$$\Delta M = \int_{x_1}^{x_2} [(\rho uA)_{t_2} - (\rho uA)_{t_1}] \, dx \tag{2.6}$$

We assume that the only important external forces acting upon the control volume in the x-direction are pressure, gravity, and frictional resistance. The pressure force F_{p^1}, is the difference of pressure forces F'_{p^1} and F''_{p^1}, applied at boundaries x_1, x_2 of the reach. At any cross section x with free surface elevation $y(x)$ the pressure force is expressed under the hydrostatic distribution hypothesis by

$$F'_{p^1} = g \int_0^{h(x)} \rho [h(x) - \eta] \, \sigma(x, \eta) \, d\eta \tag{2.7}$$

where: η = depth integration variable along the y-axis; $h(x, t)$ = water depth; $\sigma(x, \eta)$ = width of the cross section such that $\sigma(x, h) = b(x)$ = free surface width. Thus the time integral of the net pressure force F_{p^1}, when F'_{p^1} is expressed as in Equation (2.7), is

$$\int_{t_1}^{t_2} F_{p^1}\, dt = \int_{t_1}^{t_2} (F'_{p^1} - F''_{p^1})\, dt = g \int_{t_1}^{t_2} [(\rho I_1)_{x_1} - (\rho I_1)_{x_2}]\, dt \qquad (2.8)$$

where $I_1 = \int_0^{h(x)} [h(x) - \eta]\ \sigma(x, \eta)\, d\eta$

For an infinitesimal channel length dx, the increase of the pressure force due to the width variation is represented by the increase of the wetted area $d\sigma \cdot d\eta$ for constant $h = h_0$ times the distance of its centroid from the free surface $h(x) - \eta$:

$$\rho g \left[\left(\frac{\partial \sigma}{\partial x}\right) dx \cdot d\eta\right]_{h=h_0} \left[h(x) - \eta\right]$$

This force is to be integrated between $\eta = 0$ and $\eta = h(x)$ for a given cross section, and from x_1 to x_2 to obtain the total force acting on the control volume. The total integral along the contour of the control volume and for the time interval t_1 to t_2 is

$$\int_{t_1}^{t_2} \int_{x_1}^{x_2} \rho g \int_0^{h(x)} [h(x) - \eta] \left[\frac{\partial \sigma(x, \eta)}{\partial x}\right]_{h_0} d\eta\, dx\, dt$$

or

$$\int_{t_1}^{t_2} F_{p^2}\, dt = g \int_{t_1}^{t_2} \int_{x_1}^{x_2} \rho I_2\, dx\, dt \qquad (2.9)$$

where $I_2 = \int_0^{h(x)} (h - \eta) \left[\frac{\partial \sigma}{\partial x}\right]_{h=h_0} d\eta \qquad (2.10)$

Of course Equation (2.9) is not valid if a sudden width change occurs between sections x_1 and x_2. In that case supplementary forces will act upon the control volume, and they must be taken into account. In any case, in such a situation the curvature of streamlines will be non-negligible, violating one of the basic hypotheses we have adopted.

The force F_g due to gravity, that is to say the weight component along the channel axis, is evaluated by assuming that the channel bottom slope $S_0 = -\frac{\partial y_b}{\partial x} = \tan \alpha$ is small (y_b being bottom elevation above datum), so that $\tan \alpha \approx \sin \alpha$:

$$\int_{t_1}^{t_2} F_g \mathrm{d}t = \int_{t_1}^{t_2} \int_{x_1}^{x_2} \rho g A S_0 \, \mathrm{d}x \, \mathrm{d}t \tag{2.11}$$

Frictional resistance force F_f is applied to the control volume through shear along the channel bed and banks. In order to generalize the different ways in which this shear force can be treated, we follow Chow (1959) in expressing the shear force on a unit length of channel as $\rho g A S_f$ where S_f is the so-called friction slope, i.e. the energy gradient needed to overcome frictional resistance in steady flow. The time integral of the resistance force on the control volume is then

$$\int_{t_1}^{t_2} F_f \, \mathrm{d}t = \int_{t_1}^{t_2} \int_{x_1}^{x_2} \rho g A S_f \, \mathrm{d}x \, \mathrm{d}t \tag{2.12}$$

The statement of conservation of momentum thus leads to

$$\Delta M = M_f + \int_{t_1}^{t_2} F_{p_1} \, \mathrm{d}t + \int_{t_1}^{t_2} F_{p_2} \, \mathrm{d}t + \int_{t_1}^{t_2} F_g \, \mathrm{d}t - \int_{t_1}^{t_2} F_f \, \mathrm{d}t \tag{2.13}$$

or, for constant density ρ,

$$\begin{aligned} \int_{x_1}^{x_2} [(uA)_{t_2} - (uA)_{t_1}] \, \mathrm{d}x &= \int_{t_1}^{t_2} [(u^2A)_{x_1} - (u^2A)_{x_2}] \, \mathrm{d}t \\ &+ g \int_{t_1}^{t_2} [(I_1)_{x_1} - (I_1)_{x_2}] \, \mathrm{d}t - g \int_{t_1}^{t_2} \int_{x_1}^{x_2} \rho I_2 \, \mathrm{d}x \, \mathrm{d}t \\ &+ g \int_{t_1}^{t_2} \int_{x_1}^{x_2} A(S_0 - S_f) \, \mathrm{d}x \, \mathrm{d}t \end{aligned} \tag{2.14}$$

Equation (2.14) is the integral form of the momentum conservation equation for unsteady one-dimensional flow in natural channels of arbitrary shape. Equations (2.3) and (2.14) together are the integral form of the unsteady flow relations based on the de St Venant hypothesis.

Differential form of the de St Venant equations

Equations (2.3) and (2.14) are *integral* relations established without the requirement that flow variables A, Q, y, u, etc., be continuous or differentiable. Nowhere did we require that the distance $x_2 - x_1$ be infinitely small. As Liggett (1975) has pointed out, many finite difference schemes are based upon the integral relations and we shall come back to them further on. The *differential* equations of gradually varied unsteady flow may be obtained from integral equations if one assumes that the dependent variables are continuous, differentiable functions. Then, by Taylor series expansions we may write

$$(A)_{t_2} = (A)_{t_1} + \frac{\partial A}{\partial t}\Delta t + \frac{\partial^2 A}{\partial t^2}\frac{\Delta t^2}{2} + \dots$$

$$(Q)_{x_2} = (Q)_{x_1} + \frac{\partial Q}{\partial x}\Delta x + \frac{\partial^2 Q}{\partial x^2}\frac{\Delta x^2}{2} + \dots \tag{2.15}$$

By retaining only first derivatives and assuming that Δx and Δt approach zero, we can write

$$\lim_{t_2 \to t_1} \int_{x_1}^{x_2} [(A)_{t_2} - (A)_{t_1}]\, dx = \int_{x_1}^{x_2}\int_{t_1}^{t_2} \frac{\partial A}{\partial t}\, dt\, dx$$

$$\lim_{x_2 \to x_1} \int_{t_1}^{t_2} [(Q)_{x_2} - (Q)_{x_1}]\, dt = \int_{t_1}^{t_2}\int_{x_1}^{x_2} \frac{\partial Q}{\partial x}\, dx\, dt \tag{2.16}$$

And the continuity Equation (2.3) becomes

$$\int_{x_1}^{x_2}\int_{t_1}^{t_2}\left[\frac{\partial A}{\partial t} + \frac{\partial Q}{\partial x}\right] dt\, dx = 0 \tag{2.17}$$

In a similar way we may write

$$\begin{aligned}
(u^2A)_{x_2} - (u^2A)_{x_1} &= \frac{\partial (u^2A)}{\partial x}\Delta_x + \frac{\partial^2 (u^2A)}{\partial x^2}\frac{\Delta x^2}{2} + \dots \\
(uA)_{t_2} - (uA)_{t_1} &= \frac{\partial Q}{\partial t}\Delta t + \frac{\partial^2 Q}{\partial t^2}\frac{\Delta t^2}{2} + \dots \\
(I_1)_{x_2} - (I_1)_{x_1} &= \frac{\partial I_1}{\partial x}\Delta x + \frac{\partial^2 I_1}{\partial x^2}\frac{\Delta x^2}{2} + \dots
\end{aligned} \tag{2.18}$$

Substitution of the first terms of expansions (2.18) into Equation (2.14) and then passage to the limit ($\Delta x, \Delta t \to 0$) leads to

$$\int_{x_1}^{x_2}\int_{t_1}^{t_2}\left[\frac{\partial Q}{\partial t} + \frac{\partial (u^2A)}{\partial x}\right] dt\, dx$$

$$= -g\int_{x_1}^{x_2}\int_{t_1}^{t_2}\left[\frac{\partial I_1}{\partial x} - I_2 - A(S_0 - S_f)\right] dt\, dx \tag{2.19}$$

If the relations (2.17) and (2.19) are to hold everywhere in the (x, t) plane, then they must hold for an infinitely small volume, and we can write two differential equations:

continuity equation $\dfrac{\partial A}{\partial t} + \dfrac{\partial Q}{\partial x} = 0$ (2.20)

momentum equation $$\frac{\partial Q}{\partial t} + \frac{\partial (u^2 A)}{\partial x} + g \frac{\partial I_1}{\partial x} = gA(S_0 - S_f) + gI_2 \tag{2.21}$$

Combining the x derivatives in Equation (2.21) and replacing u by Q/A:

$$\frac{\partial Q}{\partial t} + \frac{\partial}{\partial x}\left(\frac{Q^2}{A} + gI_1\right) = gA(S_0 - S_f) + gI_2 \tag{2.22}$$

Equations (2.20) and (2.22) are written in a special form, often called the 'divergent' form of partial differential equations. If the right hand sides of Equations (2.20) and (2.22) are equal to zero, these equations express nil divergence of the mass and momentum vector functions in any closed contour in the (x, t) plane; mass and momentum are conserved. When the right hand side of Equation (2.22) is different from zero, momentum is no longer conserved, the free terms acting as momentum sources or sinks.

Continuing our derivations, still assuming that all dependent variables are differentiable, let us evaluate the derivative of the gI_1 term in Equation (2.22):

$$\frac{\partial}{\partial x}(gI_1) = g \frac{\partial}{\partial x} \int_0^{h(x)} [h(x) - \eta]\ \sigma(x, \eta)\, d\eta \tag{2.23}$$

Applying the Leibniz theorem for differentiation of an integral, and keeping in mind that $\sigma(x, h) = b(x)$ and $\int_0^h \sigma\, d\eta = A$, we obtain

$$\begin{aligned} \frac{\partial}{\partial x}(gI_1) &= g \frac{\partial h}{\partial x} \int_0^{h(x)} \sigma(x, \eta)\, d\eta \\ &\quad + g \int_0^{h(x)} [h(x) - \eta] \left[\frac{\partial b}{\partial x}\right]_{h = \text{const}} d\eta \end{aligned} \tag{2.24}$$

$$\frac{\partial}{\partial x}(gI_1) = gA(x) \frac{\partial h}{\partial x} + gI_2 \tag{2.25}$$

Consequently Equation (2.21) may now be rewritten

$$\frac{\partial Q}{\partial t} + \frac{\partial}{\partial x}(u^2 A) + gA \frac{\partial h}{\partial x} + gI_2 = gA(S_0 - S_f) + gI_2$$

Thus we obtain the 'momentum' equation generally used in engineering practice,

$$\frac{\partial Q}{\partial t} + \frac{\partial}{\partial x}(uQ) + gA\left(\frac{\partial h}{\partial x} - S_0\right) + gAS_f = 0 \tag{2.26}$$

which, as we shall discuss later on, is not in a momentum divergent form. We shall generally refer to the second of the two basic flow relations as the

'dynamic' equation, since it is seldom a true statement of momentum conservation.

We shall now consider some of the more often used choices of dependent variables with which engineers work, taking the continuity Equation (2.20) and dynamic Equation (2.26) as a departure point.

(i) $Q(x, t), h(x, t)$

The variable $A(h)$ in the continuity equation is eliminated by

$$\frac{\partial A(h)}{\partial t} = \frac{\partial A}{\partial h}\frac{\partial h}{\partial t} = b\frac{\partial h}{\partial t}$$

while the velocity u is replaced by Q/A in the dynamic equation.

The system of two flow equations becomes

$$\frac{\partial h}{\partial t} + \frac{1}{b}\frac{\partial Q}{\partial x} = 0$$

$$\frac{\partial Q}{\partial t} + \frac{\partial}{\partial x}\left(\frac{Q^2}{A}\right) + gA\frac{\partial h}{\partial x} + gA(S_f - S_0) = 0 \qquad (2.27)$$

where $b = b(h), A = A(h)$.

(ii) $Q(x, t), y(x, t)$

Water depth $h = y - y_b$, where $y_b(x)$ is the bottom elevation; hence

$$\frac{\partial h}{\partial t} = \frac{\partial y}{\partial t}; \quad \frac{\partial h}{\partial x} = \frac{\partial y}{\partial x} - \frac{\partial y_b}{\partial x} = \frac{\partial y}{\partial x} + S_0$$

Substitution into Equations (2.27) leads to the system

$$\frac{\partial y}{\partial t} + \frac{1}{b}\frac{\partial Q}{\partial x} = 0$$

$$\frac{\partial Q}{\partial t} + \frac{\partial}{\partial x}\left(\frac{Q^2}{A}\right) + gA\frac{\partial y}{\partial x} + gAS_f = 0 \qquad (2.28)$$

where $b = b(y), A = A(y)$.

(iii) $u(x, t), h(x, t)$

Let us put in the continuity equation $Q = uA(h)$, i.e.

$$\frac{\partial Q}{\partial x} = A\frac{\partial u}{\partial x} + u\frac{\partial A}{\partial x} = A\frac{\partial u}{\partial x} + u\left[\frac{\partial A}{\partial h}\frac{\partial h}{\partial x} + \left(\frac{\partial A}{\partial x}\right)_{h = \text{const}}\right]$$

where the last terms represent the rate of change of A when the *depth h is held constant*, and $\frac{\partial A}{\partial h} = b$. The time and space derivatives of discharge are transformed as follows:

$$\frac{\partial Q}{\partial t} = \frac{\partial (uA)}{\partial t} = u\,\frac{\partial A}{\partial t} + A\,\frac{\partial u}{\partial t} = -u\,\frac{\partial Q}{\partial x} + A\,\frac{\partial u}{\partial t}$$

$$\frac{\partial}{\partial x}\left(\frac{Q^2}{A}\right) = \frac{2Q}{A}\,\frac{\partial Q}{\partial x} - \frac{Q^2}{A^2}\,\frac{\partial A}{\partial x}$$

$$= 2\,\frac{Q}{A}\,\frac{\partial Q}{\partial x} - \frac{Q^2}{A^2}\left[b\,\frac{\partial h}{\partial x} + \left(\frac{\partial A}{\partial x}\right)_{h\,=\,\text{const}}\right]$$

Substitution of these derivatives into the system of Equation (2.27) yields, after cancelling some terms in the dynamic equation, the following system:

$$\begin{aligned} &\frac{\partial h}{\partial t} + \frac{A}{b}\,\frac{\partial u}{\partial x} + u\,\frac{\partial h}{\partial x} + \frac{u}{b}\left(\frac{\partial A}{\partial x}\right)_{h\,=\,\text{const}} = 0 \\ &\frac{\partial u}{\partial t} + u\,\frac{\partial u}{\partial x} + g\,\frac{\partial h}{\partial x} + g(S_f - S_0) = 0 \end{aligned} \tag{2.29}$$

where $A = A(h)$, $b = b(h)$

(iv) $u(x, t), y(x, t)$
The space derivative of discharge $Q = uA(y)$ is now

$$\frac{\partial Q}{\partial x} = A\,\frac{\partial u}{\partial x} + u\left[b\,\frac{\partial y}{\partial x} + \left(\frac{\partial A}{\partial x}\right)_{y\,=\,\text{const}}\right]$$

By substituting this expression and the derivatives

$$\frac{\partial h}{\partial x} = \frac{\partial y}{\partial x} - \frac{\partial y_b}{\partial x} = \frac{\partial y}{\partial x} + S_0;\ \frac{\partial h}{\partial t} = \frac{\partial y}{\partial t}$$

into Equation (2.29), we obtain

$$\begin{aligned} &\frac{\partial y}{\partial t} + \frac{A}{b}\,\frac{\partial u}{\partial x} + u\left(\frac{\partial y}{\partial x} + S_0\right) + \frac{u}{b}\left(\frac{\partial A}{\partial x}\right)_{y\,=\,\text{const}} = 0 \\ &\frac{\partial u}{\partial t} + u\,\frac{\partial u}{\partial x} + g\,\frac{\partial y}{\partial x} + gS_f = 0 \end{aligned} \tag{2.30}$$

The preceding paragraphs may seem to be dedicated to spurious 'algebraic manipulations'. As a matter of fact, these gymnastics are of some practical importance, since certain numerical techniques may be better adapted to some of the above systems of equations than others. Physical features of a given watercourse may also suggest the system which is 'better' (read: easier to integrate numerically without gross errors) than others for that particular case. For example, when the river is steep and its cross-sectional variations are small, the use of $h(x, t)$ rather than $y(x, t)$ as a dependent variable is recommended since h and $\left(\frac{\partial A}{\partial x}\right)_{h=\text{const}}$ vary slowly from one point to another. On the other hand, flat slopes and large cross-sectional variations favour the use of $y(x, t)$.

Moreover, the appearance of surges in the solution may make the use of one o the systems compulsory while rejecting others, as we shall see further on. Equations (2.27)–(2.30) are not in divergent form, as we will have occasion to re-emphasize in Section 2.3.

The systems of Equations (2.3), (2.14) and (2.27)–(2.30) are, mathematica speaking, equivalent if and only if *all* functions and variables are at least once differentiable. If it is impossible to consider the functions and variables as differentiable, the systems (2.27)–(2.30) are not equivalent. If the solutions ar discontinuous (e.g. moving hydraulic jumps appear), differential systems may not be valid at all while integral relations still will be. Neither the integral nor differential relations may be considered as valid when the basic de St Venant hypotheses are violated, as in the case of an undular jump with its train of short waves which make it impossible to neglect vertical accelerations.

Supplementary terms and coefficients

The equations often used in engineering practice are not always based on the consistent set of assumptions which we used to derive Equations (2.27)–(2.30). The desire to represent highly irregular cross sections in natural watercourses has tempted engineers to introduce corrective coefficients in order to be able to relax de St Venant's assumption of uniform velocity in the cross section. The most common example of a situation in which this appears to be necessary is flow in cross sections which include overbank areas. Because of its high resistance to flow, the overbank area may contribute only to storage, conveying virtually no discharge. In such cases the continuity equation is sometimes written

$$\frac{\partial A_{st}}{\partial t} + \frac{\partial Q}{\partial x} = 0 \tag{2.31}$$

where A_{st} is the cross-sectional area available for storage, and is generally not the same area as used in the momentum equation. Often engineers define a so-called 'storage-width' b_{st}, given by

$$\frac{\partial A_{st}}{\partial t} = b_{st} \frac{\partial y}{\partial t} \; ; \; b_{st} = b_{st}(y) \tag{2.32}$$

so that the continuity equation may be written

$$\frac{\partial y}{\partial t} + \frac{1}{b_{st}} \frac{\partial Q}{\partial x} = 0 \tag{2.33}$$

If a continuous lateral inflow q per unit length is added, Equation (2.33) becomes

$$b_{st} \frac{\partial y}{\partial t} + \frac{\partial Q}{\partial x} = q \tag{2.34}$$

As for the dynamic equation, the control volume approach we used in obtaining Equation (2.14) is replaced by a consideration of momentum conservation in a differential element in a cross section in which the velocity is not uniform. Integration over the entire cross section as described by Abbott (1979) assuming the water surface and energy slope to be everywhere the same yields another dynamic equation,

$$\frac{\partial Q}{\partial t} + \frac{\partial}{\partial x}\left(\beta \frac{Q^2}{A}\right) + gA \frac{\partial y}{\partial x} + gAS_f = 0 \tag{2.35}$$

or, if lateral inflow is considered and u_q is its downstream velocity component,

$$\frac{\partial Q}{\partial t} + \frac{\partial}{\partial x}\left(\beta \frac{Q^2}{A}\right) + gA\left(\frac{\partial y}{\partial x} + S_f\right) - \left(u_q - \frac{Q}{A}\right) q = 0 \tag{2.36}$$

where $Q = \bar{u}A$

$\bar{u}$ = cross-sectional *average* velocity, and

$$\beta = \frac{\int_0^b u_z^2 h_z \, dz}{\bar{u}^2 A} \; ; \; \beta = \beta(y) \tag{2.37}$$

the subscripts z denoting local values of depth-averaged velocity and depth at position z in the cross section. We shall come back to the meaning of β later on.

The system of two partial differential equations (2.33), (2.35) *formally* resembles Equations (2.28). The two systems, nevertheless, are founded upon basically different hypothesis. Equations (2.28) were obtained from integral relations which were derived using the assumption of *uniform* velocity in the whole cross section with a unique definition of discharge $Q = Au$, A being the cross-sectional area. Equations (2.33) and (2.35) were derived with the discharge defined as $Q = A\bar{u}$, $\bar{u}$ being an *average* velocity in the cross section and A being a 'live' cross-sectional area, different from the cross-sectional area A_{st} used in the continuity equation. Before discussing the physical meaning of the different terms of the system (2.33) and (2.35), we would like to stress that, because of these different hypotheses, Equations (2.33) and (2.35) are *not compatible* with the systems of Equations (2.27)–(2.30). One cannot pass from one to another through formal differentiation. The physical significance of this will be more clear after a discussion of the physical meaning of the resistance term (the friction slope S_f), the coefficient β, the storage width b_{st}, and lateral inflow.

Empirical resistance laws

In our developments up to this point we have expressed the force per unit channel length due to bed and bank resistance as $\rho g A S_f$ in which the 'friction slope' S_f is taken to represent any one of a number of empirical resistance laws. Most of these empirical laws are based on a relation between discharge and friction losses of the general type

$$Q = K\sqrt{S_f}$$

where $K = K(h)$ is the so-called conveyance factor of the channel and S_f is t slope of the energy grade line in steady flow. In continental Europe the mos frequently used laws are the Chezy relation

$$\bar{u} = C(RS_f)^{\frac{1}{2}};\ Q = CA(RS_f)^{\frac{1}{2}} \tag{}$$

and the Strickler relation

$$\bar{u} = k_{Str}R^{2/3}\sqrt{S_f};\ Q = k_{Str}AR^{2/3}\sqrt{S_f} \tag{2}$$

where C is the de Chezy resistance coefficient ($m^{1/2}/s$), k_{Str} the Strickler coefficient ($m^{1/3}/s$) and R the hydraulic radius, defined by the relation

$$R = \frac{A}{P} \tag{2.}$$

where P is the wetted perimeter of the cross section. In the Anglo Saxon countries, engineers are more familiar with the Manning relation

$$\bar{u} = \frac{1}{n}R^{2/3}\sqrt{S_f};\ Q = \frac{1}{n}AR^{2/3}\sqrt{S_f} \tag{2.4}$$

where n is Manning's coefficient, in metric units ($s/m^{1/3}$). Comparing the resistance laws it will be clear that the following relations link the various coefficients:

$$C = \frac{1}{n}R^{1/6}$$

and (2.43)

$$k_{Str} = \frac{1}{n} \tag{2.44}$$

In the literature the Manning relation is also found as

$$Q = \frac{1.49}{n}AR^{2/3}\sqrt{S_f} \tag{2.45}$$

where Q and R are defined in US units of cubic feet per second and feet, respectively. The n-values in both Equations (2.42) and (2.45) are given independently of the system of units.

Formulas (2.39)–(2.45) imply a constant value of the roughness coefficient across the section. In nature the coefficients k_{Str}, n and C are empirical parameters linked to the composition of the river bed (for example, the Strickler coefficient is inversely proportional to the 1/6th power of the sand grain diameter) and thus they generally vary across the watercourse width. In *compact* channels (those without overbank sections and uniform bed rough-

ness) the roughness coefficient along the wetted perimeter may be nearly constant and the mean velocity can still be computed by one of the formulae (2.39)–(2.45) without much error (*see* Chow, 1959). If the cross section has a compound shape such as shown in Fig. 2.2, common practice consists in dividing the cross section into several distinct subsections (vertical slices) with each subsection having a different roughness from the others. As we describe in more detail in Chapter 4, it is possible to define a global conveyance factor for the cross section based upon the hypothesis that the friction slope S_f is constant

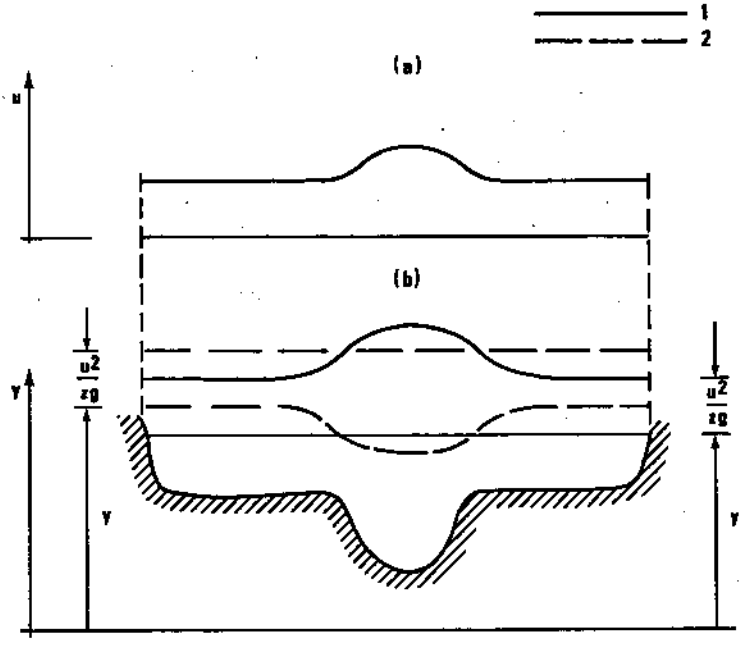

Fig. 2.2. Consequences of assumptions regarding constant energy level and horizontal water surface in channel flow: 1-horizontal water surface implies non-constant energy level, 2-constant energy level implies variable water surface. (a) Non-uniform velocity distribution. (b) Flow cross section.

across the watercourse width. Assuming that the resistance equation can be applied separately to each of several vertical slices i, we have

$$\sum_i Q_i = Q \tag{2.46}$$

or

$$\sum_i K_i \sqrt{S_f} = K \sqrt{S_f} \tag{2.47}$$

where $K_i = k_{Str} h_i^{5/3} b_i$ for the Strickler formula, and $K_i = C_i h_i^{3/2} b_i$ for the

Chezy formula, b_i being the width of slice i.

Unfortunately Equation (2.47) is in contradiction with our one-dimensional flow hypotheses: if the velocities vary across the width, the energy grade line must vary too in order to keep the free surface level constant, hence $S_f = S_f(z) \neq$ const. It would thus be more consistent to write the following equality instead of Equation (2.47):

$$\sum_i K_i \sqrt{S_{f_i}} = K \sqrt{S_f} \tag{2.48}$$

On the other hand, assuming S_f to be constant but the horizontal velocities to be non-uniform, the free water surface can no longer be horizontal. Figure 2.2 depicts this contradiction. It is only if the de St Venant hypothesis of a uniform velocity distribution is maintained, that no contradiction arises. In practice it is always assumed that both S_f is constant and the free surface is horizontal; the error thus committed may be considered as a measure of how far the real flow is from an idealized one-dimensional situation.

Following common practice and accepting the error stemming from the above contradiction, the conveyance of a compound cross section may be computed with the aid of Equation (2.47) which yields, for the Strickler formula

$$K = \sum_i k_{\mathrm{Str}_i} b_i h_i^{5/3} \tag{2.49}$$

and for the Chezy formula

$$K = \sum_i C_i b_i h_i^{3/2} \tag{2.50}$$

Coefficient of non-uniform velocity distribution

The coefficient β in Equations (2.35) and (2.36) appears as a result of the assumption of non-uniform velocity in the cross section. It reflects the fact that since local momentum flux is proportional to the square of the local velocity, the overall mean channel velocity is not representative of the overall momentum flux unless it is corrected by β. Theoretically β could be evaluated from measured velocity distributions using Equation (2.37), but this is of course impractical.

Schönfeld (1951) therefore introduces the following hypothesis: if at every point in the cross section the depth-averaged velocity u_z can be computed using the locally applied steady flow resistance law, these local velocities can then be substituted into Equation (2.37) and the integration over the cross section carried out. By analogy with non-uniform vertical velocity profiles, β is often called the Boussinesq coefficient.

If in formula (2.37) the mean velocity $\bar{u}$ in the denominator is replaced by a resistance equation using the global conveyance factor as given by Equations

(2.49) or (2.50), and if the friction slope is assumed to be constant with z, i.e. $S_f(z) = S_f$ (see once again Fig. 2.2) the integral of Equation (2.37) may be approximated by using vertical slices of finite width b_i instead of infinitely narrow tubes db. We obtain

$$\beta = \frac{\sum_i C_i^2 h_i^2 b_i}{K^2/A} = \frac{A \sum_i C_i^2 h_i^2 b_i}{\left(\sum_i C_i b_i h_i^{3/2}\right)^2} \tag{2.51}$$

for the Chezy equation, and

$$\beta = \frac{\sum_i k_{\mathrm{Str}_i}^2 h_i^{7/3} b_i}{K^2/A} = \frac{A \sum_i k_{\mathrm{Str}_i}^2 h_i^{7/3} b_i}{\left(\sum_i k_{\mathrm{Str}_i} h_i^{5/3} b_i\right)^2} \tag{2.52}$$

for the Strickler equation. The coefficients β defined according to Equations (2.51) and (2.52) are, for a given cross section, functions of water stage y and as such may be used in the dynamic equation (2.36).

Storage width b_{st}

The purpose of introducing the storage width b_{st}, or the storage cross-sectional area $A_{st} > A$, is to take into account the fact that flooded zones often act only as storage areas. They store water whose velocity is nil in the general flow direction x and, thus, does not contribute to the overall momentum flux in the cross section. If the coefficient β is used in the dynamic equation it already takes into account this phenomenon. Indeed, if for a number of vertical slices the roughness coefficient k_{Str} is assumed to be very small, the global β coefficient will increase and the term $(\beta Q^2)/A$ in Equation (2.36) will increase accordingly. It would seem superfluous in this case to admit further that $A < A_{st}$. Besides, it is not at all clear how to define the 'live' area A and width b as distinct from A_{st} and b_{st} for water stages higher than the river banks as shown in Fig. 2.3. The introduction of a 'live' width $b(y) < b_{st}$ opens the door to even more arbitrary judgements as to the model representative of reality.

Lateral inflow

Inflow (or outflow) continuously distributed along the rivercourse is seldom encountered in mathematical modelling of rivers. The most common situations in which such a lateral discharge is to be taken into account are linked to hydrological phenomena: evaporation, rainfall, and infiltration. Usually these processes can be neglected; in tropical areas, however, to neglect them may lead to important errors. A well known example is the Nile River which loses approximately 50% of its discharge between Momgalla and Malakal due to

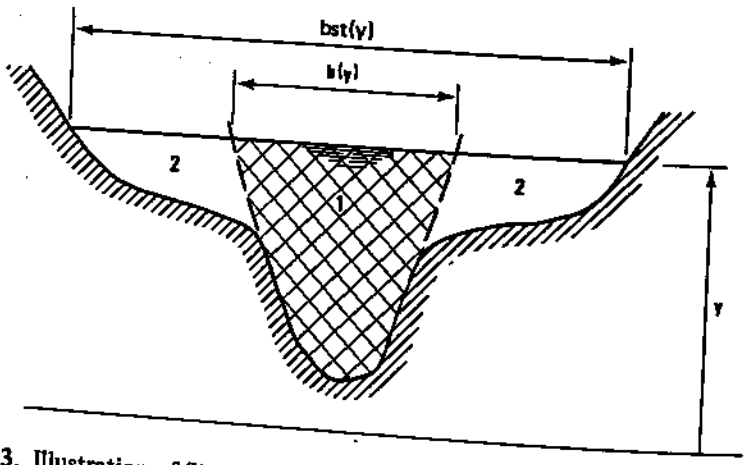

Fig. 2.3. Illustration of 'live' and 'storage' cross-sectional areas. 1, 'Live' area A in the second term of Equation (2.36); 2, Additional 'storage' area on which is based the 'storage width' b_{st} in Equation (2.33)

infiltration and evaporation. During the flooding of plains, significant amounts of water may infiltrate into the soil. Special attention has to be given in that case to previous events as the soil may be saturated by earlier floods or, on the contrary, the effects of frost on the permeability may be important in preventing infiltration. When such phenomena are modelled as continuous lateral discharge, the actual form of the function $q(x, y, t)$ should be determined from hydrological considerations and models, with dependence on the extent of inundated area, antecedent conditions, etc., taken into account.

It should be stressed that tributaries and effluents *should not* be represented by continuous lateral discharge q but rather by point inflows or outflows. Possible exceptions are lateral spillways or weirs in canals for which high accuracy in modelling is sought. The contribution of the lateral flow to the momentum in the channel is most often negligible except when relatively large amounts of water are involved. The velocity of lateral inflows and the angle they make with the main channel velocity vector are difficult to estimate and may vary with the water stage. It should be kept in mind that with all these uncertainties it may well be possible to introduce errors greater than the ones introduced by neglecting lateral inflow altogether.

2.2 CHARACTERISTICS – BOUNDARY AND INITIAL CONDITIONS

In the previous section we have described in a very general way the equations governing unsteady flow in channels. In the present paragraph we shall introduce, still in a very intuitive manner, the theory of characteristics which is most useful for understanding initial and boundary condition requirements as well as the behaviour of solutions to the differential equations.

Any disturbance which occurs at some point at time $t = 0$ in open channel

flow propagates along the channel in time and in two directions: downstream and upstream. Thus the perturbation which takes place at point Q in Fig. 2.4a

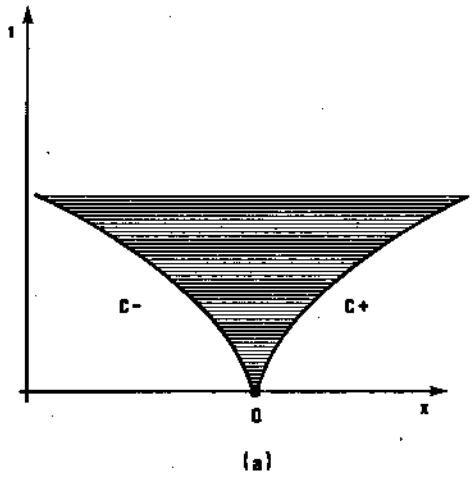

Fig. 2.4. Propagation of a disturbance in channel flow. (a) Range of influence of disturbance at point Q. (b) Domain of determinacy of point P

influences the shaded region limited by curves C_+, C_- which represent the paths of disturbance propagation. Inversely, taking a point P one can define backward in time the domain in which disturbances can influence the conditions at point P, Fig. 2.4b. Anything happening outside the shaded region will not influence the state at point P. If the perturbations form shallow water waves of small amplitude, the lines forming the boundaries of these regions are called

characteristics. They can be defined as lines in the (x, t) plane along which disturbances propagate. Coming back now to mathematical definitions, we shall define disturbances as discontinuities in the first and higher derivatives of the dependent variables and the physical parameters which appear in the flow equations. Thus the discontinuities in the free water surface slope $\partial y/\partial x$ or in the velocity gradient $\partial u/\partial x$ propagate along the characteristics with a celerity equal to that of shallow water waves,

$$\frac{\mathrm{d}x}{\mathrm{d}t} = u \pm \left(g\frac{A}{b}\right)^{\frac{1}{2}} \tag{2.53}$$

Such is not the case for discontinuities in the variables themselves. For example, Equation (2.53) cannot apply to a hydraulic bore, which is a discontinuity in the free surface between two different depths.

Depending on the direction of the two characteristics, one can distinguish three different states of fluid motion. In *sub critical* flow the celerity $\left(g\frac{A}{b}\right)^{\frac{1}{2}}$ is greater than the absolute value of the flow velocity $|u|$; the two characteristics therefore have opposite signs and the state at any point P is influenced both from upstream and downstream conditions (Fig. 2.5a). In *critical* flow $|u| = \left(g\frac{A}{b}\right)^{\frac{1}{2}}$ and one of the characteristic velocities of propagation becomes zero; for the example shown in Fig. 2.5b the negative characteristic C_ becomes a vertical line $x = x_p = \text{const}$. In *supercritical* flow $|u| > \left(g\frac{A}{b}\right)^{\frac{1}{2}}$ and the two characteristics have the same sign (Fig. 2.5c and 2.5d). In the last two cases the state at point P does not depend upon the downstream flow conditions. These statements as to the dependence of flow conditions at point P refer to a neighbourhood of the point P only. In the following paragraphs we shall briefly show how characteristic behaviour is related to the flow equations and we shall summarize the consequences of theoretical considerations. The reader will find a full treatment of the method of characteristics in mathematical treatises (e.g. Courant and Hilbert, 1953). As for application to the open channel flow equations, the basic references are Stoker (1957) and Abbott (1966, 1979). Historically speaking one should remember that the first application of the method to hydraulics is due to Massau (1889) and its development to Craya (1946).

Consider a channel of constant cross-sectional shape and constant longitudinal bottom slope S_0 (such a channel is called *prismatic*) and in which the flow is described by the differential system of Equation (2.29),

$$\begin{aligned} &\frac{\partial h}{\partial t} + \frac{A}{b}\frac{\partial u}{\partial x} + u\frac{\partial h}{\partial x} = 0 \\ &\frac{\partial u}{\partial t} + u\frac{\partial u}{\partial x} + g\frac{\partial h}{\partial x} + g(S_f - S_0) = 0 \end{aligned} \tag{2.54}$$

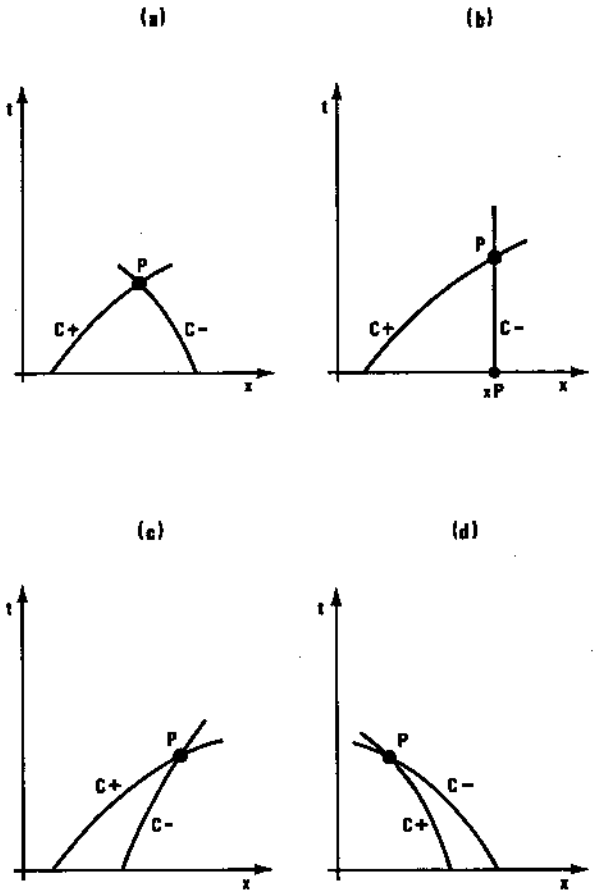

Fig. 2.5. Structure of the characteristics and their relation to the type of flow at point P. (a) Sub critical flow; (b) critical flow; (c) supercritical flow in positive direction; (d) supercritical flow in negative direction

We shall now transform Equations (2.54) into their characteristic form, closely following Stoker (1957). We introduce a new variable c to replace h:

$$c = \left(g \frac{A}{b}\right)^{\frac{1}{2}}, A = A(h) \tag{2.55}$$

Then we find by differentiating c^2 with respect to x and t, and noting that $\frac{\partial A}{\partial h} = b$,

$$2c \frac{\partial c}{\partial x} = g \frac{\partial h}{\partial x}; \; 2c \frac{\partial c}{\partial t} = g \frac{\partial h}{\partial t} \tag{2.56}$$

Substitution into Equations (2.54) leads to the following system of two equations:

$$2\frac{\partial c}{\partial t} + 2u\frac{\partial c}{\partial x} + c\frac{\partial u}{\partial x} = 0$$

$$\frac{\partial u}{\partial t} + 2c\frac{\partial c}{\partial x} + u\frac{\partial u}{\partial x} + E = 0 \tag{2.57}$$

where $E = g(S_f - S_0)$

These equations are next added, then subtracted to obtain the following pair of equations, the so-called 'characteristic form' of the flow equations:

$$\left\{\frac{\partial}{\partial t} + (u+c)\frac{\partial}{\partial x}\right\}(u+2c) + E = 0$$

$$\left\{\frac{\partial}{\partial t} + (u-c)\frac{\partial}{\partial x}\right\}(u-2c) + E = 0 \tag{2.58}$$

We observe that $u + c = W_+$ is a velocity and so is $u - c = W_-$. Indeed, according to Equations (2.58) functions c and u are differentiated along curves in the (x, t) plane which satisfy the differential equations $dx/dt = u \pm c$. The differentiation operators are nothing more than total derivatives along these curves:

$$\frac{D_+}{Dt} = \frac{\partial}{\partial t} + W_+\frac{\partial}{\partial x};\quad \frac{D_-}{Dt} = \frac{\partial}{\partial t} + W_-\frac{\partial}{\partial x} \tag{2.59}$$

Consequently we may write

$$\frac{D_+}{Dt}(u+2c) = -E \tag{2.60a}$$

$$\frac{D_-}{Dt}(u-2c) = -E \tag{2.60b}$$

Thus for any point *moving through the fluid* with the velocity $u \pm c$, the relationship (2.60a) is true *along* the characteristic curves C_+, defined by

$$\frac{dx}{dt} = u + c \tag{2.61}$$

while the relationship (2.60b) is valid *along* the characteristic curve C_-, defined by

$$\frac{dx}{dt} = u - c \tag{2.62}$$

It may be proven that Equations (2.58) and (2.60), (2.61), (2.62) are completely equivalent to the system of Equations (2.54). With the system of four differential Equations (2.60)–(2.62) one can find four partial derivatives of the dependent variables ($\partial h/\partial t$, $\partial h/\partial x$, $\partial u/\partial t$, $\partial u/\partial x$) around a line element in the (x, t) plane and then continue the solution in the vicinity of such an element.

If the channel is frictionless and horizontal (i.e. $E = 0$), Equations (2.60) state that

$$u + 2c = \text{constant} = J_+ \tag{2.63}$$

along the C_+ characteristic, while

$$u - 2c = \text{constant} = J_- \tag{2.64}$$

along the C_- characteristic. Constants J_+ and J_- are called the *Riemann invariants* whose values vary from one characteristic to another.

For a prismatic channel with a resistance shear stress ($S_f \neq 0$), expressions between two points 1 and 2 along a C_+ characteristic can be obtained from Equation (2.60a):

$$\left[u + 2 \left(g \frac{A}{b} \right)^{\frac{1}{2}} \right]_1^2 = g \int_{t_1}^{t_2} (S_0 - S_f)\, dt \tag{2.65}$$

and along a C_- characteristic from Equation (2.60b):

$$\left[u - 2 \left(g \frac{A}{b} \right)^{\frac{1}{2}} \right]_1^2 = g \int_{t_1}^{t_2} (S_0 - S_f)\, dt \tag{2.66}$$

The left-hand sides are called the Riemann quasi-invariants when the right-hand side quantities are sufficiently small, as they always can be forced to be by a suitable choice of the $t_2 - t_1$ interval (Abbott, 1979). For non-prismatic channels, the Riemann invariants under an analogous form cannot be derived; Equations (2.60) are the only ones at our disposal. The variable E in the general system contains all terms brought in because of the non-prismatic character of the channel and/or representing external forces.

Under the restrictive conditions of differentiability of all functions, the system of Equations (2.58) is equivalent to all the systems (2.27)–(2.30), since, for all of them, $Q = uA$, $h = y - y_b$, etc. Mathematically all these systems of two first order partial differential equations are of the same type and may be classified as *hyperbolic non-linear* systems. Analogous though different characteristic equations may be derived for the system of Equations (2.31) and (2.36).

A pertinent physical observation is, as can be seen from Equations (2.55), (2.61) and (2.62), that the celerities W are not *directly* dependent on bed slope, resistance or other external forces, such as wind effects and lateral flow, which might be included in the term E of Equations (2.60).

Boundary data requirements

Let us consider a line element $x(t)$ in the (x, t) plane within the domain of solution of the flow Equations (2.54). For simplicity we shall assume that the term E is zero in Equations (2.60) and consequently that the Riemann invariants are (Equations (2.63) and (2.64))

$$J_+ = u + 2\left(g\frac{A}{b}\right)^{\frac{1}{2}};\ J_- = u - 2\left(g\frac{A}{b}\right)^{\frac{1}{2}}$$

$$A = A(h);\ b = b(h)$$

We shall consider the relationship between the dependent variables u and h along the line element, which may or may not coincide with a characteristic. It is clear that when the line element corresponds over some of its length to a characteristic, only one of the functions u and h can be given independently, while the other follows from the Riemann invariant along the characteristic. When the line element and a characteristic intersect at one point only (e.g. point A situated on the line (x_0, x_1) in Fig. 2.6) the values of u and h given on that line at that point

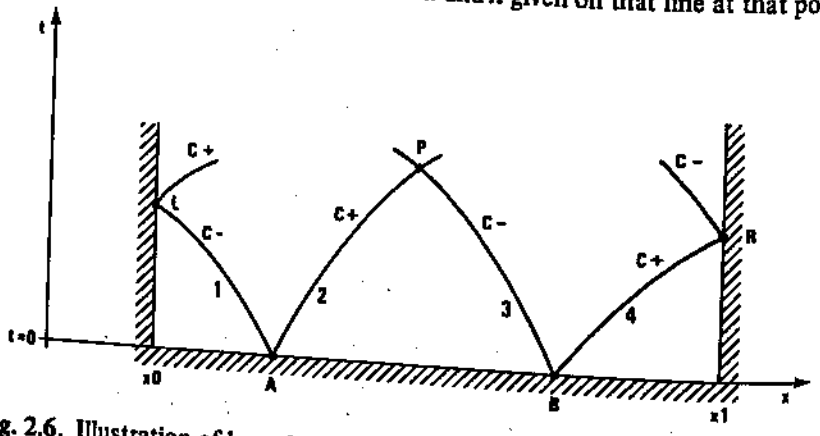

Fig. 2.6. Illustration of boundary data requirements in the (x, t) plane for subcritical flow. $1, J_-$ given at A; $2, J_+$ given at A; $3, J_-$ given at B; $4, J_+$ given at B

define the Riemann invariant at all points along the characteristic. One can imagine the (x, t) plane to be covered with an infinite set of C_+ and C_- characteristics. At every point, as for example point P, two characteristics intersect and the solution (i.e. u and h) at that point is defined through the two independent Riemann invariants J_+ and J_- derived from the values of u and h given on the line $t = 0$ at points such as A, B, etc.

In applications one is generally interested in a domain of the (x, t) plane which is bounded in space. Taking now as a line element the line composed of the two parts $t = 0$ for $x \geqslant x_0$, and $x = x_0$ for $t \geqslant 0$, we can see that this element is intersected twice by the same C_- characteristic at points A and L. When u and h are given at point A of such a characteristic, the values of u and h in the second intersection point L cannot be given independently but must satisfy the compatibility condition along the characteristic J_- given at A. The solution at point L is properly defined only when one and only one of the values u or h or a relationship between u and h independent from the invariant J_- is given. In fact this applies to all points on the line $x = x_0$, and with the other family of characteristics the same reasoning can be followed for points R on the line $x = x_1$. Thus we can say that two-point data along $(t = 0; x_0 \leqslant x \leqslant x_1)$ and one-

point data along ($x = x_0$; $t \geqslant 0$) and ($x = x_1$; $t \geqslant 0$) are necessary to define the solution in the domain bounded by the lines $x = x_0$, $t = 0$ and $x = x_1$ for the structure of the characteristics as shown in Fig. 2.6. Such data are sufficient to define the solution as long as discontinuities (mobile hydraulic jumps) do not develop within the domain of consideration.

The question arises as to whether one could not give two-point data along $x = x_1$ and one-point data along $t = 0$ and $x = x_0$. This would correspond to a physical situation in which, for example, knowing the initial canal discharge and upstream depth variation, one would like to calculate the initial depths and upstream discharge variation necessary to furnish specified downstream discharge and level hydrographs. Such a calculation would have to proceed backwards in time, which would be feasible if there were no energy losses ($E = 0$ in Equations (2.60)). But energy losses must of course be included, and in this case the so-called inverse calculation becomes virtually impossible. Physically speaking, local perturbations in the flow are smoothed out as time advances due to friction effects; a forward-in-time calculation models this behaviour. But to proceed backward in time implies the reconstruction of the particular perturbations which show up as smoothed flow features at a later time. The slightest error in flow conditions at time $t_1 > t_0$ will show up as completely artificial perturbations at time t_0. This problem of irreversibility, discussed by Abbott (1966), implies that computations can only proceed in the positive time direction and consequently two-point boundary data cannot be transferred backward in time along the characteristics. This leads in fact to another definition of data to be given at the limits of a domain in the (x, t) plane: *one boundary condition has to be given for every characteristic entering through the boundaries of the solution domain.* The above definition is illustrated in Fig. 2.7 where different subcritical and supercritical cases are shown. Considering for example supercritical flow in the positive x-direction, two characteristics enter through $x = x_0$ at the upstream side; two characteristics enter through $t = t_0$; and zero characteristics enter through $x = x_1$. Consequently, the supercritical flow computations require two-point data at the upstream boundary and two-point data along the $t = t_0$ line.

Generalizing this further, boundary data can be given as any functional relationships between the dependent variables and their derivatives with respect to x and t as long as this function adds new information to the existing information, or in other words, as long as it is *independent of existing information.* One can formulate the following restrictions for boundary data:

(i) They should be independent of each other when two-point data are required. For example on the line $t = 0$ one cannot give u and $\frac{\partial u}{\partial x}$ independently.

(ii) They should be independent of the basic equations. By virtue of the relation between $\frac{\partial h}{\partial t}$ and $\frac{\partial}{\partial x}(uh)$ in the mass equation, these two types of data or, for example, h and $\frac{\partial}{\partial x}(uh)$, cannot be given independently.

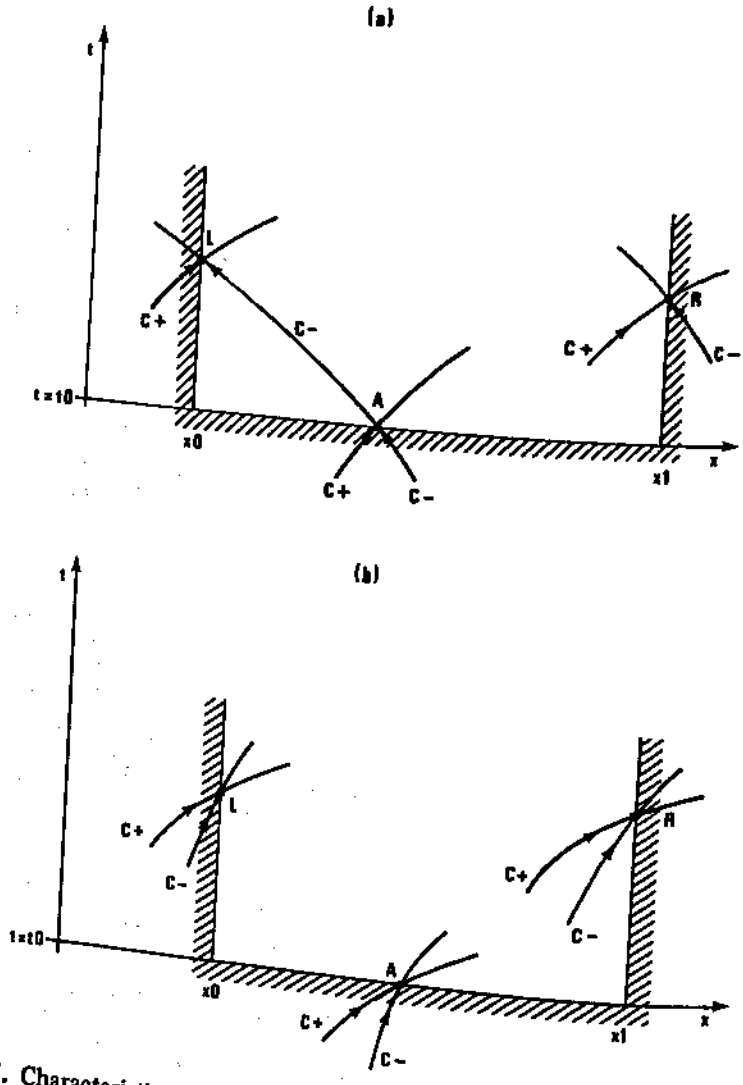

Fig. 2.7. Characteristic structure at the boundaries of the flow domain $t \geqslant t_0$, $x_0 \leqslant x \leqslant x_1$. (a) Subcritical flow: two characteristics enter the domain at every point A along $t = t_0$, and one enters at every point L, R along $x = x_0$ and $x = x_1$. (b) Supercritical flow: two characteristics enter the domain at every point A along $t = t_0$, and two enter along $x = x_0$. None enter along $x = x_1$

(iii) In the case of boundaries where one-point data are required, the condition should be independent of the Riemann invariants or of their analogues for the complete equations along the characteristics leaving the computational domain.

Up until now we have used the word boundary for every limit of the domain in the (x, t) plane. Since it is customary to use the term initial conditions (or initial

values) for conditions given along a line t = const and reserve the word boundary for limits in physical space, from now on we shall apply these terms.

Our above conclusions regarding two-point initial data apply to any of the systems of Equations (2.27)–(2.30) and (2.31), (2.36). As long as these data comply with the specifications we have laid down, they are formally acceptable. From a practical point of view, however, the most attractive approach (and the one which is nearly always used) is to give directly the two dependent variables. Thus, for example, the system of Equations (2.27) is supplemented with initial conditions $Q(x, 0), h(x, 0)$ while the system of Equations (2.30) may be supplemented with conditions $u(x, 0), y(x, 0)$, etc.

Knowing what kind of initial conditions are required, the question now arises as to how to obtain these data and what their required accuracy must be. Measuring of initial data is very difficult to carry out, because everything has to be measured at the same time. This becomes an impossible task in practice, especially for velocities and discharges. As a rule initial data must be assumed with some degree of approximation. The accuracy with which the data must be assumed depends on the type of problem to be solved. Imagine a frictionless channel closed off by vertical walls upstream ($x = 0$) and downstream ($x = L$). Suppose that at the initial time $t = 0$ the free surface is somehow perturbed along a reach, $0 < x_1 \leqslant x \leqslant x_2 < L$. The perturbation will propagate in both directions, and will be reflected at the vertical end walls. In the absence of energy dissipating effects, *the influence of the initial conditions will never disappear from the solution.* For such cases the initial condition must be given with high accuracy. A typical case is encountered in the simulation of power canals with very small roughness. For example, the Electricité de France Oraison-Manosque canal in southern France, needs nearly two days after the shutdown of turbines before all perceptible oscillations disappear! If friction plays an important role in an isolated system such as described above, evolution of the situation for $t > 0$ will still depend entirely upon the initial conditions at least until some time t_1 at which perturbations will be damped and a horizontal free surface will be re-established. If one is interested in the way the disturbances are damped along a reach $0 < x_1 \leqslant x \leqslant x_2 < L$ and if the distances x_1 and $L - x_2$ are so great that any wave will be completely damped by friction before its reflection from the boundary comes back to the reach of interest, $x_1 \leqslant x \leqslant x_2$, again, the initial conditions determine the evolution of the phenomena. In all such cases initial conditions must be given with high accuracy, and that accuracy will determine the accuracy of the final results. Typical practical examples of such situations are the simulation of power canal cascades and lock operations.

If the perturbations are maintained or induced through the boundary conditions, the initial conditions may be without importance whatsoever. Consider for example a river reach $x_1 \leqslant x \leqslant x_2$ such that the hydrographs $y(x_1, t)$ and $y(x_2, t)$ are known and imposed as boundary conditions. As depicted in Fig. 2.8 all points within the domain of determinacy of the point A (i.e. within the characteristic triangle LAR) are influenced only by the initial conditions; the

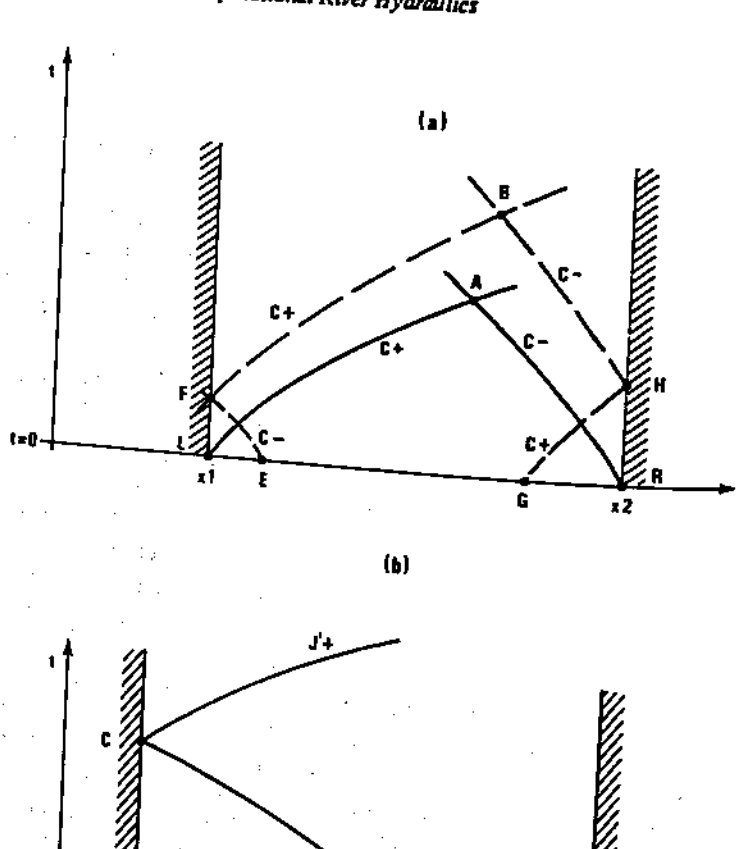

Fig. 2.8. Initial state considerations. (a) Influence of the initial state upon the solution in the presence of dominant boundary conditions. (b) Wave reflection in a frictionless canal

discharge and the water stage at point A depend exclusively upon the conditions at time $t = 0$ given along $x_1 \leqslant x \leqslant x_2$. Point B, however, depends only partially upon the initial conditions. Flow at B is defined by information along the two characteristics FB and HB. This information depends in turn on the conditions prescribed on the boundaries, i.e. y_F and y_H, and on the information reflected from the boundaries, which came originally along EF and GH from the initial state. Clearly as time progresses the information transmitted through the

boundaries becomes more and more important as compared to the initial state, whose influence on the solution is progressively damped through friction. After some time t_1, the 'memory' of the initial state is lost to the system. If the modeller is interested in the solution for $t > t_1$, the initial state can be quite inaccurate as it will not influence the solution. This is the case in tidal problems, for example; experience has shown that after two tidal periods the effect of the initial conditions has nearly completely vanished in estuaries of relatively shallow depth. The simulations can be started one day in advance with assumed initial data and even with a constant water level and zero discharges. Nonetheless, it is important to verify that such a 'start up' period is long enough so that initial state influences do indeed disappear; the higher the friction loss, the shorter the time necessary.

It is interesting to note that for certain boundary conditions the influence of the initial state disappears with time even in a system without any friction loss. Consider a canal which is closed at its upstream end (boundary condition $u = 0$ at $x = x_0$, Fig. 2.8b) and subject to a downstream rating curve type condition, $u = \alpha(c - c_0)$ at $x = x_1$ in which α is a constant $0 < \alpha < 1$, c is the celerity, and c_0 is a constant reference celerity. At point B, the arriving characteristic AB has a Riemann invariant J_+ determined from the initial conditions at point A,

$$J_+ = u + 2c$$

The value of J_- on the characteristic BC leaving point B is determined by applying the downstream boundary condition $u = \alpha(c - c_0)$, which yields

$$J_- = u - 2c = -\left(\frac{2-\alpha}{2+\alpha}\right)(J_+ + \alpha c_0) - \alpha c_0$$

At point C on the upstream boundary (Fig. 2.8b), application of the condition $u = 0$ leads to

$$J'_+ = -J_- = \left(\frac{2-\alpha}{2+\alpha}\right)(J_+ + \alpha c_0) + \alpha c_0$$

which can be reduced, by substracting $2c_0$ from both sides, to:

$$J'_+ - 2c_0 = \left(\frac{2-\alpha}{2+\alpha}\right)(J_+ - 2c_0)$$

Since $0 < \alpha < 1$, we see that after the upstream reflection the 'new' value of $J'_+ - 2c_0$ is reduced compared to the 'old' one at point A. If we were to continue the calculation, we would see that after a number of reflection cycles n, $(J^n_+ - 2c_0)$ would tend toward zero so that $J^n_+ = 2c_0$. In other words, after a certain time the value of J^n_+ would depend only on c_0 and be unrelated to the initial conditions at A, even without friction. This is a consequence of the downstream rating curve type boundary condition.

We have seen that for most practical cases (i.e. for all subcritical flow conditions) one point boundary data are needed and these data will determine the

solution to a large extent. Here again, not all the possible conditions are of practical interest, but most frequently either u, Q, h or y are given as a function of time; or a condition relating them is given. Derivatives are rarely given, mainly because it is not practical to define them. In general, boundary conditions imposed must be independent of what happens within the model, but even then their formal definition may lead to computational catastrophes. For example, a special problem with $Q(t)$ as a downstream boundary condition arises when one tries to withdraw water at a rate which exceeds the channel's delivery capacity. When discharges $Q(t)$ are imposed at both ends of a channel section, one must be careful not to withdraw more water than was initially available in the channel.

The most frequently used functional boundary relationships are discharge stage curves. A well known example is the use of a rating curve $Q(y)$ in a river, which can be single valued, or may even incorporate a correction to allow partially for unsteady effects. Another example of such a relation is the flow over a free-flowing weir for which a single valued function $Q(y)$ may be defined. Such relationships are of extreme practical importance since one seeks to impose a boundary condition which is independent of any modification within the modelled reach, a problem which we discuss in Chapter 5. Sometimes it is necessary for practical reasons to impose a downstream condition which is non-reflective in that all waves arriving at the boundary cross it without reflection. This fictitious condition corresponds to an infinite channel prolongation and may be expressed for the downstream boundary of prismatic and frictionless channels, by the Riemann invariant Equation (2.64) along the C_- characteristic entering the considered domain,

$$J_- = \frac{Q}{A} - 2\left(g\,\frac{A}{b}\right)^{\frac{1}{2}} \tag{2.64'}$$

It may be verified that such an imposed boundary condition satisfies all the requirements concerning boundary data that we stated earlier. For natural situations Equation (2.64') does nevertheless introduce some reflected waves due to the effect of dropping the term E defined in Equation (2.60).

It should be noted that a rating curve relationship $Q(y)$ *cannot* be used as an upstream boundary condition. Intuitively it can be seen why if we consider that the increase in the water stage at the upstream cross section provokes an increase in the discharge entering the modelled reach, which in turn would provoke an increase in the water stage, etc. This behaviour can be described formally if we reconsider our frictionless canal of Fig. 2.8b. If the non-reflective condition is applied at the downstream end x_1 and the rating curve $u = \alpha(c - c_0)$ at the upstream end x_0, it can be shown that the Riemann invariants are now *amplified* with each upstream reflection, leading to a continual increase in the quantity $u + 2c$.

2.3 DISCONTINUOUS SOLUTION – BORES

Up to now we have implicitly assumed that the hyperbolic partial differential system of equations such as (2.27)–(2.30) and (2.31), (2.36), have solutions in the (x, t), $t > 0$ half plane, or within a domain of that half-plane limited by boundaries $x = x_1, x = x_2$. We have also assumed that such solutions can be found if the proper boundary data and initial conditions are prescribed. Let us now consider a general system of hyperbolic partial differential equations:

$$\frac{\partial \vec{f}}{\partial t} + A \frac{\partial \vec{f}}{\partial x} + B = 0 \tag{2.67}$$

If the matrix A and the vector B are functions of x and t only and satisfy certain regularity requirements, then Equation (2.67) is a linear equation. If the initial or boundary data or their derivatives are discontinuous, the discontinuities propagate along the characteristics and the solutions are also discontinuous in the same sense. If the boundary and initial data are continuous, the solution can only be continuous. It can be proved that for such equations and their proper associated initial and boundary data, there exists a solution in the whole considered domain and, moreover, this solution is unique, i.e. at each point (x, t) there is one and only one value of $\vec{f}$ associated with a given set of initial-boundary data. If A and B are regular functions of x and t, at every point P (x, t) of the (x, t) plane exist *two* well defined characteristic directions (dx/dt). Two characteristics of the same family C_+ (or C_-) cannot intersect.

Thus at point P in Fig. 2.6 one may have only one solution $\vec{f}$, which is the solution of the relationships along the characteristics AP and BP. But when the equations are non-linear, that is to say when $A = A(x, t, \vec{f})$ and/or $B = B(x, t, \vec{f})$, then the slope of characteristics at each point of the domain (x, t) depends on the solution $\vec{f}$ itself, and the characteristics of the same family may intersect one another as seen in Fig. 2.9. Thus at point Q one may find two values for the unknown function $\vec{f}$: one resulting from the characteristics AQ, BQ and another from the characteristics DQ, BQ. The solution becomes *multivalued* and, beyond the time $t = t_1$, may no longer depend upon the initial values at time t_0.

Physically, considering the partial differential non-linear Equations (2.27)–(2.30) for unsteady flow, such a situation corresponds to a hydraulic bore or to an undular moving jump (also called a shock). It is obvious that in the neighbourhood of the jump the basic de St Venant hypotheses are violated; the streamline curvature is very strong, vertical accelerations are not negligible, and hydrostatic pressure distribution cannot be considered to be a valid assumption. However if we consider the bore to be a simple discontinuity of the water surfaces of infinitesimal length, then we can use the moving hydraulic jump relations to link the regions upstream and downstream in which the de St Venant hypotheses, and thus Equations (2.27)–(2.30) or (2.31) and (2.36), are valid. As derived by Favre (1935) (*see also* Henderson, 1966), or as can be obtained from

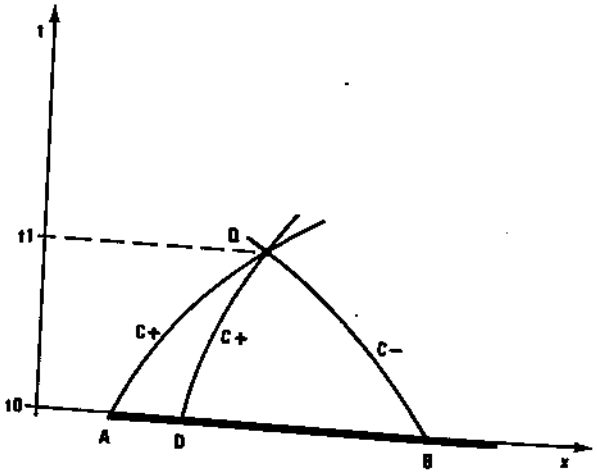

Fig. 2.9. Characteristic structure for non-linear partial differential hyperbolic equations

Equations (2.3) and (2.14), conservation of mass and momentum in a moving hydraulic jump is expressed by two relations

$$v = \frac{A_1(u_1 - u_2)}{A_1 - A_2} + u_2 \tag{2.68}$$

$$u_1 - u_2 = \pm \left(g \frac{A_1 - A_2}{A_1 A_2} (A_1 \eta_1 - A_2 \eta_2) \right)^{\frac{1}{2}} \tag{2.69}$$

where 1 and 2 denote the sections upstream and downstream of the jump, respectively, v is the celerity of the shock, and η is the distance of the centroid of the cross section from the water surface. Substituting Equation (2.69) into Equation (2.68), we obtain

$$v = u_2 \pm \left(g \frac{A_1}{A_2} \frac{A_1 \eta_1 - A_2 \eta_2}{A_1 - A_2} \right)^{\frac{1}{2}} \tag{2.70}$$

or, for rectangular channels,

$$v = u_2 \pm \left(g \frac{h_1}{h_2} \frac{h_1 + h_2}{2} \right)^{\frac{1}{2}} \tag{2.71}$$

The path of the bore in the (x, t) plane is a discontinuity separating the two continuous flow regions 1 and 2 as shown in Fig. 2.10; this path is the solution of the ordinary differential equation

$$\frac{dx}{dt} = v \tag{2.72}$$

Equations (2.68) and (2.69) are valid whatever happens *inside* the shock. They are the hydraulic equivalents of the Rankine–Hugoniot relationships for shocks in

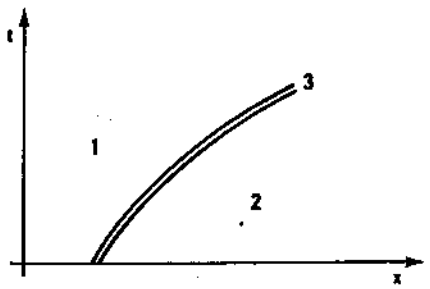

Fig. 2.10. Bore propagation path (3) separating two continuous flow regions (1 and 2).

gases. For the observer moving with the celerity v, they reduce to the equation of the stationary hydraulic jump. This schematization of a bore which may appear at some time $t > 0$ in the solution plane (x, t) is physically justified since we are not interested in the detailed structure of the discontinuity. We note that the bore celerity as defined by Equations (2.70) or (2.71) is not the same as that of 'small waves' defined by $c = (gA/b)^{\frac{1}{2}}$. Let us consider a rectangular cross section; then the bore propagation speed v, from Equation (2.71), is smaller than the propagation speed $v_1 = u_1 + c_1$ of small waves in the upstream region and greater than that $v_2 = u_2 + c_2$ in the downstream region. In Fig. 2.11 we see that positive characteristics from region (1), such as the C_+ curve GF, catch up with the bore (at point F) while all positive characteristics of region (2) are overtaken. Consider the situation at time t_E in Fig. 2.11. The solution is double-valued at the singular point E where there are two pairs of values (y_{E_1}, Q_{E_1}), (y_{E_2}, Q_{E_2}) corresponding to the two pairs of characteristics (AE, A'E and BE, B'E). Thus beginning at time $t = t_E$, there will be a bore in the system. Suppose that we would like to know the solution at some time $t_F > t_E$ and suppose also that the 'initial' state is known in all points along the line $t = t_E$. As in the case of point E, at the point F the solution will again be double-valued and we will have four unknowns $y_{F_1}, Q_{F_1}, y_{F_2}, Q_{F_2}$. There will be one positive characteristic GF which catches up with the front precisely at time t_F. Two characteristics arrive at point F from the continuous region (2): positive characteristic HF which is overtaken by the bore just at that point, and the negative characteristic H'F. The forms of these curves depend upon the solution at point F, namely y_{F_2}, Q_{F_2}, and the locus x_F. Consequently the abscissae x_G, x_H and $x_{H'}$ are unknown since they depend, through the equation of characteristics $dx/dt = u \pm c$, upon the solution at F. Thus, to define the flow at $t = t_F$ in the neighbourhood of the bore, we have to determine 8 unknowns: 4 flow variables y_{F_1}, Q_{F_1}, y_{F_2}, Q_{F_2} and 4 abscissae x_G, x_H, x_F and $x_{H'}$. The solution of the problem is possible since we have at our disposal 8 equations:

two differential equations (2.60a), (2.61) or (2.60b), (2.62) corresponding to each of the characteristics GF, HF, H'F, i.e. six altogether and

two algebraic relationships (2.68), (2.69) across the discontinuity.

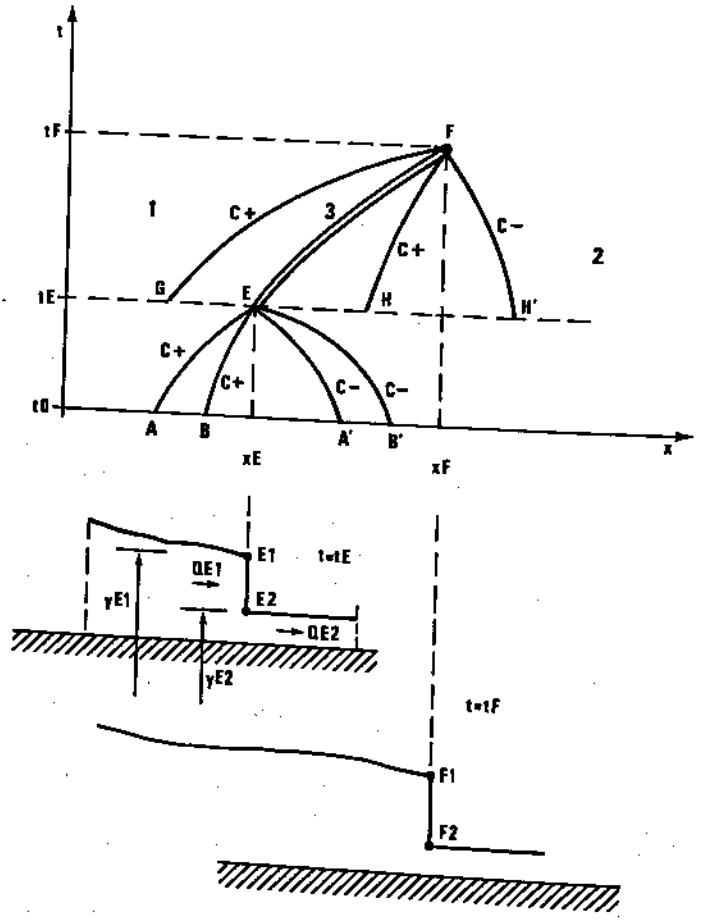

Fig. 2.11. Appearance of a bore at point E and its propagation path (3) between two continuous regions 1 (upstream) and 2 (downstream).

Thus it is possible to construct the solution with discontinuities if the latter are defined as local jumps separating continuous flow regions. It was necessary to isolate the discontinuities and treat them separately from the rest of the flow region because the differential equations (2.27)–(2.30) and (2.31), (2.36) cannot accept discontinuities in the dependent variables. This restriction is removed if the integral relations are taken as the starting point. Let us consider Equation (2.17) and the left-hand side of Equation (2.19) (gravity, frictional, and side-wall pressure forces being neglected):

$$\int_{x_1}^{x_2}\int_{t_1}^{t_2}\left(\frac{\partial A}{\partial t}+\frac{\partial Q}{\partial x}\right)\mathrm{d}t\,\mathrm{d}x=0 \tag{2.73}$$

$$\int_{x_1}^{x_2}\int_{t_1}^{t_2}\left[\frac{\partial Q}{\partial t}+\frac{\partial}{\partial x}\left(\frac{Q^2}{A}+gI_1\right)\right]\mathrm{d}t\,\mathrm{d}x=0 \tag{2.74}$$

These relations express laws of conservation of mass and of momentum in requiring that the integrals be zero within a contour in the (x, t) plane. The functions Q and A may be continuous or discontinuous within that contour. If there is a line of discontinuity in values of Q and A in the (x, t) plane as shown by the path PP' in Fig. 2.12, the discontinuity propagates along it with certain

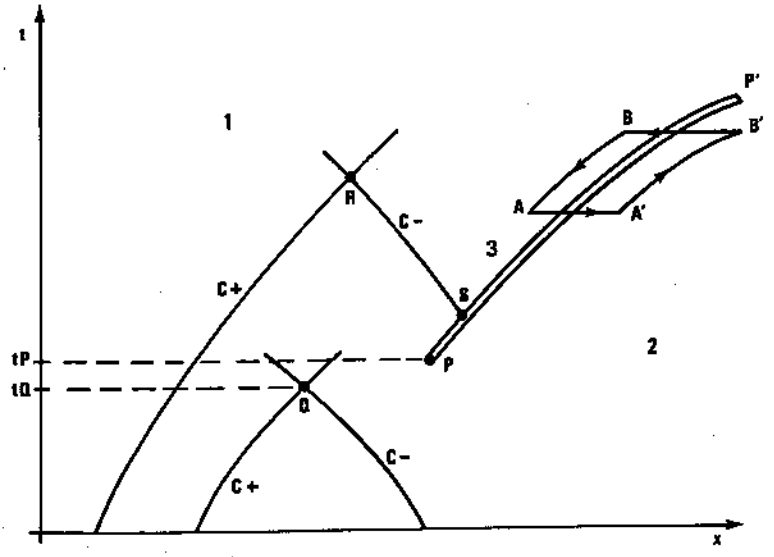

Fig. 2.12. Illustration of flow regions in which the divergent form of the momentum conservation equations must be used. 1 and 2 represent continuous flow regions, 3 is the path of the discontinuity which appears at P. Q is a point unaffected by the discontinuity, where the solution may be obtained by any form of the flow equations. R is a point in the continuous flow region which is affected by the discontinuity. The solution can be obtained only through proper representation of the influence of the discontinuity

velocity v. Equations (2.73) and (2.74) may be rewritten under the form of contour integrals

$$\oint [A\,dx + Q\,dt] = 0 \tag{2.75}$$

$$\oint \left[Q\,dx + \left(\frac{Q^2}{A} + gI_1\right) dt\right] = 0 \tag{2.76}$$

which may be integrated on the closed contour ABB'A' in Fig. 2.12. Both functions, A and Q^2/A suffer a jump, are discontinuous across the line defined by $v = dx/dt$. Consequently, there must be two different pairs of functions: (A_1, Q_1) valid in region (1) and (A_2, Q_2) valid in region (2); the solution of integral relations (2.75) and (2.76) is composed of these two pairs which also must satisfy the jump conditions defined by Equations (2.68) and (2.69).

Consider now a *differential* system of equations obtained from Equations (2.20) and (2.22) for the same conditions as Equations (2.75) and (2.76):

$$\frac{\partial f}{\partial t} + \frac{\partial g(f)}{\partial x} = 0 \tag{2.77}$$

where f and $g(f)$ are respectively the vector functions

$$f = \begin{Bmatrix} A \\ Q \end{Bmatrix}; \quad g(f) = \begin{Bmatrix} Q \\ \frac{Q^2}{A} + gI_1 \end{Bmatrix} \tag{2.78}$$

Equation (2.77) is a system of partial differential equations which represents the conservation laws (2.75) and (2.76) and therefore is called a *divergent* form (divergent free along a certain contour). It may be proved that if f_1 and f_2 are two solutions of Equation (2.77) whose domains of definition in the (x, t) plane are separated by a smooth curve, the two taken together will satisfy the integral equations (2.75) and (2.76) if, and only if, the local slope of the separating curve $dx/dt = v$ and the values of f_1 and f_2 on either side of it satisfy the condition:

$$v[f]_1^2 = [g(f)]_1^2 \tag{2.79}$$

where $[\ ]_1^2$ denotes the jump in the bracketed quantities from one side of the dividing curve to the other (see Abbott, 1979). Such a solution of Equations (2.77) which satisfies also Equations (2.75), (2.76) and (2.79) is called a *weak* solution of the differential equations.

The condition expressed by Equation (2.79) limits the validity of weak solutions of Equation (2.77) to a certain form of the flow equations. For a horizontal rectangular, frictionless channel of unit width $b = 1$ and depth h, $Q = uh$ and $I_1 = (1/2)h^2$; if all variables are continuous the vectors (2.78) may be written either under the form

$$f = \begin{Bmatrix} h \\ uh \end{Bmatrix}; \quad g(f) = \begin{Bmatrix} uh \\ u^2h + \frac{gh^2}{2} \end{Bmatrix} \tag{2.80}$$

from Equations (2.20) and (2.22) or under the form

$$f = \begin{Bmatrix} h \\ u \end{Bmatrix}; \quad g(f) = \begin{Bmatrix} uh \\ \frac{u^2}{2} + gh \end{Bmatrix} \tag{2.81}$$

from Equations (2.29). The relationship (2.79) gives then, for the form (2.80):

$$v = \frac{u_2h_2 - u_1h_1}{h_2 - h_1}; \quad v = \frac{\left(u_2^2h_2 + \frac{gh_2^2}{2}\right) - \left(u_1^2h_1 + \frac{gh_1^2}{2}\right)}{u_2h_2 - u_1h_1} \tag{2.82}$$

Elimination of u_1 from the above equations gives a shock celerity v identical to that obtained in Equation (2.71),

$$v = u_2 \pm \left(g \frac{h_1}{h_2} \frac{h_1 + h_2}{2} \right)^{\frac{1}{2}} \tag{2.71}$$

But if the form (2.81) is taken, then Equation (2.79) leads to a quite different value:

$$v = \frac{u_2 h_2 - u_1 h_1}{h_2 - h_1} \; ; \quad v = \frac{\left(\frac{u_2^2}{2} + g h_2 \right) - \left(\frac{u_1^2}{2} + g h_1 \right)}{u_2 - u_1} \tag{2.83}$$

by eliminating u_1:

$$v' = u_2 \pm \left(\frac{2 g h_1^2}{h_1 + h_2} \right)^{\frac{1}{2}} \tag{2.84}$$

Clearly, Equations (2.84) and (2.71) are not equivalent (except when $h_1 = h_2$) and quite evidently Equation (2.71) is a physically valid solution while (2.84) is not.

A significant conclusion may be obtained from non-equivalence of Equations (2.84) and (2.71); it is possible to obtain valid discontinuous (weak) solutions of the differential equations only if the latter are written under the divergent form and conserve relevant physical quantities (momentum in our case). In Fig. 2.12 before the discontinuity appears ($t < t_p$) the solutions of the two forms (2.80) or (2.81) are identical. For example it does not matter which form is used to find the solution at point Q. The solution at point R, however, is influenced by the discontinuity line PP' through the backward characteristic RS. Therefore, the physically relevant solution of the *integral relationships* (2.75), (2.76) at point R is the same as the solution of the *differential equations* (2.77) only if the momentum conservation form (2.80) is used for f and $g(f)$. If a different divergent form such as (2.81) is used, another discontinuous solution will be obtained, but corresponding to a different system of integral relations — in the case of Equation (2.81), the energy conservation equations. If a non-divergent form of partial differential equations is used, not only will the solution at point R differ from the physically relevant solution of the integral relationships, but it may not even develop a discontinuity.

It is thus clear that if bores may appear in a flow modelled using the *differential* flow equations, the latter must be written in a divergent momentum conservation form. Of all the sets of differential equations presented in this chapter, only equations (2.20) and (2.22), derived directly from the integral relations, are in the required form, and then, strictly speaking only if the free term $gA(S_0 - S_f) + gI_2$ is neglected. This free term acts as a source or sink of momentum; experience has shown that its presence does not modify the above conclusions. If, however, the discontinuous flow phenomena are described by *integral* relationships, the ambiguity disappears and there is no longer any need

to make distinctions between continuous and discontinuous solutions. Nevertheless, the proper form of integral relations (i.e. Equations (2.3) and (2.14)) should be used. The interested reader may find the theory of weak solutions of partial differential equations in specialized references, such as the original article by Lax (1954). The theory applied to open channel hydraulics is exposed in detail by Abbott (1979) and in a more intuitive form by Abbott (1975) and Cunge (1975b).

2.4. SIMPLIFIED CHANNEL FLOW EQUATIONS

Although the original set of the de St Venant hypotheses concerning channel flow is already quite restrictive, in many physical situations it is possible to obtain simpler equations by imposing additional restrictions. We shall discuss briefly some of these simplifications for two main reasons:

(i) The interpretation of results obtained with the aid of mathematical models is essentially based on simplified equations. The full equations describe a set of extremely complex phenomena, and it is very difficult to assess their global behaviour intuitively. Therefore, during the calibration process when engineering intuition is a most important factor, simplified equations most often guide our reasoning. Consequently it is important to recognize which phenomena are neglected in the process of simplification.

(ii) In spite of the continuing development of modelling systems and a steady decrease in computational costs, there are many techniques and programs in use which are based upon simplified equations. The reasons for this vary from the sheer inertia of modellers who insist on sticking with programs and methods developed years ago, to the real need of simple methods in certain situations (see Section 9.1). It is important to understand the limitations of the simplified equations.

In this section we shall take as a starting point the system of partial differential equations used most often by engineers, since it may be interpreted physically in a rather simple and natural way. This system corresponds to Equation (2.20) and the second of Equations (2.30) written for prismatic channels, and is really the original system of equations presented by de St Venant in 1871:

$$\frac{\partial y}{\partial t} + \frac{1}{b}\frac{\partial (uA)}{\partial x} = 0$$

$$\frac{1}{g}\frac{\partial u}{\partial t} + \frac{u}{g}\frac{\partial u}{\partial x} + \frac{\partial y}{\partial x} + S_f = 0 \qquad (2.85)$$

Each term in the dynamic Equation (2.86) can be considered to represent a slope. The first two terms, u being assumed uniformly distributed over the cross (2.86)

section, are the 'inertia terms' or 'acceleration slopes'. The first term, $\frac{1}{g}\frac{\partial u}{\partial t}$, represents the slope of the energy grade line due to the variations of velocity in time (acceleration). The second is the slope which corresponds to the variations of velocity head $u^2/2g$ (in steady flow) in space; for continuous functions, $\frac{u}{g}\frac{\partial u}{\partial x} = \frac{\partial}{\partial x}\left(\frac{u^2}{2g}\right)$. The third term is the slope of the water surface itself. The fourth represents the slope due to the resistance which friction forces oppose to the flow – it is called the 'friction slope'.

It is well known to hydraulic engineers that the terms of Equation (2.86) have different relative importance in different flow situations. Let us assume, for example, that in 3 h the flow velocity in a river changes from 1.0 m s^{-1} to 2.0 m s^{-1} (which is a rather rapid variation) and that, along a distance of 10 km, the velocity changes from 1.5 m s^{-1} to 1.0 m s^{-1} as the channel widens. Then the first two terms of Equation (2.86) are of the order of, respectively,

$$\frac{1}{9.81} \times \frac{1}{3 \times 3600} \approx 1.0 \times 10^{-5} \text{ and } \frac{1}{9.81} \times 1.5 \times \frac{1}{10\,000} \approx 1.5 \times 10^{-5}.$$

A typical bottom slope of the Rhône River between Lyon and Avignon (France) is about 0.7×10^{-3} while the friction slope is also of the order of 10^{-3}. These are rather typical values and they suggest that when one is interested mainly in global development of the flood, the acceleration terms may often be neglected in natural steep rivers. When $\partial h/\partial x$ is small compared to the bed slope $\partial y_b/\partial x$ it may also be dropped, and the dynamic equation is then reduced to the simple equality $S_f - S_0 = 0$. When one is interested in *steady flow*, the time dependent terms in both Equations (2.85) and (2.86) are dropped. In the following paragraphs we shall briefly look at the consequences of these simplifications.

Effect of neglecting the inertia terms

When the first two terms are dropped Equation (2.86) becomes

$$\frac{\partial h}{\partial x} + \frac{\partial y_b}{\partial x} + \frac{Q|Q|}{K^2} = 0 \tag{2.87}$$

where $K(h)$ is the conveyance factor defined in Equation (2.38). Supposing b = constant, differentiating Equation (2.85) with respect to x and Equation (2.87) with respect to t,

$$\frac{\partial^2 h}{\partial x \partial t} + \frac{1}{b}\frac{\partial^2 Q}{\partial x^2} = 0; \quad \frac{\partial^2 h}{\partial x \partial t} + \frac{2|Q|}{K^2}\frac{\partial Q}{\partial t} - \frac{2Q|Q|}{K^3}\frac{dK}{\partial t} = 0$$

Putting

$$\frac{\partial K}{\partial t} = \frac{dK}{dh}\frac{\partial h}{\partial t} = \frac{dK}{dh}\left(-\frac{1}{b}\frac{\partial Q}{\partial x}\right)$$

and eliminating $\frac{\partial^2 h}{\partial x \partial t}$ from the two equations, we obtain

$$-\frac{1}{b}\frac{\partial^2 Q}{\partial x^2} + \frac{2|Q|}{K^2}\frac{\partial Q}{\partial t} + \frac{2Q|Q|}{bK^3}\frac{dK}{dh}\frac{\partial Q}{\partial x} = 0$$

or, by rewriting:

$$\frac{\partial Q}{\partial t} + \left(\frac{Q}{bK}\frac{dK}{dh}\right)\frac{\partial Q}{\partial x} - \frac{K^2}{2b|Q|}\frac{\partial^2 Q}{\partial x^2} = 0 \tag{2.88}$$

Equation (2.88) is a classical parabolic partial differential convection-diffusion equation with one dependent variable $Q(x, t)$. Thus the quantity Q (discharge) is convected with the velocity $\frac{Q}{bK}\frac{dK}{dh}$ and diffused with a diffusion coefficient $\frac{K^2}{2b|Q|}$. If the inertia terms are in fact negligible, Equation (2.88) is a good model of flood propagation. It is capable of representing the backwater influence of tributaries, dams, etc., since it requires *two* boundary conditions one upstream and one downstream, as is the case for any diffusion equation. This feature is extremely important, since further simplifications forbid any possibility of backwater representation as we shall see below. In order to find the solution of Equation (2.88) it is necessary to prescribe not only the boundary conditions (most often of the type $Q(0, t)$, $Q(L, t)$) but also the initial condition $Q(x, 0)$. Using Equation (2.85) it is possible to determine the depths $h(x, t)$ or stages $y(x, t)$ once the solution $Q(x, t)$ is known.

Effect of neglecting the inertia terms and the $\partial h/\partial x$ term

In rivers with a sufficiently steep slope and without backwater effects one can neglect the term $\partial h/\partial x$ as being small compared to $\partial y_b/\partial x$ in Equation (2.87), which then reduces to

$$Q = K(h)\sqrt{S_0} \tag{2.89}$$

Equation (2.89) implies indeed that $Q = Q(A)$ and $A = A(Q)$, i.e. that there is a single-valued relationship between the wetted area and the discharge at a given point $x = x_0$. Consequently, the first term of the continuity Equation (2.85) may be rewritten

$$\frac{\partial A}{\partial t} = \left(\frac{dA}{dQ}\right)_{x_0}\frac{\partial Q}{\partial t}$$

and therefore

$$\frac{\partial Q}{\partial t} + \left(\frac{dQ}{dA}\right)_{x_0}\frac{\partial Q}{\partial x} = 0 \tag{2.90}$$

Equation (2.90) is the so-called *kinematic wave* equation. To get insight into its

behaviour we can express the variation of $Q(x, t)$ along a line in the (x, t) plane as

$$dQ = \frac{\partial Q}{\partial t}\, dt + \frac{\partial Q}{\partial x}\, dx \tag{2.91}$$

or

$$\frac{dQ}{dt} = \frac{\partial Q}{\partial t} + \frac{dx}{dt}\,\frac{\partial Q}{\partial x} \tag{2.92}$$

Comparison of Equations (2.90) and (2.92) shows that Q must be constant along lines

$$\frac{dx}{dt} = \frac{dQ}{dA} \tag{2.93}$$

and, consequently, $\left(\frac{dQ}{dA}\right)_{x_0}$ in Equation (2.90) is the propagation speed of a given discharge Q, a speed which is different for different sections x_0. Equation (2.93) defines the characteristics of the first-order partial differential equation (2.90), and it is clear that the slope of the characteristics may vary; as Q remains constant along them, the waves will be deformed but not damped. As long as the characteristics do not intersect, there is only one characteristic direction at each point of the (x, t) plane as depicted in Fig. 2.13. Thus the solution

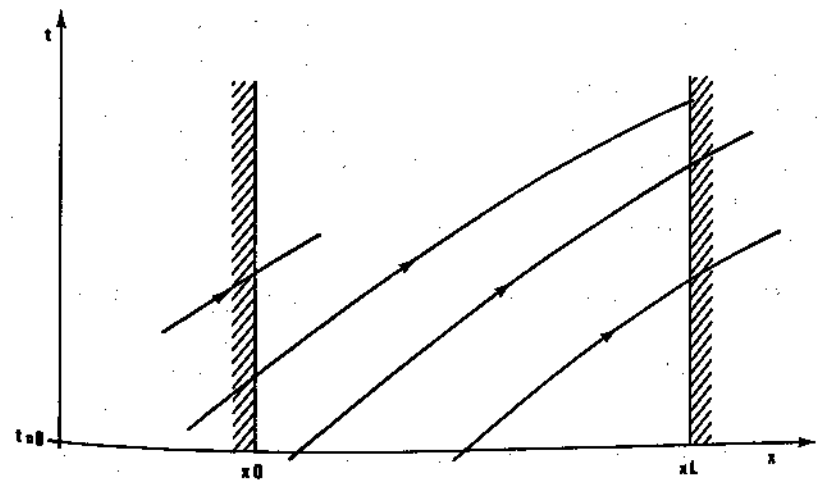

Fig. 2.13. Characteristics of the kinematic wave equation

$Q(x, t)$ of Equation (2.90) in the domain $x_0 < x < x_L, t > 0$ requires *one* initial value $Q(x, 0)$ at each point of the segment $x_0 < x < x_L$ and *one* boundary condition $Q(x_0, t)$. Since information is carried along the characteristics from the upstream boundary or initial state, the kinematic wave equation (2.90) cannot represent backwater effects.

If one considers a river reach of length L and a known input hydrograph $Q_1(t)$ for $x = 0$, then the output hydrograph $Q_2(t)$ at $x = L$ may be found, according to Equation (2.90), by a simple translation of each point of $Q_1(t)$ by a time increment $T(Q)$. That 'propagation time' $T(Q)$ has a simple physical meaning. If we trace free surface profiles in steady flow for two neighbouring values of discharge Q and $Q + \Delta Q$, and if ΔV is the volume of water stored within the reach of length L between the profiles corresponding to these two discharges, then

$$T(Q) = \lim_{\Delta Q \to 0} \frac{\Delta V}{\Delta Q} \tag{2.94}$$

The interested reader can find an excellent analysis and assessment of simplified methods and equations with criteria of choice in the *Flood Studies Report* (1975) and also in Kalinin and Miljukov (1958). A detailed analysis of simplified methods in general was given by Miller and Cunge (1975).

Steady flow equations

Since the subject of this book is the modelling of unsteady flow, the interested reader is referred to the theory of steady flow in open channels in classical references (Chow, 1959; Henderson, 1966). As for applications and mathematical modelling of steady flow, the Hydrological Engineering Centre of the US Army Corps of Engineers has developed very thorough programming systems and documentation (Corps of Engineers, 1976). It is worth noting here that the classical steady flow ordinary differential equation may be obtained from the system of Equations (2.20) and (2.22) by assuming that $Q = Q(x)$ and $A = A(x)$ so that $\partial A/\partial t = \partial Q/\partial t = 0$. Then along a given reach $\partial Q/\partial x = 0$, $Q = \text{const}$ and Equation (2.22) for non-prismatic channels becomes

$$\frac{\mathrm{d}}{\mathrm{d}x}\left(\frac{Q^2}{A} + gI_1\right) = gA\,(S_0 - S_f) + gI_2 \tag{2.95}$$

where integrals I_1 and I_2 are defined, respectively, by Equations (2.8) and (2.10).

2.5 REPRESENTATION OF SPECIAL FLOW CONDITIONS

In previous paragraphs we have described in a very general, intuitive way the equations governing unsteady one-dimensional flow in open channels. We have shown that many physical restrictions must be introduced if we wish to be able to discuss the properties of such equations or even simply to affirm that they have meaningful solutions. In practice the equations are applied to physical cases for which such restrictions obviously are not valid. In trying to adapt the basic equations to nature in all its complexity, engineers often introduce

corrective terms or coefficients – we have discussed some of them such as the Boussinesq-type coefficient related to the non-uniform velocity distribution, storage width b_{st} and conveyance factor K for compound sections (*see* Equations (2.31), (2.36) and (2.48)). Certain flow situations, however, simply cannot be described within the narrow framework of one-dimensional channel flow, whatever the corrective coefficients introduced. In this section we discuss two of the most important situations of this kind: strictly local violation of the hypotheses of one-dimensional flow, and globally quasi two-dimensional flow in the (x, z) plane.

Localized inapplicability of the channel flow equations

The original equations based on the de St Venant hypotheses may be applied to long reaches of natural river or channels but only seldom to the entire length of a modelled watercourse. We have seen, for example, that the hypotheses are not valid in the neighbourhood of a discontinuity such as a bore. It was impossible, at least as long as partial differential equations (and not integral relationships) were used, to link the flow on both sides of the discontinuity by using the original equations alone. An analogous situation, except that it is space-localized, presents itself when there is a marked discontinuity in geometrical or hydraulic characteristics of the watercourse. Typical examples are river junctions, sudden changes in cross sections, flow over weirs, singular head losses, etc. These incidents are local ones and they require hydraulic laws which, over the short length of watercourse concerned, link together the reaches in which the differential equations of unsteady flow are valid.

Thus the whole model may be considered as a set of reaches in which the de St Venant hypotheses are valid, linked by special points where different laws are introduced. These points, by analogy with true boundary conditions, are often called interior boundary conditions. The number of laws needed to link two reaches follows again from the theory of characteristics but quite obviously when two full flow equations are used in normal fluvial reaches one needs two compatibility conditions to link them: one is the discharge continuity equation at the point linking the reaches and another is the dynamic equation for the particular hydraulic features. The channel junction (shown in Fig. 2.14a) requires three independent conditions. From mass continuity it follows that at the junction point the sum of the discharges has to be zero or, in this case

$$Q_3 = Q_1 + Q_2 \tag{2.96}$$

For the other two relationships (needed to link three reaches) one could specify that the water levels are equal at the junction:

$$y_1 = y_2 = y_3 \tag{2.97}$$

A condition more applicable to some cases may be equality of energy levels

$$y_1 + \frac{u_1^2}{2g} = y_2 + \frac{u_2^2}{2g} = y_3 + \frac{u_3^2}{2g} \tag{2.98}$$

Consider next the sudden change in cross-sectional area depicted in Fig. 2.14b.

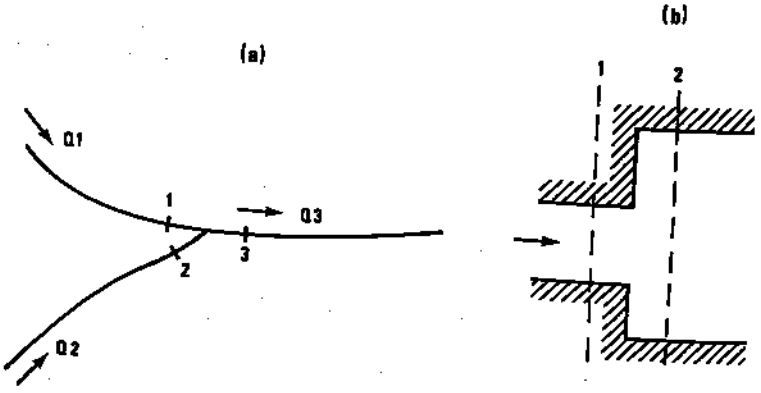

Fig. 2.14. Examples of interior boundary conditions. (a) Channel junction; (b) sudden expansion

Two proper compatibility conditions are

$$Q_1 = Q_2$$

$$y_1 + \frac{u_1^2}{2g} = y_2 + \frac{u_2^2}{2g} + \mu \frac{(u_1 - u_2)^2}{2g} \tag{2.99}$$

where the energy loss coefficient μ would be variable, depending on the flow direction for example.

Note that conditions such as Equations (2.96)–(2.99) are completely independent of the basic differential equations of unsteady flow, as was the case for moving discontinuities. We shall describe particular applications of these kinds of conditions later on in appropriate chapters.

Quasi two-dimensional flow

In the modelling of extensive inundated plains, one cannot simulate the water-course as a one-dimensional conceptual model. When the flooded area is in a coastal zone, such as in estuarial tidal flats, the water flow is most often truly two-dimensional and equations in two space dimensions (x, z), analogous to the one-dimensional Equations (2.27)–(2.30) can be established (*see*, for example, Abbott, 1979). When the flooded areas are on the other hand inundated by a river, they are most often crisscrossed by dykes, roads, groins, etc. In this case truly two-dimensional equations are not applicable and a different approach

must be used, for example, such as that proposed by Zanobetti *et al.* (1968, 1970), described in detail by Cunge (1975c), and briefly reviewed here.

We suppose that the inundated area can be represented by a series of interconnected cells of variable surface in the (x, z) plane. The area A_{s_i} of each cell i is defined by the water level y_i in the cell, and by its natural borders, such as dykes, roads, banks, etc. It is assumed that the water surface is horizontal within the cell for all free surface elevations and that the cell exchanges discharges with adjacent cells k, according to the scheme shown in Fig. 2.15. The continuity

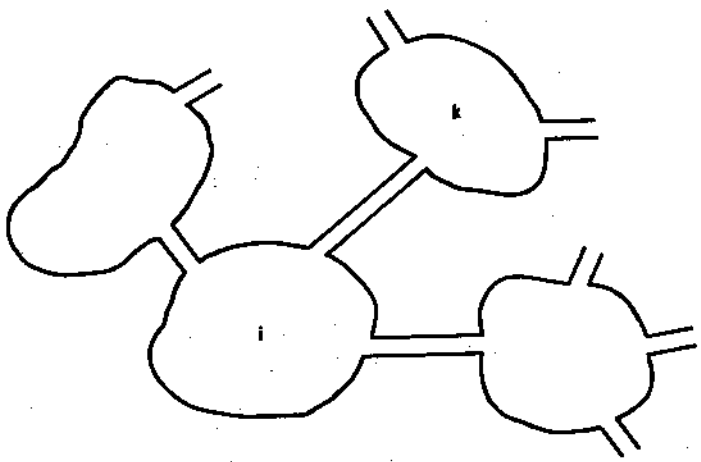

Fig. 2.15. Quasi two-dimensional representation of flooded plains by storage cells

equation for the cell i between times t_1 and t_2 can be written

$$\Delta V_i = \sum_k \int_{t_1}^{t_2} Q_{i,k}\, dt \tag{2.100}$$

where ΔV_i = change in volume stored in the cell i; $Q_{i,k}$ = discharge between cells i and k; $\sum_k$ = summation over all cells k linked with the cell i. Expressing the volume stored as function of the free surface area $A_{s_i}(y_i)$, Equation (2.100) becomes

$$\int_{y_i(t_1)}^{y_i(t_2)} A_{s_i}(y_i)\, dy_i = \int_{t_1}^{t_2} \sum_k Q_{i,k}\, dt \tag{2.101}$$

Limiting ourselves to first order terms, i.e. assuming that

$$\frac{\partial A_{s_i}}{\partial y_i} \Delta y_i \ll A_{s_i}$$

and assuming that $t_2 - t_1 = \Delta t \to 0$ and $y(t_2) - y(t_1) = \Delta y_i \to 0$, we may rewrite Equation (2.101) in the differential form

$$A_{s_i}(y_i) \frac{dy_i}{dt} = \sum_k Q_{i,k} \tag{2.102}$$

Since our purpose is to model floods which evolve fairly slowly on the flooded plain, we may assume that the discharge $Q_{i,k}$ between two cells will not be influenced by acceleration (i.e. inertia) terms. Consequently, without assuming anything about the form of such relationships, we may write that the discharge between two cells is a function only of the water surface elevation in these cells:

$$Q_{i,k} = Q(y_i, y_k) \tag{2.103}$$

For each of N cells i in the model, Equation (2.102) may be written, leading to a system of N non-linear ordinary differential equations

$$A_{s_i}(y_i) \frac{dy_i}{dt} = \sum_k Q_{i,k}(y_i, y_k); i = 1, 2, \ldots, N \tag{2.104}$$

The dependent variables in the system are the N free surface elevations $y_i(t)$. Such a system of equations requires N initial conditions (i.e. a set of $y_i(0)$ values) but no formal boundary conditions, although boundary influences may be introduced in the form of imposed water levels, introduced discharges, etc. As to the form of relationships (2.103), any appropriate hydraulic discharge formula (weir, orifice, Strickler–Manning law, etc.) may be used.

Theoretically at least, Equations (2.104) complement the full one-dimensional equations (2.20) and (2.22) and interior boundary conditions such as Equations (2.96)–(2.99). With their help nearly all unsteady river hydraulic conditions may be modelled (with some exceptions, though, such as undular moving jumps). It is of note that the discharge exchange laws defined by Equation (2.103) are *one-dimensional* relationships: the discharge is considered as being one dimensional in space, between two cells i and k. Although the full system (2.104) simulates two-dimensional flow, we call this simulation, at least in this book, quasi two-dimensional.

3 Solution techniques and their evaluation

3.1 DISCRETIZATION AND SOLUTION OF FLOW RELATIONSHIPS

The differential equations and integral relationships derived in Chapter 2 are mathematical models of real life unsteady flow. They express certain laws which are thought to be the most important ones for the phenomena under study but, as such, they furnish no direct answers as to the values of water stages and discharges, which are functions of time and space, solutions of the basic equations. The equations are too complex to be solved by analytical methods. It is possible, however, to find approximate solutions, i.e. stages and discharges at a certain number of points in the time-space domain, in such a way as to satisfy the basic laws as well as possible. We call *discretization* the process of expressing general flow laws, written for a continuous medium, in terms of discrete values at a finite number of points in the flow field. Discretized flow laws can then be numerically solved to furnish engineering solutions, i.e. stages and discharges. It must be stressed that discretization does not imply simply the replacement of derivatives by finite differences, this being only one of many possibilities. Discretization may consist, for example, in the evaluation of coefficients in polynomial expressions used for interpolation between points where flow values may be computed. A typical example of discretization is the finite element method in which the description of flow behaviour requires that one find maximum values of a function which is expressed as well as possible by a *finite* number of parameters.

As was shown in Chapter 2, there are many different forms of the basic laws, often having different domains of validity. Moreover, there may be several methods of numerical solution of each of the basic sets of relationships. To describe all of them in detail would go far beyond the material possibilities of the present book; nevertheless it would appear worthwhile to mention at least those methods which are most often employed as well as those which find application to certain special cases. Although our attention will be focused on the methods which are most commonly used, in line with our interest in the practical aspects of modelling, the reader should not misinterpret this focus as a religious attachment to certain methods. The fundamental ideas of finite difference theory, such as presented by Courant, Friedrichs and Lewy in 1928,

were considered as purely theoretical; the first serious attempts to apply them to real problems came nearly 20 years later, and the real significance of this theory began to be recognized only when digital computers became our everyday companions in the 1960s. We feel it is important to distinguish between present-day research, which may one day find its place in practical applications, and the current industrial application of mathematical modelling, which is the subject of this book.

There are three classes of numerical solution methods which one finds in the current technical literature: the finite element method (FEM), the method of characteristics, and the finite difference method (FDM). We shall not describe the *finite element method*, since, as of this writing, it has not found widespread application in mathematical modelling of river or channel hydrodynamics. As far as one-dimensional problems are concerned, the method does not show any advantage over the two others and the legitimacy of its application to time dependent problems is not always clear. *The method of characteristics* is used primarily in exceptional cases; nevertheless, because of the physical significance of its parameters and its capability of following individual perturbations, the principles of the method will be described here. The characteristic method has two important fields of applications:

- as a standard for other methods, since it is possible to prove that its solutions may be brought as close to the solution of the basic equations as one desires (or is willing to pay for . . .);
- as a means of representing the boundary conditions in methods which cannot compute all flow variables at exterior or interior boundary points of the model.

The *finite difference method* will be described in much more detail because it is the one currently used in the great majority of industrial models.

Numerical solution by the method of characteristics

Consider the system of four differential equations obtained from Equations (2.60), (2.61) and (2.62).

$$\frac{dx}{dt} = u + c \tag{3.1a}$$

$$\left\{\frac{\partial}{\partial t} + (u+c)\frac{\partial}{\partial x}\right\}(u+2c) = -g(S_f - S_0) \tag{3.1b}$$

$$\frac{dx}{dt} = u - c \tag{3.2a}$$

$$\left\{\frac{\partial}{\partial t} + (u-c)\frac{\partial}{\partial x}\right\}(u-2c) = -g(S_f - S_0) \tag{3.2b}$$

Let us assume that, in the (x, t) plane, initial data are known at points L and R (*see* Fig. 3.1). The characteristics issuing from these points and defined by

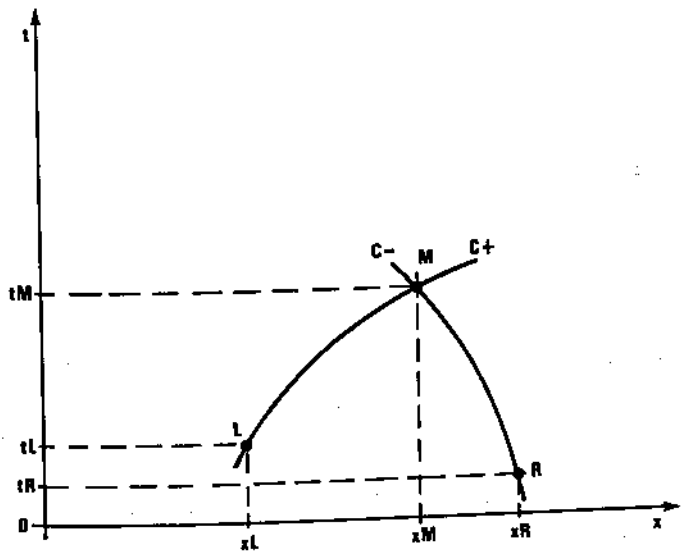

Fig. 3.1. Basis of numerical solution using the characteristic method

Equations (3.1a) and (3.2a) intersect at the point M. The coordinates t_M and x_M, and the flow variables u_M and y_M, are the unknown values to be found by solution of Equations (3.1) and (3.2). Since Equations (3.1) and (3.2) express derivatives *along* the characteristics (*see* Chapter 2), and since all variables are known at points L and R, it is possible to integrate along the characteristics as follows:

$$x_M = x_L + \int_{t_L}^{t_M} (u + c)\,dt \tag{3.3a}$$

$$u_M + 2c_M = u_L + 2c_L + \int_{t_L}^{t_M} g(S_0 - S_f)\,dt \tag{3.3b}$$

$$x_M = x_R + \int_{t_L}^{t_M} (u - c)\,dt \tag{3.4a}$$

$$u_M - 2c_M = u_R - 2c_R + \int_{t_L}^{t_M} g(S_0 - S_f)\,dt \tag{3.4b}$$

These four relations can be solved for the four unknowns x_M, t_M, u_M, y_M. In taking the integrals along the characteristics, no approximation has been made compared to Equations (3.1) and (3.2); the approximation appears in the numerical evaluation of the integrals in Equations (3.3) and (3.4). For example, numerical evaluation of the integrals in Equations (3.3) and (3.4) leads to the trapezoidal rule of integration between points L and M and R and M leads to

$$x_M - x_L = (t_M - t_L)\left(\frac{u_M + c_M}{2} + \frac{u_L + c_L}{2}\right) \tag{3.5a}$$

$$u_M + 2c_M = u_L + 2c_L + g(t_M - t_L)\left(\frac{S_{0M} - S_{fM}}{2} + \frac{S_{0L} - S_{fL}}{2}\right) \tag{3.5b}$$

$$x_M - x_R = (t_M - t_R)\left(\frac{u_M - c_M}{2} + \frac{u_R - c_R}{2}\right) \tag{3.6a}$$

$$u_M - 2c_M = u_R - 2c_R + g(t_M - t_R)\left(\frac{S_{0M} - S_{fM}}{2} + \frac{S_{0R} - S_{fR}}{2}\right) \tag{3.6b}$$

Equations (3.5) and (3.6) are four non-linear algebraic equations which may be solved by iteration. The accuracy of the values of x_M, t_M, u_M and y_M thus determined, as compared to the analytical solution of Equations (3.1) and (3.2), is subject only to the accuracy of iterations and the truncation error in the trapezoidal rule of integration. Obviously both sources of error may be made as small as desired by increasing the number of iterations and decreasing the interval $x_R - x_L$.

By choosing a number of discrete points x_1, x_2, x_3, x_4, x_5 along the line $t = 0$ as shown in Fig. 3.2a, one may compute in the way we have described a series of points M_1, M_2, M_3, M_4. Obviously, the points M_i will not all have the same ordinate t_i. The second stage of points N_1, N_2, N_3 may then be computed using the now-known computed values at points M_i, and so on. We see from Fig. 3.2a that the solution (i.e. the flow variables u, y) is found on an irregular and limited grid of points, the limits being defined by the trajectories $x_1 V$ and $x_5 V$. The solution at the grid points depends exclusively on the values of flow variables at the five points (x_i, $i = 1, \ldots, 5$) at time $t = 0$. If there is a limit to the considered domain, such as the right boundary at the abscissa $x = x_B$, in sub-critical flow a boundary condition such as $y_B(t)$ or $u_B(t)$ or $u_B = f(y_B)$ must be furnished. To describe the flow over the entire domain $x < x_B$, $t > 0$, we need to be able to compute the unknown values y_T, u_T, and t_T at point T ($x = x_B$). Supposing that the flow variables have been computed at point M_5, we have at our disposal two Equations (3.5a) and (3.5b) along the characteristic M_5 T, and the imposed boundary condition; with these three relationships we can compute the three unknowns. Knowing the flow variables at the computed points T and N_4, it is possible, using Equations (3.5) and (3.6) to compute those at the point W, and so on.

The method of characteristics fails when discontinuities appear within the considered domain. Consider Fig. 3.2b showing the case of intersection of two characteristics of the same family, LQ and MQ. The flow variables at point P_2 can be computed using characteristics MP_2 and N_1P_2. Point P_1 is computed using LP_1 and P_2P_1; point R_2 with the aid of N_2R_2 and P_2R_2; point R_1, using P_1R_1 and R_2R_1; points S_2, S_1 with the aid of N_3S_2, R_2S_2 and R_1S_1, S_2S_1 respectively. In that sequence the distances between the points LP_1, P_1R_1, R_1S_1, etc., become smaller and smaller so that the point Q will never be reached in this way. Thus, when a discontinuity is present in the flow, a special

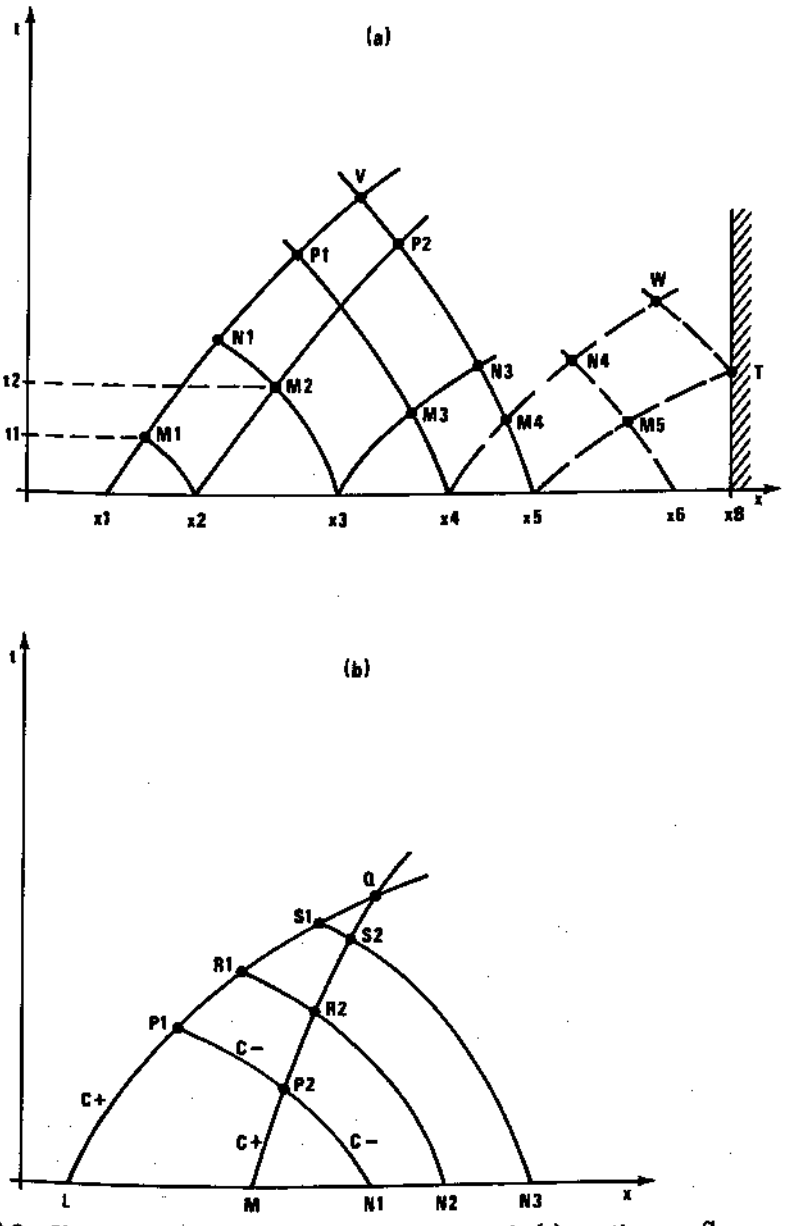

Fig. 3.2. Characteristic solution on an irregular grid: (a) continuous flow; (b) discontinuous flow

method must be used to compute its neighbourhood. The usual procedure fails to do so because the equations on which it is based are not valid any more.

The method of characteristics described above is a numerical integration method over a *variable grid of points* in the (x, t) plane. The basis of this variable-grid method is described in all standard textbooks on numerical analysis. A detailed analysis of its particular features as related to numerical

hydraulics is given by Abbott (1979); its practical implementation is described more intuitively by Liggett and Cunge (1975).

The variable-grid method requires two kinds of interpolation. The first one concerns geometric and hydraulic characteristics of the channel which are known or defined only at a limited number of sections but are needed at any point of the (x, t) plane. The second one is applied to the computed results; indeed, the latter are found at a number of (x, t) points distributed unevenly in the domain while the engineer needs to obtain results such as hydrographs $y(t)$, $Q(t)$ at a given abscissa x, or free surface profiles $y(x)$ at a given time t. Such interpolations do not introduce errors into the computational process: the first kind smoothes the geometric features, the second interpolates results already computed.

The desire to avoid interpolation of results has led to the development of techniques such as the Hartree method on specified intervals which uses the grid of points shown in Fig. 3.3. The values of dependent variables are known at the

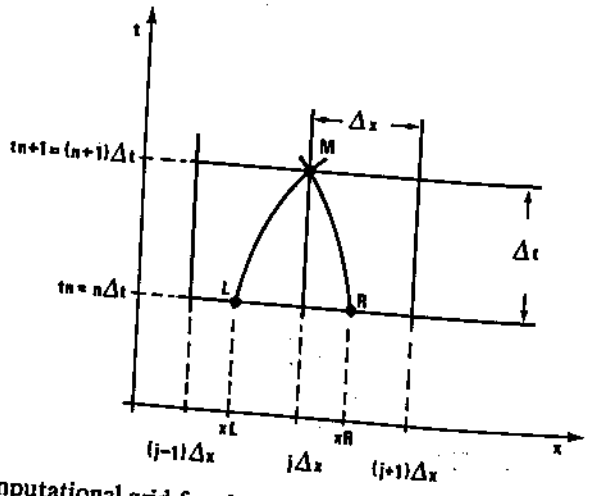

Fig. 3.3. Computational grid for the Hartree method

$n\Delta t$ time level, and their values at points such as M at time level $(n + 1)\Delta t$ are sought; the two characteristics passing through M $(j\Delta x, (n + 1)\Delta t)$ are projected backwards, where they intersect the level $n\Delta t$ at points L and R whose abscissae are unknown; the four unknowns are x_L, x_R, u_M and y_M. These unknowns may be determined with the aid of Equations (3.5) and (3.6); but since x_L and x_R do not coincide with grid points, it is necessary to interpolate between $(j-1)\Delta x$ and $j\Delta x$, and between $j\Delta x$ and $(j + 1)\Delta x$, to estimate u_L, y_L, u_R and y_R. The resulting interpolation error artificially smoothes the solution, and the clarity of the original method and its value as a quality standard are lost. Indeed, the errors are cumulative with time since the solution at the time level $(n + 1)\Delta t$ depends upon the interpolated solution at time level $n\Delta t$. The practical implementation of the Hartree method is also described by Liggett and Cunge (1975); Jolly and Yevjevich (1971) analysed the accuracy problems related to interpolation.

The original method of characteristics on a variable computational grid is not widely used for industrial modelling because of its complexity and the need to interpolate both the original topographic data and the final results. Characteristics on specified intervals are employed somewhat more frequently, but this method is complex and more costly than finite difference methods without offering any improvement in accuracy. The principal advantage of characteristic methods would seem to be their capability of dealing easily with supercritical flow, which is however rarely encountered in river modelling problems. A notable exception is the study of dam break waves (*see* Chapter 9) for which the variable-grid characteristic method is often used (Chervet and Dallèves, 1970).

Numerical solution by the method of finite differences

The foundation of the finite difference method is the following: functions of continuous arguments which describe the state of flow are replaced by functions defined on a finite number of grid points within the considered domain. The derivatives are then replaced by divided differences. Thus the differential equations, i.e. the laws describing the evolution of the continuum, are replaced by algebraic finite difference relationships. The different ways in which derivatives and integrals are expressed by discrete functions are called *finite difference schemes*. The *computational grid* is a finite set of points sharing the same domain in the (x, t) plane as the continuous argument functions. This set is the domain of definition of the discrete-argument functions which we call *grid functions*. A typical computational grid for simple one-dimensional problems is shown in Fig. 3.4. This computational grid may be uniform in space (along the

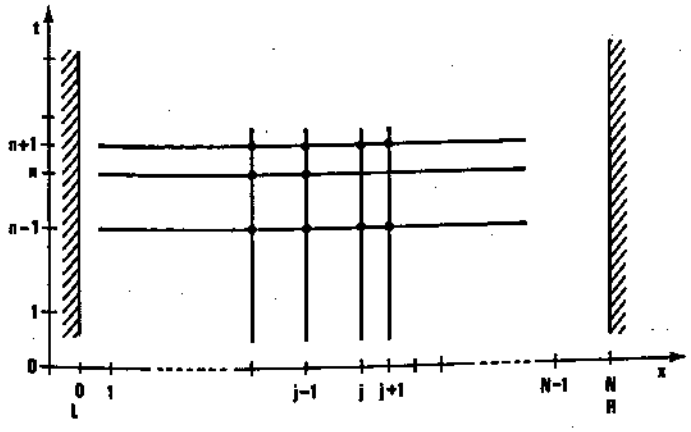

Fig. 3.4. Finite difference computational grid

x-axis) in which case there are $N-1$ equal *space intervals* Δx. If the grid is not uniform, the space intervals $\Delta x_j = x_j - x_{j-1}$ are of variable length. In general the discretization along the x-axis may be symbolically described as a set of points $w_h = \{x_j = j\Delta x, j = 1, 2, \ldots, N; \Delta x_j = x_{j+1} - x_j\}$. In the same way the dis-

cretization in time is defined by the set of points $w_\tau = \{ t_n = n\Delta t,\ n = 0, 1, \ldots;$ $\Delta t_n = t_{n+1} - t_n \}$. The computational grid in the (x, t) plane for a one-dimensional unsteady flow problem is then defined by the set $w = w_h \times w_\tau = \{ (x_j, t_n);\ x_{j+1} = x_j + \Delta x_j;\ t_{n+1} = t_n + \Delta t_n;\ j = 1, 2, \ldots, N;$ $n = 0, 1, 2, \ldots ;\}$. This set defines the *computational points*. A non-uniform computational grid is convenient when one wishes to refine the representation of the phenomena of interest in certain parts of the domain where flow parameters and/or channel geometry vary more rapidly.

In calculus the definition of differentiation of a continuous function $f(x, t)$ is

$$\frac{\partial f}{\partial x} = \lim_{\Delta x \to 0} \frac{f(x + \Delta x, t) - f(x, t)}{\Delta x} \tag{3.7}$$

In finite differences, however, Δx is never infinitely small; in fact, it represents a finite physical length of some importance. Consider three consecutive computational grid points x_{j-1}, x_j, x_{j+1} of a uniform grid (*see* Fig. 3.5) with a

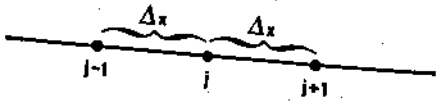

Fig. 3.5. Portion of a uniform computational grid at $t = t_n$

space interval $\Delta x = \text{const.}$ at time t_n. In order to approximate the derivative defined by Equation (3.7) *at point j*, the following relationships could be used:

$$\begin{aligned}
\frac{\partial f}{\partial x} &\approx \frac{f_{j+1}^n - f_j^n}{\Delta x} = \left(\frac{\partial f}{\partial x}\right)_h \\
\frac{\partial f}{\partial x} &\approx \frac{f_j^n - f_{j-1}^n}{\Delta x} = \left(\frac{\partial f}{\partial x}\right)_h \\
\frac{\partial f}{\partial x} &\approx \frac{f_{j+1}^n - f_{j-1}^n}{2\Delta x} = \left(\frac{\partial f}{\partial x}\right)_h
\end{aligned} \tag{3.8}$$

in which f_j^n represents the value of the *grid function* at point x_j and at time t_n, and $\left(\frac{\partial f}{\partial x}\right)_h$ symbolizes the discrete approximation to the derivative. In an analogous manner, the time derivative $\partial f/\partial t$ may be defined in several different ways (*see* Fig. 3.4):

$$\begin{aligned}
&\frac{\partial f}{\partial t} \approx \frac{f_j^{n+1} - f_j^n}{\Delta t};\quad \frac{\partial f}{\partial t} \approx \frac{f_j^{n+1} - f_j^{n-1}}{2\Delta t}; \\
&\frac{\partial f}{\partial t} \approx \frac{1}{\Delta t}\left\{ f_j^{n+1} - \left[\alpha f_j^n + (1-\alpha)\frac{f_{j+1}^n + f_{j-1}^n}{2} \right] \right\};\ 0 \leqslant \alpha \leqslant 1
\end{aligned} \tag{3.9}$$

etc.

Not only the derivatives, but also the grid functions themselves, may be defined in several different ways. The value of the function $f(x, t)$ may be approximated at the grid point j, n as $f_j^n = f(x_j, t_n)$. This is not the only way to proceed; for example one may decide that the continuous functions $f(x, t)$ are not to be defined at the points x_j, t_n but rather in the centre of the computational intervals, for example $f(x, t) \approx (1/2)(f_j + f_{j+1})$, etc. These are only two examples of the many ways one can express the grid function values at the computational points.

The replacement of differential expressions by their finite difference analogues is an approximation, the degree of which is often called 'truncation error' or 'order of approximation'. Consider the analytic function $f(x, t)$ and its derivative $\frac{\partial f}{\partial x}$. Using a Taylor series development, one can find the value of the function at the point $x_j + \Delta x$ knowing its value at the point x_j:

$$f(x_j + \Delta x, t_n) = f(x_j, t_n) + \frac{\partial f}{\partial x}\Delta x + \frac{\partial^2 f}{\partial x^2}\frac{\Delta x^2}{2} + \frac{\partial^3 f}{\partial x^3}\frac{\Delta x^3}{3!} + O(\Delta x^4) \tag{3.10}$$

where $O(\Delta x^4)$ groups all of the remaining terms, the first of which, (and presumably the greatest) is a derivative of the function f multiplied by Δx^4. We call these terms 'higher order terms', in this case 'fourth order terms'. If the definition of the grid function is $f_j^n = f(x_j, t_n)$, then from Equation (3.10) the expression for the derivative will be:

$$\frac{\partial f}{\partial x} = \frac{f_{j+1}^n - f_j^n}{\Delta x} - \frac{\partial^2 f}{\partial x^2}\frac{\Delta x}{2} - \frac{\partial^3 f}{\partial x^3}\frac{\Delta x^2}{3!} - O(\Delta x^3)$$

This may be compared with the first finite difference expression approximating the derivative $\partial f/\partial x$ in Equation (3.8). Clearly

$$\left(\frac{\partial f}{\partial x}\right)_h = \frac{\partial f}{\partial x} + \frac{\partial^2 f}{\partial x^2}\frac{\Delta x}{2} + \frac{\partial^3 f}{\partial x^3}\frac{\Delta x^2}{3!} + O(\Delta x^3) = \frac{\partial f}{\partial x} + O(\Delta x) \tag{3.11}$$

We say that the approximation of the derivative $\frac{\partial f}{\partial x}$ by the difference operator $\left(\frac{\partial f}{\partial x}\right)_h$ is of the *first order*, i.e. the first of the neglected terms, $O(\Delta x)$, is a derivative multiplied by Δx. It may be seen that the third finite difference expression in Equation (3.8) is a second-order approximation of $\partial f/\partial x$.

The order of approximation also depends on the uniformity of the computational grid. Consider a non-uniform grid and the following derivative approximation at point (x_j, t):

$$\frac{\partial f(x,t)}{\partial x} \approx \left(\frac{\partial f}{\partial x}\right)_h = \frac{1}{2}\ \frac{f_{j+1}^n - f_j^n}{x_{j+1} - x_j} + \frac{1}{2}\frac{f_j^n - f_{j-1}^n}{x_j - x_{j-1}} \tag{3.12}$$

As before, setting $\Delta x_j = x_{j+1} - x_j$ and $\Delta x_{j-1} = x_j - x_{j-1}$, and assuming that the grid function can be expanded in a Taylor series,

$$f_{j+1}^n = f_j^n + \frac{\partial f}{\partial x}\Delta x_j + \frac{\partial^2 f}{\partial x^2}\frac{\Delta x_j^2}{2} + O(\Delta x^3)$$

$$f_{j-1}^n = f_j^n - \frac{\partial f}{\partial x}\Delta x_{j-1} + \frac{\partial^2 f}{\partial x^2}\ \frac{\Delta x_{j-1}^2}{2} + O(\Delta x^3)$$

Substitution into Equation (3.12) yields

$$\begin{aligned}\left(\frac{\partial f}{\partial x}\right)_h &= \frac{1}{2\Delta x_j}\left[\frac{\partial f}{\partial x}\Delta x_j + \frac{\partial^2 f}{\partial x^2}\frac{\Delta x_j^2}{2} + O(\Delta x^3)\right] \\ &\quad + \frac{1}{2\Delta x_{j-1}}\left[\frac{\partial f}{\partial x}\Delta x_{j-1} - \frac{\partial^2 f}{\partial x^2}\frac{\Delta x_{j-1}^2}{2} + O(\Delta x^3)\right] \\ &= \frac{\partial f}{\partial x} + \frac{1}{4}\frac{\partial^2 f}{\partial x^2}(\Delta x_j - \Delta x_{j-1}) + O(\Delta x_j^2, \Delta x_{j-1}^2)\end{aligned} \tag{3.13}$$

It is immediately seen from Equation (3.13) that if the grid is uniform, i.e. $\Delta x_j = \Delta x_{j-1}$, the approximation of the derivative is of *second order*. Otherwise it is of first order. Analogous reasoning can be applied to the time derivatives $\partial f/\partial t$.

The order of approximation as defined above is the exponent of the grid interval Δx or Δt appearing in the first of the Taylor series terms which is neglected in a finite difference approximation. The greater the power n in the expression (Δx^n), the better the approximation *if Δx itself can be assumed to be small*. On coarse grids, where Δx and Δt are not small and where the solution $f(x, t)$ itself varies rapidly in time and in space, *the concept of order of approximation loses its meaning* since the product $\Delta x^n \frac{\partial^m f}{\partial x^m}$ is not small. Note that if the mth derivative does not exist, the expression makes no sense. In the analysis of difference schemes, it is indeed helpful to know that if the number of grid intervals is doubled (Δx divided by two), the error of approximation will be reduced by a factor of two for a first-order scheme and by a factor of four for a second-order scheme. But this says nothing about the *magnitude* of the error; a second-order scheme is not necessarily capable of modelling reality more accurately than a first-order one.

Some finite difference schemes

The finite difference schemes used in unsteady river flow modelling may be grouped into several distinct classes according to their main features. Within each

class the differences between competing schemes may be minor as far as the discretization principle is concerned, but these differences may have far reaching practical consequences. The main distinction among schemes belonging to the same class is related to the way in which physical coefficients in the flow equations (such as, for example, $A(y)$, $b(y)\,S_f(y, Q)$ in Equations (2.28)) are discretized. These coefficients, being functions of the dependent variables, render the equations non-linear; as a result the differences in discretization of these coefficients may have more influence upon the results than analysis based on simplified linear equations might suggest. Consequently, considerable attention must be devoted to coefficient discretization.

It is not our intention to describe all known finite difference schemes. Nor do we intend to describe the detailed development of all terms, coefficients, and algorithms for the most often used schemes, and this is for two basic reasons:

(1) these developments are usually available in other literature;
(2) the wise programmer will derive these various elements himself in order to be sure of their correctness and to adjust them to his own needs.

After describing some of the typical classes of finite difference schemes and their features using simplified systems of differential or integral relationships, we shall come back to practical problems such as discretization of non-linear terms, topological problems arising in solution algorithms, etc. Our objective is not to furnish recipes (which do not exist), but rather to stress the practical advantages and disadvantages of various approaches, pointing out their shortcuts and/or pitfalls, so that the reader can better assess their applicability to practical problems.

Family of schemes based on the integral relationships

The first possible classification of finite difference schemes is defined by the flow relationships they approximate, integral relationships or differential equations. Consider Equations (2.3) and (2.14) in which the double integrals representing free terms are dropped:

$$\begin{aligned} &\int_{x_1}^{x_2} (A_{t_2} - A_{t_1})\,\mathrm{d}x + \int_{t_1}^{t_2} (Q_{x_2} - Q_{x_1})\,\mathrm{d}t = 0 \\ &\int_{x_1}^{x_2} (Q_{t_2} - Q_{t_1})\,\mathrm{d}x + \int_{t_1}^{t_2} \left[(u^2A + gI_1)_{x_2} - (u^2A + gI_1)_{x_1} \right] \mathrm{d}t = 0 \end{aligned} \tag{3.14}$$

Referring to Fig. 3.6, it may be shown that Equations (3.14) are contour integrals taken along the path ABCD (this can be verified by setting $x_1 = x_j$, $x_2 = x_{j+1}$, $t_1 = t_n$, $t_2 = t_{n+1}$ in Equation (3.14). The system of Equations (3.14) may be written under the general vector form:

$$\oint \left[f\,\mathrm{d}x + G(f)\mathrm{d}t \right] = 0 \tag{3.15}$$

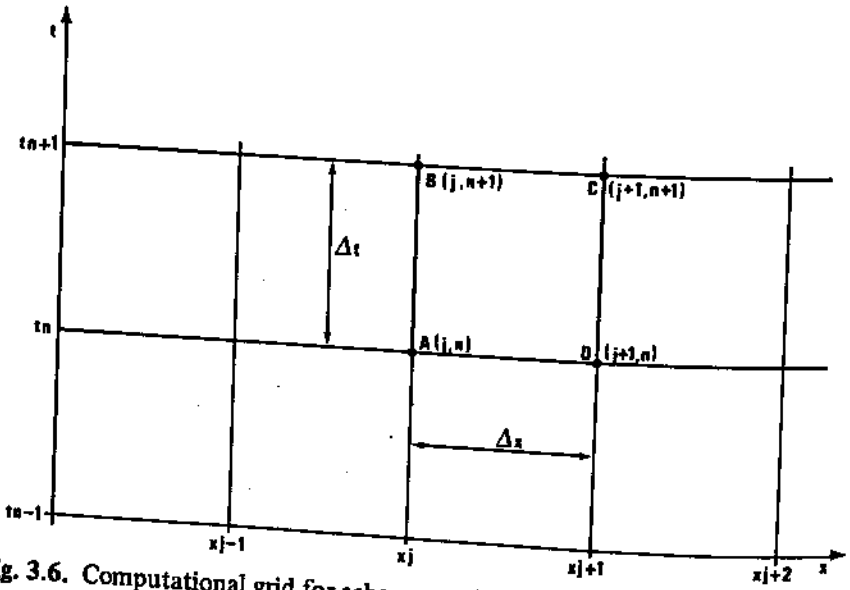

Fig. 3.6. Computational grid for schemes with both dependent variables computed at all grid points

where

$$f = \begin{Bmatrix} A \\ Q \end{Bmatrix} \quad ; \quad G(f) = \begin{Bmatrix} Q \\ \dfrac{Q^2}{A} + gI_1 \end{Bmatrix} \tag{3.16}$$

From now on we shall define the vector grid function using the following notation:

$$f(x_j, t_n) = f_j^n; \quad G\,[f(x_j, t_n)] = G_j^n; \text{ etc.} \tag{3.17}$$

The discretization of Equation (3.15) (or of Equations (3.14)) assumes that the values of the functions f and G between the computational grid points can be expressed in terms of the values of these functions at the grid points.

Let us define the following formulae in which functions f, G in intervals $j, j+1$ and $n, n+1$ are replaced by their weighted averages between these points:

for the time interval $t_n \leqslant t \leqslant t_{n+1}$

$$G(x_j, t) = \theta\, G_j^{n+1} + (1-\theta)\, G_j^n \tag{3.18a}$$

$$G(x_{j+1}, t) = \theta\, G_{j+1}^{n+1} + (1-\theta)\, G_{j+1}^n \tag{3.18b}$$

for the space interval $x_j \leqslant x \leqslant x_{j+1}$

$$f(x, t_n) = \psi\, f_{j+1}^n + (1-\psi) f_j^n \tag{3.19a}$$

$$f(x, t_{n+1}) = \psi\, f_{j+1}^{n+1} + (1-\psi) f_j^{n+1} \tag{3.19b}$$

where $0 \leqslant \theta \leqslant 1$, $0 \leqslant \psi \leqslant 1$ are weights and f_j^n, G_j^n are the grid functions defined by Equations (3.16) and (3.17). The substitution of Equations (3.18) and (3.19) into Equations (3.14) (or, equivalently, (3.15)) yields

$$\int_{x_j}^{x_{j+1}} \left\{ [\psi f_{j+1}^{n+1} + (1-\psi) f_j^{n+1}] - [\psi f_{j+1}^n + (1-\psi) f_j^n] \right\} dx + \int_{t_n}^{t_{n+1}} \left\{ [\theta G_{j+1}^{n+1} + (1-\theta) G_{j+1}^n] - [\theta G_j^{n+1} + (1-\theta) G_j^n] \right\} dt = 0 \tag{3.20}$$

Direct integration and substitution of $x_{j+1} - x_j = \Delta x$, $t_{n+1} - t_n = \Delta t$, leads to a parametric finite difference equation with weighting coefficients ψ, θ as parameters:

$$\left\{ [\psi f_{j+1}^{n+1} + (1-\psi) f_j^{n+1}] - [\psi f_{j+1}^n + (1-\psi) f_j^n] \right\} \Delta x + \left\{ [\theta G_{j+1}^{n+1} + (1-\theta) G_{j+1}^n] - [\theta G_j^{n+1} + (1-\theta) G_j^n] \right\} \Delta t = 0 \tag{3.21}$$

Clearly, Equation (3.21) is a *finite difference equation which approximates the conservation law* expressed by the integral relationship Equation (3.15) along the contour ABCD of the elementary computational mesh in the (x, t) plane.

A whole family of finite difference schemes may be obtained from Equation (3.21) by varying the parameters ψ and θ. The finite difference Equation (3.21) is not only an approximation to the integral relationship (3.15) but also to the corresponding differential system

$$\frac{\partial f}{\partial t} + \frac{\partial G(f)}{\partial x} = 0 \tag{3.22}$$

This may be immediately seen by dividing Equation (3.21) by the product $\Delta x \Delta t$. The corresponding difference scheme represents the following approximations to the derivatives:

$$\frac{\partial f}{\partial t} \approx \frac{[\psi f_{j+1}^{n+1} + (1-\psi) f_j^{n+1}] - [\psi f_{j+1}^n + (1-\psi) f_j^n]}{\Delta t} \tag{3.23a}$$

$$\frac{\partial f}{\partial x} \approx \frac{\theta (G_{j+1}^{n+1} - G_j^{n+1}) + (1-\theta)(G_{j+1}^n - G_j^n)}{\Delta x} \tag{3.23b}$$

If Equation (3.22) expresses a system of conservation laws, this finite difference scheme approximates those laws as well.

When $\psi = 1/2$, Equation (3.21) becomes the *Preissmann 4-point scheme* of finite differences in which the time derivatives are approximated by

$$\frac{\partial f}{\partial t} \approx \frac{(f_{j+1}^{n+1} + f_j^{n+1}) - (f_{j+1}^n + f_j^n)}{2\Delta t} \tag{3.24}$$

and coefficient θ is given a value between 0.5 and 1.0. The scheme was introduced by Preissmann (1961) and has been described in a number of papers (*see* for example Preissmann and Cunge, 1961a, b; Cunge and Wegner, 1964; Cunge, 1966a; Liggett and Cunge, 1975; Abbott, 1979; Amein and Fang, 1970).

The purpose of discretization is to make it possible to compute unknown flow variables at N computational grid points at time level t_{n+1},

$$f_j^{n+1} = \begin{Bmatrix} A_j^{n+1} \\ Q_j^{n+1} \end{Bmatrix}, j = 1, 2, \ldots, N-1, N$$

Since in the system of two difference equations represented by Equation (3.21) we have four unknowns A_j^{n+1}, Q_j^{n+1}, A_{j+1}^{n+1}, Q_{j+1}^{n+1}, they cannot be found directly. It is possible however to write $N-1$ systems of Equation (3.21) (or, in other words, $2N-2$ equations) for N computational points. Then, using two boundary conditions, the solution may be found at the time level $n+1$ since there are $2N$ unknowns A_j, Q_j ($j = 1, 2, \ldots, N$), $2N-2$ non-linear algebraic equations and two boundary conditions. Finite difference schemes of this type which must be solved for all points simultaneously at time t_{n+1} are called *implicit finite difference schemes*; Preissmann's scheme is one of them.

The most salient features of the Preissmann-type schemes, besides the fact that they consistently approximate integral conservation laws and are implicit, are the following:

- they compute both unknown flow variables at the same computational grid points;
- they link together flow variables at only two adjacent sections, x_j, x_{j+1}; thus the space intervals $x_{j+1} - x_j$, $x_{j+2} - x_{j+1}$, etc., may be variable while the accuracy of approximation is unaffected;
- they are schemes of first order of approximation, in the sense that the derivatives (or integrals) are approximated with first-order formulae, except for a special case when $\psi = \theta = 0.5$; then the approximation is of second order;
- for a special choice of Δx and Δt they furnish the exact solution for the fully linearized flow equations,

$$\frac{\partial h}{\partial t} + h_0 \frac{\partial u}{\partial x} = 0; \quad h_0 = \text{const.}$$

$$\frac{\partial u}{\partial t} + g \frac{\partial h}{\partial x} = 0 \tag{3.25}$$

This is an important feature because it allows us to verify the method for simple cases having exact analytical solutions.

Some explicit schemes applied to the differential equations

Explicit finite difference schemes are those in which the flow variables at any point j at the time level $n+1$ (*see* Fig. 3.6) may be computed based entirely on known data at a few adjacent points at time level n. These schemes do not lead

to a system of algebraic equations, since each point can be computed separately. Nevertheless explicit methods are seldom used in river modelling for reasons of stability which we will discuss later on. They are however useful for some special cases, and are helpful in conceptual explanations of numerical concepts; consequently we shall briefly describe two of them, probably the best known: the Lax scheme and the leap-frog scheme. One cannot discuss explicit schemes without having at least mentioned Stoker (1957) who first used such a method for real-life flood propagation computations. We would like also to mention another well-known and often applied explicit scheme of second order accuracy, the Lax–Wendroff scheme. We do not describe them here because they are very well documented in the literature and do not bring in anything new as examples. Once again, we refer the interested reader to Liggett and Cunge (1975) for more material concerning the application of explicit schemes to the open channel flow equations.

(i) *The Lax scheme*, as applied to the general vector form of the homogeneous system of Equation (3.22) is based upon the following approximation of derivatives:

$$\frac{\partial f}{\partial t} \approx \frac{f_j^{n+1} - \left[\alpha f_j^n + (1-\alpha)\,\dfrac{f_{j+1}^n + f_{j-1}^n}{2}\right]}{\Delta t} \qquad (3.26)$$

$$\frac{\partial G(f)}{\partial x} \approx \frac{G_{j+1}^n - G_{j-1}^n}{2\Delta x}\,; \quad 0 \leqslant \alpha \leqslant 1$$

Substitution into Equation (3.22) leads to an explicit formula for the unknown vector function f at the computational point (x_j, t_{n+1}):

$$f_j^{n+1} = \begin{Bmatrix} A_j^{n+1} \\ Q_j^{n+1} \end{Bmatrix} = \alpha f_j^n + (1-\alpha)\frac{f_{j+1}^n + f_{j-1}^n}{2} - \frac{\Delta t}{2\Delta x}\,(G_{j+1}^n - G_{j-1}^n) \qquad (3.27)$$

The formulation is clear and easy to analyse. Both unknown values $(A_j, Q_j)^{n+1}$ may be computed at any and all points $j = 2, 3, \ldots, N-1$ by using the known functions at the points $(j-1, n)$, (j, n) and $(j+1, n)$. The reader will note however, that it is not obvious how to compute the flow variables at the boundaries (e.g. at the right hand boundary point N where one variable is imposed but the other cannot be computed because the point $N+1$ lies outside the domain). This scheme, as in the case of the Preissmann implicit scheme, yields the exact solution of the fully linearized Equations (3.25) for a particular choice of the coefficient $\alpha = 0$ and for $\Delta x/\Delta t = (gh_0)^{\frac{1}{2}}$. For arbitrary values of α, Δx and Δt, the derivative approximations, Equation (3.26), are of the first order of accuracy.

(ii) *The leap-frog method* is probably the earliest one ever used for numerical

solution of the one-dimensional wave equations. In this method the derivatives are approximated as

$$\frac{\partial f}{\partial t} \approx \frac{f_j^{n+1} - f_j^{n-1}}{2\Delta t}\ ; \quad \frac{\partial G}{\partial x} \approx \frac{G_{j+1}^n - G_{j-1}^n}{2\Delta x} \tag{3.28}$$

Substitution into Equation (3.22) leads immediately to the explicit formulation for the unknown vector function at any point $j = 2, 3, \ldots, N-1$:

$$f_j^{n+1} = f_j^{n-1} - \frac{\Delta t}{\Delta x}(G_{j+1}^n - G_{j-1}^n) \tag{3.29}$$

Here again the problem of computation at boundary points $j = 1, j = N$ arises, as it does for *all* explicit schemes. As in the two previous schemes, the leap-frog method produces values of Q and A at all computational points and gives the exact solution of the linear Equations (3.25) when $\Delta x/\Delta t = (gh_0)^{\frac{1}{2}}$. The scheme approximates the derivatives with an accuracy of second order in Δx as well as in Δt, at least as long as $x_{j+1} - x_j = x_j - x_{j-1} = \Delta x$ and $t_{n+1} - t_n = t_n - t_{n-1} = \Delta t$.

Some implicit schemes applied to the differential equations

Sensible implicit finite difference schemes can be constructed in many different ways. Few of the possibilities, however, have been adopted as the foundation of large, industrial modelling systems. We shall outline the basic principles of four of these schemes, namely the Delft Hydraulics Laboratory scheme, the Abbott–Ionescu scheme, the Vasiliev scheme and the six-point Gunaratnam–Perkins scheme.

(i) *Delft Hydraulics Laboratory scheme*

This scheme is presented here such as described by Vreugdenhil (1973). It is based on the concept of nodes, or computational cells at the centre of which water stages are computed, and which are linked to other cells on the left and on the right through discharge laws. The continuity equation is written for each cell with discharges entering or leaving it computed according to the dynamic flow equation. The approach is the same as that described in Chapter 2 for quasi-two-dimensional situations; indeed the basic equations are the same except that the full flow equations with inertia terms are used for the discharge laws. There are 'y-points' and 'Q-points' in the computational grid, the former corresponding to the nodes, the latter to the links between them; the space derivatives are weighted between t_n and t_{n+1} time level using a weighting coefficient θ:

$$\frac{\partial f}{\partial x} \approx \theta \frac{f_{j+1}^{n+1} - f_{j-1}^{n+1}}{2\Delta x} + (1-\theta)\frac{f_{j+1}^n - f_{j-1}^n}{2\Delta x}$$
$$0.5 \leqslant \theta \leqslant 1.0 \tag{3.30}$$

The Delft scheme is identical to the Abbott–Ionescu scheme (considered in detail further on) insofar as application to the basic homogeneous flow

equations is concerned, differences appearing at the level of definition of the equation coefficients, coefficient θ, convective momentum term, and solution algorithm.

(ii) *Abbott–Ionescu type scheme*

In this scheme two dependent variables (say discharge Q and depth h) are computed at different grid points as shown in Fig. 3.7. This scheme was first

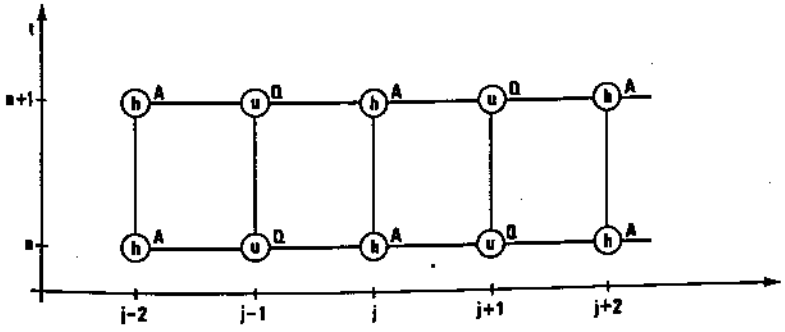

Fig. 3.7. Computational grid for the Abbott–Ionescu scheme

proposed by Abbott and Ionescu (1967) at the International Institute for Hydraulic and Environmental Engineering in Delft, the Netherlands. Because the flow variables are computed at different points, the difference approximations of the derivatives in Equations (3.22) are not applied at the same cross sections. Consider the following system of homogeneous flow equations which may be obtained from Equations (2.29):

$$g\frac{\partial h}{\partial t} - u\frac{\partial u}{\partial t} - (u^2 - gh)\frac{\partial u}{\partial x} = 0 \tag{3.31a}$$

$$h\frac{\partial u}{\partial t} - u\frac{\partial h}{\partial t} - (u^2 - gh)\frac{\partial h}{\partial x} = 0 \tag{3.31b}$$

Originally the scheme was applied to the above system by introducing into Equation (3.31a) the following derivative approximations:

$$\begin{aligned}
\frac{\partial h}{\partial t} &\approx \frac{h_j^{n+1} - h_j^n}{\Delta t} \\
\frac{\partial u}{\partial t} &\approx \frac{1}{2}\left(\frac{u_{j+1}^{n+1} - u_{j+1}^n}{\Delta t} + \frac{u_{j-1}^{n+1} - u_{j-1}^n}{\Delta t}\right) \\
\frac{\partial u}{\partial x} &\approx \frac{1}{2}\left(\frac{u_{j+1}^{n+1} - u_{j-1}^{n+1}}{2\Delta x} + \frac{u_{j+1}^n - u_{j-1}^n}{2\Delta x}\right)
\end{aligned} \tag{3.32}$$

and in Equation (3.31b):

$$\frac{\partial u}{\partial t} \approx \frac{u_{j+1}^{n+1} - u_{j+1}^{n}}{\Delta t}$$

$$\frac{\partial h}{\partial t} \approx \frac{1}{2}\left(\frac{h_{j+2}^{n+1} - h_{j+2}^{n}}{\Delta t} + \frac{h_{j}^{n+1} - h_{j}^{n}}{\Delta t}\right) \qquad (3.33)$$

$$\frac{\partial h}{\partial x} \approx \frac{1}{2}\left(\frac{h_{j+2}^{n+1} - h_{j}^{n+1}}{2\Delta x} + \frac{h_{j+2}^{n} - h_{j}^{n}}{2\Delta x}\right)$$

Thus the finite difference operator in this scheme involves eight points, i.e. four points at the same time level (from $j-1$ to $j+2$). Each of the two equations of the system (3.31) is approximated at a different point: Equation (3.31a) at point j and Equation (3.31b) at the adjacent point $j+1$.

For practical applications, such as in the System 11 SIVA developed by Verwey (1971) the scheme is applied to the flow equations (3.33) with the vector f as defined by Equations (3.16) (we are still leaving the free term out for the moment):

$$b_{st}\frac{\partial y}{\partial t} + \frac{\partial Q}{\partial x} = 0 \qquad (3.34a)$$

$$\frac{\partial Q}{\partial t} + gA\frac{\partial y}{\partial x} + \frac{\partial}{\partial x}\left(\frac{Q^2}{A}\right) = 0 \qquad (3.34b)$$

Again there are 'A-(or y-)points' (corresponding to the h-points in Fig. 3.7) and 'Q-points' (corresponding to the u-points in Fig. 3.7) within the computational grid used. The discretization is applied to Equation (3.34a) with the aid of the following approximations:

$$\frac{\partial y}{\partial t} \approx \frac{y_{j}^{n+1} - y_{j}^{n}}{\Delta t}$$

$$\frac{\partial Q}{\partial x} \approx \frac{1}{2}\left(\frac{Q_{j+1}^{n+1} - Q_{j-1}^{n+1}}{2\Delta x} + \frac{Q_{j+1}^{n} - Q_{j-1}^{n}}{2\Delta x}\right) \qquad (3.35)$$

while Equation (3.34b) is approximated using

$$\frac{\partial Q}{\partial t} \approx \frac{Q_{j+1}^{n+1} - Q_{j+1}^{n}}{\Delta t}$$

$$\frac{\partial y}{\partial x} \approx \frac{1}{2}\left(\frac{y_{j+2}^{n+1} - y_{j}^{n+1}}{2\Delta x} + \frac{y_{j+2}^{n} - y_{j}^{n}}{2\Delta x}\right) \qquad (3.36)$$

$$\frac{\partial}{\partial x}\left(\frac{Q^2}{A}\right) \approx \frac{1}{2\Delta x}\left[\left(\frac{Q^2}{A}\right)_{j+2}^{n+\frac{1}{2}} - \left(\frac{Q^2}{A}\right)_{j}^{n+\frac{1}{2}}\right]$$

The reader should note that Equation (3.36) is written symbolically; indeed, there is no time level $n+1/2$ and no discharge values Q at the computational points j, $j+2$ which are h (or A) points. Thus the Q values at $(j, n+1/2)$ and

$(j+2, n+1/2)$ must be obtained by interpolation. We shall come back to this problem when discussing the representation of equation coefficients.

The Abbott–Ionescu scheme represents *two* contour integrals, shifted one with respect to another since at the 'A-points' mass conservation is applied while the momentum equation is written for 'Q-points'. It does not produce the analytical solution for the linearized Equations (3.25), whatever the ratio $\Delta t/\Delta x$ as compared to the celerity $(gh_0)^{\frac{1}{2}}$. It does converge to the exact solution when $\Delta t, \Delta x \to 0$, but for *finite* values of the computational intervals, the two solutions cannot coincide.

The scheme is an implicit one. For N computational points, there are N unknowns (Q^{n+1} and h^{n+1}) and $N-2$ equations. Two boundary conditions close the system. However, the boundary conditions may not be applied without caution; for example, one cannot prescribe a $Q(t)$ condition at an 'h-point'. We shall come back to this problem later on.

(iii) *Vasiliev scheme*

The Vasiliev scheme was developed by a team of researchers at the Institute of Hydrodynamics, Novosibirsk (USSR), headed by O. F. Vasiliev (Vasiliev and Godunov, 1963; Vasiliev *et al.*, 1965). The scheme is a fully implicit one in which both dependent variables are computed at all grid points. It uses the following approximation of time and space derivatives (*see* Fig. 3.6):

$$\frac{\partial f}{\partial t} \approx \frac{f_j^{n+1} - f_j^n}{\Delta t} \; ; \quad \frac{\partial G}{\partial x} \approx \frac{G_{j+1}^{n+1} - G_{j-1}^{n+1}}{2\Delta x} \tag{3.37}$$

This discretization is applied to the continuity equation written under its usual form (say Equation (2.20)), and to the dynamic equation under the following form which may be obtained from Equations (2.30):

$$\frac{\partial Q}{\partial t} + 2u \frac{\partial Q}{\partial x} + (c^2 - u^2)\, b \frac{\partial y}{\partial x} = \Phi \tag{3.38}$$

where $c = (gh)^{\frac{1}{2}}$, b = width, Φ = resistance and slope terms.

Limiting ourselves to homogeneous and linear situations, the substitution of Equation (3.37) into Equations (2.20) and (3.38) leads us to

$$A_j^{n+1} - A_j^n + \frac{\Delta t}{2\Delta x}(Q_{j+1}^{n+1} - Q_{j-1}^{n+1}) = 0 \tag{3.39a}$$

$$Q_j^{n+1} - Q_j^n + u \frac{\Delta t}{\Delta x}(Q_{j+1}^{n+1} - Q_{j-1}^{n+1}) + (c^2 - u^2)\, b \frac{\Delta t}{2\Delta x}(y_{j+1}^{n+1} - y_{j-1}^{n+1}) = 0 \tag{3.39b}$$

Disregarding for the time being the representation of coefficients u, $(c^2 - u^2)$, b, etc., and keeping in mind the functional dependence $A = A(y)$, we realize that, for N computational points and $2N$ unknown dependent variables, it is possible to write $2N-4$ equations (3.39). Thus there is a boundary problem which must

be solved, since we have only two boundary conditions available. In this respect the situation here is analogous to that encountered when analysing explicit schemes.

(iv) *Gunaratnam–Perkins scheme*

This scheme (Gunaratnam and Perkins, 1970) is a finite difference approximation of the flow equations written in a linearized homogeneous characteristic form,

$$\frac{\partial y}{\partial t} + (u_0 \pm c_0)\frac{\partial y}{\partial x} - \frac{1}{b_0(u_0 \mp c_0)}\left[\frac{\partial Q}{\partial t} + (u_0 \pm c_0)\frac{\partial Q}{\partial x}\right] = 0$$

The derivatives are replaced by

$$\frac{\partial f}{\partial t} \approx \frac{1}{6}\frac{f_{j-1}^{n+1} - f_{j-1}^{n}}{\Delta t} + \frac{2}{3}\frac{f_j^{n+1} - f_j^n}{\Delta t} + \frac{1}{6}\frac{f_{j+1}^{n+1} - f_{j+1}^n}{\Delta t} \qquad (3.40)$$

$$\frac{\partial f}{\partial x} \approx \frac{f_{j+1}^{n+1} - f_{j-1}^{n+1}}{2\Delta x}$$

Consequently this is a fully implicit scheme which links together three consecutive points $j-1$, j and $j+1$, leading to a system of $2N-4$ equations for $2N$ unknowns. Two boundary conditions and two characteristic equations written for the limit points $j=1$ and $j=N$ close the system.

Discretization of boundary conditions

The number and kind of boundary conditions necessary for solution of the differential equations of open channel one-dimensional unsteady flow were described in Chapter 2. When the differential equations are replaced by finite differences, these requirements do not change since the discrete system is supposed to approximate the continuous one. The application of this principle is unfortunately not always straightforward. The ease or difficulty depends upon the discretization method chosen, which is why we shall describe in the sequel a few of the difficulties which a modeller may meet in applying exterior boundary conditions and/or interior compatibility conditions. Boundary conditions should have the same numerical properties as the scheme used for interior points. It is of no use to develop a higher order of accuracy scheme as the boundary conditions are approximated only to first order!

One obvious difficulty is common to all explicit finite difference schemes. Consider Fig. 3.8 and assume that the computation is made according to the Lax scheme. The flow variables can be easily computed for all interior points, the last of which is the point $A(N-1, n+1)$: all flow variables are known at the points L, M, R at time level $n\Delta t$. Suppose that one of the flow variables (say discharge Q) is prescribed as a known function of time at the last computational section x_N. Consequently we know the value of Q_N^{n+1} at the point B, but we still need to solve for the other dependent variable, say h_N^{n+1}. The only general

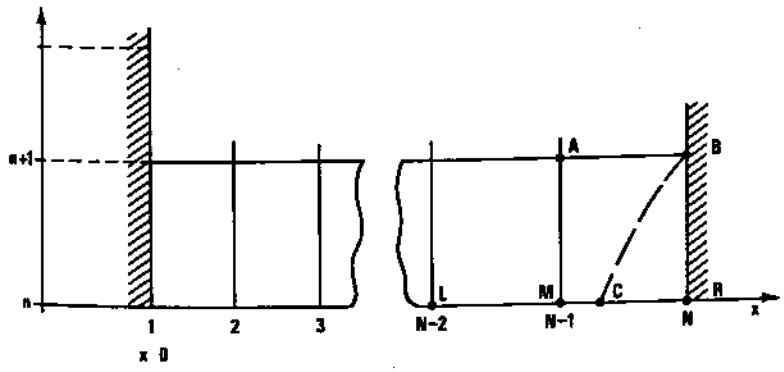

Fig. 3.8. Boundary conditions for explicit schemes. If one dependent variable is imposed at point B, the equation of the backward characteristic BC and the differential equation valid along it allow us to compute the abscissa of point C and the other dependent variable at point B

technique available for the solution of this problem is the method of characteristics, as we described it earlier (see point T in Fig. 3.2). The detailed description of this method applied to the boundary problem may be found in Liggett and Cunge (1975), and we limit ourselves here to a reminder that any other 'simplified' way of dealing with the problem may lead to serious difficulties and errors.

Explicit schemes are not the only ones which require special treatment of boundary conditions. The same situation arises when implicit schemes based on three computational points along the x-axis are used, as we mentioned when describing the Vasiliev and Gunaratnam–Perkins schemes. The latter needs the method of characteristics to compute the second variable at the boundary.

Analogous constraints are found for all these schemes when an interior boundary (or compatibility condition) is to be taken into account. Consider Fig. 3.9, in which two points L and R are linked by two compatibility

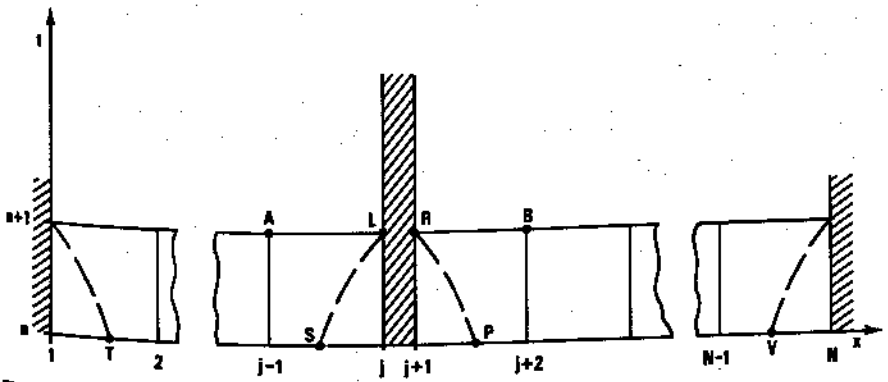

Fig. 3.9. Interior and exterior boundary conditions for implicit schemes based on three points at $t = t_n$

conditions (in this case trivial) such as $Q_R = Q_L$, $y_R = y_L$. There are four unknowns to be computed: $(y, Q)_j^{n+1}$ and $(y, Q)_{j+1}^{n+1}$. Using any of the explicit schemes, points such as A and B may be easily computed. The point L cannot be computed because we need, at the time level n, a computational point to the right of the transition. The same is true for the point R: we need a point to the left of the transition. Thus instead of using the same basic scheme as everywhere else at the interior conditions, the six following equations must be solved:

two characteristic equations on the forward characteristic LS;
two characteristic equations on the backward characteristic RP;
two compatibility equations $y_j^{n+1} = y_{j+1}^{n+1}$, $Q_j^{n+1} = Q_{j+1}^{n+1}$

for six unknown values: y_j^{n+1}, Q_j^{n+1}, y_{j+1}^{n+1}, Q_{j+1}^{n+1}, x_S and x_P. This implies the need to solve a system of six non-linear algebraic equations at each time step and at each interior boundary and transition. Generally the Newton iterative method is used, as it converges quite rapidly to the required accuracy. Still, the original simplicity of explicit schemes is compromised by this problem. An analogous situation occurs for implicit schemes such as Vasiliev or Gunaratnam–Perkins (see original papers of these authors).

Implicit staggered schemes have a different kind of boundary problem. Since the discharges (velocities) and depths (water stages, wetted surfaces) are not computed at the same points, one cannot freely prescribe the boundary conditions with respect to the grid. Put another way, the grid must be constructed in such a way that an h-point be located where $h(t)$ is imposed, and a Q-point where $Q(t)$ is prescribed. This may lead to practical difficulties, especially for the interior boundaries. Rapid modification of the computational grid during the calibration and exploitation stages of a model study may be difficult; it is not always easy to drop some grid points or to insert new ones. Finally, when the boundary condition is given as a stage/discharge rating curve, $Q = Q(y)$, it is necessary to interpolate between different computational points, since Q and y are not known at the same location. In nature the rating curve is a relationship between the discharge Q and water stage y at the same point. An example of the introduction of a rating curve using the Abbott–Ionescu scheme is given by Verwey (1971) and is shown in Fig. 3.10. Instead of approximating, let us say, a linear relationship $h_N^{n+1} = aQ_N^{n+1} + b$ (a and b being in general functions of h), the following relationship is used:

$$\frac{1}{2}\,(h_{N-2}^{n} + h_N^{n+1}) = C_1\,\frac{Q_{N-1}^{n+1} + Q_{N-1}^{n}}{2} + C_2 \tag{3.41}$$

where C_1, C_2 are coefficients.

In other words, the relationship is applied at the point P assuming that linear interpolation across two Δx steps is valid.

It should be noted that the Preissmann-type class of schemes is not at all hampered by any of the above mentioned difficulties. Any *two points* j, $j+1$ being linked by *two equations*, the representation of interior boundary

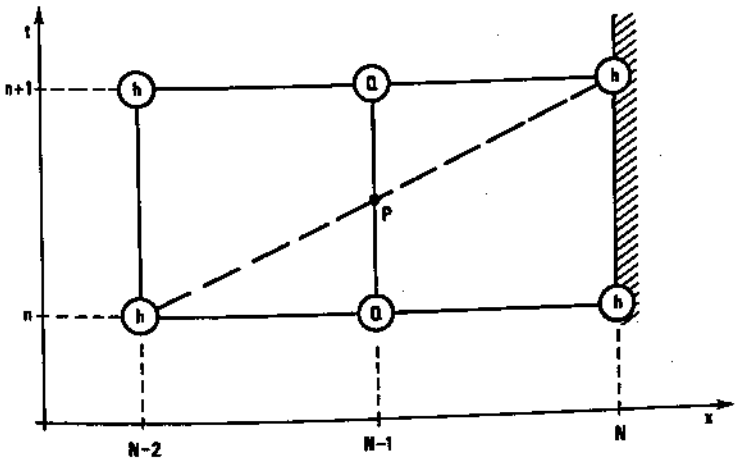

Fig. 3.10. Interpolation scheme for application of a downstream rating curve in the Abbott–Ionescu scheme

conditions by two compatibility conditions changes only the coefficients of the two equations. Thus, for any kind of model having N points there are $2N$ unknowns and $2N-2$ equations. Two boundary conditions close the system without introducing any new equations. Discharges and stages being computed at the same points, the system easily accepts modifications such as insertion of new points, its accuracy being unaffected by variations of the space interval Δx. Stage/discharge rating curves and similar relationships may be introduced at the same locations with no particular difficulty.

Discretization of the quasi-two-dimensional flow equations

The differential equations of quasi-two-dimensional flow, such as occurs over inundated plains, were derived in Chapter 2 (Equations (2.104)):

$$A_{s_j}(y_j)\frac{dy_j}{dt} = \sum_k Q_{j,k}(y_j, y_k) \tag{3.42}$$

where $A_{s_j}(y_j)$ = horizontal water surface area of the cell j, y_j = water stage in the cell j (supposed horizontal), k = index of the cells adjacent to the cell j, $Q_{j,k}(y_j, y_k)$ = discharge between cells j and k, dependent only upon the water stages y_j, y_k in these cells. The most commonly used finite difference approximation to Equation (3.42) is the following one:

$$A_{s_j}\frac{y_j^{n+1}-y_j^n}{\Delta t} = \theta \sum_k Q(y_j^{n+1}, y_k^{n+1}) + (1-\theta)\sum_k Q(y_j^n, y_k^n) \quad 0 \leqslant \theta \leqslant 1 \tag{3.43}$$

This approximation was first introduced by Preissmann and Cunge in 1961 (UNESCO/SOGREAH, 1964) and has since been widely used in the modelling systems of Delft Hydraulics Laboratory (Meijer *et al.*, 1965) and others. Note that if $\theta \neq 0$ in Equation (3.43), an implicit finite difference scheme results requiring the solution of a simultaneous system of equations for all cells in the model. If $\theta = 0$, the time step Δt is limited, as in all explicit schemes as we shall see, by the appearance of numerical instability. With $\theta > 0$ the admissible time step becomes larger and larger, the scheme becoming unconditionally stable for $\theta = 0.5$.

The discharge law $Q = Q(y_j, y_k)$ may be given under various forms which are described in available references (Zanobetti *et al.*, 1968; Zanobetti *et al.*, 1970; Cunge, 1975c). If Equation (3.43) is written for every cell $j = 1, 2, \ldots, N$ in the cell system, there will be altogether N algebraic equations which, solved by any numerical technique, furnish the N unknown values y_j^{n+1}, $j = 1, 2, \ldots, N$ of water stages in all cells. Next the discharges through the links between the cells may be computed given the known discharge laws

$$Q_{j,k}^{n+1} = Q(y_j^{n+1}, y_k^{n+1}) \tag{3.44}$$

The latter may represent either natural discharge conditions between two cells, or man-made structures. A few examples of such laws are as follows:

(i) River-like exchange law between two cells j and k, written as

$$Q = K \left(\frac{y_j - y_k}{\Delta x} \right)^{\frac{1}{2}} \tag{3.45a}$$

where K is the conveyance factor of the discharge channel and Δx is the distance between the points where y_j and y_k are computed. The conveyance is of course itself a function of elevations y_j, y_k which define the flow cross-section geometry (*see* Chapter 4).

(ii) Weir-like discharge formulae representing natural sills or man-made dykes, roads, railway embankments, etc. For example the broad crest weir formula can be used,

$$Q_{j,k} = \begin{cases} \mu_1 b (2g)^{\frac{1}{2}} (y_j - y_w)^{3/2} & \text{for a free overflow weir} \\ \mu_2 b (2g)^{\frac{1}{2}} (y_k - y_w)(y_j - y_k)^{1/2} & \text{for a drowned weir} \end{cases} \tag{3.45b}$$

where y_w is the weir elevation and $y_j > y_k$.

(iii) Discharge formula representing a submerged orifice,

$$Q_{j,k} = \mu A \left(2g(y_j - y_k) \right)^{\frac{1}{2}} \tag{3.45c}$$

where A = orifice cross-sectional area, and again $y_j > y_k$.

(iv) Discharge-elevation relationship between the cell j and a fictitious down-

stream cell (boundary condition), given, for example, as the polynomial

$$Q_{j,k} = a_0 + a_1 y_j + a_2 y_j^2 + \ldots \tag{3.45d}$$

3.2 LINEAR ANALYSIS OF THE VALIDITY OF DISCRETIZATION

Any system of computer programs for mathematical modelling of unsteady river flow is based on three fundamental elements:

- the integral or differential relationships expressing the physical laws which govern the flow, such as Equations (2.3), (2.14), (2.27)–(2.30), (2.36);
- the finite difference scheme which, when applied to the flow equations, produces a system of algebraic equations;
- the algorithm used to solve these algebraic equations.

The overall assessment of a modelling system has to be based on all three of these elements. In Chapter 2 we tried to situate the various mathematical formulations of flow laws with respect to one another and to physical reality. In Section 3.4 we shall look at various solution algorithms and the kinds of physical situations to which they are applicable. In this section we are concerned with the *convergence* of finite difference schemes to the true solutions of the flow equations. The convergence qualities of a scheme may be of decisive importance as to a modelling system's usefulness; put another way, it is useless to construct an elaborate modelling system around a basically poor scheme.

Convergence and approximation error

The fundamental notion in convergence is the following one: discrete solutions to the governing flow equations should approach the exact solutions to those same equations as the computational grid is refined (i.e. as Δx and Δt are both reduced).

In asking the question, 'Does the numerical solution (i.e. the solution of the finite difference equations) approach the solution of the differential or integral relationships?' one should not forget that the full differential equations cannot be solved exactly save for very few exceptions, and thus we never really know their solution. Therefore it is impossible to directly compare numerical and analytical results for general flow situations. What can be done, however, is to analyse the numerical method and to obtain some information concerning the behaviour of its solution as a function of certain parameters. Let $Lf = 0$ be a system of differential equations whose solution is a vector function $f(x, t)$ and let $L_h f_h = 0$ be a system of finite difference equations whose solution is the vector grid function f_h $(j\Delta x, n\Delta t)$. Then it is possible to investigate the behaviour of this solution f_h as a function of the parameters Δx and Δt, the space and time intervals. Clearly, when these intervals decrease ($\Delta x, \Delta t \to 0$), the numerical solution $f_h(j\Delta x, n\Delta t)$ must approach the analytical solution

$f(x, t)$, or it should not be used generally. In the latter case we say that the scheme is not convergent. The difference between the results it furnishes and the results of the differential equations will never be reduced, however small the computational intervals. Every proposed scheme should be submitted to convergence analysis, which incidentally has nothing whatsoever to do with the comparison of computed and observed results (e.g. water stages). Such a comparison cannot furnish criteria concerning numerical approximation error and moreover it is quite possible that a non-convergent finite difference scheme will give plausible results 'confirmed' by measurements, especially if measurements are sparse and the model is 'calibrated'.

Suppose that a series of computations is run with a given scheme while progressively decreasing Δx and Δt. A convergent scheme should give a sequence of results which approach the analytical solution at computational points. An incorrect, non-convergent scheme would furnish a sequence of solutions which either does not converge to any limit or which converge to a limit which is different than the solution of the original equations. Clearly, from a practical point of view only convergent schemes are of interest and it is of prime importance to the user to know that the scheme on which his model is based is convergent. If so, he can always improve the results by, for example, refining the computational grid and in so doing, qualitatively assess how far his solution is from the analytical one. Such an estimate is impossible with a non-convergent scheme.

We do not dispose of means to study the convergence of finite difference schemes for general problems. The only tools we can use were developed for *linear* equations which are derived from the complete non-linear expressions. We can only hope that the necessary convergence conditions for a particular scheme, derived for linearized models of the full equations, can be used as an estimate of the scheme's behaviour when applied to the full non-linear equations. The first important treatise on the convergence of finite difference methods for initial value problems (without boundary conditions) was written by Richtmyer (1957), and is still entirely applicable and timely. Godunov and Ryabenki (1964) introduced a methodology for the study of the convergence of finite difference schemes for mixed initial/boundary value problems. It is not our intention here to enter into the details and proofs of theorems and methods regarding convergence. We shall limit ourselves to a very intuitive and simple description of concepts, abstaining from the use of mathematical formalities other than elementary ones. Interested readers may find the convergence problems treated in different references at different levels of difficulty and from different points of view. In addition to the basic treatises by Richtmyer and Godunov and Ryabenki, hundreds of books and papers have been written on the subject, which has become a classical one in numerical analysis. As far as the schemes used in open channel flow modelling are concerned, the reader may find some detailed development of the ideas presented here in Abbott (1975a, b) and Liggett and Cunge (1975). A more complete theory is the subject of the first volume in the present series of books (Abbott, 1979).

For linear equations convergence is ensured if the conditions of the famous Lax theorem are satisfied:

'Given a properly posed initial-value problem and a finite difference approximation to it that satisfies the *consistency* condition, *stability* is the necessary and sufficient condition for *convergence*.'

We assume here that the problems are properly posed – such is generally the case if the boundary and initial conditions are prescribed correctly. Consistency means, very roughly, that the finite difference operators approach the differential equations when $\Delta t, \Delta x \to 0$. Numerical stability means, also very roughly, that the solutions obtained with the aid of a numerical scheme are bounded; that a small error (e.g. round-off error in the sixth place after the decimal point) should stay small during the whole computation, however long, and never become as great as the significant number (*see* the following section). The consistency condition may be explained immediately using the following example. Consider a differential equation

$$Lu = \frac{\partial u}{\partial t} + \frac{\partial u}{\partial x} = 0 \tag{3.46}$$

where $L = \frac{\partial}{\partial t} + \frac{\partial}{\partial x}$ is a differential operator and its finite difference analogue is

$$L_j u_j = \frac{u_j^{n+1} - u_j^n}{\Delta t} + \frac{u_{j+1}^n - u_{j-1}^n}{2\Delta x} = 0 \tag{3.47}$$

where L_j is the difference operator and u_j^n is a grid function satisfying Equation (3.47). Suppose that the functions u_j^{n+1}, u_{j+1}^n and u_{j-1}^n can be developed in Taylor series around the point $(n\Delta t, j\Delta x)$:

$$u_j^{n+1} = u_j^n + \frac{\partial u_j^n}{\partial t}\Delta t + \frac{\partial^2 u_j^n}{\partial t^2}\frac{\Delta t^2}{2} + \dots$$

$$u_{j-1}^n = u_j^n - \frac{\partial u_j^n}{\partial x}\Delta x + \frac{\partial^2 u_j^n}{\partial x^2}\frac{\Delta x^2}{2} - \dots$$

etc. Substitution into Equation (3.47) leads to

$$L_j u_j = \frac{\partial u_j^n}{\partial t} + \frac{\partial^2 u_j^n}{\partial t^2}\frac{\Delta t}{2} + \frac{\partial u_j^n}{\partial x} + \frac{\partial^3 u_j^n}{\partial x^3}\frac{\Delta x^2}{6} + O(\Delta t^2, \Delta x^4) \tag{3.48}$$

If the definition of the grid function u_j is such that $u_j^n = u(x = j\Delta x, t = n\Delta t)$, then we can write

$$|L_j u_j - Lu| = \frac{\partial^2 u_j^n}{\partial t^2}\frac{\Delta t}{2} + \frac{\partial^3 u_j^n}{\partial x^3}\frac{\Delta x^2}{6} + \dots = O(\Delta t, \Delta x^2) \tag{3.49}$$

When $\Delta t, \Delta x \to 0$, the difference $| L_j u_j - Lu |$ goes to zero too. Thus the finite difference analogue (3.47) is *consistent* with its differential prototype; the finite difference equation approximates the differential equation and the order of approximation is $O(\Delta t, \Delta x^2)$. This does not mean, however, that the difference solution approaches the differential one. On the contrary, it is quite possible that the sequence will diverge, that is to say that the solutions of Equation (3.47) obtained for $\Delta x, \Delta t$ smaller and smaller will be more and more different from the solutions of Equation (3.46), while the error in Equation (3.49) will be smaller and smaller. It is impossible to resolve this apparent paradox without studying the conditions of *stability* in the next section.

We may note that if convergence is ensured, its rapidity depends on the order of approximation such as defined in Equation (3.49). But we have already noted that the order of approximation of derivatives by finite differences may well be a meaningless notion for real computational grids because the time and space intervals $\Delta t, \Delta x$ and the derivatives of variables may well not be small. The same reasoning applies here, and while theoretically a higher order of approximation is better, it is not always obvious that this guarantees a better simulation of real life flow conditions.

Numerical stability

Let us consider a completely linear system of two partial differential flow equations with dependent variables $u(x, t)$ and $h(x, t)$,

$$\frac{\partial u}{\partial t} + g \frac{\partial h}{\partial x} = 0; \quad \frac{\partial h}{\partial t} + h_0 \frac{\partial u}{\partial x} = 0 \tag{3.50}$$

We seek a solution of Equation (3.50) of the type:

$$h(x, t) = H_m \exp(\mathrm{i}(\sigma_m x + \beta_m t));$$
$$u(x, t) = U_m \exp(\mathrm{i}(\sigma_m x + \beta_m t)) \tag{3.51}$$

where σ_m and β_m are constants, independent of x and t. Substituting Equations (3.51) into Equations (3.50) we obtain the homogeneous algebraic system

$$U_m \beta_m + g H_m \sigma_m = 0; \quad h_0 U_m \sigma_m + H_m \beta_m = 0 \tag{3.52}$$

whose determinant must be nil for non-trivial solutions. Applying this condition, and setting $(gh_0)^{\frac{1}{2}} = c$, we obtain a relationship between σ_m and β_m and the ratio U_m/H_m,

$$\beta_m^2 - c^2 \sigma_m^2 = 0; \quad \frac{\beta_m}{\sigma_m} = \pm c$$

$$\frac{U_m}{H_m} = -g \frac{\sigma_m}{\beta_m} = \mp \frac{g}{c} \tag{3.53}$$

To interpret this result, we first recall the physical meaning of the coefficients of Equations (3.52) and (3.53). If k is the number of waves per unit length, i.e. the inverse of the wavelength λ ($k = 1/\lambda$ is called the 'wave number'), then $\sigma = 2\pi k = 2\pi/\lambda$; if ν is the wave frequency, i.e. the inverse of the wave period T ($\nu = 1/T$) then $\beta = 2\pi\nu = 2\pi/T$; $\beta/\sigma = \lambda/T$ is thus the wave celerity. Equation (3.53) tells us that the celerity c is independent of σ_m.

Thus there are two solutions of the type (3.51) according to the sign + or − in the above ratio. Their superposition, permitted here because of the linearity of Equations (3.50), gives

$$\begin{aligned} h_m &= e^{i\sigma_m x}\left(A_m e^{i\beta_m t} + B_m e^{-i\beta_m t}\right) \\ u_m &= e^{i\sigma_m x}\left[A_m \left(\frac{U_m}{H_m}\right)_1 e^{i\beta_m t} + B_m \left(\frac{U_m}{H_m}\right)_2 e^{-i\beta_m t}\right] \end{aligned} \tag{3.54}$$

where A_m, B_m are arbitrary constants, $(U_m/H_m)_1 = -g/c$, $(U_m/H_m)_2 = +g/c$. These two sinusoidal solutions give us all liberty to choose $h(x, 0)$ and $u(x, 0)$ as independent functions. Hence we can write the development in Fourier integral of any initial repartition of u and h. Consequently the solutions h_m and u_m can be considered as Fourier series components with m indicating the harmonic.

Equation (3.54) shows that each component of the solution may be damped (or amplified) with time, the damping (or amplification) factor being $|\exp(i\beta_m t)|$. Since $\sigma_m = 2\pi/\lambda$ and $c = (gh_0)^{\frac{1}{2}}$ are both obviously real numbers, then from Equation (3.53) β_m must be real too. Consequently

$$|\exp(\pm i\beta_m t)| = |\cos\beta_m t \pm i \sin\beta_m t| = 1$$

and the components $h_m(x, t)$ of the solution are neither damped nor amplified; the exact solution to system (3.50), i.e. Equation (3.51), is energy conserving.

Now let us apply the Lax scheme (*see* Equation (3.26)) of finite differences with $\alpha = 0$ to Equation (3.50):

$$\begin{aligned} u_j^{n+1} - \frac{1}{2}(u_{j+1}^n + u_{j-1}^n) + g\,\frac{\Delta t}{2\Delta x}(h_{j+1}^n - h_{j-1}^n) = 0 \\ h_j^{n+1} - \frac{1}{2}(h_{j+1}^n + h_{j-1}^n) + h_0\,\frac{\Delta t}{2\Delta x}(u_{j+1}^n - u_{j-1}^n) = 0 \end{aligned} \tag{3.55}$$

and suppose that while $u(x, t)$, $h(x, t)$ are the exact solutions of the differential system (3.50), the grid functions u_j^n, h_j^n are the solutions of the difference system (3.55). Proceeding as we did earlier for the analytical solution to system (3.55). Proceeding as we did earlier for the analytical solution to Equation (3.50), we first express the grid functions u_{j+1}^{n+1} and h_{j+1}^{n+1} as

$$u_{j+1,m}^{n+1} = U_m \exp\{i[\sigma_m(j+1)\Delta x + \beta_m(n+1)\Delta t]\} \tag{3.56a}$$

$$h_{j+1,m}^{n+1} = H_m \exp\{i[\sigma_m(j+1)\Delta x + \beta_m(n+1)\Delta t]\} \tag{3.56b}$$

Substitution into the difference system (3.55) gives

$$U_m \left[e^{i\beta_m \Delta t} - \frac{1}{2}\left(e^{i\sigma_m \Delta x} + e^{-i\sigma_m \Delta x}\right)\right]$$
$$+ g \frac{\Delta t}{2\Delta x} H_m \left[e^{i\sigma_m \Delta x} - e^{-i\sigma_m \Delta x}\right] = 0$$

$$h_0 \frac{\Delta t}{2\Delta x} U_m \left[e^{i\sigma_m \Delta x} - e^{-i\sigma_m \Delta x}\right]$$
$$+ H_m \left[e^{i\beta_m \Delta t} - \frac{1}{2}\left(e^{i\sigma_m \Delta x} + e^{-i\sigma_m \Delta x}\right)\right] = 0$$

or using trigonometric definitions,

$$U_m \left(e^{i\beta_m \Delta t} - \cos \sigma_m \Delta x\right) + H_m g \frac{\Delta t}{\Delta x} i \sin \sigma_m \Delta x = 0$$

$$U_m h_0 \frac{\Delta t}{\Delta x} i \sin \sigma_m \Delta x + H_m \left(e^{i\beta_m \Delta t} - \cos \sigma_m \Delta x\right) = 0$$

The determinant of this system must be nil for a non-trivial solution, hence

$$\left(e^{i\beta_m \Delta t} - \cos \sigma_m \Delta x\right)^2 = -g h_0 \left(\frac{\Delta t}{\Delta x}\right)^2 \sin^2 \sigma_m \Delta x$$

and the relationship between β_m and σ_m may be found,

$$e^{i\beta_m \Delta t} = \cos \sigma_m \Delta x \pm i c \frac{\Delta t}{\Delta x} \sin \sigma_m \Delta x \tag{3.57}$$

If Equation (3.57) is satisfied, then expressions (3.56) are solutions of the difference system (3.55).

In the same way as was done for differential equations,

$$h_{j+1,m}^{n+1} = \exp\left(i\sigma_m (j+1)\Delta x\right) \left[\overline{A_m} \exp\left(i\beta_{m_1} (n+1)\Delta t\right) + \overline{B_m} \exp\left(i\beta_{m_2} (n+1)\Delta t\right)\right]$$

$$u_{j+1,m}^{n+1} = \exp\left(i\sigma_m (j+1)\Delta x\right) \left[\overline{A_m} \left(\frac{U_m}{H_m}\right)_1 \exp\left(i\beta_{m_1} (n+1)\Delta t\right) + \overline{B_m} \left(\frac{U_m}{H_m}\right)_2 \exp\left(i\beta_{m_2} (n+1)\Delta t\right)\right]$$

where $\overline{A_m}, \overline{B_m}$ are constants; β_{m_1}, β_{m_2} are two values obtained through Equation (3.57); $(U_m/H_m)_1$, $(U_m/H_m)_2$ correspond to β_{m_1}, β_{m_2} respectively.

Consequently the solutions of difference equations can be represented as Fourier series and as before, for one component m the solution h_{j+1}^{n+1} may be damped or amplified with time, so that $\exp\left(i\beta_{m_{1,2}} \Delta t\right)$ is the amplification factor. But we can no longer assume $\beta_{m_{1,2}}$ to be real numbers. Setting

$$\beta_m = \mathrm{Re}\, \beta_m + i \mathrm{Im}\, \beta_m$$

we find

$$e^{i\beta_m \Delta t} = e^{-\mathrm{Im}\beta_m \Delta t}\, e^{i\,\mathrm{Re}\beta_m \Delta t}$$

$$= e^{-\mathrm{Im}\beta_m \Delta t}(\cos \mathrm{Re}\,\beta_m \Delta t + i \sin \mathrm{Re}\,\beta_m \Delta t)$$

Our goal is to find the damping factor and the relationship between $\mathrm{Re}\,\beta_m \Delta t$ and σ_m. To that end substitution into Equation (3.57) and equating of real and imaginary parts yields

$$e^{-\mathrm{Im}\beta_m \Delta t} \cos \mathrm{Re}\,\beta_m \Delta t = \cos \sigma_m \Delta x \tag{3.58}$$

$$e^{-\mathrm{Im}\beta_m \Delta t} \sin \mathrm{Re}\,\beta_m \Delta t = \pm c\,\frac{\Delta t}{\Delta x} \sin \sigma_m \Delta x \tag{3.59}$$

Division of Equation (3.59) by Equation (3.58) gives

$$\tan \mathrm{Re}\,\beta_m \Delta t = \pm c\,\frac{\Delta t}{\Delta x} \tan \sigma_m\, \Delta x \tag{3.60}$$

Squaring and adding Equations (3.58) and (3.59) leads to

$$e^{-\mathrm{Im}\beta_m \Delta t} = \pm\, (\cos^2 \sigma_m \Delta x + c^2 \left(\frac{\Delta t}{\Delta x}\right)^2 \sin^2 \sigma_m \Delta x)^{\frac{1}{2}} \tag{3.61}$$

Thus the damping factor $|\varphi_m|$ for one step of the solution will be:

$$|\varphi_m(\beta_m n\Delta t)| = |\exp(-\mathrm{Im}\,\beta_{m_{1,2}} n\Delta t)|$$

$$= (\cos^2 \sigma_m \Delta x + c^2 \left(\frac{\Delta t}{\Delta x}\right)^2 \sin^2 \sigma_m \Delta x)^{\frac{1}{2}} \tag{3.62}$$

Having established Equation (3.62) we may now ask the two following questions:

(i) When Δx and Δt are fixed, what is the behaviour of $h_j^n - h(j\Delta x,\ n\Delta t)$ when $n \to \infty$ (i.e. when the number of time steps increases infinitely)?

(ii) Suppose σ_m is given, and suppose that the computational grid is progressively refined (i.e. $\Delta t,\ \Delta x \to 0$); does the finite difference solution h_j^n approach the analytical solution $h(j\Delta x, n\Delta t)$, i.e. what is the behaviour of $|h_j^n - h(j\Delta x, n\Delta t)|$ for a fixed value of $n\Delta t$?

We have seen that the analytical solution $h(j\Delta x, n\Delta t)$ is neither damped nor deformed with time. Such is not the case for the numerical solution. Consider Equation (3.61) and expand $\cos^2 \sigma_m \Delta x$ and $\sin^2 \sigma_m \Delta x$ in power series of small arguments $\sigma_m \Delta x$ and $\sigma_m \Delta t$. The result

$$e^{-\mathrm{Im}\beta_m \Delta t} \approx 1 + \frac{\sigma_m^2}{2}(c^2 \Delta t^2 - \Delta x^2) \tag{3.63}$$

shows that the growth (or amplification) factor of each component of the

numerical solution may approach unity with any desired accuracy, by taking Δx and Δt sufficiently small. Thus, by decreasing Δx and Δt when σ_m = const., the solution of the difference equations should approach the analytical solution of the differential equations, at least as far as damping is concerned. Actually the same may be said about the celerity. Developing Equation (3.60) in a power series of $\sigma_m \Delta x$,

$$\begin{aligned} \operatorname{Re} \beta_m \Delta t &= \arctan \left[c \frac{\Delta t}{\Delta x} \tan \sigma_m \Delta x \right] \\ &\approx c \sigma_m \Delta t \left[1 + \frac{\sigma_m^2}{3} (\Delta x^2 - c^2 \Delta t^2) \right] \\ \text{and} \quad \frac{\operatorname{Re} \beta_m \Delta t}{\sigma_m \Delta t} &= c \left[1 + \frac{\sigma_m^2}{3} (\Delta x^2 - c^2 \Delta t^2) \right] \end{aligned} \tag{3.64}$$

Thus the ratio $\operatorname{Re}\beta_m / \sigma_m$ will tend, with Δx, $\Delta t \to 0$, to the differential equation solution celerity $c = (gh_0)^{\frac{1}{2}}$.

Let us now investigate the behaviour of the growth factor of the numerical solution $|\varphi_m|$ which is a function of both the time and space steps Δt, Δx and of the coefficients σ_m, i.e. of the harmonic number m. Since while refining the computational grid (i.e. assuming that Δt, $\Delta x \to 0$) we never really approach the limit, there must be some harmonic m_0 in the solution (some sufficiently high value of m) for which the numerical solution growth factor disagrees seriously with the analytical solution growth factor. When *one has chosen* Δx and Δt so as to attain a certain degree of accuracy in the calculation, all solution harmonics above m_0 *are assumed* to be of negligible amplitude at all times. (One should not forget however that the numerical solution harmonics $m > m_0$ are always contained in the global numerical result.) The fact that the approximate solution harmonics for $m > m_0$ disagree with the corresponding analytical solution harmonics does not matter as long as the former do not become amplified to such an extent as to be no longer negligible. For example, referring to question (*i*) above, there are always truncation errors in a numerical computation, which provoke harmonics of high order in the numerical solution. If these harmonics have a growth factor such that they are amplified with time, it is conceivable that after a certain number of time steps they could destroy the solution.

Consider the growth or amplification factor defined by Equation (3.62) for the mth harmonic, $\exp(-\operatorname{Im} \beta_m n \Delta t)$ and imagine that $\operatorname{Im} \beta_m < 0$. Then the amplitude of the solution (or the growth of the amplitude of the mth harmonic) will increase exponentially with the number of time steps and with an exponent proportional to Δt! Such destructive behaviour is what is called *numerical instability*. It is intuitively evident that for Δt, Δx fixed and $n \to \infty$ the stability condition is

$$\max_m |\varphi_m| \leqslant 1 \tag{3.65}$$

Take for example Equation (3.62) for a fixed value of $\sigma_m \Delta x = \frac{\pi}{2}$ (i.e. a value for which $\sigma_m \Delta x$ is not small). Then the amplification factor will be $|\varphi_m| = |c \frac{\Delta t}{\Delta x}|$. If Δt, Δx are chosen such that $|\varphi_m| < 1$, the mth harmonic will be damped with every time step and, eventually, will disappear. If, to the contrary, $|\varphi_m| > 1$, at every time step the amplitude will be increased, being multiplied by $|c \frac{\Delta t}{\Delta x}| > 1$, a fixed quantity, independent of Δt. If we refine the grid letting $\Delta t, \Delta x \to 0$, the solution will grow without limits for a given time T.

In order to see how the stability condition Equation (3.65) constrains the time and distance steps in the Lax scheme, we apply it to Equation (3.61) to obtain

$$\cos^2 \sigma_m \Delta x + c^2 \left(\frac{\Delta t}{\Delta x} \right)^2 \sin^2 \sigma_m \Delta x \leqslant 1 \tag{3.66}$$

Quite obviously, given arbitrary values of coefficients $\sigma_m = \frac{2\pi}{\lambda_m}$ for different harmonics, the condition which ensures that Equation (3.65) is satisfied for all values of m is

$$\left| c \frac{\Delta t}{\Delta x} \right| \leqslant 1, \quad c = (gh_0)^{\frac{1}{2}} \tag{3.67}$$

This is the so called Courant–Friedrichs–Lewy (CFL) condition, established by the three authors in 1928. The value $(c\Delta t)/\Delta x$, or more precisely and for the full equations $|c + u| \frac{\Delta t}{\Delta x}$, is called throughout this book the Courant number, Cr. We would like to remind the reader that the CFL stability condition is directly linked to the theory of characteristics. Namely, with reference to Fig. 2.5b, it is seen that Equation (3.67) ($Cr \leqslant 1$) expresses the fact that the computed point $(n + 1, j)$ lies within the domain of determinacy of the point P of intersection of two characteristics drawn from two neighbouring points at the $n\Delta t$ time level. Thus if only these two points $(n, j - 1)$ and $(n, j + 1)$ enter into the computation of point $(n + 1, j)$, the time interval Δt should be less than $t_p - n\Delta t$, t_p being the time level of intersection point P. In the process of grid refinement to improve accuracy, one must obviously satisfy the stability condition at all times, i.e. there must be some relationship fixed at the beginning, between Δx and Δt whatever the Courant number value (unless the difference system is unconditionally stable).

Without developing these ideas further, we note that all explicit finite difference schemes, when applied to the hyperbolic flow equations, are *conditionally stable*. Therefore the time step Δt used cannot be chosen freely but must be small enough to satisfy the Courant (or other analogous) condition. This often leads to a computational time step which is too small as compared with the physical phenomena under consideration. Consider a river with an average depth of 3.0 m and a model of flood propagation along that river having computational

points every 1000 m. To satisfy the Courant condition the computational time step should be

$$\Delta t < \frac{1000}{(9.81 \times 3)^{\frac{1}{2}}} \approx 3 \text{ min}$$

which is small in terms of what can be used with respect to the physical phenomenon. Indeed, the flood duration may well be several days and an appropriate time step would be of the order of 1–2 h.

All finite difference methods can be analysed in terms of stability following the general procedures we have applied to the Lax scheme, and we refer the reader to the literature for detailed derivations. In general, explicit methods are conditionally stable, the Courant condition limiting the permissible time step. Implicit methods, on the other hand, can generally be made *unconditionally stable* in that the growth factor for all harmonics is never larger than 1.0 whatever the time and distance steps (or Courant number) chosen. With respect to the characteristic triangle and CFL condition one should realize that implicit schemes make the solution at any one point $(j, n+1)$ dependent upon *all* points $(j, n; j = 1, 2, \ldots)$. Thus the computed point lies always within a domain of determinacy (see Chapter 2) of the point of intersection of two characteristics issuing from the time level n. The Preissmann and Delft Hydraulics Laboratory schemes are unconditionally stable as long as $\theta \geqslant 0.5$ (Cunge, 1966a, b; Liggett and Cunge, 1975; Vreugdenhil, 1973). The Abbott–Ionescu and Vasiliev schemes are unconditionally stable (Abbott and Ionescu, 1967; Vasiliev and Godunov, 1963; Abbott, 1979).

The possible unconditional stability of implicit schemes has been one of the major reasons for their adoption in virtually all major modelling systems which are presently in use. However, implicit schemes must not be applied blindly with any arbitrary values of computational time and space intervals Δt and Δx. If it is true that an unstable scheme may yield a solution which, although satisfying the difference system, does not converge to the exact solution of the differential equations, it is also true that a stable and consistent scheme may give a solution of the finite difference system which, although bounded for a given Δx, Δt, is very far from the exact solution of the differential equations. We shall show in the next paragraph that one can approximately assess the behaviour of the scheme as a function of Δx and Δt. It must be remembered that all our conclusions, including stability criteria, stem from the analysis of linear systems such as Equation (3.50). Thus it is possible that a scheme which is declared stable based on linear analysis may be unstable when applied to the full non-linear, non-homogeneous flow equations. Later on we shall discuss the practical consequences of this problem, for which we have no formal analysis methods.

Amplitude and phase portraits

We have shown that the components m of the solution (3.51) to the linear Equations (3.50) conserve their amplitude as $|e^{I\beta m t}| = 1$ and all have the same

celerity ($c = \pm \frac{\beta_m}{\sigma_m}$) as they propagate along the channel. We have also seen that numerical solutions only approximately model this behaviour, as in the case of the Lax scheme which has the amplification factor defined by Equation (3.61). Staying on the safe side of the stability condition, i.e. considering only $Cr = c\frac{\Delta t}{\Delta x} \leqslant 1$, one finds easily that, unless $Cr = 1$,

$$|e^{-\mathrm{Im}\beta_m \Delta t}| \leqslant 1, \text{ i.e. } \mathrm{Im}\,\beta_m \Delta t > 0 \tag{3.68}$$

The conclusion is that the stable numerical solution is in fact damped with time, the damping factor over one time step being given precisely by Equation (3.61):

$$|e^{-\mathrm{Im}\beta_m \Delta t}| = (\cos^2 \sigma_m \Delta x + Cr^2 \sin^2 \sigma_m \Delta x)^{\frac{1}{2}} \tag{3.69}$$

Clearly, this factor is a function of the Courant number $Cr = c\frac{\Delta t}{\Delta x}$ and of the parameter

$$\sigma_m \Delta x = \frac{2\pi}{\lambda_m} \Delta x = \frac{2\pi}{M} \tag{3.70}$$

where M is the number of computational intervals per wavelength λ_m corresponding to the mth component of the solution. It is thus possible to compute a series of curves relating the damping to the computational grid characteristics,

$$|e^{-\mathrm{Im}\beta_m \Delta t}| = f(Cr, M) \tag{3.71}$$

In a similar way the celerity $\tilde{c}_m$ of the mth component of the numerical solution may be found from Equation (3.60):

$$\tilde{c}_m = \frac{\mathrm{Re}\,\beta_m}{\sigma_m} = \frac{1}{\sigma_m \Delta t} \arctan(\pm Cr \tan \sigma_m \Delta x) \tag{3.72}$$

Except for $Cr = 1$, the celerities $\tilde{c}_m$ will be different for different components (we refer to the distortion of the solution caused by non-uniform celerities as 'numerical dispersion'). Again one may compute a series of curves $\tilde{c}_m = f(Cr, M)$. These curves constitute what we call the 'amplitude and phase portraits' of a finite difference scheme. The detailed description and interpretation of such portraits may be found elsewhere (Preissmann, 1965; Cunge, 1966a, b; Leendertse, 1967; Abbott, 1979).

Numerical damping over one time step is described by the ratio

$$R_1 = \frac{\text{numerical solution growth factor}}{\text{exact solution growth factor}} = \frac{\exp(-\mathrm{Im}\,\tilde{\beta}_m \Delta t)}{\exp(-\mathrm{Im}\,\beta_m \Delta t)} \tag{3.73}$$

where $\exp(-\mathrm{Im}\tilde{\beta}_m \Delta t)$ is computed from formulae such as Equation (3.69), while $\exp(-\mathrm{Im}\beta_m \Delta t)$ is found from the exact solution such as Equation (3.53). In the particular case of Equations (3.50) without dissipative terms there is no

damping, and the exact solution growth factor is $\exp(-\mathrm{Im}\beta_m \Delta t) = 1$ as we have seen, but this is not always the case. In a wave period T there are $T/\Delta t$ time steps, so after one period the initial wave will be numerically damped by the factor $\delta = (R_1)^{T/\Delta t}$. If $\beta = \dfrac{2\pi}{T} = \sigma c$, $Cr = c\Delta t/\Delta x$, $\sigma \Delta x = 2\pi/M$, then:

$$\frac{T}{\Delta t} = \frac{2\pi}{\beta \Delta t} = \frac{2\pi}{\sigma c \Delta t} = \frac{2\pi}{\sigma Cr \Delta x} = \frac{2\pi}{\dfrac{2\pi}{M} Cr} = \frac{M}{Cr}$$

Thus

$$\delta = |R_1|^{M/Cr} \tag{3.74}$$

The numerical dispersion is measured by the ratio

$$R_2 = \frac{\text{numerical solution wave celerity}}{\text{exact solution wave celerity}} = \frac{\tilde{c}_m}{c}$$

where $\tilde{c}_m$ is computed from formulae such as (3.72). Over one wave period T the mth component will be delayed (or advanced) with respect to the analytical solution by the time $R_2 \times T$.

The coefficients δ and R_2, or R_1 and R_2 (called by Leendertse 'convergence coefficients'), may be plotted for the Lax scheme as a function of Cr, M and the coefficient α. In Fig. 3.11, R_1 (Cr, M, $\alpha = 0$) and in Fig. 3.12, R_2 (Cr, M, $\alpha = 0$)

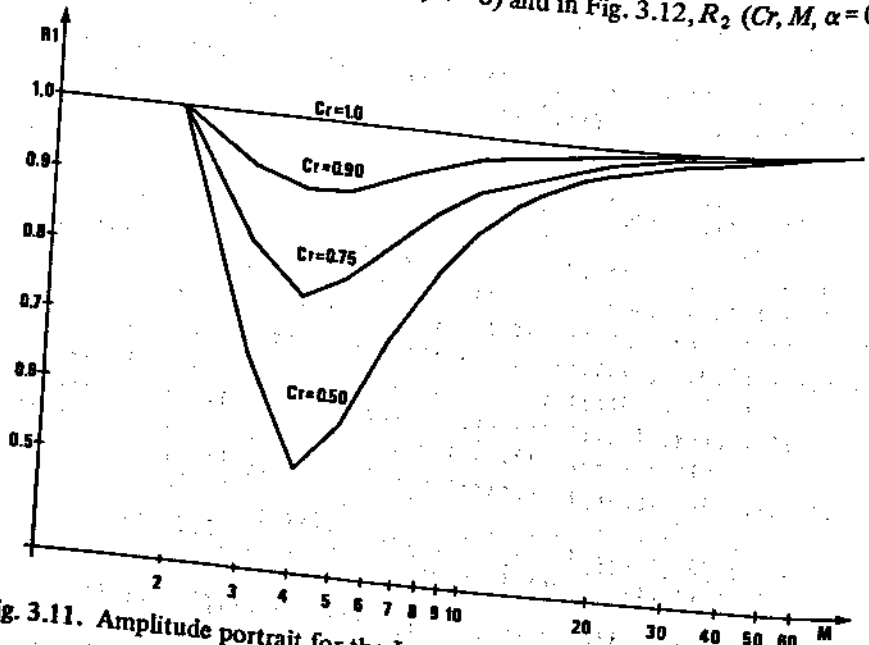

Fig. 3.11. Amplitude portrait for the Lax scheme, $\alpha = 0$

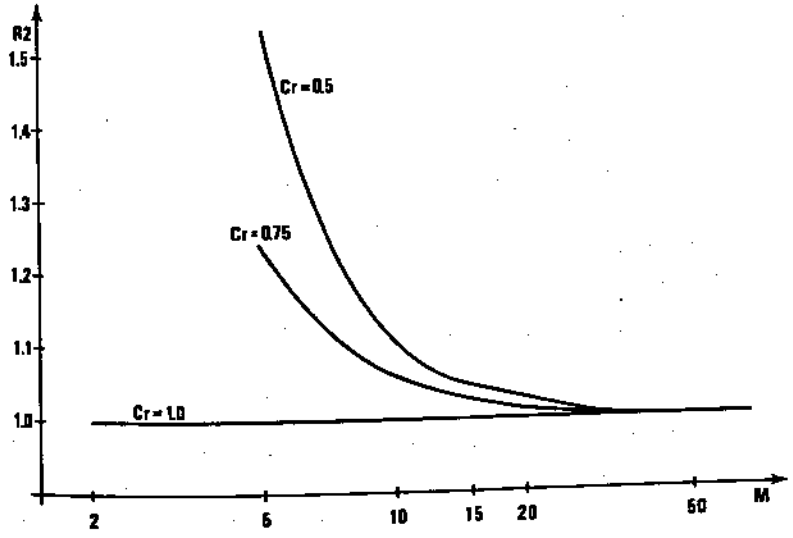

Fig. 3.12. Phase portrait for the Lax scheme, $\alpha = 0$

are shown. Such curves may be plotted for any scheme. The convergence coefficients R_1 (or, if preferred, the amplitude portraits) are extremely simple for the Abbott–Ionescu and Preissmann (with $\theta = 1/2$) schemes: $R_1 = 1$. They are not dissipative, there is no numerical damping. The Lax scheme, on the contrary, is dissipative: $R_1 \leqslant 1$ (except for $\alpha = 0$, $Cr = 1$, *see* Fig. 3.11). The Preissmann scheme may be rendered dissipative by adopting $1/2 < \theta \leqslant 1$. The Abbott–Ionescu scheme may be rendered dissipative by adopting a 'dissipative interface' (*see* Abbott, 1979). All three schemes are in general *dispersive*: the celerities of computational solution components are not equal and vary with Cr and M. However, for $Cr = 1$ both the Lax and Preissmann (for $\theta = 0.5$) schemes are non-dissipative and non-dispersive – they both give an exact solution to the linear system of Equations (3.50); such is not the case for the third scheme (*see* Fig. 3.13). For higher values of Courant number the Preissmann and

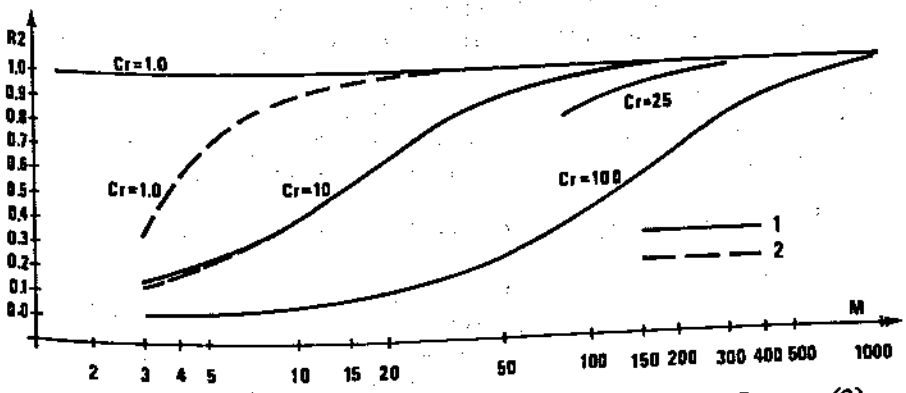

Fig. 3.13. Phase portraits for the Preissmann (1) and the Abbott–Ionescu (2) schemes

Abbott–Ionescu schemes have nearly exactly the same numerical dispersion.

It is interesting to see the kind of information one can obtain from such 'portraits', which are often considered measures of the applicability of a scheme to a particular problem. Consider the simulation of a tidal river whose tidal-influenced reach is 25 km long and assume that the tide period is 12 h. Let the average river depth be 5.0 m, i.e. $c = (gh)^{\frac{1}{2}} = 7\ \text{m s}^{-1}$. Suppose that we would like to reproduce with 95% accuracy (after simulating one tidal period) the wave whose period corresponds to the propagation time upstream of the tidal reach and back to the river mouth, i.e. along 50 000 m. That period is $50\,000/7 \approx 2\text{h}$. The total damping over 12 hours is δ^6 (Eq. 3.74) and

$$\text{damping } (\delta)^6 \leqslant 0.95, R_1 \geqslant \delta^{\Delta t/6r} = (0.95)^{Cr/6M}$$

$$\text{relative celerity } |R_2| > 0.95 \text{ (independent of } \Delta t).$$

Suppose that for practical reasons the space interval is fixed as $\Delta x = 250$ m. The wavelength of our component is $\lambda_m = 50\,000$ m, consequently $M = \lambda_m/\Delta x = 200$. From Figs. 3.11–3.13 we can choose, for each scheme, the largest Courant number Cr permitted, and then the largest possible time interval $\Delta t = 250 \times Cr/7 \approx 36 \times Cr$ (for $M = 200$)

- for the Lax scheme (Figs. 3.11, 3.12) taking any $Cr < 1$ and $M = 200$, $\Delta t < 36$ s;
- for the Preissmann and Abbott–Ionescu schemes (Fig. 3.13) $Cr = 25$ is the highest value leading to $R_2 < 0.95$ for $M = 200$.

Hence $\Delta t = 25 \times 36 \approx 900$ s.

Note that $R_1 = 1.0$ for both Preissmann and Abbott–Ionescu schemes so that Δt is not constrained by damping considerations. Inversely, one may define Δx for a given time step Δt.

This kind of estimate is valid only for the particular wave component considered. What happens to the shorter wave components? They are dispersed and damped much more severely than the longer components. If these shorter components are physically insignificant, then higher Courant numbers and time steps can be used without compromising the overall quality of the solution; however, these shorter components will disperse strongly and make the solution irregular, wavy. Oscillations will appear because some components are delayed or accelerated in the numerical solution as compared to nature. Consider as an example the propagation of the positive wave described by Equations (3.50) scaled in such a way that $(gh_0)^{\frac{1}{2}} = 1$ and subject to the following conditions:

- initial conditions: $u(j\Delta x, 0) = 0; h(j, \Delta x) = 1; j = 1, 2, \ldots, N$
- boundary conditions:

$$\text{upstream } h(0, t) = 1 + t/60 \quad 0 \leqslant t \leqslant 60$$

$$h(0, t) = 2 \quad t > 60$$

$$\text{downstream } u(N\Delta x, t) = 0$$

The analytical solution for this case is known; the entering upstream wave propagates at a celerity $c = 1.0\ \text{m s}^{-1}$ without any deformation. Numerical

solutions of this wave were obtained for $\Delta x = 10.0$ m using the Preissmann scheme with different values of Δt and θ as shown in Fig. 3.14. It is seen from

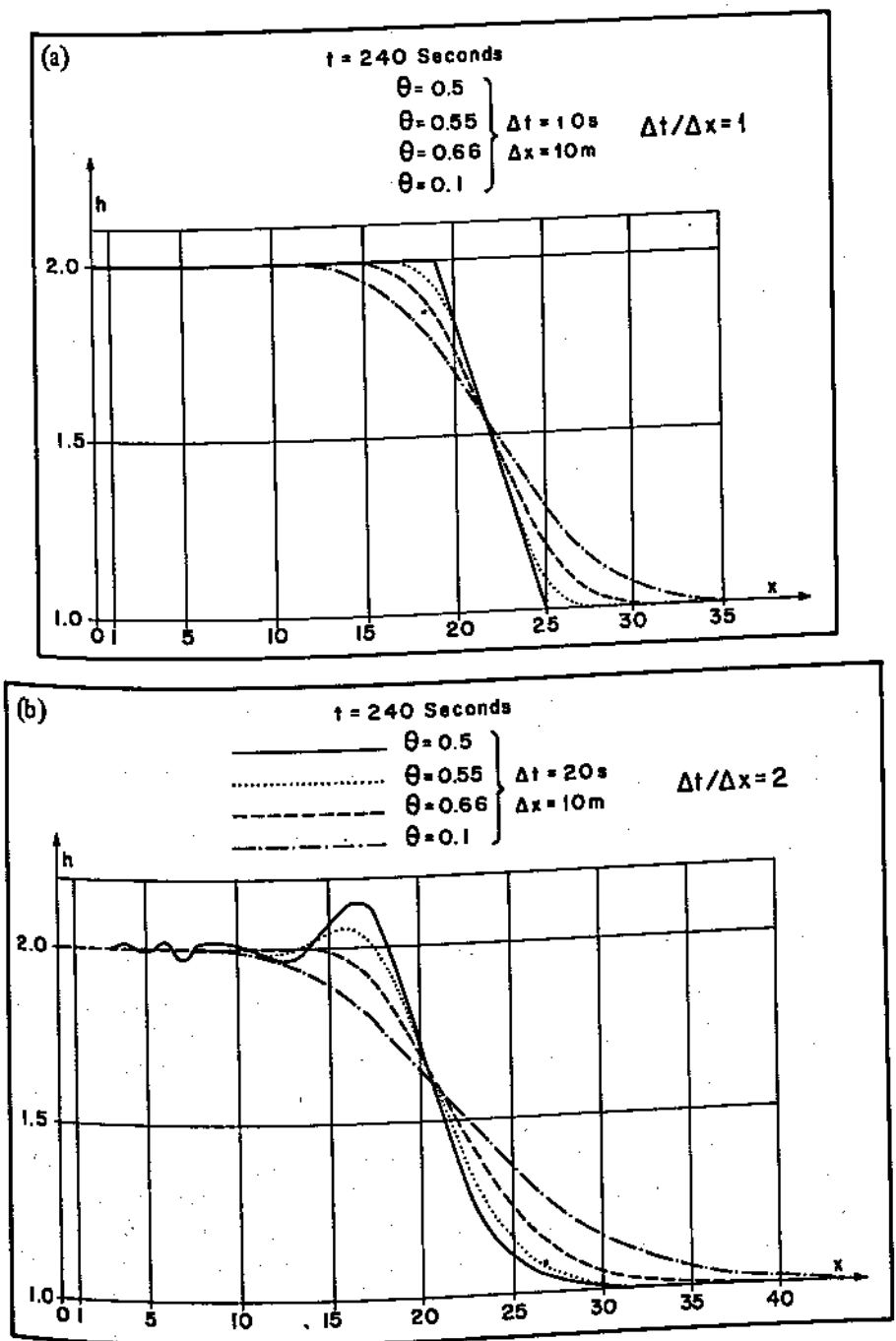

Fig. 3.14. Comparison of analytical and numerical solutions (Preissmann method) of a linear wave, Equation (3.50). (a) $\Delta t/\Delta x = 1.0$, (b) $\Delta t/\Delta x = 2.0$

these results that when $Cr = 1$ (i.e. $\Delta t/\Delta x = 1$) and $\theta = 0.5$, the scheme produces the analytical solution. When $\theta = 0.5$ and $Cr > 1$, however, the solution presents a wavy surface with oscillations. Indeed, when $\theta = 0.5$ the scheme is not dissipative but it is dispersive, the oscillations being due to the components which are delayed or accelerated. When $\theta > 0.5$, the scheme becomes diffusive and the shortest components are damped, smeared out. This damping falsifies the amplitude of these components, but often makes the numerical solution more acceptable compared to the analytical one (for example Fig. 3.14b for $\theta = 0.66$). The Abbott–Ionescu scheme has no built-in damping mechanism as we mentioned on p. 89 and, if used in its pure form, always presents some oscillations due to its dispersive feature (*see* the example given by Liggett and Cunge, 1975). Modelling systems based on this kind of non-dissipative scheme often include some sort of artificial smoothing procedure designed to remove dispersive oscillations.

Thus far we have based our analyses on the system of Equations (3.50) which does not provide for any *natural* damping. If natural attenuation and dispersion (due, for example, to the friction term in the dynamic equation) are much stronger than numerical damping and dispersion, there is no need to worry too much about them. Fortunately such is the case for many practical applications.

In conclusion, amplitude and phase portraits are useful tools for the qualitative assessment of different features of a given scheme, but cannot be considered as giving precise quantitative guidelines. Numerical damping is a nuisance only when the waves are of relatively small length and friction is negligible – such as in the case of steep front waves (surges) in canals and some tidal rivers (bores). In other cases, given the non-linearity of the full equations which thus cannot be formally analysed as well as other uncertainties, we recommend that the influence of different factors be assessed experimentally using the complete flow equations before pronouncing a definite judgement upon any considered scheme.

3.3 DISCRETIZATION OF NON-LINEAR TERMS AND COEFFICIENTS

The coefficients of the basic equations are discretized in various ways according to different authors and schemes. The variability of coefficients (their dependence upon the flow variables themselves) makes the equations non-linear, and finite difference analogues of the basic integral or differential equations become then non-linear algebraic systems. The discretization of coefficients must be done very carefully since it affects several vital features of the finite difference equations and, ultimately, of the modelling system. It is impossible to analyse here all the possible discretization methods and their consequences. We limit ourselves to the presentation of a few illustrative examples based on some of the most widely used schemes.

Preissmann scheme

In the consistent application of the Preissmann scheme to Equations (2.3),

(2.14) according to the general principles of Equations (3.18)–(3.21), the dependent flow variables are the wetted area $A(x, t)$ and the discharge $Q(x, t)$. The continuity equation does not contain any coefficients, but the dynamic equation requires discretization of the integral:

$$g \int_{t_n}^{t_{n+1}} \int_{x_j}^{x_{j+1}} [I_2 + A(S_0 - S_f)] \, dx \, dt \tag{3.75}$$

$$\text{where } I_2 = \int_0^{h(x)} (h - \eta) \left(\frac{\partial \sigma}{\partial x} \right)_{h_0} d\eta \tag{3.76}$$

$$S_f = \frac{Q \mid Q \mid}{K^2}, \quad K = K(y) = \text{conveyance} \tag{3.77}$$

Discretizing any function $f(x, t)$ such as I_2 or S_f using interpolation formulae analogous to those of Equations (3.18) and (3.19), setting the weighting parameter $\psi = 0.5$ and integrating, we obtain

$$\int_{t_n}^{t_{n+1}} \int_{x_j}^{x_{j+1}} f(x, t) \, dx \, dt = \left[\theta \frac{f_j^{n+1} + f_{j+1}^{n+1}}{2} + (1 - \theta) \frac{f_j^n + f_{j+1}^n}{2} \right] \Delta x \, \Delta t \tag{3.78}$$

Then using Equations (3.16), (3.21) and (3.78) one can write for any pair of points j, $j + 1$ two algebraic non-linear equations in terms of unknowns A and Q:

$$\frac{\Delta x}{2} (A_j^{n+1} + A_{j+1}^{n+1}) - \frac{\Delta x}{2} (A_j^n + A_{j+1}^n) + \Delta t \, [\theta (Q_{j+1}^{n+1} - Q_j^{n+1}) + (1 - \theta) (Q_{j+1}^n - Q_j^n)] = 0 \tag{3.79}$$

$$\frac{\Delta x}{2} (Q_{j+1}^{n+1} + Q_j^{n+1}) - \frac{\Delta x}{2} (Q_{j+1}^n + Q_j^n) + \Delta t \left\{ \theta \left[\left(\frac{Q^2}{A} + g I_1 \right)_{j+1}^{n+1} + \left(\frac{Q^2}{A} + g I_1 \right)_j^{n+1} \right] + (1 - \theta) \left[\left(\frac{Q^2}{A} + g I_1 \right)_{j+1}^n - \left(\frac{Q^2}{A} + g I_1 \right)_j^n \right] \right\}$$

$$+ \frac{g \Delta t \Delta x}{2} \left\{ \theta \, [(-I_2 + A S_f - A S_0)_j^{n+1} + (-I_2 + A S_f - A S_0)_{j+1}^{n+1}] + (1 - \theta) \, [(-I_2 + A S_f - A S_0)_j^n + (-I_2 + A S_f - A S_0)_{j+1}^n] \right\} = 0 \tag{3.80}$$

In these equations I_1 is a function of water stage y (*see* Equation (2.8)), and consequently of the dependent variable $A(x, t)$. Actually I_1 is the first moment of the wetted area with respect to the free surface level. I_2 is a function of the width variation between two sections and of the water stage (*see* Equation (3.76)) hence it is also, ultimately, a function of $A(x, t)$. To evaluate it one needs to know the width as a function of water stages or of wetted areas. The

friction slope S_f is a function of dependent variables $Q(x, t)$ and $A(x, t)$ according to Equation (3.77) through the conveyance K (which is a function of the wetted area or water stage). Such functions must be tabulated or represented in some other fashion for computations, *see* Section 3.6.

Because of these implicit dependencies, Equations (3.79), (3.80) form a nonlinear algebraic system. It must be stressed that in practice these particular integral relations, Equations (2.3) and (2.14), are not often used as the foundation of modelling systems except when one wants to accurately reproduce steep front waves. Indeed, it is much easier to work with $y(x, t)$ rather than with $A(x, t)$ as a dependent variable. Also the functions I_1 and I_2 require more storage and more computational efforts than the coefficients accompanying other forms of the basic equations. For example, the system of Equations (2.28)

$$\frac{\partial y}{\partial t} + \frac{1}{b}\frac{\partial Q}{\partial x} = 0 \tag{3.81}$$

$$\frac{\partial Q}{\partial t} + \frac{\partial}{\partial x}\left(\frac{Q^2}{A}\right) + gA\frac{\partial y}{\partial x} + gA\frac{Q|Q|}{K^2} = 0 \tag{3.82}$$

is most often used in spite of the fact that it is not written in a rigorously conservative form. The application of the Preissmann scheme to the derivatives in Equations (3.81), (3.82) according to Equations (3.23) and (3.24) yields, again for $\psi = 0.5$,

$$\left.\begin{aligned}
\frac{\partial y}{\partial t} &\approx \frac{y_{j+1}^{n+1} - y_{j+1}^{n}}{2\Delta t} + \frac{y_j^{n+1} - y_j^{n}}{2\Delta t} \\
\frac{\partial Q}{\partial t} &\approx \frac{Q_{j+1}^{n+1} - Q_{j+1}^{n}}{2\Delta t} + \frac{Q_j^{n+1} - Q_j^{n}}{2\Delta t} \\
\frac{\partial Q}{\partial x} &\approx \theta\frac{Q_{j+1}^{n+1} - Q_j^{n+1}}{\Delta x} + (1-\theta)\frac{Q_{j+1}^{n} - Q_j^{n}}{\Delta x}
\end{aligned}\right\} \tag{3.83a}$$

$$\left.\begin{aligned}
\frac{\partial}{\partial x}\left(\frac{Q^2}{A}\right) &\approx \frac{\theta}{\Delta x}\left[\frac{(Q_{j+1}^{n+1})^2}{A_{j+1}^{n+1}} - \frac{(Q_j^{n+1})^2}{A_j^{n+1}}\right] \\
&+ \frac{(1-\theta)}{\Delta x}\left[\frac{(Q_{j+1}^{n})^2}{A_{j+1}^{n}} - \frac{(Q_j^{n})^2}{A_j^{n}}\right] \\
\frac{\partial y}{\partial x} &\approx \theta\frac{y_{j+1}^{n+1} - y_j^{n+1}}{\Delta x} + (1-\theta)\frac{y_{j+1}^{n} - y_j^{n}}{\Delta x}
\end{aligned}\right\} \tag{3.83b}$$

The space interval in the above equations is $\Delta x = x_{j+1} - x_j$. The coefficients of Equations (3.81), (3.82), when represented according to the Preissmann formulation

$$f(x, t) \approx \frac{\theta}{2}(f_{j+1}^{n+1} + f_j^{n+1}) + \frac{1-\theta}{2}(f_{j+1}^{n} + f_j^{n}) \tag{3.84}$$

yield, together with the derivatives expressed by Equations (3.83a, b), two algebraic equations:

$$\frac{1}{2}\left(\frac{y_{j+1}^{n+1}-y_{j+1}^{n}}{\Delta t}+\frac{y_{j}^{n+1}-y_{j}^{n}}{\Delta t}\right)+\frac{2}{\Delta x}\frac{[\theta(Q_{j+1}^{n+1}-Q_{j}^{n+1})+(1-\theta)(Q_{j+1}^{n}-Q_{j}^{n})]}{\theta(b_{j}^{n+1}+b_{j+1}^{n+1})+(1-\theta)(b_{j}^{n}+b_{j+1}^{n})}=0 \tag{3.85a}$$

$$\frac{1}{2}\left(\frac{Q_{j+1}^{n+1}-Q_{j+1}^{n}}{\Delta t}+\frac{Q_{j}^{n+1}-Q_{j}^{n}}{\Delta t}\right)+\frac{\theta}{\Delta x}\left[\left(\frac{Q^2}{A}\right)_{j+1}^{n+1}-\left(\frac{Q^2}{A}\right)_{j}^{n+1}\right]+\frac{(1-\theta)}{\Delta x}\left[\left(\frac{Q^2}{A}\right)_{j+1}^{n}-\left(\frac{Q^2}{A}\right)_{j}^{n}\right]$$
$$+g\left[\theta\frac{A_{j+1}^{n+1}+A_{j}^{n+1}}{2}+(1-\theta)\frac{A_{j+1}^{n}+A_{j}^{n}}{2}\right]\left\{\left[\theta\frac{y_{j+1}^{n+1}-y_{j}^{n+1}}{\Delta x}+(1-\theta)\frac{y_{j+1}^{n}-y_{j}^{n}}{\Delta x}\right]+\left[\theta\frac{Q_{j+1}^{n+1}|Q_{j+1}^{n+1}|+Q_{j}^{n+1}|Q_{j}^{n+1}|}{2}+(1-\theta)\frac{Q_{j+1}^{n}|Q_{j+1}^{n}|+Q_{j}^{n}|Q_{j}^{n}|}{2}\right]\left[\theta\frac{(K_{j+1}^{n+1})^2+(K_{j}^{n+1})^2}{2}+(1-\theta)\frac{(K_{j+1}^{n})^2+(K_{j}^{n})^2}{2}\right]^{-1}\right\}=0;\quad 0.5\leqslant\theta\leqslant 1.0 \tag{3.85b}$$

Here again we find two non-linear algebraic equations in terms of y_j^{n+1}, Q_j^{n+1}, y_j^n and Q_j^n. The way the coefficients leading to Equations (3.85) are expressed also influences the way in which the non-linear system is solved. In SOGREAH's applications of the Preissmann method, it is supposed that all functions $f(y, Q)$ in the discretized non-linear algebraic equations are known at time level $n\Delta t$ and are differentiable with respect to y and Q. Then one can evaluate any such function at the time level $(n+1)\Delta t$ by a Taylor series expansion of the form

$$f_j^{n+1}=f_j^n+\Delta f=f_j^n+\frac{\partial f_j}{\partial y}\Delta y_j+\frac{\partial f_j}{\partial Q}\Delta Q_j+\frac{\partial^2 f_j}{\partial y^2}\frac{\Delta y_j^2}{2}+\cdots$$

where Δy, ΔQ are y and Q increments during the time step Δt. The substitution of such expansions into the finite difference approximations leads to a system of two non-linear algebraic equations in terms of Δy_j, ΔQ_j, Δy_{j+1}, ΔQ_{j+1} for every pair of points $(j, j+1)$. For N computational points there will be a system of $2N-2$ such equations for $2N$ unknowns. With the addition of two boundary conditions the system can be solved by a Newton iteration method, and for that purpose it is first linearized in terms of unknowns Δy_j, ΔQ_j, $j=1, 2, \ldots, N$ as described by Liggett and Cunge (1975). For a pair of adjacent points $(j, j+1)$ the linearized system may be written as follows:

$$A\Delta y_{j+1} + B\Delta Q_{j+1} + C\Delta y_j + D\Delta Q_j + G = 0$$
$$A'\Delta y_{j+1} + B'\Delta Q_{j+1} + C'\Delta y_j + D'\Delta Q_j + G' = 0 \qquad (3.86)$$

Using the known values of y_j^n, Q_j^n the coefficients $A, B, C, \ldots, G'$ can be computed, and the linearized system of Equations (3.86) written for N points can be solved, furnishing the second approximation to the unknowns at the new time $(n+1)\Delta t$. (The first approximation in the iteration process was $\Delta y_j = \Delta Q_j = 0$, since $n\Delta t$ values were adopted to initialize it.) The coefficients $A, B, C, \ldots$ can then be updated and the linear system can be solved again, furnishing the third approximation, etc. The significant feature of the system is that in most cases the second approximation (i.e. first iteration) is so good, that there is no need for further iterations (thus the system of Equations (3.86) for N points is solved only *once* for one time step Δt). The explanation is, of course, that when the coefficients $A, B, \ldots$ are derivatives of the functions $f(y, Q)$, the solution benefits from the quadratic convergence characteristics of the Newton method. On the other hand the full implicit discretization of coefficients ensures numerical stability of the computation.

Verwey's variant of the Preissmann scheme

Verwey derived a scheme of the Preissmann type using a different discretization principle for some terms, as shown below:

$$\frac{\partial}{\partial x}\left(\frac{Q^2}{A}\right) \approx \frac{1}{\Delta x}\left(\frac{Q_{j+1}^n\, Q_{j+1}^{n+1}}{A_{j+1}^{n+1/2}} - \frac{Q_j^n\, Q_j^{n+1}}{A_j^{n+1/2}}\right) \qquad (3.87a)$$

$$b \approx \frac{b_{j+1}^{n+1/2} + b_j^{n+1/2}}{2}; \quad A \approx \frac{A_{j+1}^{n+1/2} + A_j^{n+1/2}}{2} \qquad (3.87b)$$

$$\frac{Q|Q|}{K^2} \approx \frac{1}{2}\left\{\frac{|Q_j^n|\, Q_j^{n+1}}{(K_j^{n+1/2})^2} + \frac{|Q_{j+1}^n|\, Q_{j+1}^{n+1}}{(K_{j+1}^{n+1/2})^2}\right\} \qquad (3.87c)$$

The superscript $n + 1/2$ means that the function is evaluated between two time levels $n\Delta t$ and $(n+1)\Delta t$. The computation begins with the evaluation of the coefficients superscripted with $n + 1/2$ at time level $n\Delta t$, i.e. by setting $b_j^{n+1/2} = b_j^n$, $A_j^{n+1/2} = A_j^n$; $K_j^{n+1/2} = K_j^n$. The resulting system of linear equations in y_j^{n+1}, Q_j^{n+1}, $j = 1, 2, \ldots, N$ is solved to give a second approximation to these values, $\tilde{y}_j^{n+1}$, $\tilde{Q}_j^{n+1}$, and to the coefficients,

$$b_j^{n+1/2} \approx \frac{1}{2}\left[b_j(\tilde{y}_j^{n+1}) + b_j(y_j^n)\right] \text{ etc.}$$

Then the second iteration leads to the third approximation of the unknowns, and so on.

Experience with this scheme has shown that most problems can be treated satisfactorily with a weighting coefficient $\theta = 1/2$. As a rule two iterations per

time step (i.e. *two* solutions of the algebraic system of $2N$ equations) are needed to give a sufficiently accurate simulation. Application of this scheme without iterating generally leads to unstable behaviour.

Abbott–Ionescu scheme

The Abbott–Ionescu scheme applied to the system of Equations (3.81), (3.82) with the discretization of derivatives according to Equations (3.32), (3.33) leads to:

$$b_j^{n+1/2}\,\frac{y_j^{n+1}-y_j^n}{\Delta t}+\frac{1}{2}\left(\frac{Q_{j+1}^{n+1}-Q_{j-1}^{n+1}}{\Delta 2x_j}+\frac{Q_{j+1}^{n}-Q_{j-1}^{n}}{\Delta 2x_j}\right)=0 \qquad (3.88a)$$

$$\frac{Q_{j+1}^{n+1}-Q_{j+1}^{n}}{\Delta t}+\frac{1}{\Delta 2x_{j+1}}\left[\left(\frac{Q^2}{A}\right)_{j+2}^{n+1/2}-\left(\frac{Q^2}{A}\right)_{j}^{n+1/2}\right]$$
$$+g\,\frac{A_{j+1}^{n+1/2}}{2}\left[\frac{y_{j+2}^{n+1}-y_j^{n+1}}{\Delta 2x_{j+1}}+\frac{y_{j+2}^{n}-y_j^{n}}{\Delta 2x_{j+1}}\right]$$
$$+g\left(\frac{A}{K^2}\right)_{j+1}^{n+1/2}\left[f Q_{j+1}^{n}\,|\,Q_{j+1}^{n+1}\,|+(1-f)\,|\,Q_{j+1}^{n}\,|\,Q_{j+1}^{n}\right]=0 \qquad (3.88b)$$

where

$$\Delta 2x_j=x_{j+1}-x_{j-1};\ \Delta 2x_{j+1}=x_{j+2}-x_j;\ f=\text{weighting coefficient} \qquad (3.88c)$$

in which the discretization chosen for the coefficients is evident. This discretization is used in System 11 SIVA developed by Verwey of the Danish Hydraulic Institute. Since in this scheme water stages y and discharges Q are not computed at the same points, the values of Q^2 in the $\frac{\partial}{\partial x}\left(\frac{Q^2}{A}\right)$ terms of Equation (3.88) have to be evaluated at the y-points j, $j+2$. They are interpolated from the values at neighbouring Q-points with a weighting defined by storage. The parameter f in the resistance term has been introduced because of the possible rapid variation and reversal of discharge. The solution of Equations (3.88) requires iterations; in the first iteration f is taken equal to 1.0, while in the later iterations it is given the value

$$f=\frac{Q_j^{n+1/2}\,Q_j^{n+1/2}-Q_j^{n}\,Q_j^{n}}{Q_j^{n}\,(Q_j^{n+1}-Q_j^{n})} \qquad (3.89)$$

If the coefficients of Equations (3.88) with superscript $n+1/2$ are considered as known functions of flow variables computed at time level $n\Delta t$, these equations may be rewritten under the following form:

$$\alpha_j\,Q_{j-1}^{n+1}+\beta_j y_j^{n+1}+\gamma_j\,Q_{j+1}^{n+1}=\delta_j$$

$$\alpha_{j+1}^{*}\,y_j^{n+1}+\beta_{j+1}^{*}\,Q_{j+1}^{n+1}+\gamma_{j+1}^{*}\,y_{j+2}^{n+1}=\delta_{j+1}^{*}$$

where coefficients $\alpha, \beta, \gamma, \delta, \alpha^*, \beta^*, \gamma^*, \delta^*$ are known functions of flow variables. Equations (3.90) are two linear algebraic equations in terms of values Q_{j-1}, y_j, Q_{j+1}, and y_{j+2}; for each pair of points $(j-1, j), (j+1, j+2)$ a system of Equations (3.90) can be established. Thus these equations are analogous to the system of Equations (3.86) but, of course, with different coefficients and variables on a staggered grid.

The coefficients $b_j^{n+1/2}$, $A_{j+1}^{n+1/2}$, $\left(\frac{A}{K^2}\right)_{j+1}^{n+1/2}$ are evaluated during iterations in the same way as in Verwey's variant of Preissmann's scheme. It is of note that the coefficients A_{j+1} and $\left(\frac{A}{K^2}\right)_{j+1}$ are to be evaluated at the Q-points, where water stages are unknown. Hence these functions must be interpolated. Assuming as a first approximation $b^{n+1/2} = b^n$, $A^{n+1/2} = A^n$, $K^{n+1/2} = K^n$, $Q^{n+1/2} = Q^n$, Equations (3.88) are linear algebraic equations which, when solved, furnish a first approximation to the variables y_j^{n+1}, Q_{j+1}^{n+1} $(j = 1, \ldots, N)$ and, hence a second approximation to the coefficients $A^{n+1/2} = (A^n + A^{n+1})/2$, $K^{n+1/2} = (K^n + K^{n+1/2})/2$, etc. The substitution in (3.88) and second resolution of the linear system (second iteration) leads to a new, second, approximation for y_j^{n+1}, Q_{j+1}^{n+1}, $j = 1, 2, \ldots, N$. The scheme gives satisfactory results with two iterations at every time step. Whenever oscillations due to phase errors (see preceding paragraphs) have to be damped, a special dissipative interface (smoothing) used between two successive time steps.

The detailed developments of other schemes can usually be found in the literature. (*See* for example Liggett and Cunge, 1975 for the discretization of coefficients in some explicit schemes and for the Vasiliev scheme; Gunaratnam and Perkins, 1970, for the MIT six-point scheme.) The reader should however be aware that original publications sometimes describe only the discretization principle applied to derivatives, with no detail on how non-linear terms and coefficients are discretized in operational modelling systems.

Comments

The above three examples show that the coefficients may be represented in very different ways indeed. A first important comment is related to the linear analysis of basic finite difference equations which we presented in the previous sections. Quite obviously such an analysis, especially concerning the magnitude of numerical damping and dispersion, must be recognized as incomplete unless all interpolations, iterations and dissipative interfaces of investigated schemes are taken into account. Moreover, the influence of non-constant time and space intervals is neglected in such linear analyses.

We would like to bring in the following example (Preissmann, private communication 1979) concerning the value of the weighting coefficient θ in implicit schemes. The linear analysis shows, at least for certain schemes, that the highest accuracy is obtained with $\theta = 1/2$. Suppose that the modelled river is such that the inertia terms in the basic dynamic equation are negligible as compared to other terms:

$$\frac{1}{g}\underbrace{\left(\frac{\partial u}{\partial t}+u\,\frac{\partial u}{\partial x}\right)}_{\text{negligible}}+\frac{\partial y}{\partial x}+\frac{Q\,|Q|}{K^2}=0$$

Thus the dynamic equation is, in reality, reduced to the following one, which must be satisfied at every time level $n, n+1, n+2, \ldots$:

$$\frac{\partial y}{\partial x}+\frac{Q\,|Q|}{K^2}=0$$

Suppose that at initial time $t=0$ this equation was not satisfied *exactly* (typical case in practice). Then, at the time level $n\Delta t=0$,

$$\left(\frac{\partial y}{\partial x}\right)^n+\left(\frac{Q\,|Q|}{K^2}\right)^n=\Delta$$

where Δ is the error due to the initial state. Let us now use the following implicit schematization:

$$\theta\left(\frac{\partial y}{\partial x}\right)^{n+1}+(1-\theta)\left(\frac{\partial y}{\partial x}\right)^n+\theta\left(\frac{Q\,|Q|}{K^2}\right)^{n+1}+(1-\theta)\left(\frac{Q\,|Q|}{K^2}\right)^n=0$$

If $\theta=1$ is used, the initial error will be corrected after one time step since, at the $(n+1)\Delta t$ time level, the equation will be satisfied. If, however, $\theta=1/2$, then

$$\left(\frac{\partial y}{\partial x}\right)^{n+1}+\left(\frac{Q\,|Q|}{K^2}\right)^{n+1}=-\left[\left(\frac{\partial y}{\partial x}\right)^n+\left(\frac{Q\,|Q|}{K^2}\right)^n\right]$$

i.e.

$$\left(\frac{\partial y}{\partial x}+\frac{Q\,|Q|}{K^2}\right)^{n+1}=-\Delta$$

and

$$\left(\frac{\partial y}{\partial x}+\frac{Q\,|Q|}{K^2}\right)^{n+2}=-\left(\frac{\partial y}{\partial x}+\frac{Q\,|Q|}{K^2}\right)^{n+1}=\Delta$$

The solution will continuously oscillate. For $1/2<\theta\leqslant 1$ the oscillations will disappear with time. One may ask if a number of the 'non-linear instability' cases described in the literature are not due to the above phenomenon which can be avoided by putting $\theta=1$ at least in the portions of a model in which inertia terms are negligible.

A second comment concerns the relative ease with which discretization mishaps can be made. We would like to describe in some detail an instructive example encountered during recent years. A model was built based on a dynamic equation derived from Equations (3.81), (3.82) and using by differen-

tiation of the term $\frac{\partial}{\partial x}\left(\frac{Q^2}{A}\right)$ written as $\frac{2Q}{A}\frac{\partial Q}{\partial x} - \frac{Q^2}{A^2}\frac{\partial A}{\partial x}$

$$\frac{\partial Q}{\partial t} + \frac{2Q}{A}\frac{\partial Q}{\partial x} - \frac{Q^2}{A^2}\frac{\partial A}{\partial x} + gA\frac{\partial y}{\partial x} + g\frac{AQ|Q|}{K^2} = 0 \tag{3.91}$$

Preissmann's scheme was applied and the third and fourth terms were discretized in the following manner:

$$\begin{aligned}
\frac{Q^2}{A^2} &\approx \frac{\theta}{2}\left[\left(\frac{Q^2}{A^2}\right)_{j+1}^{n+1} + \left(\frac{Q^2}{A^2}\right)_j^{n+1}\right] + \frac{1-\theta}{2}\left[\left(\frac{Q^2}{A^2}\right)_{j+1}^{n} + \left(\frac{Q^2}{A^2}\right)_j^{n}\right] \\
\frac{\partial A}{\partial x} &\approx \frac{\theta}{\Delta x}\left(A_{j+1}^{n+1} - A_j^{n+1}\right) + \frac{1-\theta}{\Delta x}\left(A_{j+1}^{n} - A_j^{n}\right) \\
A &\approx \frac{\theta}{2}\left(A_{j+1}^{n+1} + A_j^{n+1}\right) + \frac{1-\theta}{2}\left(A_{j+1}^{n} + A_j^{n}\right) \\
\frac{\partial y}{\partial x} &\approx \frac{\theta}{\Delta x}\left(y_{j+1}^{n+1} - y_j^{n+1}\right) + \frac{1-\theta}{\Delta x}\left(y_{j+1}^{n} - y_j^{n}\right)
\end{aligned} \tag{3.92}$$

Consider a steady flow situation. Equation (3.91) reduces to the energy equation,

$$\frac{\partial y}{\partial x} - \frac{1}{gA}\frac{Q^2}{A^2}\frac{\partial A}{\partial x} + S_f = 0 \tag{3.93}$$

or, for two cross sections j, $j+1$, to the following discrete form

$$y_{j+1} = y_j + \frac{u_j^2 - u_{j+1}^2}{2g} - \Delta x\, S_f \tag{3.94}$$

Let us now see if the discretization (3.92) of Equation (3.93) leads indeed to Equation (3.94). To that end we may take the $(n+1)\Delta t$ time level, i.e. $\theta = 1$, since we are concerned with a steady flow situation. Then, dropping the superscript $n+1$, the discretized Equation (3.93) is written

$$\frac{y_{j+1} - y_j}{\Delta x} - \frac{2}{g(A_{j+1} + A_j)} \times \frac{1}{2}\left(\frac{Q_{j+1}^2}{A_{j+1}^2} + \frac{Q_j^2}{A_j^2}\right)\frac{A_{j+1} - A_j}{\Delta x} + S_f = 0 \tag{3.95}$$

Putting $Q_j = Q_{j+1}$ for steady flow,

$$y_{j+1} = y_j + \frac{A_{j+1} - A_j}{A}\quad\frac{u_{j+1}^2 + u_j^2}{2g} - \Delta x\, S_f \tag{3.96}$$

where $A = (A_j + A_{j+1})/2$.

Comparing Equations (3.96) and (3.94), we see clearly that in steady flow simulations the energy equation is not satisfied when such a discretization is

used. As long as the difference in wetted area (and thus velocity) between two adjacent cross sections is small, the error is very difficult to detect in unsteady flow computations. Fortunately the model in question included a section of dyked river with a weir as shown in Fig. 3.15. Two computational points J

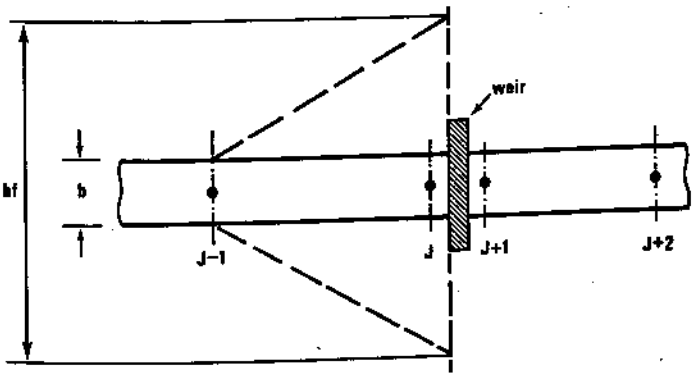

Fig. 3.15. Schematization used to replace the approach velocity head in the weir formula by an artificial increase in water stage: b = actual river width; bf = fictitious river width at point J

and $J+1$ were linked by two compatibility equations: $Q_J = Q_{J+1}$, and the weir discharge equation $Q_J = \mu(y_J - y_w)^{3/2}$, ($y_w$ = weir crest level), an equation which neglects the velocity head at the location J, in ordinary circumstances quite a reasonable assumption. During high water, however, and because of dyking, the weir approach velocity was of the order of 3.7 m s^{-1}, corresponding to a head of 0.72 m, too much of a difference to be neglected as seen in the impossibility of obtaining a satisfactory upstream calibration. The modeller thought of an expedient to avoid having to reprogram the weir subroutine: since he was not interested in the exact reproduction of water stages in the immediate upstream vicinity of the weir, he decided to change the cross section of the point J for high stages, by widening it considerably as shown in Fig. 3.15. As a consequence the velocity u_J should become negligible and the fictitious water stage $\bar{y}_J$ should be

$$\bar{y}_J \approx y_{J-1} + \frac{u_{J-1}^2}{2g} - \Delta x\, S_f$$

i.e. much higher than the natural level y_J. Since Δx was very small there would be virtually no energy loss, and the water level used in the weir equation would be then

$$\bar{y}_J \approx y_J + \frac{u_{J-1}^2}{2g}$$

Consequently the velocity head would be taken into account, at least approximately. The error in volume due to the artificial section widening would be

small, since Δx is small, and of no consequence whatsoever for steady flow calculations.

The results of model runs with the new, fictitious section J were so strange that the modeller proceeded with steady state simulation for high discharges, only to find that the total head at the point J was higher than that at the point $J-1$! This physically absurd result is completely consistent with Equation (3.96); further investigations showed that the problem was in the approximation of the coefficient $\frac{Q^2}{A^2}$ which should be discretized not as shown in Equation (3.92), but rather in the following way:

$$\frac{Q^2}{A^2} \approx \frac{\theta}{4}\left[\left(\frac{Q}{A}\right)_{j+1}^{n+1} + \left(\frac{Q}{A}\right)_{j}^{n+1}\right]^2 + \frac{1-\theta}{4}\left[\left(\frac{Q}{A}\right)_{j+1}^{n} + \left(\frac{Q}{A}\right)_{j}^{n}\right]^2 \tag{3.97}$$

Then the steady flow Equation (3.95) is replaced by

$$\frac{y_{j+1}-y_j}{\Delta x} - \frac{2}{(A_{j+1}+A_j)g} \times \frac{1}{4} \times \left(\frac{Q_{j+1}}{A_{j+1}} + \frac{Q_j}{A_j}\right)^2 \times \left(\frac{A_{j+1}-A_j}{\Delta x}\right) + S_f = 0 \tag{3.98}$$

as before, putting $Q_{j+1} = Q_j$,

$$y_{j+1} - y_j - \frac{1}{2g}\frac{A_{j+1}-A_j}{A_{j+1}+A_j}(u_{j+1}+u_j)^2 + \Delta x\, S_f = 0 \tag{3.99}$$

Now

$$\begin{aligned}(A_{j+1}-A_j)(u_{j+1}+u_j)^2 &= (A_{j+1}-A_j)(u_{j+1}^2 + 2u_j u_{j+1} + u_j^2\\ &= A_{j+1}u_{j+1}^2 + A_{j+1}u_j^2 + 2u_j u_{j+1}A_{j+1} - A_j u_{j+1}^2 - A_j u_j^2 - 2u_{j+1}u_j A_j\\ &= Qu_{j+1} + A_{j+1}u_j^2 + 2u_j Q - A_j u_{j+1}^2 - Qu_j - 2u_{j+1}Q\\ &= Q(u_j - u_{j+1}) + Q\left(\frac{u_j^2}{u_{j+1}} - \frac{u_{j+1}^2}{u_j}\right)\end{aligned}$$

and Equation (3.99) becomes

$$y_{j+1} - y_j - \frac{1}{2g}\frac{Q}{A_{j+1}+A_j}\left[(u_j - u_{j+1}) + \frac{u_j^2}{u_{j+1}} - \frac{u_{j+1}^2}{u_j}\right] + \Delta x\, S_f = 0$$

Since $\frac{A_{j+1}+A_j}{Q} = \frac{1}{u_{j+1}} + \frac{1}{u_j} = \frac{u_j + u_{j+1}}{u_{j+1}u_j}$, the second term of the equation is transformed into

$$-\frac{1}{2g}\frac{u_j^2 u_{j+1} - u_j u_{j+1}^2 + u_j^3 - u_{j+1}^3}{u_j + u_{j+1}} = -\frac{1}{2g}\frac{u_j^2 - u_{j+1}^2}{u_j + u_{j+1}}(u_j + u_{j+1})$$

And finally

$$y_{j+1} - y_j - \frac{1}{2g}\,(u_j^2 - u_{j+1}^2) + \Delta x\, S_f = 0 \tag{3.100}$$

which is the proper approximation.

Several remarks may be made concerning the above 'post mortem' example.

(a) When considering Equation (3.91) alone, it is not obvious that the coefficient $\frac{Q^2}{A^2}$ should be represented in discrete form by

$$\left[\frac{1}{2}\left(\frac{Q}{A}\right)_j + \frac{1}{2}\left(\frac{Q}{A}\right)_{j+1}\right]^2 \text{ rather than by } \frac{1}{2}\left(\frac{Q^2}{A^2}\right)_j + \frac{1}{2}\left(\frac{Q^2}{A^2}\right)_{j+1}.$$

Only by appealing to another hydraulic law can one choose the proper form, although the two forms are clearly not equivalent.

(b) The error does not affect either the order of the finite difference scheme or its stability; it could not have been detected *a priori* by examination of phase and amplitude portraits.

(c) it was necessary to look through the FORTRAN statements to find, in this particular case, the formulation actually used (!).

(d) The formulation was programmed following published material in which, by negligence, the improper discretization was indicated.

The experience shows to what a large extent the engineer's judgement and action can influence modelling results, whose value often depends upon the trituration of terms and coefficients.

3.4. ALGORITHMIC ASPECTS OF MODELLING SYSTEMS

A convergent discretized form of the basic relationships, together with appropriate boundary conditions, furnishes a system of algebraic equations in terms of unknown flow variables at the time level $(n+1)\Delta t$. The equations resulting from explicit schemes are uncoupled; there is no need for complex solution algorithms since the unknown values at the time level $(n+1)\Delta t$ may be computed separately for every computational grid point.

Implicit schemes lead to large systems of non-linear algebraic equations which can only be solved by successive approximation (iteration) methods. Present-day models often contain hundreds, and sometimes thousands, of computational points. The advantages of using implicit schemes are lost unless efficient methods for the solution (at every time step) of such systems of non-linear algebraic equations are used.

In order to solve a non-linear system by iterations, the system is first linearized, i.e. the coefficients are evaluated on the basis of known values of flow variables at the time level $n\Delta t$. Then this linear system is solved, furnishing a

first approximation to the flow variables at the time level $(n + 1)\Delta t$. The coefficients, which render the equations non-linear, are then re-evaluated using the new, estimated values of the flow variables at time $(n + 1)\Delta t$, and then the linear system is solved again to furnish a still better approximation to the flow variables, which then can be used to improve the estimate of the coefficients, and so on. For example, the coefficients $b^{n+1/2}$, $A^{n+1/2}$, $K^{n+1/2}$ in the Abbott–Ionescu Equations (3.88) or the coefficients $A, B, C, \ldots, G'$ in the Preissmann Equations (3.86) are updated in such a way. This general approach raises two important problems.

The first problem concerns the definition of updated coefficients – indeed, the speed of convergence of successive solutions of linear systems to the non-linear solution depends upon this definition. We mentioned in Section 3.3 that if the coefficients are defined as derivatives of updated functions with respect to dependent variables, the iteration procedure amounts to a Newton-like method, and its convergence will be of second order. In most cases the first approximation to the flow variables obtained from just one solution of the linear system is sufficient; when a second iteration is required, it furnishes an approximation which is very nearly the exact solution to the non-linear system. Preissmann's scheme as used in SOGREAH's general purpose modelling systems CARIMA and CAREDAS is solved in this way; the Delft Hydraulics Laboratory modelling system is based upon the same principle (Vreugdenhil, 1973).

A demonstration of the rapid convergence of Newton-type iterations with Preissmann's method was made by simulating wave propagation in a horizontal, prismatic canal 10 km long. The canal had a trapezoidal section, with a base width of 10 m, bank slopes of 2 horizontal to 1 vertical, and a Strickler coefficient of 25; computational points were placed at 1 km intervals. One end of the canal was closed by imposing a zero discharge condition. At the other end a time varying discharge was introduced. The simulation, which used a Δt of 6 min, began with the system at rest at a depth of 7.0 m; then during 6 h one full period of a sinusoidally varying discharge was introduced into the canal, so that the net inflow was exactly zero. After 6 h, the input discharge was held at zero until all wave propagation disappeared and the system returned again to rest. Since the net inflow to the canal was zero, the final depths should have been exactly equal to the initial depth, 7.0 m. But in fact, since only one iteration was used (i.e. coefficients and their derivatives were evaluated at time $n\Delta t$), volume was added to the canal: the depth was 7.14 m at the end of the calculations, representing a 3% volume error. The same calculation was then repeated with one additional iteration (i.e. one correction of the coefficients) per time step; at the end of the simulation, the depth had returned to 7.000 m. In Chapter 4 we describe a similar iteration test using the Preissmann method applied to a model of a real river.

The Abbott–Ionescu scheme as used in the Danish Hydraulic Institute's System 11 SIVA updates coefficients by averaging them between time $n\Delta t$ and the last approximation at time $(n + 1)\Delta t$; its convergence rate is slower than that of a Newton-like method (one needs in general two approximations, i.e. two

resolutions of the linear system to obtain a sufficiently accurate approximation).

In the above we have assumed that the iteration process is always convergent. But this may not always be the case, especially when interior compatibility conditions at constrictions, weirs, dams, junctions, etc., are modelled without sufficient care, or if the first approximation is too far from the sought solution. Non-convergent behaviour of an iteration algorithm is sometimes attributed to instability in the difference scheme, and summarily declared 'non-linear unstable behaviour'. Proper identification of the source of trouble is most important if a remedy is to be found, and it is dangerous to jump to hasty conclusions as to the identity of the guilty party.

The second problem concerns the solution of the linearized system of equations, the result of which furnishes successive approximations to the solution of the non-linear system. One could use standard matrix inversion techniques, but this is precisely the best way to nullify all the potential benefits of implicit schemes. Since the number of operations in standard inversion algorithms (and thus the cost) is proportional to N^3, where N is the number of equations, matrix inversion cost for a large model could become prohibitive. This is why all existing modelling systems used for models having more than 50 computational points or so are based on one of two techniques: iterative matrix methods, or double sweep methods.

Iterative matrix methods

The only major example of iterative matrix methods known to the authors is the Delft Hydraulics Laboratory modelling system (Vreugdenhil, 1973). Vreugdenhil uses the Gauss–Seidel method of successive relaxation: each equation i is written with only the main element z_i on the left hand side of the equation in the form:

$$z_i = \frac{1}{a_{ii}} \left(b_i - \sum_{k=1}^{N} a_{ik} z_k \right), \quad k \neq i. \tag{3.101}$$

where z_i, $i = 1, 2, \ldots, N$ are unknowns, and a_{ik} are matrix coefficients. At first, z_k values corresponding to the situation at the time level $n\Delta t$ are adopted, and then they are successively improved by substitution into the right hand side of Equation (3.101). As soon as a new value is computed, it is taken into account for subsequent computations, this being a method of successive relaxation. The iteration process is continued until the absolute value of the difference between two successive iterations for all elements z_i is smaller than an accuracy criterion. According to Vreugdenhil the number of iterations usually necessary is of the order of 5 – 10 (but no indication concerning the corresponding matrix size is furnished). In general, it is not easy to predict *a priori* the number of iterations needed by an iterative matrix method, and it is therefore difficult to anticipate the computer effort needed.

Double sweep methods

These methods are much more often used in industrial modelling systems. A computational point of a model is not linked directly to all other points, but only to adjacent ones. In a one-dimensional river model a point j is linked only to the adjacent points $j-1$ and $j+1$. In quasi-two-dimensional inundated plain models, a cell j may well be linked to several neighbouring cells $k = 1, 2, \ldots, K$, but still their total number K is usually less than six, ten at the most. Thus the matrix of the linear system of equations is sparse, and in the case of one-dimensional, one-reach models, the sparse matrices are banded and three- or five-diagonal.

Double sweep methods use the banded matrix structure of the linear system of equations to compute the solution with a number of operations proportional to N. Thus for a given number of points, the computer effort may be precisely estimated and, moreover, it increases from one model to another in proportion to the number of points N and not to N^3. The double sweep method is quite straightforward, and has been used for years in models composed of series of one-dimensional reaches. But the method requires complex algorithms and considerable programming effort when applied to looped (or multiply connected) channel networks or two-dimensional models. In the following paragraphs we shall briefly summarize the features of a single channel double sweep method, then its application to a branched network of channels. After a description of double-sweep methods applied to quasi-two-dimensional inundated plain models, we shall then outline the principles of double-sweep algorithms for looped networks of channels and inundated plains.

Single channel solution algorithms

For single channels with one boundary condition given at each end, the coefficient matrices contain elements only in the band along the main diagonal. To demonstrate the double sweep procedures, we take the Abbott–Ionescu type scheme with Equations (3.90) written in matrix form as

$$\begin{bmatrix} \alpha_1 & \beta_1 & & & & & \\ A_2 & B_2 & C_2 & & & & \\ & A_3 & B_3 & C_3 & & & \\ & & \cdot & \cdot & \cdot & & \\ & & & \cdot & \cdot & \cdot & \\ & & & & A_{jj-1} & B_{jj-1} & C_{jj-1} \\ & & & & & \alpha_{jj} & \beta_{jj} \end{bmatrix} \begin{bmatrix} Z_1 \\ Z_2 \\ Z_3 \\ \cdot \\ \cdot \\ Z_{jj-1} \\ Z_{jj} \end{bmatrix} = \begin{bmatrix} \gamma_1 \\ D_2 \\ D_3 \\ \cdot \\ \cdot \\ D_{jj-1} \\ \gamma_{jj} \end{bmatrix} \tag{3.102}$$

where α, β, γ are coefficients describing the boundary conditions at the first grid point $j = 1$ and the last point $j = jj$. Z_j represents the dependent variable at grid point j (either Q_j^{n+1} or y_j^{n+1}, depending on the grid point). The coefficients A_j, B_j, C_j and D_j are coefficients in the continuity and dynamic Equations (3.90) corresponding to the coefficients $\alpha, \beta, \gamma, \delta$ or $\alpha^*, \beta^*, \gamma^*, \delta^*$.

Introducing the auxiliary relation

$$Z_{j-1} = E_j Z_j + F_j \tag{3.103}$$

and substituting it into the equation at a gridpoint j,

$$A_j Z_{j-1} + B_j Z_j + C_j Z_{j+1} = D_j \tag{3.104}$$

one obtains an expression relating Z_j and Z_{j+1}:

$$Z_j = \frac{-C_j Z_{j+1} + (D_j - A_j F_j)}{B_j + A_j E_j}$$

By anology with Equation (3.103) we see the recurrence relationships

$$E_{j+1} = \frac{-C_j}{B_j + A_j E_j} \quad ; \quad F_{j+1} = \frac{D_j - A_j F_j}{B_j + A_j E_j} \tag{3.105}$$

To initialize a forward sweep, the E_2, F_2 values are evaluated from the equivalence of Equation (3.103) and the relation at the boundary. Equation (3.103) is written for the two first points as:

$$Z_1 = E_2 Z_2 + F_2 \tag{3.106a}$$

and the first equation of the system (3.102) is

$$\alpha_1 Z_1 + \beta_1 Z_2 = \gamma_1$$

$$\text{or} \quad Z_1 = \frac{-\beta_1}{\alpha_1} Z_2 + \frac{\gamma_1}{\alpha_1} \tag{3.106b}$$

Comparison of Equations (3.106a) and (3.106b) gives the general form of the first coefficients,

$$E_2 = -\frac{\beta_1}{\alpha_1} \quad ; \quad F_2 = \frac{\gamma_1}{\alpha_1} \tag{3.107}$$

The boundary condition could, of course, have been treated in a less general way. For example when the value of Z is known directly at the first point, the starting values obtained are simply $E_2 = 0$ and $F_2 = Z_1$.

The forward sweep can now be carried on to compute the pairs of coefficients $(E_3, F_3), (E_4, F_4) \ldots, (E_{jj}, F_{jj})$ by applying the recurrence relations of Equations (3.105). At the last point $j = jj$, Equation (3.103) may be written again together with the last equation of the system (3.102).

$$Z_{jj-1} = E_{jj} Z_{jj} + F_{jj} \tag{3.108a}$$

$$\alpha_{jj} Z_{jj-1} + \beta_{jj} Z_{jj} = \gamma_{jj} \tag{3.108b}$$

From these equations the value of the boundary condition prescribed (by means of α_{jj}, β_{jj} and γ_{jj}) is obtained by elimination of Z_{jj-1}:

$$Z_{jj} = \frac{\gamma_{jj} - \alpha_{jj} F_{jj}}{\beta_{jj} + \alpha_{jj} E_{jj}} \tag{3.109}$$

Next a second return sweep is made computing $Z_{jj-1}, Z_{jj-2}, \ldots, Z_2, Z_1$ values in successive grid points by using Equation (3.103).

In physical terms this algorithm is a procedure in which the forward sweep transfers information given at one boundary to the other boundary where it is combined with the imposed condition there. Now enough information is available to define the solution in a return sweep. As long as the flow is subcritical, the direction of the two sweeps with respect to that of the flow is of no importance: a forward sweep may be initiated at the upstream or at the downstream limit, the method is symmetrical. The supercritical flow situation is more complex and requires more care -- *see* Abbott (1979).

More details on the double sweep algorithm as applied to the Abbott–Ionescu type scheme may be found in the original references (Abbott and Ionescu, 1967; Verwey, 1971; Abbott, 1979). Readers interested in theoretical justifications of the double sweep method, accuracy and stability considerations are invited to consult Richtmyer (1957), Abramov (1961), Abramov and Andrieyev (1963), Gelfand and Lokutsievski (1964). The method was first applied to open channel hydraulics by Preissmann and Cunge (1961a, b) and described in more detail by Cunge and Wegner (1964). A more recent description of the method as applied to the Preissmann scheme (Equations (3.86)) is given by Liggett and Cunge (1975).

The application of the method to the Preissmann scheme may be explained very briefly as follows: suppose, in Equations (3.86), that we can write the relationship

$$\Delta Q_j = E_j \, \Delta y_j + F_j$$

and eliminate from the system of these two equations the unknown increment Δy_j, then express the discharge increment ΔQ_{j+1} as a function of Δy_{j+1}. Two recurrence relationships will result:

$$E_{j+1} = E(E_j); \quad F_{j+1} = F(E_j, F_j)$$

Thus, if the linearized boundary condition furnishes (E_1, F_1), all coefficients $(E_j, F_j), j = 2, 3, \ldots, N$ may be computed. On the other hand the elimination from Equations (3.86) of ΔQ_j leads to

$$\Delta y_j = L_j \, \Delta y_{j+1} + M_j \, \Delta Q_{j+1} + N_j$$

where L_j, M_j and N_j can again be computed for all points $j = 1, 2, \ldots, N-1$. The known boundary condition at the point N should let us express Δy_N, then $\Delta Q_N = E_N \Delta y_N + F_N$, $\Delta y_{N-1} = L_{N-1} \Delta y_N + M_{N-1} \Delta Q_N + N_{N-1}$, etc.

The essential principles of the double sweep method can be applied to any type of scheme resulting in a banded matrix. For example, the Vasiliev scheme may be rewritten as an equation linking three grid points,

$$A_j Z_{j-1}^{n+1} + B_j Z_j^{n+1} + C_j Z_{j+1}^{n+1} = D_j \tag{3.110}$$

where A_j, B_j, C_j are 2×2 matrices, D_j is the free term vector of two components and

$$Z_j = \begin{pmatrix} Q_j^{n+1} \\ y_j^{n+1} \end{pmatrix}$$

The system of Equations (3.110) is then solved by the double sweep method using a procedure equivalent to those described above, with operations performed on matrices and vectors instead of on single elements.

Interior one-dimensional flow boundary conditions link two subsequent computational grid points, often located at the same geographical section, with the aid of two flow equations which differ from the usual difference analogue of differential or integral relationships. These two compatibility equations are usually discretized at the time level $(n + 1)\Delta t$, since the compatibility conditions should be satisfied at that time. When the difference scheme computes water stages and discharges at the same points (as do the Preissmann or Vasiliev type schemes, for example), the resulting algebraic compatibility equations may be incorporated easily into the system: they are just another pair of relationships such as Equation (3.86), with coefficients $A, B, C, \ldots, G'$ which come from the compatibility conditions instead of the usual flow equations. The algorithm itself is unchanged. A detailed description of the procedure used for interior conditions with the Preissmann scheme is given by Liggett and Cunge (1975). Most interior boundaries in the CARIMA modelling system developed by SOGREAH are treated as described in that reference. The treatment of these conditions is more complex with staggered schemes.

Branched channel solution algorithms

A model of a branched channel system (also called 'tree-like'), includes tributaries and/or distributaries. As long as the network of channels is not looped, the basic double sweep algorithm can still be applied, provided that a certain computation order is respected. Let us consider the 'junction' algorithms for two implicit schemes: Abbott–Ionescu and Preissmann.

A junction of two channels simulated with the Abbott–Ionescu scheme is shown in Fig. 3.16a. The flow direction does not matter, the important thing being the section where the double sweep algorithm was initiated. Suppose that the first sweep was initiated at ① where, for example, a water stage as a function of time is given. The schematization should be made in such a way that the junction coincides with a y-point of the computational grid. Carrying the forward sweep from point ① to the junction along branch A, one can compute with Equations (3.105) all E and F coefficients, including the last two E_{11+1}, F_{11+1} in the relationship

$$Q_{11}^{n+1} = E_{11} y^{n+1} + F_{11} \tag{3.111}$$

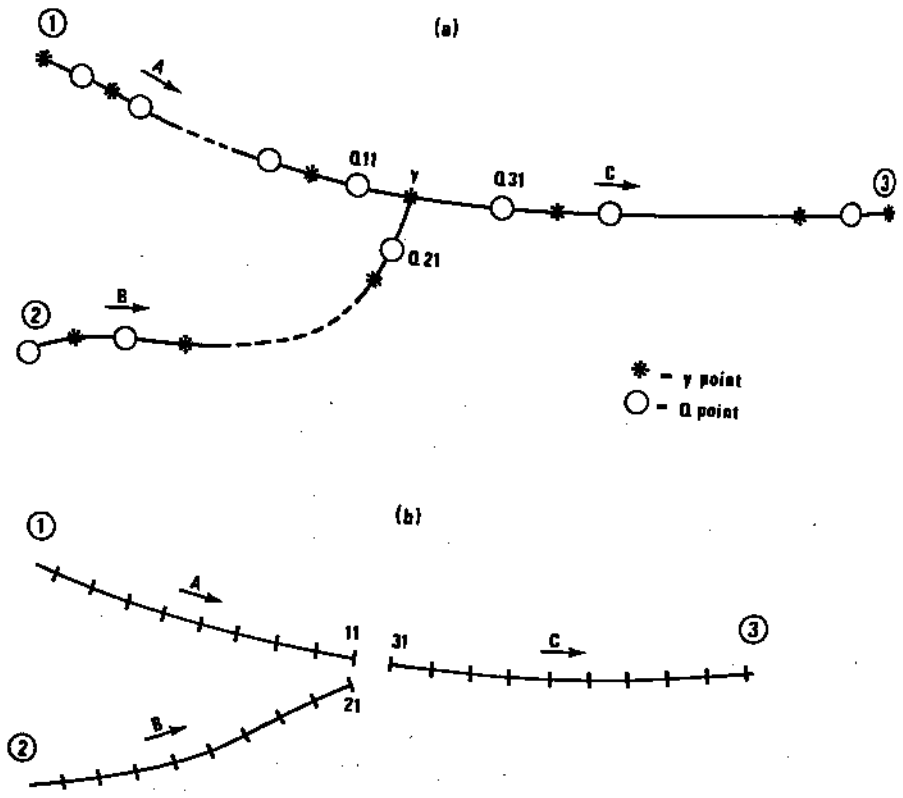

Fig. 3.16. Double sweep algorithms for junctions. A, B, C = order of forward sweep. (a) Abbott–Ionescu type scheme; (b) Preissmann type scheme

It is impossible however to continue the sweep along branch C, for example by computing the E_{31}, F_{31} coefficients linking y and Q_{31}; had this been possible, the complete solution in branch C could have been defined in the return sweep independently of the influence of channel B, which is physically absurd. For that reason the forward sweep is interrupted at the junction and another first sweep is initiated at the limit ② of branch B. All E, F coefficients are computed along branch B up through E_{21+1}, F_{21+1}, which define the relationship

$$Q_{21}^{n+1} = E_{21+1} y^{n+1} + F_{21+1} \tag{3.112}$$

It was implicitly assumed in Equations (3.111) and (3.112) that the water stage y is the same for all three branches at the junction (to assume equality of energy heads at the junction, as is done in the SIVA system, introduces complications in the staggered scheme: discharges are not computed at the junction, and velocities there are thus unknown). The continuity equation at the junction may be written in the form of Equations (3.90),

$$\alpha' Q_{11}^{n+1} + \alpha'' Q_{21}^{n+1} + \beta y^{n+1} + \gamma Q_{31}^{n+1} = \delta \tag{3.113a}$$

or, under the general algorithmic form of Equation (3.102):

$$A_1 Q_{11}^{n+1} + A_2 Q_{21}^{n+1} + B y^{n+1} + C Q_{31}^{n+1} = D \tag{3.113b}$$

Discharges Q_{11}^{n+1} and Q_{21}^{n+1} may be eliminated by substitution of Equations (3.111) and (3.112) into (3.113b); then the stage y^{n+1} may be expressed as a function of Q_{31}^{n+1},

$$y^{n+1} = E_{31} Q_{31}^{n+1} + F_{31} \tag{3.114}$$

where

$$E_{31} = \frac{-C}{B + A_1 E_{11+1} + A_2 E_{21+1}} \tag{3.115a}$$

$$F_{31} = \frac{D - A_1 F_{11+1} + A_2 F_{21+1}}{B + A_1 E_{11+1} + A_2 E_{21+1}} \tag{3.115b}$$

The forward sweep along the branch can now be carried on down to point ③ where the appropriate boundary condition is applied. Then the return sweep computes Q^{n+1} and y^{n+1} values from ③ back to the junction. The return sweeps along the two other branches may then be initiated by Equations (3.112) and (3.111), respectively, since y^{n+1} at the junction is known.

When the Preissmann scheme is used, discharges and stages are computed at the same points (*see* Fig. 3.16b). The forward sweep is initiated at, say, point ① and the recurrence coefficients are computed along branch A. In the Preissmann scheme, however, the recurrence relations between adjacent points are expressed as

$$\Delta Q_j = E_j \Delta y_j + F_j \tag{3.116}$$

$$\Delta y_j = L_j \Delta y_{j+1} + M_j \Delta Q_{j+1} + N_j \tag{3.117}$$

Where

$$E_j = E(E_{j-1}); \quad F_j = F(E_{j-1}, F_{j-1}) \qquad L_j = L(E_j); \quad M_j = M(E_j); \quad N_j = N(E_j, F_j) \tag{3.118}$$

The forward sweep along branch A computes E_{11}, F_{11} and the forward sweep along branch B computes E_{21}, F_{21}. Three compatibility conditions at the junction are now applied:

$$\begin{aligned} y_{11}^{n+1} + \frac{1}{2g}\left(\frac{Q_{11}^{n+1}}{A_{11}^{n+1}}\right)^2 &= y_{21}^{n+1} + \frac{1}{2g}\left(\frac{Q_{21}^{n+1}}{A_{21}^{n+1}}\right)^2 \\ y_{11}^{n+1} + \frac{1}{2g}\left(\frac{Q_{11}^{n+1}}{A_{11}^{n+1}}\right)^2 &= y_{31}^{n+1} + \frac{1}{2g}\left(\frac{Q_{31}^{n+1}}{A_{31}^{n+1}}\right)^2 \\ Q_{31}^{n+1} &= Q_{11}^{n+1} + Q_{21}^{n+1} \end{aligned} \tag{3.119}$$

The equal energy level condition is expressed with no difficulty, since in the Preissmann method each branch has its own distinct cross section at the junction. Substitution into Equations (3.119) of

$$y^{n+1} = y^n + \Delta y; \quad Q^{n+1} = Q^n + \Delta Q$$

$$f^{n+1} = f^n + \left(\frac{\partial f}{\partial y}\right)^n \Delta y + \left(\frac{\partial f}{\partial Q}\right)^n \Delta Q \tag{3.120}$$

and linearization in terms of Δy and ΔQ leads to the following system of equations:

$$\begin{aligned} A_1 \Delta y_{11} + B_1 \Delta Q_{11} + C_1 \Delta y_{31} + D_1 \Delta Q_{31} &= H_1 \\ A_2 \Delta y_{21} + B_2 \Delta Q_{21} + C_2 \Delta y_{31} + D_2 \Delta Q_{31} &= H_2 \\ \Delta Q_{31} - \Delta Q_{11} - \Delta Q_{21} &= Q_{11}^n + Q_{21}^n - Q_{31}^n \end{aligned} \tag{3.121}$$

The discharge increments ΔQ_{11} and ΔQ_{21} may be eliminated by

$$\Delta Q_{11} = E_{11} \Delta y_{11} + F_{11}; \quad \Delta Q_{21} = E_{21} \Delta y_{21} + F_{21} \tag{3.122}$$

using the coefficients $E_{11}, F_{11}, E_{21}, F_{21}$ computed during the forward sweeps along A and B. Then Equations (3.121) represent a system of 3 linear equations in terms of 4 unknowns: $\Delta y_{11}, \Delta y_{21}, \Delta y_{31}$ and ΔQ_{31}. By eliminating Δy_{11} and Δy_{21} one easily finds the relationship $\Delta Q_{31} = E_{31} \Delta y_{31} + F_{31}$ with explicit expressions

$$\begin{aligned} E_{31} &= E(E_{11}, E_{21}) \\ F_{31} &= F(E_{11}, E_{21}, F_{11}, F_{21}) \end{aligned} \tag{3.123}$$

Now the forward sweep along branch C can be continued to point ③ as before.

At the end of the return sweep from ③ back to the junction, elimination of $\Delta Q_{11} = E_{11} \Delta y_{11} + F_{11}$ from the first of Equations (3.121) gives

$$\Delta y_{11}(A_1 + B_1 E_{11}) + C_1 \Delta y_{31} + D_1 \Delta Q_{31} = H_1 - B_1 F_{11}$$

and then

$$\Delta y_{11} = \frac{-C_1 \Delta y_{31} - D_1 \Delta Q_{31} + (H_1 - B_1 F_{11})}{A_1 + B_1 E_{11}} \tag{3.124}$$

Equation (3.124) furnishes the return transfer coefficients

$$L_{11} = \frac{-C_1}{A_1 + B_1 E_{11}}; \quad M_{11} = \frac{-D_1}{A_1 + B_1 E_{11}}$$

$$N_{11} = \frac{H_1 - B_1 F_{11}}{A_1 + B_1 E_{11}}$$

for branch A. Analogous expressions are easily found for the coefficients L_{21},

M_{21} and N_{21} permitting the return sweep along branch B.

Similar double sweep procedures can be developed for other implicit schemes, and can easily be extended to junctions of more than 3 channels.

Two-dimensional solution algorithms

There are two basic differences between models of one-dimensional channel flow and quasi-two-dimensional flood plain flow insofar as solution algorithms are concerned.

(i) The flow direction in channels is well defined, and the computational points are aligned in branches, while the flow direction in flooded areas is undetermined so that the computational cells and links form a very complex interconnected network; the very concept of a channel disappears as seen in the network of computational cells and discharge links of the two-dimensional Mekong Delta mathematical model built by SOGREAH and shown in Fig. 3.17.

(ii) The flow equations are usually fundamentally different. For channel flow, one retains all inertia terms, so that the discharge between two points is a function of water levels at those points *and* of the discharge itself, and discharge cannot be eliminated from the computation. Since two-dimensional flow over inundated plains is most often a slow phenomenon, the equations may be simplified by neglecting the inertia terms. If the levels are known, the discharges can be computed. Therefore the discharges may be eliminated from the computation routine and the levels are the only unknown variables.

These two differences are reflected in the algorithms developed to solve the linear systems of equations resulting from the discretization of flow equations. For both kinds of models linearization is used to furnish successive approximations to the non-linear equations, as explained in the previous sections. But one-dimensional discretization always leads to banded matrices; the narrow bands are only a few elements wide and the number of elements adjacent to the diagonal is always the same. In two-dimensional models a cell j may be linked to other cells k in various ways and the number of links, while usually limited to less than 10, is really arbitrary. Thus even if the overall matrix is a sparse one, the number of elements around the diagonal is variable and may not be negligible. (A cell j linked to 10 cells k will be represented by something like 21 elements in an overall matrix of, say, 400 x 400; thus in a j row there will be 21 elements and 379 zeros.) On the other hand, the possibility of eliminating discharges as unknown variables makes it possible to express the unknown level in cell j solely in terms of the unknown levels in the neighbouring cells, which makes the solution algorithm more efficient as we will show further on.

To the authors' best knowledge there is only one published method dealing with the problem of implicit schemes applied to models of inundated areas. The principle of the double sweep matrix elimination algorithm, which is the basis of the method's solution algorithm and which will be explained here, is of course a very general technique and has nothing to do with hydraulics or mathematical models. The scheme used to transform the flow equations into a form tractable

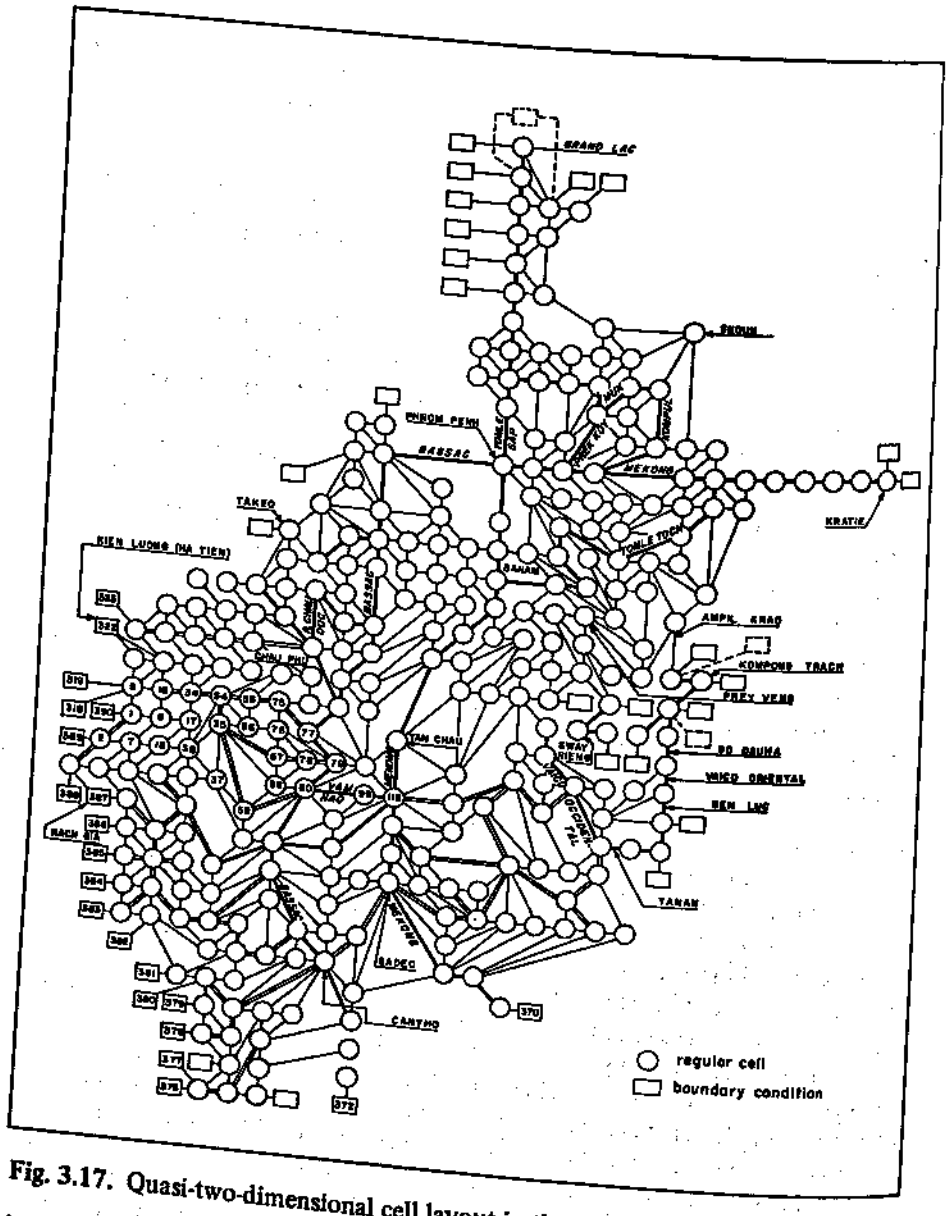

Fig. 3.17. Quasi-two-dimensional cell layout in the Mekong model

by the algorithm was developed between 1961 and 1962 at SOGREAH by Preissmann and Cunge (UNESCO–SOGREAH, 1964; Zanobetti *et al.*, 1968; Zanobetti *et al.*, 1970). It was then adopted by the Delft Hydraulics Laboratory (Meijer *et al.* 1965). A detailed description of the Mekong model structure and of the particular simulation and calibrating problems can be found in Cunge (1975c).

Consider a network of cells i ($i = 1, 2, \ldots, N$), as shown in Fig. 3.17. For each of them we can write a non-linear algebraic continuity Equation (3.43):

$$\Delta y_i \frac{A_{s_i}}{\Delta t} = \theta \sum_k Q_{i,k}^{n+1} + (1-\theta) \sum_k Q_{i,k}^{n} + P_i \tag{3.125}$$

where, we recall, A_{s_i} = horizontal water surface, $Q_{i,k}$ = discharge between the cell i and an adjacent cell k, and P_i is a direct inflow into the cell (such as rainfall). The discharges $Q_{i,k} = f(y_i, y_k)$ are defined by Equations (3.45) and are functions only of y_i and y_k. By developing the discharge formulae in Taylor series around the time level $n\Delta t$, and dropping higher order terms, we obtain

$$Q_{i,k}^{n+1} = Q_{i,k}^{n} + \frac{\partial Q_{i,k}^{n}}{\partial y_i} \Delta y_i + \frac{\partial Q_{i,k}^{n}}{\partial y_k} \Delta y_k \tag{3.126}$$

Substitution of Equation (3.126) into Equation (3.125) yields a system of N linear algebraic equations for Δy_i, $i = 1, 2, \ldots, N$:

$$\frac{A_{s_i}}{\Delta t} \Delta y_i = \theta \left(\sum_k \frac{\partial Q_{i,k}}{\partial y_i} \Delta y_i + \sum_k \frac{\partial Q_{i,k}}{\partial y_k} \Delta y_k \right) + \sum_k Q_{i,k}^{n} + P_i \tag{3.127}$$

The sparse matrix representing the system of Equation (3.127) can of course be solved by any direct matrix inversion method. An iterative method could be used, such as the one employed by Delft Hydraulics Laboratory. Another solution algorithm can be developed if the cells forming the model are arranged in a certain number of groups as shown in Fig. 3.18. A cell i in a certain group j

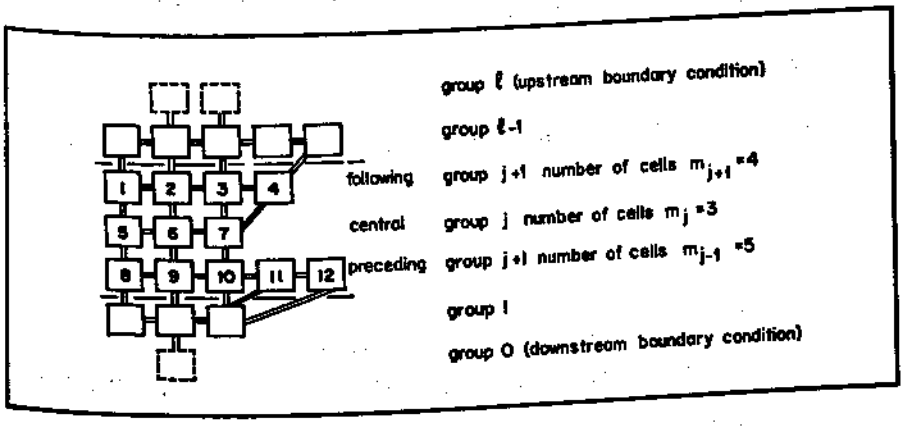

Fig. 3.18. Arrangement of cell groups in a quasi-two-dimensional model

can only exchange water with the cells in the same group j, or the preceding group $j-1$, or the following group $j+1$. Such a grouping is possible because of the sparseness of the matrix. Equation (3.127), rewritten as

$$\Delta y_i \left(-\frac{A_{s_i}}{\Delta t} + \theta \sum_k \frac{\partial Q_{i,k}^n}{\partial y_i} \right) + \theta \sum_k \frac{\partial Q_{i,k}^n}{\partial y_k} \Delta y_k + L_i = 0 \qquad (3.128)$$

in which the free term $L_i = P_i + \sum_k Q_{i,k}^n$ is known, is now applied to the central group j, the preceding group $j-1$ and the following group $j+1$ of the example shown in Fig. 3.18. Using matrix notation, the three continuity Equations (3.128) for the cells 5, 6 and 7 in Fig. 3.18 belonging to the group j, are

$$[M_{j,j-1}]\{\Delta y_j\} + [M_{j,j+1}]\{\Delta y_{j+1}\} + [M_{j,j-1}]\{\Delta y_{j-1}\} + \{L_j\} = 0 \qquad (3.129)$$

in which: $[M_{j,j}]$ = a square matrix, $m_j \times m_j$ (in the example 3 x 3), whose elements are derivatives of discharges between the cells within group j, and $A_{s_j}/\Delta t$; $[M_{j,j+1}]$ = a rectangular matrix $m_{j+1} \times m_j$ (in the example 4 x 3), whose elements are derivatives of discharges between group j and $j+1$; $[M_{j,j-1}]$ = a rectangular matrix (in the example 5 x 3), whose elements are the derivatives of discharges between the cells of group j and $j-1$; $\{\Delta y_j\}$, $\{\Delta y_{j+1}\}$, $\{\Delta y_{j-1}\}$ = the corresponding vector unknowns; $\{L_j\}$ = the free term vector. Equation (3.129) may be written for each group j, including group 1:

$$[M_{11}]\{\Delta y_1\} + [M_{12}]\{\Delta y_2\} + [M_{10}]\{\Delta y_0\} + \{L_1\} = 0 \qquad (3.130)$$

There are $l-1$ equations of this type and $l+1$ vector unknowns Δy_j, the downstream and upstream boundary conditions closing the system.

Once the cells are thus grouped, the double sweep matrix algorithm can be used exactly as is the one-dimensional double sweep method. Assuming a functional relationship between $\{\Delta y_{j-1}\}$ and $\{\Delta y_j\}$,

$$\{\Delta y_{j-1}\} = [E_{j-1}]\{\Delta y_j\} + \{F_{j-1}\} \qquad (3.131)$$

where $[E_{j-1}]$ is a rectangular matrix and $\{F_{j-1}\}$ a corresponding vector, one may find from Equation (3.129)

$$\{\Delta y_j\} = [E_j]\{\Delta y_{j+1}\} + \{F_j\}$$

where

$$[E_j] = -[[M_{j,j}] + [M_{j,j-1}][E_{j-1}]]^{-1}[M_{j,j+1}] \qquad (3.132a)$$

$$\{F_j\} = -[[M_{j,j}] + [M_{j,j-1}][E_{j-1}]]^{-1}\left\{[M_{j,j-1}]\{F_{j-1}\} + \{L_j\}\right\} \qquad (3.132b)$$

Clearly, with the aid of the recurrence Equations (3.132) one can compute in a forward sweep the matrices $[E_j]$ and the vectors $\{F_j\}$ for all groups up until $l-1$ provided the first values $[E_0]$, $\{F_0\}$ are evaluated from the boundary condition. The other boundary condition provides the vector $\{\Delta y_l\}$. Then, in a return sweep, using Equations (3.131), the increments Δy_j and the levels $y_j^{n+1} = y_j^n + \Delta y_j$ are computed. The discharges $Q_{i,k}^{n+1}$ can be computed once the levels y_i^{n+1}, y_k^{n+1} are found.

This algorithm requires the inversion of the $m_j \times m_j$ matrix

$$[[M_{j,j}] + [M_{j,j-1}]\,[E_{j-1}]]$$

for every group j of cells and for every time step. As the number of operations is proportional to $(m_j)^3$ (these matrices have no zero elements), the efficiency of the algorithm depends on having as few cells per group as possible. Experience with current computers has shown that the desired size is $m_j < 20$ but this depends of course upon the speed of computer used. Depending upon the shape of the modelled domain, such a grouping may be more or less difficult; we shall come back to that problem in the next section. If the grouping is made in such a way that all groups have the same number of cells m_j, the computational time is proportional to $I \times (m_j)^3 < N^3$, N^3 relating to the time needed for a standard matrix inversion without the use of a double sweep matrix algorithm.

Looped network solution algorithms

The fundamental difference between 'branched' and 'looped' networks is shown in Fig. 3.19. From a given point in a branched network there is only one possible

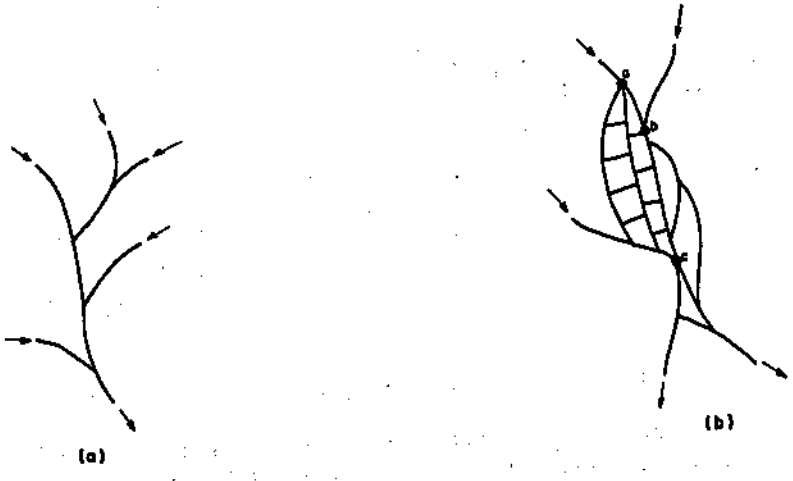

Fig. 3.19. Branched (a) and looped (b) networks

flow path to another point, while there are in general several possible paths in a looped network. It is not difficult to program a looped solution algorithm using an explicit finite difference scheme, but, as we have already indicated, implicit schemes are usually preferred for engineering applications. Consequently efficient algorithms capable of solving the equations resulting from an implicit finite difference scheme applied to a looped network have recently been developed. The generally adopted procedure is the reduction of the matrix corresponding to the complete model by local elimination of internal grid points along branches between nodal points (i.e. points where several branches meet). It must be stressed that this principle, which we shall demonstrate for a few types of schemes, is not universally used. Some modelling systems used an iteration method applied to the original complete system of equations.

The looped solution algorithm for the Preissmann scheme developed at SOGREAH is based on the fact that a looped network contains elements known as nodes which represent the confluence of several flow paths, some of which originate from other nodes, some from boundary points. In Fig. 3.19b, the confluences labelled a, b, and c are examples of nodes. The principle of the looped solution algorithm is as follows: a system of simultaneous linear equations is developed which has as unknowns only the water level changes Δy at each node. The solution of this relatively small system by any matrix inversion (or iteration) technique yields the Δy values at each node. The Δy and ΔQ values at all intermediate points on the links between nodes are then obtained using a variation of the branched network sparse matrix technique. The number of simultaneous linear algebraic equations to be solved by matrix inversion is limited to the number of nodes.

In order to explain the algorithm, we consider Fig. 3.20 and, in particular,

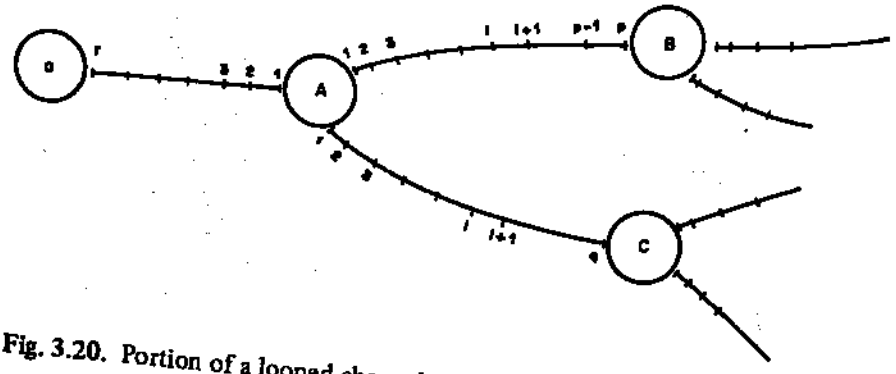

Fig. 3.20. Portion of a looped channel network

links AB, AC, and Aa. Suppose that there are p computational points along a link AB and q points along link AC. Consider first AB. For any pair of points $(i, i+1)$ Equation (3.86) may be written and, by eliminating ΔQ_{i+1}, one finds:

$$\Delta y_{i+1} = L_{i+1}\ \Delta y_i + M_{i+1}\ \Delta Q_i + N_{i+1} \tag{3.133}$$

where L, M, N are known functions of coefficients A, B, C, etc.; suppose now that for any computational point $i+1$ there exists the following relationship:

$$\Delta Q_{i+1} = E_{i+1}\ \Delta y_{i+1} + F_{i+1} + H_{i+1}\ \Delta y_p \tag{3.134}$$

where E, F, H are known coefficients. Equation (3.134) expresses the partial dependence of the unknown variables ΔQ and Δy at any point $i+1$ on the value of Δy_p adjacent to the node B. It may be easily verified that by elimination of ΔQ_{i+1} and Δy_{i+1} from the three linear Equations (3.86) and (3.134), it is possible to write the linear recursive formulae:

$$E_i = E(E_{i+1}, F_{i+1}, H_{i+1}); \quad F_i = F(E_{i+1}, F_{i+1}, H_{i+1}) \qquad (3.135)$$
$$H_i = H(E_{i+1}\, F_{i+1}, H_{i+1})$$

If coefficients E_{p-1}, F_{p-1} and H_{p-1} are known by elimination of ΔQ_p from Equations (3.86), it is possible to compute in a first sweep from B to A the groups of coefficients $(E, F, H)_{p-2}, \ldots, (E, F, H)_1$. Consequently one finds that:

$$\Delta Q_{1\,AB} = E_{1\,AB}\, \Delta y_{1\,AB} + F_{1\,AB} + H_{1\,AB}\, \Delta y_p \qquad (3.136)$$

where $(E,F,H)_{1\,AB}$ are known values. Equation (3.136) shows, through the coefficient $H_{1\,AB}$, the influence of the nodal point p on the nodal point 1AB along the link BA.

The same process may be repeated with respect to the branch AC: beginning with the point q the sweep from C to A leads to:

$$\Delta Q_{1\,AC} = E_{1\,AC}\, \Delta y_{1\,AC} + F_{1\,AC} + H_{1\,AC}\, \Delta y_q \qquad (3.137)$$

An analogous formula is obtained by the sweep from a to A:

$$\Delta Q_{1\,Aa} = E_{1\,Aa}\, \Delta y_{1\,Aa} + F_{1\,Aa} + H_{1\,Aa}\, \Delta y_r \qquad (3.138)$$

At node A a compatibility condition must be satisfied. The most simple one is that of discharge continuity and common water levels,

$$\sum_{k=1}^{m} Q_{1k}^{n+1} = 0 \qquad (3.139)$$

$$y_{11}^{n+1} = y_{12}^{n+1} = \ldots = y_{1k}^{n+1} = \ldots = y_{1m}^{n+1} \qquad (3.140)$$

where $n+1$ = superscript to indicate the $(n+1)\Delta t$ time level in the solution, k = index of the links which emanate from the node A, and m = the number of such links. If $\Delta y_{1\,AB} = \Delta y_{1\,AC} = \Delta y_{1\,Aa} = \Delta y_A$, it is clear that if Equations (3.136), (3.137) and (3.138) are substituted into the discharge continuity condition of Equation (3.139) (recalling that $Q^{n+1} = Q^n + \Delta Q$), we obtain a linear algebraic equation in terms of 4 unknowns, namely

$$f(\Delta y_A, \Delta y_p, \Delta y_q, \Delta y_r) = 0 \qquad (3.141)$$

Equation (3.136) shows how the node B (through nodal point p) influences the node A. The reciprocal is also true: one can express the influence of node A on node B. To do this, a second sweep along the link A to B is effected through a procedure identical to the first sweep but in the opposite direction. Analogous sweeps along other links leading to the node B provide similar expressions which can be introduced into the compatibility condition, Equation (3.139), at this node.

Relations of the form of Equation (3.141) written for each of M nodes leads to a system of M linear equations having as unknowns the water level changes Δy at each node,

$$[S]\{\Delta y\} = \{T_L\} \tag{3.142}$$

where $[S]$ = coefficient matrix, $M \times M$ elements; $\{\Delta y\}$ = vector of unknowns, M elements; $\{T_L\}$ = vector of the free terms, M elements.

The system represented by Equation (3.142) may be solved by any matrix inversion technique. Once the increments of water stages Δy are known at the nodes, Equations (3.133) and (3.134) are used to compute Δy_i, ΔQ_i values for all intermediate computational points in a generalized return sweep.

The principles of the above looped algorithm were published by Friazinov (1970) who described it and proved its numerical stability for a system of finite difference equations of the following type:

$$a_i Z_{i+1} - b_i Z_i + c_i Z_{i-1} + d_i = 0, \quad 1 < i < p \tag{3.143}$$

where a, b, c, d = known coefficients, Z = unknown variable.

The local elimination method explained above can also be applied to the equations resulting from the Abbott–Ionescu scheme for a reach,

$$A_j Z_{j-1} + B_j Z_j + C_j Z_{j+1} = D_j \tag{3.144}$$

where again Z_j represents either y_j or Q_j depending on the point. In a forward sweep from left ($j = 1$) to right ($j = jj$) between two nodes the coefficients in the auxiliary relation analogous to (3.136) are defined as:

$$Z_{j-1} = C'_{j-1} Z_j + E'_{j-1} Z_1 + G'_{j-1} \tag{3.145a}$$

Eliminating Z_{j-1} from Equation (3.144)

$$Z_j = C'_j Z_{j+1} + E'_j Z_1 + G'_j \tag{3.145b}$$

where

$$C'_j = \frac{-C_j}{A_j C'_{j-1} + B_j}; \quad E'_j = \frac{-A_j E'_{j-1}}{A_j C'_{j-1} + B_j}$$

$$G'_j = \frac{D_j - A_j G'_{j-1}}{A_j C'_{j-1} + B_j} \tag{3.146}$$

With the aid of Equation (3.145) the coefficients at point $j = 1$ can be initialized,

$$C'_2 = -\frac{C_2}{B_2}; \quad E'_2 = -\frac{A_2}{B_2}; \quad G'_2 = \frac{D_2}{B_2}; C'_1 = G'_1 = 0; E'_1 = 1 \tag{3.147}$$

and one can compute all coefficients C'_j, E'_j, G'_j up to $j = jj$ with the recurrence relations of Equations (3.146). In the return sweep the coefficients defined by another auxiliary relationship are determined,

$$Z_j = E_j Z_1 + F_j Z_{jj} + G_j \tag{3.148}$$

Substitution of Equation (3.148) into (3.145b) gives

$$\begin{aligned} E_{j-1} &= E'_{j-1} + C'_{j-1} E_j \\ F_{j-1} &= C'_{j-1} F_j \\ G_{j-1} &= G'_{j-1} + C'_{j-1} G_j \end{aligned} \tag{3.149}$$

Since at the gridpoint $j = jj$, $Z_j = Z_{jj}$ in Equation (3.148), we see immediately that $E_{jj} = 0$, $F_{jj} = 1$ and $G_{jj} = 0$. These values initiate the recurrence computations of E_j, F_j and G_j according to Equations (3.149) for all points $j = jj - 1, \ldots, 3, 2$.

Introducing again the generalized boundary conditions, we have

$$\begin{aligned} \alpha_1 Z_1 + \beta_1 Z_2 &= \gamma_1 \\ \alpha_{jj} Z_{jj-1} + \beta_{jj} Z_{jj} &= \gamma_{jj} \end{aligned} \tag{3.150}$$

Z_2 and Z_{jj-1} are eliminated from Equation (3.150) by use of Equation (3.148);

$$Z_2 = E_2 Z_1 + F_2 Z_{jj} + G_2; \quad Z_{jj-1} = E_{jj-1} Z_1 + F_{jj-1} Z_{jj} + G_{jj-1}$$

giving, for a reach between two nodes adjacent to the points 1 and jj,

$$\begin{bmatrix} \alpha_1 + \beta_1 E_2 & \beta_1 F_2 \\ \alpha_{jj} E_{jj+1} & \beta_{jj} + \alpha_{jj} F_{jj-1} \end{bmatrix} \begin{Bmatrix} Z_1 \\ Z_{jj} \end{Bmatrix} = \begin{Bmatrix} \gamma_1 - \beta_1 G_2 \\ \gamma_{jj} - \alpha_{jj} G_{jj-1} \end{Bmatrix} \tag{3.151}$$

Referring again to Fig. 3.20, for the reach AB, the points 1 and jj in Equations (3.151) correspond to the points 1 and p. It is seen that as for the previous scheme, the systems of two Equations (3.151) form an overall system of linear algebraic equations for unknowns Z at the points adjacent to nodes. Using a compatibility condition at nodes such as equality of levels in branches arriving at a junction, a system of equations in water stages y^{n+1} analogous to Equation (3.142) is obtained.

Still another local elimination algorithm is used by Wood *et al.* (1975). The algorithm is based upon the six-point Gunaratnam–Perkins implicit scheme of finite differences.

3.5 COMPUTATIONAL PRINCIPLES OF STEEP FRONT SIMULATION

When the flow conditions are such that a steep front (or a bore) occurs, the basic equations founded upon the de St Venant hypotheses are not valid in the neighbourhood of the discontinuity. As we described in Chapter 2, this is mainly because of the existence of vertical accelerations as reflected in strong streamline curvature. When the steep front forms as a roller, or mobile hydraulic jump, the zone it affects and in which the de St Venant hypotheses are invalid is very narrow, most often narrower than the distance Δx between two com-

putational points. In such cases it is possible to assume that the discontinuity is a boundary between two regions in which the de St Venant hypotheses are valid. These upstream and downstream regions are linked by the roller compatibility equation. It was mentioned in Chapter 2 that the integral relationships (2.3) and (2.14) over a contour in the (x, t) plane implicitly take into account such a discontinuity. It was also mentioned that the differential equations written under the divergent form compatible with integral relationships have weak (or generalized) solutions which tend to discontinuous solutions. In practical terms the above statements mean that if the solutions of the integral relationships (2.3) and (2.14) or the divergent differential Equations (2.20), (2.22) can be found in the immediate neighbourhood of the discontinuity, they will implicitly satisfy the compatibility relationships across the discontinuity.

We will now describe three practical methods for the computation of steep fronts: the shock fitting, pseudoviscosity, and through methods.

Shock fitting method

In this approach, the propagation of the discontinuity is computed for one time step independently of the computation in the two adjacent de St Venant regions. Consider Fig. 3.21a which depicts a computational grid $j\Delta x, n\Delta t$. At time level $n\Delta t$, the position of the discontinuity x_A corresponds to four flow variables as shown in Fig. 3.21b: $(y_A, Q_A)_1$ at the upstream side of the discontinuity, and $(y_A, Q_A)_2$ at the downstream side. (The abscissa x_A does not correspond to a computational point location). If we can find the new position of the front at time level $(n + 1)\Delta t$ and the flow variables on both sides of it, then flow variables at all computational points can be obtained by any method of numerical solution of the usual flow equations, using the new, $(n + 1)\Delta t$, values of flow variables on either side of the discontinuity as internal boundary conditions.

The two shock compatibility conditions are (*see* Equations (2.68) and (2.71))

$$v - \frac{Q_1 - Q_2}{A_1 - A_2} = 0 \tag{3.152}$$

$$\frac{Q_1}{A_1} - \frac{Q_2}{A_2} - \left(g \frac{A_1 - A_2}{A_1 A_2} \left(A_1 \eta_1 - A_2 \eta_2 \right) \right)^{\frac{1}{2}} = 0 \tag{3.153}$$

where v is the (unknown) shock celerity and 1, 2 represent the upstream and downstream sides of the shock. The shock path in the (x, t) plane is defined by the ordinary differential equation

$$\frac{dx}{dt} = v \tag{3.154}$$

Consequently we have 3 equations and 6 unknowns: the new shock position x_B at the time level $(n + 1)\Delta t$, the shock celerity v, and two variables (y, Q) on each

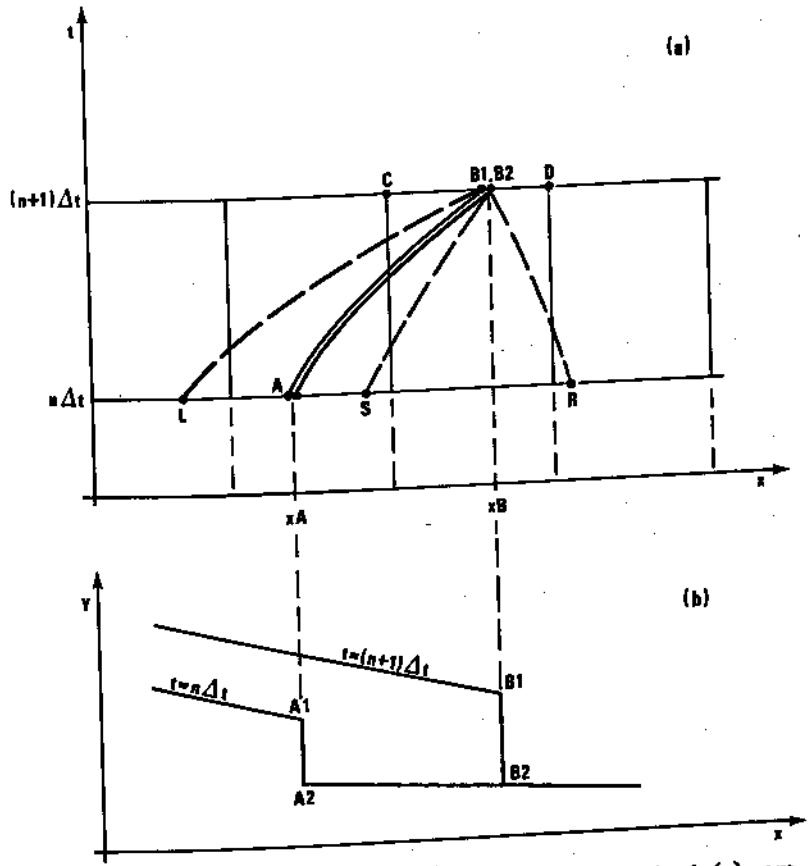

Fig. 3.21. Steep front calculation using the shock fitting method; (a) computational grid; (b) physical situation

side of it. The solution is possible because the shock celerity v satisfies the following inequality:

$$c_1 + u_1 > v > c_2 + u_2$$

Consequently the perturbations created upstream of the shock catch up with it, which means that one can trace a characteristic such as B_1L. The abscissa x_L is unknown, so one new unknown is introduced, along with two new equations analogous to Equations (3.6a), (3.6b) for the characteristic B_1L. In the same way two characteristics B_2R, B_2S may be drawn on the downstream side of the shock introducing two new unknowns x_R, x_S and 4 new equations. In all a system of 9 non-linear algebraic equations for 9 unknown variables y_{B1}^{n+1}, Q_{B1}^{n+1}, y_{B2}^{n+1}, Q_{B2}^{n+1}, v, x_B, x_L, x_R and x_S is obtained and may be solved by, for example, the Newton–Raphson method. Once $(y, Q)_{B1}^{n+1}$ and $(y, Q)_{B2}^{n+1}$ are known, the reaches to the left (beginning with the point C) and to the right (point D) of the shock may be solved by any method of numerical integration;

the basic equations in those regions do not need to be conservative. The only problem is to compute the boundary values at points C, D based upon the shock solutions AB_1 and AB_2. This kind of method is used most often to compute dam break waves (*see* for example Vasiliev *et al.*, 1965).

Pseudoviscosity method

The pseudoviscosity method, used by von Neumann and Richtmyer (1950), was adapted to open channel flow computations by Preissmann and Cunge (1961a, b). It can best be explained using the simplified differential equations (2.29) to which one new term $\frac{1}{n}\frac{\partial q}{\partial x}$ is added:

$$\frac{\partial h}{\partial t} + \frac{\partial (uh)}{\partial x} = 0 \tag{3.155a}$$

$$\frac{\partial u}{\partial t} + \frac{\partial}{\partial x}\left(\frac{u^2}{2}\right) + g\frac{\partial h}{\partial x} + \frac{1}{h}\frac{\partial q}{\partial x} = 0 \tag{3.155b}$$

where the pseudoviscosity q is defined by

$$q = \begin{cases} l^2 h\left(\dfrac{\partial u}{\partial x}\right)^2 & \text{when } \dfrac{\partial u}{\partial x} < 0 \\ 0 & \text{when } \dfrac{\partial u}{\partial x} > 0 \end{cases} \tag{3.156}$$

$l = a\Delta x$, a = const.

The result of this modification is a smoothing, or diffusion, of discontinuities. Discontinuous fronts cannot appear – the steeper the front, the stronger the artificial viscosity, the stronger the diffusion. Variations in depth or discharge are smeared over a length whose order of magnitude is that of coeffient l in Equation (3.156); a should be taken as 2 or 3.

The pseudoviscosity method is most often used with non-dissipative schemes of finite differences. As we showed in Section 3.2, dissipative schemes, such as the Preissmann method for $\theta \neq 0.5$, Vasiliev, or Lax schemes, introduce numerical damping of different components of the solution. Other methods, such as the leap-frog or Abbott–Ionescu schemes, are not dissipative: no numerical damping is introduced, even though these schemes are dispersive. When the front steepens, short wave components in the solution appear and propagate with different celerities. As the front gets steeper and steeper, the solution may thus become uncontrollable. In Fig. 3.22a is shown a computation of a steep wave using the explicit leap-frog scheme *without* the pseudoviscosity term, while in Fig. 3.22b is shown the same case *with* the term. The explicit formulae used were the following ones (*see* Equations (3.155) and the leap-frog discretization Equations (3.28), (3.29)):

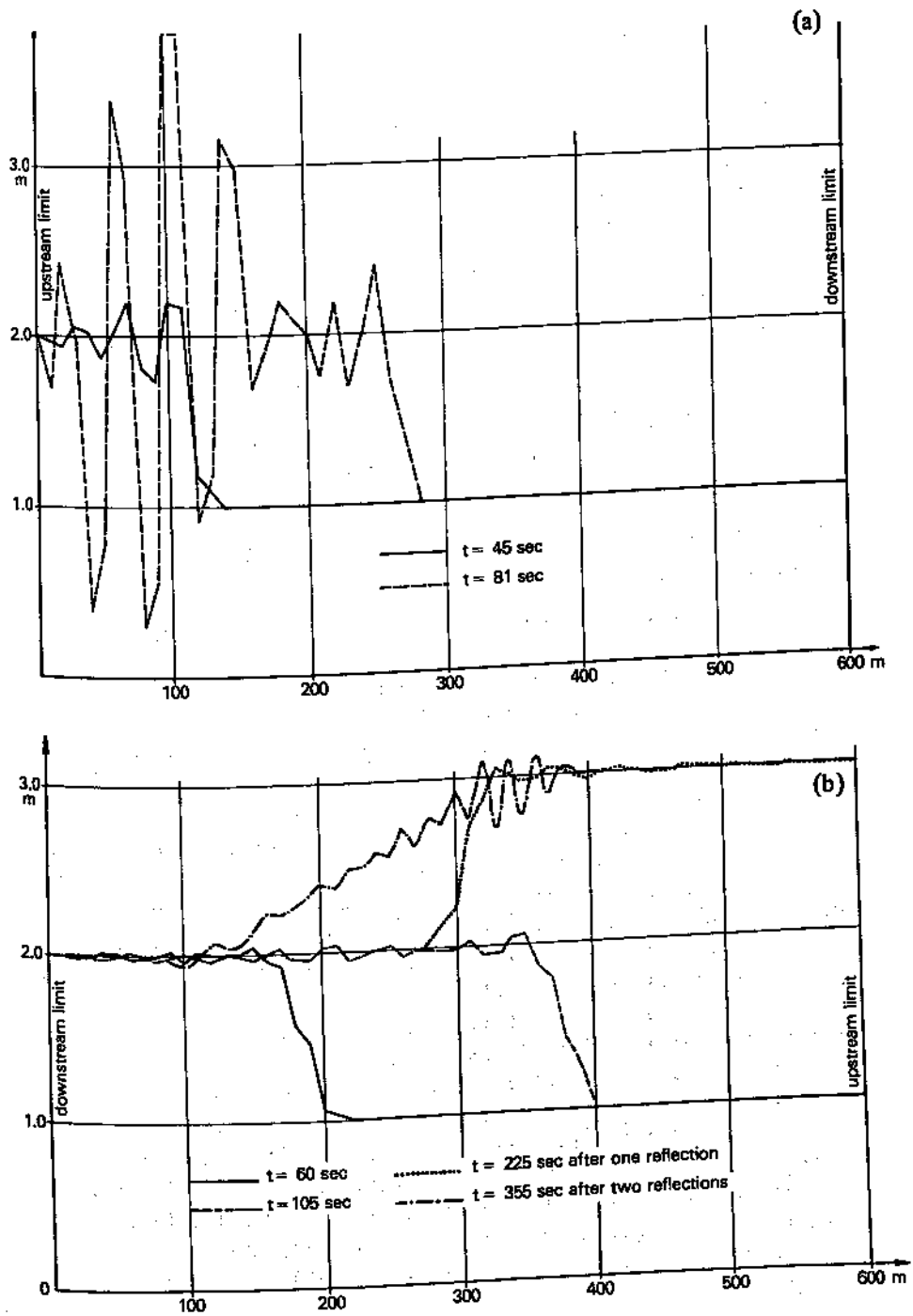

Fig. 3.22. Steep front wave propagation using the explicit leap-frog scheme without (a) and with (b) pseudoviscosity (courtesy La Houille Blanche, 1961)

$$h_j^{n+1} = h_j^{n-1} + \frac{\Delta t}{\Delta x}\left(h_{j+1}^n u_{j+1}^n - h_{j-1}^n u_{j-1}^n\right) \tag{3.157a}$$

$$u_j^{n+1} = u_j^{n-1} + \frac{\Delta t}{\Delta x}\left[(u_{j+1}^n)^2 - (u_{j-1}^n)^2\right] + g\frac{\Delta t}{\Delta x}\left(h_{j+1}^n - h_{j-1}^n\right) + \frac{\Delta t}{\Delta x}\frac{2}{h_{j+1}^n + h_{j-1}^n}\left(q_{j+1}^n - q_{j-1}^n\right) \tag{3.157b}$$

$$q_j^n = \begin{cases} a^2\Delta x^2 \dfrac{h_{j+1}^n + h_{j-1}^n}{2}\dfrac{(u_{j+1}^n - u_{j-1}^n)^2}{4\Delta x^2} & \text{for } u_{j+1}^n - u_{j-1}^n < 0 \\ 0 & \text{for } u_j^n - u_{j-1}^n > 0 \end{cases} \tag{3.157c}$$

The results shown in Fig. 3.22 are self-explanatory as to the effect of a pseudo-viscosity term upon the steep wave computations.

Through methods

The most important advantage of the so-called 'through' methods of shock computations is that they compute the shock without any special treatment of the algorithm. The idea in itself is extremely simple: since any dissipative scheme introduces damping of individual Fourier components of the solution, as we saw in Section 3.2, this diffusion prevents the formation of a steep front – the latter is replaced by a 'smeared' front, by a smooth variation of levels and discharges. If the damping is stronger for shorter components, they are then smoothed rather quickly; this avoids the wavy water surface behind the front which would otherwise be due to the dispersion of shorter components which must be present to represent the front curvature. If a scheme is not dissipative, but only dispersive, the differences in component celerities may well destroy the value of the solution. Consider for example Fig. 3.23, given by Cunge (1975b) which shows a surge computation in a power canal. The surge was due to rapid turbine closure at the downstream end of the canal. Five simulations were run using the Preissmann scheme; the Courant number was kept constant, $Cr \approx 1$, but the coefficient θ was varied. The results clearly show the oscillations at $\theta = 0.5$ (when the scheme is non-dissipative) due to numerical dispersion. These oscillations are damped through numerical dissipation when $\theta > 0.5$.

Non-dissipative schemes (such as the leap-frog or Abbott–Ionescu methods) need either a pseudoviscosity term or some other artificial damping to simulate steep fronts as a through computation. This is one reason why the theory of 'dissipative interfaces' (*see* Abbott, 1979) was developed; indeed, not any arbitrary diffusive term is appropriate, and a proper diffusive influence must be carefully chosen.

At this point an important question may be asked – how do we know that a smeared front approximates the real solution? Is its celerity correct and are the values of flow variables on both sides of the front (at least at some distance from

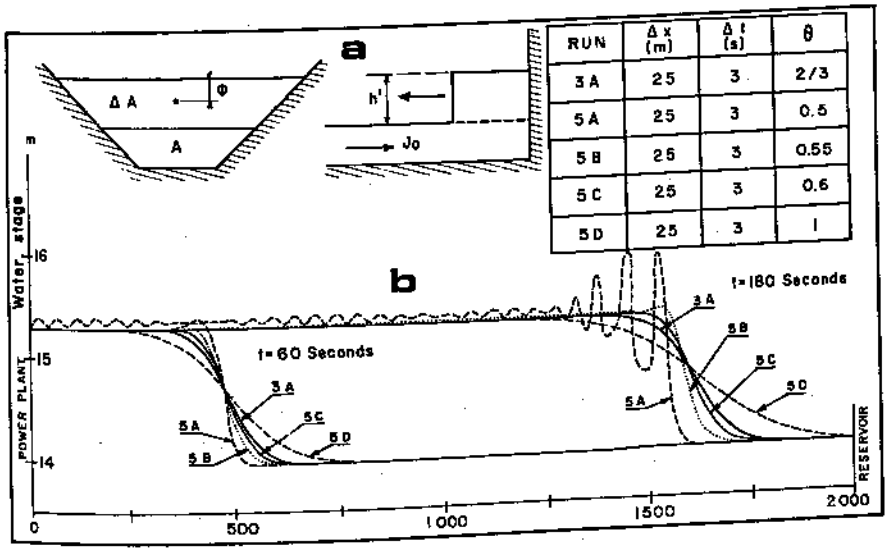

RUN	Δx (m)	Δt (s)	θ
3A	25	3	2/3
5A	25	3	0.5
5B	25	3	0.55
5C	25	3	0.6
5D	25	3	1

Fig. 3.23. Surge computation in a power canal using a through method (Preissmann's scheme). Source: Cunge, 1975b. (a) Favre solution. (b) Numerical experiment, turbine closure from 2500 m^3s^{-1} to 250 m^3s^{-1} in 15 s

the supposed discontinuity) the right ones? The answer to these questions is not evident. The reader interested in the theoretical aspect of the questions should consult Abbott (1979) and, for a less theoretical interpretation, Cunge (1975b). We can nonetheless point out a few requirements here.

To begin with, the basic flow relationships must have the correct discontinuous solution. As was shown in Chapter 2, the discontinuous solutions to the integral relationships (2.3) and (2.14) are precisely the right ones. Moreover, it has been proven (see Lax, 1954; Abbott 1979) that the weak solutions of homogeneous differential equations written under the divergent form tend to the discontinuous solutions of the integral relationships. However we cannot expect that equations written under non-divergent form will have a solution which, for $\Delta x, \Delta t \to 0$, converges to the proper discontinuous solution. And we know nothing about equations whose left-hand sides are written under the divergent form but which have non-homogeneous terms on the right-hand side, even though we hope that non-differential terms do not change the equation's basic properties. Thus our first conclusion is that only the integral relationships (2.3) and (2.14) and the system of Equations (2.20), (2.22) should be used if one expects shocks to appear. Recalling Equations (2.20) and (2.22)

$$\frac{\partial A}{\partial t} + \frac{\partial Q}{\partial x} = 0 \tag{3.158}$$

$$\frac{\partial Q}{\partial t} + \frac{\partial}{\partial x}\left(\frac{Q^2}{A} + gI_1\right) = gA\,(S_0 - S_f) + gI_2$$

we observe on their left hand sides a divergent form similar to the formal

representation (*see* Abbott, 1979):

$$\frac{\partial f}{\partial t} + \frac{\partial G(f)}{\partial x} = 0 \tag{3.159}$$

But equations such as the system of Equations (2.28):

$$\frac{\partial y}{\partial t} + \frac{1}{b}\frac{\partial Q}{\partial x} = 0$$

$$\frac{\partial Q}{\partial t} + \frac{\partial}{\partial x}\left(\frac{Q^2}{A}\right) + gA\left(\frac{\partial y}{\partial x} + S_f\right) = 0 \tag{3.160}$$

are obviously *not* written under the conservative form. If they are used and give plausible results, it is thanks to the small variability of certain terms, but they have a built-in danger of error for general conditions.

Quite obviously, the differential equations which are derived from energy conservation rather than from the momentum conservation principle should not be used under any pretext when discontinuities may appear (*see* Abbott, 1979; Abbott, 1975b; Cunge, 1975b). For example, the following dynamic equation, based on energy conservation, must not be used:

$$\frac{1}{g}\frac{\partial u}{\partial t} + \frac{u}{g}\frac{\partial u}{\partial x} + \frac{\partial y}{\partial x} + S_f = 0 \tag{3.161}$$

Once the proper analytical form of flow equations has been selected, a proper finite difference approximation of that form must be used. Finite difference schemes which approximate the integral relationships (2.3), (2.14) are the best choice for such simulation (for example the Preissmann scheme). Other schemes must be applied to the divergent form of differential equations, and one has to be sure that they are consistent with and convergent to these equations before using them in practical applications.

3.6 REPRESENTATION OF TOPOGRAPHIC AND HYDRAULIC DATA

We have seen in Sections 3.2 and 3.3 that the topographic and hydraulic nature of the flow situation to be modelled is represented in the numerical procedures by a certain number of functions of water level y_j for each computational point j, such as:

wetted area $A(y)$
conveyance factor $K(y)$
cell surface area $A_s(y)$, etc.

Some equations use the width $b(y)$ as a variable, which may be furnished separately as such or computed from the function $A(y)$, since $b = \mathrm{d}A/\mathrm{d}y$. When the flow equations are written under the divergent form, Equations (2.20),

(2.22) (Equations (3.158)), one also needs the function $I_1(y)$. Finally, either the bed slope S_{0j} or the bottom elevation y_{bj} must be given at each point j.

One possibility is to store such data in their raw form, such as $y_b(x, z)$, $k_{Str}(y, x, z)$ (we recall that z is the transversal coordinate and k_{Str} is the Strickler coefficient) and then compute each needed function at every point and at every time step – obviously too time-consuming a procedure. Another more common but dangerous solution consists in fitting polynomials to the above functions for every computational point. Such a procedure saves space in computer storage, but may yield false values near inflexion points, by extrapolation, and near zero depth. The most common procedure, and one which represents a tradeoff between the inaccuracy of polynomial representation and the memory needs of raw data storage, is the use of tabulated functions. In the model construction stage, the raw data are used to develop tabulated functions such as $A(y), K(y), A_s(y)$, etc. During the calculation these tabulated functions are consulted for each point and for each time step (or each iteration) with the water level y as argument. Linear (or possibly non-linear in the case of conveyances, see Vreugdenhil, 1973) interpolation between tabulated values yields the needed values with a minimum of computational effort and good accuracy.

It should be noted that a fully divergent scheme requires that at least *four* tables be stored for each point: $A(y), b(y), I_1(y)$ and $K(y)$. If divergent schemes are not always used, it is partially because of the effort and storage required to manipulate this considerable mass of data.

In staggered-grid schemes or in models in which the cross section is not known at all points, longitudinal interpolation of data is sometimes necessary. Again, tables are more convenient than polynomials.

In any model based on the de St Venant hypotheses, the energy slope S_f which appears in, for example, Equation (2.14), is assumed to be representative of the reach between two computational points. But since S_f is usually expressed in the form

$$S_f = \frac{Q^2}{K^2} \tag{3.162}$$

and the conveyances K are properties of the cross sections at either end of the reach, the problem arises as to how to interpolate between them in expressing S_f. To the authors' knowledge no definitive procedure has been developed, different modelling organizations using their own methods. It is nonetheless worthwhile to see how the different formulae differ one from another. Let us consider the four following interpolation formulae:

$$S_{f1} = \frac{Q^2}{\alpha K_1^2 + (1-\alpha) K_2^2} \quad \text{(weighted average of } K^2\text{)} \tag{3.163a}$$

$$S_{f2} = Q^2 \left(\frac{\alpha}{K_1^2} + \frac{1-\alpha}{K_2^2} \right) \quad \text{(weighted average of } S_f\text{)} \tag{3.163b}$$

$$S_{f3} = \frac{Q^2}{K_1^{2\alpha} K_2^{2-2\alpha}} \quad \text{(weighted geometric mean of } K^2\text{)} \tag{3.163c}$$

$$S_{f4} = \frac{Q^2}{[\alpha K_1 + (1-\alpha) K_2]^2} \quad \text{(weighted average of } K\text{)} \tag{3.163d}$$

in which we have assumed a steady flow situation in writing $Q_1 = Q_2 = Q$, 1, 2 = upstream and downstream sections, α = weighting coefficient.

If $K_2 = \eta K_1$, each of these expressions can be written as

$$S_f = \frac{Q^2}{K_1^2} f(\alpha, \eta) \tag{3.164}$$

with

$$f_1 = \frac{1}{\alpha + \eta^2 (1-\alpha)} \tag{3.165a}$$

$$f_2 = \frac{1 + \alpha(\eta^2 - 1)}{\eta^2} \tag{3.165b}$$

$$f_3 = \eta^{2(\alpha-1)} \tag{3.165c}$$

$$f_4 = \frac{1}{(\alpha + \eta - \alpha\eta)^2} \tag{3.165d}$$

Figure 3.24 shows the behaviour of these functions for $\eta = 1$ and $\eta = 2$. With a factor of two difference in conveyance between two adjacent points and $\alpha = 0.5$, the friction slope for the reach could vary by some 50% depending on the conveyance interpolation chosen; this difference becomes even more striking as η increases. It is important however, to remember that large differences in adjacent sections are incompatible with the de St Venant hypotheses, which assume basically one-dimensional flow with small streamline curvature. If two adjacent sections have such differential conveyances that the results are highly sensitive to the interpolation formula used, intermediate computational points should be introduced to bring the model into line with the de St Venant hypotheses.

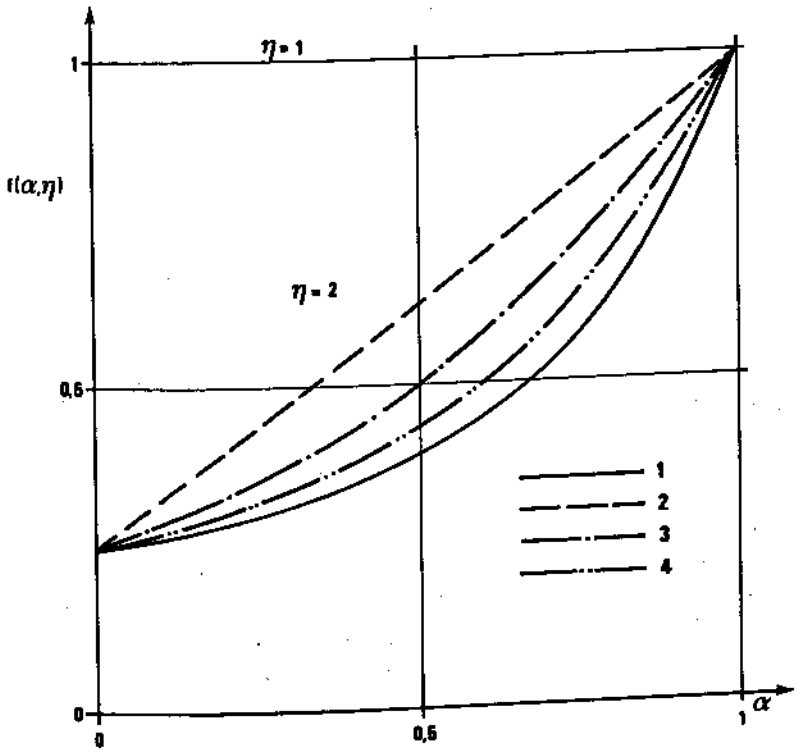

Fig. 3.24. Comparison among several energy slope interpolating formulae; $K_2 = \eta K_1$, $S_f = \dfrac{Q^2}{K_1^2} f(\alpha, \eta)$. (1) Equation (3.165a); (2) Equation (3.165b); (3) Equation (3.165c); (4) Equation (3.165d)

4 Flow simulation in natural rivers

4.1 INTRODUCTORY REMARKS

When we speak of mathematical modelling of flow in 'natural rivers', we are really using a misnomer. Rivers which can be considered to be in a truly natural state, in the sense that their flow is unaffected by man's intervention in one form or another, are few in number and rapidly disappearing. Although some of the large watercourses in northern Canada, South America, and Africa can be considered to be more or less in natural state, most of the world's rivers have been to some extent modified by man through dam construction, channelization, dredging, etc.

Nevertheless, most rivers have been modified only locally, such that over a major part of their length, water flows through natural cross sections and at a natural channel slope, in a valley which is periodically flooded in spite of the presence of man-made dykes. These rivers are still subjected to extended low-flow periods and at times exceptional flooding, both of which can have major effects on the economies of riparian countries. Thus even though few rivers can be considered to be fully natural, they are still subject to quite natural flow events, and as such present mathematical modelling problems which do not arise in the case of completely artificial channels or canals (*see* Chapter 6).

Man's interest in river flow stems from his need to protect human life, property, and economic systems from the capriciousness of natural flow events, and to exploit their potential benefits in terms of energy, agriculture, and navigation. In this overall context, mathematical modelling provides a tool by means of which man can study and gain an understanding of hydraulic flow phenomena, select and design sound engineering projects, and predict extreme situations so as to be able to provide advance warning of their occurrence and importance. Let us consider these three general objectives in more detail.

The understanding of hydraulic phenomena implies gaining an appreciation of how water exchanges between different areas occur, which portions of the river carry the flow and which merely store water, how the flow is distributed in multiple channels, etc. Not only is such an understanding essential to the intelligent planning and design of engineering projects, but it also is indispensable to the study of water quality control in the watercourse. The very act of model

construction and calibration leads to the perception of topographic and hydraulic data inadequacies; subsequent data collection and survey campaigns can be planned in an optimal manner with the aid of a mathematical model. The initial phase of the study of the Niger River in Niger and Mali is an example of the use of modelling to understand flow phenomena. The flow pattern in the Mali Lake region (the so-called 'interior delta', *see* Fig. 4.1), is of such complexity that it simply could not have been understood without the aid of detailed modelling and associated surveying. Other examples are the Nigerian Delta region of the lower Niger River and the Brahmapoutra–Ganges deltas. The economic development of countries which are riparian to such watercourses (Niger, Mali, Nigeria, and Bangla Desh for the examples cited above) cannot be disassociated from the beneficial and destructive potential of these great rivers. Mathematical modelling is essential to the understanding of flow patterns in such complex systems.

The study and design of large river engineering projects and their consequences requires not only that the present hydraulic situation be understood, but also that the effect of the project itself on flow patterns be predicted. It is only by comparing the long-term effects of alternative engineering projects on flow patterns that intelligent choices can be made with regard to river development. Mathematical modelling is the tool which makes such predictions and comparisons possible.

The prediction of exceptional natural events and their consequences implies the use of mathematical modelling because past observations of such events are so often non-existent. A model which is constructed to produce the 'observation' desired must first of all be able to reproduce known flow events, then extrapolate beyond them. The capability of a properly constructed mathematical model to perform this extrapolation rests on the fact that it uses physically correct, deterministic hydraulic equations whose validity is not limited to the known flow events used to adjust their empirical (and strictly physical) coefficients.

The essential quality of a mathematical model is its predictive capacity. In order that model predictions be accurate and useful, the model must of course be based on hydraulic equations which represent the most important flow phenomena. But even if the flow equations used are appropriate, the model is useless unless real hydraulic and topographic features are introduced into it and simulated in a sound manner. This is perhaps the distinguishing feature of river modelling; it is incumbent upon the modeller to provide a numerical description of physical reality which is consistent with the flow equations used, and with the purpose of the model study.

Assuming that all necessary data have been collected (*see* Chapter 5), the engineer who wishes to construct a mathematical model of a river must follow three basic steps:

(1) Selection of the type of model and modelling system software used to construct it. We discuss in Section 4.2 the relationships between flow equations adopted and physical situations to be modelled, and in Section 4.3 we consider

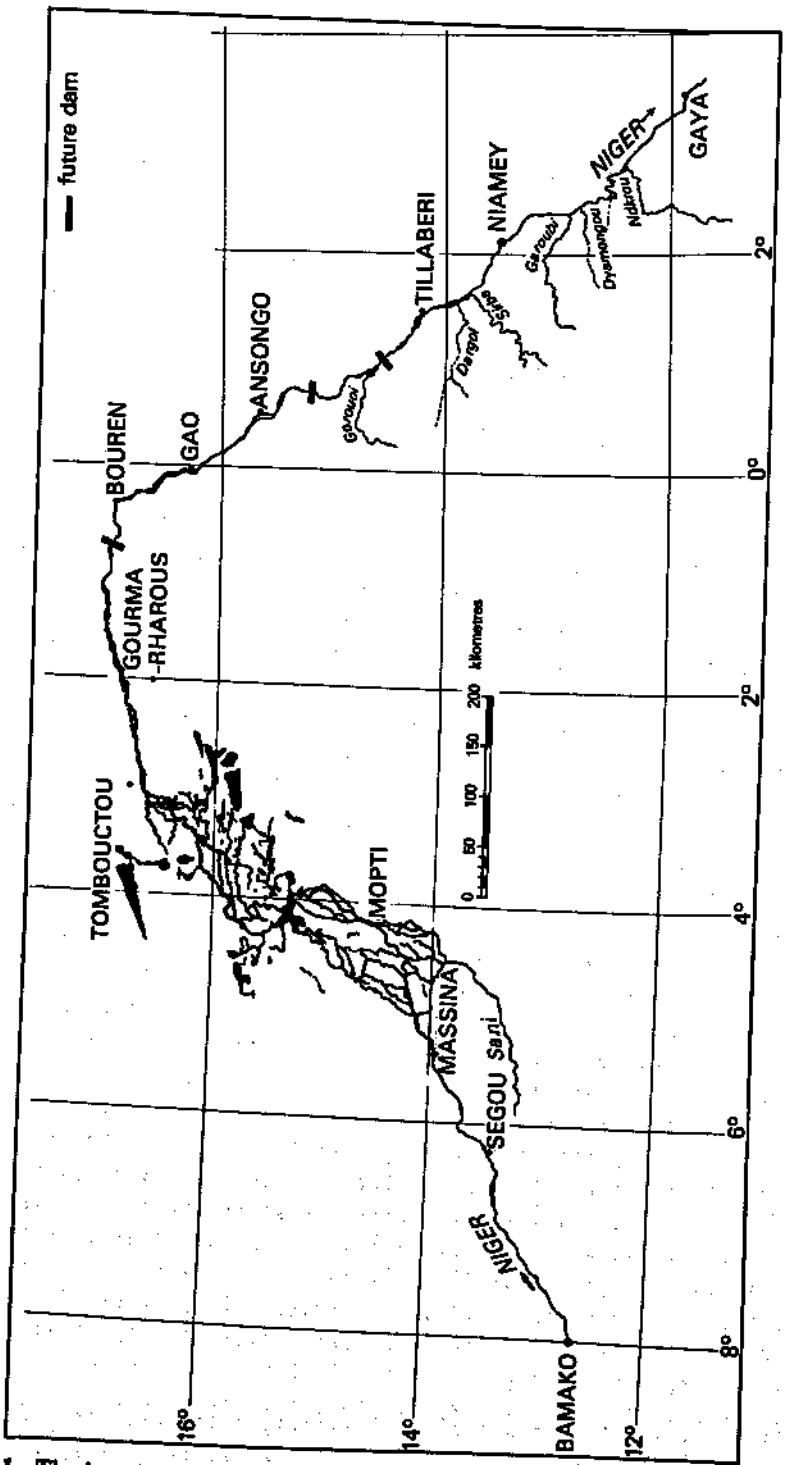

Fig. 4.1. The interior delta of the Niger River

the problem of deciding whether one-dimensional or two-dimensional modelling is necessary.

(2) Schematization of the hydraulic and topographic features of the watercourse and inundated area to be modelled. In Sections 4.4 and 4.5 we deal with the notions of topologic and hydraulic discretization of flow situations.

(3) Calibration of the model. We leave this important subject to Chapter 5.

In Section 4.6 we discuss some aspects of computational problems associated with river modelling.

4.2 CHOICE OF EQUATIONS FOR CHANNEL FLOW

In river channel modelling it is extremely important to base the model on appropriate flow equations. The physical nature of a river and its floods suggest the appropriate equations to be used to model the situation. As has been stressed in Chapter 2, the various terms in the equations of unsteady flow as established by de St Venant may be of quite different order of magnitude, and under certain conditions some of them may be dropped. For example, if a river to be modelled has a steep slope and its flow is primarily influenced by the bed roughness, one may drop the inertial terms from the dynamic equation. The River Rhône, in France, is typical of those for which simplified equations are well suited for the representation of its floods, the natural bed slope being a relatively steep 0.70 m km^{-1}. The rise of the flood wave is relatively slow and the acceleration terms

$$\frac{1}{g}\left(\frac{\partial u}{\partial t} + u\,\frac{\partial u}{\partial x}\right)$$

are small as compared to the water surface slope $\dfrac{\partial y}{\partial x}$.

The effect of neglecting the acceleration terms has been demonstrated by constructing two mathematical models of a reach of the Rhône; the first model used the full unsteady flow equations, the second one the Muskingum method. Computed hydrographs could not be distinguished one from another (SOGREAH, 1961). However, these models simulated a river reach before river canalization was achieved along its lower course, and the studies undertaken at that time (1960) were directed toward the prediction of the influence of future structures upon flood propagation. Figure 4.2 shows the location and nature of completed and planned structures along the Rhône. It is obvious from this figure that the river can no longer be considered as being in its natural state. The free surface slope, except during catastrophic floods, is very small and quite different from that of the longitudinal bed profile. Thus the inertial terms

$$\frac{1}{g}\left(\frac{\partial u}{\partial t} + u\,\frac{\partial u}{\partial x}\right)$$

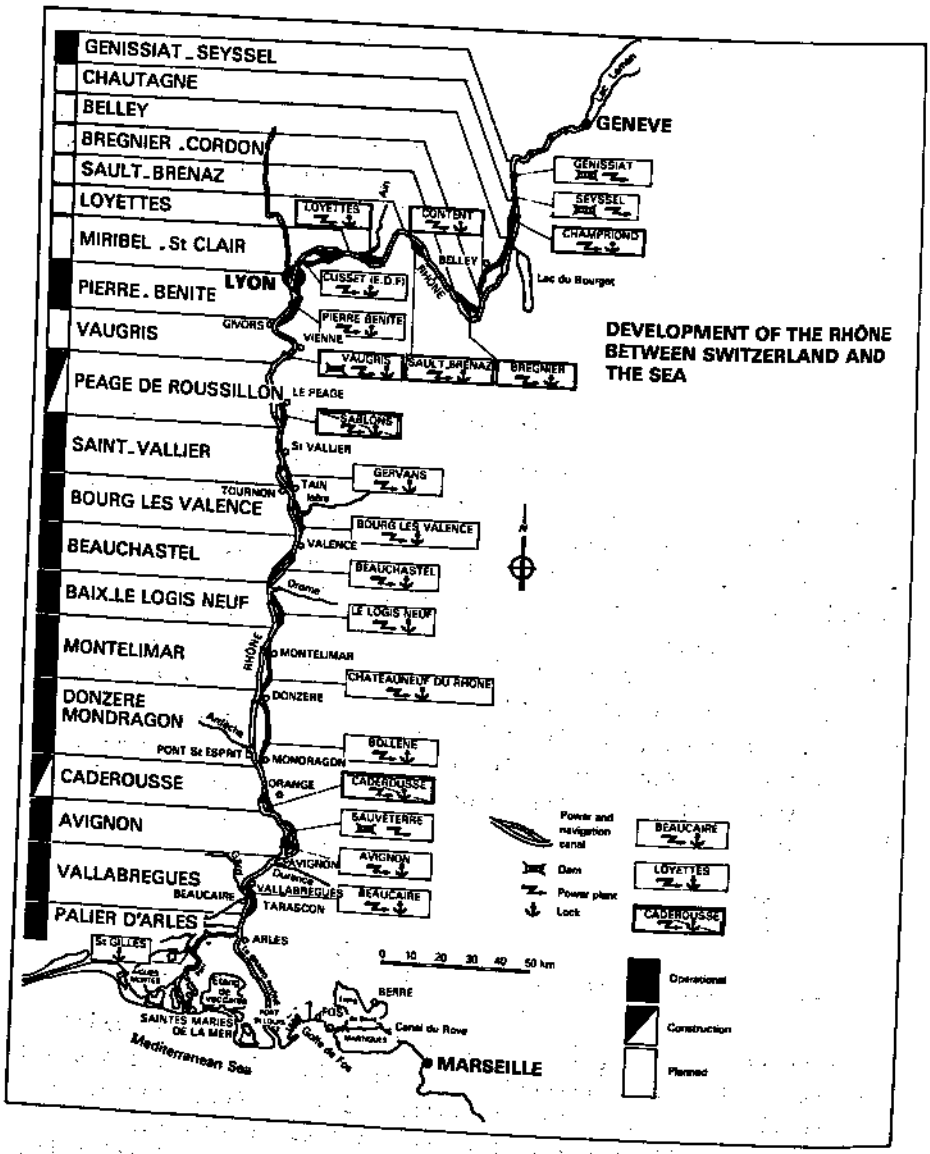

Fig. 4.2. Present and proposed development on the Rhône River in France

cannot be neglected as compared to $\frac{\partial y}{\partial x}$, especially when dam and power plant manoeuvres are considered – in fact steep front waves, which are essentially inertial phenomena, can develop in the derivation channels (Favre, 1935). Moreover, water management problems on the Rhône have changed since 1960. Responsible authorities are now interested in the optimization of energy

production by cascade releases, in detailed prediction and control of water levels for industrial and domestic consumption, and in pollutant transport. Had the model been built on the basis of the Muskingum or another simplified method, none of these model applications would have been possible, as such simplified methods not only neglect inertial terms, but also preclude the possibility of extrapolation of existing situations towards new ones, notably those incorporating new structures.

Another example is that of the Parana River. The upper reaches of the Argentinian Parana can be simulated using simplified equations, and thus if interested in simple flood prediction, one could well build a model based upon simplified relationships. However, large dam projects are foreseen, such as Apipe-Yaciyreta and Corpus. The characteristics of these proposed structures are such that the river will be transformed into what is essentially a wide canal flowing within its dykes with a minimum possible slope. The flow in such canals, or in fact reservoirs, will no longer be governed by resistance, but rather by inertial forces. To choose simplified equations for a flood prediction model would render this model useless for the simulation of the future influence of large dams.

In the above examples, we have been trying to point out that the purpose of the modelling must be kept in mind when choosing the equations. One can identify two general classes of applications in engineering practice:

(i) those in which the flood is not modified by the structures or developments under study. In this class of applications we find problems based on the 'project flood', flood prediction in present conditions, and estimates of flood damage.

(ii) Those in which the influence of developments and structures upon the flood itself is of interest as well. Examples are studies of dams, reservoirs, flood control projects, etc.

In general, simplified equations can be used in class (i) when permitted by the type of river and flow; on the other hand, the full equations would be advised for class (ii). It should not be forgotten that problems of type (i) may well be transformed into problems of type (ii) with time, and in that case the wrong choice at the beginning could lead to a considerable increase in expense in the future if one is led to completely rebuild the mathematical model based on different equations.

An excellent monograph concerning flood routing in natural rivers using simplified equations has been published by the Hydraulic Research Station, Wallingford, England (Flood Studies Report, 1975). In this chapter we restrict our attention, as far as channel flow is concerned, to models based on the full equations of Barré de St Venant, which have few built-in limitations as to river and flood types and as such are more universally applicable. We discuss in Chapter 10 the cost implications of opting for a complete equation model over a simplified equation one.

4.3 ONE-DIMENSIONAL AND TWO-DIMENSIONAL MODELLING

The unsteady one-dimensional channel flow equations, as established from the de St Venant hypotheses (*see* Chapter 2) have been experimentally confirmed in laboratory flumes and in full scale confined channels. But the use of these equations to simulate river flood wave propagation is a rather audacious extrapolation of their intended role, and the modeller must be aware of the limitations of this practice.

We seldom observe in nature truly straight channels in which the flow can be considered to be strictly one-dimensional. Natural river flow is most often curvilinear, following the channel bed which meanders within the valley limits. The valley can seldom be considered to be a series of cross sections representing simple overbank extensions of the main channel; it widens and narrows in an irregular manner, contains depressions, oxbow lakes, secondary valleys, etc. In some uncomplicated valleys, flood waters simply inundate the overbank extension of the channel, all the while flowing in a basic downstream direction defined by the main channel. But it is more often the case that overbank flows go their own way, filling up the flood plain in a manner dictated by local topography, sometimes never returning to the main channel during the falling flood.

Let us consider Fig. 4.3 in which we see a river and its adjacent flood plain. It is evident from the photograph that once flood waters leave the main channel by overflowing its dykes, their subsequent behaviour is completely independent of flow between the submerged dykes. In fact, valley inundation can even begin from a downstream low-dyke location, such that flood plain waters actually flow in an upstream direction, at least for a certain period of time. In this case it is only between the dykes that the flow might be considered as one-dimensional.

Another quite different situation is depicted in Fig. 4.4 where the overbank flow of the Mekong River inundates the entire flood plain; only part of the overbank flood waters ever find their way back into the main channel, and the direction of flow on the flood plain has absolutely nothing to do with the direction of flow in the Mekong. Figure 4.5 presents a more detailed view of the situation. The notion of one-dimensional flow has no meaning here, except for very short channel reaches between the ponded reservoirs.

It was in response to the need to model vast inundated plains such as in Fig. 4.5 that so-called two-dimensional modelling techniques were developed (Zanobetti *et al.*, 1970). It is understood that by 'two-dimensional' we do not refer to the unsteady flow equations in two spatial dimensions, but rather to the physical situation in which channels and storage cells form a two-dimensional network in the horizontal (x, z) plane.

As described in Chapter 2, the flood plain in practical models is divided into a number of cells, or storage basins, in each of which the water surface is assumed horizontal (although its surface area depends on the water level in the cell) and each of which communicates with its neighbours and/or the main channel. The flow in links between cells is calculated according to a chosen hydraulic law (Manning/Strickler, weir, orifice, etc.), neglecting inertial forces; this simplifi-

cation renders complicated problems more tractable computationally. Although it is possible to take into account the term $\frac{1}{g}\frac{\partial y}{\partial t}$ and still have a reasonably efficient modelling system (Abbott and Cunge, 1975), we assume in this chapter that two-dimensional river modelling neglects inertial effects. When these effects must be taken into account, a looped network of one-dimensional reaches can be used for the simulation.

Fig. 4.3. Adour River (France) main channel and flood plain

In two-dimensional models, the division of the flood plain into cells is not at all arbitrary, but is based on natural boundaries such as elevated roads, embankments, dykes, etc. We discuss two-dimensional modelling in more detail in Section 4.5; it is important to realize that, in river hydraulics, when an area is modelled with such a two-dimensional tool, the main channel flow is computed in the same way as the flood plain, i.e. without inertial forces due to temporal and spatial accelerations. Such a model cannot simulate a delta region influenced by the tide during the dry period, nor can it represent water releases or levee failure wave propagation, saline front propagation, etc. Inertial terms are also

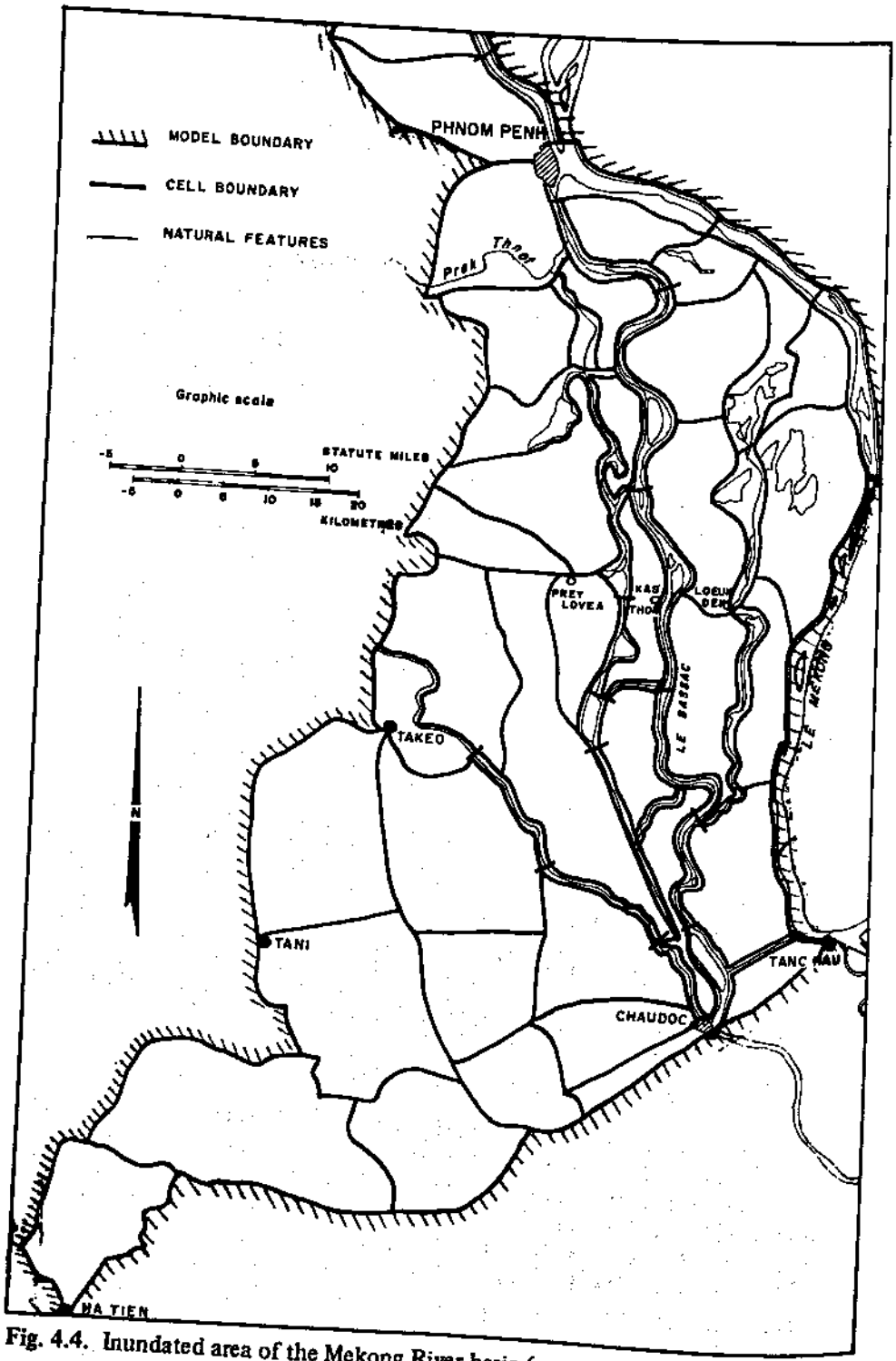

Fig. 4.4. Inundated area of the Mekong River basin (courtesy UNESCO)

Fig. 4.5. Detailed view of Cambodian rice paddies (courtesy UNESCO)

important in large reservoirs in which friction slopes are negligible as compared to the acceleration slopes, which are then the most important driving forces.

This separation of the engineer's tools into either one-dimensional models (correctly representing inertial forces but only very crudely simulating flood plain flows), or two-dimensional models (unable to correctly simulate the river flow), has historically hampered progress in the application of mathematical models. Indeed, in more practical situations, flow in both the river and the adjacent flood plain must be simulated, and for all possible situations: dry period flow, partial inundation, completely flooded valley, etc.

It was necessary to treat the two situations separately because of the fundamental difference between 'branched' and 'looped' networks, as shown in Fig. 4.6. From a given point in a branched network (also called 'dendritic', 'simply connected', or 'tree-like'), there is only one possible flow path to another point (Fig. 4.6a), while there are in general several possible paths in a looped network (also called 'multiply connected'), Fig. 4.6b. (We have repeated Fig. 3.19

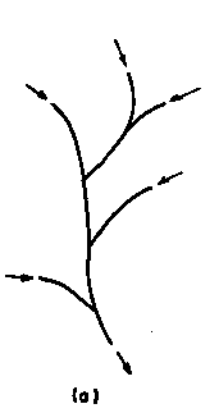

(a)

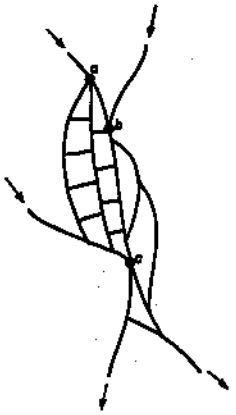

(b)

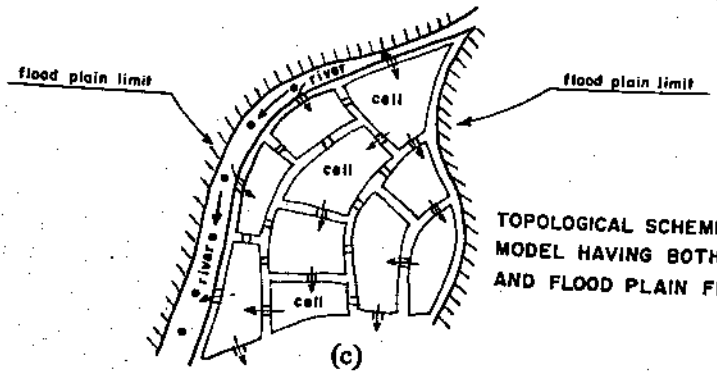

(c)

TOPOLOGICAL SCHEME OF A MODEL HAVING BOTH RIVERINE AND FLOOD PLAIN FLOW.

TOPOLOGICAL SCHEME OF A MODEL FOR NAVIGATION STUDIES

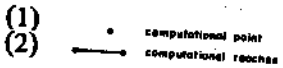

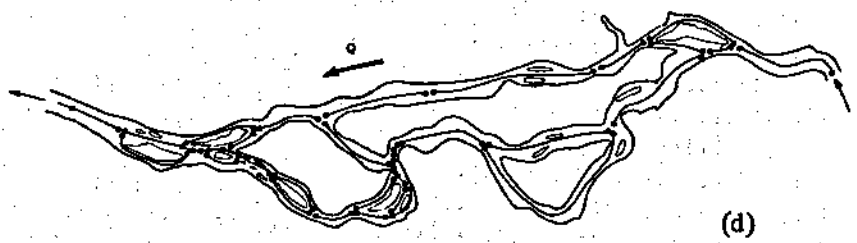

(d)

Fig. 4.6. Illustration of different topological schemes: (a) simply connected network; (b) looped network; (c) two-dimensional looped model; (d) one-dimensional looped model, (1) computational point, (2) computational reach

here for the sake of clarity.) As shown in Fig. 4.6c, two-dimensional flow over flood plains is usually modelled as a looped network of cells, for which an efficient solution algorithm using the simplified flow equations has been available for some time (Preissmann and Cunge, 1968). Efficient solution algorithms for complete-equation one-dimensional flow have also been available, but only for branched networks (Preissmann, 1961). As long as there was no interaction between the two types of flow, they could be combined in one overall simulation model; this would be the case when, for example, flood waters overflow the channel banks and never return to the main channel. But if there was river-flood plain interaction including return flow, Fig. 4.6c, or if the channel flow itself was looped, in that parallel flow paths existed, Fig. 4.6d, the two types of flow could not be treated in a single model based on a unique, implicit algorithm. It is not difficult to program a looped solution algorithm using an explicit finite difference scheme, and indeed, such modelling systems do exist (for example, the one described by Balloffet *et al.* (1976)), but such schemes are generally far too costly for current engineering applications.

In the mid-1970s economic solution algorithms for the solution of the full inertial equations in looped networks using implicit methods began to appear. This marked an important point in the history of river modelling, because for the first time the hydraulic engineer could construct models in which both one-dimensional channel flow (possibly looped), and two-dimensional flood plain flow could be simulated economically using a unique algorithm.

4.4 TOPOLOGICAL DISCRETIZATION

Whether the engineer uses a one-dimensional, two-dimensional, or mixed model, he cannot expect to obtain useful results unless his representation of physical reality by model elements is correct. The need for correct representation intervenes at two levels of the model construction process, which for lack of better terms we call *topological discretization* and *hydraulic discretization*. Topological discretization refers to the process of selecting the kinds of model elements which will be used to represent nature; one-dimensional channel links, two-dimensional flood plain cells, hydraulic structures, looped or branched networks, etc. Hydraulic discretization refers to the detailed hydraulic and topographic descriptions of flow cross sections, flood plain cells, weir characteristics, etc., as well as the choice of appropriate hydraulic equations. In this section we consider some of the more important aspects of topological discretization and in Section 4.5 we consider hydraulic discretization.

In Section 4.3 we spoke as if certain problems were evidently either one-dimensional or two-dimensional. But this is rarely the case. Nature is in fact three-dimensional, and the engineer can only use his judgement and experience in deciding which portions of his river system should be modelled as one-dimensional and which as two-dimensional flow.

We defined one-dimensional flow in Section 4.3 as flow which follows a preferential direction in a confined channel, modelled using the Barré de St Venant equations which include inertial effects. In one-dimensional modelling the inundated areas along the main channel must be represented in a way which is consistent with the fact that only one spatial coordinate, x (which follows the main channel axis), is considered. We defined two-dimensional flow in Section 4.3 as flow which is not confined to a preferred direction. Two-dimensional modelling of inundated plains takes into account the two horizontal space coordinates x, z in a discrete manner, in simulating flooded areas as a complex network of storage cells defined by roads, dykes, etc., and exchange links between cells. Since velocities are usually small, inertial forces can be safely neglected in the hydraulic flow equations for links between cells.

Topological discretization begins with the definition of zones which should be modelled as one-dimensional and two-dimensional flow. The modeller must assemble maps, aerial photos of the river basin, and field observations, and decide how the physical system will be represented in his numerical model by assigning computational points and storage cells to channel and flood plain zones. Then he must establish the ways in which the various points and cells communicate hydraulically, and based on this determination he can assign to the communication links appropriate flow elements chosen from the arsenal of elements available in the modelling system software he is using; fluvial reaches, weirs, singular head losses, flood gates, spillways, etc. In this sense it is really artificial to think of topological and hydraulic discretization as being two different activities, since the modeller cannot possibly design his model topologically without considering the hydraulic characteristics of the river and its flood plain. Put another way, no amount of cheating in later hydraulic discretization can compensate for errors made in the initial topological discretization. For this reason we treat 'topological' and 'hydraulic' discretization as separate concepts for description purposes.

If in most situations purely one-dimensional models are used, it is because two-dimensional ones have historically been either too difficult or too expensive to construct. It is fortunate that most often the overall results of these models do not seriously differ from reality, although they cannot always reproduce complicated details of flow which are all but one-dimensional.

Let us consider a flood wave propagating along the river valley as shown in Fig. 4.7: during the rising flood, the positive wave advancing along the river will have higher celerities and higher stages along the thalweg. Thus, there will be a transverse slope which will fill up the inundated plain with water, Fig. 4.7a, c. Clearly the same water stage will not occur simultaneously in the main channel and on the inundated plain. During the falling flood, the inverse situation will be observed: the main channel will tend to drain first and the transverse slope will then cause water to flow from the inundated plain back into the main channel, Fig. 4.7b. But the consideration of flood propagation in one dimension as described by the de St Venant equations written for non-prismatic channels implies that the transverse slope is nil (horizontal water surface) and the water

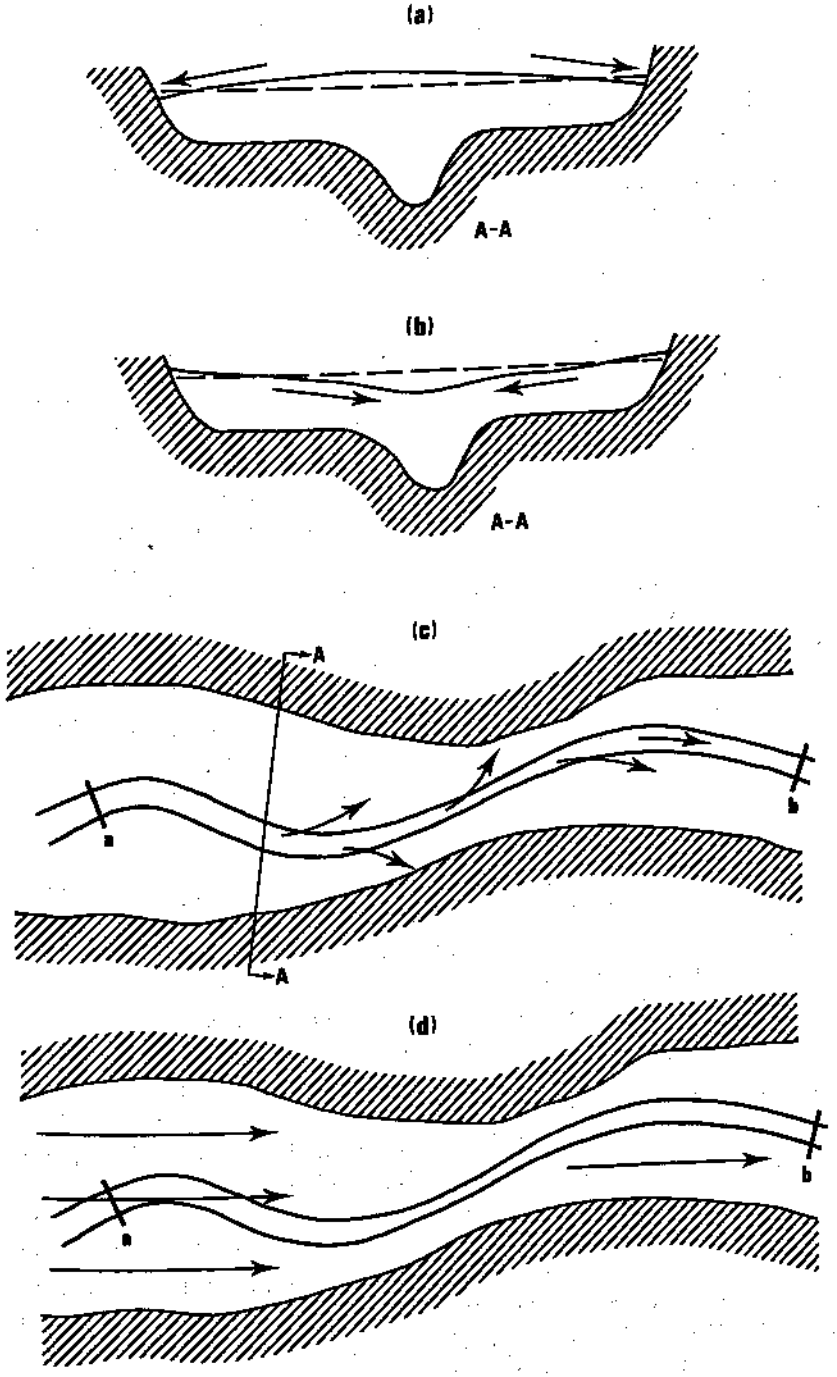

Fig. 4.7. Channel and valley flow in one-dimensional models. (a) Rising flood; (b) falling flood; (c) beginning of overbank flow; (d) high flood valley flow

velocity is uniform within the cross section. Thus one does not, when using the de St Venant hypotheses compute the actual local velocity u and water elevation y since, in reality, they both vary within the cross section. The use of the average water velocity $\frac{Q}{A}$ also falsifies the kinetic energy term $u\frac{\partial u}{\partial x}$. The exchange of momentum across the banks (between the main channel and the adjacent valley) is not taken into account at all (*see* Myers, 1978), and the conveyance K is assumed to absorb many physical phenomena which are not represented in the basic relations. As long as the main channel banks are not overflowed, the de St Venant hypotheses are reasonably well satisfied. This is also the case when water stages are very high; then, if the valley width is limited, there is no great difference between the average velocity and the local water velocities within the section. The general flow direction is then such as shown in Fig. 4.7d and the main channel is nothing but a deep trench in the middle of the valley section, a trench which slightly increases the flow capacity but is of no great importance compared to the overall flow conveyance.

For these two extreme cases (less-than 'bankful' flow or fully valley flow) one-dimensional schematization is reasonable; however, the distance between two computational points a and b as shown in Fig. 4.7 will be much smaller during floods than at 'bankful' flow. Hence, if the same model is used to simulate both cases, the flood wave propagation speed and longitudinal bed slope will be wrong in one or the other of the two situations. Between the extreme cases is the intermediate case, which is also the most common situation encountered. Here the flow patterns during partial inundation and drainage of the valley, and the momentum exchange mechanisms which result, bear little resemblance to what we call one-dimensional flow.

Another remark relating to one-dimensional models concerns the use of fictitious physical parameters to compensate for model inadequacy. For example, the velocity u is sometimes computed from the discharge Q and a wetted area corresponding to a fictitious 'active width' instead of the full width (*see* Chapter 2). Some modellers replace real sections and reach lengths by fictitious ones in order to obtain better coincidence between computed and observed values in flow situations which the basic equations were not designed to handle in the first place. This kind of tinkering is justified only if the modeller has a good understanding of the limits of application of his fictitious representation of reality, and of how the model responds to it. Such an understanding is especially important during model calibration, during which it is incumbent upon the modeller to test the sensitivity of his model to individual fictitious parameters (*see* Chapter 5).

In summary, then, one-dimensional schematization may be perfectly acceptable for engineering purposes if one is not interested in differences in free surface elevations and discharges across the flooded valley, and if these differences are small enough that the flow can still be considered to be confined to a preferential direction. Sometimes it is possible to improve the topological representation of a channel-flood plain system while staying within the overall framework of a one-dimensional model. One example is the use of storage 'pockets' which model

flooded areas adjacent to the main channel, as described further on in this section.

There are many cases in which the engineer's primary interest is focused on the flood plain itself. A typical example is the study of highway crossings of wide flood plains. The highway structure blocks the valley except for bridge openings, and the flood plain flow pattern can be profoundly transformed. Other such examples are flood protection and flood insurance studies, reclamation and dyking projects, backwater effects of dams and tributary junctions, etc. In these cases, it is a question of studying the flow adjacent to and dependent on flow in the main channel; moreover it is usually a two-dimensional problem, since one is precisely interested in transverse variations of water surface elevation. The de St Venant equations are inapplicable to this problem.

As an example, consider Fig. 4.8 showing a more complete photo of a portion of the flooded valley of the Adour river in southwestern France, *see* Fig. 4.3. Such a system cannot be simulated by a one-dimensional model alone, since water exchanges between flooded areas and the main stream cannot be defined within a one-dimensional framework. It should be stressed that if one is interested not in the flooded reach shown in Fig. 4.8, but rather in the flood hydrograph 50 km downstream, a one-dimensional model is still possible, but obviously its results along the reach shown would be false insofar as flow details are concerned. Thus for this system one can imagine two possible discretizations: a one-dimensional, branched model as sketched in Fig. 4.8 or a two-dimensional, looped one, Fig. 4.9a, b.

The Cambodian rice paddies as shown in Fig. 4.5 represent a two-dimensional looped network of links with dyked water storage reservoirs which cannot be reproduced by any one-dimensional model. The water depths are, however, small, and so is the flow velocity. The flood lasts a long time: it rises and falls slowly and the influence of inertial forces is negligible as compared to that of the water surface slope. Thus the two-dimensional system of equations, as developed in Chapter 2, may be used here. A portion of the Mekong Delta model (UNESCO/SOGREAH, 1964) is shown in Fig. 4.10. Such a schematization corresponded to the technical possibilities of the 1960s, and was acceptable even though the Mekong river itself flows through the modelled region, since the flood variations in the river are very slow.

In Section 4.3 we drew a distinction between branched and looped models, a distinction which was historically necessary because of the fundamentally different calculation problems presented by the two cases. But there are important hydraulic differences as well between branched and looped models. All two-dimensional models are looped since, by definition, the flow may circulate through the links in any direction. One-dimensional models may be branched or looped. Consider Fig. 4.11a; at first glance it would appear to be a looped model. But in reality it all depends on the conditions imposed at the power plant. The discharge continuity condition implies that if the discharge through the turbines is imposed as a function of time, then our model of Fig. 4.11a can

Fig. 4.8. Adour River (France) main channel and flood plain with one-dimensional discretization (courtesy SOGREAH)

(a)

(b)

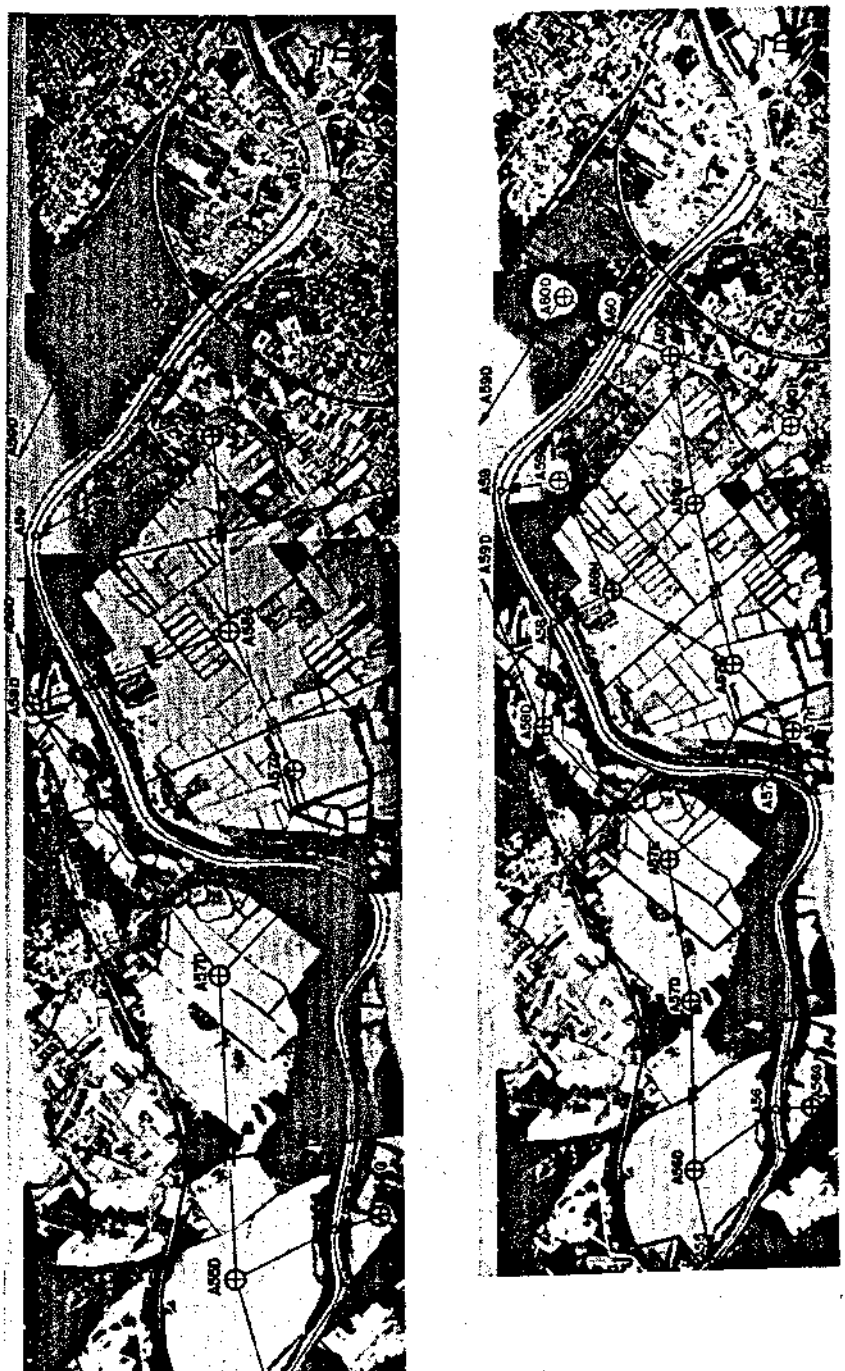

Fig. 4.9. Adour River alternative discretizations: (a) two-dimensional looped model; (b) alternative two-dimensional looped model (courtesy SOGREAH)

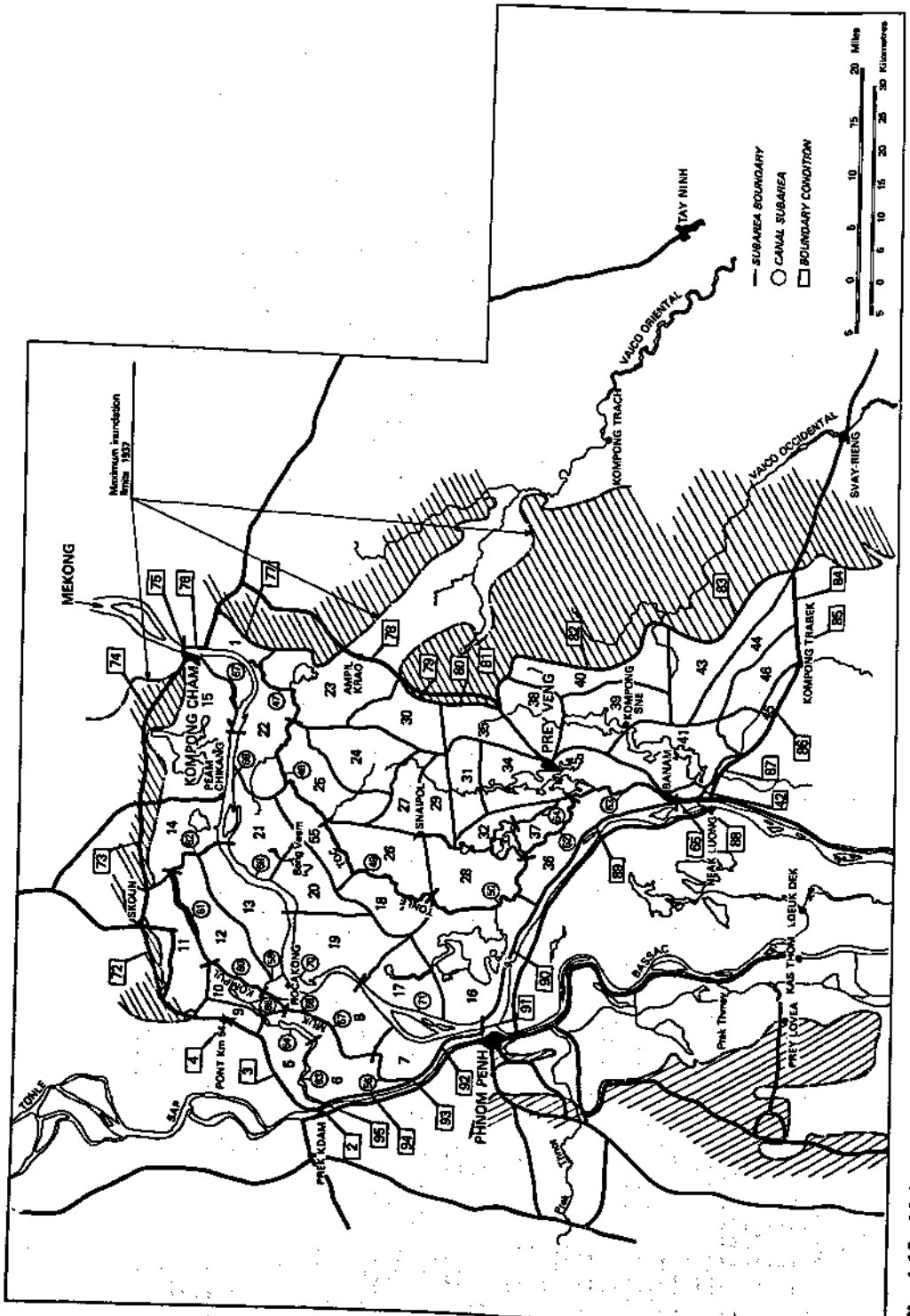

Fig. 4.10. Mekong River model — left bank (courtesy UNESCO): (a) physical location of computational cells

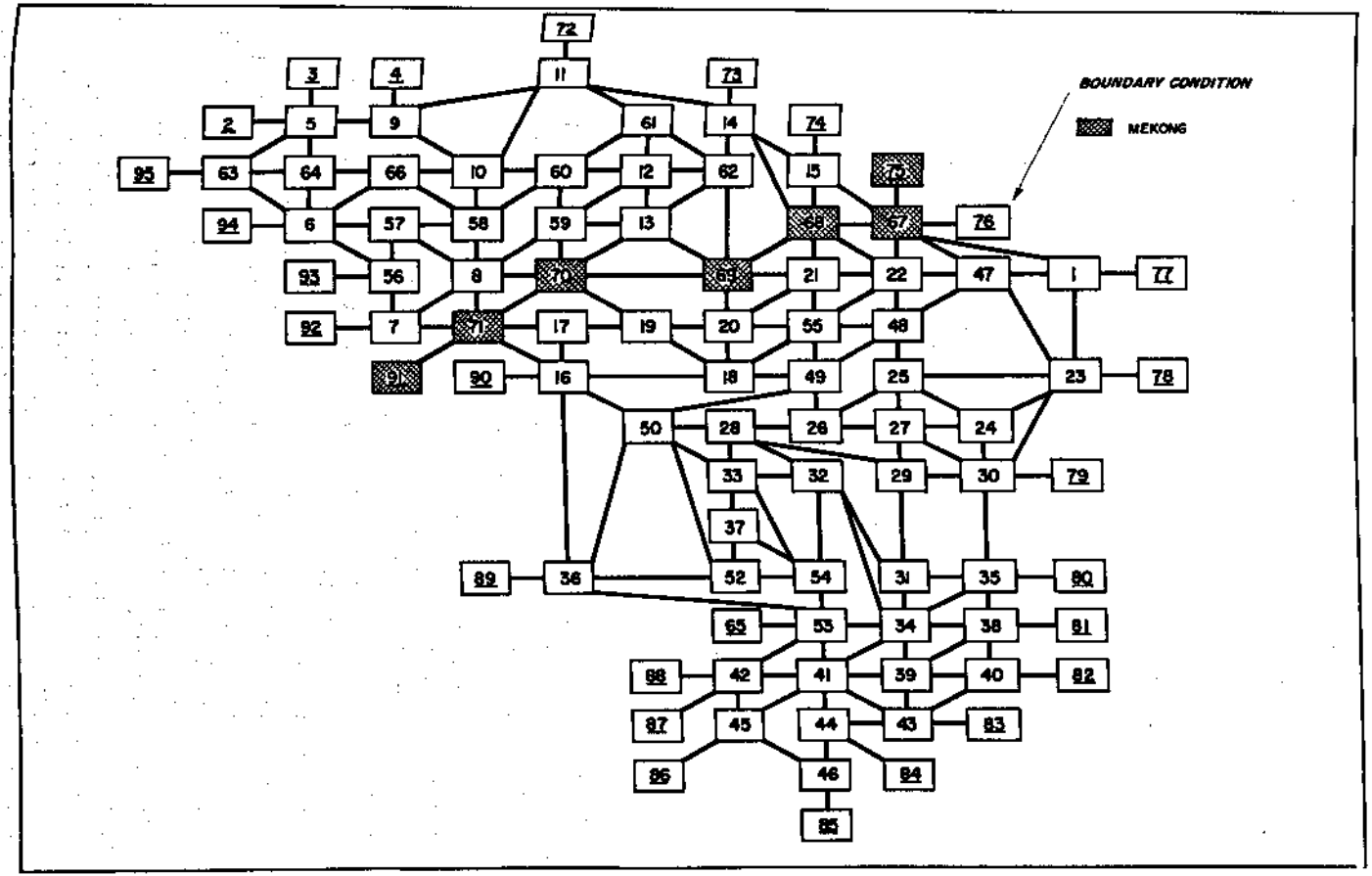

Fig. 4.10. Mekong River model – left bank: (b) topological breakdown of computational cells (courtesy UNESCO)

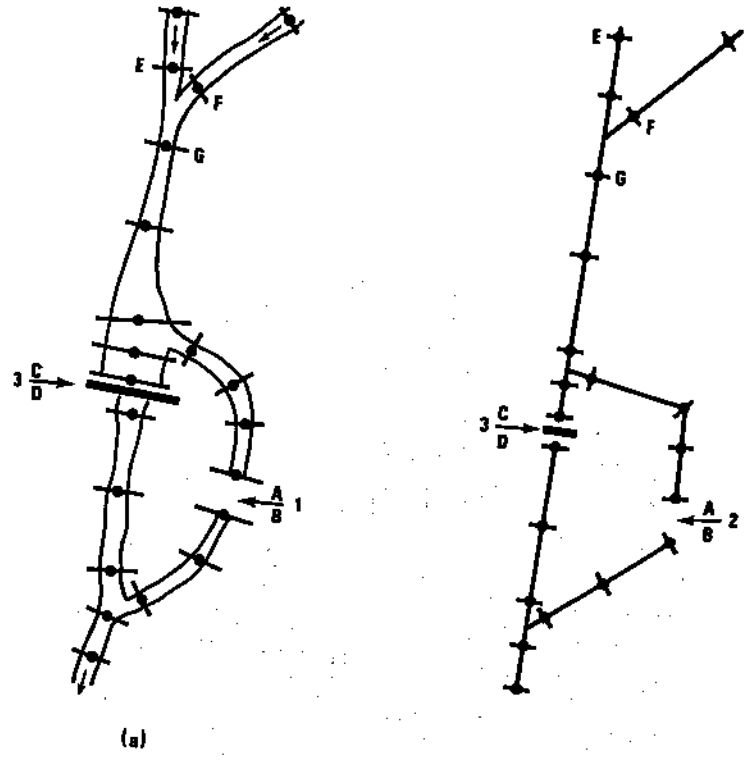

Fig. 4.11. Example of apparent looped model which is in fact branched. (a) Physical situation. (b) Topological model representation: (1) power plant; (2) boundary conditions $Q_A = Q_B = Q(t)$; (3) dam

be represented schematically as shown in Fig. 4.11b. Thus in reality the model is branched. Such is not the case for the model shown in Fig. 4.12. This model is still one-dimensional but there is no possibility of using a branched topology since the flow on both sides of the island depends on conditions upstream and downstream of it, nodes A and B.

Some engineering projects require detailed modelling of looped networks of natural channels in which the flow velocity varies rather quickly, and the de St Venant equations must be used, as in navigation studies of large rivers (Fig. 4.6d) or deltaic channels influenced by tidal fluctuations. Now that techniques for constructing and running economical looped models exist and have been industrialized, such systems can be correctly simulated.

Unfortunately it is most often the case that, within the same modelled area, one encounters some regions where inertial forces can be neglected, others for which such simplification is not possible. Moreover, considering river flow, inertial forces must usually be taken into account along extensive reaches of one-dimensional flow which communicate with vast areas of two-dimensional

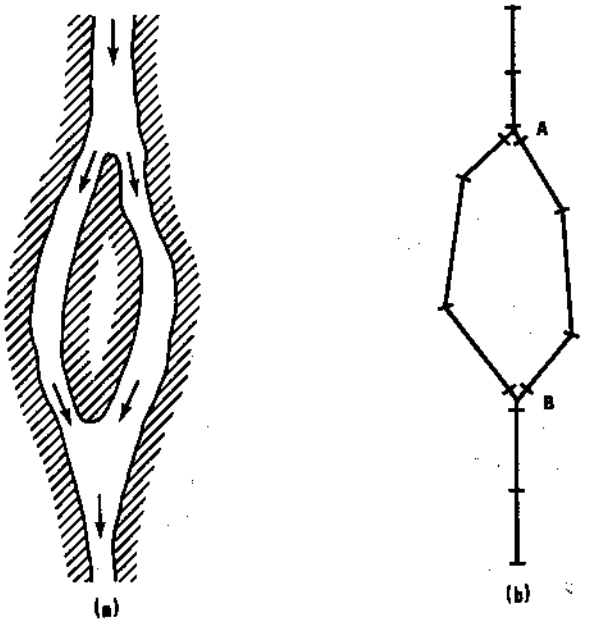

Fig. 4.12. Example of physically looped model. (a) Physical situation. (b) Topological model representation

inundation where inertial forces are small. Topological discretization thus implies also the process of determining how to link overbank, flood plain, and channel flow. When a cross section has a composite shape as shown in Fig. 4.13, this shape may be associated with two different plan views of the river, as shown in Fig. 4.14, and for both of which there can be two different free surface levels within the same cross section as shown in Fig. 4.15.

With respect to Fig. 4.14a it may be seen that this is essentially a one-dimensional situation. Indeed, the areas marked by 2 are really storage 'pockets' linked with the main stream through some sort of a law (e.g. a weir equation), but separated one from another. Such a situation may be topologically schematized as shown in Fig. 4.16a. The situation depicted in Fig. 4.14b

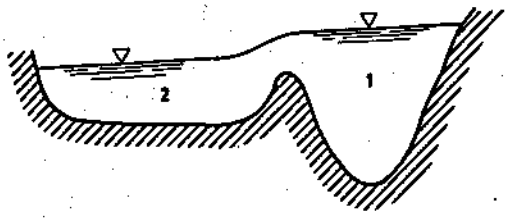

Fig. 4.13. Composite channel cross-section. 1, Main channel; 2, Flood plain

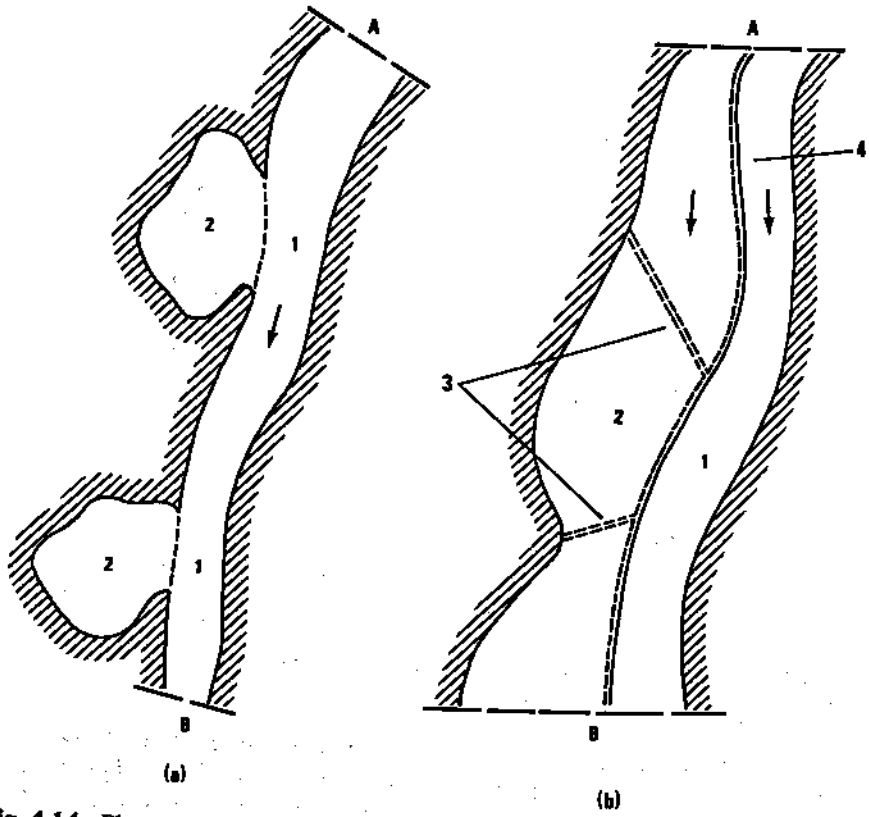

Fig. 4.14. Plan view of composite channel discretization. (a) One-dimensional channel with storage pockets. (b) Mixed one-dimensional and two-dimensional model: (1) main channel; (2) storage areas; (3) ditches, roads, transverse dykes; (4) main channel banks

however is essentially two-dimensional. It may be simulated as shown in Fig. 4.16 either by a combination of a one-dimensional inertial reach and two-dimensional inertia-less reach, Fig. 4.6b, or when the inertia terms are not negligible within the storage areas by a one-dimensional looped network

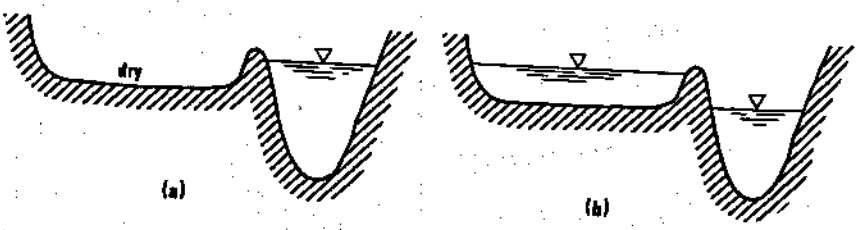

Fig. 4.15. Possible water surface differences in composite section. (a) Rising flood. (b) Falling flood.

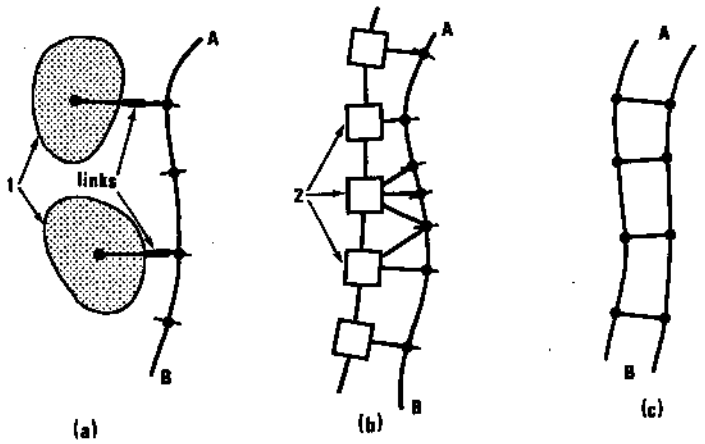

Fig. 4.16. Possible schematizations of Fig. 4.14. (a) One-dimensional model with storage pockets. (b) Combined one-dimensional inertial plus two-dimensional non-inertial model. (c) Looped one-dimensional inertial model: (1) storage pockets; (2) two-dimensional cells

Fig. 4.16c. What must be stressed is the general notion that the schematization of a given real-life situation is seldom unique (e.g. as in Fig. 4.9). Most often there are many possibilities and even if for a given situation there are good and bad solutions, there is probably no *one* best way.

In composite models containing channel and flood plain flow, it is important to model correctly both the overflow of flood waters from the channel to the flood plain and the exchanges between flood plain elements along the valley. In the case of massive inundation, where water completely fills the flood plain and the water level is nearly horizontal across the valley, the error induced by improper exchange laws will not be significant as far as filling up of the flood plain is concerned. But in the case of a minor event such as a 5-year flood, where channel flow is only moderately higher than bankful and the flood plain is only partially inundated, simulation results (in terms of extent of flooded area, for example) can be quite sensitive to the channel overflow representation used. In the following paragraphs we give a few examples of the kinds of difficulties which come up in such representations.

When overflow occurs only at well defined locations where the bank is particularly low or where controlled overflow spillways have been built into the levee, the physical situation clearly dictates the appropriate model representation. In most cases a weir section is called for, as shown in Fig. 4.17. In such a situation the weir section in the model would be given the crest elevation, width, and discharge coefficient which correspond to the physical situation as closely as possible. As long as the overflow section is relatively short compared to the river length over which a significant water surface elevation change occurs, then it is appropriate to base the weir discharge calculation on the unique water level at A (and at B, if the weir is flooded).

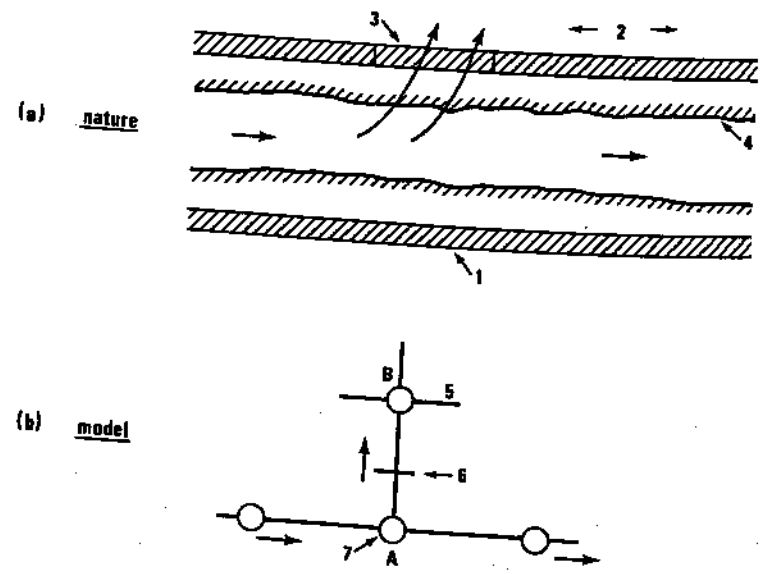

Fig. 4.17. Model representation of localized levee overflow. (a) Physical situation. (b) Model representation: 1, levee; 2, flood plain; 3, overflow section; 4, channel bank; 5, cell; 6, weir section; 7, fluvial calculation point

A more difficult modelling situation occurs when there are no well defined overflow sections, the bank or levee elevations being at a more or less consistent height above the channel bed. Overflow then occurs as a general shallow spilling from channel to flood plain, which in spite of its continuous (with respect to longitudinal river distance) character must be discretely modelled, and this is where problems arise. The physical situation is schematized in Fig. 4.18a, b. If measured cross sections are available at short intervals, and if there is no practical limit on the number of points in the model, the modelling option shown in Fig. 4.18c is appropriate. The fluvial computational points are spaced close enough together so that the drop in water level between them is small; each point is linked to a flood plain cell by a single rectangular weir whose crest elevation is the same as the average bank or levee elevation along the channel length attributed to the computational point. In this way the flow depth on each weir corresponds roughly to the physical flow depth across the bank or levee.

It may not always be possible, however, to introduce enough fluvial points to correctly model the overflow in this fashion. Measured cross sections may be few and far between and the total number of points in the model may be limited by program capacity or economic constraints. In such cases one might be tempted to retain the basic scheme shown in Fig. 4.18c but with several kilometres between computational points, so that each weir would be several kilometres wide at a single crest elevation. This is very dangerous, not only because the details of the filling up of the flood plain are lost, but also

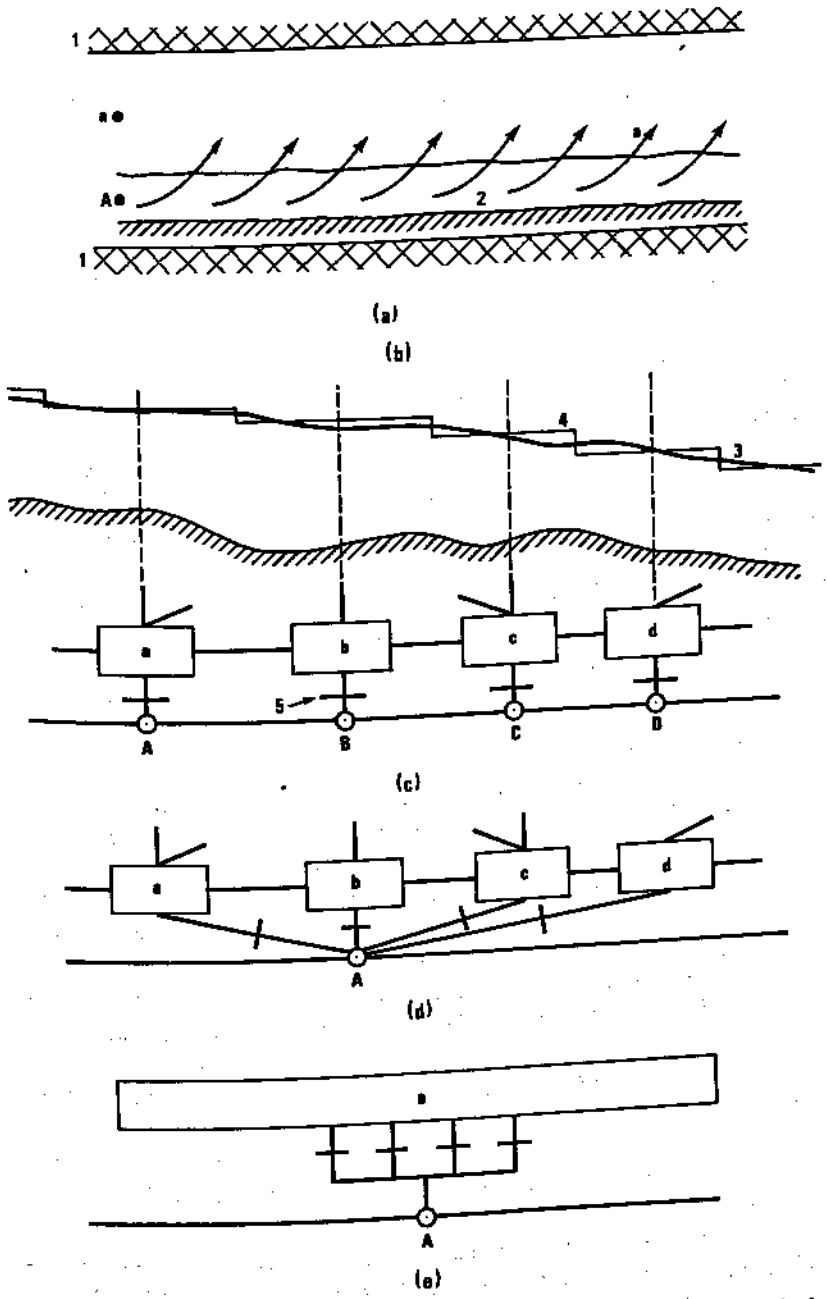

Fig. 4.18. Model representation of generalized levee overflow. (a) Physical situation – plan view. (b) Physical situation – longitudinal section. (c) First model representation, plan view. (d) Second model representation, plan view. (e) Third model representation, plan view: 1, flood plain limits; 2, river; 3, physical bank elevation; 4, discrete weir elevations; 5, rectangular weir sections

because it introduces a potential computational instability. Imagine that during a simulation using a fairly large time step, the water level at a fluvial point passes from 10 cm below the weir crest at time step n to 10 cm above the crest at step $n + 1$. Such an increment in the surface elevation is quite normal for a typical computational time step of, say, 2 h. If the weir is several kilometres wide, this seemingly innocuous depth of 10 cm may correspond to a tremendous discharge which, pouring into a nearly dry cell, may cause the cell water level to jump much too high, falsifying continuity and possibly destroying the calculation if iterations are not used (*see also* Section 4.6).

The best way to avoid this problem is to try if at all possible to have closely enough spaced computational points so that no individual weir discharge can be very large, even if it means interpolating between known cross sections to create artificial computational points. If there is no alternative to having widely spaced points, the second modelling option shown in Fig. 4.18d will at least avoid computational instabilities; the bank or levee is modelled as a series of small rectangular sections at different crest elevations as in Fig. 4.18b. Then either each weir section serves as a link between the single fluvial computational point A and a particular cell a, b, c, or d, Fig. 4.18d, or the unique link between the point A and a single large flood plain cell a, comprises the several different weir sections, Fig. 4.8e. The important thing is to avoid a situation in which a small increase in water surface elevation in the river could provoke a sudden large discharge to the flood plain, since it is not only dangerous for the computation but also false physically.

The cost of this multiple-weir alternative in terms of model accuracy is nothing less than the complete falsification of the details of flood overflows. In Fig. 4.18c, overflow would normally progress in time from cells a to d as the flood wave travels down the river from A to D. But in Fig. 4.18d, the weir from A to d will be first to flow, as it has the lowest crest elevation, so that in the model the flood plain will first receive water in the downstream portion instead of the upstream portion as in nature. This being the case, what then is the sense of breaking the flood plain into several cells, since the flow details cannot be correct in any case? A single cell linked to a single computational point, as in Fig. 4.18e, is a much more consistent compromise which makes no illusion about being able to model the details of overflow, while correctly simulating gross flood plain volume and avoiding possible computational troubles.

A final point concerns dynamic effects. In all of the preceding discussion we have been assuming that a frontal weir between the river and flood plain can successfully model what is really a lateral weir situation, in which overflow discharges depend on both the water level *and* the velocity in the river. The modeller must not forget that he has ignored these effects in the model, and accordingly he needs possibly to adjust weir coefficients and widths to account for the approximation.

The important thing to remember in modelling channel-flood plain overflows is that if one wishes to simulate not only the volume, but also the localization of overflows, he must have closely spaced fluvial computational points. If on the

other hand only the volume of overflow is of interest, much more widely spaced points with multiple-weir links to the flood plain are adequate. The channel overflow example shows how artificial is our division of schematization problems into 'topological' and 'hydraulic' ones. Indeed, while discretizing the modelled domain one has to keep in mind at all times the hydraulic consequences. To complete the description of the weir-like link given above, one has to think of the exceptional event, when the whole valley cross section is filled up and the water flows along a common valley axis. In that situation the head loss between the points A and a in Fig. 4.18a is very small indeed, while it may have been very important at low levels. The schematization must not hamper the representation of these differences and, moreover, the adopted weir discharge law must have a general physical form which retains its validity during extrapolation to high floods.

The above discussions of schematization problems are only examples of a multitude of such problems which come up during the planning and construction of a mathematical model. It is by no means our intention to furnish a catalogue of solutions to such problems. What we want to emphasize is that topological discretization represents a trade-off between the user's need to represent nature as faithfully as possible on the one hand, and the built-in limitations of discrete modelling techniques on the other hand. The more correct the topological discretization, the freer will be the user to concentrate on physical, hydraulic aspects of his model during hydraulic discretization.

4.5 HYDRAULIC DISCRETIZATION

One-dimensional modelling requires that a series of so-called computational points be selected along the water course. The flow equations (for example, de St Venant or simplified equations) represent hydraulic laws according to which the flow variables (discharge Q, velocity u, free surface elevation y, etc.) are related from one point to another. Thus, for a natural river reach which approximately satisfies the basic de St Venant hypotheses, and for a numerical scheme defined on only two computational points, a finite difference approximation to the flow equations can be given between two points a and b distant Δx_{ab} one from another as in Fig. 4.19a. Each of the points may be then considered as representative of an elementary physical reach of length, say, $\frac{1}{2}(\Delta x_{ab} + \Delta x_{bc})$.

It is not always possible, however, to consider the de St Venant equations as representative of the change of flow variables between two computational points, even in a one-dimensional situation. This is obviously the case for cross-channel weirs, power plants, etc., but a more subtle example is a sudden increase in cross-sectional area over a short length, Fig. 4.19b. The appropriate law governing the flow between points b and c is not the dynamic equation, but a relation for singular head loss. In such a case point b must be representative of the reach Δx_b rather than Δx_c, and the singular head loss law between b and c must be explicitly specified.

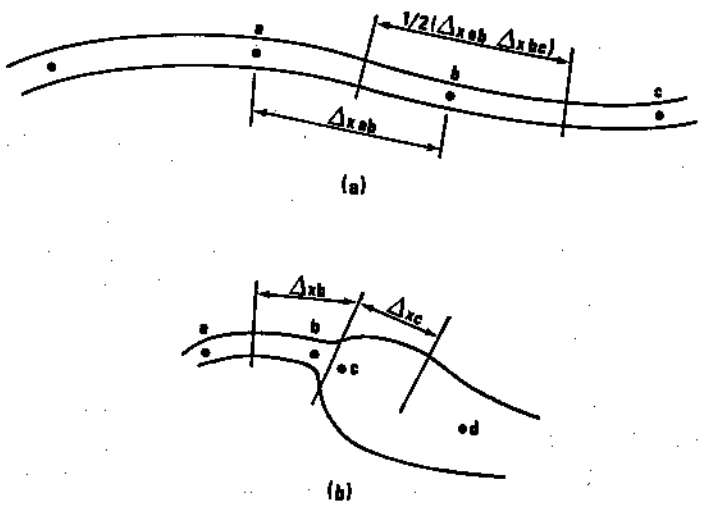

Fig. 4.19. One-dimensional discretization: (a) reach over which the de St Venant equations apply; (b) treatment of singular head loss

Thus each computational point must correspond to a cross section which is representative of the reach of length Δx, and the modeller must define this section in such a way that it represents as faithfully as possible all the important topographical and hydraulic features of the reach. For gradually varied unsteady one-dimensional flow, these features are:

cross-sectional area
width
conveyance
} as functions of water level

The topographical features of the reach must be defined in such a way that the volume of water within the reach will be correctly represented and the wave propagation speed, which depends notably on the width, will not be biased. An essential requirement from this point of view is the correct emplacement of computational points. Rozenberg and Rusinov (1967) demonstrated clearly a consideration which would seem obvious but has not always been respected: the computational points must be chosen in such a way that the channel and flood plain width variation along the river be accurately represented (Fig. 4.20). The importance of this consideration is that it is the width which most influences the wave propagation speed, and yet one is often tempted to replace such a reach by a fictitious one whose constant but artificial width is assigned on the basis of volume considerations alone (Fig. 4.21). This type of simplification can completely distort the true wave propagation speed through the reach. A related notion is the use of an 'active width' (*see* Chapter 2), which should not be adopted without special precautions and careful analysis of the possible consequences of such a decision as explained in Chapter 5 regarding the calibration of models.

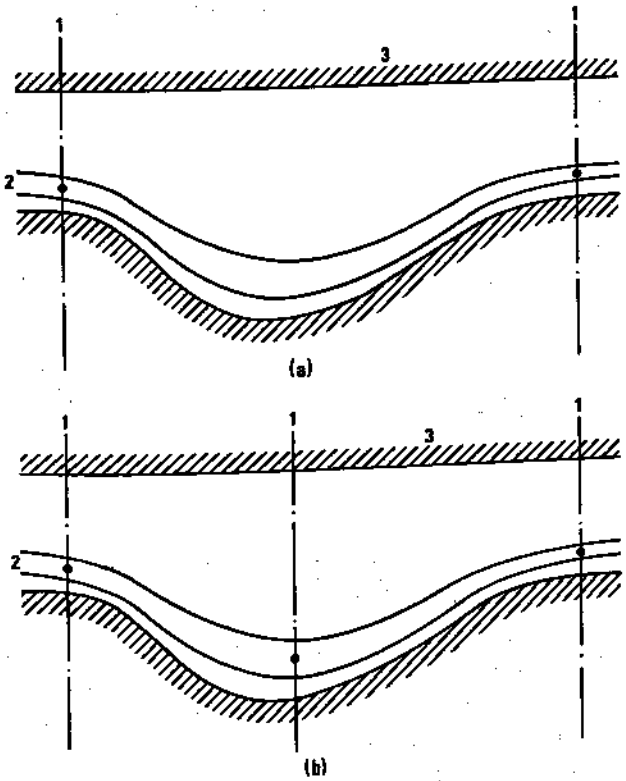

Fig. 4.20. Emplacement of computational points so as to represent flood plain width correctly. (a) Incorrect. (b) Better: 1, computational point; 2, channel; 3, flood plain limits

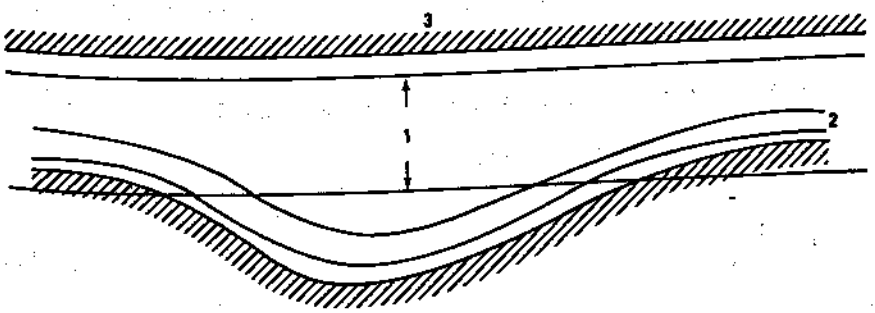

Fig. 4.21. Use of fictitious width to represent average valley width—wrong! 1, Fictitious reach limits; 2, channel; 3, real flood plain limits

Of course computer storage and cost limitations induce the user to minimize the number of computational points, and moreover one does not always have

sufficient field data on which to base a large number of points. Nevertheless the user must always be aware of the need to incorporate true reach characteristics in the computational points he selects. A somewhat amusing but very real danger is that cross-sectional data may exist only for the narrowest, most confined section of a river, since these data are easiest to measure in such cases (Fig. 4.22).

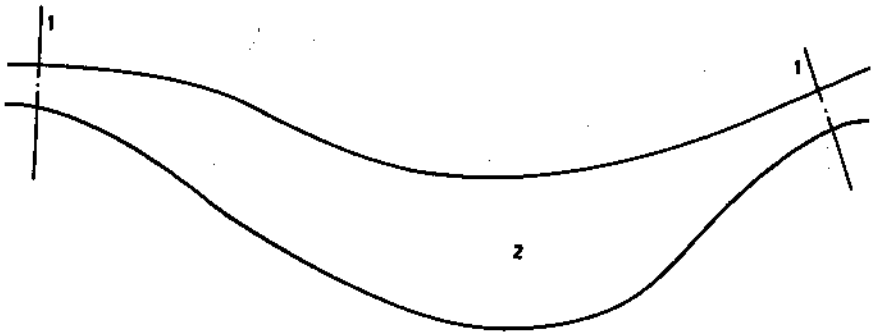

Fig. 4.22. Emplacement of computational points at narrowest parts of valley – wrong! 1, Measured cross sections; 2, Channel

Obviously a model based only on these measured cross sections would only remotely resemble the real river, not only in terms of celerities but also in terms of volume. The user must always use aerial photographs, maps, and field visits if necessary to verify that his measured cross sections are truly representative of the actual river.

The hydraulic features of the river reach represented by the computational point are generally lumped into the resistance term of the dynamic equation as we described in Chapter 2. This resistance term is of utmost importance because it is based on an empirical law and as such is the only truly 'adjustable' term during model calibration. For steady flow, the discharge Q can be expressed as

$$Q = K\,(S_f)^{\frac{1}{2}} \tag{4.1}$$

where: K = conveyance factor; S_f = slope of the energy line, $S_f = -\dfrac{\mathrm{d}}{\mathrm{d}x}\left(y + \dfrac{u^2}{2g}\right)$; y = water surface elevation; u = velocity.

The energy slope in the dynamic equation can then be replaced by

$$S_f = \frac{Q\,|Q|}{K^2} \tag{4.2}$$

The meaning of the conveyance factor K when the most often used empirical laws are adopted is given in Equations (2.38)–(2.45).

In practical application the function $K(y)$ may absorb all kinds of head losses such as those due to groins, unidentified singular losses, etc., which is a rather dangerous situation. Modelling systems should always have the capacity to represent the most important of these kinds of losses by special features and not

try to represent them by conveyances, lest the predictive capability of the function $K(y)$ be lost. It is always useful to be able to introduce a singular head loss proportional to $u^2/2g$.

The overall conveyance factor for a cross section is a function of the depth, and may incorporate transverse variations of roughness in a single channel as well as the dependence of the roughness coefficient on depth as observed in some rivers. As described by Chow (1959), the total section conveyance can be considered to be the sum of the conveyances in several subsections (Fig. 4.23),

$$K(y) = \sum_{i=1}^{m} K_i = \sum_{i=1}^{m} k_{\mathrm{Str}_i} A_i R_i^{2/3} \tag{4.3}$$

where: m = number of subsections, each of which has its own distinct roughness characteristics. Thus the function $K(y)$ can be tabulated for each computational point.

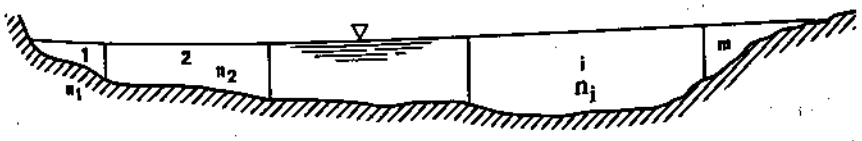

Fig. 4.23. Division of natural cross section into discrete elements

It is only by treating the conveyance factor in this manner that we can obtain predictive capacity in a model. Let us consider the simple cross section shown in Fig. 4.24. We shall represent the conveyance in two different ways, first using Equation (4.3) and then Equation (4.4),

$$K(y) = \overline{k}_{\mathrm{str}} \overline{A}\, \overline{R}^{2/3} \tag{4.4}$$

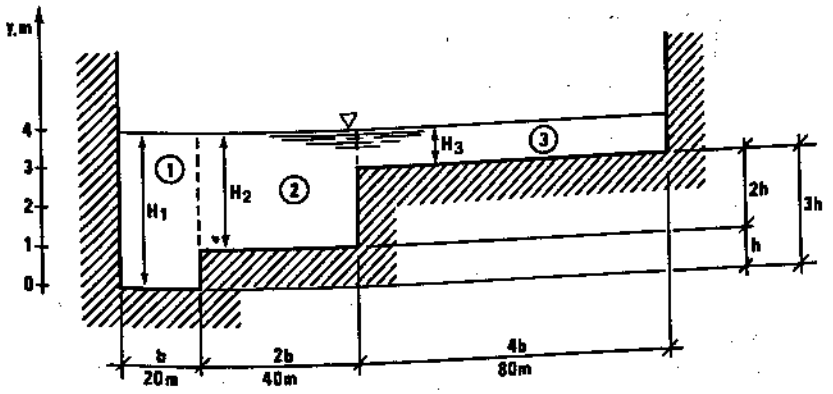

Fig. 4.24. Simplified cross section composed of three rectangular elements

in which we assume that $\bar{k}_{str}$, $\bar{A}$ and $\bar{R}$ correspond to the whole section.

For the application of Equation (4.3), we assume that the Strickler coefficients k_1, k_2, k_3 are representative of the bed materials in each subsection; for example $k_1 = 35, k_2 = 30, k_3 = 20$. Then, using Equation (4.3) and putting $b = 20m$, $R_l = H_l$, $h = 1$ m, we can construct Table 4.1 and calculate the $K(y)$ function.

If we were reasonably confident of the roughness values k_1 and k_2, perhaps because we had past observations of flows which did not exceed $y = 3$ m, we would not hesitate to sum up the section 1 and 2 conveyances up to $y = 3$ m, and consider this sum as representative of the entire section. But we might hesitate to continue our calculation above $y = 3$ m because of uncertainty as to the value of k_3, which in our simplified section represents the overbank section or flood channel. Even though the value of k_3 is related much more to overbank vegetation and obstructions than to bed material grain diameter, we can estimate it without too much difficulty, *see* Chow (1959). If we continue our calculations above $y = 3$ m, this being the only rational way of extending the $K(y)$ function upwards, we see that slice number 3 and thus the value of k_3, has very little influence below $y = 6$ m where it contributes only 24% of the total conveyance; thus any error in the estimate of k_3 will only slightly affect the section conveyance up to that level. Obviously for higher and higher levels, the conveyance of slice 3 will become more and more dominant compared to slices 1 and 2. Figure 4.25 shows the total $K(y)$ function from Table 4.1, which may be extrapolated upwards with some confidence since it represents an integration of all three slices.

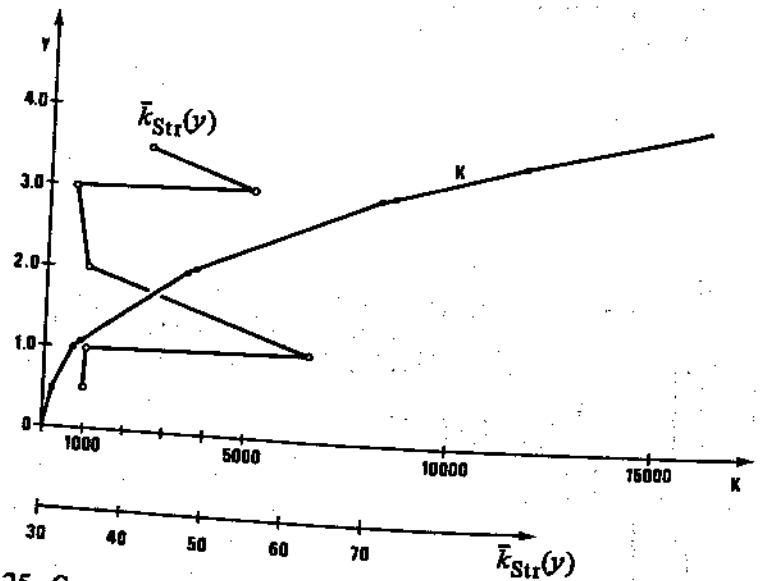

Fig. 4.25. Composite section conveyance function and corresponding global roughness coefficients

Table 4.1. *Construction of composite conveyance function using Equation (4.3)*

	Section 1			Section 2			Section 3			Total	Section 3
y m	A m^2	$H^{2/3}$	K	A m^2	$H^{2/3}$	K	A m^2	$H^{2/3}$	K	$\sum_{i=1}^{3} K_i$	% of total conveyance
0.5	10	0.63	220	0	0	0	0	0	0	220	0
1.0	20	1.0	700	0	0	0	0	0	0	700	0
1.05	21	1.033	759	2	0.136	8	0	0	0	767	0
2.0	40	1.587	2222	40	1.0	1200	0	0	0	3422	0
3.0	60	2.08	4368	80	1.587	3810	0	0	0	8178	0
3.05	61	2.103	4490	82	1.614	3970	4	0.136	10.86	8471	0.1
3.5	70	2.305	5648	100	1.842	5326	40	0.63	504	11 678	4.3
4.0	80	2.52	7056	120	2.08	7488	80	1.0	1600	16 144	9.9
5.0	100	2.92	10 234	160	2.52	12 095	160	1.587	5080	27 409	18.5
6.0	120	3.302	13 868	200	2.92	17 544	240	2.08	9984	41 396	24.1
7.0	140	3.659	17 930	240	3.302	23 744	320	2.52	16 127	57 801	27.9
8.0	160	4.00	22 400	280	3.659	30 733	400	2.92	23 392	76 530	30.6
10.0	200	4.64	32 491	360	4.327	46 729	560	3.66	40 984	120 204	34.1

Let us now consider Equation (4.4). It is not possible to estimate the *global* Strickler coefficient beyond the water elevation $y = 1$ m; indeed, if the three slices present different characteristics, how can we estimate one common coefficient? In practice, one usually knows the slopes S which correspond to several steady discharges Q. With these values one can compute a global $K(y)$ using Equation (4.1) and then, since $\bar{A}(y)$ and $\bar{R}(y)$ are known, one can find the global Strickler or Manning coefficient using Equation (4.4). Let us suppose that this method is used to compute the global $\bar{k}_{str}(y)$ values for which the conveyance $K(y)$ from Equation (4.4) would be equal to $K(y) = \sum_{i+1}^{m} K_i(y)$ from Equation (4.3) and Table 4.1. The computation is made in Table 4.2 and the corresponding curve is plotted in Fig. 4.25. Let us suppose again that one would like to extend the curve $\bar{k}_{str}(y)$ beyond the water surface elevation $y = 3$ m; we simply cannot make any such extrapolation in a rational manner. Suppose next that known, observed water surface slopes were available for water levels only up to 1.99 m. The $\bar{k}_{str}(y)$ and $K(y)$ curves cannot reasonably be extrapolated without properly taking into account the increasing influence of the slice no. 3 with increasing depth.

Table 4.2. Calculation of global roughness coefficients using Equation (4.4)

y m	ΣK_i from Table 4.1	Global $\bar{A}$ m^2	$P = b$	$\bar{R} = \frac{\bar{A}}{P}$	$\bar{R}^{2/3}$	Global $\bar{k}_{str}$
0.5	220	10	20	0.50	0.63	35
1.0	700	20	20	1	1	35
1.05	767	23	60	0.383	0.528	63
2.0	3422	80	60	1.333	1.211	35.32
3.0	8178	140	60	2.333	1.759	33
3.05	8471	147	140	1.050	1.033	56
3.5	11678	210	140	1.50	1.310	42

It is possible to compute an overall $K(y)$ function on the basis of observed steady state discharges and slopes, and use this *conveyance* function directly for the simulation of flows which do not exceed the observed range. It is quite another thing to extract global roughness values from this conveyance function and to try to extrapolate them above observed flows.

We shall come back to this question in Chapter 5, but we feel very strongly that conveyance representation using a global roughness coefficient is unacceptable in mathematical modelling, except for compact channels of nearly constant width.

Hydraulic discretization of one-dimensional models also requires that

boundary conditions be correctly imposed. Models based on the complete de St Venant equations require two general kinds of boundary conditions (*see* Chapter 2): exterior (at end points of the model), and interior. The de St Venant equations form a hyperbolic system of two non-linear partial differential equations, and the existence and uniqueness of their solution along a reach for a finite interval of time are subject to certain restrictions:

the initial conditions must be specified along the reach, i.e. all water levels and discharges must be known at time zero;

one boundary condition as a function of time must be given at each end of the reach for subcritical flow, and two conditions at the upstream end for super-critical flow.

These exterior boundary conditions are usually of three different kinds: $y(t)$, $Q(t)$ and $Q = f(y)$, and are subject to certain restrictions as described at the end of Section 2.2.

Interior boundary conditions generally express compatibility conditions such as continuity of discharge and energy level or water surface elevation. They intervene at points where the original de St Venant equations are not applicable, *see* Section 2.5. Several examples are:

- sudden variation in cross section between two reaches. We require that the discharge and energy levels (with perhaps a local head loss) be compatible;
- junction of two rivers. We require continuity of discharge and compatibility of energy levels or water levels;
- weir flow. We require that the discharge be the same on both sides of the weir, and we calculate this discharge using the free-flowing or flooded formula;
- imposed discharge as a function of time. This is the case of a hydroelectric plant or a particular reservoir operating rule;
- imposed water level as a function of time. This would be the case of a reservoir or automatic irrigation control system;
- imposed water level or discharge as a function of one or more flow variables at other points of the model. This is the case of automatic regulation used in irrigation systems or in power plant cascades.

It is again quite impossible to furnish here a catalogue of cases and solutions. Some of them are explained in more detail by different authors, usually as solved for a particular scheme (*see*, for example, Liggett and Cunge (1975), Verwey (1971)).

When we speak of interior boundary conditions, we really should note that there are two kinds: those which replace the normal flow equations by special relationships (singular head losses, junctions, flooded weirs), and those which are completely analogous to exterior boundary conditions (discharge or level imposed as a function of time). Strictly speaking, points at which these latter types of conditions are applied could be modelled as normal, exterior points; we saw in Fig. 4.11 that a power plant through which $Q(t)$ is applied can be

modelled as one point at which $Q(t)$ is withdrawn from the model, another at which the same $Q(t)$ is introduced into the model. The water levels associated with each point (one in the upstream reservoir, the other in the tailrace) need not be (indeed cannot be) specified; they are dependent variables in the overall solution of the flow equations.

For the case of water level imposed as a function of time, say in a reservoir, the situation is similar. Again referring to Fig. 4.11, imagine that $y_A(t)$ is to be imposed at point A. We can treat this point as an exterior point with $y(t)$ specified, and for each time step the model solution will yield the discharge $Q_A(t)$ which must flow out of the reservoir in order that the flow equations be satisfied. This same discharge, $Q_A(t)$ becomes the $Q(t)$ condition at point B, treated again as a simple exterior point (we will come back to the problem of how to simultaneously impose these two conditions). The same reasoning can be applied to the case of a free-flowing weir, which represents essentially a rating curve $Q_A = f(y_A)$ in our example, since the discharge depends only on the upstream water level. Point A can be treated as a downstream rating curve boundary condition, and point B as an imposed discharge condition, $Q_B = Q_A$.

Thus we see that certain types of interior boundary conditions can in principle be treated as exterior conditions, since they represent physical disconnections of the model. But from a practical point of view, it is at best inconvenient, and at worst impossible in some cases, to disconnect the model in this way. For example, how would we treat a weir which passes from free-flowing to flooded conditions during the course of a calculation? Or for the case of $y(t)$ imposed in the reservoir at A in a model based on an implicit finite difference scheme, how can we impose $Q_B(t + \Delta t) = Q_A(t + \Delta t)$ when $Q_A(t + \Delta t)$ cannot be known until the end of the time step? The solution is to treat all such conditions as truly interior ones, replacing the normal equations by whatever special ones are necessary to represent the condition. This implies that, whatever the numerical method used, we must link two points, most often located at the same or nearly the same physical location by *two* equations expressing continuity of discharge and the particular exchange law. Sometimes it is not at all easy to devise the appropriate equations for such conditions; the ease or the difficulty depends upon the modelling system, the algorithm or even the finite difference scheme used. In this respect six-point schemes, the method of characteristics, explicit schemes, and schemes which compute levels and velocities at different points present some practical difficulties (*see* Chapter 3) as compared with four-point schemes computing levels and discharges at the same sections.

As an example of the kind of situation to which the modeller must be alert in terms of hydraulic discretization, let us consider the inclusion of dynamic effects in weir computations. River flow simulation systems usually use the weir flow equations which result from neglecting the upstream approach velocity and assuming that the flow over the weir is critical in the free-flowing case, or that the water level over the weir is the same as the downstream level in the flooded case:

$$\text{flooded: } Q = \mu_1 (2g)^{\frac{1}{2}} (y_{ds} - y_w)\,(y_{us} - y_{ds})^{1/2} \tag{4.5}$$

$$\text{free flowing: } Q = \mu_2 (2g)^{\frac{1}{2}} (y_{us} - y_w)^{3/2} \tag{4.6}$$

where: y_{us} = water surface elevation on the upstream side of the weir; y_{ds} = water surface elevation on the downstream side of the weir; b = rectangular weir width; y_w = weir crest elevation; μ_1, μ_2 = discharge coefficients.

In some simulation systems it is possible to include the upstream approach velocity in the weir calculation directly; note that a velocity of 3 m s^{-1} corresponds to a velocity head of nearly 46 cm, which cannot be neglected in a weir calculation. In other systems, only the upstream water level is used in the calculation, in which case the localized error in neglecting a velocity head such as 46 cm may be unacceptable. One way to avoid this error is to create an artificial and extremely large section just upstream of the weir in which the velocity is negligible, as shown in Fig. 4.26.

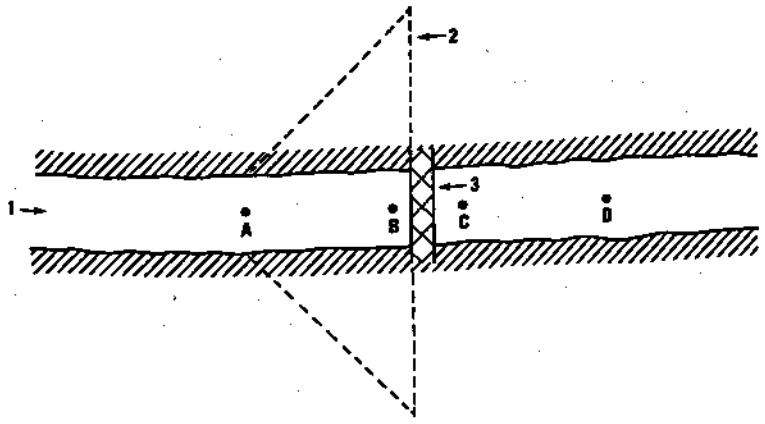

Fig. 4.26. Use of artificial channel section to incorporate the effect of approach velocity in a weir calculation. 1, Channel; 2, artificial section; 3, weir

The reach from A to B could be either a very short fluvial reach along which the de St Venant equations would be assumed valid, or a special reach which ensures equal head at both ends, so that:

$$y_A + \frac{u_A^2}{2g} \approx y_B; \quad Q_A = Q_B \tag{4.7}$$

The water level at B will then be higher than at A by $\frac{u_A^2}{2g}$ so that the weir calculation using y_B will implicitly take the approach velocity into account.

It is possible to incorporate into one-dimensional codes a more sophisticated treatment of the weir flow problem, in which the upstream and downstream velocities, as well as possible Borda type head losses, are taken into account.

However, it is important not to lose sight of the purpose of modelling a weir in a river model. The goal is simply to provide an approximately correct local interior boundary condition in a model which may extend from tens to hundreds of kilometres upstream and downstream of the weir. If the engineer really needs to model the details of flow over the weir with all its dynamic effects, then a river system mathematical model is not the place to do it.

We now turn our attention to hydraulic discretization problems in two-dimensional flood plain flow modelling. Recall that we suppose that the flood plain can be divided into a number of cells in each of which the water surface is assumed horizontal and each of which communicates with its neighbours and/or the main channel as shown in Fig. 4.6c. The flow between cells and between the channel and the cells is represented as a link for which a discharge will be calculated in the simulation according to a fluvial-type or weir-type or other discharge law.

The division of the flood plain into cells is not at all arbitrary, but is based, as far as possible, on natural boundaries such as elevated roads, embankments, dykes, etc. If the absence of natural obstacles leads to cells of unwieldy size, their further subdivision is no longer based on natural features, but simply allows for the slope of the flood plain to be represented more precisely. The cell centres must moreover be defined in such a way that the direction of flow can be correctly represented during the passage of a flood. Figure 4.27 illustrates this point. The area ABCD could be considered as a single cell as far as natural features are concerned, but since the water level is assumed constant in the cell and equal to the value at P_1, the water surface slope between sections AB and CD could not be reproduced in the model. Thus the area should be subdivided into two cells, ABEF and EFDC. The area then will be represented by two water levels, at P_2 and P_3, and the slope will be defined by:

$$S = \frac{y_{P_2} - y_{P_3}}{l} \tag{4.8}$$

Once the model is divided into cells in this fashion, the discharge laws between cells must be formulated. When the inertial terms may be dropped completely because they are of small importance compared to the water surface slope and friction slope, the laws of exchange between cells become single-valued expressions relating discharge to the water levels in the two communicating cells. The first Mekong River model was constructed using this type of formulation (Zanobetti *et al.*, 1970), as were the flood plain portions of models of the Adour, Garonne and Rhône rivers in France.

The hydraulic discretization of such a case has two aspects: one must furnish, for each cell, the function $V(y)$ (volume of the cell as a function of water elevation in the cell) and the geometry and discharge or roughness coefficients of exchange law links between the cells. Although both aspects seem straightforward, let us consider some difficulties related to each of them. They will show that even a seemingly obvious situation should be approached with caution.

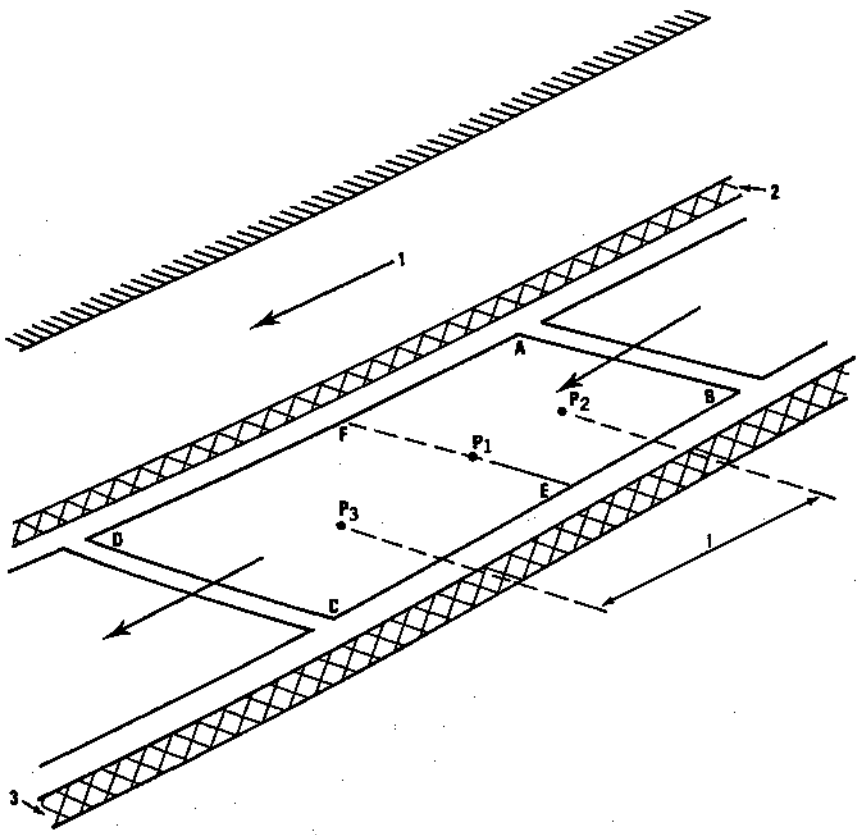

Fig. 4.27. Subdivision of flood plain cells in order to better represent the water surface slope. 1, River; 2, levee; 3, road

The simplest way to define the storage function $V(y)$ for a given cell i is to extract it from a detailed map with the help of a planimeter, measuring the cell surface area function $A_s(y)$ and integrating it vertically to obtain volume. The limits of the cell being defined by topological discretization, the operation is explicit and the accuracy of the $A_s(y)$ function is limited only by the accuracy of the map, at least theoretically (*see* Chapter 5).

As is shown in more detail in Chapter 3 the storage equation on which two-dimensional modelling is based has the following form:

$$\frac{dV_i}{dt} = \theta \sum_{k=1}^{L} Q_{i,k}^{n+1} + (1-\theta) \sum_{k=1}^{L} Q_{i,k}^{n} \tag{4.9}$$

where: V_i = volume stored in the cell i; $Q_{i,k}$ = discharge between the cell i and an adjacent cell k; L = total number of adjacent cells; n = the time step index; θ is a weighting coefficient, $0.5 \leqslant \theta \leqslant 1.0$.

Suppose, for a fully implicit scheme that $\theta = 1$, and that volumes can be expressed as the product of surface area A_s and a water level increment. Then

$$\frac{dV_i}{dt} = A_{si}\frac{dy_i}{dt} \text{ and } A_{si}\frac{y_i^{n+1} - y_i^n}{\Delta t} = \sum_{k=1}^{L} Q(y_i^{n+1}, y_k^{n+1}) \qquad (4.10$$

Such a formulation being fully implicit, the computation should be unconditionally stable from a formal numerical point of view. Suppose further that the water surface A_{si} in Equation (4.10) is evaluated at time $n\Delta t$, i.e. $A_{si} = A_{si}(y_i^n)$, and imagine a cell of the cross section shown in Fig. 4.28. The conscientious modeller, wishing to represent correctly the true volume of his

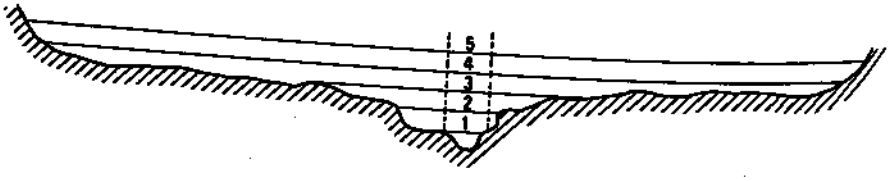

Fig. 4.28. Flood plain cell including local drainage

cell, furnishes a surface area for each level shown, so that the local drainage ditch volume shows up as a very small surface area at level 1. At the beginning of the simulation the cell is nearly dry, its water level having been initialized at the level 1. For the first few time steps there is no inflow or outflow to or from the cell, whose water level thus remains at 1. But at the first time step for which some water flows into the cell, the computation only 'sees' the volume indicated by the dashed lines in the sketch, and consequently the calculated water level y^{n+1} will be much too high; the increase in storage volume in the cell will be completely out of line with the net inflow, all because the method as expressed in Equation (4.10) cannot integrate the volume over the change in water level.

Even if this sudden jump in the cell water level does not destroy the calculation by inducing oscillations (*see* below), the stored volume in the simulation is completely false, and the calculation is invalid. There are two ways in which the program can be protected against the consequences of this type of error: to abort the calculation whenever the errors in volume or stage (in one time step) exceed a specified value; or to perform an iterative solution which allows volume errors to be corrected within a time step (*see* Chapter 3).

The Adour model provides us with an example of the use of an iterative procedure to avoid this kind of cell volume error. SOGREAH's CARIMA simulation system, which combines the Preissmann method for solution of inertial channel flow with non-inertial flood plain storage and flow, was designed to perform iterations automatically during time steps in which the largest water level change in the system exceeds a specified value, in this case 20 cm. Figure 4.29 shows the rising flood in the main channel at point A35, and the gradual filling up of cell A35M which is separated from the main channel by a low dyke. We note

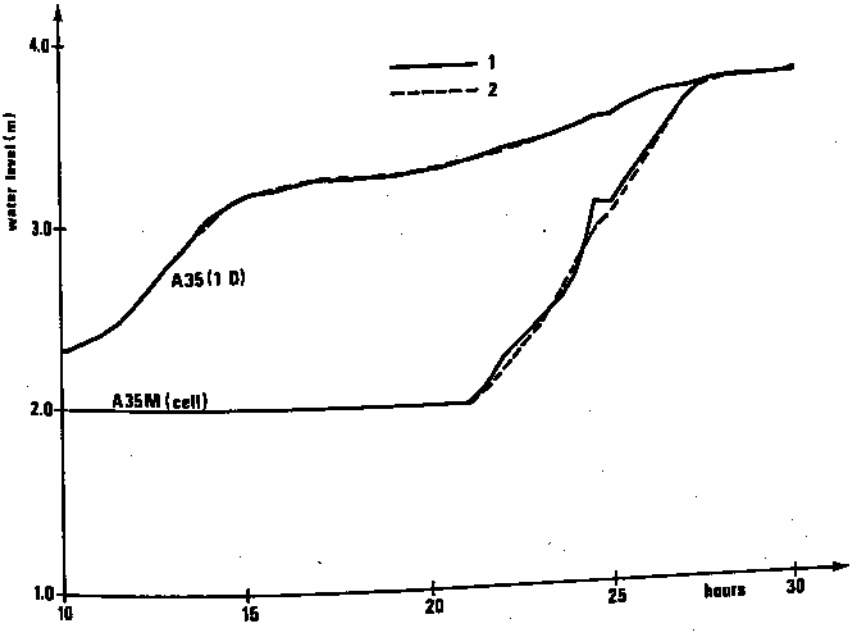

Fig. 4.29. Effect of the use of iterations on calculated water levels in the Adour model. 1, Results without iterations; 2, results with one iteration

first of all that in the main channel, the calculation with one iteration maximum per time step predicts water levels which differ by less than 5 cm from those calculated with no iterations (the time step, limited by the downstream tidal boundary condition, is a relatively small 30 min). In cell A35M on the flood plain, the apparently anomalous water level jump of nearly 40 cm between times 24 and 24.5 h nearly disappears when one iteration is used. Moreover, the level in the cell rises generally more smoothly than without iterations.

Another way to improve cell volume accuracy would be to express the water surface A_{si} differently, for example by writing

$$A_{si} = A_{si}(y^n) + \frac{dA_{si}}{dy}(y^{n+1} - y^n)$$

which would lead to a new equation replacing Equation (4.10),

$$\left[A_{si} + \frac{dA_{si}}{dy} \frac{(y^{n+1} - y^n)}{2} \right] \frac{y^{n+1} - y^n}{\Delta t} = \sum_{k=1}^{L} Q_{l,k}^{n+1} \qquad (4.11)$$

Such a formulation would allow a much better representation of cell volume changes over a time step but the price to pay is high in terms of computer cost since an iterative method would be then needed to solve the non-linear system of algebraic equations for all time steps and not just those in which water levels are changing rapidly.

Over and above these questions of stability and error in the simulation, is it really reasonable to try to reproduce the cell volume as precisely as our conscientious modeller wished? Let's consider three possible situations:

(1) The local drainage is of no consequence during dry periods, and the modeller wishes simply to incorporate the volume it represents in his cell definition. In this case, why not simply start the cell definition at level 3 in Fig. 4.28? This will probably eliminate any possibility of oscillation or gross volume error, and the loss of resolution below level 3 is of no importance compared to the overall volume storage during floods.

(2) The local drainage channels flow all the time, and their effect on the overall system is considered important. In this case the engineer should model the local drainage as a subnetwork of one-dimensional channels, on either side of which the flood plain cells dominate the flow situation during floods.

(3) The local drainage is of itself unimportant as in case (1), but the cell is drained by a flood gate whose invert corresponds to local drainage conditions. Since the calculation of flow through the flood gate requires that the upstream water level be correctly represented compared to its invert, and since it is not possible to allow a cell to drain itself below its 'dry' level, one would be tempted once more to try to model the local drainage volume, with the associated problems we have described. A much simpler and correct solution is to impose zero discharge through the flood gate when the water level in the cell drops below a certain specified level; in this way the cell is defined without the troublesome local drainage and the flood gate flow is calculated with a true upstream head.

Once the flood plain has been divided into cells, the modeller must define and hydraulically describe the links, or flow paths, between cells. Here again, the physical situation dictates the type of link to be introduced. If two cells are separated by an elevated road, low dyke, or locally higher terrain, a weir-type link is most appropriate. A composite weir section can be introduced, in which the width and crest elevation of each rectangular section corresponds to a portion of the flow section between the cells as obtained from road profiles, maps, etc. There is no length associated with such a link; the water levels at the centres of the adjacent cells are assumed to exist on either side of the weir linking them.

If adjacent cells have no particular physical feature separating them, as would be the case between cells ABEF and EFCD of Fig. 4.27, a fluvial-type link is generally called for. The modeller uses topographic maps or field surveys to define the flow cross section, whose overall conveyance properties can be constructed as described earlier for one-dimensional composite sections. In general, the modeller uses the cross section halfway between the two cell centres; but it is most important to be sure that the cross section adopted is representative of flow conditions along the entire distance between the two cell centres. The length associated with the fluvial-type link is simply the distance between the two cell centres. We will come back to the fluvial link discretization problem later when we discuss small depth considerations.

4.6 SOME COMPUTATIONAL PROBLEMS IN RIVER AND FLOOD PLAIN FLOW SIMULATION

It is obviously impossible to recapitulate in a single document all the possible computational problems associated with river flow modelling. Our intention in this section is to alert the model user and the programmer to the kinds of problems that can arise, and the kinds of approaches used to solve them. Our concern here is not with the formal mathematical behaviour of various numerical schemes, but with the numerical treatment of particular situations related to the fact that we try to simulate continuous nature with a discontinuous, or discrete, model. One should keep in mind the fact that the difficulties such as described below may not appear at all in certain modelling systems and, on the contrary, other troubles may occur in such systems which are not mentioned here. Modellers are always faced with questions of how to deal with hydraulic anomalies which do not follow the general flow equations.

Small depths

In certain situations, computational difficulties develop when physical flow depths are small, usually when flood waters first appear in dry channels or on the flood plain, and we refer to these difficulties when we speak of the 'small depth problem'. In fact there are several different facets to 'the' small depth problem, and we shall consider a few of the more important ones from the point of view of simulation system design and programming. This is a prime example of a problem which should be handled by the program to as great an extent as possible. Nature has no problem when depths are low, and the model user shouldn't either, though he should be aware of why the programmer may have to adjust his procedures to compensate for the computational difficulties.

A small depth situation usually precedes or follows a 'zero depth' situation, that is to say a dry bed condition, either on the flood plain or in a channel. Let us first consider the zero flow case from a topological point of view. Most solution algorithms are based on the supposition that there is a continuous transfer of information through a model network, be it from one boundary condition to another (branched models) or from one node to another and from nodes to boundary conditions (looped models). This transfer takes place through the hydraulic equations linking computational points or cells, which in general permit discharge to be related to water levels in a continuous fashion (*see* Chapter 3).

In a branched model which includes only channel flow, a zero flow situation is only seldom encountered. But in looped models, flow in the flood plain or in certain channel branches can be nil during low flow periods, and as a consequence the computational algorithm may find itself disconnected in certain places, since the discharge does not depend at all on adjacent water levels. If no special precautions are taken, this disconnection may invalidate the solution algorithm: the symptoms may be division-by-zero messages on the computer or patently false results. One solution would be to require the model user never to

allow zero flow situations to occur by introducing small base flows on the flood plain, weir leakage, etc. But a better solution, and one which frees the user from an artificial constraint on his model representation, is to design the solution algorithm to detect computational disconnections and compensate for them automatically.

Apart from the topological problem then, where do small depths perturb the numerical solution of the hydraulic equations? The problem is in fluvial reaches, whether they be calculated with the full equations in the main channel, or with non-inertial relationships on the flood plain. Imagine for the moment that the inertial terms are dropped and the flow is expressed by a resistance equation such as Manning/Strickler written for a rectangular flow cross section,

$$Q = k_{str} b h^{5/3} \left(\frac{y_{us} - y_{ds}}{\Delta x} \right)^{1/2} \tag{4.12}$$

Suppose that the upstream level y_{us} is constant while the downstream water level y_{ds} may be variable. Now, normally the discharge should increase as the downstream water level decreases due to the steepened slope. We can see this by taking the derivative of (4.12) with respect to y_{ds},

$$\frac{\partial Q}{\partial y_{ds}} = \frac{k_{str} b}{\Delta x^{1/2}} \left[\frac{5}{3} h^{2/3} \frac{\partial h}{\partial y_{ds}} (y_{us} - y_{ds})^{1/2} - \frac{1}{2} h^{5/3} (y_{us} - y_{ds})^{-1/2} \right] \tag{4.13}$$

This derivative should be negative if the discharge is to increase as the water surface slope steepens due to a falling downstream level, and in Equation (4.13) is obviously the case when the flow depth varies slowly with y_{ds}, i.e. when $\frac{\partial h}{\partial y_{ds}} \approx 0$. Then the derivative $\frac{\partial Q}{\partial y_{ds}}$ is always negative, and the discharge can only increase as the slope steepens. But in fact the flow depth *does* depend on the downstream water level, namely the flow area (or depth) decreases when y_{ds} decreases and as a result there is a downstream water level at which the discharge is a maximum (i.e. when $\frac{\partial Q}{\partial y_{ds}} = 0$). If the downstream level drops still further, the discharge actually decreases as the reduction in flow area more than compensates for the increase in slope, as shown in Fig. 4.30.

Thus the assumed flow equation models a perfectly realistic physical situation (*see* Chow, 1959, Chapter 11) but one which can cause problems in a numerical solution, because the same discharge can occur at two different downstream water levels for small depths, and the calculation is likely to oscillate between the two discharges, possibly with catastrophic results for the overall simulation.

The key to avoiding this small depth oscillation is in the definition of the flow depth h which intervenes in the resistance term of the non-inertial or inertial equations. Of course one could systematically avoid the problem by relating h only to y_{us}, but at the risk of poorly modelling the low flow situations

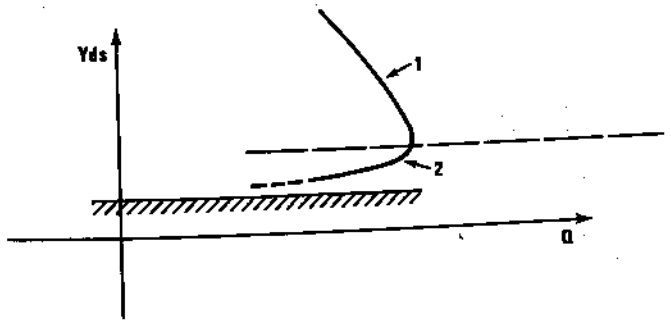

Fig. 4.30. Relationship between discharge and downstream level in small depth situations. 1, Increasing slope dominates; 2, decreasing cross section dominates

in which both upstream and downstream levels play an important role. A better solution is to introduce a parameter which permits the depth, or conveyance perhaps, to be calculated as the weighted average of upstream and downstream values. The user would generally specify a weighting parameter of 0.5, adopting a simple average between upstream and downstream conditions. The program then tests the sign of $\frac{\partial Q}{\partial y_{ds}}$, and if it is positive, shifts automatically to fully upstream weighting (one example worked out in detail is given by Cunge, 1975c), or perhaps attempts to calculate the weighting necessary so that $\frac{\partial Q}{\partial y_{ds}}$ would be strictly zero. The exact procedure adopted depends on the weighting system chosen. The important thing is to detect the anomaly automatically, modify the weighting factor as necessary, print a warning message so the user will know that it was not possible to use his desired weighting factor, and continue the computation. The user must be warned since such a procedure locally changes his basic hypotheses, and knowledge of the fact is essential for the interpretation of results.

This type of procedure is sure to avoid an instability for flood plain flow calculated without inertial terms. But for full equation channel flow the protection is not guaranteed from a formal point of view, since the inertial terms are also in the calculation whereas only the resistance term would have been used to detect the problem and adjust the weighting factor. On the other hand, when flow depths are small enough for the problem to appear, the inertial terms are usually unimportant compared to the resistance term. A resistance-based procedure usually provides good protection, the efficiency of which depends upon the general characteristics of the modelling system and algorithm used.

A final comment concerns the possibility of supercritical flow occurring because of small depths. If at a section which is subject to small depths, the depth decreases only a small amount in each time step, there is normally no risk of the flow becoming supercritical, unless the natural slope of the channel is greater than the critical slope. We do not deal here with the latter case which is

exceedingly rare in river modelling and requires a special algorithm. Most modelling systems have no such provisions and, if they are based on implicit finite difference schemes, they develop unstable numerical oscillations whenever supercritical flow appears. Usually the resistance term dominates the inertial terms and the Strickler formula may be used to estimate flow velocity, $u = k_{str} h^{2/3} S_f^{1/2}$. Its substitution into the Froude number definition formula, $Fr = u/(gh)^{1/2}$, leads to

$$Fr = k_{str} h^{2/3} S_f^{1/2} g^{-1/2} h^{-1/2} = k_{str} \left(\frac{S_f}{g}\right)^{\frac{1}{2}} h^{1/6} \tag{4.14}$$

Thus the Froude number decreases with decreasing depth and subcritical flow should remain subcritical during the process. However, in a computation which takes into account inertia terms and if the time step is relatively large, the change in these terms may be greater than in nature and they may dominate the resistance term. Then the flow depth may drop into the supercritical range, for numerical reasons only. This would provoke a computational catastrophe even though the numerical incident is a local one and should be of no consequence to the overall simulated phenomena. Some action should be taken automatically by the modelling system, for example suppression of the convective acceleration term $\frac{\partial}{\partial x}(u^2/2g)$ whenever depths are small. Once again, the dominance of the resistance term for small depths means that the suppression of the convective acceleration term will have little effect on the results.

Weir oscillations

Closely related to the dry bed problem, as far as flood plain cells are concerned, is the weir oscillation problem. In certain situations and for certain modelling systems which do not use an iterative solution procedure, the direction of flow over the weir at a given time step can be in the opposite sense from the water surface slope, and the persistence of the anomaly can destroy the calculation. Figure 4.31 shows how this may come about. Flood overflows first arrive in cell A, then flow into cell B across a low weir. Cell B, due to the inattention of the modeller or perhaps for some real physical reason, has been given a very small surface area near the bottom (*see* Section 4.4); moreover in the pre-flood condition this cell is dry or nearly so.

The sketches (a), (b), and (c) in Fig. 4.31 represent three consecutive time steps, situations computed by a modelling system which does not use an iterative procedure. In (a), flood overflows arrive for the first time in A, so that its level rises above the weir crest at the end of the time step. During the next time step, the program calculates a discharge from A to B, but due to the small surface area in B, its level jumps to the position shown in (b) at the end of the time step. Iterative procedures would correct it of course, but if they are not used, then at the beginning of the third time step (c), the situation is anomalous in that the flow is from the lower to the higher water level. At the end of time step (c) the

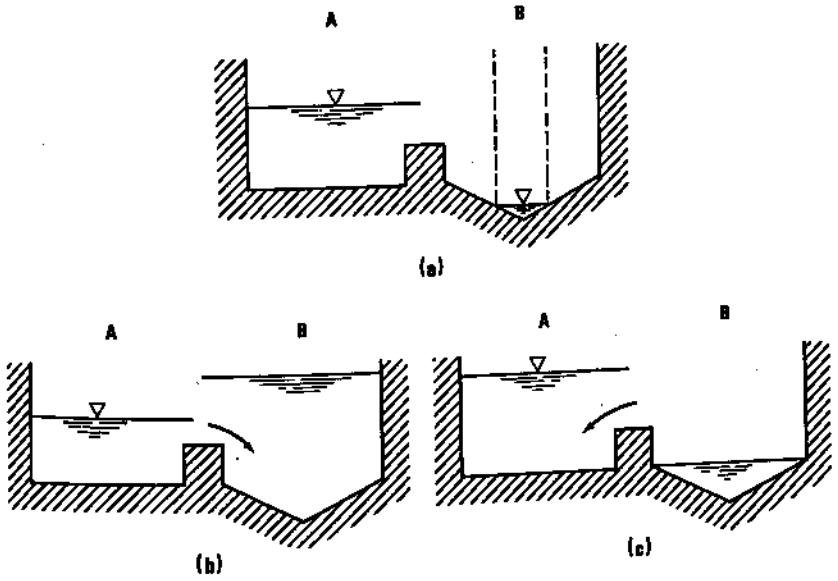

Fig. 4.31. Illustration of oscillations in weir flow between two cells. (a) At end of time step n, the level in cell A has for the first time risen above the weir crest elevation. (b) At end of time step $n + 1$, the discharge from A to B causes the level in B to jump too high. (c) At end of time step $n + 2$, the high level in B has caused a large discharge toward A, whose level rises too high

flow will again be from B to A, still opposite to the water surface slope.

This type of oscillation generally calms down after a few cycles, especially if each of the two cells communicates with others so that the system can absorb the oscillations. But if the cells are isolated from others, and if one or both have surface areas which are just too small compared to the time step, the oscillation can become unstable and destroy the calculation.

Why does this situation occur? Because given the magnitude of the discharges, the time step is too large compared to the cell surface areas. In most non-iterative simulation methods the program only 'sees' the surface area at the present water level, as we have described earlier. Once the water level jumps too high as in (b) above, the simulation is already false and one could argue that it should be stopped.

But in the early stages of a modelling effort it is sometimes useful to try to go as far as possible in the simulation, detecting as many anomalous situations as possible for correction all at once. The weir discharge water surface anomaly should *always* provoke a warning message, since it is a symptom of something being wrong. The oscillation can then be artificially damped by appropriately adjusting the weir formula for one time step if desired, simply so that the calculation may be continued.

Clearly one solution to this kind of problem is to use iterative procedures to

avoid oscillations, but it may mean a considerable increase in computation time. Usually it is less costly to accept some inconsistency like the above oscillations, provided that volume continuity is not violated beyond reasonable limits and that the oscillations disappear quickly. A possible remedy is to decrease the time step during the filling up of such critical cells. If an explicit finite difference scheme is used, one may never run into such troubles since the permissible time step Δt is usually quite small anyway.

Flooded weir linearization

Consider a flooded rectangular weir (Fig. 4.32a), for which the non-inertial flow equation is

$$Q = \mu(y_k - y_w)(y_i - y_k)^{1/2} \tag{4.15}$$

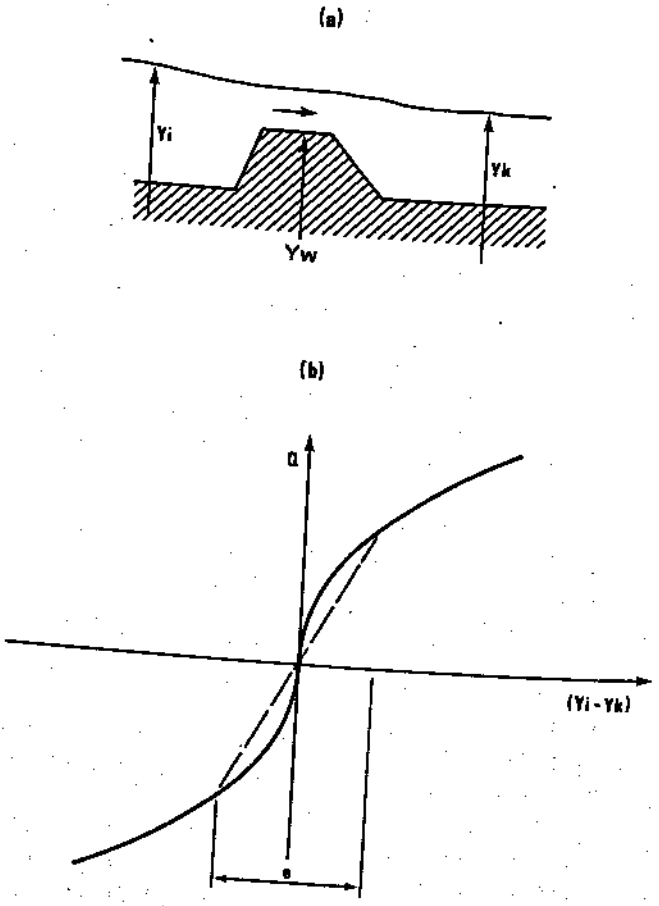

Fig. 4.32. Flooded weir relationships. (a) Definition sketch; (b) dependence of Q on $y_i - y_k$ for $y_k - y_w$ fixed

in which K is a constant coefficient, and y_i and y_k are levels immediately upstream and downstream of the weir whose crest elevation is y_w. Figure 4.32b shows the general form of the relationship between Q and the water level difference across the weir, $y_i - y_k$, when $y_k - y_w$ is held fixed.

We see that as $(y_i - y_k)$ approaches zero, the derivative $\frac{\partial Q}{\partial (y_i - y_k)}$ approaches infinity even though Q approaches zero. Consider a finite difference scheme which uses a truncated Taylor series to express the unknown discharge at the future time step, for example

$$Q^{n+1} = Q^n + \frac{\partial Q}{\partial y_i} \Delta y_i + \frac{\partial Q}{\partial y_k} \Delta y_k \tag{4.16}$$

When y_i and y_k are very nearly equal, the derivatives $\frac{\partial Q}{\partial y_i}$ and $\frac{\partial Q}{\partial y_k}$ will be very large in absolute value, even infinite if $y_i = y_k$, as seen in Fig. 4.32b. This is troublesome since Equation (4.16) will yield much too large a value of Q at the new time step if $y_i \approx y_k$ and one of the two levels changes appreciably. It is interesting to note that an iterative procedure is not a remedy for this problem; it may simply not converge at all but just oscillate around the origin of the $(Q, y_i - y_k)$ coordinate system in Fig. 4.32. This situation can be avoided by linearizing the function $Q(y_i, y_k)$ when y_i and y_k are nearly equal. The dashed line in Fig. 4.32b shows how such a linearization still yields $Q = 0$ for $y_i = y_k$, but avoids the extremely large derivatives in the original function when $y_i - y_k < \epsilon$ where ϵ is of the order of a centimetre.

It should be recognized that this problem is usually one of the time step being too large, for as long as Δy_i and Δy_k are small, the error introduced by the large derivatives near the origin will not be too important. But use of an automatic linearization frees the modeller from having to adjust his time step because of a purely computational anomaly when the water levels on either side of a weir are nearly equal, be it in the initial state, a no-flow equilibrium condition between two cells, or a momentary situation during flow reversal.

Steady flow calculations

Why is it necessary to mention steady flow calculations in the context of *unsteady* flow? Because unsteady flow techniques are often used to calculate steady flow profiles, and there are a few special problems associated with this procedure.

For many projects, only steady flow calculations are performed; for example to establish water surface profiles for levee design, to establish flooded area limits for flood insurance studies, to establish the backwater curve changes caused by bridge construction, etc. For this purpose engineering organizations often develop their own backwater curve programs or use industrialized systems such as the US Army Corps of Engineers' HEC-2 program, 'Water Surface Profiles'. In either case, flow simulation is based on one form or another of the

energy equation. But there are some situations in which classic steady flow techniques cannot be used to furnish steady flow conditions. For example, the one-dimensional energy equation does not apply to two-dimensional flow over flood plains. Nor can it be used directly in looped channel networks, since the discharge distribution in various reaches is not known *a priori*. Steady flow calculations are often required as part of an overall unsteady flow simulation study, either to generate water surface profiles for rough data checks during the calibration stage (*see* Chapter 5), or to provide a reasonable initial condition from which an unsteady simulation can be started up.

The de St Venant unsteady flow equations reduce to the energy equation for steady flow conditions. The same is true of their finite difference representation if done correctly – *see* Section 3.3 for some important remarks in this respect. Therefore an unsteady flow modelling system can be used to obtain steady conditions if the boundary conditions are held fixed and initial flow perturbations are allowed to dissipate or propagate out of the system. Once the modeller has verified that his modelling system does indeed furnish a correct solution to the energy equation for steady conditions, he must then find a way to obtain it economically.

In physical terms, we impose a fairly arbitrary initial state on the model, consisting of depths and discharges (or velocities) which are generally inconsistent with the flow equations. Then we impose the desired boundary conditions, and 'release' the system. The initial inconsistency between flow conditions, the governing equations, and the boundary conditions causes transient waves to propagate about the system as described in Chapter 2, and a steady state is obtained only after the simulation of a physical time period long enough for the flow conditions to adjust themselves to the imposed boundary conditions. In a large model, the physical time represented can be prohibitively long if modelled with normal unsteady flow simulation time steps.

Obviously the most direct way to minimize the number of time steps required is to furnish an initial condition which is very close to the desired steady state. This is unfortunately usually impossible, first of all because one has only a very rough idea of the steady flow water levels, secondly because it is a waste of time for the engineer to try to furnish a precise water level at each of the possibly hundreds or thousands of points in the model. A normal procedure is to start with constant depths, or straight-line water surface slopes, or if possible the results of a previous steady or unsteady flow calculation.

Since the initial state is in general inconsistent with the flow equations, the series of time steps which hopefully will stabilize in a steady flow must begin with several small time steps; this allows initial discharge and water level discontinuities, as well as other violations of the governing equations, to be smoothed out gradually without destroying the calculation. The dissipative character of the finite difference scheme employed should be used to the utmost in this stage, so that discontinuities will be smoothed as rapidly as possible. In the Preissmann scheme, for example, we would put $\theta = 1.0$. Once the initial flow errors have been thus allowed to correct themselves, the model must be run for

a long enough prototype time so that the volume excess or deficiency in the initial state, as compared to the final steady state, can be self-corrected through natural water wave propagation in the river. The number of time steps required for this process can be minimized by increasing the length of the time step to larger and larger values as the flow stabilizes into steady conditions.

This procedure of systematic time step variations can always be performed manually, the engineer using his common sense and judgement to decide at what points in the stabilization process it will be 'safe' to increase the time step. If he allows the time step to become too great too soon, the calculation may break down because of weir or cell oscillations, for example, as we have described previously. It is thus highly desirable to have an automatic programmed procedure for the management of time step variations, to free the engineer of this responsibility. The time step could be increased by a certain factor whenever the maximum change in water levels or discharges becomes inferior to a specified value, the value itself becoming smaller and smaller as the time steps increase. If there is danger of the flow passing locally and temporarily into supercritical regime during the stabilization phase, the convective acceleration terms $u^2/2g$ in the de St Venant equations can be suppressed for a preliminary volume stabilization; then the process can be repeated retaining $u^2/2g$, to let the water surface slope adjust itself to differences in velocity from one section to another.

The success of this type of automatic procedure seems to depend on the amount of 'dead' flood plain storage in the system. For the 200-point one-dimensional branched model of the Seine River upstream of Paris, steady flow conditions were obtained after first imposing a constant water depth and zero discharge throughout the 300 km model, then executing some 30 time steps varying from 6 min to 25 h. In Table 4.3, the time step Δt was maintained until the maximum water level change between two successive cycles was less than ϵ; then the next larger time step was adopted, and so on.

Table 4.3

Δt (min)	6	15	30	60	150	300	600	900	1200	1500
ϵ (cm)	25	25	25	7.5	3.5	2.5	2.0	1.5	1.0	0.5

At the end of this procedure the flow was fully stabilized. For a much smaller branched one-dimensional model of the Rivière Salée in Martinique (SOGREAH, private communication), only 11 cycles were required for complete stabilization.

But for the Adour and Garonne models built by SOGREAH, both of which contain considerable flood plain storage modelled as two-dimensional cells, it was not possible to obtain economically true steady flow using the above procedures. The cause appeared to be that the water level in a large cell responds quite slowly to net excesses or deficits in inflowing discharges. The time step must be increased to a large value at an early time, so that the volume

adjustment in large cells can take place in as few cycles as possible. But this time step may be too large to avoid a calculation incident elsewhere in the model, since 'things are still happening' in the flow. It turned out to be much less expensive to manage the time step variations manually, never using an extremely large Δt as in the case of the Seine. The stabilization was considered satisfactory before a true steady flow condition was obtained, because the minor flow adjustments still taking place on the flood plain were of no real consequence.

4.7 CONCLUDING REMARKS

The industrialization of modelling systems for river flow simulation has made it possible for models to be used more and more often in engineering studies. Whereas in the early days models were constructed and exploited by the same specialists who developed the solution techniques and associated software, many of today's modellers are hydraulicians who use existing software as routine tools. The advantages of this situation are evident: state-of-the-art developments in modelling techniques are made available to the engineer charged with solving a particular problem, without his having to fully understand the computational details used in the modelling system.

But on the other hand, the user of a program does not always share its developer's healthy scepticism toward the correctness of the results, a scepticism born of awareness of the approximate nature of the numerical simulation. The more automatic the program, and the more extensive its error detection capability, the more vigilance is required on the part of the user in guarding against what might be called the 'authority of printed output'. River models tend to be rather insensitive to minor errors in basic data and to the kinds of computational 'tinkering' we described in Section 4.6, in the sense that a simulation may continue without formal incident even though serious flow anomalies exist. Thus it is incumbent upon the user, especially in the early stages of model calibration, to study the flow patterns predicted by the model carefully and in detail, point by point and reach by reach. Any strange situations should be traced back to the basic data if necessary, and any unresolvable questions referred to the program's developer.

The benefits of this kind of analysis are twofold. First, any major errors in topological or hydraulic discretization can be corrected early in the study. Second, the user cannot help but develop a detailed understanding of how his river system functions, an understanding from which he will gradually develop an intuitive appreciation of how the river reacts to proposed modifications.

5 Model calibration and data needs

A mathematical model is a simplified, discrete representation of a complex and continuous physical flow situation. Three-dimensional terrain features are represented by one-or two-dimensional equivalent elements, and the physics of flow are assumed to obey differential equations in which certain empirical coefficients appear. Model calibration is the process of adjusting the dimensions of simplified geometrical elements and the values of empirical hydraulic coefficients so that flow events simulated on the model will reproduce as faithfully as possible the comparable natural events. A model's potential for reproducing and predicting real flow events, and the potential quality of its calibration, depend on the amount and quality of topographical, topological and hydraulic data available for the watercourse under study. Thus the questions of model calibration and data needs cannot really be separated. In this chapter we first consider some of the detailed procedures which must be confronted in calibrating a model, and then we give an overview of data needs and their relation to model calibration. We assume throughout this chapter that the modelling method being used is appropriate for the problem being studied, and that numerical parameters such as time and distance steps have been correctly chosen as described in Chapter 3. In other words, we are interested in calibration as the process of obtaining a correct physical description of reality, and not as the force-fitting of a physical situation to an overly simplified modelling technique.

5.1 MODEL CALIBRATION

We have seen in Section 3.6 that the geometric and hydraulic characteristics of a river reach are usually represented, at least in one-dimensional mathematical models, by three functions of water stage: width $b(y)$, wetted area $A(y)$ and conveyance $K(y)$. These functions provide an appropriate representation of all relevant physical influences at any river *cross section*, as long as the flow resistance may be represented by the same conveyance factor as in uniform, steady flow. In actual modelling practice, two rather extreme extensions of this

notion are introduced. First, the above functions are assumed to represent not only one cross section, but in fact *the entire length* Δx between two computational points. Second, composite cross sections are used to construct these functions even though the water velocity is assumed to be uniform within the entire section and flow is assumed to be truly one-dimensional. As long as these two assumptions are acceptable, one-dimensional schematization may be used; otherwise a two-dimensional model must be built. The choice between the two types of models is based primarily on the engineering common sense of the modeller, who considers the purpose of the model and the physical situation in making the choice, as we discussed at some length in Chapter 4. But another constraint on this choice comes from the calibration process itself. Indeed, it may prove impossible to calibrate a one-dimensional model correctly (or with the required accuracy) when the physical situation calls for a two-dimensional schematization, as is shown further on. In this section we consider in detail first the difficult and controversial process of calibration of one-dimensional river models. Then we describe some special problems associated with the calibration of two-dimensional models.

Steady flow

One-dimensional steady-state calibration consists in the systematic adjustment of the conveyance factor $K(y)$ at computational points so as to obtain coincidence between observed and computed flow events. The 'observed events' are generally recordings of water stages for different steady state conditions; discharges are normally measured only in order to construct rating curves at a limited number of stations along the river. These rating curves are nearly always defined as single-valued relationships between discharge and water stage, and are not always representative of real life, unsteady (hence multi-valued) flow relationships, as we shall see further on. Nevertheless, these rating curves are the first, and sometimes the only, data available to the modeller. Hydrographic services often prepare longitudinal 'steady state' water surface profiles. Acting upon the assumption that $Q(y)$ rating curves are correct, water stages y which correspond at different stations to a given discharge Q are joined by straight lines to define the profile. Although such longitudinal profiles are not at all representative of unsteady flow situations, they reflect the overall hydraulic characteristics of most rivers, with the possible exception of those having a small longitudinal slope and those which are strongly influenced by the downstream boundary condition (tidal rivers or rivers flowing into reservoirs subject to rapid water level changes). Therefore any calibration procedure should begin with the simulation of a series of steady state profiles for the whole range of discharges to be considered.

The downstream boundary condition of the model in steady state is defined as the local steady state rating curve $Q(y)$; the upstream boundary condition is a series of discharges Q = constant. A number of simulations are run, each of sufficient duration to obtain steady flow conditions along the entire river (*see*

Section 4.6 for a discussion of how this can be done economically). The resulting series of free surface longitudinal profiles may then be compared with those obtained from the rating curves along the river. In the early stages of calibration, obvious model errors can be detected through close examination of these computed profiles. Indeed, in uniform flow, profiles should be parallel one to another and to the longitudinal river bed profile. In non-uniform steady flow the profiles are not parallel, but still, marked irregularities represent either real physical perturbations or errors in the data – hence the need to examine the results very closely. It is advisable to plot the functions $b(y)$, $A(y)$ and $K(y)$ for all computational points, since the visual examination of these functions immediately highlights obvious data errors and, moreover, may point out the physical reasons for irregularities in longitudinal free surface profiles.

Once the obvious errors are eliminated, the calibration is conducted by varying the conveyance in such a way as to obtain computed profiles which agree reasonably well with the 'observed' steady flow ones. Let us consider a situation such as is depicted in Fig. 5.1, in which computed and observed water surface slopes do not agree. The composite cross-section representative of the reach Δx would have a conveyance factor K'_{11} computed, for the water surface elevation corresponding to the discharge Q_1, as follows:

$$Q_1 = K'_{11}\sqrt{S'_1} \tag{5.1}$$

$$K'_{11} = k'_{str1}\, A'_{11} h'^{2/3}_{11} \approx k'_{str1}\, b'_1 h'^{5/3}_{11}$$

where k'_{str1} = Strickler coefficient attributed to slice (1) of the cross section. It is seen from the longitudinal profiles that the computed free surface slope S'_1 does not coincide with the observed slope S_1, while the discharges are of course the same. Therefore we can write

$$K'_1\ \sqrt{S'_1} = K_1\ \sqrt{S_1} \tag{5.2}$$

where K_1, S_1 = 'observed' values; K'_1, S'_1 = computed values, which are incorrect.

From Equations (5.1) and (5.2),

$$k'_{str1}\, b'_1\, h'^{5/3}_{11}\ \sqrt{S'_1} = k_{str1}\, b_1\, h^{5/3}_{11}\ \sqrt{S_1} \tag{5.3}$$

Assuming that the geometry is correct (hence $b'_1 \approx b_1$), the necessary value of the Strickler coefficient for the slice (1) of the cross section is given by

$$k_{str1} = k'_{str1} \left(\frac{h'_{11}}{h_{11}}\right)^{5/3} \left(\frac{S'_1}{S_1}\right)^{1/2} \tag{5.4}$$

All values on the right-hand side of Equation (5.4) are known (most often $h'_{11} \approx h_{11}$) and the correction of our first guess of the Strickler coefficient k'_{str1} is easily computed.

Let us consider now the free surface profile corresponding to the discharge Q_2. The conveyance is defined by

$$Q_2 = K'_2 \sqrt{S'_2} = (K'_{12} + K'_{22})\sqrt{S'_2} \tag{5.5}$$

where K'_{12} = computed conveyance for slice (1) and depth h_{12}, K'_{22} = computed

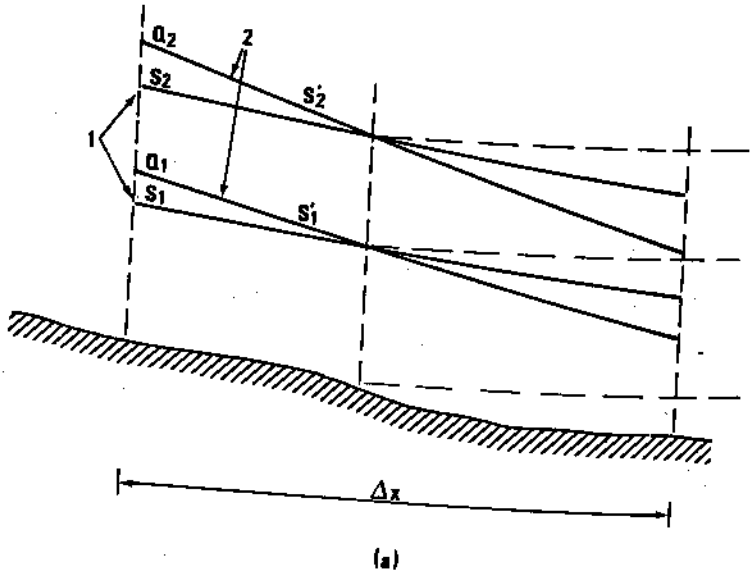

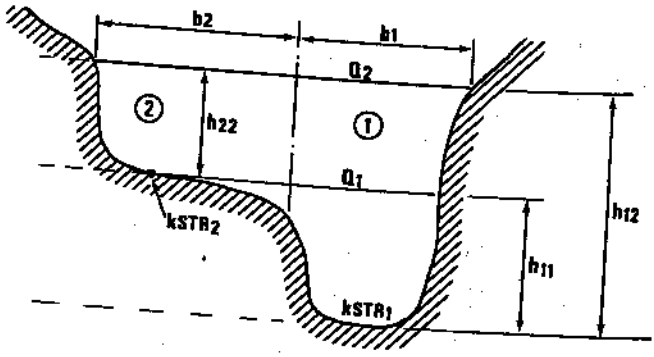

Fig. 5.1. Steady flow water surface slope dependence upon conveyance. (a) Longitudinal bed and water surface profiles. (b) Associated cross-sectional view: 1, observed profiles; 2, computed profiles

conveyance for slice (2) of the cross section and depth h_{22}. Thus we may write

$$K'_{12} = k'_{str1}\, b_1\, h_{12}^{'5/3}$$
$$K'_{22} = k'_{str2}\, b_2\, h_{22}^{'5/3} \tag{5.6}$$

For equality of computed and observed discharges, we have

$$\sqrt{S_2'}\ (k'_{str1}\ b'_1\ h'^{5/3}_{12} + k'_{str2}\ b'_2\ h'^{5/3}_{22})$$
$$= \sqrt{S_2}\ (k_{str1}\ b_1\ h^{5/3}_{12} + k_{str2}\ b_2 h^{5/3}_{22})$$

Assuming that $h' \approx h$ and $b' \approx b$ and using Equation (5.4), we can write

$$\sqrt{S_2'}\ (k'_{str1}\ b_1\ h^{5/3}_{12} + k'_{str2}\ b_2\ h^{5/3}_{22}) = \sqrt{S_2}\ \left[k'_{str1}\left(\frac{S_1'}{S_1}\right) b_1\ h^{5/3}_{12} + k_{str2}\ b_2\ h^{5/3}_{22}\right] \tag{5.7}$$

or

$$k_{str2} = \left\{\left[\left(\frac{S_2'}{S_2}\right)^{1/2} - \left(\frac{S_1'}{S_1}\right)^{1/2}\right] k'_{str1}\ b_1\ h^{5/3}_{12} + \left(\frac{S_2'}{S_2}\right)^{1/2} k'_{str2}\ b_2\ h^{5/3}_{22}\right\} \frac{1}{b_2\ h^{5/3}_{22}}$$

The above procedures may be repeated for all the steady flow profiles and for each computational point. In practice one usually begins with the smallest discharge; corrections are introduced until the main channel portion of all model cross sections is furnished with correct roughness values. Then the profile for the next value of Q is adjusted, and so on.

If the comparison of observed and computed profiles shows that they are parallel but shifted vertically with respect to one another, the equal discharge condition is again the basis for the necessary roughness corrections:

$$k'_{str}\ A'\ h'^{2/3}\ \sqrt{S'} = k_{str}\ A h^{2/3}\ \sqrt{S}\ ; \quad S' = S \tag{5.8}$$

or
$$k_{str} = k'_{str}\ \frac{A'}{A}\left(\frac{h'}{h}\right)^{2/3} \tag{5.9}$$

In applying the quantitative roughness correction procedures we have been describing, the modeller must be careful not to violate his subjective, hydraulic sense of what are appropriate values for the reach under consideration. During the original model construction, the engineer has to estimate roughnesses throughout the modelled zone, and he uses all his experience and intuition in the choice of values which hopefully will not have to be changed too much during the calibration. Implicit in this original estimation is the observance of certain common-sense rules; two reaches of essentially the same bed material and cross-sectional shape should not have significantly different roughnesses, for example. During calibration, the modeller must not violate these same rules when he adjusts roughnesses, quantitatively or otherwise, unless a clear physical justification for doing so exists. If good agreement between observed and measured levels cannot be obtained with physically realistic roughness values, then a closer look should be given to model discretization, accuracy of topographic and hydraulic data, etc. In the calibration of the one-dimensional portion of the Garonne model

(France), the modellers were unable to remove a glaring discrepancy between observed and computed levels in one portion of the otherwise well calibrated model, unless a roughness value inconsistent with adjacent reaches was adopted. A verification of cross-sectional data in this particular reach revealed that the bed elevation for one section furnished to the modellers was in error by nearly 1 m. When the corrected section was introduced into the model, the water level discrepancy disappeared.

We have been assuming that the conveyance factors of composite cross sections are always computed according to the classical rules of hydraulics (Chow, 1959). As has been shown in Section 4.5, such a computation is a basic requirement for extrapolation beyond observed stages. Indeed, suppose that the cross section shown in Fig. 5.1 was flanked by vertical walls (dyked river). The Strickler coefficients k_{str1} and k_{str2} having been calibrated, the conveyance factor may be computed for any water stage with Equation (4.3). Nevertheless it is sometimes more convenient to work with an overall conveyance factor $K(y)$. Such a function may be obtained from the steady flow profiles; for a given cross section and a given series of discharges Q and corresponding levels y, the values of K can be computed by

$$K = \frac{Q}{\sqrt{S}} \tag{5.10}$$

where S is the observed free surface slope. In such cases there is no adjustment and no steady state calibration necessary, but it is impossible to extrapolate the $K(y)$ curve obtained beyond the highest observed water stage (Cunge, 1975a; *see* again Section 4.5). Hence this method is applicable only when the model will be used within the range of known water levels. In addition to this limitation, one may not be able to obtain high accuracy in unsteady flow calibration when using such a relationship, as we shall see further on.

In Section 4.5 we demonstrated the dangerous implications of computing an overall variable Strickler or Manning-like coefficient instead of the conveyance. In this method, which is all too frequently used, instead of constructing a monotonic function $K = K(y)$, one constructs another kind of relationship, namely $n = n(y)$ or $k_{str} = k_{str}(y)$. This function is obtained from 'observed' steady state profiles; for every discharge Q at a given cross section and for a corresponding water stage y Equation (5.11) is used to compute for example, n:

$$n = \frac{AR^{2/3}\sqrt{S}}{Q} \tag{5.11}$$

where n = overall cross-sectional Manning coefficient; A = cross-sectional area corresponding to water stage y; R = total hydraulic radius for the cross section, $R = A/P$; P = total wetted perimeter.

The 'roughness' values computed by Equation (5.11) are not really roughnesses at all, but numerical coefficients which relate the overall section

properties (hydraulic radius and cross-sectional area) to the discharge and the energy slope. In a compact section, such as a closed conduit or a lined trapezoidal or rectangular channel, these 'roughness' values can be considered to represent physical roughness. But in a typical composite natural channel section, containing zones of different bed roughnesses and/or overbank flow areas, they reflect bed roughness *and* hydraulic radius effects. Any procedure which attempts to use these values as true roughnesses, for example in the construction of a conveyance function treating the channel now as a composite section, is absolutely wrong. In a case known to the authors, this procedure yielded conveyance functions which actually *decreased* with increasing stage, which is of course physically ridiculous. Since the modelling system being used did not provide for automatic plotting of $K(y)$ functions, the error went undetected well into the calibration stage; it was the difficulty in obtaining a reasonable calibration which led the modellers to verify the $K(y)$ functions and thus uncover the anomaly. The calibration phase had to be repeated from the beginning.

One of the main difficulties in obtaining a good steady state calibration comes from lack of data at computational points between surveyed stations where the rating curves are known. There is a danger that during the calibration, the roughness adjustments will be made only in the vicinity of such surveyed stations, and that the model accuracy between them will not be improved. Let us consider a river reach between two surveyed stations where rating curves are known. There may be several computational points between the stations and, even if the cross-sectional shape is known at these points (as obtained, for example, using ultrasonic depth sounding equipment), their absolute bottom elevations and their roughnesses may be unknown. One way to compensate for the lacking information was suggested by Jobson and Keefer (1976); we describe here a modified version of their technique.

Suppose there are N computational points ($i = 1, 2, \ldots$) between two surveyed stations. We shall consider two typical situations:

(i) the absolute bed elevations at each computational point are known as a result of a survey, but the conveyances are not;

(ii) neither elevations nor conveyances are known.

Consider first the situation in which the *bed elevation is known at each point*. The dynamic de St Venant equation reduced to steady flow conditions may then be written, for the interval between two computational points (i, $i+1$)

$$u_i^2/2g + h_i + (y_{bi} - y_{bi+1}) = u_{i+1}^2/2g + h_{i+1} + \frac{Q^2\,\Delta x_{i,i+1}}{K_{i,i+1}^2} \tag{5.12}$$

Therefore

$$K_{i,i+1} = Q\sqrt{\Delta x_{i,i+1}}\left\{\frac{u_i^2 - u_{i+1}^2}{2g} + (h_i + y_{bi} - h_{i+1} - y_{bi+1})\right\}^{-1/2} \tag{5.13}$$

If the conveyance factor is attached to a point i rather than to the interval between points i, $i+1$ then we may assume one of the averaging formulae cited in Section 3.6, for example

$$K_{i,i+1} = \left(\frac{2K_i^2 K_{i+1}^2}{K_i^2 + K_{i+1}^2} \right)^{1/2} \quad \text{(average energy line gradient)}$$

or

$$K_{i,i+1} = \frac{1}{2}(K_i + K_{i+1}) \quad \text{(average conveyances)} \tag{5.14}$$

The total conveyances at each computational point are then estimated as follows. For each discharge Q for which the steady-state water surface profile is known, i.e. for which the water level is known at each computational point i, we execute a recursive computation from point N to point 1. For the interval between $i+1$ and i, the conveyance $K_{i,i+1}$ is calculated from Equation (5.13) (note that knowing h_i and the shape of the cross section, we also know A_i and thus $u_i = Q/A_i$, etc.). Then using an averaging expression such as one of those in Equation (5.14), K_i can be calculated in terms of $K_{i,i+1}$ and the known K_{i+1} (we assume K_N is known). This process is carried out for each Q; the result is a tabulated function $K_i(y)$ for each point i from N to 1. If there are no errors in the bed elevations y_{bi}, the cross-section shapes, and the measured water surface profile, and if the formula relating $K_{i,i+1}$ to K_i and K_{i+1} is appropriate, the computed and measured functions $K_1(y)$ should be in good agreement. If this is not the case, the problem is either in faulty measurements or, more likely, in inappropriate conveyance averaging. If the conveyances at two adjacent sections are not very nearly the same, the value of $K_{i,i+1}$ can be very sensitive to the type of averaging assumed, *see* Fig. 3.24. Therefore if there is significant disagreement between computed and observed $K_1(y)$ values, and if measured data are not suspect, the engineer should reconsider the conveyance averaging used for each reach; special attention should be given to adjacent points having significantly different computed conveyance values for the same discharge.

Once the conveyance functions $K_i(y)$ for all intermediate points have been thus calculated, each section can be decomposed into composite subsections, for each of which the bed roughnesses can be adjusted so that the composite conveyance function will be the same as the objective $K_i(y)$ calculated.

When the *absolute bed elevations are known only at points $i = 1$ and $i = N$*, it is possible to estimate the bed elevations for intermediate points with relatively small error insofar as the quality of later flow simulation is concerned. Suppose that the conveyances $K'(h)$ for all points $i = 2, 3, \ldots, N-1$ have been estimated as described in Section 4.5. Although these conveyances are based on estimated roughness values, it is likely that, for a reasonable length $x_N - x_1$, the estimated roughness coefficients all have the same relative error compared to true values, high or low (Jobson and Keefer, 1976). Then we may write for two neighbouring points i, $i+1$ and for a given discharge Q,

$$y_{bi} - y_{bi+1} = \frac{Q^2 \Delta x_{i,i+1}}{C^2 (K'_{i,i+1})^2} + \frac{u_{i+1}^2 - u_i^2}{2g} + h_{i+1} - h_i \tag{5.15}$$

and $$K_{i,i+1} = CK'_{i,i+1} \tag{5.16}$$

where C = error factor defined by Equation (5.16); $K_{i,i+1}$ = real conveyance factor; $K'_{i,i+1}$ = initially assumed value.

Equation (5.16) simply states the hypothesis that estimated conveyances are uniformly shifted with respect to the real ones for a given value of Q. The sum of partial elevation drops $y_{bi} - y_{bi+1}$ as defined by Equation (5.15), for the entire reach must be equal to the total drop $y_{bN} - y_{b1}$, which is of course known; we express this condition as

$$y_{b1} - y_{bN} = \sum_{i=1}^{N-1} (y_{bi} - y_{bi+1})$$

$$= \frac{u_1^2 - u_N^2}{2g} + h_1 - h_N + \frac{Q^2}{C^2} \sum_{i=1}^{N-1} \frac{\Delta x_{i,i+1}}{(K'_{i,i+1})^2} \tag{5.17}$$

From Equation (5.17) the value of the error coefficient C may be computed and then, using Equation (5.15), the values of y_{bi} $(i = 2, 3, \ldots, N-1)$ may be calculated. As Jobson and Keefer observed, the errors in relative values of the assumed conveyances† are compensated for by artificially changing the bed elevation values, that is to say the local bed slope. The bed slope and the friction slope (a function of the conveyance K for constant discharge) are always additive (*see* Equation 2.21) so the errors in bed slope should not seriously affect the accuracy of the model.

The above procedure should be applied for several different discharges, in order to obtain estimates of $K(y)$ for a wide range of levels in the composite sections.

Unsteady flow

A model calibrated for the full range of steady flows satisfies the simplified steady flow relationship

$$\frac{\partial}{\partial x}\left(y + \frac{u^2}{2g}\right) + S_f = 0 \tag{5.18}$$

discretized on a certain computational grid as in Equation (5.12), for example. If the modelled river satisfied all the one-dimensional flow hypotheses, the

†It is to be noted that Jobson and Keefer (1976) worked not with conveyances but rather with global Manning-like coefficients $n(y)$; therefore we do not recommend their original formulae for the reasons we described earlier regarding overall $n(y)$ or $k_{str}(y)$ functions.

unsteady flow calibration would be straightforward. Unsteady flow calibration consists in adjusting model features in such a way as to obtain coincidence between observed and computed time dependent hydrographs of water stages. We stress the use of stage hydrographs in unsteady calibration because measured discharges are never very accurate and are virtually never measured continuously during a flood. Recorded stage variations as a function of time are, on the other hand, usually quite reliable and available at many locations along the river. Measured unsteady discharges can of course be used as a supplementary calibration check. But discharge 'hydrographs' obtained from measured stage hydrographs using a steady-state rating curve must never be compared with computed discharge hydrographs; we will see why shortly.

If the numerical method used to integrate the de St Venant equations is a good one and is correctly applied, the inertia term $\frac{1}{g}\frac{\partial u}{\partial t}$ added to Equation (5.18) should take care of the unsteady character of the flow insofar as dynamic effects are concerned. In compact prismatic channels the geometrical features $A(y)$, $b(y)$ can be easily represented with high accuracy, and with a correct integration method, a good approximation to the solution of the full dynamic equation and continuity equation can be obtained (*see* Chapter 3). Under these idealized conditions the only calibration needed in unsteady flow is a correction of the friction slope formula (or roughness coefficient) in unsteady flow as compared with steady flow.

Coming back now to the real world, we know that the one-dimensional hypotheses are never completely satisfied and that natural river beds can rarely be considered as prismatic channels. In this paragraph we shall consider first the unsteady flow features in a river of 'compact' cross section, like the one shown in Fig. 5.2a, then in a compound section, Fig. 5.2b. In both cases we shall

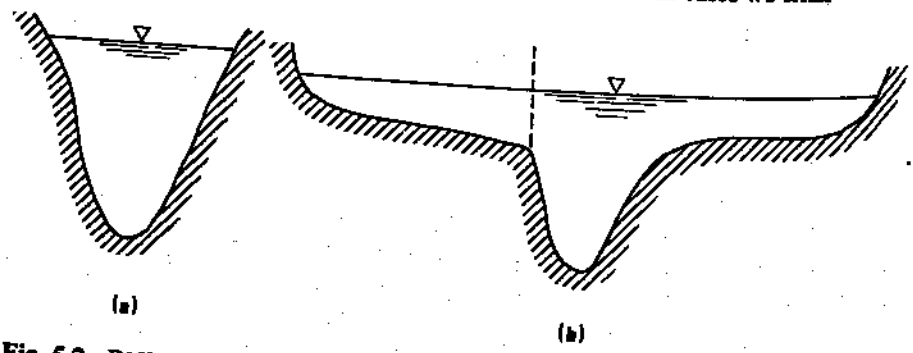

Fig. 5.2. Different types of river cross section: (a) compact one-dimensional section; (b) compound (or composite) one-dimensional section

discuss the distinctive characteristics of unsteady flow in such sections as compared to steady flow, for which the model is assumed already calibrated. Both sections shown in Fig. 5.2 are assumed to convey one-dimensional flow, i.e. during the computations the *average* flow velocity $u = Q/A$ is considered

constant over the entire cross section. When the flow is truly two-dimensional and a schematization such as shown in Fig. 5.2b is therefore unacceptable, a two-dimensional model must be used.

Before entering the subject in detail we would like to stress two important points which should be remembered when calibrating a model in unsteady flow:

(i) The calibration is obtained by varying a limited number of parameters, essentially, the roughness coefficients. If the equations integrated by the modelling system used are not the full equations but simplified ones, the changes in roughness leading to better reproduction of observed stages may really be implicit corrections of some other terms, such as neglected inertia effects. Such a 'calibration' might be excellent for a given flood, but could not reproduce a flood of different characteristics (e.g. a flood having steeper or milder hydrographs).

(ii) Observed hydrographs to be reproduced by the model are recorded at a limited number of stations along the river, and it is often impossible to interpolate for the computational sections located between them. Unless these interior points are also taken into account in the calibration process, there is a danger that an acceptable fit of computed and observed curves be obtained at the price of adopting unrealistic hydraulic features in the immediate vicinity of the calibrated stations.

Compact sections

We begin by reviewing some of the characteristic differences between steady and unsteady flow in rivers. The unsteady character of flood flow is in principle incompatible with the hypothesis of a single-valued rating curve. When the $Q(y)$ relationship is plotted at a given station during the passage of a flood wave, a multi-valued curve is observed; for a single-peak flood wave the curve takes the shape of a loop as shown schematically in Fig. 5.3. Its form indicates that there

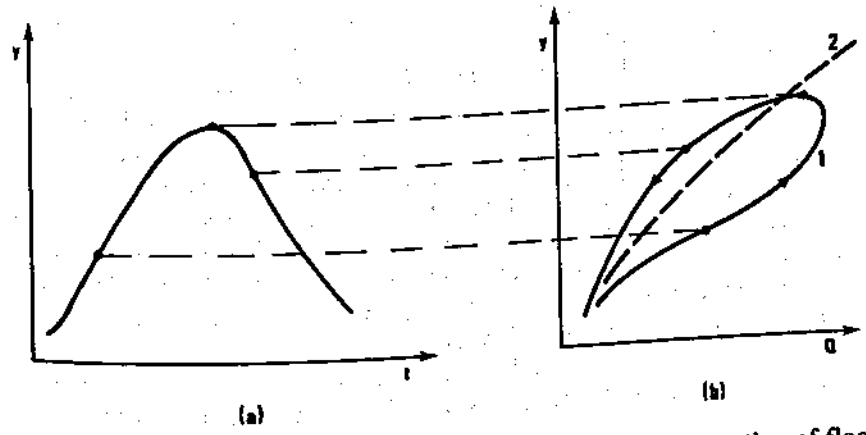

Fig. 5.3. Unsteady flow $Q(y)$ relationship: (a) schematic representation of flood hydrograph; (b) associated rating curve $Q(y)$

is not one discharge value Q for a given depth, but two or more; indeed, every recorded flood will produce a particular loop†. For slow natural floods the rising and falling branches of the loop are more or less symmetric with respect to the steady flow rating curve; deviations from it may be large but are nearly equal in absolute value during rising and falling levels. When the flood wave varies quickly with time, however, this symmetry may disappear. In Fig. 5.4 are shown $Q(y)$

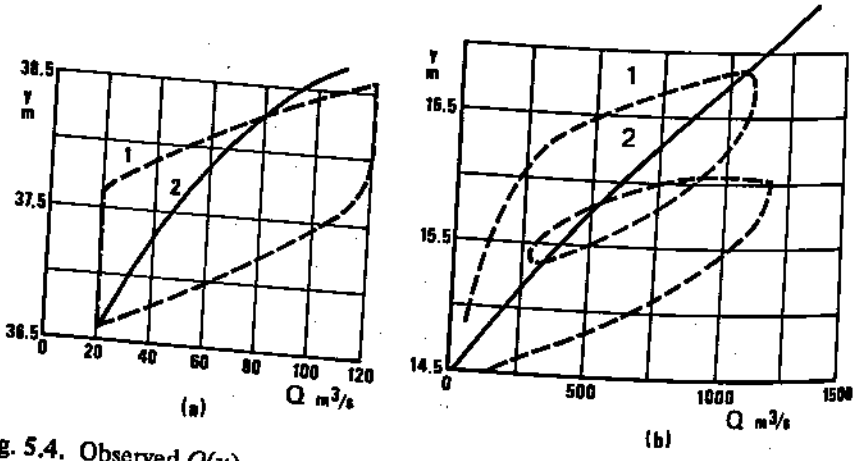

Fig. 5.4. Observed $Q(y)$ curves in natural rivers subject to rapid water level changes (after Ivanova, 1967). (a) Single peak power station release in the river Tvertsa (USSR). (b) Two-peak flood in the river Svir (USSR): (1) unsteady flow $Q(y)$ curve; (2) steady flow rating curve

curves measured in two fixed-bed natural rivers for rapid variations of water stages during single and double-peak floods with the corresponding steady state rating curve shown for comparison. As in Fig. 5.3, in unsteady flow the free surface elevations are lower during the rising flood and higher during the falling flood compared with steady flow stages corresponding to the same discharges, but there is now a strong asymmetry in the unsteady curves.

The form of multi-valued rating curves for compact channels depends upon the energy line slope evolution during the unsteady event. (As we shall see further on, the phenomenon is even more complex for natural main-channel–flood valley composite cross sections.) Factors which intervene are: acceleration of the flow in time and space, longitudinal bed slope, roughness (or conveyance), and evolution of downstream water stages (for example, dynamic reservoir operations or tidal conditions producing dynamic backwater effects). Depending on these different factors, the loop may be more or less spread out, or 'open' as compared to the steady flow rating curve.

The modeller engaged in the task of calibration of a river model must be well aware of the model's possible responses to different actions, for example, the

†In this chapter we consider only fixed-bed models, so that rating curve loops are due only to unsteady water flow effects, river bed form development being neglected.

modification of roughness coefficients. To illustrate the different types of responses we shall primarily use the results of numerical experiments conducted by the researchers from the State Hydrologic Institute of Leningrad (USSR). The experiments consisted of a large number of computational runs with models of artificial channels having compact and composite cross sections. In such experiments it is possible to vary one factor at a time (e.g. roughness, slope, width of the flood plain, etc.) and then observe its effect on the results.

In the Russian experiments there are three factors which influence the shape of $Q(y)$ curves: intensity of the discharge variation $\Delta Q/\Delta t$, longitudinal bed slope S_0, and the roughness coefficient.

(i) *Intensity of discharge variation.* Numerical experiments using artificial upstream releases (Ivanova, 1967) have shown that the increase in the discharge variation intensity, as measured by the ratio $\Delta Q/\Delta t$, tends to damp the flood peak and also to increase the 'unsteadiness'† of the flow. In Fig. 5.5 are shown

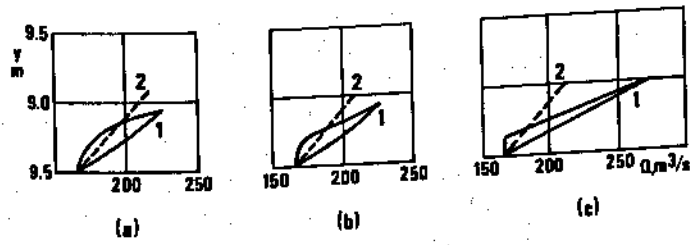

Fig. 5.5. Influence of flood rise intensity on the shape of the $Q(y)$ curve. (a) $\Delta Q/\Delta t = 0.015$ m^{3}s^{-2}: (b) $\Delta Q/\Delta t = 0.030$ m^{3}s^{-2}: (c) $\Delta Q/\Delta t = 0.600$ m^{3}s^{-2}: 2, steady flow rating curve; 1, unsteady flow $Q(y)$ relationship

different forms of loops due to triangular hydrographs released in a reach of a prismatic canal with different values of $\Delta Q/\Delta t$. The influence of the $\Delta Q/\Delta t$ intensity is taken into account, in the de St Venant equations, by the acceleration term $\frac{1}{g}\frac{\partial u}{\partial t}$ and should not be subject to calibration when the modelling system used takes this term into account and properly incorporates the $A(y)$ relationship. However, if the model cross sections are not representative of reality, the inertia term $\frac{1}{g}\frac{\partial u}{\partial t}$ may be poorly approximated because of inaccurate estimates of the increment Δu during the time step Δt. Difficulties in calibrating can sometimes be explained by this influence.

Consider, for example, the composite cross section of Fig. 5.2b. As long as flow is confined to the main channel, i.e. the water level is below the flood plain elevation, the mean velocity $u = Q/A$ is reasonably representative of flow in the section. But suppose that the water stage passes from below the flood plain

†By 'unsteadiness' we mean the persistence and enlargement of the $Q(y)$ loop compared to the steady flow rating curve.

elevation at time t to just above it at time $t + \Delta t$. Physically, the main channel velocity will increase, so that $\frac{1}{g}\frac{\partial u}{\partial t}$ will contribute to an increase of the energy line slope. Numerically, however, since $A(t + \Delta t) > A(t)$ while $Q(t + \Delta t) \approx Q(t)$, there is a good chance, depending upon the numerical method and cross-sectional representation used, that $u(t + \Delta t) < u(t)$, so that the term $\frac{1}{g}\frac{\partial u}{\partial t}$ as well as the energy slope will be falsified. The problem can persist until the flood rises sufficiently for the velocity to be once more approximately uniform in the entire section.

(ii) *Bed slope* S_0 is an important factor as far as unsteady behaviour of the flow is concerned. The greater the slope the smaller the deviation of the unsteady $Q(y)$ relationship from the single-valued steady state rating curve. If there is no downstream backwater effect due to tributaries, dams, etc., the loop may in fact never exist in natural conditions, and could be relatively unimportant even in artificial release conditions. Numerical experiments have shown that in usual river flow conditions, $Q(y)$ loops always exist during floods when $S_0 < 0.0001$. If the longitudinal slope is large (say $S_0 > 0.001$), loops are practically never observed. However, these conclusions are not valid in backwater conditions, for which the role of the bottom slope decreases. In these conditions it affects the results mainly through the increase of the wetted area in the downstream direction, with a corresponding decrease in water velocity and thus in the energy loss. The bed slope should not be subject to calibration in unsteady flow.

(iii) *The roughness* is an essential factor of unsteady calibration. An increase in the roughness tends to increase the unsteadiness of the flow. In the absence of backwater influence, the differences in discharge hydrographs and $Q(y)$ relationships computed with two different values of the Manning coefficients $n_1 < n_2$ would be typically as shown in Fig. 5.6. The flood peak decreases (the damping increases) with higher values of n, but the $Q(y)$ loop opens up somewhat. One should keep this in mind when trying to calibrate a model for a real life hydrograph: the increase of roughness leads not only to a decrease in peak discharge but also to a modification of the rising and falling branches of the rating curve.

Downstream boundary conditions

In unsteady flow calibration the downstream boundary condition plays an important role. A condition of the type $y(t)$, i.e.. water stage as a function of time, might be the most convenient one to apply at the downstream boundary. On the other hand, a single-valued $Q(y)$ condition is needed for steady state calibration. Moreover, during eventual model exploitation runs, the condition $y(t)$ will not generally be available, unless the downstream limit of the model is a reservoir or tidal condition. For these reasons it is more convenient to work always with the same $Q(y)$ downstream boundary condition, whether it be during steady flow calibration, unsteady flow calibration, or model exploitation.

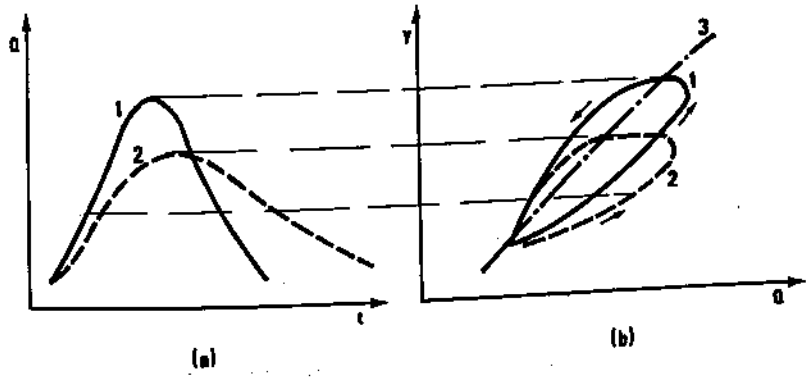

Fig. 5.6. Influence of roughness coefficient on the shape of the hydrograph and $Q(y)$ curve at a station (same upstream hydrograph). (a) Hydrographs. (b) $Q(y)$ relationships: 1, roughness n_1; 2, roughness $n_2 > n_1$; 3, steady flow rating curve

This is analogous to having a free overflow weir at the downstream cross section since flow conditions downstream of it cannot be felt upstream. The unsteady character of the flow is perturbed along a certain distance upstream of this artificial condition, as schematically shown in Fig. 5.7. The perturbation is due

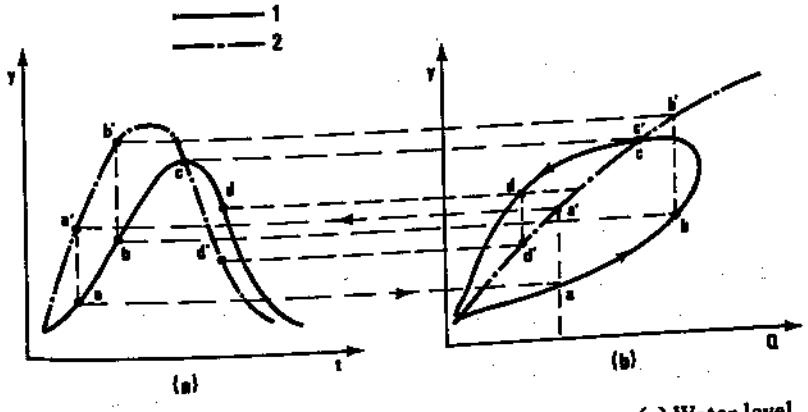

Fig. 5.7. Influence of single valued downstream $Q(y)$ curve. (a) Water level hydrographs at a calibrated station upstream of model limit. (b) $Q(y)$ relationships at model limit: 1, physical, unsteady flow situation; 2, imposed $Q(y)$ single valued curve and corresponding computed upstream hydrograph

to the waves which would propagate on downstream of the model limit in nature, but which are reflected backward from the unrealistic boundary condition in the model. If these waves are damped over a short distance, the false backwater influence is limited to a small distance upstream from the down-

stream boundary. Thus the downstream boundary condition should be sufficiently far downstream from the last gauging station being used in the calibration so that the perturbations do not reach that station.

Care must be taken even in the case when the downstream portion of the model has a roughness and/or slope such that the relationship $Q(y)$ is physically single-valued at the downstream model limit for all intensity ratios $\Delta Q/\Delta t$ of the upstream hydrograph. One is tempted to think that since the $Q(y)$ relationship is physically single-valued at the last calibrated section, its influence on upstream computed hydrographs will be of no consequence. This is so only if the imposed downstream rating curve $Q(y)$ is defined accurately enough in the model. Otherwise it will still introduce perturbations which propagate upstream, and there is no point in calibrating the model reach which lies within this influence.

Composite main channel/flooded valley sections

In order to simplify an otherwise extremely complex phenomenon, we may consider a flood to be described by three characteristic features: peak discharge Q_{max} (or, alternatively, peak stage y_{max}), peak celerity c_p and the shape of the stage hydrographs. In order to be able to calibrate a composite section model in unsteady flow, it is essential to understand how the above features are affected by the composition of a cross section such as that shown schematically in Fig. 5.8. The most important characteristics of composite cross sections are

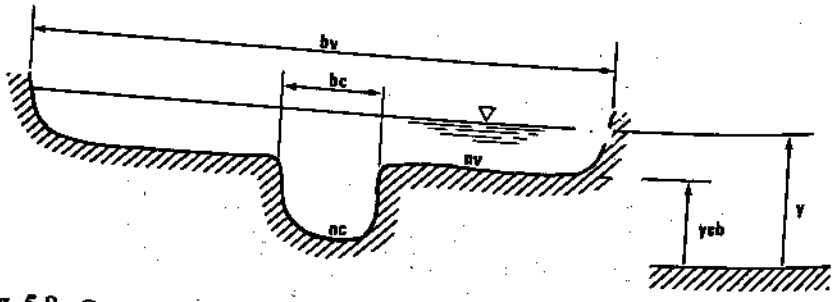

Fig. 5.8. Composite cross section of a flooded valley. n_c, n_v = respectively main channel and valley Manning coefficients

y_{cb} (the elevation at which overbank flooding begins), the width ratio b_v/b_c, and the flooded area roughness coefficient n_v.

In Fig. 5.9 are shown the results of a series of real life experiments conducted on the river Tvertsa in the Soviet Union (Rusinov, 1967) whose cross-sectional shape, though natural, is essentially that shown in Fig. 5.8. The experiments consisted of a number of artificial floods (releases from an upstream reservoir) with flood peaks which were well defined and at different stages from one flood to another. Flood hydrographs were recorded along the river, and cross-sectional average peak flow velocities u_p were measured at the time of occurrence of each flood peak. Steady state cross-sectional average flow velocities u were computed from steady state rating curves using the corresponding flood peak stages. The

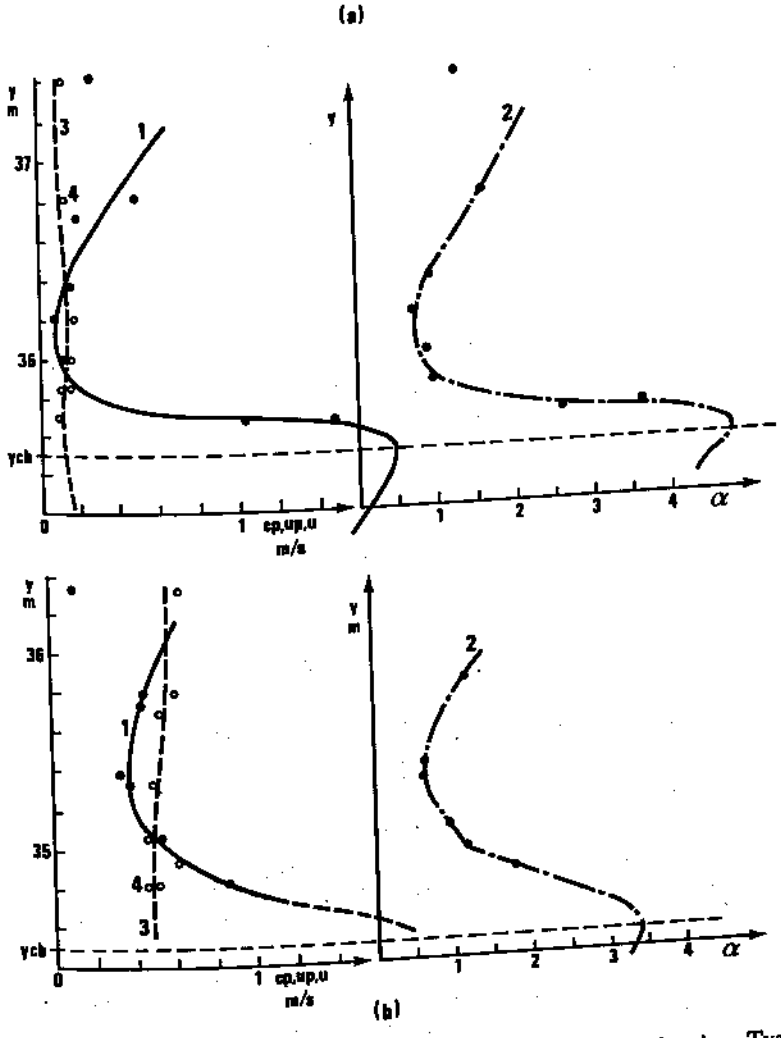

Fig. 5.9. Velocity and celerity relationships at two stations in the river Tvertsa (USSR), after Rusinov (1967). (a) Upstream cross section. (b) Downstream cross section: 1, peak celerity c_p; 2, celerity ratio $\alpha = c_p/u_p$; 3, steady flow velocity u; 4, peak velocity u_p

results of these experiments are expressed as plots of the following variables against water stage y for two stations along the river:

- flood peak celerity, $c_p(y)$
- peak flow velocity $u_p(y)$ (measured)
- steady state flow velocity at the same depth, $u(y)$ (from rating curve)
- the ratio of flood wave celerity to water flow velocity at the peak $\alpha(y) = c_p/u_p$

The curves shown in Fig. 5.9 are typical for composite cross sections of the general shape shown in Fig. 5.8. The equality of velocities $u \approx u_p$ (a result suggested also by other experiments) is confirmed as is the sudden decrease in peak celerity when the water stage reaches the level of the main channel banks and overbank flow begins. In order to investigate the influence of the b_v/b_c ratio upon the flood characteristics, a number of releases propagating along a prismatic channel of constant slope and cross section shown in Fig. 5.10a were

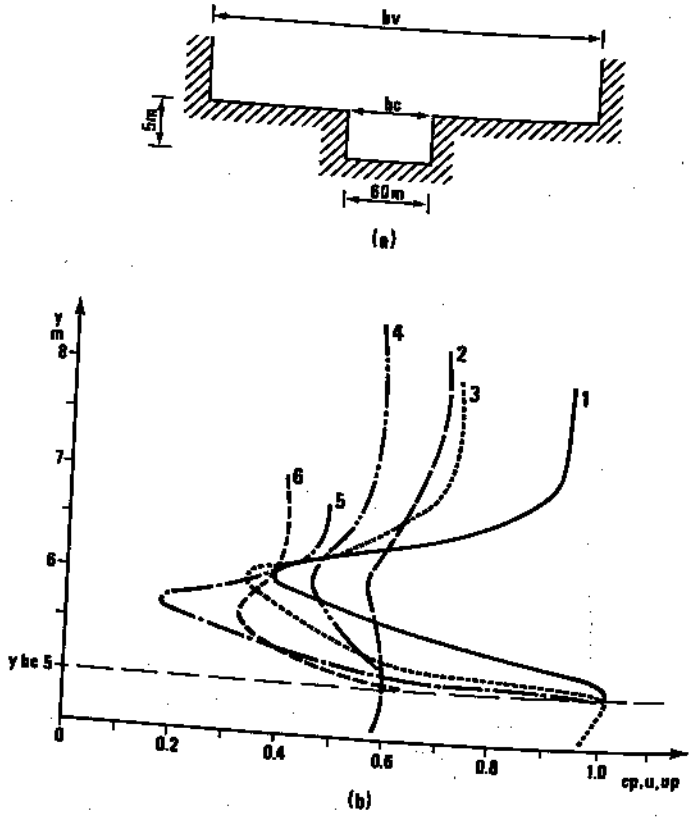

Fig. 5.10. Effect of valley width to channel width ratio (after Rusinov, 1967). (a) Prismatic channel used for numerical experiments. (b) c_p and $u_p = u$ as functions of b_v (b_c = 60 m, constant): 1, c_p for b_v = 160 m; 2, $u_p = u$ for b_v = 160 m; 3, c_p for b_v = 260 m; 4, $u_p = u$ for b_v = 260 m; 5, c_p for b_v = 660 m; 6, $u_p = u$ for b_v = 660 m

simulated numerically (Rusinov, 1967). In Fig. 5.10b are shown the corresponding curves $c_p(y)$ and $u(y)$ for different values of b_v, thus b_v/b_c. For all computations a constant Manning coefficient $n = 0.07$ was adopted for the flooded valley.

Examination of the curves shown in Fig. 5.10 leads to some interesting remarks concerning the behaviour of c_p as a function of b_v variations.

- The celerity c_p of the flood peak varies with the depth of water in the flooded valley.
- The greatest values of c_p correspond to bankfull flow.
- c_p decreases as the water depth in the flooded valley increases; as b_v increases, the minimum value of c_p decreases and occurs at lower stages.
- c_p decreases more rapidly from its bankful maximum to its flooded valley minimum when b_v is large.
- The minimum value of c_p occurs at nearly the same depth as the minimum value of the steady flow velocity in the flooded range.
- For greater depths in the flooded valley, the values of c_p and u_p increase at about the same rate, so that $\alpha = c_p/u_p$ remains nearly constant.

The above observations are of considerable importance as to the non-coincidence of observed and computed parameters (y_{max}, c_p, and hydrograph shape) during the calibration procedure. Our conclusions based on the simplified section shown in Fig. 5.8 are somewhat synthetic, but they show that in addition to the head loss problem, discrepancies between observed and computed hydrographs may well be due to overbank flow geometry, namely:

(i) a wrong estimate of the flooded valley width b_v assigned to computational points and assumed to be representative of intermediate reaches;
(ii) a wrong estimate of the true main channel bank elevation at which valley inundation begins, due to differences between the longitudinal slope of the main channel and the flooded valley or to a simple lack of topographic data.

The modeller obviously is not at liberty to distort known geometrical data so as to obtain a better calibration. On the other hand, he must attribute to each computational point both channel and valley data which, in a one-dimensional model, are representative of the reaches between computational points, reaches over which parameters such as channel bank elevation y_{cb} and valley width b_v can vary considerably. Thus thoughtful (and physically justified) corrections to the y_{cb} and b_v values at particular cross sections are sometimes needed to bring computed hydrographs into better agreement with observed ones. Using the results of several hypothetical floods run on the model, $c_p(y)$ curves can be constructed for various computational points. Stage hydrographs recorded during past floods can be used to determine physical $c_p(y)$ curves at the same points. The differences between the observed and computed $c_p(y)$ functions can be used as a guide to the correction of b_v as in Fig. 5.10b. Since the general *shape* of the $c_p(y)$ function is not too sensitive to b_v/b_c, b_v can be slightly modified without risk of fundamentally altering the characteristics of flood propagation through the reach. In the same manner, comparison of $c_p(y)$ curves can suggest whether or not and in what direction y_{cb} should be modified, since the level at which c_p decreases rapidly corresponds to the average bank elevation.

It is by no means our intention to propose cookbook rules for the variation of valley width to obtain a better calibration – the procedures to be followed

depend on the particular calibration problems faced. But it is important that the modeller appreciate the role of valley width as it affects flood wave celerity and hydrograph shape. In this respect the modeller must be careful not to limit his attention to a single characteristic of the flood hydrograph – the changes which seem necessary to correct the arrival time of peak stage may very well worsen the calibration insofar as the rest of the hydrograph is concerned.

If significant lateral storage exists along a one-dimensional channel, and this storage cannot be modelled as a two-dimensional zone for one reason or another, it may be impossible to correctly reproduce observed flood peak discharges and volume without introducing lateral storage 'pockets' as described in Section 4.4. The principal effect of such pockets is to flatten the flood peak downstream by temporarily storing water during the rising flood and re-releasing it into the main channel after passage of the peak. In some situations these pockets are distinct physical features, in which case their elevation volume characteristics are known and are not subject to calibration. More often, discrete pockets are assumed to be the equivalent of continuous lateral storage as in Fig. 4.14; in this case, their elevation–volume relationships as well as their assumed physical location may have to be adjusted during calibration so as to correctly account for observed hydrograph flattening downstream.

We now pass from channel width considerations to bed roughness. The relationship between the roughness and the width in uniform flow suggests that roughness variation acts in a manner analogous to width variation. For two different wide cross sections conveying the same discharge with the same friction slope, we can write

$$\frac{1}{n_1}\, b_1\, h_1^{5/3} = \frac{1}{n_2}\, b_2\, h_2^{5/3} \tag{5.19}$$

or

$$\frac{n_2}{n_1} = \frac{b_2}{b_1}\left(\frac{h_2}{h_1}\right)^{5/3} \tag{5.20}$$

Consequently we would expect the reactions of the flow to changes in width and to changes in roughness to be analogous. In Fig. 5.11 are shown the plots $c_p(y)$, $u_p(y)$, $u(y)$ and $\alpha(y)$ obtained from numerical experiments using a constant composite cross-sectional shape (Fig. 5.10a) but varying the Manning coefficient n (Rusinov, 1967). The increase in n-value has the effect of reducing the peak celerity, which is indeed the same type of response as observed for valley widening (*see* Fig. 5.10). Thus a change in roughness coefficients for the flooded valley may lead the modeller to re-examine the choice of valley width b_v. Indeed, if an increase in roughness is thought necessary in order to obtain more damping of the flood peak, though the peak celerity c_p is approximately correct, one should also decrease the valley width to compensate for the modification in c_p caused by higher roughness. Such an action is obviously not justified if the inundated valley geometry is well known and when the future use of the model requires its correct representation. In such a case one cannot manipulate the topography, and if there is no other possible cause of non-

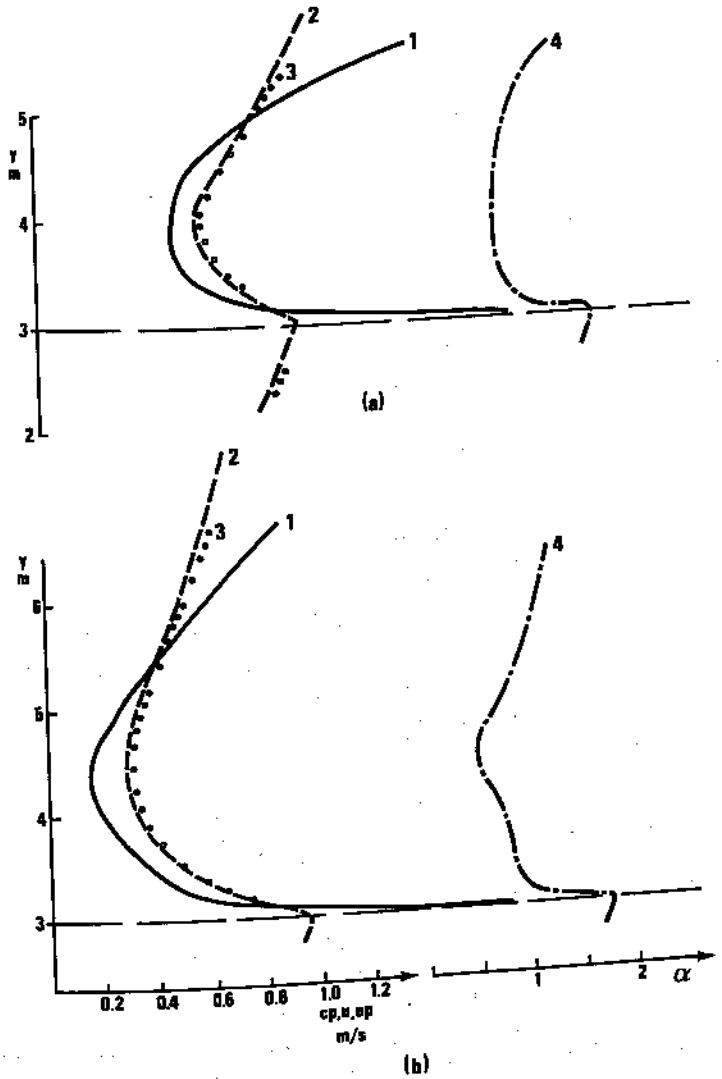

Fig. 5.11. Effect of roughness variation in unsteady flow (after Rusinov, 1967) in prismatic channel shown in Fig. 5.10a. (a) $b_v = 260$ m, $n_v = 0.04$. (b) $b_v = 260$ m, $n_v = 0.10$: 1, $c_p(y)$; 2, $u(y)$; 3, $u_p(y)$; 4, $\alpha(y)$

coincidence, a two-dimensional representation may be mandatory.

In models for some parts of which the longitudinal bed slope is subject to some uncertainty, it is important to recognize that the flood peak celerity c_p increases with the longitudinal slope; but, as is shown in Fig. 5.12, the increase is not the same for different values of the valley width b_v. It is worthwhile to note that since the friction slope S_f is proportional to n^2 and since in the dynamic equation the longitudinal bed slope and friction slope are additive, the

increase in the manning coefficient will act in the same sense as an increase in the longitudinal slope.

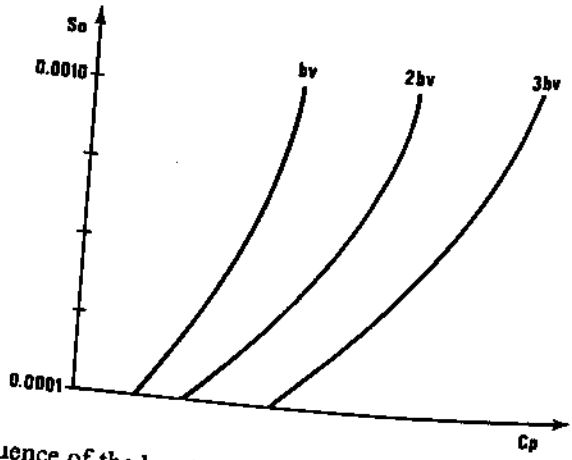

Fig. 5.12. Influence of the longitudinal slope S_0 on peak celerity c_p for increasing values of valley width b_v

In conclusion, it is possible, through careful modification of various physical parameters, to obtain a satisfactory model calibration in one-dimensional unsteady flow. A successful calibration is possible, however, only if the modeller acts carefully and with an appreciation of the various interactions between flow parameters. In particular, he should remember that:

(i) Given the widely varying shape of the $c_p(y)$ relationship, the calibration process should be based on floods which cover a sufficient range of depths if the model is to be considered calibrated.

(ii) The hydraulic considerations we have discussed are general physical principles which are not related to the type of model; comments on hydrograph shape are valid even for very simple methods of computation, e.g. the Muskingum method. However, these principles enable us to adopt detailed, physical modifications which can turn the model into a predictive tool only if the modelling system provides for detailed representation of physical phenomena.

(iii) In tidal river flows or in reservoirs, the inertia term $\frac{1}{g}\frac{\partial u}{\partial t}$ is much more important than the friction slope, and it is often impossible to obtain good calibration of hydrograph shape through simple variations of roughness coefficients. Only detailed analysis of the cross-sectional geometry and velocity variations can lead to a successful calibration.

Two-dimensional model calibration

Two-dimensional models do not require special calibration techniques as compared to one-dimensional models, but more caution is needed in the choice of physical parameters. As shown in Section 2.5, such models consist of a

number of fluvial and weir-like links connecting storage cells. Supposing that a sufficient number of recorded hydrographs of past floods are available, the calibration of fluvial links is subject to the same considerations we have discussed earlier for one-dimensional models. Weir-type links, on the other hand, pose a different problem: that of calibrating the discharge coefficient. The weirs may well be composed of multiple rectangular sections if the cell dimensions are large, in which case the elevations of the 'steps' in such a weir may also be subject to calibration. As in one-dimensional models, two-dimensional models should first be calibrated for steady state flows, and then for unsteady flows (observed floods). There are a number of difficulties specifically related to two-dimensional model calibration which we describe briefly below.

(i) A physical change introduced into a river reach or a weir-like link can have much greater repercussion in a two-dimensional zone than a one-dimensional one; this is mainly due to the relatively small slopes in two-dimensional zones, as a result of which a minor modification can cause changes in flow patterns a large distance away.

(ii) Even small modifications may have far reaching effects on the flow pattern. In a one-dimensional model, water only flows upstream in cases of very strong downstream influence (tide, gate or turbine closure, tributary flood, etc.). In two-dimensional models, on the other hand, reverse flow is not only possible but even common as flood waters leave the main channel, then return to it.

(iii) One never has at one's disposal enough gauges and recorders to be absolutely sure as to what goes on in each cell and at every computational point. Since it is impossible to install a gauge in every cell, 'observed' water levels in cells are often somehow interpolated between points at which water surface elevations are recorded. Such interpolations may be completely pointless given the influence of roads, dykes, canals, etc., which may be located between two recorders. Therefore the calibration requires of the modeller a good knowledge of the topography of the modelled domain, of the general flow pattern during floods, and also the courage to refuse to go too far in calibration when such physical knowledge is lacking.

(iv) The modeller must resist the temptation to go back to one-dimensional schematization because of lack of data otherwise necessary for an accurate two-dimensional model calibration. If the flow pattern is truly two-dimensional, a one-dimensional schematization will be useless as a predictive tool, as we have already mentioned. It is better to have a two-dimensional model partially calibrated in such situations than a one-dimensional one which is unable to predict unobserved events. Indeed, the latter is of very little use while the former is an approximation which may always be improved by complementary surveys.

A detailed example of calibration techniques applied to the Mekong two-dimensional model is presented in a previous publication (Cunge, 1975c). In the next paragraph we give another example, although more general, of calibration of a two-dimensional model.

Example: calibration of the Senegal Valley model†

The Senegal Valley model, constructed by SOGREAH in 1969–1970 for the United Nations Food and Agriculture Organization (FAO), was subject to many of the calibration needs and difficulties we have discussed in this chapter. As we shall see, it was the lack of basic hydraulic and topographic data which conditioned the calibration process. After a brief description of the model and its objectives, we will describe some of the more illustrative problems encountered during model calibration.

Figure 5.13 shows the 1000 km course of the Senegal from its headwaters in Mali to the Atlantic Ocean, flowing along the border between the Republics of Senegal and Mauritania. The upper portion of the river, from the headwaters to Bakel, is fairly steep, flowing through occasional rapids and falls. There is no particular flooding along this reach. From Bakel to Saint-Louis the river slope is relatively flat, and the valley, whose width gradually increases from Bakel downstream, is flooded annually to a width of from 10 to 30 km. Flood-plain farming in the valley is dependent on the annual flooding cycle, and certain crops such as rice are cultivated under submerged conditions as flood waters recede. The lower Senegal from Bakel to Saint-Louis can be subdivided into three distinct zones; Bakel to Kaedi, which is characterized by predominantly left-bank flooding; Kaedi to Dagana, over which distance the river splits into two branches, the Doué and the Senegal, separated by the island of Morphil; Dagana to Saint-Louis, where delta flooding is limited by a left-bank dyke constructed in 1964.

The purpose of the Senegal model was to be able to simulate the river and valley between Gouina and Saint-Louis with sufficient precision to be able to provide good and rapid prediction of the effect of proposed hydropower and agricultural development (including at least one major dam) on flood propagation in the system. It was necessary to use two-dimensional modelling techniques because water levels on the flood plain are often quite different from those in the channel; moreover it was important to be able to simulate the details of flow from one part of the flood plain to another as influenced by local water levels, dykes, roads, etc. For this purpose the model was constructed using the method applied to the Mekong River (Zanobetti *et al.*, 1970), that is to say that both the flood plain and the channel were modelled using non-inertial water exchange between storage cells. Such an assumption was justified since tidal influences were negligible during flood periods. Of course, had a modelling system such as CARIMA been available (Chapter 1), it would have been used to construct a model which simulated main channel flow using the full de St Venant equations and flood plain flow using storage cells, thus permitting a better representation of flood propagation in the river itself.

The model was constructed using only the data which were available at the time: recent 1:50 000 maps of good reliability, older 1:20 000 maps of questionable elevation accuracy, river cross sections which were in general not

†Courtesy FAO and SOGREAH, Grenoble, France.

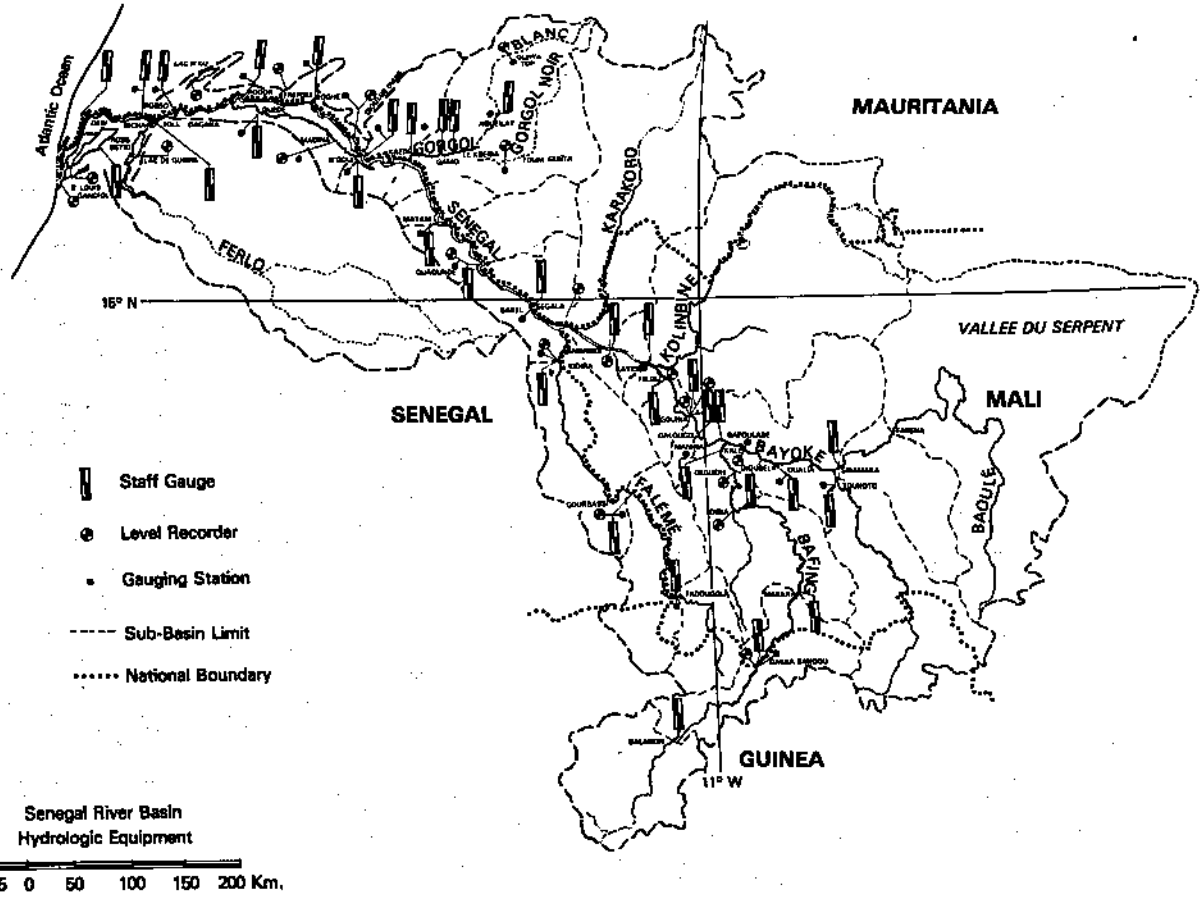

Fig. 5.13. Senegal River basin (Source: FAO – SOGREAH)

perpendicular to the flow direction and of questionable vertical control, and engineering reports on the right-bank delta flow conditions. Over the 1000 km length of the model there were some 21 stations at which water levels were observed with differing degrees of regularity, and 14 stations having discharge observations. Fluvial computational points were placed at each of the water level observation stations as well as at other stations where measured cross sections were available. Flood plain cell limits were plotted on maps based on natural boundaries, then elevation–volume functions were constructed by planimetering. As finally constructed, the model contained 87 fluvial cells (of which 15 were in the Doué) and 157 flood plain cells. The topological plan of the model is shown in Fig. 5.14. Boundary conditions comprised known water levels at Saint-Louis (tidal condition), known discharges at Gouina, known tributary inflows and lake or structure outflows at 12 locations, and evaporation/precipitation data.

Main channel conveyance factors were taken directly from a preliminary one-dimensional model of the channel which had been constructed to identify problem areas and data needs. Flood plain cell volumes were of course fixed topographically and thus not subject to change during the calibration phase. But exchange laws between cells, and between the channel and the flood plain, were virtually unknown and thus subject to definition during the calibration process. As we will see further on, it was this feature which limited the generality of the model calibration.

The terms of the model construction contract called for calibration based on two floods, with a third flood to be simulated as a calibration check. The calibration floods chosen were those of 1964 and 1968, representing relatively high and low flood years, respectively. The model was run for the complete 1964 and 1968 floods at each stage of the calibration process. The analysis of each run was performed by choosing several different days during the flood, and closely examining the calculated water levels and discharges in four general reaches:

(1) Gouina to Bakel, where the one-dimensional calibration results were more or less applicable.
(2) Bakel to Kaédi, the reach within which overbank flooding begins.
(3) Kaédi to Dagana, where the Doué parallels the Senegal.
(4) Dagana to Saint-Louis, the tidal delta.

The adjustment procedure was performed from upstream to downstream, each reach being approximately adjusted before passing to the next. The adjustment was performed by noting on the topological map of the model (*see* Fig. 5.14) observed and calculated water levels, and discharges, for the particular days chosen. From the known levels in the main channel, objective levels on the flood plain were estimated; then the distributions of discharge needed to meet these objectives were estimated. Finally, the changes in conveyance factors, weir elevations, etc., necessary to meet the target discharges were estimated and introduced into the model.

The model adjustment process for each run was a tedious process, since any

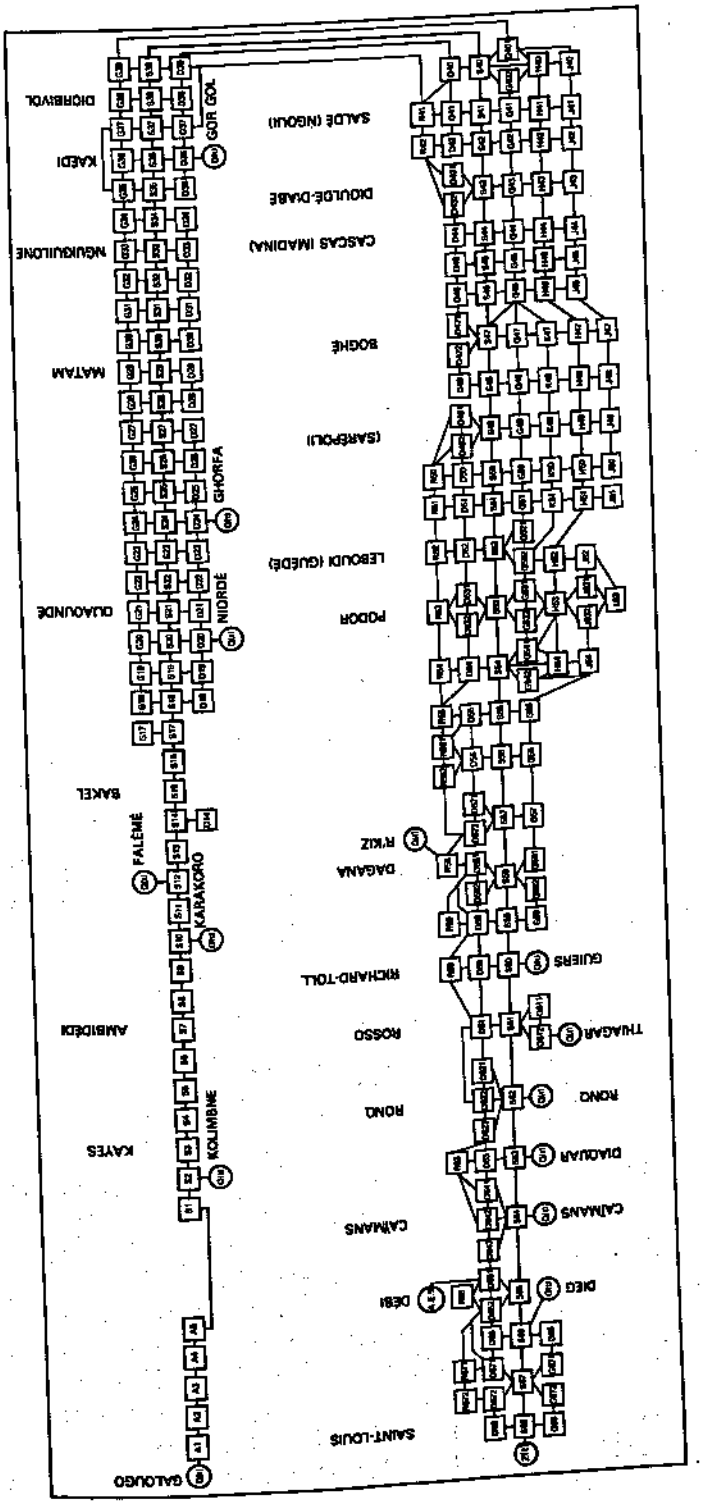

Fig. 5.14. Topological plan of the Senegal valley two-dimensional model (courtesy SOGREAH, Grenoble, France)

changes had an effect on other parts of the system. Moreover, it was often not obvious in what direction to modify a parameter; one flood's results might suggest a particular sill be raised, the other flood's results suggesting the same sill should be lowered, etc. It was often necessary simply to wait for the next simulation to see how the system reacted to various changes. Each adjustment of the model took from two to three days; the model was modified some 40 times in all for the 1964–1968 calibration.

Three of the major problems encountered in calibration were as follows.

Storage between Félou and Bakel

Although it had been hoped that the one-dimensional model calibration results could be used directly for this reach, such was not to be the case. Figure 5.15a shows the calibrated one-dimensional model results for main channel water levels during the 1964 flood at Bakel and Ambidedi. We see that the calculated flood peaks arrive several days before the observed ones at Bakel and that the

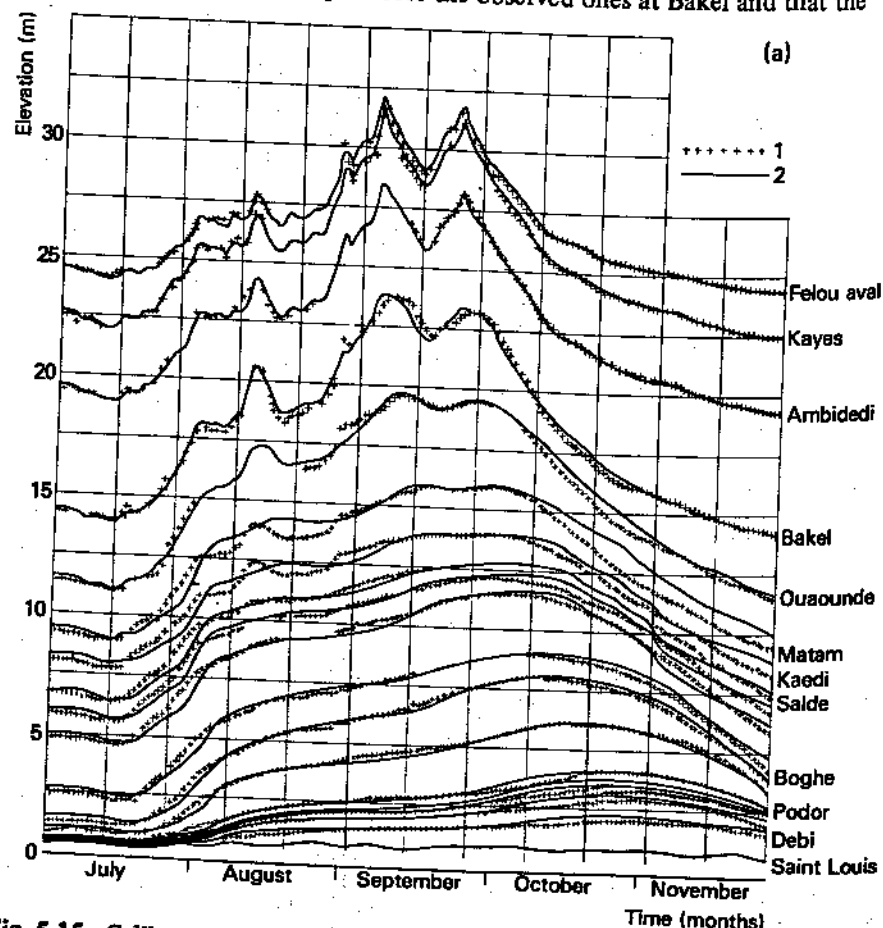

Fig. 5.15. Calibration of the mathematical model of the Senegal Valley (courtesy SOGREAH). 1964 Flood. (a) One-dimensional model: 1, recorded levels; 2, computed levels.

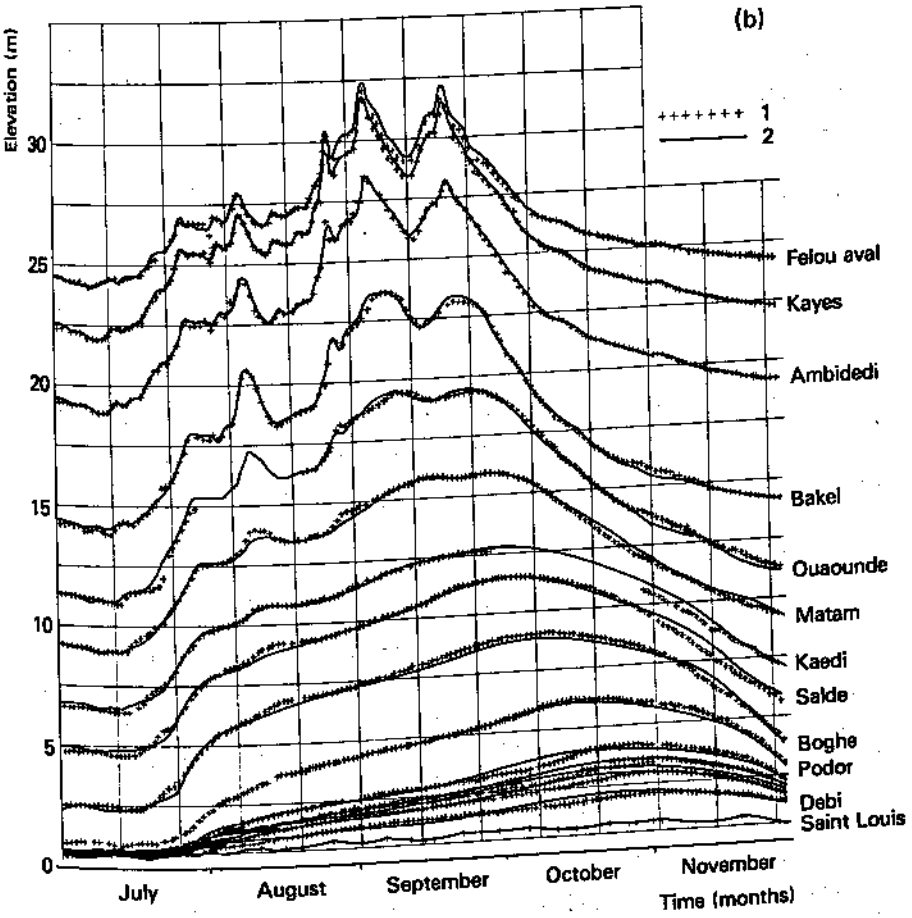

Fig. 5.15. Calibration of the mathematical model of the Senegal valley (Courtesy SOGREAH). 1964 Flood. (b) Two-dimensional model: 1, recorded levels, 2, computed levels

computed water level hydrograph is generally less rounded than the observed one. The engineers responsible for the calibration concluded that there must be some overbank flooding upstream of Bakel which delays and diffuses somewhat the flood peak, even though it was not obvious from the maps whether or not there could be overbank flooding in this region. But the good prediction of levels at Ambidedi using the same one-dimensional model suggested the model was basically sound, and thus that there must indeed be some overbank flooding between the two stations. Therefore an attempt was made to construct a storage cell, or lateral 'pocket' in the model whose law of volume as a function of elevation would schematically represent flood plain storage and permit a better reproduction of levels at Bakel. Figure 5.15b shows the two-dimensional model results with the storage element included; we see that both the arrival time and

the general shape of level variations at Bakel are much more faithfully simulated. We would like to stress that this kind of creation of physical features is conceivable only when the topography is unknown and more information is expected at a later date. It would be unthinkable otherwise. The adoption of a physically reasonable element (storage cell) rather than some arbitrary 'lumped' parameter lets the model maintain its predictive capacity within the adopted schematization.

Divided flow below Kaédi

There were no data available on flow exchange between the Doué and the Senegal across the island of Morphil. Yet it was obvious that significant exchange existed, since observations showed that during floods, the Doué carries most of the discharge near Kaédi, but the Senegal carries most of the discharge near Dagana. Therefore the calibration process for this reach consisted in schematically representing old channels depicted on maps which cut across the island in such a way as to provide for the needed flow exchange.

Eroding sills

It was often the case that different channel–overbank exchange sill elevations were needed to simulate high (1964) and low (1968) flood plain levels equally well. The problem appeared to be related to the fact that these overflows take place through ancient channel beds which are separated from the main channel by natural sandy or silty sills. These sills appear to erode to different levels during floods of different intensity, thus explaining the difficulty of establishing unique sill levels. Since a calibrated fixed-bed model cannot contain parameters which depend on the severity of the flood, compromise sill elevations were adopted for the Senegal model.

Once the model was considered to be adequately calibrated for the 1964 and 1968 floods, the 1966 flood was run as a check. Based on those results it was decided to refine the calibration using the 1966 flood, and to use the 1969 flood as an independent check, after which the calibration was considered to be satisfactory. Table 5.1 outlines the timetable of the calibration process.

Table 5.1. Senegal Model Calibration Timetable (courtesy SOGREAH)

Date	Action
Feb. 1969	First run using two-dimensional model
Aug. 1969	1964–1968 calibration completed
Dec. 1969	1966 check run, additional calibration requested
May 1970	1966 calibration completed
June 1970	1969 check run

At this point it is worth noting the calibration criteria chosen for the Senegal model. The contract specified that the arithmetic average of differences in daily computed and observed water levels during 6 months of flood and at 16 measuring stations should be ± 10 cm or less. In addition, it was required that maximum water levels be reproduced within ± 10 cm. These rather severe requirements were tempered by a clause in the contract which foresaw the possibility of the client obtaining additional data if the ± 10 cm standard simply could not be met with existing data. In fact, the existing data were insufficient, and the client accepted an average precision of ± 14 cm for the four floods tested, of which three (1964, 1966, 1968) were used for the calibration. Table 5.2 (Courtesy SOGREAH) shows the precision obtained for the 1969 check flood; the values in parentheses are corrected values which take into account suspected but unconfirmed data errors. The precisions shown are not as good as those for the three floods used for the calibration itself.

Table 5.2. Senegal model verification – 1969 flood

Station	Average absolute level precision (cm)	Maximum level precision (cm)
Félou	15.1 (12.0)	– 10
Kayes	10.6	+ 7
Bakel	17.1	+ 25
Oaoundé	15.8	– 2
Matam	17.2	– 2
Kaédi	26.5 (23.2)	– 9
Saldé	28.3 (24.5)	– 28 (–12)
N'Goui	25.5 (18.7)	– 1
Boghé	32.5 (29.9)	– 13
Podor	20.0	– 9
Dagana	13.6	– 12
Richard-Toll	10.0	– 7
Rong	11.9	0

The general lack of topographic and hydraulic data in the Senegal valley limited the generality of the calibration; that is to say, the calibration could not be considered to be valid for flows which greatly exceed the range used for the calibration. The model represents an average state of the river and its calibration was considered to be quite good in a relative sense (i.e. for comparing alternative river development schemes), but less satisfactory in an absolute sense (i.e. for reproducing absolute water stages during floods). The only way to improve the calibration in the absolute sense would be to obtain much more complete and precise data. In fact, the recommendations at the end of the study insofar as

data needs were concerned were the following:

- Verification of several staff gauges whose vertical elevation control appeared suspect based on calibration difficulties.
- Establishment of regular staff gauge reading times, or installation of automatic level recorders.
- Exploitation of existing gauging stations on several tributaries.
- Completion of topographic surveys in the upper portions of the valley.
- Installation of staff gauges at important slope changes.
- Measurement of discharges in the Doué and Senegal to better understand the flow division around the island of Morphil.
- Survey of the right bank delta.
- Installation of staff gauges at some critical flood plain locations.

Example: calibration of the upper Rhône model†

The problems encountered in calibration of the Senegal model are typical of those faced for large, undeveloped river basins where data are scarce and of questionable quality. The modeller's task is essentially one of compensating for missing data with reasonable physical assumptions. The upper Rhône river model (France) provides us with an example of a different sort – one in which the basic data are very dense and of high quality. The purpose of the upper Rhône model is to study and design a comprehensive automatic flow regulation system similar to the one presently in operation on the lower Rhône. The regulation system will optimize hydroelectric energy production in eight low-head power plants totalling 800 MW maximum power, while maintaining minimum low flow discharges and respecting rather narrow limits on permissible reservoir water level fluctuations. The design of such a regulation system requires a particularly accurate model calibration.

In this example we consider only a small portion of the upper Rhône model, a reach of about 25 km length above Lac du Bourget as shown on Fig. 5.16. The physical locations of various channel computational points and flood plain cells are also shown in Fig. 5.16, and their topological representation can be seen in Fig. 5.17.

Flooding in this portion of the model proceeds by an inundation of the marsh region on the left bank called the Marais de Chautagne. These flood waters partially return to the river and partially flow, through openings in a railroad embankment, into the Lac du Bourget. The marsh region is represented by a series of two-dimensional cells; AG 26, AG 29, AG 30, AG 31, AG 34, AG 35, AG 36 and AG 37. The flow into the Lake is from cells AG 35 and AG 36. Another marsh region on the right bank (Marais de Lavours) is represented by two-dimensional cells AD 35, AD 36, AD 38 and AD 41. The river itself is represented by a sequence of one-dimensional computational points as is the canal of Savières through which the Lac du Bourget drains into the Rhône.

†Courtesy Compagnie Nationale du Rhône and SOGREAH, Grenoble, France.

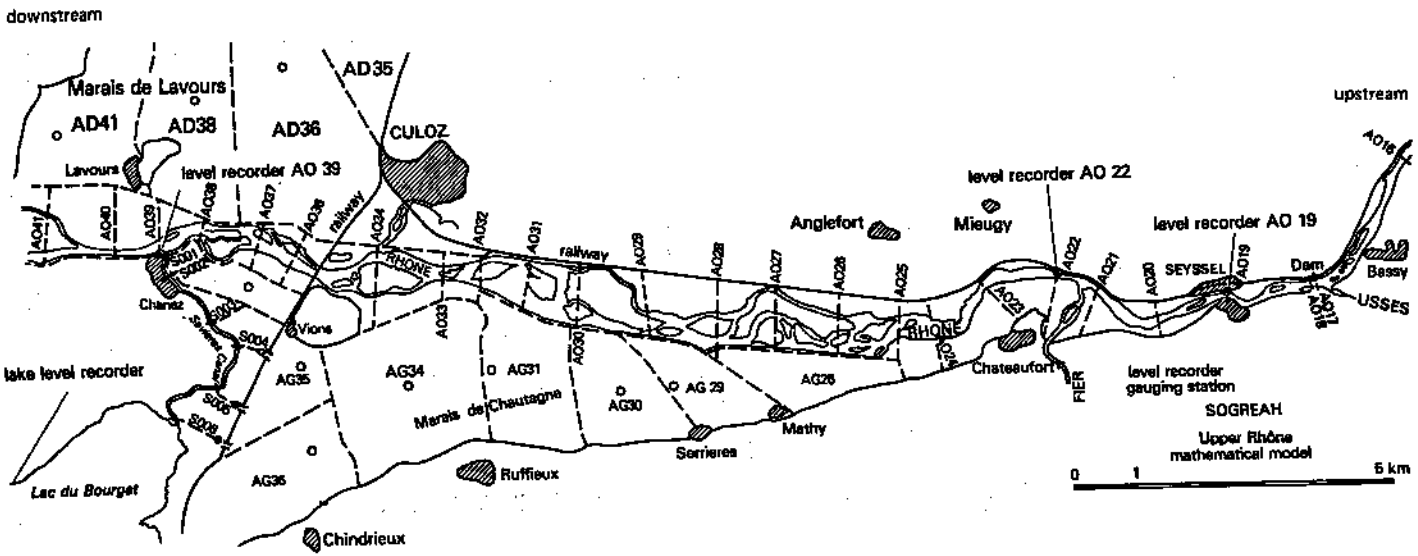

Fig. 5.16. Upper Rhône river mathematical model; two-dimensional schematization of the Chautagne region (courtesy SOGREAH, Grenoble, France)

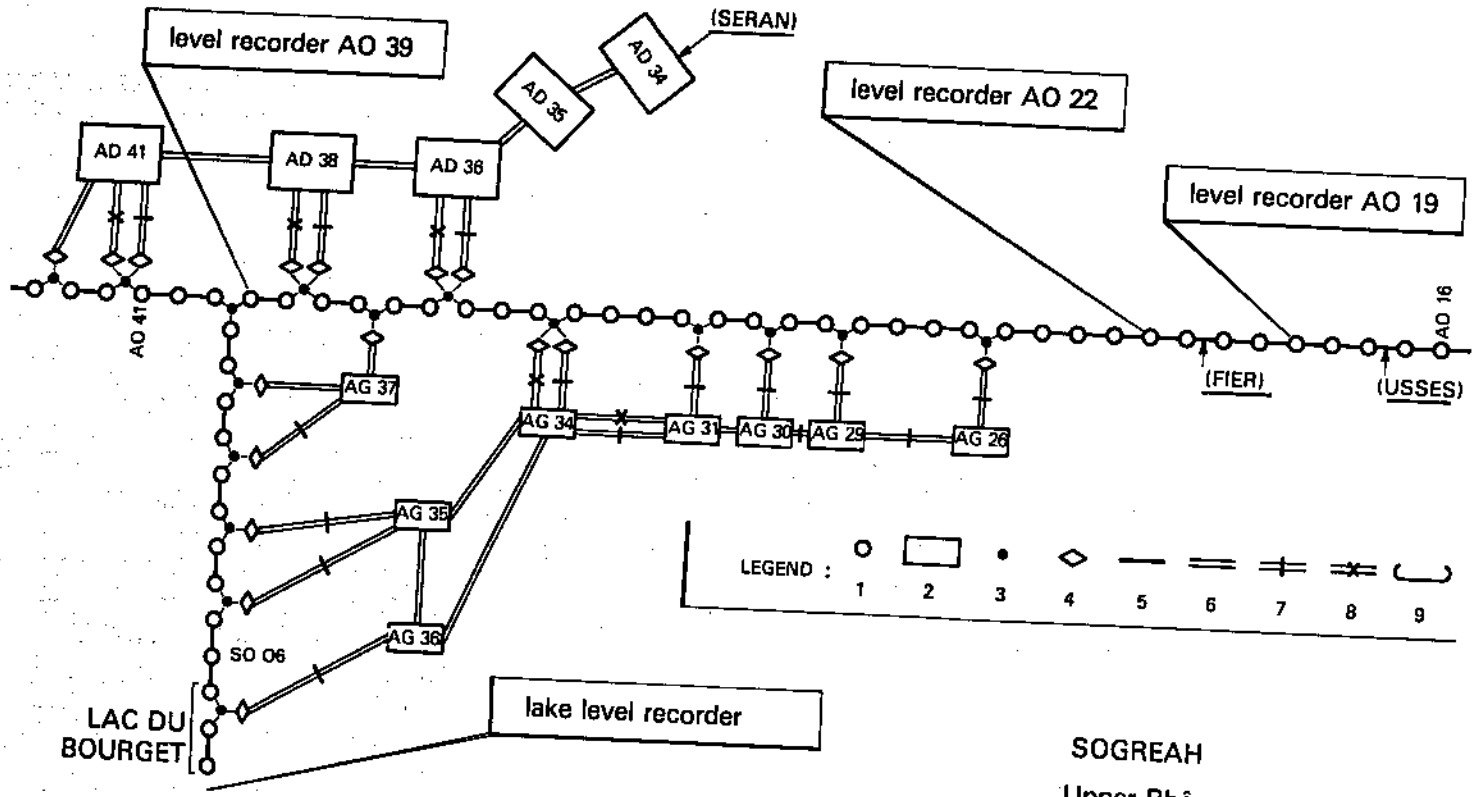

Fig. 5.17. Upper Rhône river mathematical model; topological representation of looped network of computational points and cells in Chautagne region (courtesy SOGREAH, Grenoble, France). 1, 1-D computational point; 2, 2-D cell; 3, nodal point; 4, 2-D point linking 2-D zone to nodal point; 5, 1-D fluvial reach (with inertia); 6, 2-D fluvial reach (without inertia); 7, 2-D weir; 8, flood gate; 9, tributary inflow

The modelling system used was CARIMA, enabling one-dimensional flow along the main river channel to be represented using the full equations (with all inertia terms) and flood plain flow to be represented using two-dimensional, non-inertial equations. The Lac du Bourget was modelled using the one-dimensional inertial equations because of its oblong river-like shape.

Based on steady-state calibration of this portion of the model, a uniform Strickler coefficient of $k_{str} = 25$ was adopted for the entire main channel reach shown; slightly higher values of 30 and 32 were needed in reaches further downstream. Discharge coefficients and roughnesses for the inundated areas were estimated based on site visits and experience. Unsteady calibration was then undertaken; in what follows we shall describe the sequence of events during the first three calibration runs at points A019, A022, A039, and the Lac du Bourget; the calibration was still in progress as of this writing.

Figure 5.18 shows the observed stage hydrographs at the four stations and the results of calculations C1, C2 and C3, all for the flood of 1976.

Calculation C1

Analysis of this calculation led to the following actions.

Main channel dyke elevations were verified and modified in some cases. The relatively large distance step of 1–2 km made it necessary to choose dyke heights which are representative of the entire reach taking the longitudinal slope into account.

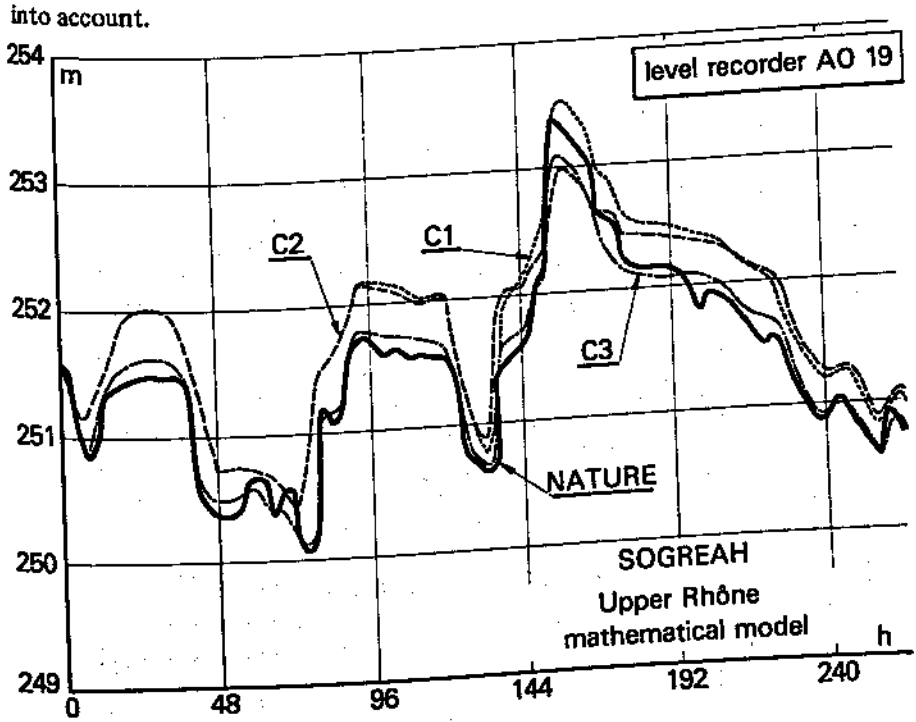

Fig. 5.18. (a) *see page 221*

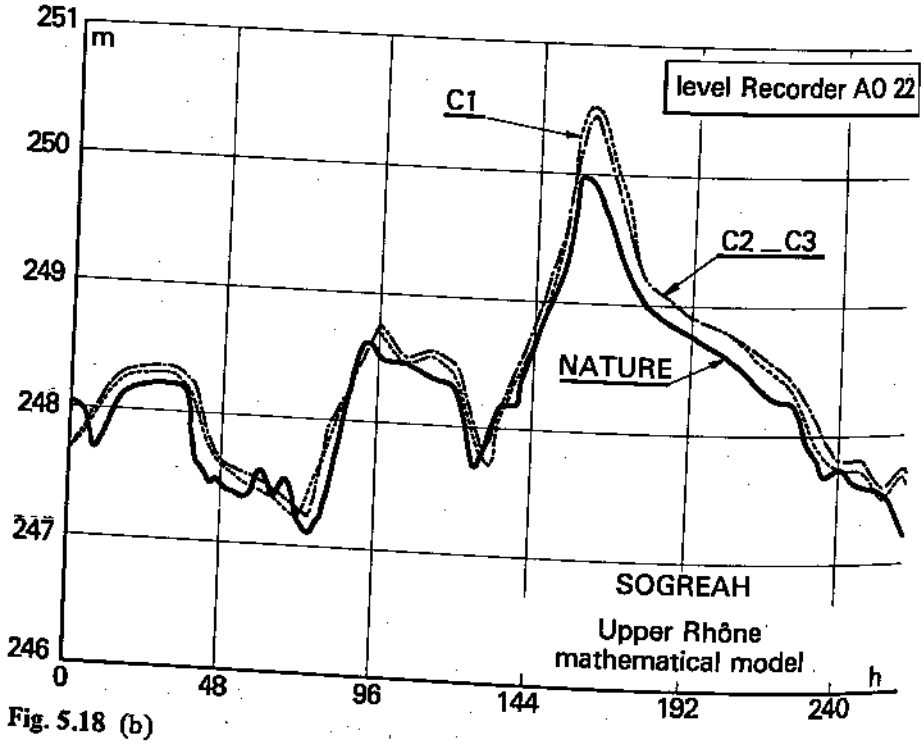

Fig. 5.18 (b)

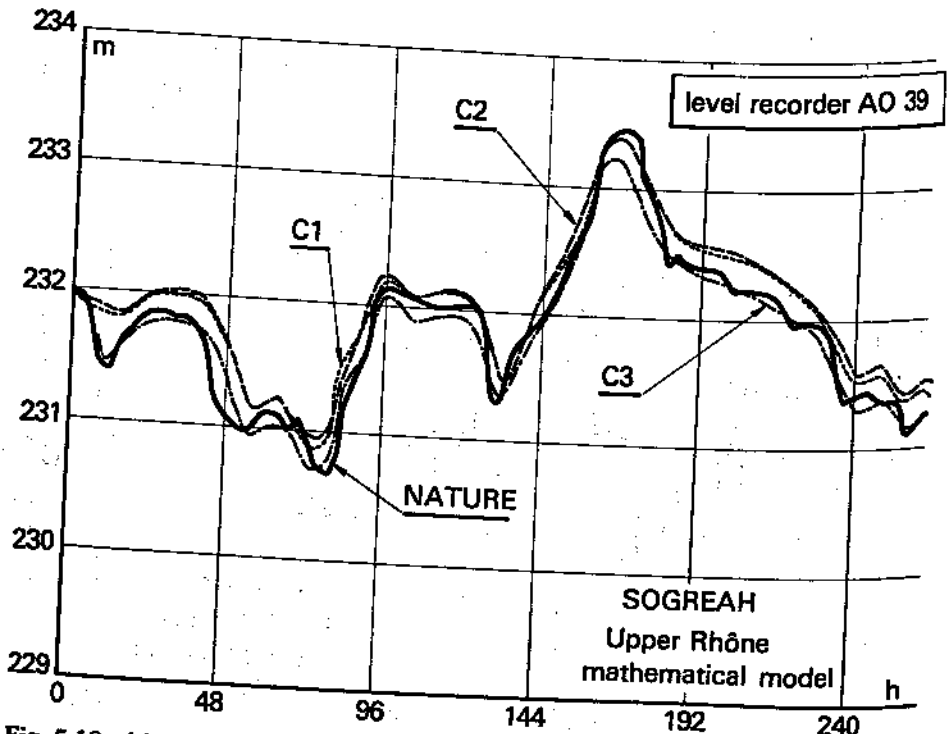

Fig. 5.18. (c) *see page 221*

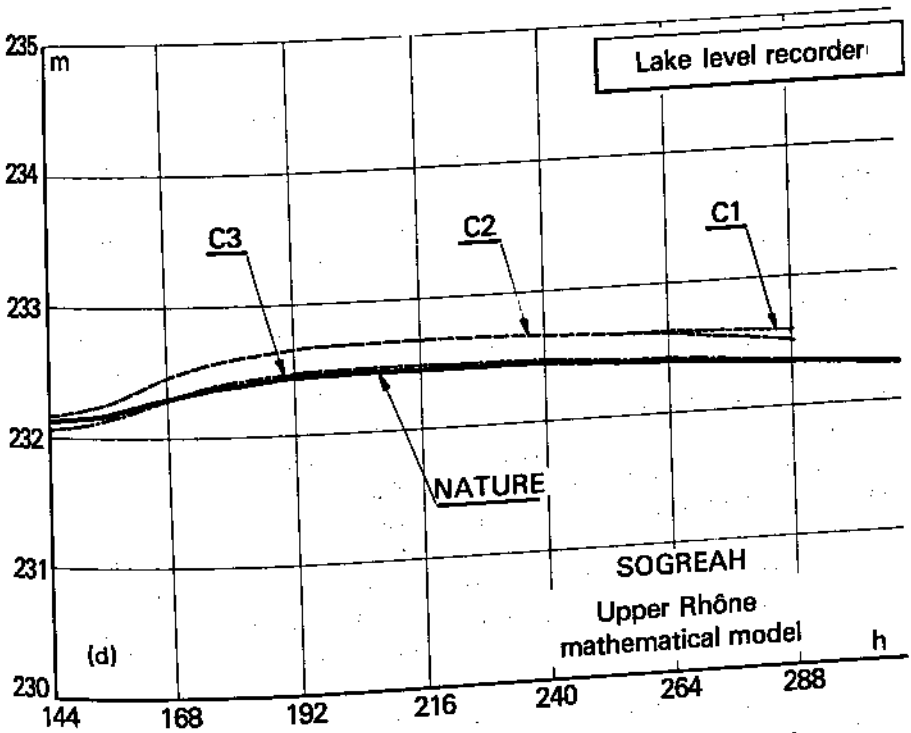

Fig. 5.18. Upper Rhône river mathematical model; 1976 flood calibration sequence of first three unsteady runs for four stations in Chautagne region (courtesy SOGREAH, Grenoble, France). Modelling system CARIMA. (a) Computational point A019; (b) computational point A022; (c) computational point A039; (d) Lac du Bourget point. C1, C2, C3 = subsequent computations

Minor tributary inflows into the Lake were added to the model, even though at first they had been thought to be negligible.

The effect of inflow into the Rhône from the Fier (between points A021 and A022) was analysed in detail. The available rating curve for the Fier was based on daily mean discharges, and thus considered to be of poor accuracy. Unfortunately it was impossible to obtain better information.

Several fluvial and weir-type links between cells on the Chautagne inundated plain were modified. While there is no stage recorder on the plain, maximum water levels during the flood were known for a number of points. Energy losses in some reaches, such as AG26 to AG29, were too high, requiring correction of the equivalent weir section between the two cells.

One of the sections in the canal of Savière was modified. The canal evacuates spills from cells AG37 and AG35 into the Rhône, but the section was apparently too narrow and too high, preventing proper flow patterns between the cells, the Lake and the Rhône.

Calculation C2

The above corrections and several others were incorporated into the model and calculation C2 was run. Based on the results, the following actions were taken:

The main-channel roughness was increased from 25 to 30. The energy losses with $k_{str} = 25$ appeared to be too high, causing overestimation of upstream water levels. Careful examination of contour maps and site reconnaissance showed that in spite of the apparently braided form of the channel, a preferential channel exists with a higher k_{str} than the rest of the cross section.

A reassignment of computational point locations in the main channel was effected. A careful examination of the envelope of maximum water surface elevation of the 1976 flood compared with the observed nearly steady state profile corresponding to a mean low discharge of 300 $m^3 s^{-1}$, showed that the two profiles were parallel nearly everywhere, except at a few sections where the computed levels seemed to show localized energy losses which were too high. Cross-sectional profiles in the Rhône River are available every 100 m. It was discovered that at several particular locations, narrow cross sections were adopted as being representative of an entire reach, while the sections immediately upstream or downstream may have been a better choice. This redefinition of several cross-sections was in the vicinity of point A022.

Between the gauges A019 and A022 a new computational point was added in order to represent a section acting as a natural sill upstream of the Fier tributary. This sill was not represented in the original model, and its existence was discovered only after careful analysis following the calculation C2.

Calculation C3

After the above modifications were introduced into the model, calculation C3 was run. It can be seen from Fig. 5.18 that the intermediate computed levels are now in acceptable agreement with the observed ones, but that the peak levels are too low at gauges A019 and A039, while the peak is too high at gauge A022. Subsequent calibration efforts are proceeding, with particular attention being given to the influence of inundated zone roughnesses.

Accuracy of calibration

It is tempting to try to establish objective criteria concerning model calibration quality. Such an objective system would free the modeller and his client from constant concern as to how well their model is calibrated. But no such quantitative criteria can really be objectively applied to all models, because each has its own set of particular problems which must be treated subjectively. To seek a formal, rigid accuracy in calibration is to be tempted to obtain that accuracy at all cost – even if unrealistic physical parameters must be introduced. If after a reasonable calibration effort a model is still not capable of reproducing observed flood events satisfactorily one or more of the following kinds of problems may exist:

(i) The basic equations are correct and the finite difference method used is appropriate, but the integration is inaccurate because the time step Δt and/or the distance step Δx are too large. This kind of error should not normally get past the model construction stage, during which the modeller must define computational points spaced closely enough to be consistent with both the precision expected of the model and the distance over which significant changes in water surface elevation and discharge occur. The time step must be chosen small enough to adequately describe the input conditions – tidal variations, flood hydrographs, etc. The only definitive way to see whether the time step is too large or not is to simulate the same event on the model using successively smaller values of Δt. If the size of the time step significantly affects computed results, it is too large.

Another calibration problem related to the time step concerns tributary inflow. If the time step is not small enough to provide good resolution not only of hydrographs in the main river, but also those of important tributaries, then a proper calibration cannot be obtained. A good example of this problem is the lower Rhône River downstream of its confluence with the Ardeche, a mountain tributary. The average discharge in the lower Rhône is 1500 $m^3 s^{-1}$, with a 10-year peak flow of 8000 $m^3\ s^{-1}$. Floods rise rather slowly, and last 10–20 days. The Ardeche is, on the other hand, a capricious mountain river subject to nearly flash flooding. The discharge can rise from a few cubic metres per second to 3000 $m^3\ s^{-1}$ in just a few hours, and drop back down again just as fast. The mathematical model of the lower Rhône is usually run with a time step of 2 h; this value is completely appropriate as far as the time scale of flooding in the Rhône itself is concerned, but it is much too large for a good resolution of the rapid rise in the Ardeche flood, which is modelled as a tributary inflow. Figure 5.19 demonstrates how the Rhône model would 'see' a very distorted picture of the Ardeche flood if the time step was kept at 2 h. At a downstream calibration station, the calculated hydrograph would be too low compared to the real one, since the full Ardeche flood volume would not have been input into the model. The danger is that a good agreement between observed and calculated level hydrographs for a particular flood event might still be obtained by modifying roughness values to compensate for the missing volume. The obvious solution is to reduce the time step to something like 30 min for the duration of the Ardeche flood.

(ii) The basic equations are overly simplified; for example important inertial terms are neglected, or one-dimensional schematization is used to represent two-dimensional situations. It is better in such a case to accept the discrepancy than to try to satisfy statistical accuracy criteria in the calibration.

(iii) The data measurement techniques or frequency of observations are inadequate. Errors may be due to inaccurate levelling or to incorrect implantation of gauges (near bridges, etc.). During the passage of a flood all measurements are difficult and thus more subject to error than during low flow.

(iv) Information concerning tributaries and exchange of volume between the river and ground water is unavailable or was not taken into account in the model.

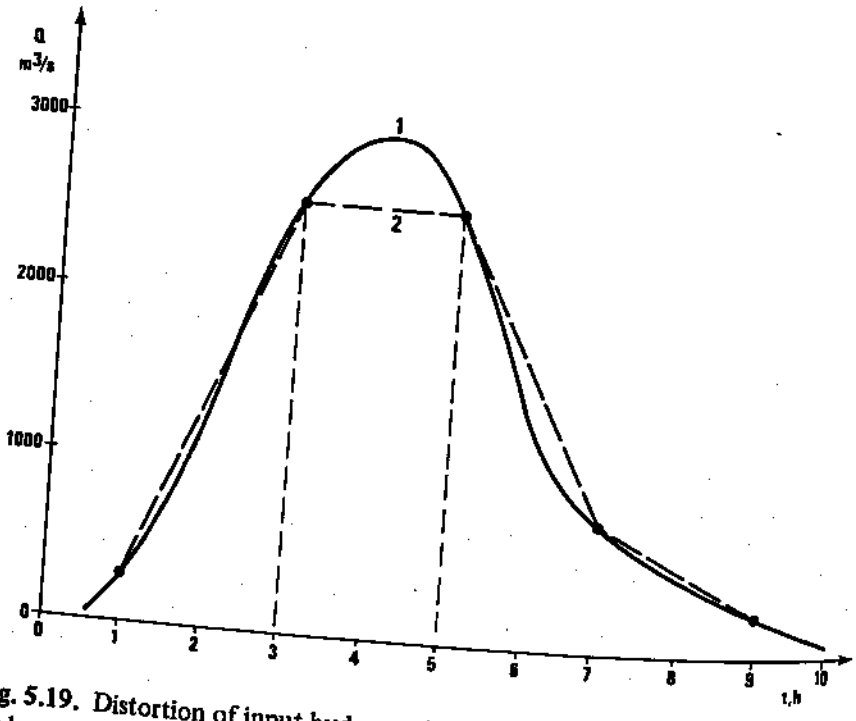

Fig. 5.19. Distortion of input hydrograph when Δt is too large: 1, true hydrograph; 2, hydrograph 'seen' by model using $\Delta t = 2$ h

A discussion of ways in which this infiltration loss can be taken into account is given by Cunge (1975a).

As for tributary inflow, the main problem is that in many situations neither the overall volume nor the shape (and timing) of the inflow hydrographs are available, and the modeller must often estimate these parameters. As long as the tributary inflow is relatively small compared to the main river flow, errors in the estimation will be of no great consequence in the calibration process. But in the lower Rhône example we described above, the Ardeche can flood during relatively low flow in the Rhône itself; in this case the agreement between measured and observed water levels downstream will be highly sensitive to errors in the assumed Ardeche inflow. Even if the inflow volume is correctly estimated or measured, the precise timing of the hydrograph may be subject to some uncertainty (poor synchronization of stage recorders, for example). In such case one might observe a time-shift between observed and calculated level hydrographs downstream, as indicated in Fig. 5.20. It is obvious that an 'objective' statistical measure (such as standard deviation of differences between calculated and observed levels at fixed times) of the comparison in Fig. 5.20 would disqualify an otherwise well calibrated model.

(v) Some phenomena are not taken into account at all by the formulation, such as:

- Absorption of water by dried up soil of inundated areas, or evaporation;

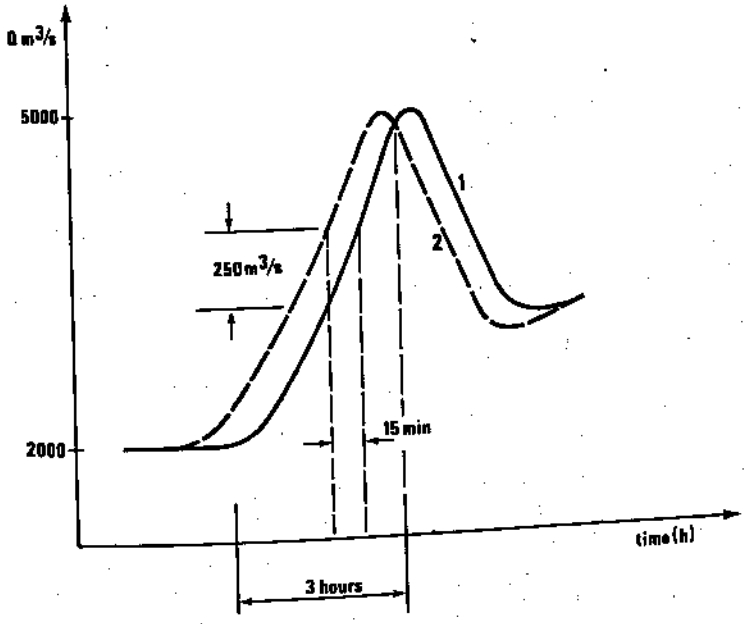

Fig. 5.20. Example of hydrograph time shift due to uncertain tributary inflow data: 1, observed flood; 2, computed flood

- lateral dead storage of flood waters;
- bed variation due to erosion;
- seasonal roughness variation due to vegetation cover.

In conclusion, if statistical measures of calibration accuracy are not to be rejected entirely, they should not be considered as the most important criteria. Visual examination of computed and observed hydrographs and their interpretation based on physical analysis of hydraulic features is the decisive factor as far as model calibration quality is concerned.

5.2 DATA NEEDS

General remarks

The reader's first reaction to the term 'data needs' may be one of scepticism; indeed, one could easily say that data needs are infinite. The more data one can obtain, the better, and all of it can be used to improve the quality of a model. On the other hand, it is very difficult to establish the minimum data needs for the construction of a model. If the old (by now!) data processing proverb 'garbage in – garbage out' is still valid, the question 'in the absence of anything else, what is the garbage you are willing to accept?' must be answered in every

specific case. In what follows, instead of giving a list of needed data – an impossible task without knowing the model purpose – we consider a certain number of general questions concerning topographical and hydraulic data for mathematical models: data collection difficulties, inherent limitations, data consistency, etc.

Theoretically any physical situation can be simulated with as high an accuracy as desired within the limits of validity of the physical hypotheses represented in the flow equations. Simulation methods which allow for looped networks of main channels and inundated plains, as described in Chapter 3, offer such a possibility; if the topography and hydraulic characteristics of the modelled watercourse are described with as high a precision as desired, the model will simulate reality with the same degree of precision, at least as long as the basic laws expressed by the equations used include all the pertinent phenomena. However the purpose of a model must be considered in deciding what resolution is to be sought. A mathematical model of a physical reduced scale laboratory model might require a computational grid resolution of the order of several centimetres; the necessary geometric data, measured directly on the scale model, would need to be quite precise, especially if the model represents a natural river and is intended to simulate the physical model with high accuracy. It would be clearly absurd, however, to introduce cross-sectional profiles every 20 m in a mathematical model which represents 100 km of natural river. In such a case the modeller is probably interested in the description of natural phenomena whose length scale corresponds to something like 1000 m. Most likely the introduction of cross sections every 20 m would not significantly increase the model accuracy as compared to using cross sections every 200 m, provided that their locations along the river are correctly chosen.

Thus there is no such thing as a criterion for 'ideal data', since the data which are needed depend fundamentally upon the model purpose. If a flood prediction model or a dam break wave propagation model is built with the purpose of implementing a flood warning system and determining design dyke heights, the accuracy and density of the data must be very high. If the model is to be used as one component of a general basin development study in which the characteristic land areas studied by the planners is of the order of 1000 km^2, the accuracy and density requirements will be different.

It is instructive to note the basic difference between general data needs for flood wave and dam break wave propagation models. The flood model requires considerable hydraulic data (measured levels and discharges) in order to be calibrated as well as possible, while it can get along with topographic data which are relatively sparse and coarse. Indeed, floods are slow phenomena and they usually propagate along rather smoothly varying valleys, hence the topographic features which influence them may be simulated by a small amount of discrete information. The dam break model requires, on the other hand, very accurate and dense topographic data while measurements of hydraulic data most often are not even needed. Dam break waves often propagate in mountain valleys of very complex topography, and simulated water stages are much higher

than anything observed in the past; therefore it is more important to introduce precise valley geometry and soil cover conditions beyond the main channel than to obtain records of past floods.

Since in this book we are not dealing with intuitive studies by consultants who lack the necessary tools for mathematical modelling, but rather with the art of building and running models of predictive capacity, we would like to warn the reader against the following fallacious but quite frequent argument: 'Since accurate and dense data are not available, the use of "sophisticated" (read: based on physically sound equations) models would be inconsistent with our knowledge of the physical situation'. According to this line of reasoning, some sort of 'global', or 'empirical', formula or oversimplified equation would be more 'consistent' with the sparse data (read: cheaper or within the grasp of the interested contractor) than would a model based on the simulation of physically meaningful laws of water flow. While it is quite legitimate to opt for simplified methods when the model purpose and known physical situations justify such a decision, to forsake the physically sound flow equations under the pretext that the data are insufficient means most often the compounding of two poor representations of reality.

The data required for flood propagation models can be grouped into two classes: topographic and hydraulic.

Topographic data describe the geometry of the simulated river system. By this we mean that they supply the elements necessary to define width, cross-sectional areas, volumes of inundated plains, etc. Moreover, they should permit the establishment of the topology of the model: the definition of cells in inundated areas, channel loops, the characteristic cross sections along channels where the computational points are to be established, the limits between main channels and flooded plains, the network of discharge exchange between the cells, etc. (*see* Chapters 3 and 4). The topography of river valleys may be measured with an accuracy and completeness which is limited only by its cost and can be directly carried over into the model in the precise definition of cross sections, cells, weirs, etc.

Hydraulic data consist of measurements of stage and discharge hydrographs, tidal records, spot measurements of stage, discharge and velocity, high water marks for flood events, rating curves, flooded area limits and depths, etc. These data serve two purposes: the establishment of model boundary conditions, and the indirect determination of channel conveyances (roughnesses), weir coefficients, and other hydraulic parameters which cannot be determined on the basis of topographic data alone.

Supplementary data are needed for certain kinds of models. For example, tidal river models may require salinity distributions along the river, for use in calibrating, validating and exploiting the model. For calibrating movable bed models, data concerning sediment discharge and river bed deformation (deposition or erosion) are essential, along with the usual topographic and hydraulic characteristics required for flood propagation models.

In the following paragraphs we will go into some detail regarding topographic and hydraulic data needs, and their relation to model calibration and exploitation.

Topographic data

The topographic data used to build mathematical models of rivers may be divided into two basic categories:

(i) Qualitative, reconnaissance type descriptions of the river, its tributaries, and inundated plains. This involves the identification of the physical conditions which determine flood development patterns; the existence of berms within the flood plain, dykes, breach formation, elevated roads, localized obstacles within inundated zones, preferential flow axes, etc. Qualitative data may be obtained by field investigation, inquiries, satellite and aerial photographs, newspaper reports, etc. It is next to impossible to enumerate 'what is needed', since the more that is known, the better. The essential objective is to learn enough about general flood patterns in the modelled area to be able to intelligently locate cells, computational points, weirs, and other model elements, and to be able to recognize anomalous model predictions during simulation. The better the modeller's 'feel' for the terrain and its floods, the more faithful will be his model's representation of physical reality.

(ii) Quantitative topographic data which are needed for the model representation of the river and its flooded plains. There are essentially three factors which, in the course of flow simulation, depend directly upon the topography, namely: preferential flow directions (which depend on conveyance variations, breach elevations, dykes and roads), the wave celerity (which depends on the cross-sectional characteristics), and the volume of water stored in the system. Accordingly, three kinds of quantitative topographic information are required: longitudinal profiles along banks, dykes, roads, etc., transverse profiles across the watercourse, and contour imagery of the inundated area.

In theory all three types of data could be obtained from a series of maps of sufficiently large scale. In practice it is not as easy as that. In what follows we assume that the river valley can be divided into three zones: a main channel (dry season bed, conveying low flow discharges), flood channel (flooded areas in which water flows only during the flood period but more or less follows the general direction of the main channel) and inundated plains, where the flow direction cannot be determined in advance. We shall try, with reference to these three zones, to describe the data which the modeller needs to obtain either from existing maps or from a special survey -- the goal being to build a reliable and detailed model.

Longitudinal profiles

Longitudinal profiles are needed along the *flood channel banks* which are

nearest the inundated plain. Profiles should also be established along the flood channel banks of tributaries and their inundated plains, keeping in mind that the latter may well be flooded through backwater effects in the main river.

Longitudinal profiles should be defined along the *main channel banks* (separation between main and flood channels).

Longitudinal profiles of *transverse roads and dykes* within the flood channel and the inundated plain should be established and tied into the longitudinal profiles of flood channel banks. All important breaches and structures, as well as depressions in dykes, banks and roads must be described in enough detail so that they may be assigned appropriate overflow widths, elevations, and discharge coefficients in the model.

Transverse profiles

Transverse profiles across *flood channels* are established at more or less equal distances one from another except where the particular features of the valley require irregular spacing. The average interval between transverse profiles (or sections) depends on the required model accuracy and on the steepness of the valley; the order of magnitude is from 1 to 10 km. Transverse profiles should also be obtained for the *tributaries* which are included in the model.

Main channel transverse profiles are needed at an average distance which depends upon the model purpose, the range being from 200 m to 5000 m. These transverse profiles should be located so as to reflect all special features of the river such as narrows, pools, etc., as well as average section properties.

Inundated area maps

Longitudinal and transverse profiles are not sufficient for the determination of stored water volumes on flooded plains modelled as two-dimensional zones. When flooded zones are modelled as a network of interrelated cells, the modeller must establish for each cell not only the elevation of dykes, roads, and other natural limits around the cell (furnished by profile surveys), but also the storage versus water elevation curve. Unless the cell bottom is horizontal and the cell itself completely dyked, the construction of this curve requires contour maps, the scale and vertical contour interval of which should be consistent with the desired model accuracy. The distance between cell centres being of the order of 1 km to 10 km, a horizontal scale of 1:20 000 or 1:50 000 (1 cm = 200 m or 1 cm = 500 m) would be generally sufficient. A vertical contour interval of 1 m or less would be necessary to be consistent with the usual modelled water surface elevation accuracy of between 15 and 50 cm.

In estimating that we need maps of 1:20 000 or 1:50 000 scale with a maximum contour interval of 1 m, we have been considering model needs independently of mapping possibilities. In a detailed analysis of mapping techniques, Carrère (1977) arrives at a rather unfortunate conclusion as far as modelling needs are concerned: it is impossible to have a contour interval as small as 1 m for maps of smaller than 1:10 000 scale (unless a detailed ground survey is performed). Even in industrialized countries, it is generally impossible

to obtain maps of 1:10 000 scale over any significant area. In France, for example, only 1:20 000 maps with a contour interval of 5 or 10 m are available except for Paris and certain regions of the Maritime Alps. By comparison, the largest map scale available in the countries riparian to the Niger River is 1:200 000 with a contour interval of 50 m or more.

In a river valley such as that of the Rhône River, the flooded valley is delimited by relatively steep banks. In this case the horizontal distance between contour lines on a 1:20 000 map is relatively small, and the valley storage volume can be estimated with small error by interpolation between contours. The existing cartography, supplementing existing longitudinal and transverse profiles which are tied into the vertical control datum of the maps, provides a perfectly adequate basis for the construction of a reliable mathematical model. On the other hand in large, flat inundated plains such as for the Niger and Mekong rivers, where detailed cartography is unavailable, the horizontal distance between 5-m contour lines may be as great as 50 km, and a reliable model cannot be constructed unless a certain amount of special mapping is commissioned.

It would be too easy to conclude from the above that since sufficiently precise topography is not available, we can do without mathematical modelling and go back to qualitative shamanism in flood prediction and hydraulic studies. We are saved from such a fate by the fact that since civilization has usually developed along natural watercourses, topographic data are generally much more abundant and precise in river valleys than elsewhere. Transverse profiles in main channels are abundant in large rivers, especially navigable ones, and are of considerable value in constructing a mathematical model even if not tied into a vertical control survey. And experience has shown that even with 1: 20 000 or 1:50 000 maps, augmented occasionally by detailed local surveys, models can be successfully constructed, calibrated, and exploited as far as stored volume on the flood plain is concerned.

Hydraulic data

Hydraulic data needs fall into two general categories; boundary conditions, and discharge and water level observations which are needed for indirect bed roughness estimation and model calibration.

Boundary conditions

All models require boundary conditions. Upstream stage or discharge hydrographs are always required for natural rivers and can usually be obtained without too much difficulty. As for the downstream boundary condition, one should keep in mind the remarks we made in Section 5.1 concerning the influence of a steady flow rating curve. Since the real stage/discharge relationship is multi-valued in unsteady flow, the results along downstream reaches of the model will be distorted if a steady flow (single-valued) rating curve is applied at the downstream limit. Therefore it may be more advantageous to search for data such as

water stage hydrographs at the downstream boundary. However one should not forget that while water stage hydrographs may be available for some past floods, and can be used for model calibration, they will not be known *a priori* for the exploitation runs unless the model ends at a lake, reservoir, or tidal condition.

Additional boundary condition data may be required for special kinds of models: a tidal river model requires tide recordings and perhaps salinity measurements at the river mouth as well as the inland fresh water inflow hydrographs; movable bed models require the sediment transport rate at the upstream boundary.

Tributary inflows, which can also be considered as boundary conditions, are seldom gauged, and it is not uncommon to read that their 'average discharge is negligible as compared to the main river'. This may be so, but if during the passage of a calibration flood a flash flood occurs on a tributary, and this event was not taken into account during the calibration process, the modeller may choose wrong roughness coefficients for the main watercourse only because of his ignorance of the additional flow as we described earlier. Thus it is most important to collect flow data on any tributaries whose contribution to the mainstream flow could have a significant influence on calibration accuracy and model exploitation.

Discharge and level observations

This second category of hydraulic data is of a fundamentally different nature from topographic or boundary condition information. Discharge and level observations are not substantive data which are necessary for the construction and operation of a model; they are associated information which is needed for the calibration of bed roughnesses, discharge coefficients, and other hydraulic parameters which cannot be directly measured. These parameters can be roughly estimated on the basis of the modeller's experience combined with field reconnaissance, but their true values can be determined only throughout indirect calculation using discharge and level observations.

As far as steady flow calibration is concerned, the essential hydraulic data are rating curves (i.e. $Q(y)$ relationships) at as many points as possible along the main channel. As we described in Section 5.1, these rating curves can be used to construct approximate longitudinal water surface profiles on the basis of which overall section conveyances, and thus bed roughness values (Manning, Chezy, or Strickler coefficients), can be calibrated. Available rating curves are not generally defined for flood discharges (which are usually quite unsteady in any case), but overall section conveyance functions can be extrapolated upwards for flood flows if bed roughness values are correctly assigned, as we described in Sections 4.5 and 5.1. In undeveloped river basins, it may be necessary to conduct special surveys to tie in uncontrolled staff gauges and their rating curves to a common elevation datum. In all rivers, it is important to verify whether or not significant channel erosion or deposition has taken place since rating curves were established.

Unsteady flow observations, on the other hand, are all too often funda-

mentally incompatible with the needs of mathematical (and physical) models. The kinds of data which are usually available are geared to the extreme-event needs of statistical hydrology: maximum annual discharges, high water marks on the flood plain, maximum flood stages, etc. These kinds of observations are indeed extremely valuable for checking model calibration, but they are of little use for the detailed calibration process itself. Models are calibrated for a small number of flood events; 100 years of observed maximum discharges and the well defined flood frequency curve which has been developed are of no use to the modeller who needs to have the detailed structure of a *particular flood*.

Thus the kind of data we need for unsteady calibration is systematic and continuous measurements of water levels and discharges (if possible) at various points in the main channel and on the flood plain during the full duration of several flood events. Even when this type of data exists, it is all too often still inadequate; daily observations of channel water level, and widely separated and occasional observations of flood depth on the inundated plain, are insufficient for the definition of flood wave celerity in the channel and flooding patterns on the flood plain. What is needed are

- continuous recordings of stage in the main channel during the entire flood event and at stations spaced closely enough to permit a good resolution of the flood wave celerity and shape; a few measurements of discharge distribution in different channel;
- frequent observations of flood plain water level (and/or limits of inundation) and flow directions at locations which are spaced closely enough to define flow patterns during the entire flood event.

These two kinds of data, with all levels related to a common datum, are worth their weight in gold (perhaps literally) to the modeller. Observation networks temporarily installed for just one flood season but synchronized over the basin can provide more useful information than years of spotty, maximum-event type data. Once a model is well calibrated, it can then be used in conjunction with statistical hydrologic data to generate flood statistics throughout the modelled region.

We have been talking about ideal data needs, obviously; many predictive mathematical models have been successfully constructed, calibrated, and exploited with only a minimum of the kinds of unsteady flow observations we have described. This is a tribute to the basic soundness of the de St Venant flow equations and the numerical techniques used to solve them, which provide a correct description of physical reality and require only physically meaningful parameters as data. Nonetheless, the more detailed information on particular floods that is available, the better will be the predictive capacity of the model. This view is becoming more and more frequently recognized by various organizations and has modified the system of data collection in many countries. For example, the U.S. geological survey is involved in a program automatization of data collection *for mathematical modelling purposes*. This is only the beginning of an evolution which may indeed revolutionize the future of mathematical river modelling (see, for example, Schaffranek and Baltzer, 1978).

6 Modelling of flow regulation in irrigation canals and power cascades

The present chapter is mainly descriptive, its purpose being to show some specific characteristics of models used to simulate flow in canalized and entirely controlled systems, and to point out the ways in which this type of modelling differs from the essentially natural river simulation we have treated in the two previous chapters. We shall make use of examples to as great an extent as possible, and avoid delving into mathematical developments, at least when the latter may be found in Chapters 2, 3 or elsewhere. We consider three kinds of flow control systems corresponding to different kinds of physical situations:

(i) irrigation canals with automatic control devices;
(ii) power and navigation canals;
(iii) power plant cascades on canalized rivers.

6.1 FLOW CONTROL IN IRRIGATION AND WATER SUPPLY CANALS

The most important aspects of water supply through an open channel system may be illustrated by a simple example of a single canal reach with upstream water storage from which the discharge into the canal is controlled by a gate called the regulator, Fig. 6.1. Suppose that there is a single diversion of water at the downstream end of the channel, $Q_d(t)$.

The discharge Q_d may vary, depending on irrigation needs, from $Q_d = 0$ to some value $Q_d = Q_{max}$. Hence the channel reach has to be designed for that maximum discharge Q_{max}. The diverted discharge Q_d varies with time, and the purpose of the regulator is to assure that the discharge Q in the channel will satisfy the demand.

Suppose that Q_d decreases from its maximum value Q_{max} to some smaller value, Q_i. A positive wave will then be created at the downstream end and propagate upstream as shown in Fig. 6.1. Suppose that the regulator is connected to a sensor A in such a way that when the free surface water level varies at that point, the regulating mechanism will close or open the regulator so as to maintain some constant reference level at section A, $y_A = y_{ref}$. In our

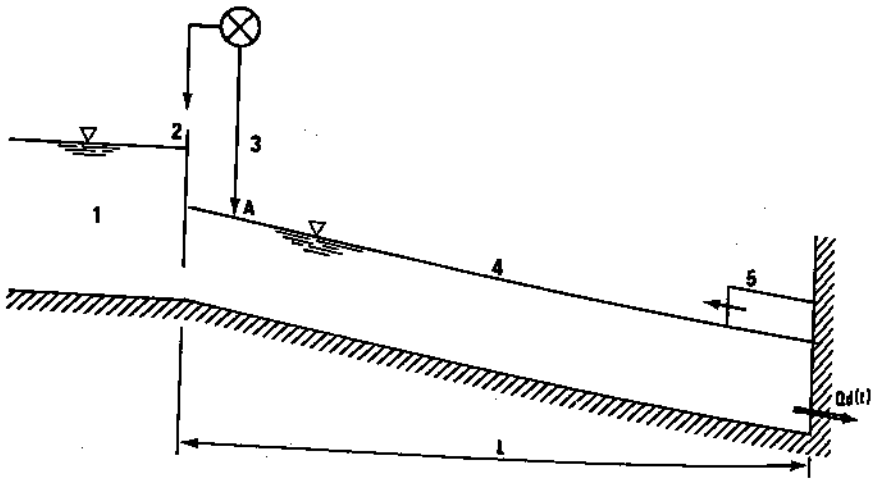

Fig. 6.1. Downstream regulation system. 1, Upstream storage; 2, regulator; 3, sensor; 4, water level at $Q = Q_{max}$; 5, positive wave

example, when the positive wave arrives at point A, the water level there will increase and it will cause a partial closure of the regulator. This action will in turn decrease the discharge at the head of the canal.

Such a system should, after a certain time, adapt the upstream discharge to the downstream diversion demand. It is called a downstream regulating system, since it maintains a level downstream of the gate constant, and is a very simple but not very economic system. Indeed, when $Q = 0$ in the channel, this system leads to a horizontal free surface as shown in Fig. 6.2, which requires very high dykes

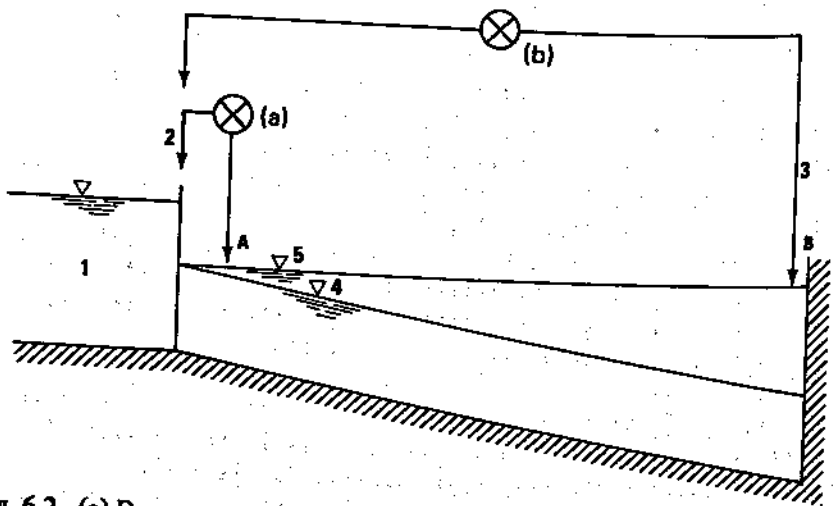

Fig. 6.2. (a) Downstream regulating system. 1, Upstream storage; 2, regulator; (b) Upstream regulating system. 3, sensor, 4, water level at $Q = Q_{max}$; 5, water level at $Q = 0$.

along the channel. Moreover, the time of response is long; the upstream regulator cannot react until the wave generated at the diversion arrives at point A. When the diverted water discharge increases from 0 to some Q_i value, the negative wave thus created must arrive at point A before the regulator can open and generate a positive wave to feed the increased demand. Until this wave arrives at the downstream end, the diverted discharge must be supplied by the volume stored in the canal itself. That volume must be large enough to satisfy the demand during the time $2L/c$ (c being the wave celerity) necessary to bring the water from upstream storage.

One obvious solution to this difficulty is to install a sensor at the downstream point B as shown in Fig. 6.2. The time of response of the system is then divided by two. Such an upstream regulation principle requires that a new parameter be specified: the reference level to be maintained at point B. Moreover, this scheme is not as easy to implement as may be thought. In downstream regulation, the opening of the regulator has an immediate influence upon the measured water level at A; hence the system is inherently stable. This inherent stability does not exist in upstream regulation systems. Suppose that there is an increase in the demand Q_d; the level at section B decreases and the regulator opens immediately, sending a positive wave from point A towards point B with a celerity of, say, 2–3 m s^{-1}. If the channel length is 3000 m, it will take about 20 min for that wave to arrive downstream. During that time the level at B will continue to decrease, thus provoking further opening of the upstream gate. When the level at section B stops decreasing, there is a pretty good chance that the upstream regulator will be completely open and $Q = Q_{max}$ injected into the channel. Conversely, if the downstream sensor requests that the upstream regulator be closed, it may cut the discharge off completely before its influence could be felt downstream. Thus the upstream regulating system, as we have described it, is inherently unstable. When water supply systems become highly complicated, including a great number of reaches, turnouts, and regulators, the stability question is of prime importance.

Sophisticated control systems have been developed in recent years, and interested readers may find the description of such systems in the literature (Cunge, 1975b; Clément, 1966; Combes, 1968; ASCE, 1968; Harder *et al.*, 1972). The stability question was thought for years to be the only aspect of control system design which was really important. Hence classical mathematical methods were used to study stability conditions; the de St Venant equations were linearized, as were the regulator laws, and then the behaviour of the solution to the resulting system of equations was investigated: if the system damped induced oscillations, it was considered stable. The details of such methods and of their applications may be found elsewhere (IAHR, 1976).

Stability analyses, in neglecting non-linear phenomena altogether, are incomplete in several respects. For example, they cannot predict system behaviour due to finite discharge variations (breakdown of a gate, general voltage cut, pump group cut off, etc.) which create rapidly varying flow conditions, and they are unable to simulate the cumulative effect of several regulators. In engineering

practice it is becoming more and more customary to replace strictly mathematical analyses of control systems with mathematical models which are based on the de St Venant equations, since such models are able to properly simulate regulators and structures along the canals while taking important non-linear phenomena into account.

Let us look at two particular examples of such use of mathematical models. Consider an irrigation channel of five reaches, each containing three diversion points as described by Bagnérès (1972) and shown in Fig. 6.3. The 50 km

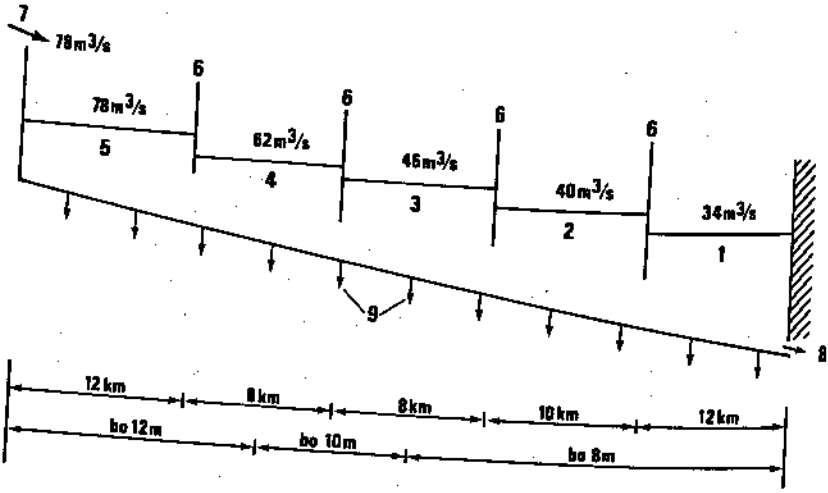

Fig. 6.3. Regulated irrigation canal (after Bagnérès, 1972). 1, Reach 1; 2, Reach 2; 3, Reach 3; 4, Reach 4; 5, Reach 5; 6, gate; 7, upstream pumping station (8 units @ 10 $m^3\ s^{-1}$ each); 8, downstream intake; 9, turnout diversions

channel has a trapezoidal cross section with a bank slope of 3:2 and invert widths b_0 as shown; The discharge at the head of the system is 78 $m^3 s^{-1}$ and falls to 34 $m^3 s^{-1}$ in the downstream reach.

First of all, a classical downstream constant level regulation system was considered (the constant level is maintained on the downstream side of the gate which is at the *upstream* end of the reach, as shown in Fig. 6.1). As applied to the 5-reach canal, this scheme will try to maintain a constant free surface elevation y_{ref} on the downstream side of each gate. In order to study the canal behaviour beyond the simple statement of its stability, a mathematical model of it was built using a standard modelling system for translatory wave propagation in channels. It was based on the full de St Venant equations, using Preissmann's implicit finite difference scheme; the time step was carefully chosen so as to avoid as much numerical damping as possible (*see* Section 3.2). The gates were simulated by special subroutines into which were introduced data such as gate width, sill elevation, speed of gate opening, insensitivity range, etc. The model simulated a sudden discharge variation at the downstream limit of the canal from 0 to 20 $m^3\ s^{-1}$ while all other diversions discharged at their maximum

capacity. In Fig. 6.4a are shown computed water stages at three points in the downstream reach (No. 1) and in Fig. 6.4b the stages computed at three points in the upstream reach (No. 5). It is evident from the curves that the upstream regulators do not begin supplying water until the negative wave propagating upstream arrives; the initial downstream demand change occurred between time 0 and 6 min, but the reach 5 regulator does not sense the demand until 2.5 h later. The curves show also that free surface oscillations are of greater amplitude in reach 5 than in the downstream reach 1, though according to the conclusion of a theoretical study of a reach, these oscillations are eventually damped. Nevertheless, the maximum elevation in reach No. 5 due to these oscillations is 8.3 m while the y_{ref} at the upstream end of that reach (pumping station) is 7.97 m, obtained only 12 h or more after the initial perturbation.

The behaviour of the same canal was also studied using a different type of

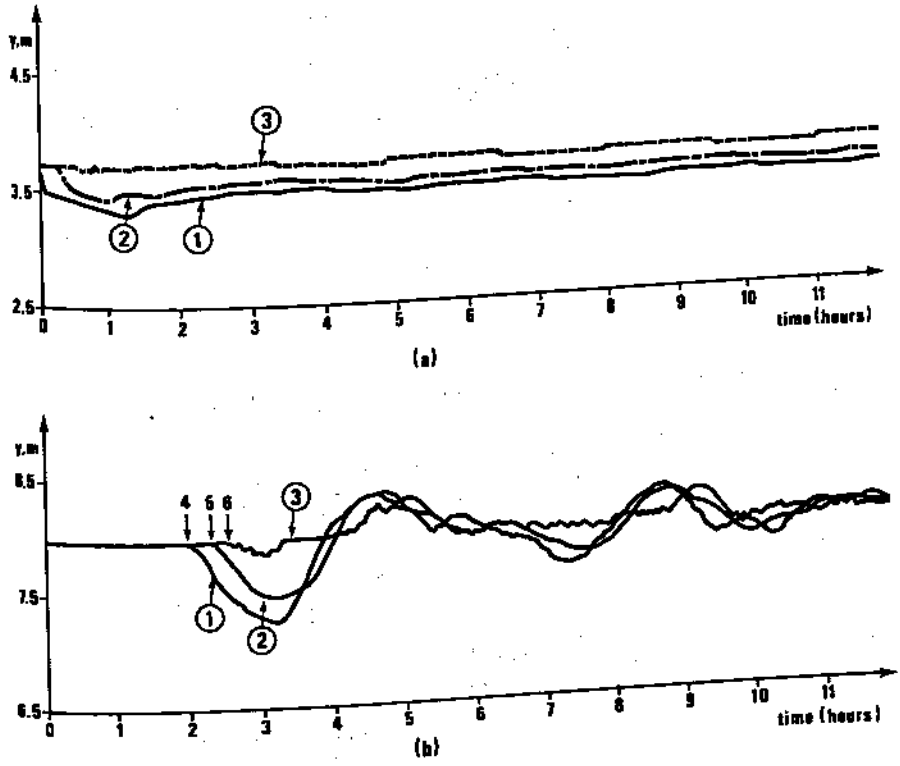

Fig. 6.4. Modelled water level variations in regulated irrigation canal (downstream regulation). (a) Reach 1. (b) Reach 5. 1, water level at downstream end of reach; 2, water level at middle of reach; 3, water level at upstream end of reach; 4, negative wave arrives at downstream of Reach 5; 5, negative wave arrives at middle of Reach 5; 6, negative wave arrives at upstream of Reach 5

regulator; the BIVAL (or associated elevation) type of gate control system. The system, described in detail by Cunge (1975b), functions as schematically described in Fig. 6.5. The BIVAL system introduces a weighting factor α between two sensor indicators A and B, making it possible to use a y_{ref} level which is

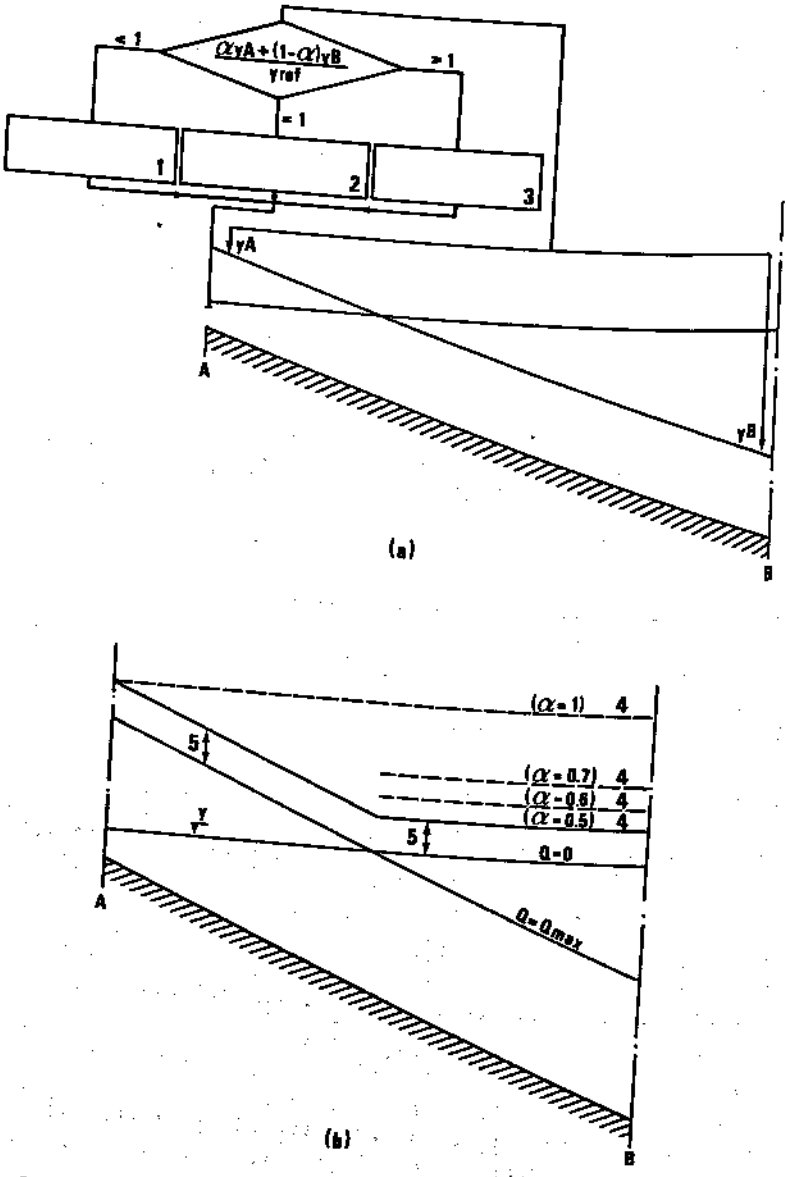

Fig. 6.5. BIVAL Control System. (a) Schematic representation. (b) Required bank level for different values of α. 1, gate opens; 2, no action; 3, gate closes; 4, maximum bank level for different values of α; 5, freeboard

situated between the reach limits. When $\alpha = 1$, BIVAL reduces to simple upstream regulation. Use of the BIVAL system requires that the engineer determine parameters such as the weighting coefficient α, reference level y_{ref}, insensitivity range, speed of gate closure, positioning of the sensor B, etc. Since our purpose is only to show how a mathematical model can intervene, the reader is invited to refer to the cited references for more details of the system.

In Fig. 6.6a and Fig. 6.6b are shown the computed stage hydrographs for the

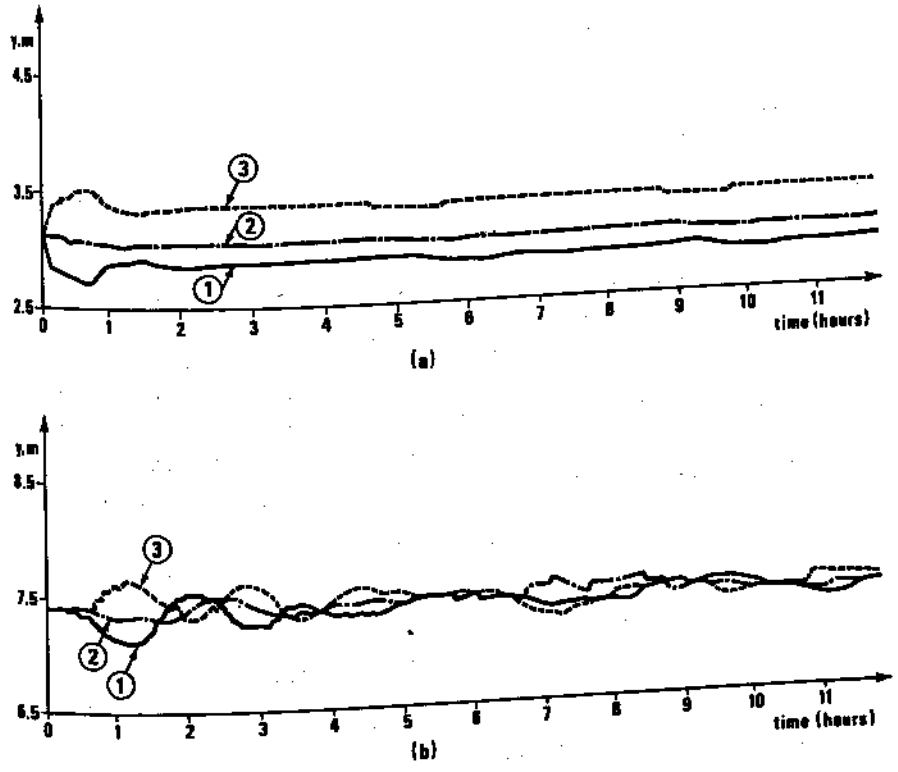

Fig. 6.6. Modelled water level variations in regulated irrigation canal (BIVAL system). (a) Reach 1. (b) Reach 5. 1, water level at downstream end of reach; 2, water level at middle of reach; 3, water level at upstream end of reach

same canal as in Fig. 6.4, but with the BIVAL system being simulated. The picture is strikingly different as to the dynamic behaviour of the two systems. The reader should closely examine the highest levels attained by the free surface in both cases. In Fig. 6.7 are shown the envelopes of maximum water levels along the channel for the two cases. It is not our purpose to discuss the respective merits of the described systems; that is done, for example, by Bagnérès. But we would like to stress, before going on to review another example, that it would not have been possible to compare the two systems, and even less to examine the

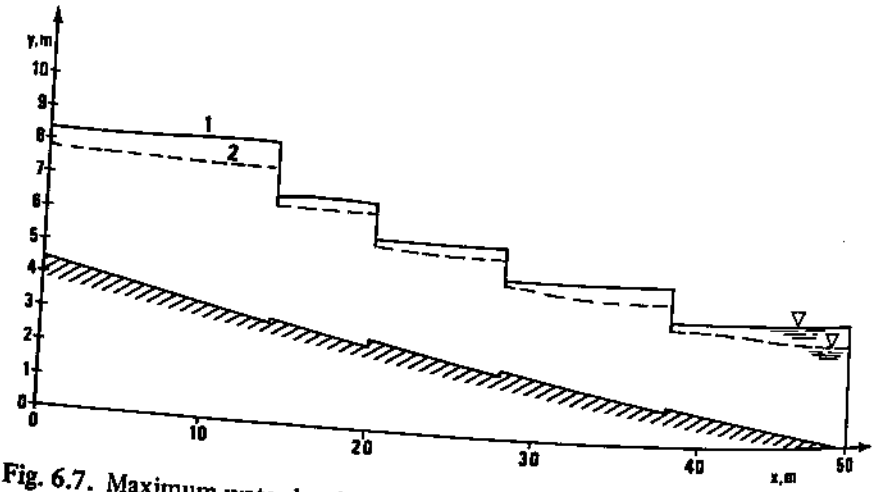

Fig. 6.7. Maximum water levels in regulated irrigation canal using downstream regulation and the BIVAL system. 1, downstream regulation; 2, BIVAL system

influence of such factors as weighting coefficients, decrements, etc., without the use of the full mathematical model.

The Kirkuk–Adhaim (Iraq) irrigation project is another example of the engineering application of mathematical modelling to flow control problems†. The project consists of a 37 km Feeder Canal on a rather steep slope bringing water from Dibbis diversion dam on the Lesser Zab River, followed by the 40 km Main canal of much milder slope, Fig. 6.8. Maximum discharge at the

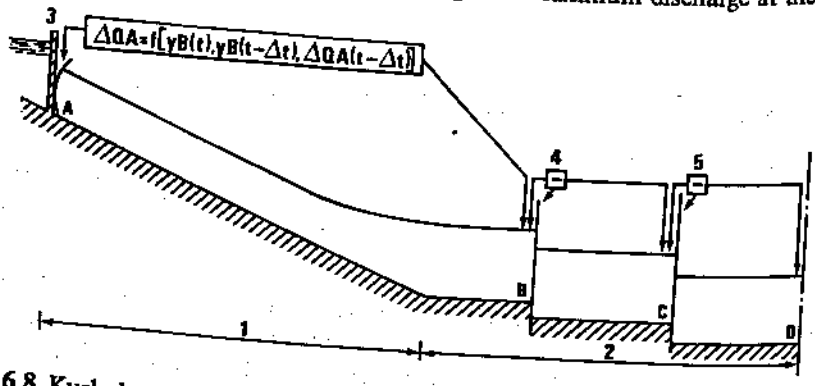

Fig. 6.8. Kurkuk–Adhaim Project regulation system (courtesy SOGREAH, Grenoble, France). 1, feeder canal; 2, main canal; 3, Dibbis dam with upstream gate; 4, Regulator R1; 5, Regulator R2

head of the Feeder canal is 280 $m^3 s^{-1}$; the irrigated area is 3000 km^2. At first, upstream control of the flow was thought to be appropriate, and it was to be executed with the aid of a dam at Dibbis, the upstream limit. Such a regulation system, had it been built and implemented, would have led to two major problems:

†Courtesy SOGREAH, Grenoble, France.

(1) Considerable loss of water during the periods of irrigation water refusal.
(2) Lack of water if the demand was higher than the programmed discharge.

As originally planned, the system could therefore have been inefficient and/or a source of water waste.

Mathematical modelling techniques made it possible to develop a design which reduced the system's problems to an acceptable level (Chevereau and Gauthier, 1976). The new control system consists of two regulators R1 and R2 whose role is to maintain a constant difference in free surface elevation between two points located at the downstream limits of consecutive reaches ($y_B - y_C$ = constant, $y_C - y_D$ = constant in Fig. 6.8). The action of the two regulators creates a buffer volume in the canal itself; this volume is used to supply water during the initial period of increasing demand. The upstream gate at Dibbis dam must maintain that reserve and it is open or closed depending on the free surface elevation at section B. The gate position is checked at time intervals Δt and its opening supplies, at time t, a discharge variation defined by the formula

$$\Delta Q_A = \alpha [y_B(t - \Delta t) - y_B(t) + \beta (y_{B\,ref} - y_B(t))] - \gamma \Delta Q_A(t - \Delta t) \tag{6.1}$$

where y_B = free surface elevation at point B; ΔQ_A discharge increase (or decrease) at the upstream section A; α, β, γ = coefficients to be adjusted; $y_{B\,ref}$ = free surface elevation to be maintained.

In Equation (6.1) the coefficient β damps the influence of the difference between the sought and actual free surface levels; the coefficient α depends on the surface area of the main canal; the coefficient γ depends upon the flow in the feeder canal. All conceivable operating procedures were simulated with the aid of the mathematical model which was built using the full de St Venant equations and solved by the Preissmann implicit finite difference scheme; special care was taken to properly simulate the regulator movements. The model made it possible to study the Kirkuk system behaviour under exceptional circumstances, such as sudden demand cutoff. It was possible to define the various regulating coefficients so as to ensure that the demand would be satisfied without loss of water as long as the difference between that demand and the programmed demand is less (in absolute value) than 15% of the maximum canal discharge (i.e. less than $\pm$ 42 $m^3 s^{-1}$).

Other examples of similar applications of mathematical models are available in the literature. The technique is especially well suited for the simulation of such complicated upstream control systems as Hyflo used for the regulation of the California Water Project irrigation system (Harder *et al.*, 1972), or to check the efficiency of dynamic regulation systems such as that implemented by the Société du Canal de Provence in Southern France. The latter is based on the use of an industrial computer which periodically adjusts all regulators with the goal of maintaining volumes of water in different reaches which are as close as possible to certain reference volumes. The reference volumes themselves are established by statistical studies of consumptive water demand by the users,

taking into account seasonal variations.

The modelling techniques used for such studies must be selected with the greatest possible care if the simulation is to provide a faithful reproduction of reality. The friction slope is usually very small in irrigation systems, and inertia forces thus play an important role. As was shown earlier, stability is an important factor in the functioning of such systems; it may thus be dangerous to simulate them with modelling schemes which introduce a great amount of numerical damping which could mask real-life unstable behaviour. Hence proper finite difference schemes should be chosen, and that choice has to be accompanied by a proper choice of the $\Delta t/\Delta x$ ratio during simulation. It is always advisable to run several tests before beginning the real simulation, in order to check the damping characteristics of the model. For example, the propagation of water releases can be simulated while suppressing the energy loss term and varying the time step, in order to appreciate how the wave attenuation depends on the time step.

One important application of such models is in the planning of water releases. Indeed, one would often like to be able to prescribe the opening of upstream gates in such a way as to obtain the desired downstream hydrograph. Such a problem is, mathematically speaking, an 'inverse' problem and as such is ill-posed, at least for non-linear equations of the hyperbolic type (*see* Chapter 2). Nevertheless some researchers have attempted to solve this inverse problem for practical applications (Bodley and Wylie, 1978). It is possible to obtain *reasonable* upstream flow variables (stage and discharge hydrographs) using downstream ones if the following conditions are satisfied: friction must be very small (negligible); non-linearity of the convective velocity term must not be strong; the distance between the regulators must be small. Even then the only method which can be used is the method of characteristics with all its complexity and unwieldiness. In order to define upstream releases it is better to run several test cases using a model built with the aid of a standard, efficient modelling system instead of a specially written inverse problem program. The celerities thus obtained for different volumes stored within the system of canals and for different discharges will be a sufficient guide for the planning of the release, whose propagation along the channel can then be checked using the same model.

6.2 SURGES IN POWER CANALS

The evolution of free surface elevations and flow discharges in irrigation canals usually proceeds rather slowly in time, the only exception being wave propagation following a sudden accidental closure of flow regulators. Except for this special case, the de St Venant equations are valid for the simulation of flow throughout canal systems. Such is not the case for power canals, in which the flow is characterized by very rapid variations of discharge and water level. Since the de St Venant equations are not valid in such situations, special modelling techniques are necessary.

Let us consider an upstream propagating positive wave in a trapezoidal channel. Such a wave, caused by the sudden closure of gates or turbines, may have a mild initial curvature, but it will become steeper and steeper as it propagates. The mechanism by which an initial wave steepens is described in Chapter 2, and recapitulated in Fig. 6.9. Suppose that the initial wave was of the

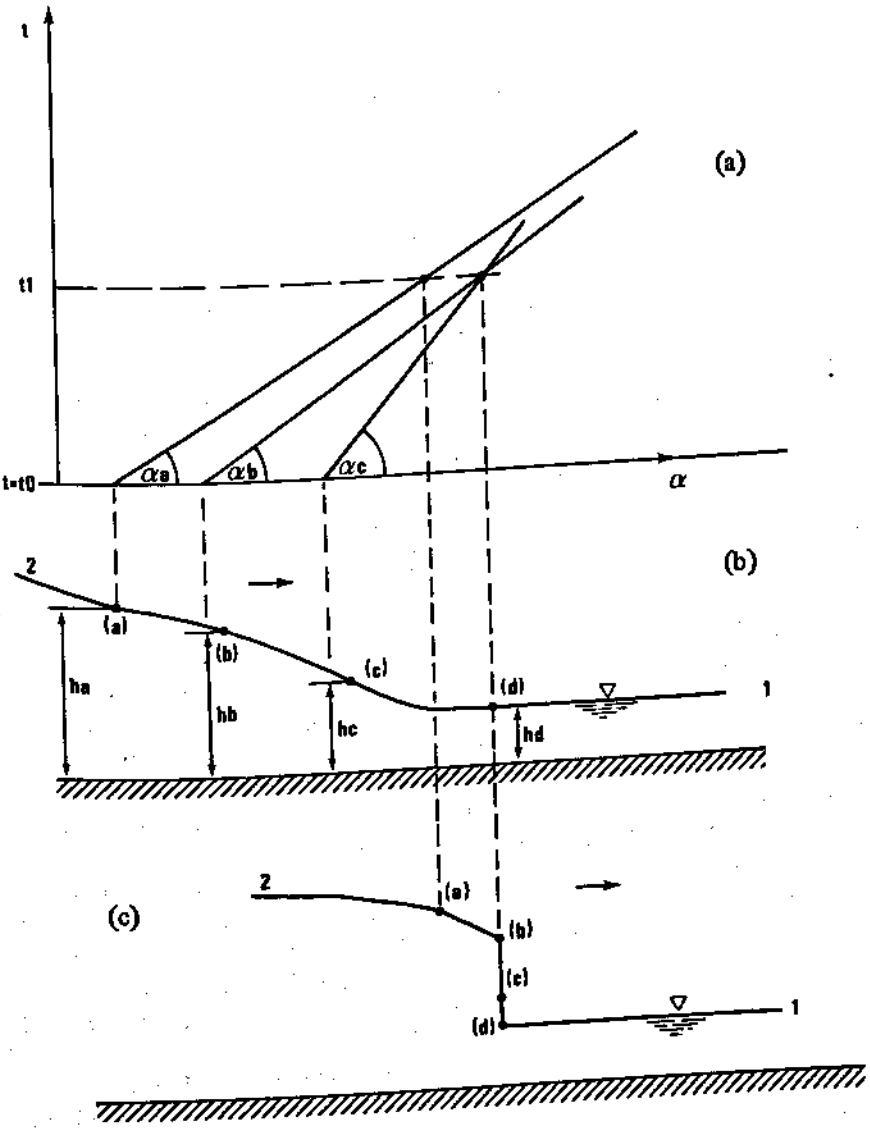

Fig. 6.9. Surge formation in a power canal. (a) Trajectories from points a, b, and c. (b) Initial surge shape. (c) Steep-ended surge shape. $\tan \alpha_a = (gh_a)^{-1/2}$; $\tan \alpha_b = (gh_b)^{-1/2}$; $\tan \alpha_c = (gh_c)^{-1/2}$; 1, initial level; 2, advancing surge

shape shown in Fig. 6.9b. The celerities of each of the three points (a), (b), (c) shown in that figure are not the same and if friction is negligible, they are nearly proportional to the shallow wave celerities $(gh)^{\frac{1}{2}}$ at these points. In Fig. 6.9a are shown the propagation paths of the three points in the (x, t) plane. Obviously, the tangent of the angle between each path and the x-axis is $dt/dx \approx (gh)^{-1/2}$. After some time (let us say at $t = t_1$) the point (b) will catch up with point (c) as shown in Fig. 6.9c. In the (x, t) plane this phenomenon is shown by the intersection of the propagation paths of points (b) and (c). In hydraulics such a situation is called a 'surge' or a 'steep front wave'. In gas dynamics it would be called a shock wave, while in computational hydraulics we often call it a discontinuity, although the other names are used as well.

Physically, something special should happen in such situations and indeed hydraulic engineers are quite familiar with the two forms of such a surge. The first one is simply a 'roller', or a 'bore', a mobile hydraulic jump which propagates along the channel with a celerity smaller than that of the points behind it (hence the point (a) will be able to catch up with such a front) but greater than that of the points in front of it. The de St Venant hypotheses are not valid in the neighbourhood of such a front (as they are not valid within any hydraulic jump) since vertical accelerations are not negligible, the pressure distribution is not hydrostatic, and a certain amount of energy is dissipated in the highly turbulent roller which propagates with a nearly constant celerity. For the observer who runs along the canal at a speed equal to the bore celerity, there is no difference between the surge and a stationary hydraulic jump. Such a form, however, is only seldom encountered. Indeed, in order to create a roller the free surface elevation of the surge above the initial level should be more than 20% of the average initial depth.

When the incident wave height is smaller, quite a different situation prevails. The front of the positive surge remains a smooth, continuous surface and as it propagates, it creates a train of short waves behind it. These waves all have nearly the same crest elevation along the canal – they are extremely slowly damped. The occurrence of such undulations instead of a discontinuous steep wave front cannot be explained satisfactorily by the de St Venant hypotheses. The hydrostatic pressure distribution assumption, and possibly also that of uniform longitudinal velocity in a section, must be discarded in accounting for real phenomena along the whole length of the wave train. The details of a travelling undular surge are depicted in Fig. 6.10, which is a photograph of an advancing undular mobile jump in the Oraison (France) power canal, see Cunge (1966b).

Figure 6.11 defines the nomenclature we use to quantitatively present the Oraison power canal (France) undular jump observations in Figs. 6.12 and 6.13; h^* and h_* are, respectively, the free surface superelevations of wave crests and troughs as compared to the initial free surface level. Figure 6.12 shows an instantaneous observation of 19 waves at the bank of the trapezoidal canal following an abrupt intake discharge change of 210 $m^3 s^{-1}$. The non-symmetric, almost cnoidal character of the waves is evident, as is their persistence; the 19th

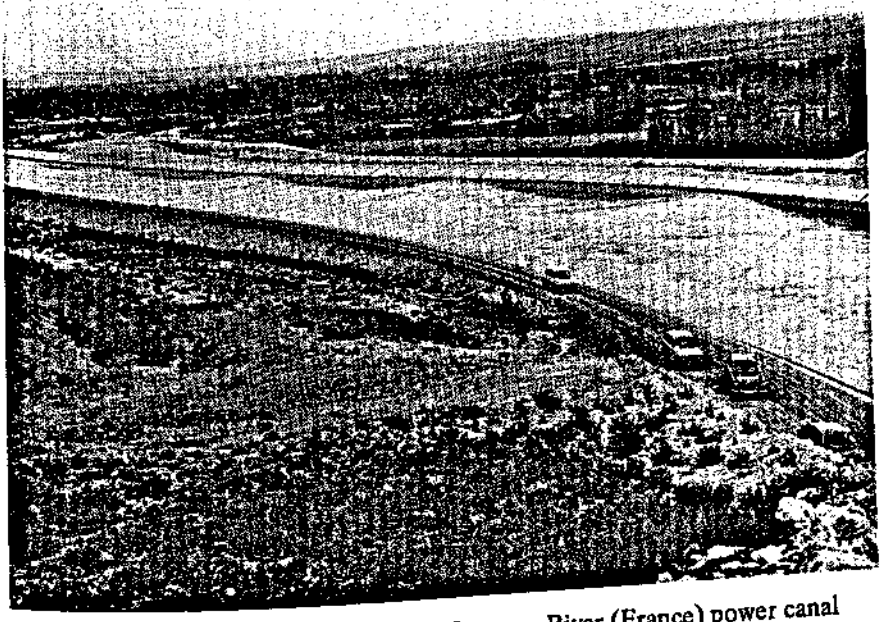

Fig. 6.10. Advancing undular surge in a Durance River (France) power canal (courtesy Electricité de France)

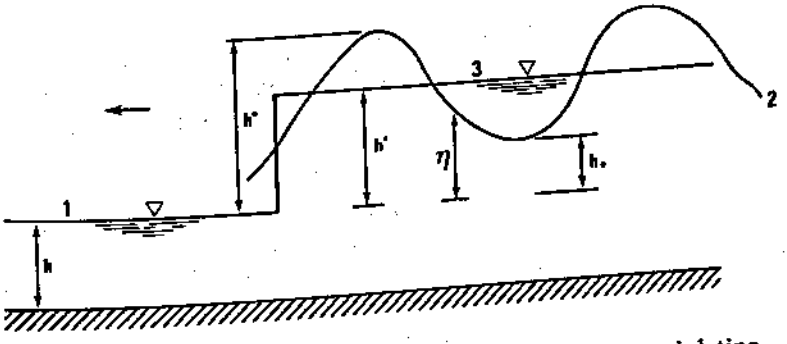

Fig. 6.11. Definition sketch for surges. 1, initial water level; 2, undulating surge; 3, equivalent steep front surge

crest is only 40 cm lower than the first one. Figure 6.13 shows the envelopes of crest and trough superelevations divided by the initial flow depth. Also shown is the volumetric equivalent average superelevation as compared to the equivalent steep front wave (i.e. a discontinuous surge of the same celerity and volume as the undular mobile jump). We see that at the centre of the canal, there is very little damping of the waves, the 15th crest being virtually as high as the first one.

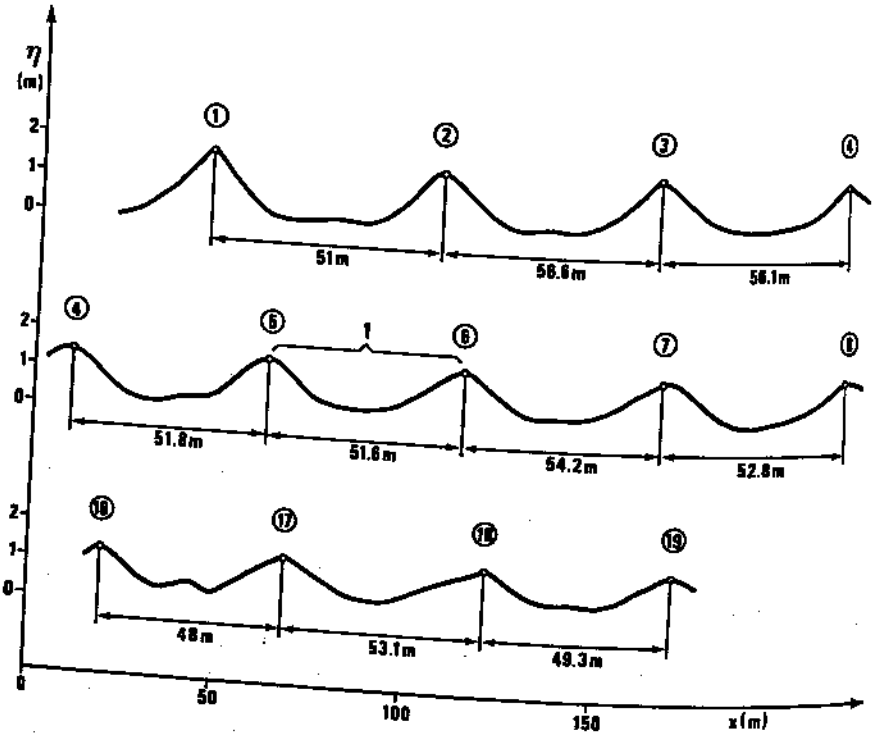

Fig. 6.12. Undular surge water surface at a given instant as observed on one bank of the Oraison (France) power canal. 1, Cnoidal character of the surge wave. ⑦ Indicates wave crest number

An extremely important observation from the canal design point of view is that the undular wave crest elevations are significantly higher than the equivalent discontinuous surge, with obvious consequences for canal free board elevations.

The engineering interpretation of the mobile hydraulic jump links the wave train to the energy of the surge. When a roller is created, energy is dissipated by turbulence and transformed into heat. When a mobile undular jump occurs this energy is used to radiate a wave train behind the surge (Lemoine, 1948). Roller propagation may be simulated by the discontinuous front approach through numerical solution of the flow equations as we describe later on. The wave train propagation phenomenon has not been solved, either analytically or numerically. First described by Favre (1935), its solution was sought by Lemoine (1948) for rectangular channels and by Preissmann and Cunge (1967) for trapezoidal channels. Both attempts used short wave linear theory and thus were not capable of closely predicting the behaviour of the essentially cnoidal (non-linear) wave train. Abbott and Rodenhuis (1972) tried to approach the solution by numerical integration of the Boussinesq equation – their methodology, applied to a rectangular cross section, was never used for engineering projects. The interested reader can find the description of steep front surge phenomena in classical books on hydraulics such as Favre (1935), Henderson (1966), Chow

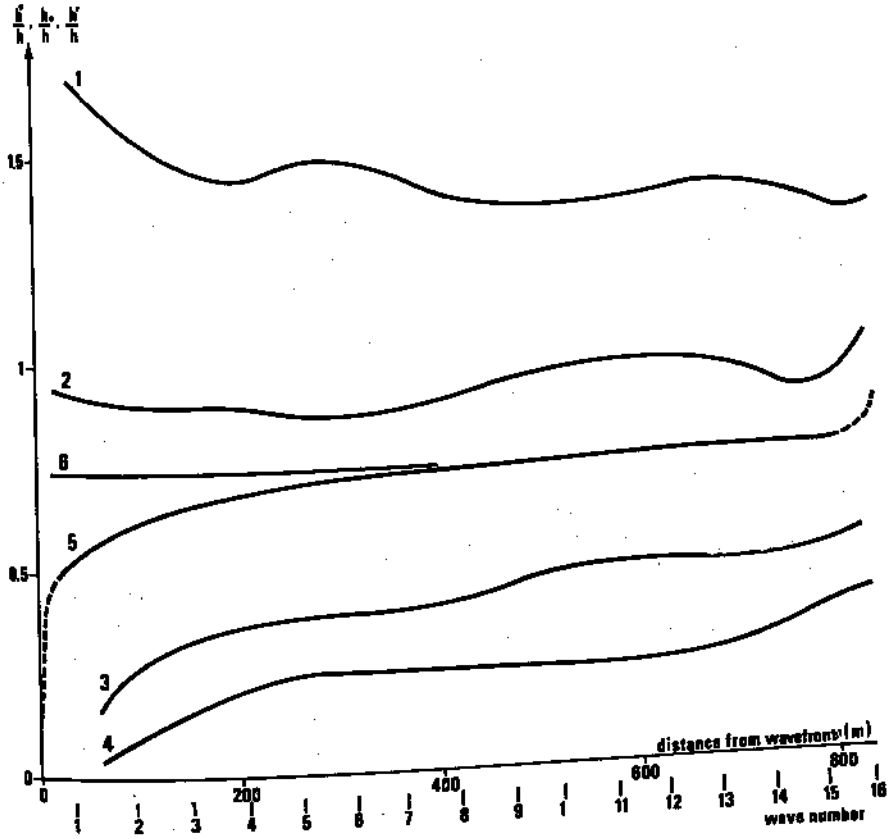

Fig. 6.13. Observed undular surge maximum, minimum, and equivalent steep front surge elevations in the Oraison canal (courtesy Electricité de France). 1, Relative maximum superelevation at banks, h^*/h; 2, relative maximum superelevation at centre, h^*/h; 3, relative minimum superelevation at centre, h_*/h; 4, relative minimum superelevation at banks, h_*/h; 5, volumetric relative wave elevation, h'_{av}/h (h'_{av} = wave volume/initial free surface area); 6, equivalent steep front wave relative elevation, h'/h

(1959). Details on the mobile undular jump are to be found in previously cited publications and in Benet and Cunge (1971) and Ponsy and Carbonnell (1972).

Observations of real-life wave trains behind undular jumps, scale hydraulic model testing, and partially successful numerical studies such as those referenced above have led to the development of a methodology applicable to the solution of engineering problems. The wave train characteristics must depend upon the amount of available energy, which otherwise would have been dissipated in the equivalent roller. Techniques which permit us to compute the propagation of such a roller (shock, bore, discontinuity) along the channel are available (*see* Chapters 2 and 3). Hence once the path of propagation and the

height of the equivalent bore have been computed, the undulations then can be estimated. The estimated undulation may be superimposed on the 'main' wave as shown in Fig. 6.11. The consultant's experience, laboratory tests which he commissions and analyses, and observed water levels will help to define the maximum water surface elevations *above* computed discontinuous solutions.

The use of mathematical modelling to simulate surge propagation is a well proven technique; it has been shown that the results obtained are as good as those obtained on reduced scale models and, moreover, that real life observed phenomena confirm the results of computations (Cunge, 1966b). Theoretical considerations have made it possible to guarantee that the coincidence between the computed and observed results is not merely fortuitous (Lax and Wendroff, 1960; Abbott, Marshall and Ohno, 1969; Cunge 1975b; Abbott, 1979).

The role of mathematical modelling in power canal design may be illustrated by using as an example one of the more spectacular achievements of Electricité de France: a hydroelectric plant and its associated derivation and tailrace canals at Sisteron (Southern France)†. The Sisteron plant is only a part of the overall system of canals running in parallel with the Durance River. The entire system, beginning with the Serre Ponçon reservoir of 1.27×10^9 m^3 capacity, has a mean annual energy production of 6360 GWh (roughly 725 MW installed).

The Sisteron plant is unique because of its derivation canal, which brings the water from the small reservoir La Saulce (the compensation reservoir of the Curbans power plant) to the power house itself over a distance of 32 km as shown in Fig. 6.14. The small longitudinal slope of the canal, 8 cm per km, makes it possible to obtain 116.40 m head above the underground plant where the turbines of 228 MW power are installed. The discharge of 245 m^{3}s^{-1} is then evacuated through a 1020-m long free surface tunnel to the river Buech. At the upstream end of the canal the intake structure is designed to isolate the canal itself by closing the gates at La Saulce dam, but there are no control structures between the gates and the plant 32 km further downstream.At one point the canal passes through a 700 m long siphon under the Deoule River.

The closing or opening of turbines causes waves to propagate along the canal, whose cross section is trapezoidal, with an invert width of 8.60 m and a bank slope of 2:1. The concrete lining ensures a very small friction coefficient and induced waves may persist for days, propagating back and forth along the channel with only very weak dissipation. Consider the case when the power plant at Sisteron sheds load after a period of established flow regime at maximum discharge of 245 m^{3}s^{-1}. A positive wave is then created, and it propagates upstream while the Curbans power station (located upstream of the intake of Sisteron canal) discharge is still 245 m^{3}s^{-1}. The celerity of small waves $((gh)^{\frac{1}{2}})$ is of the order of 6 m s^{-1}, thus the time of propagation along the channel is about 1.5 h. The free surface level upstream of the Sisteron power house will suddenly rise, and then will continue to increase more gradually during a certain time. The increase of the free surface elevation at the power plant may be of the order of 1.5 m even if the upstream La Saulce gates close

†Courtesy Electricité de France and SOGREAH, Grenoble, France.

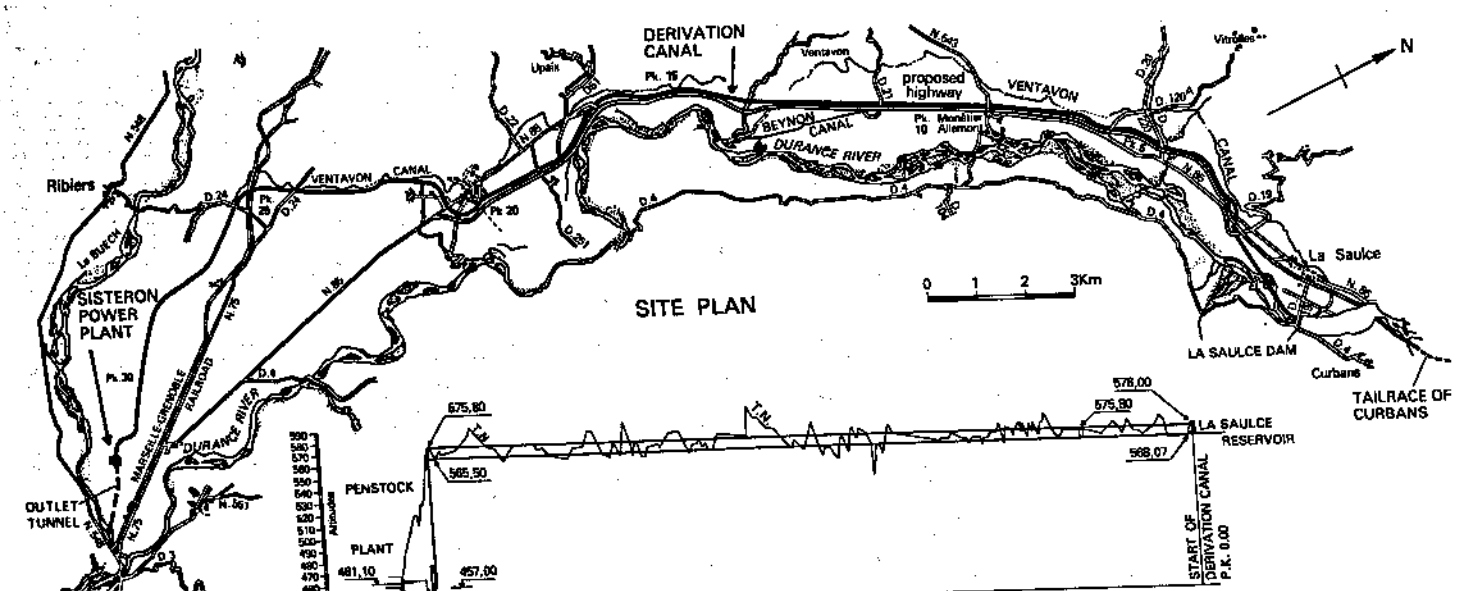

Fig. 6.14. Sisteron Canal layout (Courtesy Electricité de France); TN = natural terrain elevation

immediately. Suppose now that the power plant takes on load (a negative wave is then created), then sheds it again. A very complex hydraulic situation develops along the canal where the positive and negative waves interact and may cause an unfavourable situation with high water surface elevations and resultant overbank spilling.

The following aspects of the Sisteron power canal design were studied with the aid of a mathematical model:

(i) Freeboard elevation of the canal banks over its entire 32 km length.
(ii) Operation rules for the Sisteron and Curbans power plants including upstream safety gates, whose purpose is to avoid bank overflow.
(iii) Utility of a special discharge structure (lateral weir) near the downstream power plant.

When the power plants are working normally, load shedding can happen at any time, and is unpredictable. Sensible manoeuvring of the upstream power station gates and/or the La Saulce safety gates can, however, limit the height of the final water level, enabling subsequent load resumption to take place in better conditions.

After a series of simulations of various La Saulce operating procedures, it was possible to define operating rules which would eliminate the need for a special canal overflow structure under normal conditions of exploitation, and with reasonable canal freeboard elevations. Once the freeboard elevation had been defined, operation rules were then designed with the goal of avoiding overbank spilling in exceptional situations. An example of such an exceptional situation is the following sequence of events:

(i) Downstream Sisteron power plant sheds load at the maximum discharge ($245\ m^3 s^{-1}$) at time $t = 0$.
(ii) Curbans (upstream power plant) is ordered to close its turbines progressively in, say, 10 min.
(iii) Upstream safety gates close in 15 min.
(iv) Both power plants begin to take on load again, at half discharge: Sisteron at $t = 55$ min, Curbans at $t = 65$ min. At the same time the safety gates open progressively from $t = 55$ min to $t = 70$ min.
(v) Both plants (Sisteron at time $t = 125$ min, Curbans at $t = 135$ min) take on full load, increasing the discharge to $245\ m^3 s^{-1}$.
(vi) Sisteron sheds load again at $t = 140$ min, Curbans closes its turbines between $t = 140$ and $t = 150$ min, the safety gates close at the same time.

The sequence of hydrographs along the canal as computed with the mathematical model (built and run by SOGREAH) is shown in Fig. 6.15. In Fig. 6.16 are shown several computed free surface profiles, which are helpful in interpretation of the results. Such computations made it possible to determine the envelopes of extreme elevations along the canal for different operating rules (time of closure and opening of turbines and gates) for exceptional situations.

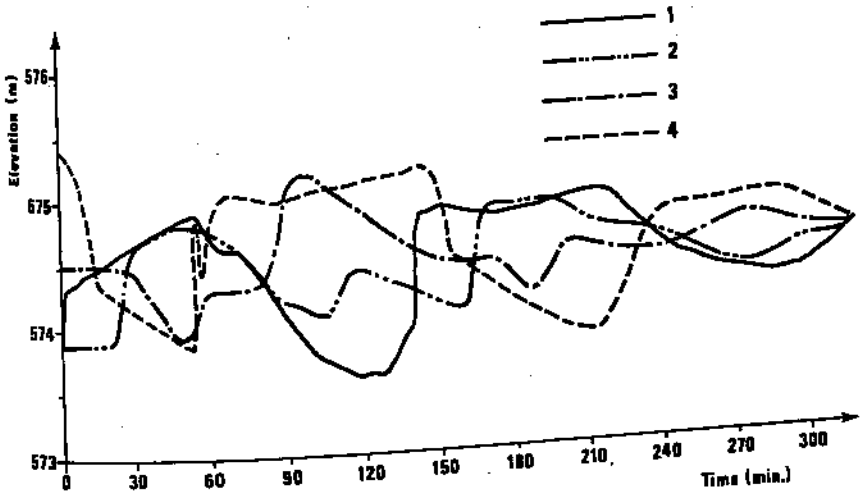

Fig. 6.15. Sisteron Canal computed stage hydrographs (Courtesy Electricité de France and SOGREAH). 1 = Sisteron power plant, station 0.0; 2 = station 9.48 km; 3 = station 19.0 km; 4 = station 26.95 km, downstream of siphon

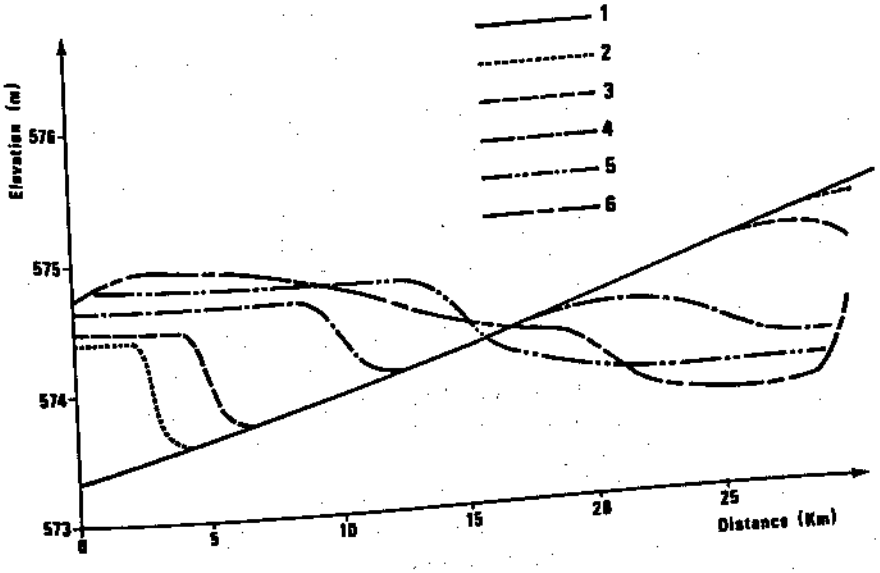

Fig. 6.16. Sisteron canal computed free surface profiles (Courtesy Electricité de France and SOGREAH); 1—time = 0; 2 = 10 min; 3 = 15 min; 4 = 30 min; 5 = 45 min; 6 = 60 min.

Figure 6.17 shows the envelopes of computed levels and estimated elevations due to the undular jumps along the canal.

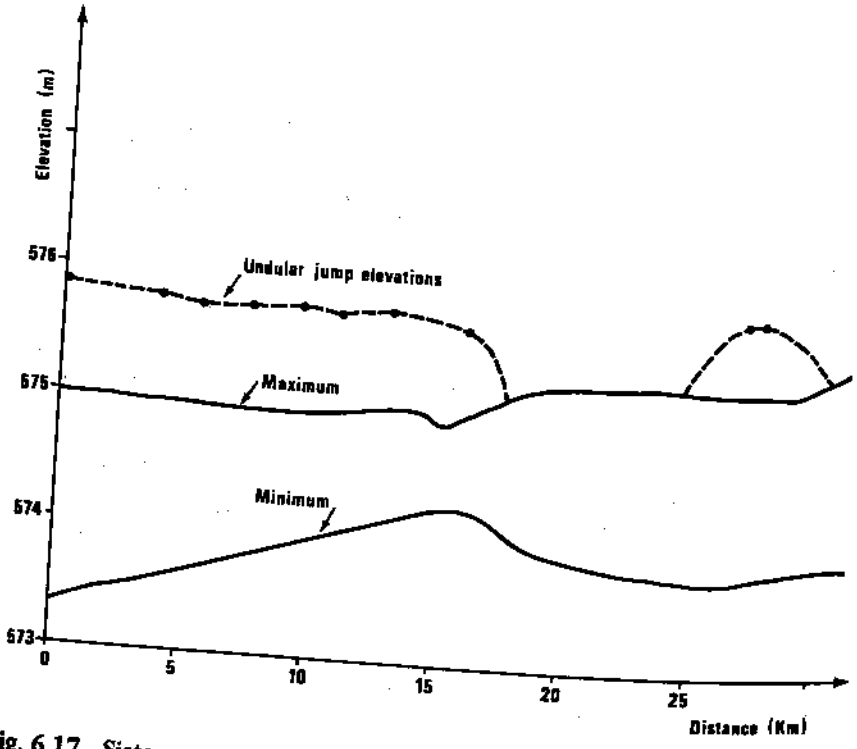

Fig. 6.17. Sisteron canal computed level envelopes (maximum and minimum) and estimated undular jump elevations (Courtesy Electricité de France and SOGREAH)

As for the model itself, it consisted of 213 computational points. The distance step was of the order of 200 m and boundary conditions chosen were discharges as a function of time at the downstream point S001 (PK 0.000, Sisteron power house) and at the upstream point C995 (PK 36.652, Curbans power house). La Saulce dam and its gates were represented by special computational points; the siphon under Deoule River was represented as two 'special' points linked by the siphon dynamic equation

$$\frac{L}{g}\frac{\mathrm{d}u}{\mathrm{d}t} = y_{\mathrm{us}} - y_{\mathrm{ds}} - \Delta H \tag{6.2}$$

where L = siphon length, u = siphon velocity, y_{us}, y_{ds} = respectively upstream and downstream siphon free surface elevations, $\Delta H(u^2/2g)$ = head loss along the siphon. Strickler coefficients were assumed as follows: 65 along the canal, 75 in the tailrace tunnel of Curbans power station, 30 in the La Saulce reservoir. The time step was chosen in such a way as to keep the Courant number $((gh)^{\frac{1}{2}}\Delta t/\Delta x)$ close to unity; the value of $\Delta t = 30$ s adopted kept the Courant number between 0.9 and 1.1.

6.3 FLOW AND ENERGY PRODUCTION CONTROL IN POWER CASCADES ON CANALIZED RIVERS

Canalized rivers have several particular features which set them apart from natural rivers as far as mathematical modelling is concerned. Although the main channel usually retains its natural cross section (at least between dykes), the free surface slope is usually small compared to the bed slope. This is in contrast to many natural situations, in which the bed and water surface slopes are approximately the same. Due to low water velocities, the friction slope is also small compared to the bed slope, and hence inertia forces in varied flow become important. One manifestation of this is that in steady (or nearly steady) flow, the water surface elevation is quite sensitive to the water stage at the downstream section of the reach.

The exploitation of a system of dams, locks and power stations along a canalized river is always an attempt to satisfy contradictory requirements: energy production, flood control and protection, navigation, domestic and agricultural water supply. This is why operations research techniques have been used in order to 'optimize' the exploitation of such systems; we have in fact seen during the last few years a veritable explosion of studies on the subject. Nearly all of them, however, have been made from an economic standpoint, sometimes in the total absence of hydraulic considerations. It is amazing to see that even when hydraulicians have evidently taken part in such studies, there usually is no link between the econometric model and hydraulic considerations. And, most often, the modern tools of computational hydraulics (mathematical models of propagation) have not been used to provide the econometric model with data which would have made its prediction more realistic. In this section, we shall try to show, using the Rhône River (France) as an example, how mathematical modelling of unsteady flow may be applied to such systems. Readers who are familiar with operations research modelling will, most likely, see the way in which the link between two kinds of modelling may be established. Given the increasing number of canalized rivers and cascade power stations in the world (Rhine, Columbia, Danube, Ohio, etc.), such engineering applications are bound to become more and more numerous.

The lower Rhône River cascade schemes†, located as shown in Fig. 4.2, consist generally of a dam and a diversion canal terminating at the power plant-lock structure at the downstream boundary, fed at the upstream limit by a reservoir whose volume is relatively small. Although the reservoir cannot play a flood control role, its volume is sufficient to enable the power station to turbine, during a limited time, a discharge which is much higher than the natural Rhône flow. When such a mode of releases is used, every power plant can turbine more discharge than the one situated immediately upstream by using the volume stored in its own reservoir. Hence the double possibility of producing more peak energy than the river discharge would normally permit, and of providing peaking power to supply network shortages.

†Courtesy Compagnie Nationale du Rhône and SOGREAH, Grenoble, France.

All power stations along the Rhône River are equipped with automatic regulation centres from which computers control turbines and gates in order to attain the best possible trade-off between different objectives. Energy production targets correspond to various power plant–dam functioning modes, each of which is recognized by the computer, which then regulates the turbine and gate discharges in such a way as to attain the objective. Some of the possible modes are:

(i) Run-of-the-river mode, requiring that the average river discharge be turbined with the highest possible water elevation in the reservoir.
(ii) Release-like mode, which produces peak energy according to demand during a certain time and then brings the reservoir level back to the initial (or otherwise specified) elevation.
(iii) Exceptional emergency-like mode, designed to furnish maximum power very quickly and for a short time (of the order of 1 h).

The functioning mode is defined by the dispatching centre as a function of power grid needs and given to the power house computer as the strategy to be followed on a daily basis, though the strategy may be modified at any time. There are security limitations, however, which constrain the attempt to satisfy the objective mode (e.g. maximum energy production during release mode). The security constraints are, for example:

- protection against inundations, hence limits on maximum reservoir levels;
- limits put upon the speed of water level variations which would disturb navigation conditions and endanger the dykes and other works;
- protection against unpredicted incidents, for which the system must function without catastrophic consequences until personnel can intervene.

The power plant computer is given a certain number of operation rules and limits such as maximum and minimum water elevations at given points, the objective turbine discharge as a function of time, water stage to be maintained at given cross sections, etc.

The difficulties in designing such automatic systems are increased by the fact that one of the goals is to be able to let the power stations work automatically, thus reducing personnel cost. There are only a few supervisors along the river, and they intervene only if incidents are detected by the computer. Hence the absolute necessity of simulating every power plant system and of testing all possible imaginable incidents with the aid of a mathematical model. The core of the simulation system is of course a detailed model of the reservoir, derivation and tailrace canals. The model must have a very high accuracy (of the order of a few centimetres) and be able to represent the flows and waves with excellent resolution. A long calibration period was needed for each reservoir in the lower Rhône system, and is presently (1980) underway in the upper Rhône as we described in Chapter 5.

To the calibrated model of the reservoir and canals, two additional components are added:

- a program simulating the action of the on-site computer (called also 'automaton') with all its strategies, operating rules and possible dispatching centre orders;
- a program simulating the power house, spillway gates and data acquisition system. This program simulates possible equipment incidents or failures, unknown or random perturbations, delays in manoeuvring, discretization of real life measurements, etc. A very thorough simulation is needed because of the multiplicity of possible incident sources.

Once the overall model of the system, comprising all three components (reservoir, automaton, power house–gates data acquisition ensemble) is built, then it may be run in order to test the behaviour of the system in different natural discharge conditions (flood, dry season, etc.). While once more referring the reader to the literature (see Chevereau and Gauthier, 1976), we shall show how such modelling is applied to a real life case using the example of the Avignon (France) hydroelectric power plant on the lower Rhône.

A map of the Avignon power complex is shown in Fig. 6.18a, and a schematized layout is shown in Fig. 6.18b. There are two inflows to the reservoir, both from the upstream Caderousse complex; one through the dam and another through the tailrace canal as seen in Fig. 6.18b. The outflow from the Avignon complex is through three sections: the Villeneuve dam, the Avignon power station, and the Sauveterre dam–power station structure. These outflows are subject to regulation by the automatic system which obtains data from Caderousse, from the three outflow locations, and from two continuously measured water stages at Roquemaure and Defluent (where the derivation to Sauveterre dam begins).

The general reservoir regulation principle is depicted in Fig. 6.19. In all situations, the regulation system tries to maintain, or return to, a fictitious reference water stage

$$y_{\text{ref}} = \alpha y_{\text{D}} + (1-\alpha) y_{\text{R}}$$

where y_{D} and y_{R} are stages at Defluent and Roquemaure, respectively. As long as inflow from Caderousse is smaller than 3300 m^3s^{-1}, the weighting coefficient is $\alpha = 0$; in this case the regulation system manoeuvres gates and turbines at Sauveterre, Avignon, and Villeneuve in such a way as to try to maintain the level at Roquemaure at a reference level of 26.00 m, with the level at Defluent free to vary depending on power demand. For discharges which exceed 3300 $\text{m}^3\,\text{s}^{-1}$, the system progressively shifts the point at which it tries to regulate the water level from Roquemaure to Defluent. The coefficient α and the fictitious reference level vary with the discharge from 3300 to 4200 $\text{m}^3\,\text{s}^{-1}$ in such a way as to respect various safety, power production, and equipment constraints. At any given instant, the regulators compare the weighted level $\alpha y_{\text{D}} + (1-\alpha) y_{\text{R}}$ with y_{ref} and modify the outflow so as to respect y_{ref}. Once the discharge exceeds 4200 $\text{m}^3\,\text{s}^{-1}$, $\alpha = 1$ and the regulators operate so as to follow the natural state stage–discharge relationship at Defluent (y_{ref} as a

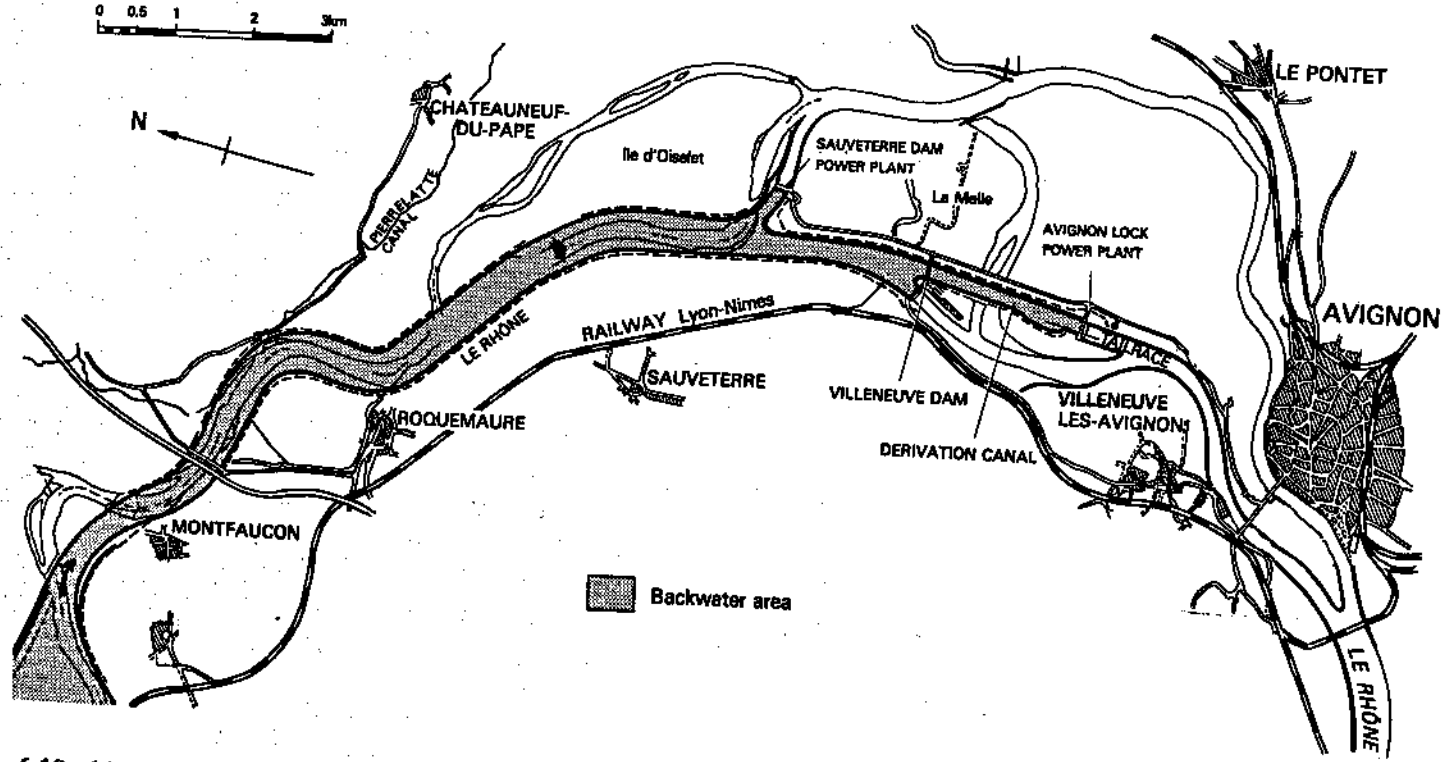
0 0.5 1 2 3km
N
CHATEAUNEUF-DU-PAPE
PIERRELATTE CANAL
Ile d'Oiselet
SAUVETERRE DAM
POWER PLANT
La Melle
LE PONTET
AVIGNON LOCK
POWER PLANT
AVIGNON
RAILWAY Lyon-Nimes
LE RHONE
SAUVETERRE
VILLENEUVE DAM
VILLENEUVE LES-AVIGNON
DERIVATION CANAL
ROQUEMAURE
MONTFAUCON
Backwater area
LE RHÔNE

Fig. 6.18. (a)

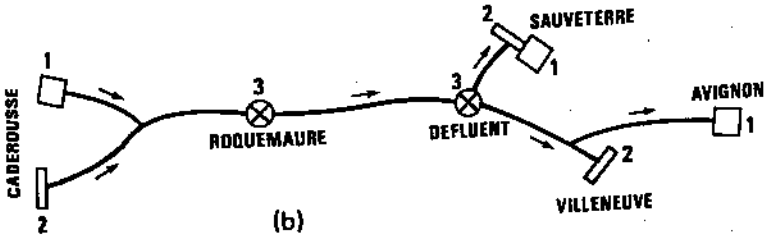

Fig. 6.18. Avignon hydroelectric power plant. (a) Physical layout. (b) Model schematization. 1, power plant; 2, dam; 3, water stage recorder

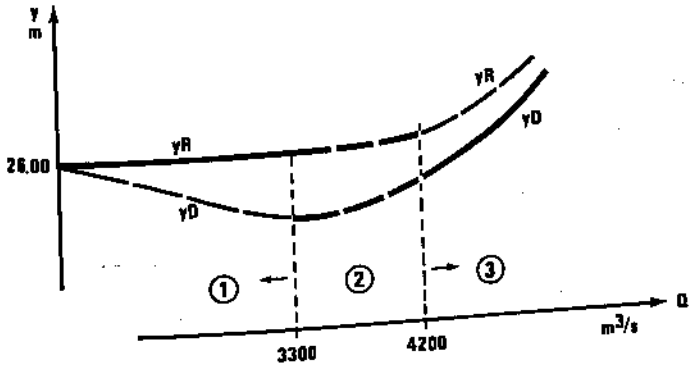

Fig. 6.19. Avignon regulation principle. 1, $y_{ref} = y_R$, $\alpha = 0$; 2, $y_{ref} = \alpha y_D + (1-\alpha) y_R$, $0 < \alpha < 1$; 3, $y_{ref} = y_D$, $\alpha = 1$; y_R = water level at Roquemaure; y_D = water level at Defluent

function of Q). During the falling flood, the inverse procedure is followed. The entire system is studied on a mathematical model so as to determine parameters such as y_{ref}, α, and outflow distribution among the various works.

In the so-called release-like mode, the regulators take into account wave propagation times in the reservoir, head losses, turbine operating limits, etc., in trying to maximize energy production while replacing the water volume used in a power peaking operation. Figure 6.20a shows the mathematical model simulation of such a case. The inflow from Caderousse is a constant $1200\ m^3\ s^{-1}$, so that the Avignon peaking production between time 1 h and 1 h 45 min must be fed by reservoir volume as reflected in the rapid drop in level at Defluent. At time 6 h, the level at Roquemaure is on its way back to 26.00 m, the regulator having been programmed to replace the used volume before the next peaking operation.

An example of a constant-volume cascade release operation is shown in Fig. 6.20b. The objective is to turbine as much of as possible of the inflowing discharge from Caderousse without exceeding a level of 26.00 m at Roquemaure.

We see that the reference level is maintained within a few centimetres for discharge variations of the order of 100 $m^3 s^{-1}$ in 20 min. Flood operation is shown in Fig. 6.20c, where the system passes from trying to maintain a level of 26.00 m at Roquemaure to following the stage–discharge curve at Defluent and returns to a stabilized situation after 24 h.

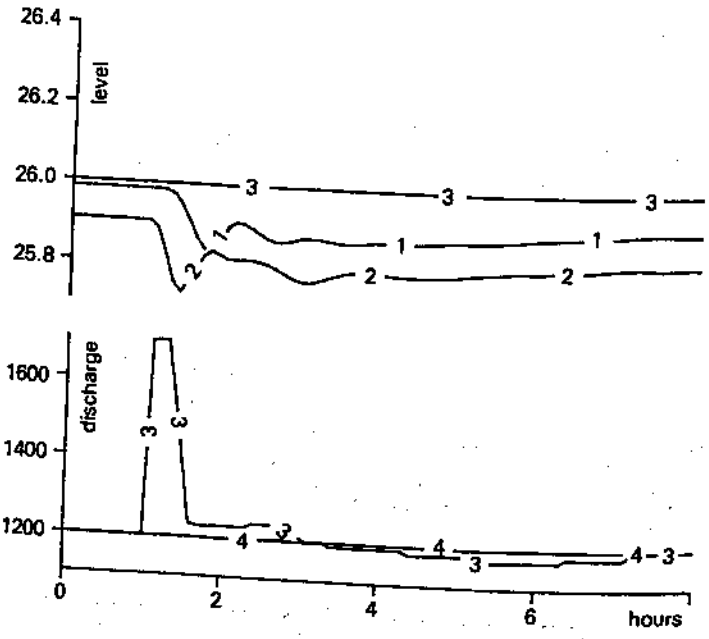

(a)

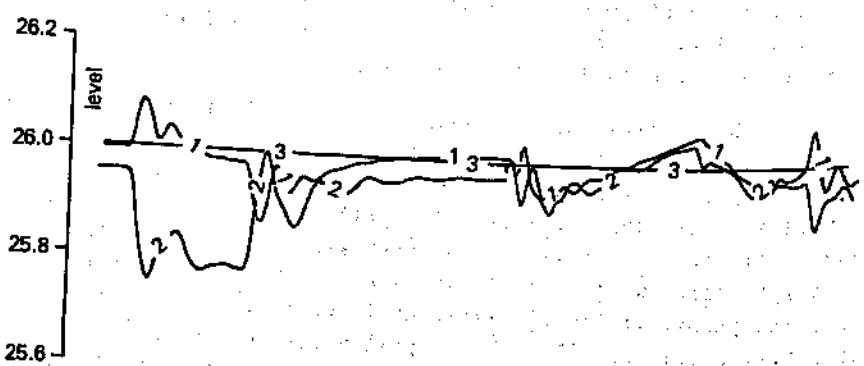

(b)

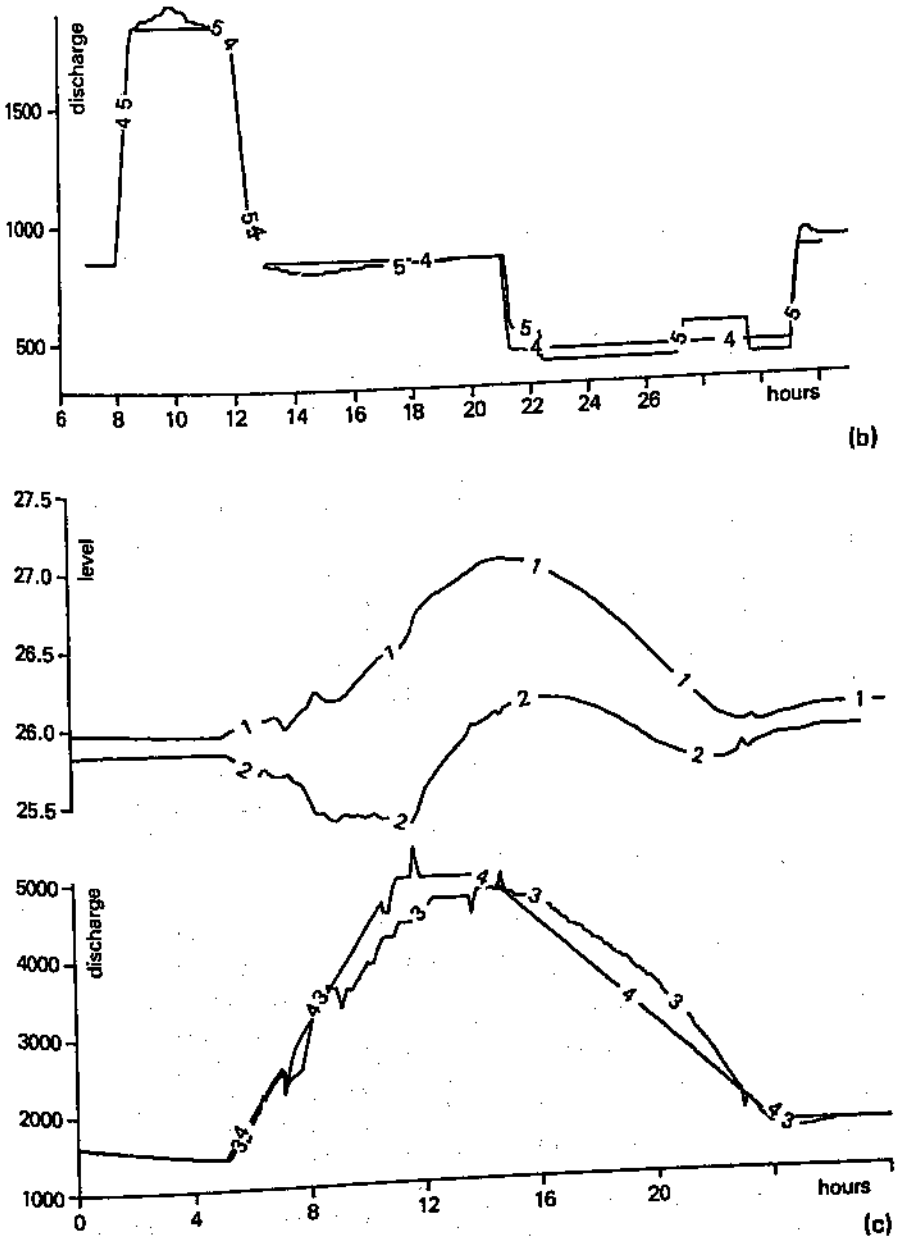

Fig. 6.20. Avignon regulation simulation (courtesy Compagnie Nationale du Rhône and SOGREAH). (a) Peak energy production during a short period. (b) Simultaneous releases. (c) Flood operation. 1, water level at Roquemaure; 2, water level at Defluent; 3, target level at Roquemaure and total system outflow; 4, inflow from Caderousse; 5, total system outflow

6.4 COMPUTATIONAL AND MODELLING CONSIDERATIONS

Modelling of discontinuous fronts

The basic requirement for a modelling system of wave propagation in canals is the capacity to represent the propagation of discontinuous fronts. Indeed, as was shown theoretically in Chapter 2 and has been confirmed in practice, when the bed resistance is small and the canal sufficiently long, manoeuvres of flow control devices (turbines, gates) will always create surges. The distance needed for surge development may be large if the manoeuvres are slow; but even in irrigation systems, there can always be rapid emergency gate closures. The surge thus created may be an undular one or a roller, but, as has been explained earlier, only the latter form may be directly simulated, unless the de St Venant hypotheses are abandoned. In practice these hypotheses are retained and the following solution strategy is used. One assumes that there is only a limited number of discontinuities (or shocks) which propagate and interact within the hydraulic system. Each discontinuity is a mobile hydraulic jump such as described in Chapter 2, and assumed to be 'narrow', i.e. the zone affected by it (the zone within which the de St Venant equations are not valid) is of negligible length as compared to the distance between discontinuities. In the numerical integration process advancing from time t to time $t + \Delta t$, the discontinuous fronts may be computed first; their new positions and flow variables (water stages and discharges in front of and behind the shocks) are determined for time $t + \Delta t$. Then the flow between the shocks is computed by any appropriate method (finite differences, characteristics). This method is called the 'shock fitting' method – the shock computation during time interval Δt is independent of the future $(t + \Delta t)$ situation between the shocks; the exact shock position as well as its configuration (Q_1, y_1, Q_2, y_2) are calculated independently of the computational grid (*see* Section 3.5).

An alternative approach to the problem is to use numerical integration methods for which the precise locations and characteristics of the shocks are not computed. It is assumed that the discontinuity spreads over several space intervals Δx and that the front is 'smeared' over that distance. Hence there is not a true discontinuity where double values of water stage y and discharge Q exist as we showed in Chapter 3. This method, known as the 'through' method, can be used to approach a true discontinuous front only when $\Delta x \to 0$.

Quite clearly the 'shock fitting' method is attractive since it enables us to find 'accurate' values of flow variables (needed, for example, to define the undular jump height). Let us suppose that a study such as that of the Sisteron canal (Section 6.2) is made using the shock fitting method. Consider Fig. 6.21a which schematically shows the discharge hydrograph at the downstream limit of the canal. It represents a sudden load shedding at time t_0, load resumption at time t_2, and a new shedding at time t_4. Figure 6.21b shows the interaction of different discontinuities thus created in the (x, t) plane, while the sketches in Fig. 6.21c show the increasingly complicated pattern of shocks. In Fig. 6.21b the computational grid is also symbolically shown – the regions of continuous

flow between the shocks must be computed on such a grid, since the shocks propagate across it as they please. Moreover, a shock may appear at any point in the plane, just as it may disappear (due to the interaction with a negative wave, for example). Each such transition creates new shock reflections of course, just as does a shock 'collision' (points C in Fig. 6.21b).

The development of a program code capable of simulating all such phenomena would be possible using the principles described in Chapter 3. Indeed, for some particular cases (such as dam breaking) partial codes of that type have been used (Dracos, 1970, Chervet and Dallèves, 1970). Nevertheless the necessary complexity of the program, as well as computer speed and the necessary capacity requirements, act as a deterrent, even more so since such a program

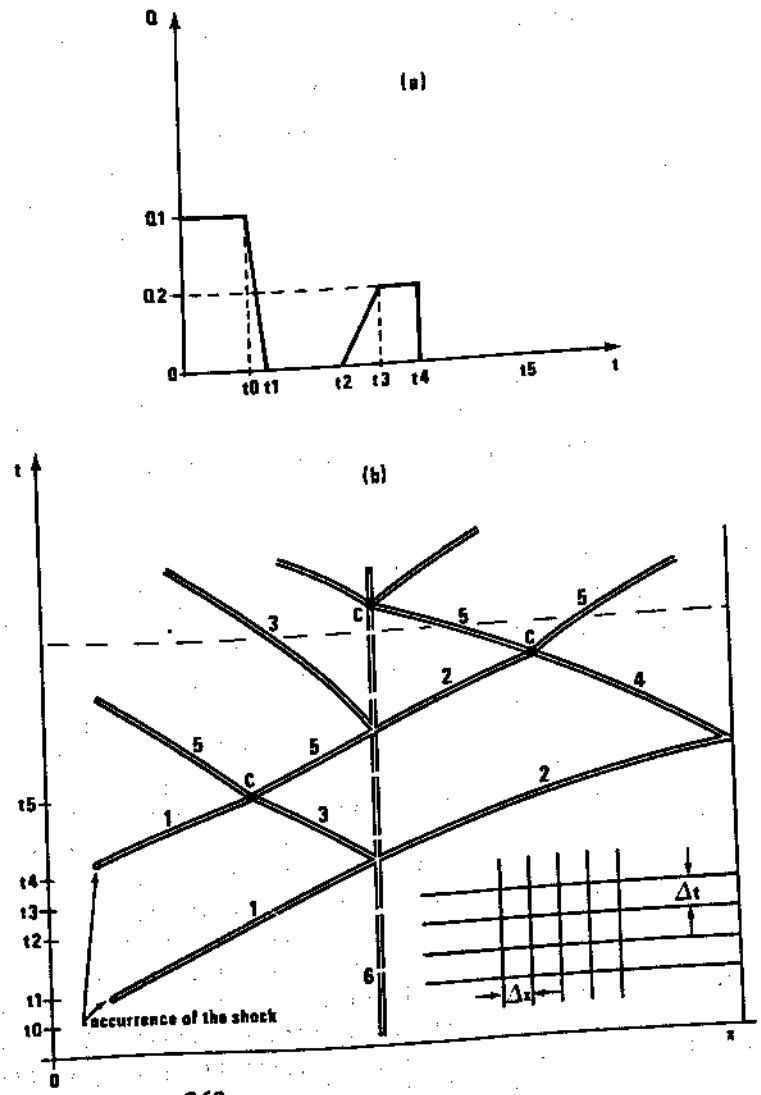

Fig. 6.21. *See page 262*

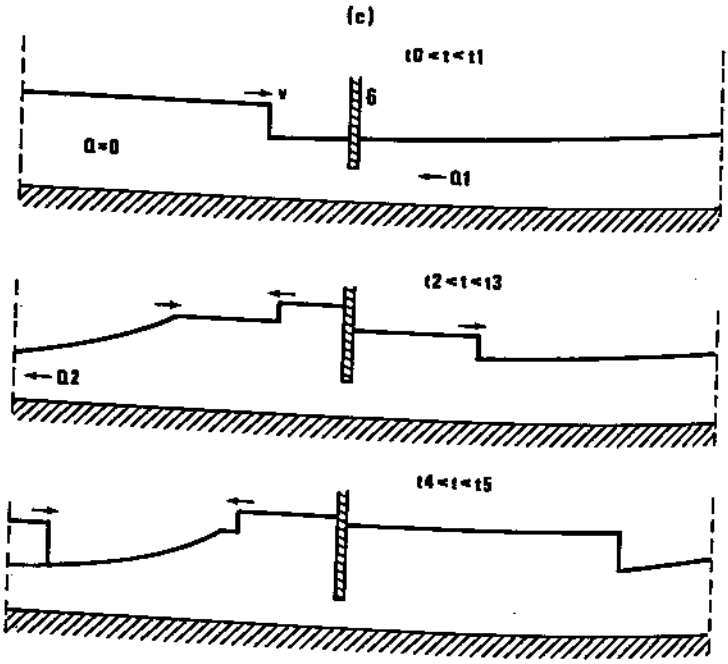

Fig. 6.21. Schematic representation of surge propagation in a power canal. (a) Discharge hydrograph at downstream canal limit (turbine flow). (b) Propagation paths of discontinuities in the (x, t) plane. (c) Successive free surface profiles. 1, incident shocks created at downstream boundary; 2, incident shocks transmitted through siphon; 3, shocks reflected from siphon; 4, shocks reflected from upstream limit of canal; 5, shocks reflected from collisions C; 6, siphon

cannot be economically justified when applied to ordinary river flow problems. While a certain number of codes based on the method of characteristics may be found in the literature, they do not take discontinuous fronts into consideration. 'Through' methods are the only ones presently used on an industrial scale, since they do not require special treatment of shocks; moreover, the same codes may be used for river and canal simulation. There are, however, some special requirements concerning the codes used and great care must be taken to ensure quality results. The numerical integration method producing the 'smeared' front must be such that the smeared solution tends to the discontinuous front solution when $\Delta x \to 0$. As is shown in Chapters 2 and 3, this is possible only when the original differential flow equations are written in momentum-divergent form and, moreover, when the numerical solution of these equations ensures the conservation of momentum across the diffused front. The choice of the finite difference scheme must be conditioned by considerations such as the amount of 'smearing' (or the width of the shock zone), which depends upon the numerical damping introduced into the computation. Such numerical damping acts in the same way

as viscosity; it introduces diffusion which allows a continuous and smooth transition from the state behind the shock to that in front of it. Damping may be explicitly introduced when non-dissipative schemes are used, in the form of 'pseudo-viscosity' or a 'dissipative interface' (*see* Chapter 3). Or again damping may be included implicitly in dissipative schemes.

For most schemes, numerical damping is a function of the Courant number

$$Cr = ((gh)^{\frac{1}{2}} + |u|)\,\Delta t/\Delta x$$

and of the number of computational points per wavelength. The wavelengths which one would like to simulate in rapidly varying flow are usually short, hence the necessity of choosing small values of the space interval Δx. For the same physical reason the time step Δt must be small as well. It is, however, important to obtain some amount of dissipation at the discontinuity, while the damping should be minimized elsewhere. To achieve this, the Courant number Cr should be as close to unity as possible – for a given depth, velocity and space interval Δx, the Courant condition gives guidance as to the choice of Δt.

Modelling of transitions and control structures

Transitions and control structures represent interior boundary conditions which cannot be treated with the usual equations based on the de St Venant hypotheses. Their numerical representation must furnish two relationships replacing the two normal flow equations and linking the flow variables (stages and discharges) on both sides of the structure or transition. For example, when an abrupt change of cross section is simulated, the relationships come from the continuity equation (stating that the discharges at any given time $t + \Delta t$ are equal upstream and downstream of the singularity) and by the dynamic equation which relates energy line elevations on both sides to the discharge through the section change. It is interesting to note that the discontinuous front (bore, mobile jump) could be treated in the same way, i.e. as just another transition, since there are two relationships (Equations (2.68) and (2.69)) which link its back and front sides. But a particular feature of such an interior boundary is that it propagates and changes its location. Hence, if it is to be treated like a transition, a mobile computational grid must be used allowing for dynamic change in the number of computational points (or for a change of the space interval) behind and in front of the bore (Alalykin *et al.*, 1970).

The way a transition calculation is approached is important and cannot be separated from the type of computational grid; often the choice of grid imposes the way in which the transition must be simulated, and vice versa. Consider two canal reaches separated by a gate which regulates the discharge between them (Fig. 6.22). As long as the gate is open, the two equations which represent it may be symbolically written as

$$\begin{aligned} &Q_u = Q_d \\ &\Phi(u_u, u_d, a, y_u, y_d) = 0 \end{aligned} \qquad (6.3)$$

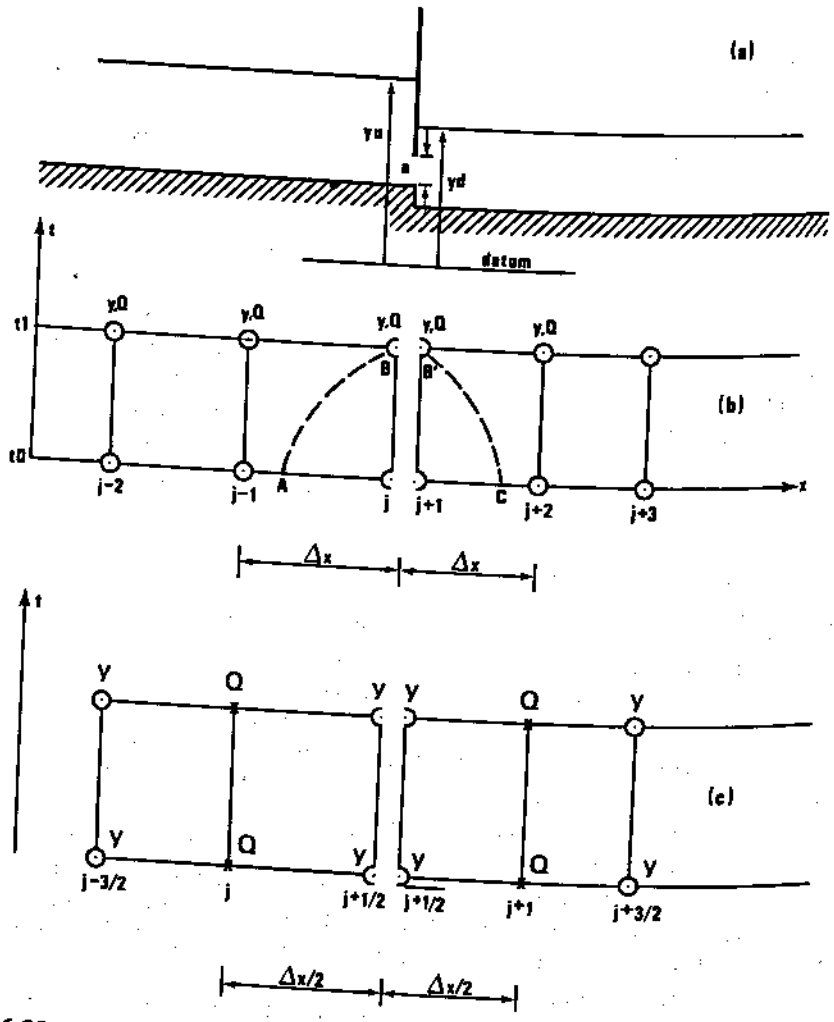

Fig. 6.22. Sluice gate schematization. (a) Physical situation. (b) Computational grid having y, Q at same points. (c) Computational grid having y, Q at different points

where subscripts u and d mean upstream and downstream, respectively. From the programming point of view, the second of Equations (6.3) requires the introduction of a new parameter (as compared to usual transitions): the gate opening a, which is variable, being prescribed either as a function of time or of some other information. For example, the opening may be a function of the water stage immediately downstream from the regulator.

Let us consider first a computational grid in which free surface elevations and discharges are computed at the same points and time levels. A regulator such as shown in Fig. 6.22a may be represented by two computational points $(j, j+1)$

geographically situated at the same location (i.e. immediately upstream and downstream of the gate) but having different cross sections. As far as the computation is concerned, no particular difficulty arises since $y_j = y_u$ and $y_{j+1} = y_d$ are water stages immediately upstream and downstream of the regulator in Fig. 6.22b and the discharge formula (Equation (6.3)) may be used directly. When flow through a gate has to be described on a staggered grid the best description is obtained with y-points immediately at the upstream and downstream side, as depicted in Fig. 6.22c. The discharges at the gate are obtained by applying off-centered finite difference schemes of the continuity equation for the steps $\Delta x/2$ at both sides of the weir. Although such an off-centering may introduce some error, a Taylor series expansion of the terms in the difference scheme shows that the errors at both sides have opposite signs in the dominant terms and the overall approximation may be quite reasonable. At the gate, the discharges at both sides have to be set equal and together with the gate discharge formula the problem is well defined. In the solution algorithm for the system of equations the treatment of the gate then becomes very similar to the treatment of a nodal point, connecting in this case only two channels. As for computational grids where both variables are calculated at the same points, an example is given at the end of this chapter showing how a regulator may be simulated both by implicit and explicit finite difference methods.

When implementing the software which simulates regulators, one should not forget that it is not at all necessary to reproduce exactly the characteristics of a particular gate. Indeed, if a regulator of a given head loss coefficient and a given speed of opening ensures the required discharges, another regulator with a different head loss coefficient will do the same job provided that the discharge law is analogous for both regulators (although the velocity of opening and opening itself would be different). This feature is important since the characteristics of future regulators are usually not known when the studies are carried out. An example illustrating this point is given by Cunge (1975b); a regulator maintaining a prescribed upstream level furnished the same transitory discharge for head loss coefficients φ and 10φ, but its velocities were quite different in both cases.

Example of gate simulation

Suppose that the transition depicted in Fig. 6.22 is a gate whose purpose is to maintain a constant reference level y_{ref} downstream. It does not matter how y_{ref} was defined; it may well be the water stage immediately below the gate, or again the weighted elevation as in the BIVAL system of water stages measured at the limits of the downstream reach (Fig. 6.5). We shall assume that the possible hydraulic situations are as represented in Fig. 6.23.

Let us first consider Fig. 6.23a. The flow under the gate is supercritical, and it may be approximately computed with the formula†

†All classical formulae may be found in handbooks of hydraulics, e.g. Kiselev, 1957.

$$Q = \varphi \epsilon ab\,(2g\,(y_u - y_w - \epsilon a))^{\frac{1}{2}} \tag{6.4}$$

where Q = discharge under the gate; φ = discharge coefficient (0.85 – 0.95); ϵ = contraction coefficient, which depends on the ratio a/h, so that $\epsilon = f(a/h)$; a = gate opening; b = width under the gate; y_u, y_w = upstream free surface and weir elevations respectively (to simplify the formulation we shall neglect the influence of the velocity head $u^2/2g$ upstream of the gate). Equation (6.4) is valid as long as the following inequality is satisfied:

$$h_{test} > h_d; \quad h_{test} = \frac{h_c}{2}\left[\left(1 + \frac{8Q^2}{gb^2h_c^3}\right)^{\frac{1}{2}} - 1\right] \tag{6.5}$$

$$h_c = ae$$

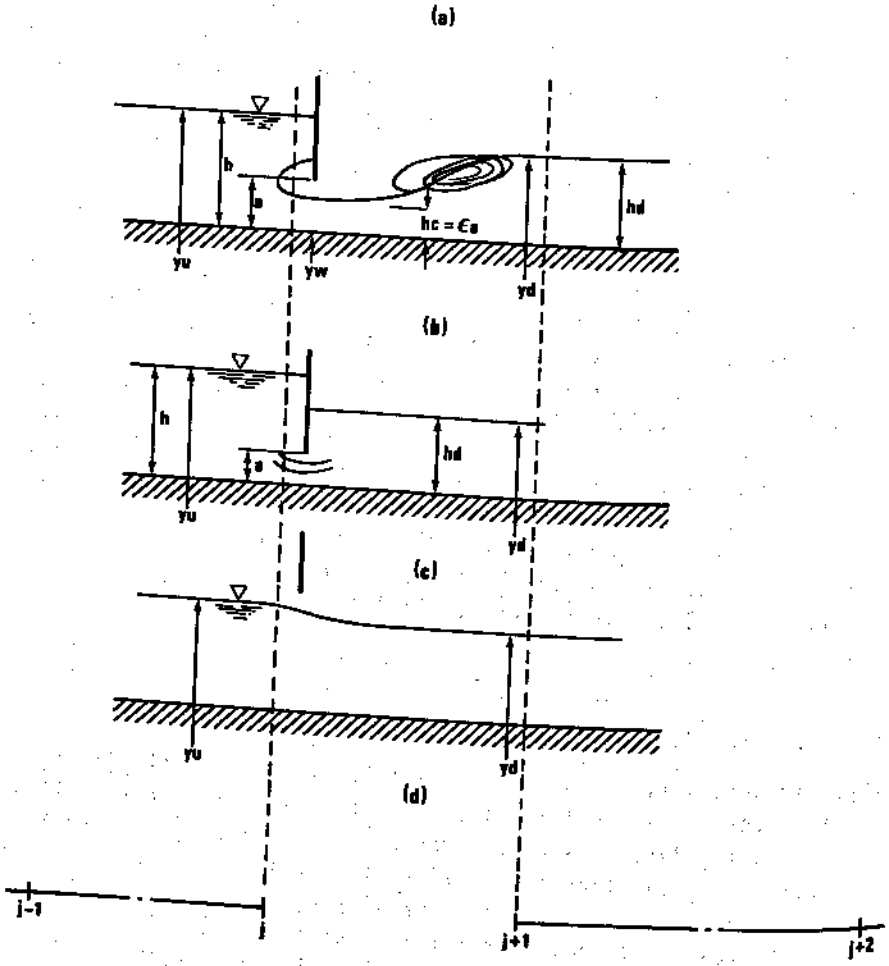

Fig. 6.23. Sluice gate flow conditions. (a) Free flow, $h_{test} > h_d$. (b) Drowned flow, $h_{test} < h_d$. (c) Gate in fully raised position. (d) Computational grid

When $h_{test} < h_d$ a different relation must be used:

$$Q = \mu\, ba\, (2g\,(y_u - y_d))^{\frac{1}{2}} \tag{6.6}$$

where μ = discharge coefficient $(0.65 - 0.70)$, y_d = downstream free surface elevation. Equation (6.6) is simplified as compared to analogous equations sometimes used in actual engineering practice.

When the gate is completely open, the structure may be represented by a simple broad crested weir for which the discharge formula for drowned conditions is analogous to Equation (6.6),

$$Q = \psi b\,(y_d - y_w)\,(2g\,(y_u - y_d))^{\frac{1}{2}} \tag{6.7}$$

Let us consider Equations (6.4) and (6.6) only; in order to avoid numerical oscillations during transitory flow simulation, both equations should give the same discharge when $h_{test} = h_d$:

$$\varphi\, \epsilon\, (y_u - y_w - \epsilon a)^{\frac{1}{2}} = \mu (y_u - y_d)^{\frac{1}{2}} \tag{6.8}$$

Setting, from Equation (6.5)

$$h_d = \frac{\epsilon a}{2}\left[\left(1 + \frac{8Q^2}{gb^2(\epsilon a)^3}\right)^{\frac{1}{2}} - 1\right] \tag{6.9}$$

and using Equation (6.4) for Q, elimination of h_d leads to

$$\varphi^2 \epsilon^2 (y_u - y_w - \epsilon a) = \mu\left\{y_u - y_w - \frac{\epsilon a}{2}\left[-1 + \left(16\varphi^2\left(\frac{y_u - y_w}{\epsilon a} - 1\right)\right)^{\frac{1}{2}}\right]\right\} \tag{6.10}$$

in which $\epsilon = f\left(\frac{a}{y_u - y_d}\right)$ and μ = const. Hence, for each pair of values $\left(y_u, \frac{a}{y_u - y_d}\right)$ the coefficient φ may be computed.

In transitory flow, the above formulae are applied in the following sequence of programmed operations:

- supposing that the computational points $(j, j+1)$ correspond to sections immediately upstream and downstream of the gate, the h_{test} value is computed according to Equation (6.5) using a^n, $\epsilon^n = f\left(\frac{a^n}{y_j^n - y_w}\right)$ and Q^n (we recall that the index n signifies time level $t = n\Delta t$ at which all flow variables are known).
- if $h_{test}^n \leq y_{j+1}^n - y_w$, then formula (6.8) may be used (with an adopted value μ = const.).
- if $h_{test}^n > y_{j+1}^n - y_w$, the discharge coefficient φ is numerically computed (for example by the Newton method) from Equation (6.10), and formula (6.4) may be used.

Within the program the transition must be represented by a system of two relations linking points j and $j+1$. One of two equations is the continuity equation,

$$Q_j^{n+1} = Q_{j+1}^{n+1} \tag{6.11}$$

Another equation depends upon the type of flow under the gate. For drowned flow Equation (6.12) must be satisfied:

$$Q_j^{n+1} = \mu b a^{n+1} \left(2g\left(y_j^{n+1} - y_{j+1}^{n+1}\right)\right)^{\frac{1}{2}} \tag{6.12}$$

where $a^{n+1} = a^n + \Delta a$ is given according to the operation rule which closes (or opens) the gate by an amount Δa during one time step Δt. For free underflow Equation (6.13) is to be used,

$$Q_j^{n+1} = \varphi^n \epsilon^n a^{n+1} b \left(2g\left(y_j^{n+1} - y_w - \epsilon^n a^{n+1}\right)\right)^{\frac{1}{2}} \tag{6.13}$$

where φ^n is computed from Equation (6.10), and $\epsilon^n = f\left(\dfrac{a^n}{y_j^n - y_w}\right)$ is interpolated from the appropriate tables. One may even replace ϵ^n and φ^n values in Equation (6.13) by

$$\epsilon^{n+1} = \epsilon^n + \frac{d\epsilon}{da}\left(a^{n+1} - a^n\right) + \frac{d\epsilon}{dy_j}\left(y_j^{n+1} - y_j^n\right) \tag{6.14}$$

and

$$\varphi^{n+1} = \varphi^n + \frac{d\varphi}{da}\left(a^{n+1} - a^n\right) + \frac{d\varphi}{dy_j}\left(y_j^{n+1} - y_j^n\right) \tag{6.15}$$

but that would appear to be extravagant for most cases given the small variations of φ and ϵ.

We shall now describe how the above formulation may be incorporated in two algorithms: one using an explicit method, and another using an implicit method.

Explicit finite difference algorithm

Consider again Fig. 6.22b showing the transition and the computational grid in the (x, t) plane. Since the explicit method is used, one wishes to compute discharges Q_j^{n+1}, Q_{j+1}^{n+1} and water stages y_j^{n+1}, y_{j+1}^{n+1} using solely the information known at time level n at points $j-1, j, j+1, j+2$. Thus there are four unknowns and supposing that the new gate opening a^{n+1} is given, there are only two equations (6.11), (6.12) (or (6.13)). If the forward characteristic BA is followed from the point B$(n+1, j)$ until it intersects the time level $n\Delta t$ at point A, two more equations are obtained, and one new unknown, the abscissa x_A, is added (*see* Chapters 2 and 3).

The backward characteristic traced from point B′ at time level $(n+1)\Delta t$ to

point C at time level $n\Delta t$ furnishes two more equations and one more unknown, x_C.

Since there are 6 unknowns ($Q_j^{n+1}, y_j^{n+1}, Q_{j+1}^{n+1}, y_{j+1}^{n+1}, x_A, x_C$), and 6 non-linear algebraic equations (namely, (6.11), (6.12), or (6.13) and 4 characteristic equations), the problem may be solved by any appropriate iterative method for each time level $(n+1)\Delta t$, $(n+2)\Delta t$, etc.

Implicit finite difference algorithm

Consider Preissmann's implicit scheme (*see* Chapter 3) which provides, as an approximation to the de St Venant equations, a system of two algebraic equations for every pair of computational points $(j, j+1), j = 1, 2, \ldots, N-1$, where N = number of computational points,

$$A\Delta y_{j+1} + B\Delta Q_{j+1} + C\Delta y_j + D\Delta Q_j = G \qquad (6.16)$$
$$A'\Delta y_{j+1} + B'\Delta Q_{j+1} + C'\Delta y_j + D'\Delta Q_j = G'$$

where $A, B \ldots$ are the coefficients which may be computed using $n\Delta t$ time level information while Δy, ΔQ are flow variable increments such that

$$\Delta y = y^{n+1} - y^n; \quad \Delta Q = Q^{n+1} - Q^n$$

Clearly, if our system of Equations (6.11) and (6.12) (or (6.13)) may be reduced to the form (6.16), it can be then solved with all the other equations of that form established for the set of ordinary computational points. Equation (6.11) gives immediately

$$Q_j + \Delta Q_j - Q_{j+1} - \Delta Q_{j+1} = 0 \qquad (6.17)$$

Equation (6.6) may be rewritten by assuming that all functions f are differentiable so that

$$f = f^{n+1} \approx f^n + \frac{df}{dy}\,\Delta y + \frac{df}{dQ}\,\Delta Q \qquad (6.18)$$

Hence Equation (6.6) becomes

$$Q_j^n + \Delta Q_j = \frac{\mu b a^{n+1} g}{(2g\,(y_j^n - y_{j+1}^n))^{\frac{1}{2}}}\,(\Delta y_j - \Delta y_{j+1}) + \mu b a^n\,(2g\,(y_j^n - y_{j+1}^n))^{\frac{1}{2}} \qquad (6.19)$$

In the same way Equation (6.4) may be written in the form

$$Q_j^n + \Delta Q_j = \varphi^n a^n \epsilon^n b\,(2g\,(y_j^n - y_w - \epsilon^n a^n))^{\frac{1}{2}} + \frac{Q^n b\,\epsilon^n a^{n+1} g}{(2g\,(y_j^n - y_w - \epsilon^n a^n))^{\frac{1}{2}}}\,\Delta y_j \qquad (6.20)$$

We note that the derivation is not accurate as far as ϵ, φ and a are concerned. If these functions vary rapidly with water elevation, they should be differentiated too. Equation (6.17) has the same form as the first of Equations (6.16) as long as

$$A = C = 0, B = -1, D = 1, G = Q_{j+1}^n - Q_j^n \tag{6.21}$$

Equations (6.19) or (6.20) may be written in the form of the second of Equations (6.16) by putting either

$$A' = \frac{\mu b a^{n+1} g}{(2g\,(y_j^n - y_{j+1}^n))^{\frac{1}{2}}}, B' = 0, C' = -A', D' = 1,$$

$$G' = \mu b a^n\,(2g\,(y_j^n - y_{j+1}^n))^{\frac{1}{2}} - Q_j^n \tag{6.22}$$

or

$$A' = B' = 0, C' = \frac{-\varphi^n b\,\epsilon^n a^{n+1} g}{(2g\,(y_j^n - y_w - \epsilon^n a^n))^{\frac{1}{2}}},$$

$$D' = 1, G' = \varphi^n a^n \epsilon^n b\,(2g\,(y_j^n - y_w - \epsilon^n a^n))^{\frac{1}{2}} - Q_j^n \tag{6.23}$$

Thus we see that once the flow equations for the transition are written in discrete form, they can be directly incorporated in the overall implicit solution. The system of having levels and discharges calculated at the same points lets us define the flow equations for any 'link' $(j, j+1)$ independently of the others.

7 Movable bed models

7.1 THE ROLE OF MOVABLE BED MATHEMATICAL MODELS IN ENGINEERING PRACTICE

Sediment transport in rivers is a very special problem in fluvial hydraulics. Transported sediments may render nearly any man-made structure useless. By 1973, 33% of the U.S. reservoirs built before 1935 had lost from 25% to 50% of their original capacity while another 14% of these reservoirs had had their capacity reduced between 25% and 50%. One out of ten reservoirs lost all usable storage (ASCE, 1975). Other problems due to sediment transport are structural or morphological deterioration due to degradation below dams, deterioration of water intake entrance conditions, filling up of irrigation channels, and shifting of stream alignment, not to mention pollution and ecological consequences. The essential difficulty of dealing with the situation is the present human incapacity to obtain a satisfactory quantitative description of sediment transport phenomena.

One can find voluminous literature on particular aspects of transport, such as particle suspension, fall velocity and initiation of motion, but there are only two ways to predict the consequences of human intervention on sediment transport: a laboratory scale model or an expert appraisal, possibly using a mathematical model.

When properly built and run, scale models provide the answer to the engineer's eternal question 'what will happen if . . .'. Unfortunately, they can only model the immediate neighbourhood of the structures being studied and when large scale and long term consequences of man's intervention are concerned (hundreds of kilometres of river course, tens of years of morphological variations), a study made by an expert consultant is the only solution.

The expert has at his disposal a large number of sediment transport formulae, detailed descriptions of microprocesses (at the level of one sand grain), numerous descriptions (in geographic terms) of observed global phenomena and, last but surely not least, his own experience. It is worth mentioning that there are a score or so of sediment transport formulae in use, all of them founded upon the same basic hypotheses: uniform flow (energy line parallel to the bed and steady water flow), river bed in equilibrium, and negligible washload

transport. The results furnished by these formulae may vary by an order of magnitude or more from one to another for the same input data. In most engineering problems, it is difficult to determine which formula best applies to a given river, since flow is never uniform and seldom steady, and washload can often be an important factor. Hence it is recommended (ASCE, 1975) that the engineer try to make use of all of the potentially viable tools at his disposal, that he should be guided by available experience with similar streams, and should base his conclusions on the results obtained from several methods. The computations using some of the formulae are lengthy, especially when the river reach under consideration is several hundred kilometres long. If the specialist wishes to predict changes over a period of 20–30 years, he must obviously limit himself to one or two of the formulae which he knows well, study one or two 'typical' situations, and then resort to global estimates. If he is an experienced engineer, he will be able to use his intuition and knowledge of physical situations to ensure that his results allow an adequate safety margin.

Movable bed river hydraulics is in a situation analogous to that of fixed bed hydraulics in the 19th century before Boussinesq and de St Venant formulated the flow equations taking into account the most important features of long waves in open channels. Until a similar breakthrough takes place in the movable bed domain, subjective procedures and judgements will have to be accepted. But even if the basic subjective methodology remains essential, new computational techniques are changing the way it is applied. Moreover, these techniques bring with them the need for new concepts and developments in the methodology. Thus, the application of computational hydraulics to this field is an incentive to progress.

Existing mathematical models are nearly all based upon the idea that it should be possible to simulate hydrological flow conditions and the concomitant change in longitudinal profile of a river over a period of 20–50 years, using a chosen sediment transport formula. A single simulation should require only a reasonable amount of computer time and the results, taking into account different alternative operating policies for man-made structures, should be available in a neat, plotted form a matter of hours after the initial data were submitted to the computer. Of course, there will be as many different conclusions as formulae used. However, instead of a few computations with a limited number of formulae made for 'typical situations', an engineer can try a number of formulae, take into account the hydrology of the river and actually defining operating policies. He can better choose the proper formulation and even, by simulating the river evolution recorded in the past, adjust the particular coefficients in a given formula. Consequently the 'coefficient of ignorance' which separates the engineers' conclusion from reality may be considerably reduced.

The mathematical models described in this chapter are one dimensional, representing only longitudinal bed profiles, longitudinal free surface profiles and sediment transport as a function of time and hydraulic flow conditions. Nevertheless they can be used to solve numerous problems associated with river bed evolution in response either to natural conditions or to man-made developments.

The following natural phenomena are examples of what has been or can be successfully simulated with such models:

- Bed variations during floods in the lower reaches of rivers flowing into the sea (Perdreau and Cunge, 1971; Bouvard, Chollet and Cunge, 1977; Chollet, 1977).
- Delta formation at river mouths, alluvial fan formation below foothills (Chang and Hill, 1977).
- Bed variations during floods in the vicinity of gorges (Blanchet, 1971) or at river crossings (de Vries, 1973a).
- Bed variations downstream of tributaries or at bifurcations (de Vries, 1973b).
- Long term natural evolution of a river bed (Chen and Simons, 1975).

Some of the river improvement problems which may be studied with the help of such mathematical models are:

- Modifications of water flow and sediment transport due to dam construction (Chollet and Cunge, 1979).
- Establishment of long term operating rules for dams in order to preserve useful reservoir volume by flushing operations; determination of necessary reservoir volume (Lugiez, 1976; Chollet and Cunge, 1979).
- Modifications of river morphology in response to river training works, cutoffs or alignment changes (Verdet, 1975).
- Deposition of materials, and dredging operations (Verdet, 1975).
- Modifications to river morphology due to the withdrawal of water for irrigation, industrial use, etc. (de Vries, 1973a).

7.2 BASIC HYPOTHESES AND FORMULATION OF EQUATIONS

In this chapter our attention will be focused on modelling non-uniform and unsteady sediment transport phenomena. Programmes developed to solve the sediment transport formulae in uniform flow, or those developed for steady state situations only, are considered as common engineering aids, which do not enter into the subject of unsteady flow modelling. The purpose of this chapter is not to develop the theory of sediment transport modelling. Nonetheless, we will find it necessary to review the mathematical behaviour of some of the equations whose particular characteristics must be taken into account in developing modelling techniques.

Sediment transport and water flow are interrelated in such a way that they can never be completely disassociated. There are many formulations expressing the interrelation of the two phenomena in unsteady situations; the simplest acceptable mathematical description is summarized by the following system of equations (*see* Fig. 7.1).

Continuity equation for liquid flow:

$$\frac{\partial h}{\partial t} + u \frac{\partial h}{\partial x} + h \frac{\partial u}{\partial x} = 0 \tag{7.1}$$

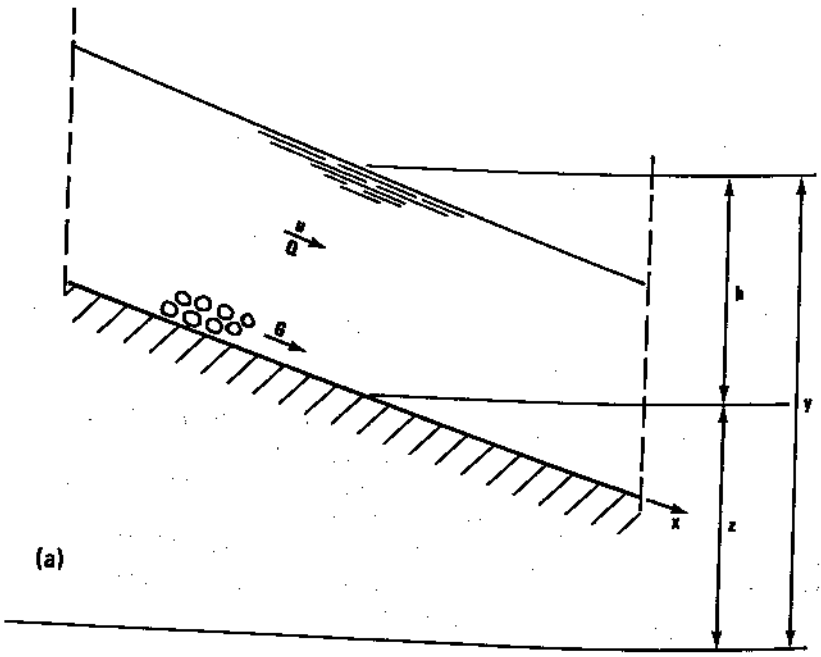

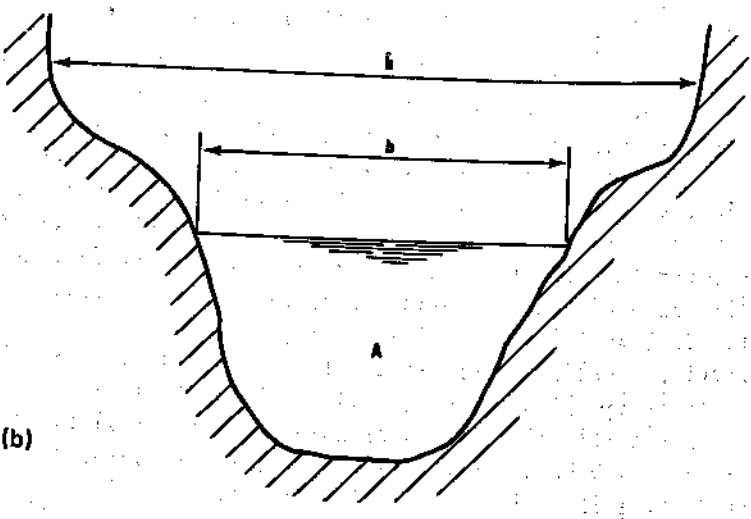

Fig. 7.1. Definition sketch for one-dimensional flow in a movable bed river. (a) longitudinal profile (b) cross section

Dynamic equation for liquid flow:

$$\frac{\partial u}{\partial t} + u\,\frac{\partial u}{\partial x} + g\,\frac{\partial h}{\partial x} + g\,\frac{\partial z}{\partial x} + gS = 0 \tag{7.2}$$

Continuity equation for solid discharge:

$$(1-n)\,\tilde{b}\,\frac{\partial z}{\partial t} + \frac{\partial G}{\partial x} = 0 \tag{7.3}$$

together with the sediment transport formula:

$$G = G(u, h) \tag{7.4}$$

where x is the abscissa measured along the river axis, t is time, h the depth of water, u the average velocity within a section, z the level of the river bed, S the steady state energy line slope, G the solid load transported, in units of volume per time, b the width of the free surface, $\tilde{b}$ the width of the section affected by the bed load transport, and n the porosity of the bed material. In the formulae of this chapter we shall change the general meaning of the symbol z: instead of being a transverse horizontal coordinate, it will represent the bed elevation above the datum.

The set of differential equations (7.1)–(7.3) links the three unknown functions $h(x, t)$, $u(x, t)$, $z(x, t)$ with the independent variables x and t. Since these equations are representative of all basic physical phenomena and have all the mathematical properties of more complex equations, we shall use them throughout this chapter. They incorporate a series of hypotheses concerning both water flow and solid transport. The de St Venant hypotheses, i.e. the hydrostatic distribution of pressure and the uniformity of velocity within a section, are accepted for the liquid phase. The phenomena of erosion and material deposition are of course of a three-dimensional nature due to secondary currents, but the simulation of this complex phenomenon is at present not feasible, at least not over long reaches of river. Thus the sediment transport, like water flow, is schematized as a one-dimensional phenomenon for the purpose of modelling.

Any conceptual model based on Equations (7.1)–(7.4) should be completed by laws relating the variation of cross sections to deposits or erosion (i.e. as a function of variation of the bed elevation z). All known operational models assume that cross sections are eroded or filled within their own alluvia, which is supposed homogeneous. Any other hypotheses would require the introduction of a law to cover the separation of eroded or deposited materials and a further law to cover their lateral distribution over the bed. Even within these limits there are several ways of describing the variation in the cross-sectional area, A, with the bottom elevation, z. One way is to assume that the cross section rises or falls without changing its shape, as shown in Fig. 7.2a. Another is to suppose that only those parts of the cross section which are below the water level y move up and down (Fig. 7.2b). In some models, an attempt is made to introduce a lateral distribution of deposits or erosion (Fig. 7.2c) related to the tractive force (Chang and Hill, 1977) or according to an arbitrary assumption, based on empirical

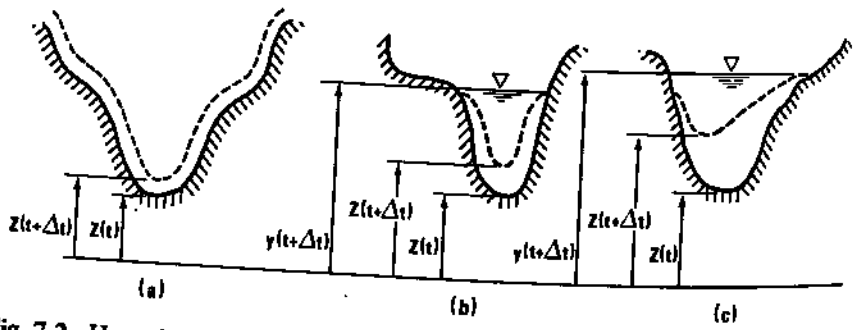

Fig. 7.2. Hypotheses relating cross-sectional changes to bed elevation changes. (a) Entire cross section rises; (b) cross section is affected only below the water surface; (c) lateral distribution of deposition assumed

information (Chen and Simons, 1975). Whether the use of a complicated lateral distribution law is justified or not is a matter of engineering judgement concerning particular applications; our knowledge of such laws is usually severely restricted. It is enough to say here that any of the above concepts can easily be introduced into any mathematical model if thought necessary. The only limitation is that such a concept, or law, must be consistent with the basic assumption of the one-dimensional nature of the phenomena.

Equations (7.1)–(7.4) represent a complex physical process; it is important to be aware of the significance of certain of their terms. S, the steady state energy line slope, can be an explicit function of the flow and river bed characteristics; that is the case in the Manning–Strickler formula:

$$S = \frac{u^2}{k_{str}^2 R^{4/3}} \tag{7.5}$$

where k_{str} = Strickler coefficient and R = hydraulic radius. When this concept is used, the river bed resistance to the flow depends only upon the diameter of the bed material, liquid discharge and flow depth.

We know, however, that for alluvial streams the hydraulic relations in steady flow should allow for the existence of bed forms (ASCE, 1975) and that the overall resistance coefficient depends upon the type of these bed forms (dunes, flat bed, etc.). In that case the simple Equation (7.5) should be replaced by an implicit relationship of the type:

$$\varphi(S, u, h, d, \ldots) = 0 \tag{7.6}$$

where d represents river bed characteristics, possible experimental coefficients and other special criteria that may enter into the relationship. In fact, such an implicit relationship may be expressed by a system of one or more non-linear algebraic equations (e.g. Einstein, 1950; Engelund and Hansen, 1967) from which it is impossible to extract the slope S as a function of other parameters. In that case the system of equations (7.6) must be added to

Equations (7.1)–(7.4) and the simulation program must be designed to solve the whole set.

Equation (7.4) is nothing more than a symbolically stated sediment discharge formula. It may be a simple one, expressing G explicitly as a function of the flow and material characteristics, or, again, it may be a system of equations such as those proposed by the full Einstein theory (1950).

Equations (7.1)–(7.4) form a non-linear partial differential system. It cannot be solved analytically, but numerical methods of integration using computers can be used to obtain solutions. Because of the complexity of the differential system, a complete numerical solution is both tedious and expensive. Experience has shown, however, that the typical time scale of liquid wave propagation phenomena is much shorter than the time scale of longitudinal profile modification. The propagation time of a flood peak along a 100 km reach may be of the order of one or two days, while it would take many years for a bed perturbation to cover such a distance. Although there are situations when the bed level variations are nearly as rapid as free surface changes (Perdreau and Cunge, 1971), this is not a common case. Consequently the system of equations (7.1)–(7.4) is often simplified, as shown further on in this chapter, by assuming quasi-steady state of the liquid phase (Vreugdenhil and de Vries, 1967; Perdreau and Cunge, 1971). This makes the solution easier while preserving the essential coupling between the liquid and solid phase equations, even if such a simplification introduces some minor violation of the liquid phase continuity equation.

Thus we see that there are two possible ways to classify one-dimensional mathematical formulations of movable bed phenomena. The first one is based on the type of equations used and includes two classes of models:

(i) Those based on the full equations of unsteady flow and suitable for simulating rapidly varying phenomena (Equations (7.1)–(7.4)).

(ii) Those based on simplified equations and suitable for the study of slow variations in longitudinal profiles (Equations (7.15), (7.16) in the following paragraphs).

The second classification is based upon the representation of the term S (energy line slope) in Equation (7.2). Here again there are two classes of models:

(iii) Those based on the Manning–Strickler or Chezy resistance formulae, the roughness coefficient being assumed constant and the energy slope taken as an explicit function of the roughness and of other flow parameters.

(iv) Those using a more complicated resistance relationship which includes the influence of bed forms (dunes) and their variation with discharge.

Clearly, at least in principle, a class (i) or (ii) model can be used with class (iii) or class (iv) expression for S.

7.3 BOUNDARY CONDITIONS IN MOVABLE BED MODELLING

All mathematical models of sediment transport need upstream and downstream boundary conditions. Not all methods need the same number of such conditions, as we shall see, but all should be able to accept internal boundary conditions, which are needed at all sections where the basic flow equations (such as Equations (7.1)–(7.4)) are not valid, e.g. rapid variations in cross-sectional area, weirs, dams, gates, confluences, tributaries. Typically an industrialized program would be able to treat the following external and internal boundary conditions:

(i) sediment discharge and water discharge as a function of time imposed at the upstream end of the model:

$$G(x = 0) = f_1(t); \quad Q(x = 0) = f_2(t)$$

(ii) water stage as a function of time imposed at the downstream end of the model:

$$y(x = L) = f(t)$$

(where $x = L$ represents the downstream limit)

(iii) relationship between the depth and discharge at the downstream end of the model:

$$h(x = L) = f(Q)$$

(iv) bottom elevation as a function of time imposed at one end of the model, $z(x = L) = f(t)$ or $z(x = 0) = f(t)$ (condition which represents an unerodable bed, or dredging, etc.)

(v) abruptly varying river cross section as shown in Fig. 7.3a, represented by three compatibility conditions:

$$Q_{i+1} = Q_i; \quad G_{i+1} = G_i; \quad y_{i+1} + \frac{u_{i+1}^2}{2g} + \Delta H = y_i + \frac{u_i^2}{2g}$$

where ΔH is the expansion or contraction energy loss

(vi) tributary sediment inflow; in this case, as shown in Fig. 7.3b, the time-dependent variation of $Q(t)$ and $G(t)$ to be imposed must be known. Dredging can be simulated by putting $G(t) < 0$, $Q(t) = 0$. The compatibility conditions for this case are:

$$Q_{i+1} = Q_i + Q(t); \quad G_{i+1} = G_i + G(t);$$

$$y_{i+1} + \frac{u_{i+1}^2}{2g} + \Delta H = y_i + \frac{u_i^2}{2g}$$

(vii) tributary confluence shown in Fig. 7.3c and represented by the following conditions:

$$Q_c = Q_a + Q_b$$

$$G_c = G_a + G_b$$

$$y_c + \frac{u_c^2}{2g} + \Delta H = y_a + \frac{u_a^2}{2g} = y_b + \frac{u_b^2}{2g}$$

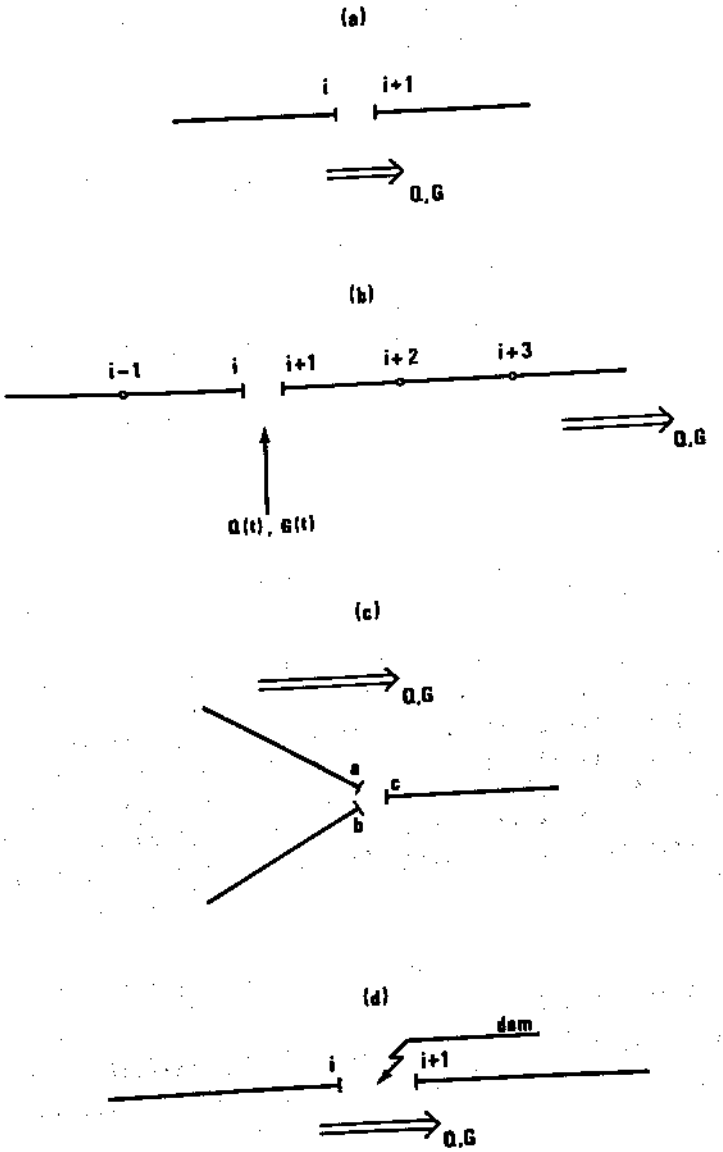

Fig. 7.3. Internal boundary conditions for movable bed models. (a) Abrupt change in cross section (case v); (b) tributary water and sediment inflow (case vi); (c) confluence (case vii); (d) control structure or dam (case viii)

(viii) dam, requiring two discharge compatibility laws $Q_{i+1} = Q_i$, $G_{i+1} = f(G_i)$ and one concerning the water levels which is either given as the water stage imposed as a function of time $y_i = f(t)$ or as a discharge formula through the dam gates (*see* Fig. 7.3d)

The conditions (i)–(iv) are external boundary conditions which apply to the limits of the model. Clearly, a model may have several such limits, e.g. the model shown in Fig. 7.4 has 5 sections where external boundary conditions are to be

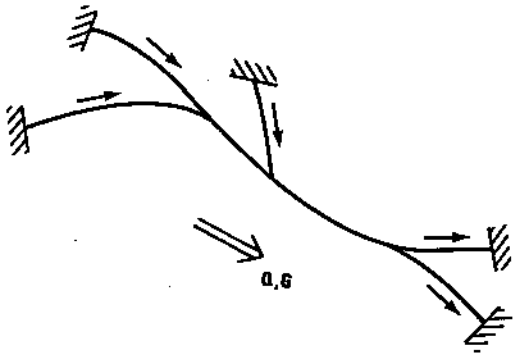

Fig. 7.4. Boundary conditions in branched transport model

imposed. Conditions (v)–(viii) are internal boundary conditions, and a model may require several of each kind. Obviously the above list of conditions is not exhaustive.

The various kinds of internal boundary conditions, and the ways in which they are represented numerically, depend on the needs of particular models. One general remark is that all compatibility laws must be programmed with the same care as the basic equations; for example, they must be expressed in proper implicit form if such a scheme of finite differences is used elsewhere. The equality of energy levels at junctions seems to be an extreme requirement for nearly all practical cases: the equality of free surface levels is usually quite sufficient.

7.4 DATA REQUIREMENTS

The basic data needs of a sediment transport model are the same as those of a river flood propagation model (Chapter 5) to which must be added the following additional data:

- particle size distribution of sediment transported including both the bed load and the suspended load;
- sediment discharge vs. time data whenever this can be obtained along the simulated reach. These data are compulsory for the upstream boundary conditions

of the model;
- variation in bottom elevations observed in the past at different stations and overall changes in the longitudinal profile over a long period of time.

Basically, mathematical modelling of movable bed rivers requires the same kind of topographic and hydraulic data as flood propagation models do, and the representation of cross sections and conveyances may be the same as that described in Chapter 4. However, a movable bed model may require less precision than a flood propagation model; since one does not usually know how to distribute laterally the deposited or eroded material, it may be superfluous to represent cross-sectional features in a sophisticated way, especially when only slow changes in the longitudinal profile are to be studied. For example, engineers often prefer to use a rectangular cross section as representative of the real one in movable bed models since they are unable to formulate physically sound lateral transport laws. A very sophisticated representation of the deposits within a section and of the section itself may be inconsistent with other qualities of a simplified model.

7.5 MATHEMATICAL ANALYSIS OF THE EQUATIONS

Full unsteady flow equations

Using Equation (7.4) it is possible to express the derivative of the solid discharge $\partial G/\partial x$ as a function of velocity u and depth h:

$$\frac{\partial G}{\partial x} = \frac{\partial G}{\partial h}\frac{\partial h}{\partial x} + \frac{\partial G}{\partial u}\frac{\partial u}{\partial x} \tag{7.7}$$

Let $b = \tilde{b} = 1$ and $n = 0$ in Equations (7.1)–(7.3). By substituting Equation (7.7) into Equation (7.3), and by adding the expressions for the total derivatives of the three dependent variables $u(x, t)$, $h(x, t)$ and $z(x, t)$ to the system of equations (7.1)–(7.3), a set of six equations is obtained:

$$\frac{\partial h}{\partial t} + h\frac{\partial u}{\partial x} + u\frac{\partial h}{\partial x} = 0 \tag{7.8a}$$

$$\frac{\partial u}{\partial t} + u\frac{\partial u}{\partial x} + g\frac{\partial h}{\partial x} + g\frac{\partial z}{\partial x} + gS(u, h) = 0 \tag{7.8b}$$

$$\frac{\partial z}{\partial t} + \frac{\partial G}{\partial u}\frac{\partial u}{\partial x} + \frac{\partial G}{\partial h}\frac{\partial h}{\partial x} = 0 \tag{7.8c}$$

$$\frac{\partial u}{\partial t}\,dt + \frac{\partial u}{\partial x}\,dx - du = 0 \tag{7.9}$$

$$\frac{\partial h}{\partial t}\,dt + \frac{\partial h}{\partial x}\,dx - dh = 0 \tag{7.10}$$

$$\frac{\partial z}{\partial t}\,dt + \frac{\partial z}{\partial x}\,dx - dz = 0 \tag{7.11}$$

The condition which enables us to determine the characteristic directions of the set of equations (7.1)–(7.3) is that the determinant of the set of equations (7.8)–(7.11) be zero:

$$\begin{vmatrix} 0 & h & 1 & u & 0 & 0 \\ 1 & u & 0 & g & 0 & g \\ 0 & \partial G/\partial u & 0 & \partial G/\partial h & 1 & 0 \\ dt & dx & 0 & 0 & 0 & 0 \\ 0 & 0 & dt & dx & 0 & 0 \\ 0 & 0 & 0 & 0 & dt & dx \end{vmatrix} = 0 \tag{7.12}$$

which can be expanded to yield:

$$-dx^3 + 2u dx^2 dt + \left(gh - u^2 + g\frac{\partial G}{\partial u}\right) dx dt^2 + g\left(h\frac{\partial G}{\partial h} - u\frac{\partial G}{\partial u}\right) dt^3 = 0 \tag{7.13}$$

Let $dx/dt = c$, the characteristic velocity:

$$-c^3 + 2uc^2 + \left(gh - u^2 + g\frac{\partial G}{\partial u}\right) c + g\left(h\frac{\partial G}{\partial h} - u\frac{\partial G}{\partial u}\right) = 0 \tag{7.14}$$

Equation (7.14) has three roots c_1, c_2, c_3, hence the set of equations (7.1)–(7.3) has three characteristics in the plane (x, t). Equation (7.14) was first presented by Vreugdenhil and de Vries (1967) and analysed by Kyozo Suga (1969). According to Equation (7.14), each point in the solution domain, including the boundaries, is an intersection of three characteristic curves whose directions correspond to the three roots of the system. As shown in Fig.7.5, in subcritical flow conditions ($u^2 < gh$) a characteristic C_2 originating within the domain and two characteristics C_1 and C_3 originating outside the domain will pass through each upstream boundary point. Characteristic C_2, originating outside the domain, and two characteristics C_1 and C_3, originating within the domain, will pass through each downstream boundary point. Consequently, if the complete mixed (i.e. within the bounded space domain) problem of sub-critical flow is to be well posed from a mathematical standpoint it is necessary to furnish:

- three initial condition functions $u(x, 0)$, $h(x, 0)$ and $z(x, 0)$ over the interval $0 < x \leqslant L$ at the initial time $t = 0$;
- two time-dependent conditions at the upstream boundary of the model, $x = 0$;
- a time dependent condition at the downstream boundary of the model, $x = L$.

Simplified system of unsteady flow equations

It is physically obvious that the two first roots of Equation (7.14) (free-surface

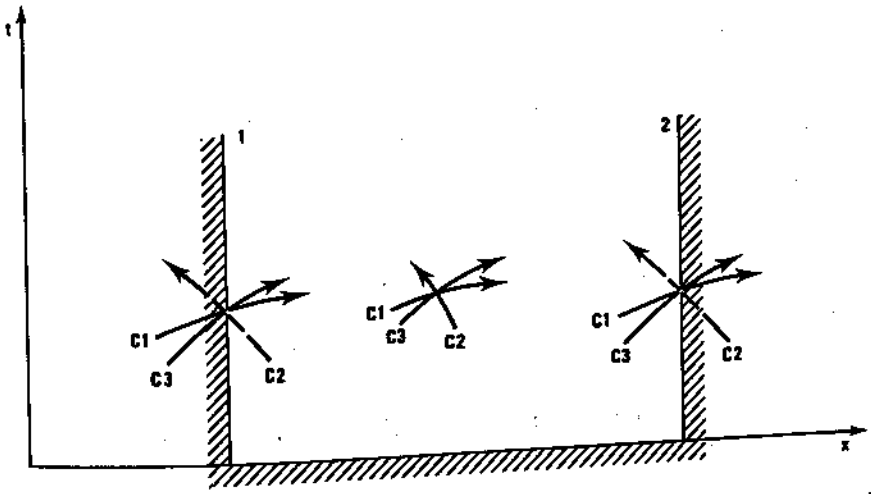

Fig. 7.5. Interior and boundary characteristics in subcritical unsteady water and sediment flow. 1, upstream boundary; 2, downstream boundary

wave celerities) should be far greater than the third root (celerity of bottom perturbations). This intuitive conclusion has been confirmed by an analysis of Equation (7.14) (Vreugdenhil and de Vries, 1967; Kyozo Suga, 1969), which shows, at least for flows with Froude number $Fr \neq 1$, that the first two roots are very close to the free surface wave celerities $u \pm (gh)^{\frac{1}{2}}$, and that they are indeed far greater than the third root. Thus it is often possible to study bed perturbations while neglecting the terms $\frac{\partial h}{\partial t}$ and $\frac{\partial u}{\partial t}$ in Equations (7.8a) and (7.8b). A simplified system of equations is obtained with $Q(t) = \text{const}$ resulting from the continuity equation (7.8a). By putting $h = y - z$ in Equations (7.8b) and (7.8c) and using (7.8a), a set of two partial differential equations is obtained:

$$(1 - Fr^2)\frac{\partial y}{\partial x} + Fr^2\frac{\partial z}{\partial x} + S(u, h) = 0 \tag{7.15}$$

$$\left(\frac{\partial G}{\partial h} - \frac{u}{h}\frac{\partial G}{\partial u}\right)\frac{\partial y}{\partial x} + \frac{\partial z}{\partial t} - \left(\frac{\partial G}{\partial h} - \frac{u}{h}\frac{\partial G}{\partial u}\right)\frac{\partial z}{\partial x} = 0 \tag{7.16}$$

where $Fr = u/(gh)^{1/2}$ is the Froude number and y is the water surface elevation. In this system the unknown functions are $y(x, t)$ and $z(x, t)$.

The system of equations (7.15), (7.16) is a hyperbolic system of equations except when $Fr = 1$, in which case it becomes parabolic; for $Fr \neq 1$ it possesses two characteristic directions which define the small wave propagation paths.

By adding to Equations (7.15), (7.16) the expressions for the total derivatives of dependent variables $y(x, t)$ and $z(x, t)$:

$$\frac{\partial y}{\partial t}\,dt + \frac{\partial y}{\partial x}\,dx - dy = 0 \tag{7.17}$$

$$\frac{\partial z}{\partial t}\,dt + \frac{\partial z}{\partial x}\,dx - dz = 0 \tag{7.18}$$

and by setting equal to zero the determinant of the set of equations (7.15)–(7.18):

$$\begin{vmatrix} 0 & 1-Fr^2 & 0 & Fr^2 \\ 0 & \left(\frac{\partial G}{\partial h} - \frac{u}{h}\frac{\partial G}{\partial u}\right) & 1 & -\left(\frac{\partial G}{\partial h} - \frac{u}{h}\frac{\partial G}{\partial u}\right) \\ dt & dx & 0 & 0 \\ 0 & 0 & dt & dx \end{vmatrix} = 0 \tag{7.19}$$

we obtain the equation for the two characteristic directions of the set of equations (7.15), (7.16),

$$(1-Fr^2)\,dx\,dt + \left(\frac{\partial G}{\partial h} - \frac{u}{h}\frac{\partial G}{\partial u}\right)dt^2 = 0 \tag{7.20}$$

The first solution may be obtained by letting dt tend toward zero,

$$c_1 = \lim_{dt \to 0} \left(\frac{dx}{dt}\right)_1 = \infty \tag{7.21}$$

Equation (7.21) expresses the fact that the characteristic C_1 is parallel to the x axis, i.e. that the velocity of the liquid surface waves is infinite. Equation (7.20) also provides the second characteristic direction:

$$c_2 = \left(\frac{dx}{dt}\right)_2 = \frac{u\,\frac{\partial G}{\partial u} - h\,\frac{\partial G}{\partial h}}{h(1-Fr^2)} \tag{7.22}$$

The value c_2 expressed in metres per second represents the velocity of the small bed waves. The simplified set of equations (7.15) and (7.16) differs from the complete set (7.8a)–(7.8c). Each point of the domain considered in the plane (x, t) is a point of intersection of two curves: a straight line C_1 parallel to the abscissa x and a characteristic C_2 defined by Equation (7.22) (Fig. 7.6). To ensure that the problem is well posed, we must furnish:

- two functions $y(x, 0)$ and $z(x, 0)$ over the interval $0 \leqslant x \leqslant L$ at the initial time $t = 0$;
- a time dependent condition at the upstream limit of the model $x = 0$;
- a time dependent condition at the downstream limit of the model, $x = L$.

The fact that one of the characteristics is parallel to the x-axis has a direct and practical consequence, because the system of equations (7.15) and (7.16) is not

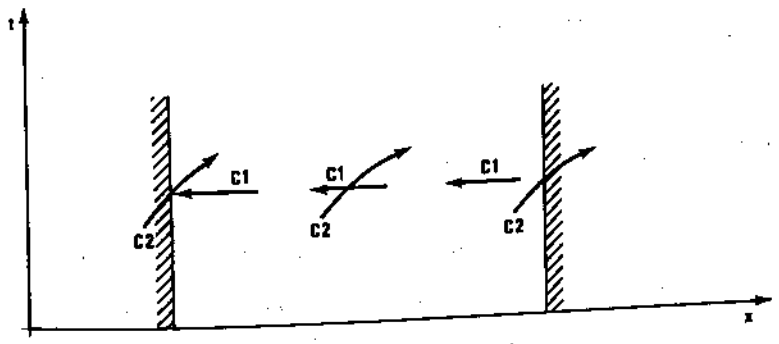

Fig. 7.6. Interior and boundary characteristics in subcritical steady water flow and unsteady sediment flow

the same problem, mathematically speaking, as that discussed in Section 2.2. It is the so-called Goursat problem: the initial data are given *on the characteristic.* The problem is not well posed unless the initial conditions $y(x, 0)$, $z(x, 0)$ and $u(x, 0)$ satisfy Equations (7.15) and (7.16), and computational difficulties develop if this is not the case.

Since the replacement of Equations (7.1)–(7.3) by the system of equations (7.15), (7.16) is a considerable simplification, it is important to understand its physical ramifications.

Let us consider the following system of equations:

$$\begin{aligned} &u\frac{\partial u}{\partial x} + g\frac{\partial h}{\partial x} + g\frac{\partial z}{\partial x} + g\frac{1}{C^2}\frac{u|u|}{h} = 0 \\ &\frac{\partial z}{\partial t} + \frac{\partial G}{\partial x} = 0 \\ &uh = q = \text{const} \\ &G = f(u, h) \end{aligned} \tag{7.23}$$

obtained from Equations (7.1)–(7.4) for $n = 0$ and a channel of unit width by neglecting terms $\partial u/\partial t$, $\partial h/\partial t$ as we did in obtaining Equations (7.15) and (7.16), and assuming that the steady state energy line slope can be computed with the Chezy formula:

$$S = \frac{u|u|}{C^2 h} \tag{7.24}$$

We shall linearize Equations (7.23) in the neighbourhood of steady uniform flow, i.e. by assuming that the dependent variables u, h and z can be replaced by:

$$u = U + \tilde{u}; \quad h = H + \tilde{h}; \quad z = Z + \tilde{z} \tag{7.25}$$

The resulting equation,

$$\frac{\partial \tilde{z}}{\partial t} - \frac{(1-Fr^2)\,HC^2}{3g\,Fr^2}\,\frac{\partial^2 \tilde{z}}{\partial x \partial t} + \frac{\dfrac{\partial G}{\partial h} - \dfrac{q}{H^2}\,\dfrac{\partial G}{\partial u}}{3g\,Fr^2}\,C^2 H\,\frac{\partial^2 \tilde{z}}{\partial x^2} = 0 \tag{7.26}$$

is a hyperbolic partial differential equation of second order with a damping term. Thus the effect of neglecting $\frac{\partial u}{\partial t}$ and $\frac{\partial h}{\partial t}$ is to simulate an initial perturbation damping process, and this conclusion is of utmost importance with respect to the application of dissipative finite difference schemes. Indeed, if there were no natural damping due to the physical phenomena, the choice of numerical methods applied to solve Equations (7.15) and (7.16) would be much more difficult as is the case for any purely convective process, *see* Chapter 8. Since Equation (7.26) is an equation with damping term depending upon coefficient

$$D = \left(\frac{\partial G}{\partial h} - \frac{\partial G}{\partial u}\,\frac{q}{H^2}\right)\,\frac{C^2 H}{3g\,Fr^2} \tag{7.27}$$

any dissipative finite difference scheme for the solution of Equations (7.15) and (7.16) is acceptable as long as the artificial damping introduced by it is negligible as compared to the damping resulting from Equation (7.27).

Nonetheless, we must stress that this simplification $\left(\text{dropping } \frac{\partial u}{\partial t} \text{ and } \frac{\partial h}{\partial t}\right)$ represents an important physical approximation. Dropping the $\frac{\partial h}{\partial t}$ term from Equation (7.8b) leads to $\frac{\partial Q}{\partial x} = 0$, hence $\frac{\partial h}{\partial t} = 0$ and $h(t) = \text{const}$. This is physically false. Suppose that a dam is built and that the water discharge and water stage at the dam are maintained constant. Then material will deposit at the bottom, and quite clearly at a given section x_0, the water depth $h(x_0, t)$ will vary with time as shown in Fig. 7.7. Thus, $\frac{\partial h}{\partial t} \neq 0$ and, since the hypothesis $\frac{\partial Q}{\partial x} = 0$ was adopted, the continuity equation is not satisfied. The discrepancy is usually very small however, its magnitude being given by the ratio of the volume filled up by the sediment to the total volume of the flow which passes through the reservoir during the same period.

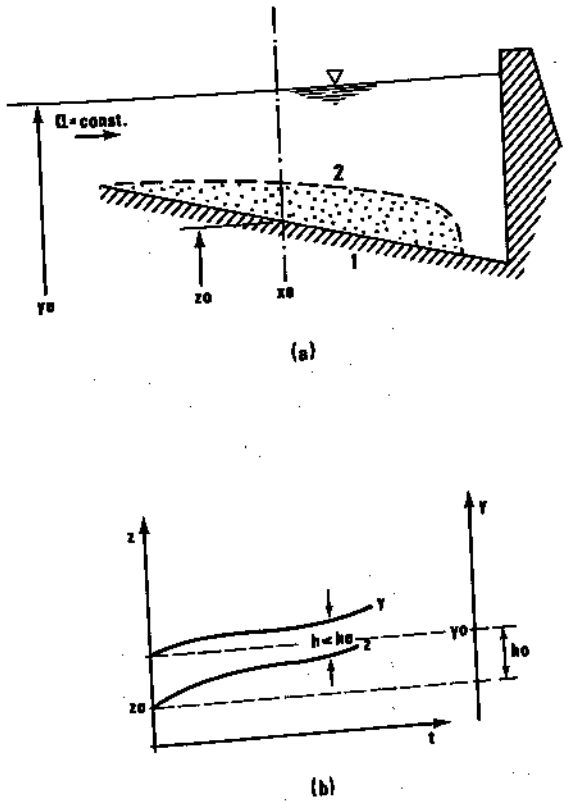

Fig. 7.7. Continuity equation violation using simplified equations (7.15) and (7.16). (a) Longitudinal profile in reservoir before (1) and after (2) deposition. (b) Variation of y and z with time at point x_0; $h < h_0$ shows that $\partial h/\partial t = 0$ is physically wrong

7.6 NUMERICAL SOLUTIONS

Full system of three equations

All existing practical applications of movable bed modelling are based on the finite difference approach which leads to the replacement of Equations (7.1)–(7.3) by a system of algebraic equations. In practice, this may be done in two different ways: either by solving all three equations simultaneously, or by separating the solution of the system of Equations (7.1), (7.2) (related to the liquid flow phase) from that of Equation (7.3) (representing the sediment flow phase).

Separation of liquid and solid phase equations (uncoupled solution)

In the uncoupled formulation, for a computational time step $\Delta t = t_1 - t_0$, first the finite difference equivalents of Equations (7.1), (7.2) are solved along the

water course. This is a classical flood or surge wave propagation problem such as is dealt with in Chapters 4 and 6. Its solution consists of water stages, water discharges, and mean water velocities computed at time t_1 at all computational grid points of the model. It is assumed for this first calculation that the bottom elevations $z(x)$ do not change during Δt.

The water depths $h(x, t_1)$ and velocities $u(x, t_1)$ found from the first step are first used in the sediment transport formula Equation (7.4) and then the first-order partial differential equation describing propagation of the bottom sediment wave, Equation (7.3), is solved numerically, usually on the same computational grid as the flood propagation calculation.

Equation (7.3) has one family of characteristics in the (x, t) plane (*see* Fig. 7.8) and consequently requires one upstream boundary condition, while initial values $z(x, t_0)$ must be imposed along $0 \leqslant x \leqslant L$.

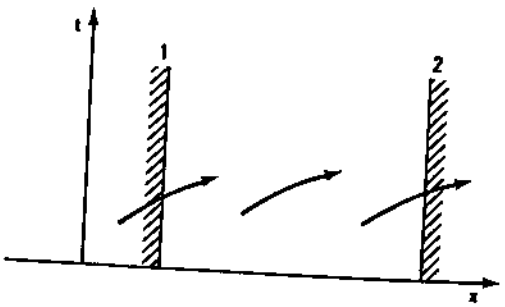

Fig. 7.8. Characteristics of Equation (7.3). 1, upstream boundary; 2, downstream boundary

The uncoupled solution method has its origins in the general concept of explicit finite difference schemes: it is assumed that one dependent variable (here the bottom elevation z and consequently the depth h) can be, during one time step, computed independently from the other dependent variables. If this is not the case, computational instabilities will appear whatever numerical method is chosen for the solution of Equation (7.3), even when the method of solution of Equations (7.1), (7.2), is unconditionally stable from a strictly numerical viewpoint. This was shown by Perdreau and Cunge (1971) who used two different schemes to solve Equation (7.3). The first was explicit, the derivatives being approximated as

$$\frac{\partial f}{\partial t} \approx \frac{f_{j+1}^{n+1} - f_{j+1}^{n}}{\Delta t}; \quad \frac{\partial f}{\partial x} \approx \frac{f_{j+1}^{n} - f_{j}^{n}}{\Delta x} \tag{7.28}$$

(*see* Fig. 7.9). This explicit scheme is subject to the usual numerical stability condition

$$c \frac{\Delta t}{\Delta x} \leqslant 1 \tag{7.29}$$

where c is the celerity of bottom perturbations, *see* Equation (7.22).

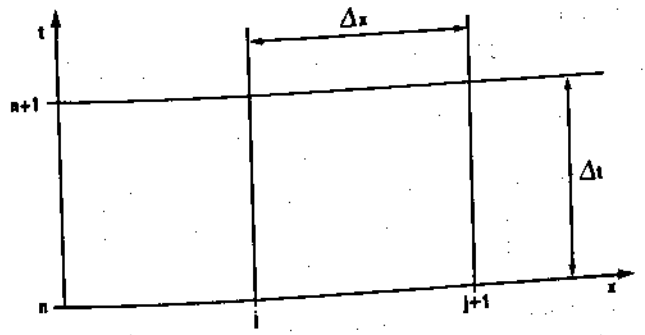

Fig. 7.9. Computational grid for Preissmann's implicit scheme

The second scheme was an implicit one,

$$\frac{\partial f}{\partial t} \approx \frac{f_{j+1}^{n+1} - f_{j+1}^{n}}{\Delta t} \; ; \quad \frac{\partial f}{\partial x} \approx \frac{f_{j+1}^{n+1} - f_{j}^{n+1}}{\Delta x} \tag{7.30}$$

ensuring unconditional stability for the solution of Equation (7.3).

Nevertheless, for both methods, wherever increments $\Delta h = h^{n+1} - h^n$ computed with the full system of equations (7.1)–(7.3) ceased to be negligible compared with $h(x, t)$ itself, numerical instability appeared in the uncoupled model.

An analogous uncoupled method was used by Chen (1973) and was applied to a reach of the Mississippi River; the condition $\Delta h \ll h$ was satisfied in that case.

Three coupled equations

Preissmann's four-point implicit scheme of Chapter 3 may be applied to Equations (7.1)–(7.3), replacing the derivatives by finite differences. Putting $f_j^{n+1} - f_j^n = \Delta f_j$, substituting this definition into Equations (7.1)–(7.3), and dropping second-order values (based upon the hypothesis that $\Delta f \ll f$), yields the following system of three linear algebraic equations in Δy, Δu and Δz written in matrix form

$$[A]\,\{\Delta w_{j+1}\} + [B]\,\{\Delta w_j\} + \{C\} = 0 \tag{7.31}$$

where $[A]$, $[B]$ are 3×3 matrices of coefficients known at time t_n, $\{C\}$ is a vector of known coefficients, and $\{\Delta w\}$ is the unknown vector:

$$\{\Delta w_j\} = \begin{Bmatrix} \Delta u_j \\ \Delta y_j \\ \Delta z_j \end{Bmatrix} \tag{7.32}$$

In Equation (7.31) the unknown variable Δu_j is usually replaced by ΔQ_j, where Q is the water discharge, since Q is a computationally more convenient variable than the velocity u.

For a given reach of river represented by N computational points, there are $3(N-1)$ Equations (7.31) and $3N$ unknowns $\{\Delta Q_j, \Delta y_j, \Delta z_j\}, j = 1, 2, \ldots, N$. Two upstream and one downstream boundary condition close the system which can then be solved by the double sweep method (*see* Chapter 3).

As long as the coefficient θ of Preissmann's scheme is greater than 0.5, the method is numerically stable. It is also a dissipative method and thus introduces numerical diffusion and phase error. Without going into the details of the analysis, it may be shown that for usual situations, numerical error does not destroy the solution even for large values of the time step.

A reach of a mountain river (River Drac near Grenoble, France) was computed with the coupled equation method. The reach considered was modelled as a rectangular channel having the following characteristics: length = 10 km, width = 100 m, Strickler coefficient $k_{str} = 30$, $d_{50} = 35$ mm.

The assumed initial conditions which represent the river in equilibrium were the following: bottom longitudinal slope $S_0 = 0.004$, depth $h = 3$ m, water discharge $Q = 1187\ \mathrm{m^3 s^{-1}}$, sediment discharge $G = 0.719\ \mathrm{m^3 s^{-1}}$.

The Meyer–Peter bed load formula was used during the computation, and the following boundary conditions were imposed:

- at the point $j = 1$ (downstream): free overflow weir defining a $y = f(Q)$ relationship;
- at the point $j = N$ (upstream): $Q = 1187\ \mathrm{m^3 s^{-1}} = \text{const.}$ and the sediment discharge varying linearly according to the hydrograph shown in Fig. 7.10.

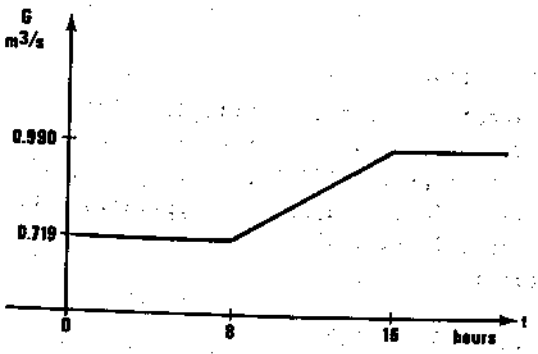

Fig. 7.10. River Drac upstream sediment inflow hydrograph

The river reach was represented by 101 computational points with a constant $\Delta x = 100$ m. Two computations were made, both with $\theta = 1$: one putting $\Delta t = 16$ h and another with $\Delta t = 100$ h. In Fig. 7.11 are shown the longitudinal profiles of the reach computed with both values of Δt after 1116 h, at which time the perturbation arrived at the downstream limit. It may be seen that the increase in time step did not significantly change the results.

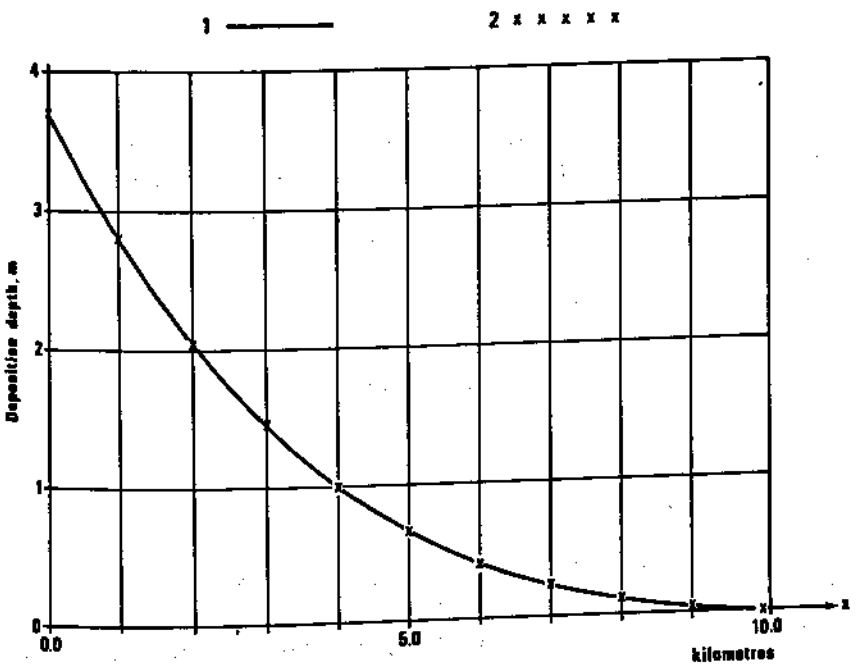

Fig. 7.11. River Drac computed bed profiles after $t = 1116$ h. 1, $\Delta t = 16$ h; 2, $\Delta t = 100$ h

The implicit method described above was first used to solve the full system of equations (7.1)–(7.3) in 1971 (Cunge, 1972). It was further described in detail by Chen and Simons (1975) who used a constant value of $\theta = 1$ for the weighting coefficient.

Simplified system of two equations

There are two well described numerical methods of solving the system of equations (7.15), (7.16). Both are finite difference methods and both were developed by institutions using mathematical models on an industrial scale as consultancy tools: the Delft Hydraulics Laboratory and SOGREAH.

SOGREAH method (Cunge and Perdreau, 1973)

The simplified system derived from Equations (7.1)–(7.3) by neglecting $\frac{\partial h}{\partial t}, \frac{\partial u}{\partial t}$ may be written

$$\frac{\partial}{\partial x}\left(\frac{Q^2}{2A^2} + gy\right) + \frac{gQ\,|Q|}{K^2} = 0$$

$$\frac{\partial z}{\partial t} + \frac{1}{b}\frac{\partial G}{\partial x} = 0 \tag{7.33}$$

where: K = conveyance factor; $Q = Au$ = const, A = wetted area. Application of Preissmann's four-point scheme as described in Chapter 3 and linearization of the resulting expressions with respect to increments in time of the dependent variables leads to the following system of linear equations in Δz_j, Δy_j, $j = 1, 2, \ldots, N$:

$$[A_j]\ \{\Delta w_j\} + [B_j]\ \{\Delta w_{j+1}\} + \{C_j\} = 0 \tag{7.34}$$

where $[A_j]$, $[B_j]$ are 2×2 matrices; $\{C_j\}$ is a two-component vector, and $\{\Delta w_j\}$ is the unknown vector

$$\{\Delta w_j\} = \begin{Bmatrix} \Delta y_j \\ \Delta z_j \end{Bmatrix}$$

The coefficients of $[A_j]$, $[B_j]$ and $\{C_j\}$ are functions of values known at time t_n at points j and $j + 1$. If there are N computational points j in the model, there are $2(N - 1)$ Equations (7.34). Two boundary conditions close the system, which can then be solved by the double sweep method as described in Chapter 3. (Note that the corresponding non-linear algebraic system of equations in Δy_j, Δz_j can be solved by iterations if desired.)

It was shown by Cunge and Perdreau (1973) that the finite difference scheme is always stable within linear analysis limits when $0.5 \leqslant \theta \leqslant 1.0$, this result being true for a frictionless system; Cunge and Perdreau also give estimates of relative numerical damping and dispersion as compared to the analytical solution of linear systems.

For most practical cases, when the typical wavelength of the bottom perturbation to be represented stretches over a great number of computational points, numerical damping is negligible as compared to the physical damping even for very high Cr (Courant number) values. The advantage of this feature of the method, which is a consequence of the implicit scheme used, is that time steps can be chosen which are compatible with the time scale of the phenomena simulated: hours during the flood and weeks during the low flow periods in the same run. The method also allows variable spacing of computational points: the accuracy of the solution is not affected. The system of Equations (7.34) and its boundary conditions is symmetric: it can be solved by the double sweep method from downstream to upstream or vice versa. This feature is useful in certain circumstances, as will be shown further on. The solution fails, however, if critical flow is encountered along the river reach.

Delft Hydraulics Laboratory method (de Vries, 1973a)

The system of equations to be solved is the following:

$$\left(u - \frac{gQ}{bu^2}\right)\frac{\partial u}{\partial x} + g\frac{\partial z}{\partial x} = g\frac{u|u|}{C^2 h} \tag{7.35}$$

$$\frac{\partial z}{\partial t} + \frac{1}{b}\frac{\partial G}{\partial x} = 0 \tag{7.36}$$

The Delft method is based upon the hypothesis that, as in the case of explicit schemes, the two dependent variables $u(x, t)$ and $z(x, t)$ can be computed in two separate steps. In the first step z is considered to be constant during the time interval Δt and $u(x, t_n + \Delta t)$ is computed from Equation (7.35). Since $z(x) = z(x, t_n)$ is assumed to be known, Equation (7.35) becomes an ordinary differential equation which can be solved by any conventional method over the time interval Δt. Vreugdenhil and de Vries (1967) used the following (*see* Fig. 7.12) implicit scheme to solve Equation (7.35):

$$f(x, t) \approx f_j^{n+1}; \quad \frac{df}{dx} \approx \frac{f_{j+1}^{n+1} - f_{j-1}^{n+1}}{2\Delta x} \tag{7.37}$$

Later De Vries (1973a) indicated that the Ralston standard method was used to solve the non-linear algebraic equation which results from the substitution of Equation (7.37) into Equation (7.35).

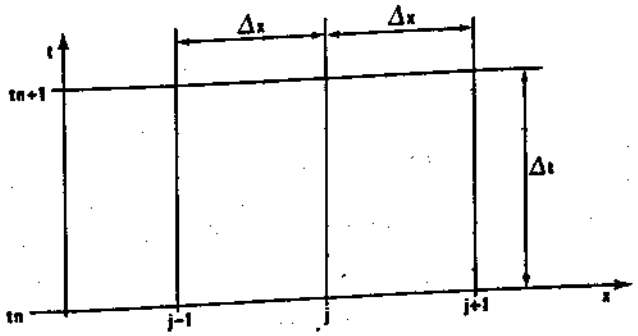

Fig. 7.12. Computational grid for the Delft scheme

In the second step, Equation (7.36) is solved for $z(x, t_{n+1})$ using known values of $u(x, t_n)$ and the following explicit finite difference approximation:

$$\frac{\partial z}{\partial t} \approx \frac{1}{\Delta t}\left\{z_j^{n+1} - \left[(1-\alpha)z_j^n + \alpha\frac{z_{j+1}^n + z_{j-1}^n}{2}\right]\right\} \tag{7.38}$$

$$\frac{\partial G}{\partial x} \approx \frac{G_{j+1}^n - G_{j-1}^n}{2\Delta x}; \quad \alpha > 0 \tag{7.39}$$

Putting $\alpha > 0$ is equivalent to introducing a dissipative interface (Abbott, 1979), stabilizing an otherwise numerically unstable scheme. Thus, when new values of $z(x, t_{n+1})$ are computed:

$$z_j^{n+1} = (1-\alpha)\, z_j^n + \alpha\, \frac{z_{j+1}^n + z_{j+1}}{2} - \frac{\Delta t}{2\Delta x}\,(G_{j+1}^n - G_{j-1}^n) \tag{7.40}$$

the equation which has to be solved is really a finite difference equivalent of the following parabolic equation:

$$\frac{\partial z}{\partial t} + \frac{\partial G}{\partial x} - \frac{(\Delta x)^2}{2\Delta t}\,(\alpha^2 - \mu^2)\,\frac{\partial^2 z}{\partial x^2} = 0 \tag{7.41}$$

where $\mu = c_2\,\dfrac{\Delta t}{\Delta x}$ is a number similar to Courant number Cr if C_2 is the celerity of bottom sand waves in a frictionless system. De Vries (1973a) defines this celerity as

$$c_2 = \frac{\dfrac{1}{b}\,\dfrac{\mathrm{d}G}{\mathrm{d}u}}{1 - Fr^2} \tag{7.42}$$

Equation (7.41) shows that by choosing α nearly equal to μ the dissipation can be minimized (but must not be fully eliminated, for in this case the method becomes unstable). According to De Vries (1973a) the stability condition is:

$$\mu^2 < \alpha < 1 \tag{7.43}$$

and one should choose (De Vries, private communication, 1974)

$$\alpha - \mu^2 \approx o(10^{-2}) \tag{7.44}$$

The Delft method differs from the SOGREAH method in several respects which are of practical importance. The time step cannot be chosen arbitrarily, since it is limited by the greatest value of Cr, i.e. by the celerity of sand waves and the smallest space interval Δx in the system. It is not symmetric with respect to the x axis: Equation (7.35) (the backwater curve equation) must be solved starting from the downstream limit (except for supercritical flow reaches) while Equation (7.36), on the other hand, is solved from upstream to downstream. Also care must be taken that the finite difference schematization as shown in Equations (7.38) and (7.39) does not introduce supplementary error if the computational points are not spaced at equal intervals. Indeed, Equations (7.38) and (7.39) involve variables at three points $j-1$, j and $j+1$ and if the distance between the points is not the same, additional errors are introduced.

On the other hand the method presents an important advantage if Equation (7.35) is solved properly for the backwater curve: it enables river reaches with critical sections to be simulated more easily, an important feature when dealing with mountain streams or flushing operations of reservoirs.

7.7 MODELS OF ALLUVIAL CHANNEL RESISTANCE

Physical aspects

As was stressed at the beginning of this chapter, the resistance of the river bed may be more complex than as described by the Manning–Strickler or Chezy laws. Figure 7.13 shows the longitudinal profile of a 0.7 mile reach of the

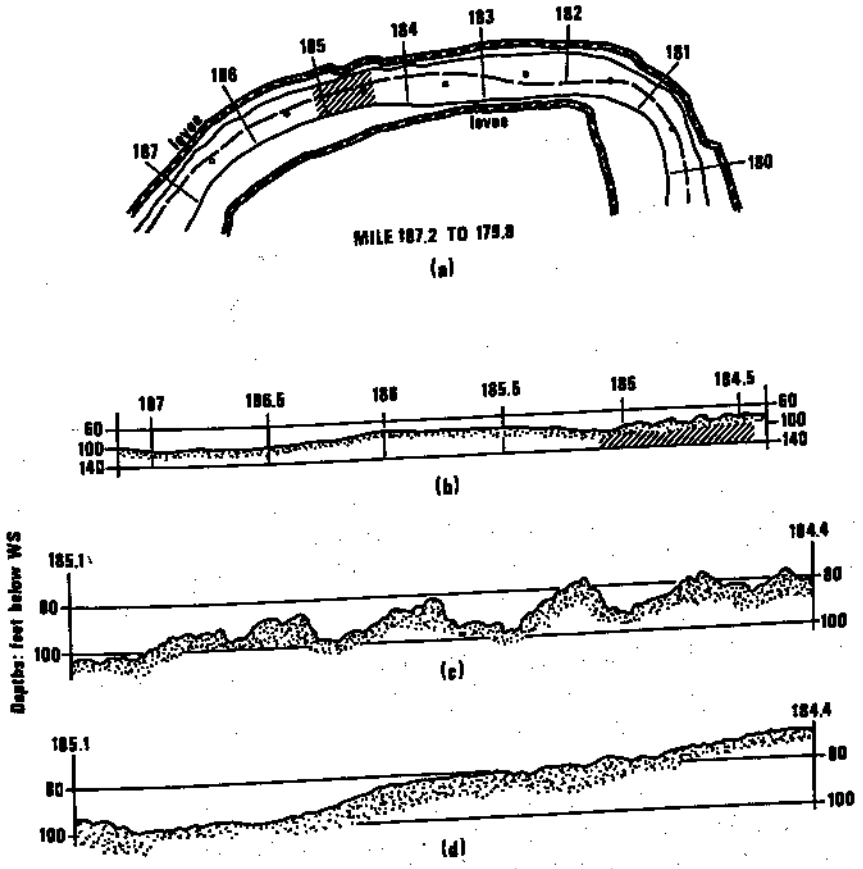

Fig. 7.13. River bed form variations in the Mississippi River, mile 187.2 to 179.8 (after Walters, private communication, 1973). (a) Study area; (b) sailing line profile, 10 April 1956; (c) detailed bed profile, 10 April 1956 (Donaldsonville gauge = 18.3 ft); (d) detailed bed profile, 10 July 1956 (Donaldsonville gauge = 5.8 ft)

Mississippi River at two different times: 10 April and 10 July 1956. The profoundly different profiles shown demonstrate the problem faced by engineers trying to model alluvial streams whose beds are composed of fine grain material (say $d < 1$ mm).

The resistance which such river beds present to flow can be considered to be composed of two parts, one linked to the classical grain roughness (well described by the Manning formula) and another due to the bed forms. The latter is provoked by the wakes created behind the dunes as is shown schematically in Fig. 7.14. The main difficulty arises from the fact that the dunes are washed out

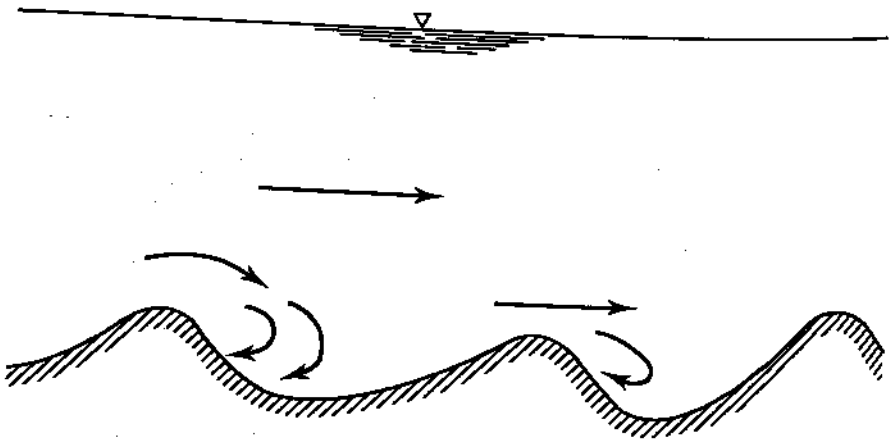

Fig. 7.14. Wakes behind dunes

completely or partially when the discharge increases during floods, and appear again during the lower water period. Thus there are two regimes which are possible within the same section: lower regime (with dunes) and upper regime (flat bed). Clearly, the upper regime presents a smaller resistance than the lower regime. This situation has led some engineers to define a 'variable Manning coefficient' computed according to the formula

$$n = \frac{S_{fs} R^{2/3}}{u} \tag{7.45}$$

where S_{fs} = free surface slope; R = hydraulic radius (*see also* Section 4.5).

The coefficient n in Equation (7.45) is a global roughness coefficient which, in uniform flow, is equal to the Manning coefficient in the upper regime but in the lower regime reflects both forms of resistance. Such a coefficient n varies with the discharge. If it is computed for a wide river it absorbs an additional phenomenon: lower regime may well be established across one part of the width while upper regime is observed across another part, as shown in Fig. 7.15. During rising flood conditions in such a river, the values of the coefficient n will decrease gradually until the whole cross section conveys the flow in the upper regime (and then n will be constant, equal to that of Manning's definition related to bed material size).

This phenomenon is well known (corresponding references can be found in the ASCE Manual (1975)) and is being considered more and more frequently

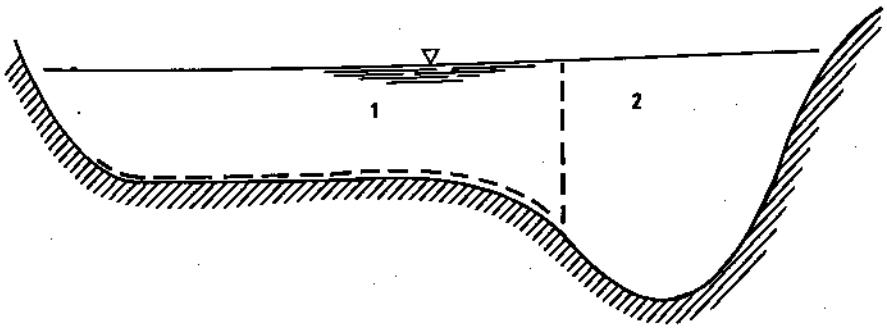

Fig. 7.15. Lateral variation of river bed regime. 1, Low velocity, low regime (dunes); 2, high velocity, upper regime (flat bed)

although it affects only those rivers which flow in very fine alluvia. Many rivers in Asia, Africa and South America are of this kind and the need for mathematical modelling of these streams has raised the question of how to express the relationship for the energy line gradient stated symbolically by Equation (7.6),

$$\varphi(S, u, h, d, \ldots) = 0 \tag{7.6}$$

This problem is the subject of considerable research at present (1979). Operational models based upon complex relationships rather than the Manning–Strickler law were developed in 1975–1977 for the simplified system of equations (7.15), (7.16), but could only represent rectangular cross sections. One of them uses the full Einstein (1950) theory for the stage/discharge relationship, another is founded upon the Engelund–Hansen (1967) formulations. The reader who is interested may consult the relevant references (Cunge and Simons, 1975; Bouvard, Chollet and Cunge, 1977; Chollet and Cunge, 1979).

In these models it was assumed that the head loss relationships established in uniform flow conditions by Engelund and Einstein were also valid in unsteady flow conditions. It must be said that the original formulations of both Einstein and Engelund theories do not make clear the relationship between the energy line gradient, the flow characteristics and bed parameters. Consequently, when these missing relationships were finally defined (Chollet, 1977), it was found that they were double valued in some ranges and could not be applied to a model which represents the full range of discharges and depths along the same river reach (as is the case when a river flowing into a reservoir is simulated). This double-valued relationship caused no difficulties for engineers who use the formulae developed by Einstein and Engelund for specific cases and for sample computations as used in classical expert consulting. But advances made in mathematical modelling have necessitated a better understanding of the theories which have been used for years, and this has led to more consistent interpretations of both theories (Chollet and Cunge, 1978).

In the following paragraphs the discretization of the energy line gradient

Equation (7.6) and of the solid transport formulae are described in more detail.

Energy line gradient formulation

The same approach is used for both the Einstein and Engelund methods; in Equation (7.6) one considers three dependent variables y, z and S. Equation (7.6) should then be written in future time $t_{n+1} = t_n + \Delta t$ which implies that each dependent variable f is replaced, following the implicit scheme, by:

$$f(x, t_{n+1}) \approx \frac{f_j^n + \theta\, \Delta f_j + f_{j+1}^n + \theta\, \Delta f_{j+1}}{2} \tag{7.46}$$

while the variables $\Phi(y, z, S)$ which are functions of the dependent variables should be written

$$\Phi(y, z, S) \approx \frac{1}{2} \left\{ \theta \left[\frac{d\Phi_j}{dy}\, \Delta y_j + \frac{d\Phi_j}{dz}\, \Delta z_j + \frac{d\Phi_j}{dS}\, \Delta S_j \right] + \Phi_j^n + \theta \left[\frac{d\Phi_{j+1}}{dy}\, \Delta y_{j+1} + \frac{d\Phi_{j+1}}{dz}\, \Delta z_{j+1} + \frac{d\Phi_{j+1}}{dS}\, \Delta S_{j+1} \right] + \Phi_{j+1}^n \right\} \tag{7.47}$$

Actually, as may be seen from published details (Chollet and Cunge, 1979), it was assumed that $\theta = 1$ and that

$$f(x_j, t_{n+1}) \approx f_j + \Delta f_j \tag{7.48}$$

As a result, for each computational point j, Equation (7.6) is replaced by a certain number of algebraic equations which then are added to the system (7.34).

Solid transport formulation

The relationships expressed by Equation (7.4), $G = G(u, h)$, represent any one of the many equations for evaluating solid transport. Einstein's and Engelund's formulae were chosen in the examples shown here for model homogeneity in spite of the fact that, for both formulations, the expressions for solid transport are practically independent of those for energy dissipation. As with all solid transport formulations, these methods were originally developed for beds in equilibrium. They cannot be used to represent significant and rapid evolution of bed profiles if prior experimental checks and, if necessary, adjustment of coefficients, have not been made.

Einstein's formula

Einstein (1950) deduced his formulation from a probabilistic interpretation of the movement of solid grains transported on the river bed by the flow. The

method incorporated in our examples corresponds exactly to the one formulated by Einstein, allowance being made for all correction parameters, separate evaluation of solid transport on the river bed and in suspension, and for different grain size distributions. The corresponding formulae are given by Chollet and Cunge (1979). The calculations made using this method are lengthy since, in addition to evaluating the solid transport intensity for each grain size range, it is also necessary to determine the derivatives of this intensity with respect to S and h, and numerically evaluate the integrals involved in the calculation of transport by suspension.

Engelund and Hansen's formula

Engelund and Hansen (1967) established this formula from a dunal bed load model extended to make allowance for solids in suspension and a flat bed. The expression for the total solid discharge, G_s, is simple, leading to a direct calculation for the incremental solid transport intensity with respect to the gradient S and the depth h. The detailed discretized formulae are given by Chollet and Cunge (1979).

Examples of application (Chollet and Cunge, 1980)

In the examples discussed here, unless stated to the contrary, the Engelund method was used in preference to Einstein's to represent energy dissipation and solid transport in order to reduce calculation times.

Example of a development study

The implementation of a given river development scheme inevitably leads to changes in river bed and bottom profiles. These perturbations may extend over considerable distances and their evolution may continue for long periods of time. The mathematical model is a powerful means of forecasting changes in bed configuration; it can also contribute to the definition of measures to be taken to solve certain engineering problems created by the planned development works.

In this example, we shall evaluate the changes in the longitudinal profile of a river following the construction of a dam. Our example concerns an imaginary river for which the cost of data preparation is not excessive; we have nevertheless made every effort to approximate an actual prototype river as closely as possible, namely, the Setit River, tributary of the Atbara river in the Sudan. The characteristics of the model are as follows:

- constant width: $b = 150$ m;
- constant longitudinal gradient: $S_0 = 0.00053$;
- uniform grain size: $d = 0.20$ mm;
- liquid and solid discharge hydrographs were deduced from the natural hydrographs of the Setit River; however the duration of floods has been increased in order to reduce the calculation times required for a significant modification of bed configuration.

The model consists of 41 computational points at 2000-m intervals. The time-dependent water and sediment discharge variation laws are presented in discretized form in Fig. 7.16.

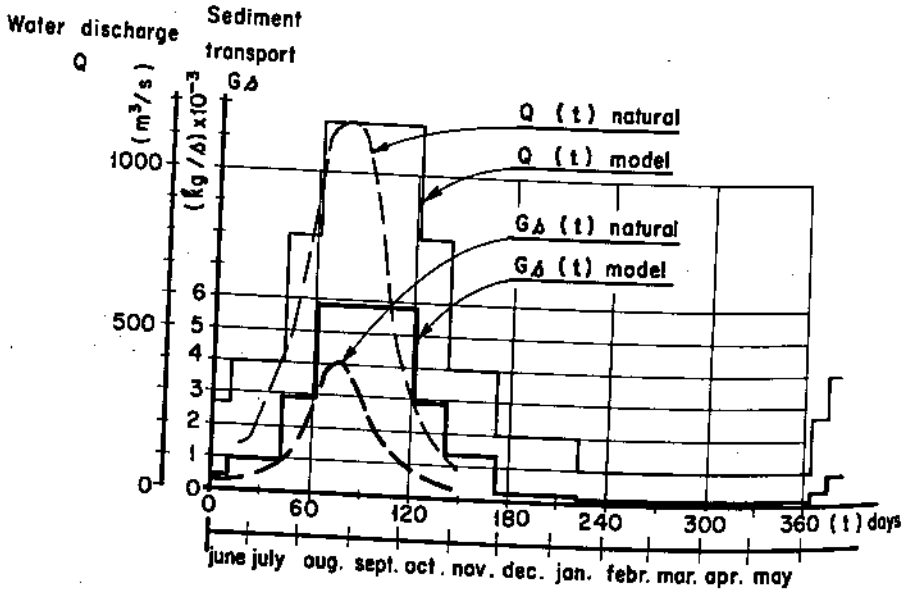

Fig. 7.16. Water and sediment discharges at the upstream model limit

Simulation of natural conditions

The aim of this first calculation is to determine whether the solid discharge relationships used are appropriate for the river under study. For the downstream boundary condition, the bed level z is assumed to remain constant.

After simulation of a two-year period, a slight tilting of the bed about the downstream end may be observed: in Fig. 7.17, the deposition at calculation point 11 (20 km downstream of the upstream boundary) has reached 50 cm. The river being near its equilibrium conditions, the representation of solid transport would seem to be fairly good and could be adjusted for practical applications by modifying coefficients and by repeating the calculations until a stable bed configuration is achieved over a period of several years.

Flow simulation with a dam maintaining a constant free-surface level at the downstream end

The upstream boundary condition remains unchanged with respect to the simulation of natural conditions; at the downstream boundary, the free-surface level is maintained at a constant value, $y = 20$ m. In the initial state, represented in Fig. 7.18, the flow regime varies over the 80 km length of river studied; upper regime over the first 45 km, lower regime corresponding to a bed covered with dunes over a distance of about 5 km, and regime too low for material transport near the dam.

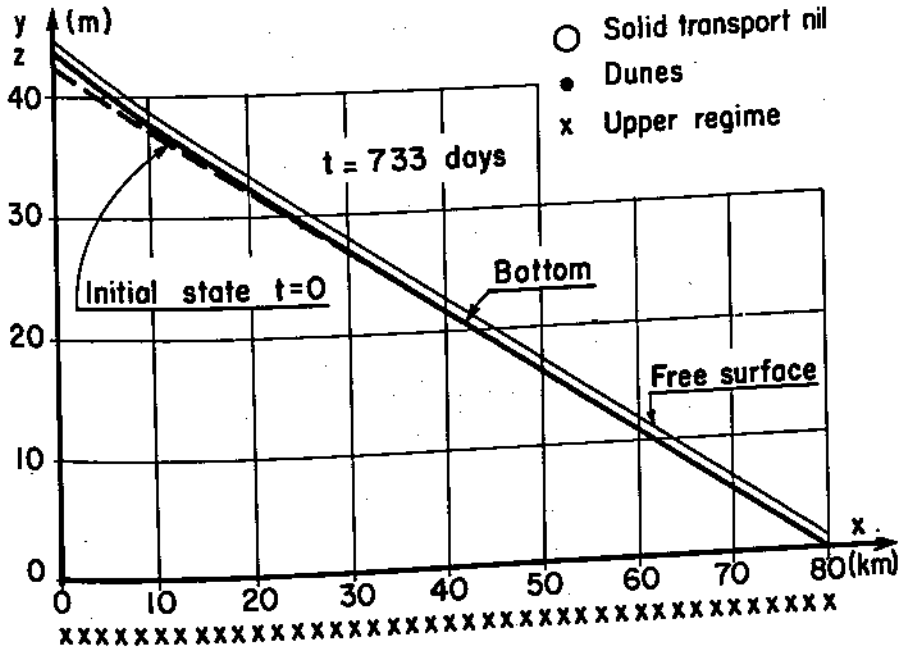

Fig. 7.17. Simulation of natural conditions

Successive longitudinal bed profiles are illustrated in Fig. 7.18; the progressive filling of the reservoir by sand can be seen in the gradual movement of a very distinct solid deposit front.

Protection of the live capacity by means of a sedimentation reservoir
The advantage of a mathematical model is not only in forecasting the rate of sedimentation in the reservoir, but also in defining ways of maintaining the live capacity. A dam constructed upstream can be used to collect the sediment transported; at the upstream boundary, the solid discharge then becomes zero, i.e. the sedimentation reservoir is assumed to collect all the materials transported by the river without changing the liquid discharge distribution with time. The downstream boundary condition remains the same as for the previous case: $y = 20$ m. The river bed profiles illustrated in Fig. 7.19 show that the utility of the upstream dam is very limited if it is built too far upstream of the main reservoir, since eroded material from just below the sedimentation reservoir can be deposited in the downstream reservoir.

Protection of live capacity by low-level flushing
This technique consists in suddenly lowering the downstream reservoir level, thus considerably increasing the flow velocity at the start of the flood season, for example as shown in Fig. 7.20. This method of protecting the reservoir from siltation appears to be more promising than the method described above; the mathematical model can be put to good use to assess the efficiency and

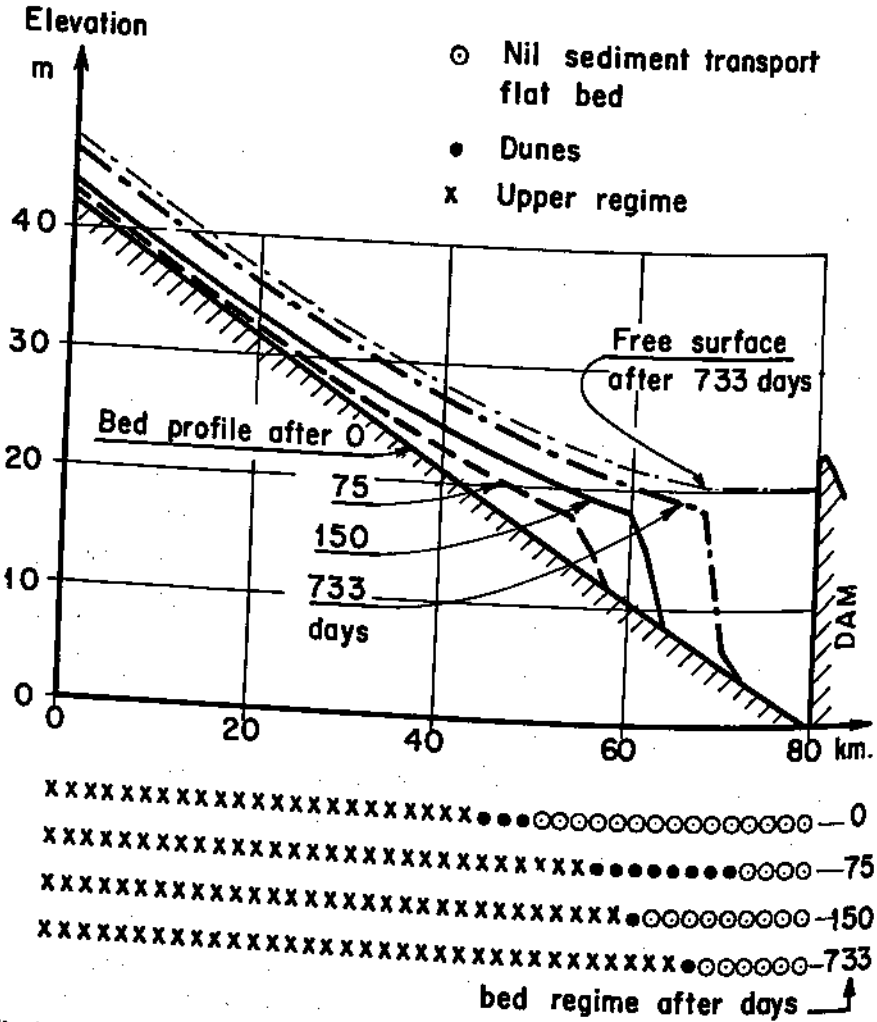

Fig. 7.18. Bed evolution in time with a constant downstream reservoir water level

determine the optimum procedure of such flushing operations. The upstream boundary condition is the 'natural' previously defined hydrograph of the solid discharge. The downstream boundary condition is the flushing procedure described in Fig. 7.20a. The effect of the flushing operations on the longitudinal bed profiles is clearly apparent in Fig. 7.20b; the typical steep sediment front advancing and filling the reservoir is practically non-existent.

Einstein's method and Engelund's method

Another reservoir simulation calculation was made while representing energy dissipation and solid transport by Einstein's method. The boundary conditions remain unchanged: 'natural' solid discharge upstream, constant free-surface level downstream ($y = 20$ m). The situation obtained after 150 days is shown in Fig. 7.21.

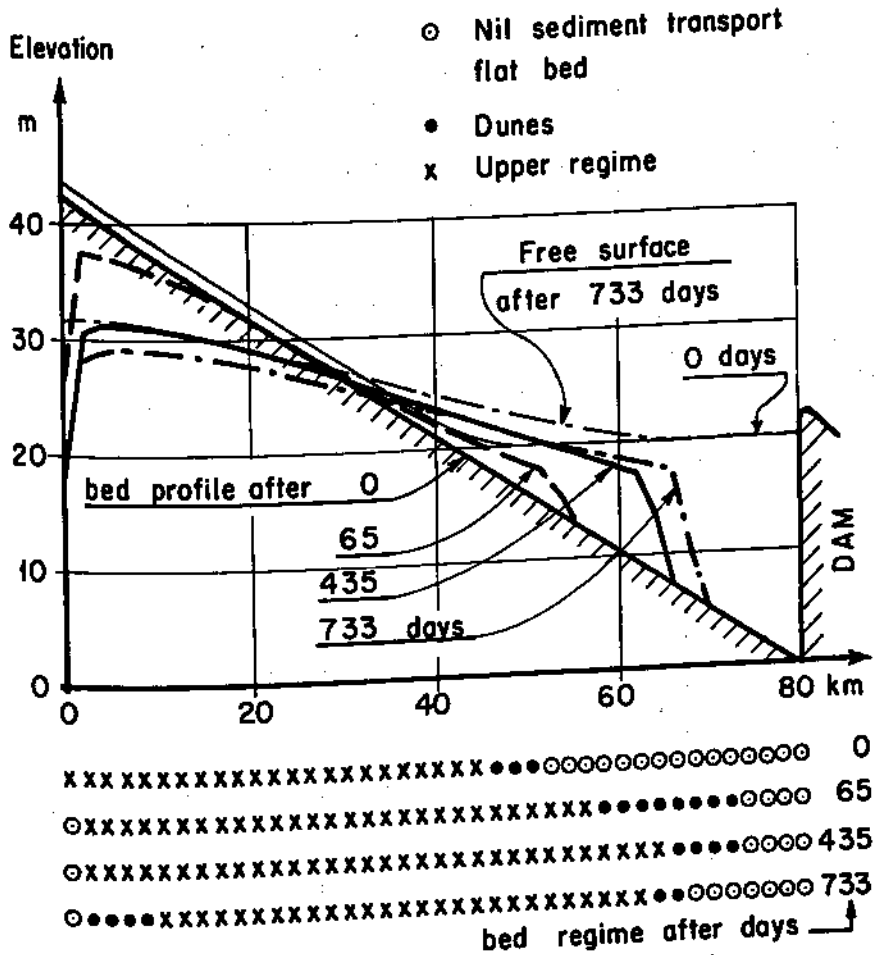

Fig. 7.19. Bed evolution in time with an upstream sedimentation reservoir

The longitudinal bed profiles shown in Fig. 7.21a illustrate that, using Einstein's method, the mathematical model operates satisfactorily and gives the same progression of the solid front. On the other hand, the rate at which the bed level rises (Fig. 7.21b) is much faster than in Engelund's representation.

Simulation of a large alluvial river

The mathematical model used in these examples can also simulate the flow of large alluvial rivers in which the bed configuration changes with variation in liquid discharge. The example dealt with here is based on the Padma river in Bangla Desh, formed by the confluence of the Brahmaputra and Ganges rivers. The model characteristics are as follows: constant width $b = 1110$ m, longitudinal bed gradient $S_0 = 0.000015$, uniform grain size $d = 0.245$ mm.

The model consists of 41 points at 5000-m intervals, simulating a 200-km stretch of river. At the upstream end, the bed elevation is assumed constant, and at the downstream end, a 'sea' type boundary condition is imposed in the simplified form of a constant value for the free-surface level y.

The simulation of two years of identical hydrological regimes with upstream conditions shown in Fig. 7.22a, as deduced from observations, produced a slight tilting of the bed about the upstream end; Fig. 7.22b shows that the mean bed gradient over the first 100 km increased from 0.000015 to 0.000022. During the course of the year, the bed configuration varies, the simulation clearly showing the change from dunes at low regime to flat bed at higher regimes when the discharge increases.

On the basis of measurements taken on the stretch of the Padma river between Goalundo and Bhagyakul, Stevens and Simons (1973) constructed the

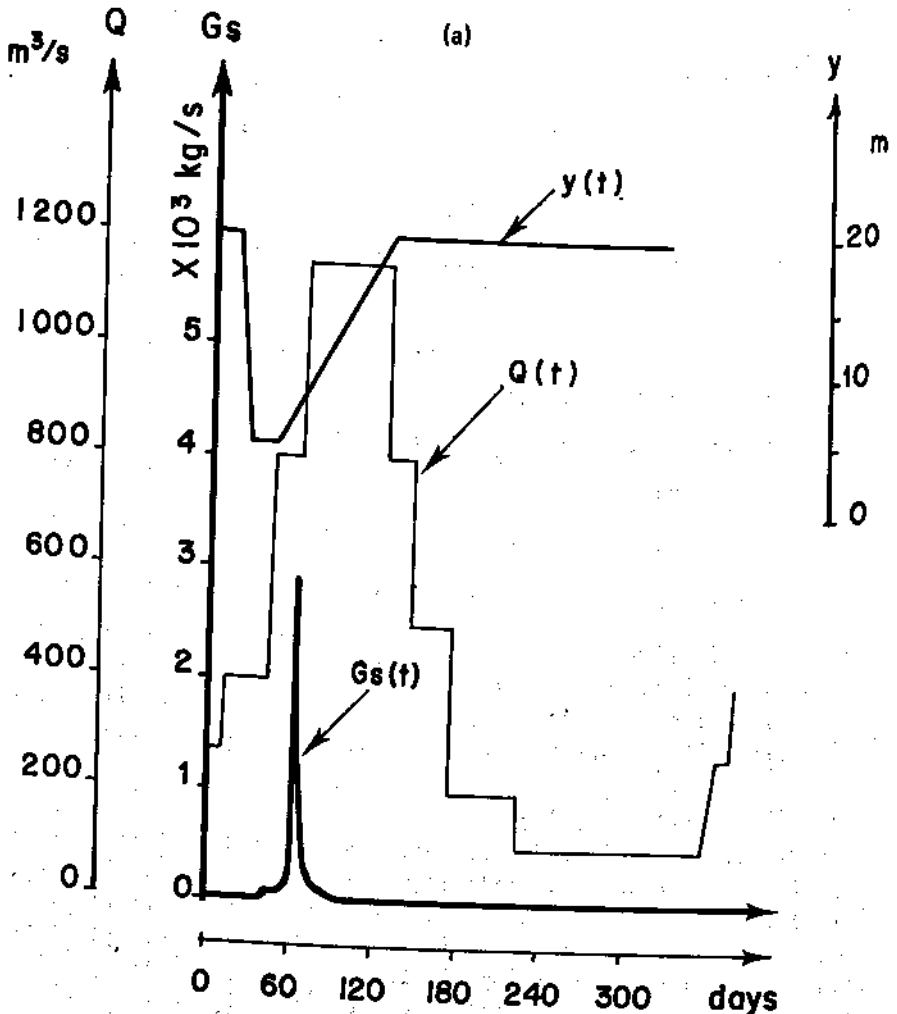

Fig. 7.20

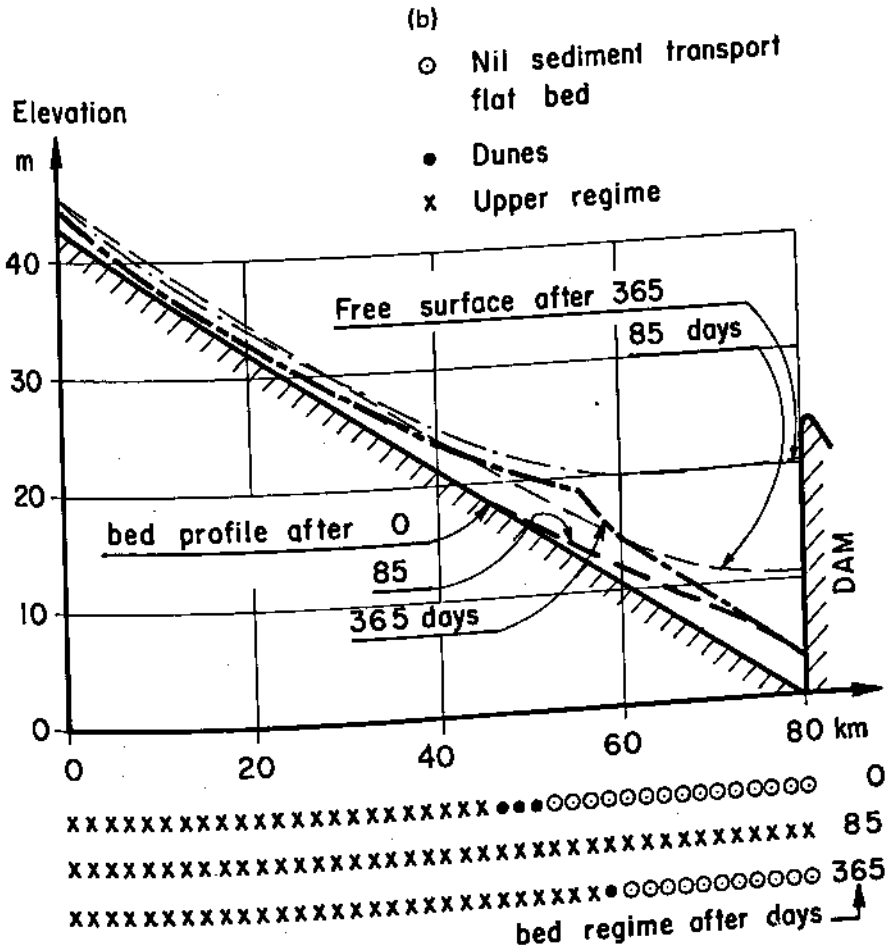

Fig. 7.20. Reservoir flushing operation. (a) Downstream water level, discharge, and sediment hydrographs. (b) Bed evolution in response to the flushing operation

relationship between the overall Manning coefficient n related to the cross section, and the liquid discharge Q:

$$n = \frac{AR^{2/3}\,S^{1/2}}{Q} \tag{7.49}$$

where: A = wetted cross section, R = hydraulic radius, S = free surface gradient.

This relationship has been plotted in Fig. 7.23 together with the points calculated in the same manner from the results of the mathematical model for the zone situated 50 km downstream of the upstream end. There is a remarkable similarity between the calculated results and the field observations, at least until all the cross section is in the upper regime. For very high regimes, the

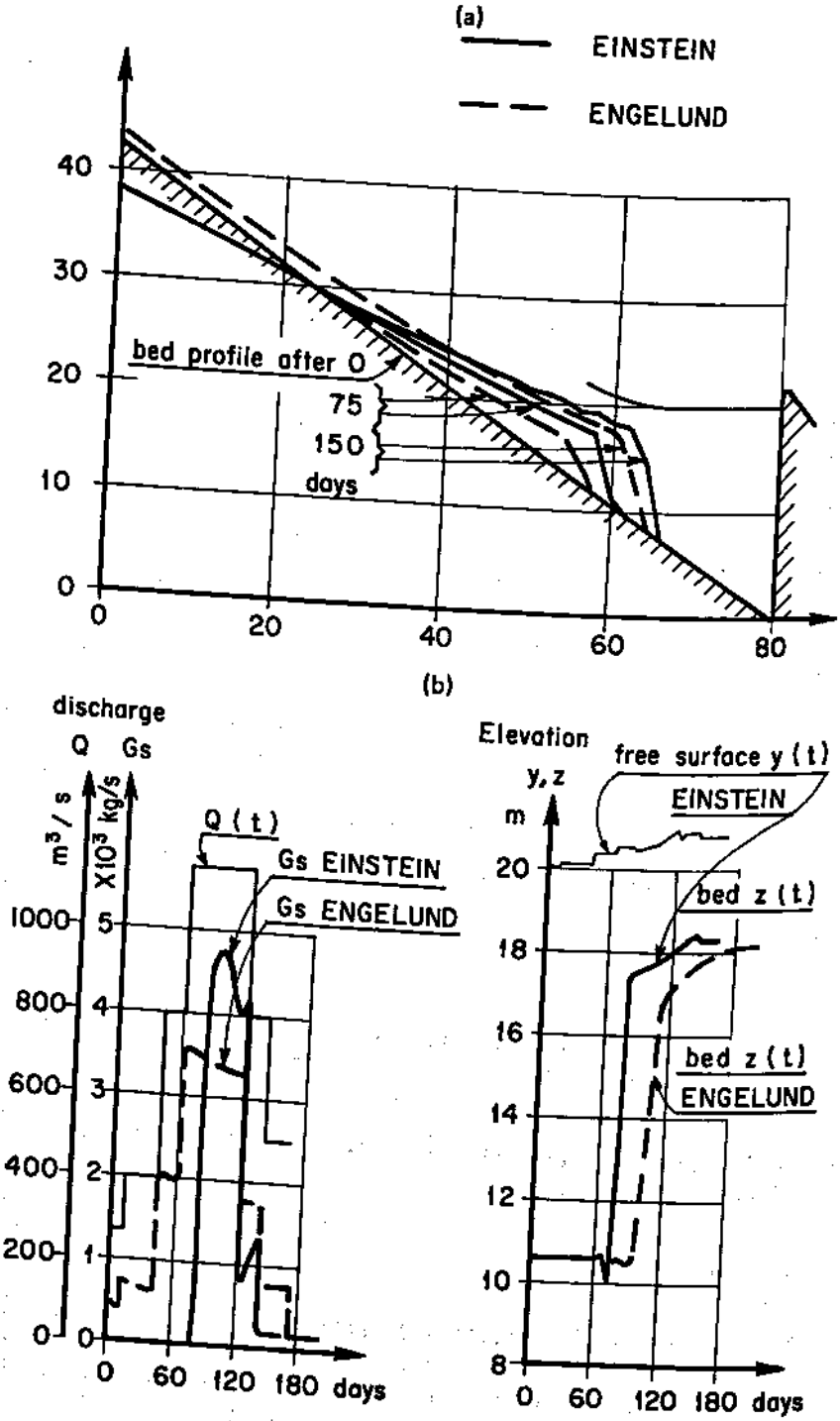

Fig. 7.21. Comparison of Einstein and Engelund methods for a constant downstream water level. (a) Bed evolution in time. (b) Transport rates and bed evolution at an intermediate point

comparison obviously does not have any meaning since the rectangular cross section of the model no longer corresponds to the natural cross section of the actual river.

7.8 CRITERIA INVOLVED IN CHOOSING A MODELLING METHOD

There is no way of giving a clear-cut answer to the simple question: which modelling technique should I use? As in all mathematical modelling, the answer should be the result of trade-off, since there is no ideal technique which can satisfy all possible needs. It is impossible to try to class the different methods according to their usefulness or advantages; after eliminating those which are obviously incorrect or impractical, all that remains is to consider their flexibility, ease of application, computer-time economy, and the engineering experience and mathematical knowledge of their creators.

We can nonetheless try to list the factors which should determine the criteria choice for movable bed models. While this choice depends on the specific situation and its trade-offs, two classes of factors may be considered: those linked to the physical phenomena and those related to numerical methods. Whatever the factor discussed below, its importance must be measured in terms of the basic consideration: what is the purpose of the model? This point must be kept constantly in mind and complemented by a second consideration: later on, is it possible that I may want to go beyond the primary purpose? If so, does my present choice exclude that possibility? What is the price of keeping my options open?

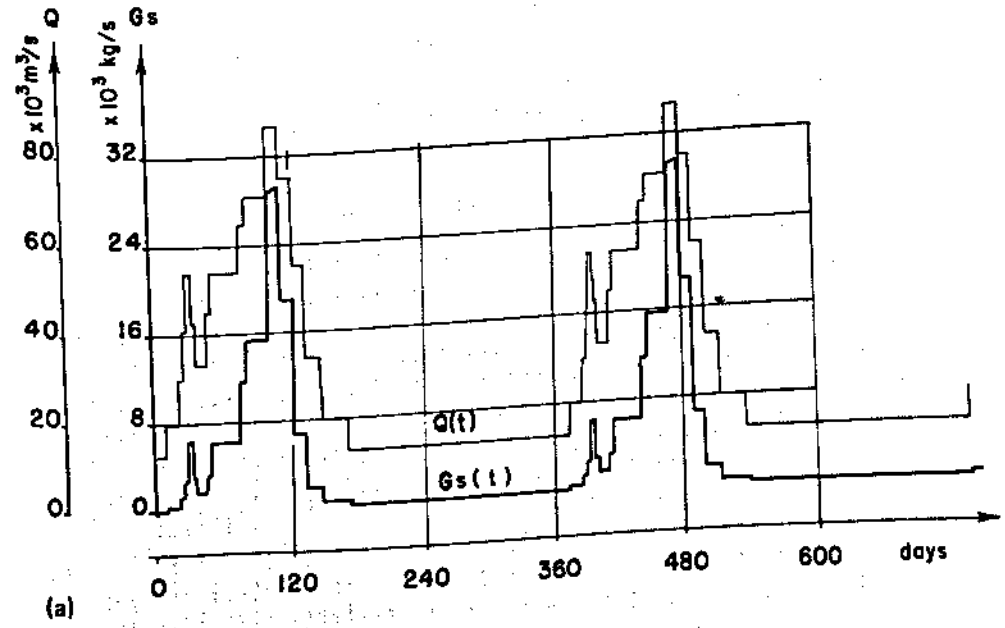

Fig. 7.22 *see page 308*

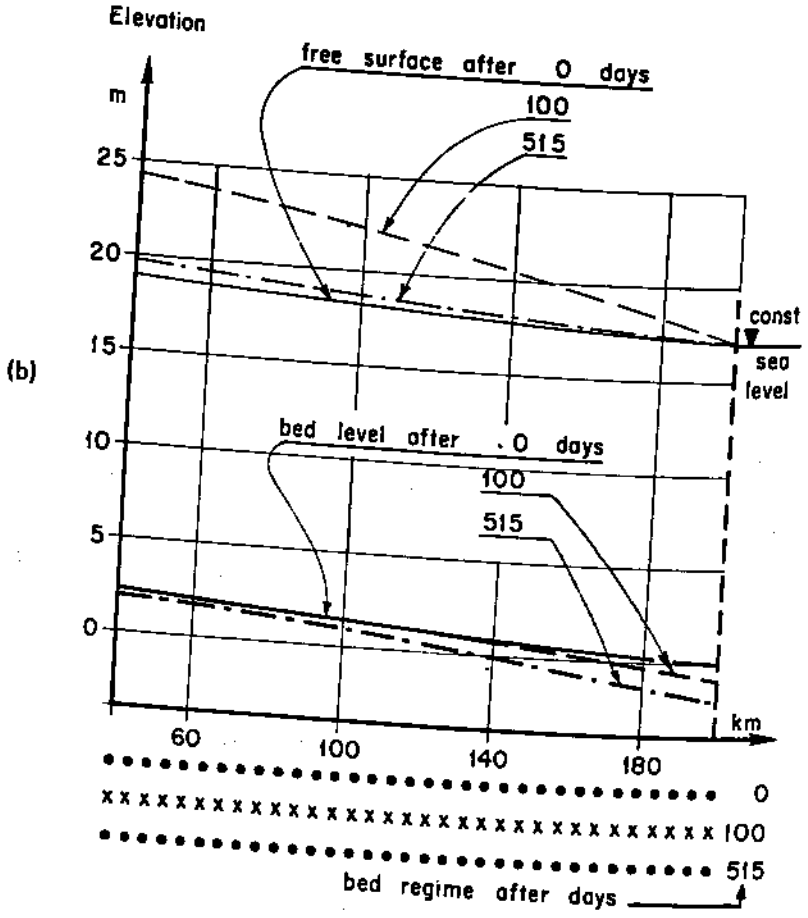

Fig. 7.22. Padma river model. (a) Upstream sediment and water hydrographs. (b) Bed and water surface profile evolution

Factors linked to the physical phenomena simulated

(i) Rapidity of variation of processes studied. If all dependent variables change quickly with time it may be necessary to use a model based on the full system of Equations (7.1), (7.2) and (7.3). Sometimes one is interested in long-term variations, but essential river bed changes occur during the very short high water periods each year. In this case use of the full system of equations might be advantageous. Another point is related to a possible downstream tidal limit. Are daily tidal variations an important factor for the bed evolution? If yes, use of the full system of equations (7.1)–(7.3) is compulsory. But if only slow variations of mean sea level are to be reproduced, the simplified equations (7.15), (7.16) can be used.

(ii) Type of river to be simulated: is it an alluvial stream transporting fine sediments and with varying resistance according to changing bed forms, or can

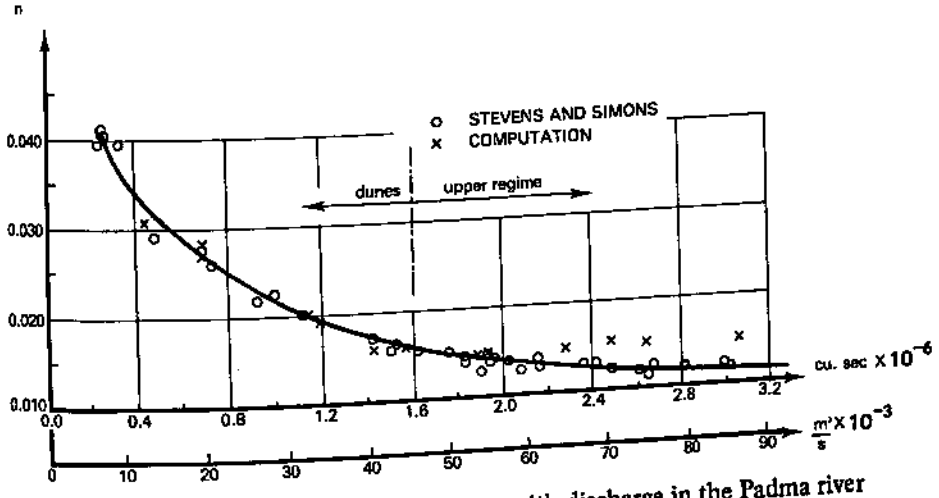

Fig. 7.23. Variation of resistance coefficient with discharge in the Padma river

the energy line gradient be represented by a Manning-type law? As for point (i) above, the answers are far from obvious. For example, Chen and Simons (1975) simulated a Mississippi reach using the Manning formulation, and yet bed forms play an important role in that river (Fig. 7.13). But since the existence of dunes had little influence on the global phenomena simulated, it was not necessary to use alluvial stream resistance theories.

(iii) Topology of the river system under consideration. All modelling techniques can be applied to single reaches, but when a network of tributaries is to be represented, the situation is not the same. Some models have inherent difficulties in simulating such situations; for example, models based on the system of full Equations (7.1), (7.2), (7.3) require two upstream boundary conditions and one downstream condition. In the case of bifurcated flow, shown in Fig. 7.24, the problem of partition of the sediment discharge at the bifurcation arises, and this difficulty may be serious enough to prevent use of the technique.

There are some programs which cannot treat branched river networks, and others which cannot accept internal boundary conditions which allow the simulation of natural morphological singularities or man-made structures. It should be stressed that a looped network of rivers (Fig. 7.24) poses special computational problems as in the case of flood propagation modelling, *see* Chapters 3 and 4.

Factors linked to numerical methods

(i) Convergence of the method to the true solution of the differential equations. This must be ensured and the use of any method which gives results which do not converge to the analytical solution for the linearized case when

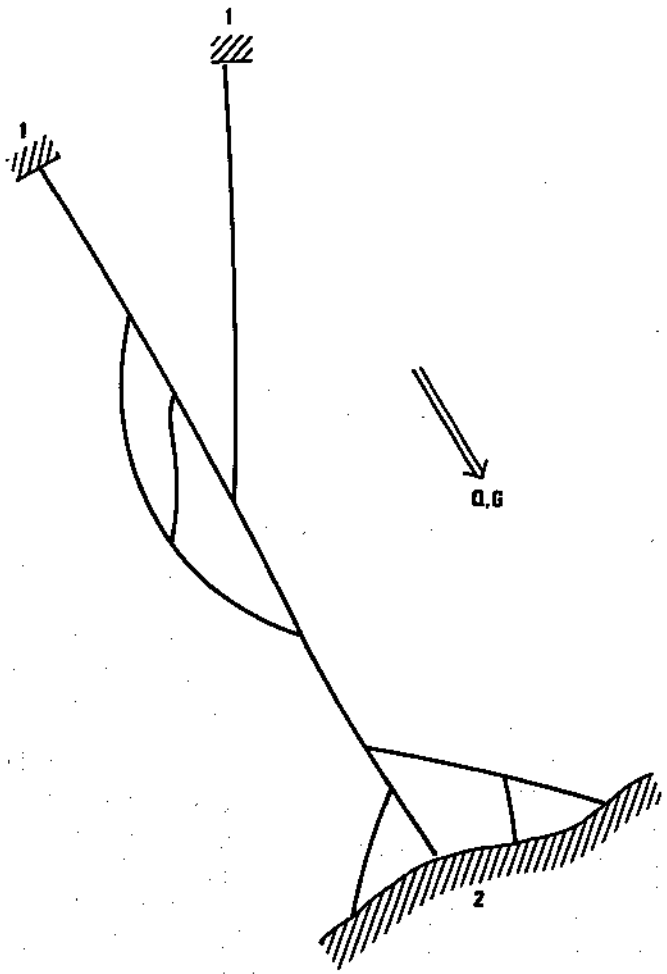

Fig. 7.24. Looped channel network in a deltaic area. 1, Upstream boundary points; 2, ocean

$(\Delta t, \Delta x) \to 0$ is to be avoided. But even when the convergence is certain, several additional factors should be investigated.

The influence of the 'Courant-like' number linking Δx and Δt steps must be known and the error characteristics analysed. If the spacing between points, Δx, is not constant, the finite difference scheme should not be sensitive to its variations. Schematization of singular points (morphological singularities or man-made structures) and boundary conditions should be of the same order of approximation as the scheme used to solve the basic equations.

(ii) Which is better, the implicit or explicit method? There is no direct answer to this question. However, the authors' preference lies with the implicit schemes since they are, in the end, more economical, and more convenient; if there is

one very small space step Δx, this particular Δx will define the time step Δt for the whole model if an explicit method is used even if otherwise, for physical reasons, the time step could have been several times greater.

8 Transport of pollutants

8.1 INTRODUCTION

The general subject of water quality modelling is a vast one which is to be treated in detail in a separate book later in this series. Although many aspects of water quality modelling can be considered to be completely independent of unsteady flow modelling in open channels, one essential factor links the two disciplines: transport of dissolved or suspended substances. By transport we refer to the hydrodynamic process of dispersion, that is to say, the interaction between differential convection and turbulent diffusion which are both dependent upon the flow velocity field. We find it necessary to treat the dispersion process in the present book for two reasons:

The results of unsteady channel flow simulations are often used as the hydrodynamic basis for water quality models. Sometimes flow models are built only for that purpose. Thus the needs of water quality models must be often taken into account in the construction of hydrodynamic models.

The numerical representation of physical reality in transport models is subject to the same kinds of constraints as in river flow modelling, and it is essential that the modeller be aware of them.

Consequently we shall deal in this chapter with mathematical modelling of transport of neutrally buoyant conservative substances by the river flow. We shall be interested in the time dependent evolution of concentration in river flow which is known – either computed by a flood propagation model, or measured. Since the time scale of the mixing phenomena which interest us here is generally much shorter than the time over which significant changes in water discharge occur, the steady-flow approach, which simplifies the transport equations, is usually justified. If in some cases unsteady river flow must be taken into account, we assume nonetheless that the discharge is constant over the entire reach being studied during a certain time during which pollutant transport is modelled as in steady flow. The unsteady flow is represented as a series of increasing (or decreasing) quasi-steady flow steps of this type; the transport results at the end of each steady flow step are used as initial conditions for the next step, as described by Jobson and Keefer (1979).

8.2 THE DISPERSION PROCESS

We begin with a review of the dispersion process considered from a physical point of view. Then later on we will be able to better appreciate the consequences of numerical simplification of physical reality. The phenomenon of molecular diffusion in fluids is well described in all physics textbooks. The 'marked' molecules of one fluid will diffuse in the other 'neutral' fluid according to the law established by Fick: their flux is proportional to their concentration gradient. Mathematically the law is formalized, in three dimensions, by Equation (8.1) for molecular diffusion in a fluid at rest:

$$\frac{\partial C}{\partial t} = \frac{\partial}{\partial x}\left(\epsilon_m \frac{\partial C}{\partial x}\right) + \frac{\partial}{\partial y}\left(\epsilon_m \frac{\partial C}{\partial y}\right) + \frac{\partial}{\partial z}\left(\epsilon_m \frac{\partial C}{\partial z}\right) \tag{8.1}$$

where C is the concentration of the 'tracer', ϵ_m is a coefficient of molecular diffusion, expressed in $m^2\ s^{-1}$. This molecular diffusion is very weak, ϵ_m being of the order of the dynamic viscosity coefficient, i.e. $10^{-6}\ m^2\ s^{-1}$. A point source of dye in still water takes about 24 h to attain a diameter of 1 m. But when water is flowing in turbulent conditions, i.e. such that the Reynolds number is higher than about 2000, another phenomenon appears: turbulent diffusion.

If one observes a particular point P (*see* Fig. 8.1) somewhere in the cross

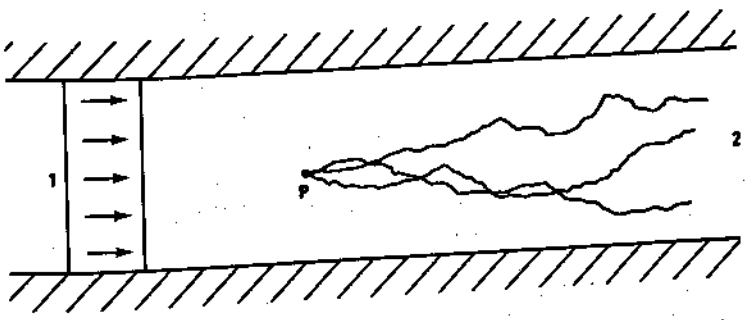

Fig. 8.1. Individual particle diffusion in turbulent flow. 1, Mean velocity distribution; 2, individual particle paths

section of a river in which the flow is steady but turbulent, and if he measures the current direction and velocity at the point by some averaging process (such as counting the revolutions of a current meter), he will conclude that the current velocity and direction do not vary with time. But if he were able to obtain a series of *instantaneous* observations of velocity at point P (using a laser or hot-wire anemometer, for example), he would note that the velocity varies in a more or less random manner in magnitude and direction (compared to the long-term average value) from one moment to the next. If he were to release a number of small particles of some neutrally buoyant substance at P, he would note that at some distance downstream the particles were quite dispersed one from another. This is the process of turbulent diffusion, whereby individual fluid particles are

subject to random fluctuations of velocity, and their paths wander around the flow field as shown in Fig. 8.1.

If we release a small quantity of pollutant at the point P, rather than a number of particles, we will observe that it has grown into an ever-expanding cloud as it moves downstream; this is simply equivalent to the behaviour of an extremely large number of particles released instantaneously at P. The mathematical description of this dispersion process is based on a semi-empirical theory which begins with a partial differential equation for the conservation of tracer in a differential volume element (*see*, for example, Sayre, 1968),

$$\frac{\partial C}{\partial t} + u\,\frac{\partial C}{\partial x} + v\,\frac{\partial C}{\partial y} + w\,\frac{\partial C}{\partial z} = \frac{\partial}{\partial x}\left(\epsilon_m\,\frac{\partial C}{\partial x}\right) + \frac{\partial}{\partial y}\left(\epsilon_m\,\frac{\partial C}{\partial y}\right) + \frac{\partial}{\partial z}\left(\epsilon_m\,\frac{\partial C}{\partial z}\right) \tag{8.2}$$

in which u, v and w are the instantaneous velocity components in the x, y and z directions.

It is possible to consider a turbulent 'steady' flow as resulting from the superposition of turbulent fluctuations on a steady time averaged flow. Thus we consider that at a given point the velocity field is composed of two parts: the time averaged velocity ($\overline{u}$, $\overline{v}$, $\overline{w}$) and the instantaneous velocities u', v', w' (the latter having zero time averages); $u = \overline{u} + u'$; $v = \overline{v} + v'$; $w = \overline{w} + w'$.

The motion of a 'marked', neutrally buoyant particle can then be considered as subject to three influences: molecular diffusion, time-averaged velocity, and turbulent velocity fluctuations. The displacement of such a particle is the resultant of the three processes. As we shall see further on, molecular diffusion can usually be safely neglected in the modelling of transport in rivers, and the time averaged velocity field is usually known or can be estimated. The main difficulty is relating transport due to turbulent velocity fluctuations to the measurable properties of the mean flow.

In order to relate the turbulent transport to the mean flow field, we apply Reynolds averaging in expressing the concentration at a point as the sum of a time averaged value and a fluctuating component, $C = \overline{C} + C'$. We substitute this definition and the comparable ones for u, v and w into Equation (8.2), and average the resulting expression over a time period which is long compared to the turbulent fluctuations but short compared to the time scale of the dispersion event being modelled. Using the subscript i to denote the x, y or z axis and following the usual tensor summation conventions, we obtain

$$\frac{\partial \overline{C}}{\partial t} + \overline{u}_i\,\frac{\partial \overline{C}}{\partial x_i} = \frac{\partial}{\partial x_i}\left(\epsilon_m\,\frac{\partial \overline{C}}{\partial x_i} - \overline{u_i' C'}\right) \tag{8.3}$$

The terms $\overline{u_i' C'}$ represent turbulent transport due to fluctuating local velocities. As in the case of a comparable averaging procedure applied to the dynamic flow equation, which produces energy dissipation terms related to $\overline{u'v'}$, $\overline{u'w'}$ and $\overline{v'w'}$, it has not yet been possible to link these so-called correlation terms to the mean

flow field properties in a formal manner. The semi-empirical approach consists in supposing that turbulent transport can be described in a manner analogous to molecular diffusion,

$$\overline{u_i' C_i'} = 1 - \tilde{\epsilon}_i \frac{\partial \overline{C}}{\partial x_i} \tag{8.4}$$

where $\tilde{\epsilon}_i$ is a coefficient of turbulent diffusion. These turbulent diffusion coefficients may be evaluated if terms such as $u_i' C_i'$ can be evaluated semi-empirically. This evaluation is based on the basic concepts of Prandtl:

(i) The turbulent fluctuations are related to a characteristic velocity known as the 'friction' velocity u_*,

$$u_* = \left(\frac{\tau_0}{\rho}\right)^{\frac{1}{2}}$$

where τ = tangential stress on the wall, ρ = fluid density.

(ii) A 'mixing length' l plays the same role as the mean free path in molecular gas diffusion theory, and is proportional to the distance of the particle from the wall y,

$$l = \kappa y$$

where κ = von Karman's constant and y is the distance from the wall.
The application of these two fluid mechanics principles to the development of a semi-empirical diffusion theory uses the so-called Reynolds analogy between transport of momentum and mass. The essential result is that the turbulent diffusivity in open channel flow can be directly related to the bed shear velocity u_* (Fischer, 1966).

Turbulent diffusivities are much greater than molecular ones, which thus may be safely neglected in turbulent flow. Indeed, the weakest values of turbulent diffusivities are of the order of a few $cm^2\ s^{-1}$, while molecular diffusivities are of the order of $10^{-2}\ cm^2\ s^{-1}$. The distribution of the turbulent diffusivities in the flow field is not uniform, but depends upon the orientation of fluctuating velocities and the distance from the walls. In general the turbulent diffusion coefficients in Equation (8.4) are not the same in all directions and, moreover they vary as a function of the independent space variables x, y, z.

Dropping the overbars in Equation (8.3), we can now write the transport (or flux) equation for a neutrally buoyant substance in a three-dimensional velocity field

$$\frac{\partial C}{\partial t} + u \frac{\partial C}{\partial x} + v \frac{\partial C}{\partial y} + w \frac{\partial C}{\partial z} = \frac{\partial}{\partial x}\left(\tilde{\epsilon}_x \frac{\partial C}{\partial x}\right) + \frac{\partial}{\partial y}\left(\tilde{\epsilon}_y \frac{\partial C}{\partial y}\right) + \frac{\partial}{\partial z}\left(\tilde{\epsilon}_z \frac{\partial C}{\partial z}\right) \tag{8.5}$$

The substance will be convected by time averaged velocities, u, v, w and diffused by turbulent diffusivities $\tilde{\epsilon}_x, \tilde{\epsilon}_y, \tilde{\epsilon}_z$. We refer to the overall process as *dispersion*.

Equation (8.5) is the three-dimensional, time averaged dispersion equation. In principle, if the full three-dimensional velocity field and the three diffusivities $\tilde{\epsilon}_x, \tilde{\epsilon}_y, \tilde{\epsilon}_z$ were known, Equation (8.5) could be solved by analytical or numerical methods to yield the function $C(x, y, z, t)$ for any appropriate initial and boundary conditions. But in fact the three-dimensional averaged velocity field is generally not known. Moreover, because the river depth is usually small as compared to the width, a neutrally buoyant substance becomes fully mixed over the depth of flow in a river in a relatively short time. Consequently the concentration distribution in the vertical dimension becomes uniform very quickly, long before uniformity in the horizontal direction is attained.

Therefore it is considered reasonable to average Equation (8.5) vertically over the flow depth. We note in passing that this simplification is analogous to our neglect of the vertical velocity component in the hydrodynamic flow equations. It should be stressed, however, that mixing in a river, especially transverse mixing, is influenced by secondary helicoidal flows which of course cannot be represented without taking into account the vertical velocity component. This remark is an important one as it reminds us that we work with schematized situations which are modelled conceptually, and that we have to keep in mind the consequences of the simplifications adopted when deciding to what extent the model is applicable to the solution of the engineering problem at hand.

The depth-averaged dispersion equation is obtained by integrating Equation (8.5) over the depth of flow (Holly, 1975) using the hypotheses (Holley, 1971) that differential convective transport and turbulent diffusion processes may be combined in gradient diffusion terms. The result is the two-dimensional, depth-averaged dispersion equation,

$$h\frac{\partial C}{\partial t} + \frac{\partial}{\partial x}(huC) + \frac{\partial}{\partial z}(hwC) = \frac{\partial}{\partial x}\left(h\epsilon_x \frac{\partial C}{\partial x}\right) + \frac{\partial}{\partial z}\left(h\epsilon_z \frac{\partial C}{\partial z}\right) \tag{8.6}$$

in which u, w and C are understood to be depth averaged values, and ϵ_x and ϵ_z are empirical mixing coefficients which should not be confused with the turbulent diffusivities $\tilde{\epsilon}_i$ of Equation (8.5).

In general ϵ_x and ϵ_z are much larger than $\tilde{\epsilon}_x$ and $\tilde{\epsilon}_z$, since they incorporate dispersion due to differential convection as well as turbulent diffusion. To better explain the physical meaning of these coefficients let us consider a small cloud of dye on the water surface. If its diameter is so small that the water velocities are the same near its centre and its outer limit, the cloud will be simply transported by the current and its dimensions will grow symmetrically under the effect of turbulent diffusion alone. Once the cloud becomes large enough so that the velocity varies across it, its shape will become distorted and its dimensions will increase faster than before. Thus the *apparent* diffusion (which includes the effects of both diffusion and differential convection) will be much stronger than

turbulent diffusion and depend upon the dimension of the cloud itself. Figure 8.2 illustrates the above concepts for the case of an initial vertical dye distribution in a parabolic flow profile. When depth-averaged coefficients such as ϵ_x and ϵ_z are used in dispersion modelling, they take into account this interaction between differential convection and turbulent diffusion.

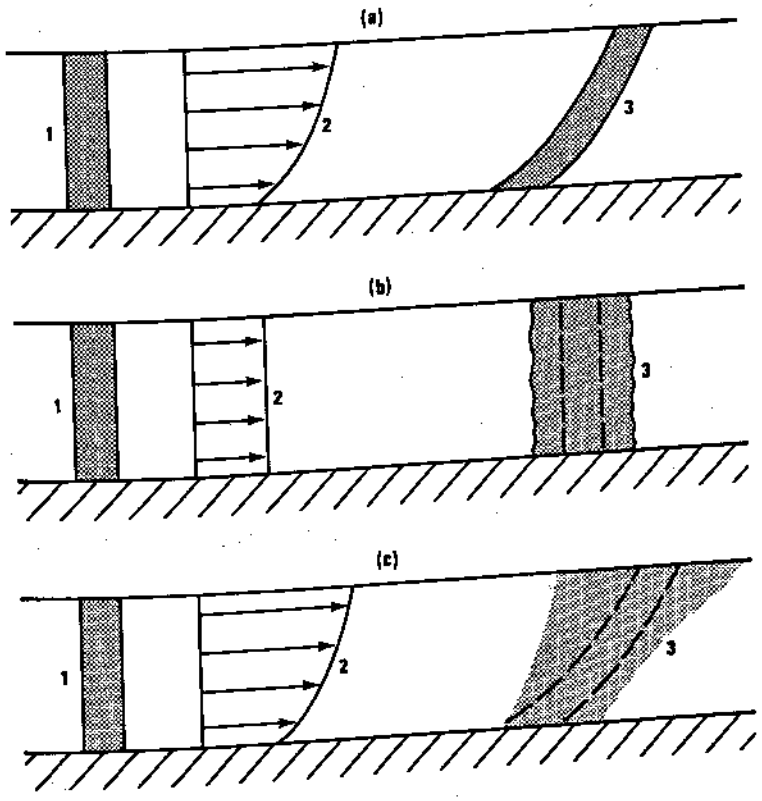

Fig. 8.2. The components of dispersion. 1, Initial tracer distribution; 2, velocity profile; 3, tracer distribution at a later time. (a) Differential convection without diffusion. (b) Diffusion without differential convection. (c) Combined differential convection and diffusion = dispersion

The experimental and theoretical bases for estimating ϵ_x and ϵ_z were provided by Elder (1959). The reader is advised to refer to his work for details; the essential results for our needs in this chapter are that, for uniform flow in a wide open channel,

$$\epsilon_z = 0.23\, u_* h$$

$$\epsilon_x = 5.93\, u_* h$$

Here ϵ_x is much larger than ϵ_z because it incorporates differential convection

due to the logarithmic vertical velocity profile in established flow (as in Fig. 8.2).

Equations (8.5) and (8.6) describe the time-dependent dispersion of a neutrally-buoyant, conservative tracer substance in a natural channel subject to steady but non-uniform flow. Analytical solutions to these equations exist for some particular simplified flows and tracer injection configurations (*see* Holly, 1975; Cleary and Adrian, 1973; Shen, 1978), but for most practical situations only numerical solution methods can be used to construct a useful mathematical model of dispersion in a waterway.

Attempts to model the dispersion process in natural rivers have been concentrated in two areas:

- one-dimensional simulation of the dispersion downstream from an instantaneous plane source injection;
- two-dimensional simulation of the dispersion downstream from an arbitrary source.

8.3 ONE-DIMENSIONAL DISPERSION MODELLING

The theoretical basis for the one-dimensional modelling concept was elaborated by Taylor (1954), who showed that in the case of fully developed pipe flow, the longitudinal dispersion of a tracer which is fully mixed over the cross section should behave as a Fickian diffusion process, at least at large distances from the point at which the tracer is injected instantaneously. The dispersion equation is assumed to be of the form

$$\frac{\partial}{\partial t}(AC_a) + \frac{\partial}{\partial x}(AUC_a) = \frac{\partial}{\partial x}\left(AK_x \frac{\partial C_a}{\partial x}\right) \tag{8.7}$$

where C_a and U are the cross-sectional average concentrations and velocities respectively, A is the flow area and K_x is the longitudinal mixing coefficient. This coefficient K_x is not to be confused with the mixing coefficient ϵ_x of Equation (8.6), since it accounts for *differential convection within the entire cross section* and is generally much larger than ϵ_x.

If U, A and K_x are known and assumed constant, the analytical solution to (8.7) is a Gaussian distribution,

$$C_a(x, t) = \frac{C_0 V_0}{2A(\pi K_x t)^{\frac{1}{2}}} \exp\left[-\frac{(x - Ut)^2}{4K_x t}\right] \tag{8.8}$$

in which C_0 and V_0 are the concentration and volume of the tracer injected instantaneously over the entire cross section. However this solution is generally of little practical use for engineering purposes, for three reasons:

(1) U, K_x and A are never constant over any appreciable reach of a natural river;

(2) as shown by Nordin and Sabol (1974), experimental data taken in natural

rivers do not support the assumption that the one-dimensional mixing process can be considered to be Fickian, and thus Equation (8.8) is a poor model of the phenomenon;

(3) the one-dimensional process implied by Equation (8.7) cannot be assumed until the tracer has progressed a distance from the source greater than (Fischer, 1966)

$$L = \frac{1.8\,l^2}{R}\,\frac{U}{U_*}$$

where l = characteristic mixing length (e.g. the channel half width), R = hydraulic radius, U_* = shear velocity. This distance is often well beyond the range of interest in water quality studies. In the lower Mississippi River, for example, L = 240 km (McQuivey and Keefer, 1976).

These inadequacies of the analytical solution have led engineers to solve Equation (8.7) numerically in order to obtain dispersion predictions. If such a procedure is adopted it must not be forgotten that the model is, in principle, still limited to distances greater than L from the source. The river is divided into a series of elementary reaches and an appropriate finite difference method is used to solve Equation (8.7) and obtain the value of C_a at each computational cross section and for each time step. If the value of K_x is known, and if the finite difference method adopted introduces very little numerical error (*see* below), one can expect to be able to obtain useful predictions of cross-sectional average concentration at relatively large distances from the source.

8.4 EVALUATION OF THE LONGITUDINAL MIXING COEFFICIENT

The coefficient K_x is assumed to incorporate the effects of differential convection within the cross section. Fischer (1966) developed a method of estimating K_x if the shape of the cross section and the distribution of velocity and turbulent mixing coefficients within it are known. Fischer's formula for K_x is

$$K_x = -\frac{1}{A}\int_0^b u''(z)\,h(z)\int_0^z \frac{1}{\epsilon_z h(z)}\int_0^z\int_0^{h(z)} u''(z)\,dy\,dz\,dz\,dz \qquad (8.9)$$

in which $u''(z)$ is the local deviation of longitudinal velocity from the cross-sectional average, and $h(z)$ is the local depth. That K_x represents differential convection is seen by observing that if the velocity in the section is everywhere the same, then $u''(z) = 0$ for all z, and $K_x = 0$. Likewise if $\epsilon_z = 0$, that is to say if there is no turbulent transfer between zones of different velocity, $K_x \to \infty$.

The integration of Equation (8.9) can be carried out numerically if one knows for each cross section the complete velocity distribution, and the resulting values of K_x for each section can be introduced into the numerical solution of Equation (8.7). The problem is that one generally has at his disposal only the one-dimensional average value of flow velocity at a given section from which he must estimate the distribution of $u''(z)$.

In some studies the value of K_x is determined by field experiments in which a slug of tracer, such as Rhodamine dye or a radioactive substance, is dumped across the entire cross section upstream of the reach of interest. By measuring and analysing the concentration–time distributions at several downstream sections, the value of K_x can be determined (Fischer, 1966). But if the reach studied is not far enough downstream from the injection point to be beyond the initial mixing distance L, then the apparent K_x which has been determined may have no value whatsoever in a one-dimensional model of the reach. If K_x is on the other hand valid in this respect, then one must not forget that it is valid only for the discharge at the time of the experiment. We see from Equation (8.9) that K_x depends on the velocity distribution within the cross section, and this distribution depends, sometimes quite strongly, on the discharge. K_x is really a global, catch-all coefficient which is extremely variable and too far removed from elementary physical processes to be used in situations for which it is not calibrated.

Some authors have proposed empirical formulae for K_x which are thought to reflect the existence of a global transverse distribution of velocity as related to a few flow parameters such as shear velocity, hydraulic radius, width-to-depth ratio, etc. Examples of such procedures can be found in Fischer (1973), Liu (1977), Jain (1976).

8.5 NUMERICAL SOLUTION OF THE ONE-DIMENSIONAL CONVECTION EQUATION

The numerical solution of the one-dimensional dispersion equation must be approached with a great deal of care. Mechanically speaking, it is not difficult to formulate a solution to Equation (8.7), which is a linear parabolic partial differential equation requiring one upstream and one downstream boundary condition as well as an initial state. But most finite difference methods for the calculation of the convection portion of Equation (8.7) are plagued by an artificial, or numerical, diffusion which is sometimes stronger than the physical diffusion, rendering the calculation useless. Since this question has been addressed in numerous publications, we limit ourselves in this section to a brief review of the problem and the presentation of a few examples.

The transport equation represents two physical mechanisms: convective longitudinal transport and longitudinal diffusion. We are interested here in the convection which is expressed for the flow area A = constant† as

†We assume A = constant only to describe the method. Note that for steady flow, the convection portion of Equation (8.7) can be written

$$\frac{\partial AC_a}{\partial t} + \frac{\partial}{\partial x}(AUC_a)$$

which represents the convection of the product AC_a, or the mass of tracer per unit length of channel. The numerical schemes we describe in this section can be written for AC_a as well as C_a.

$$\frac{\partial C_a}{\partial t} + U \frac{\partial C_a}{\partial x} = 0 \tag{8.10}$$

It is well known that some finite difference approximations to (8.10) actually represent a different equation,

$$\frac{\partial C_a}{\partial t} + U \frac{\partial C_a}{\partial x} = K_n \frac{\partial^2 C_a}{\partial x^2} \tag{8.11}$$

where K_n is an *artificial* diffusion coefficient introduced by the approximate nature of the finite difference scheme. As long as K_n is much smaller than K_x, this artificial diffusion does not compromise the simulation results. But if K_n is of the same order of magnitude as K_x, or greater than K_x, the simulation results may well appear plausible but be unrelated to the natural phenomena being modelled. Thus an essential quality criterion of a numerical scheme for the calculation of convection is the value of K_n.

As an example, we consider the scheme described by Dobbins and Bella (1968) which was analysed in some detail by Chevereau and Preissmann (1971). Figure 8.3 represents the space–time grid on which a finite difference scheme for the solution of Equation (8.10) is applied.

If we consider the point $(i+1, n+1)$, we can pose the convection problem as follows: the particle of water which arrives at point $i+1$ at the future time $n+1$ departed from the point ξ at time n and followed the trajectory shown as a dashed line. Therefore since in pure convection the concentration of marked fluid particles does not change, we can write

$$C_a(i+1, n+1) = C_a(\xi, n) \tag{8.12}$$

and the problem becomes one of following the trajectory back to time n, then evaluating the concentration at that point (recalling that at the previous time step n, the concentrations are known at all points $i-1, i, i+1$, etc.). In the special case in which ξ coincides with i, that is to say

$$U\Delta t = \Delta x \tag{8.13}$$

this procedure yields

$$C_a(i+1, n+1) = C_a(i, n) \tag{8.14}$$

which represents a simple transposition of the concentration at point (i, n) to $(i+1, n+1)$ (Fig. 8.3a). But in general applications U is not the same at all grid points, and Δx and Δt may also vary, such that $U\Delta t \neq \Delta x$ as a rule, as shown in Fig. 8.3b. The most direct way to estimate $C_a(\xi, n)$ in this case is to interpolate linearly between $C_a(i-1, n)$ and $C_a(i, n)$, which is the basis of the Dobbins and Bella scheme. It is precisely this interpolation process which yields numerical diffusion, as we now illustrate.

Application of the linear interpolation principle to the case shown in Fig. 8.3b, in which we assume U = constant, yields

$$C_a(i+1, n+1) = C_a(\xi, n) = \frac{(\Delta x - \alpha)\, C_a(i, n) + \alpha\, C_a(i-1, n)}{\Delta x} \tag{8.15}$$

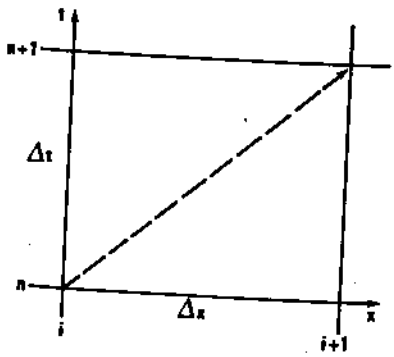

(a)

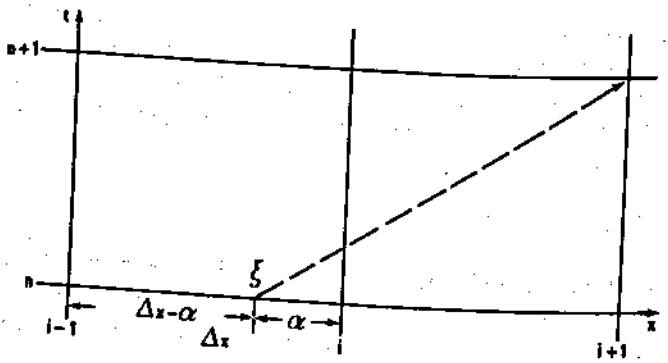

(b)

Fig. 8.3. Convection scheme of Dobbins and Bella (1968). (a) $\Delta x = u\Delta t$; (b) $\Delta x \neq u\Delta t$

If we expand $C_a(i+1, n+1)$, $C_a(i, n)$ and $C_a(i-1, n)$ in a Taylor series around the point $i+1, n$, dropping terms which are higher than second order, we obtain

$$C_a(i+1, n+1) \approx C_a(i+1, n) + \frac{\partial C_a}{\partial t}\Delta t + \frac{\partial^2 C_a}{\partial t^2}\frac{\Delta t^2}{2}$$

$$C_a(i, n) \approx C_a(i+1, n) - \frac{\partial C_a}{\partial x}\Delta x + \frac{\partial^2 C_a}{\partial x^2}\frac{\Delta x^2}{2}$$

$$C_a(i-1, n) \approx C_a(i+1, n) - \frac{\partial C_a}{\partial x} 2\Delta x + \frac{\partial^2 C_a}{\partial x^2} 2\Delta x^2$$

We substitute these expressions into Equation (8.15), which after simplification using the identity $\Delta x + \alpha = U\Delta t$ and the relation $\frac{\partial^2 C_a}{\partial t^2} = U^2 \frac{\partial^2 C_a}{\partial x^2}$ becomes

$$\frac{\partial C_a}{\partial t} + U \frac{\partial C_a}{\partial x} = \frac{\alpha(\Delta x - \alpha)}{2\Delta t} \frac{\partial^2 C_a}{\partial x^2} \tag{8.16}$$

Thus for this scheme

$$K_n = \frac{\alpha(\Delta x - \alpha)}{2\Delta t} \tag{8.17}$$

In terms of the Courant number†:

$$Cr = \frac{U\Delta t}{\Delta x} \tag{8.18}$$

we can express K_n as

$$K_n = \frac{\Delta x^2}{2\Delta t}(1 - Cr)(Cr - 2) \tag{8.19}$$

which shows that $K_n = 0$ for $Cr = 1$ or $Cr = 2$, but it reaches a maximum of $\frac{\Delta x^2}{8\Delta t}$ for $Cr = 1.5$.

The same analysis for the case of $Cr \leqslant 1$, that is to say for a trajectory which cuts the x-axis between points $i + 1$ and i, yields

$$K_n = \frac{Cr\,\Delta x^2}{2\Delta t}(1 - Cr) \tag{8.20}$$

which again gives $K_n = 0$ for $Cr = 0$ and $Cr = 1$, and $K_n = \frac{\Delta x^2}{8\Delta t}$ for $Cr = 0.5$.

The severity of this problem can be seen by considering a numerical example. One-dimensional dispersion is to be modelled in a river having a mean velocity of 1 m s^{-1} and a depth of 5 m. It is necessary to use $\Delta x = 1$ km so as to minimize the cost of the simulation. The worst case is for $Cr = 0.5$, as we have seen, which implies $\Delta t = 500$ s, from Equation (8.18) and

$$K_{n\max} = \frac{\Delta x^2}{8\Delta t} = \frac{(1000)^2}{8(500)} = 250 \text{ m}^2 \text{ s}^{-1}$$

By comparison, some observations of Fischer (1973) suggest that

$$\frac{K_x}{RU_*} = 250 \tag{8.21}$$

†The Courant number was originally derived from the Courant–Friedrichs–Levy stability condition for hyperbolic equations and equal to $\Delta t(gh)^{\frac{1}{2}}/\Delta x$. We refer here to the Courant number as an analogous parameter for the first-order convection equation.

If we take $R \approx h$ and $U_* \approx \dfrac{U}{20} = 0.05 \text{ m s}^{-1}$, we obtain

$$K_x = (250)(5)(0.05) = 62.5 \text{ m}^2 \text{ s}^{-1}$$

Thus we see that K_n can easily become larger than K_x, so that the solution is dominated by numerical, rather than physical, diffusion.

Another more graphic illustration of the potential severity of numerical diffusion is shown in Fig. 8.4, which presents the results of the application of

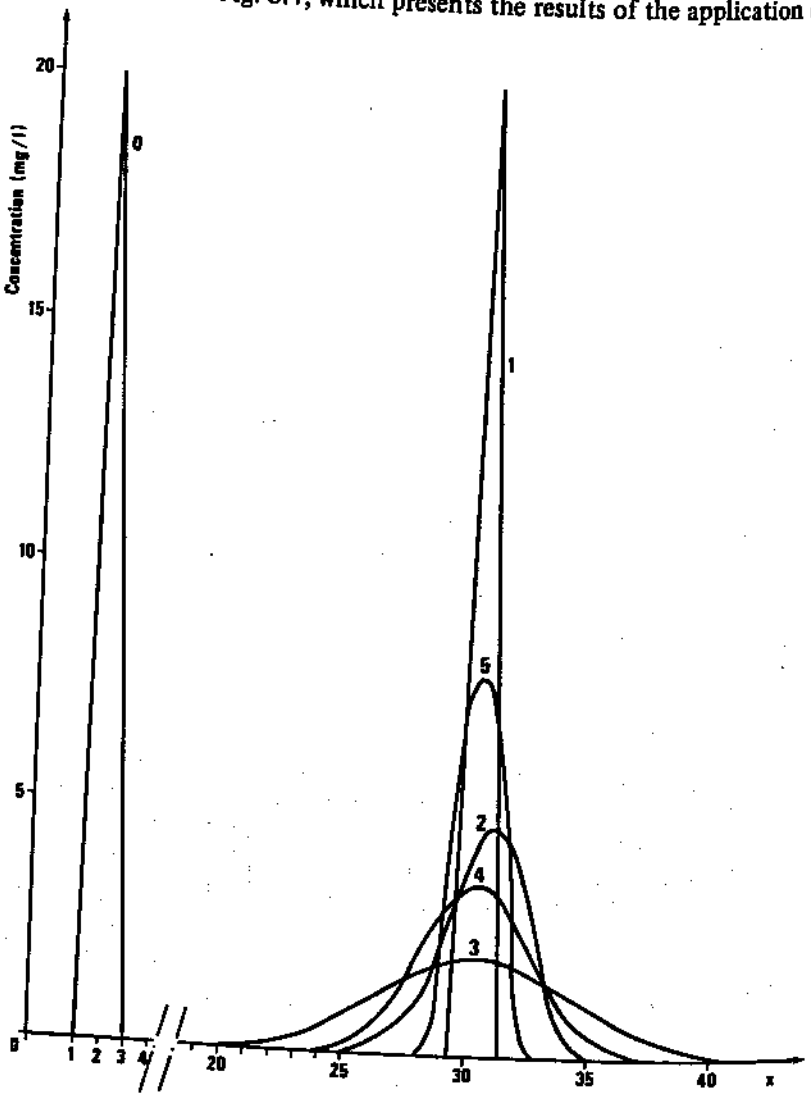

Fig. 8.4. Numerical diffusion in the Dobbins and Bella (1968) scheme. 0, initial concentration distribution; 1, 2, 3, 4, 5, *see* Table 8.1

Equation (8.15) to convection in the following idealized channel; a rectangular section, 2 m wide and 1 m deep, slope 0.1%, Strickler coefficient 25, discharge 1 $m^3\ s^{-1}$, velocity 0.5 $m\ s^{-1}$. The channel's 10 km length was divided into 50 computational reaches of $\Delta x = 200$ m each.

The upstream concentration distribution shown as curve 0 on the left was transported downstream for approximately 3 hours using the conditions given in Table 8.1. Only case 1, in which the Courant number is an integer value,

Table 8.1

Curve	Δt (s)	Cr	K_n ($m^2\ s^{-1}$)	Calculation interval (s)
1	400	1.0	0.0	11 400
2	360	0.9	5.0	11 520
3	200	0.5	25.0	11 400
4	600	1.5	8.33	11 400
5	3800	9.5	1.32	11 400

reproduces pure convection with no artificial diffusion. The other curves demonstrate the strong diffusion introduced by the numerical scheme, a diffusion which can be taken to be physical if the user is not well aware of the numerical problem and chooses Δt and Δx accordingly.

Land (1978) suggests that K_x be set equal to zero if $K_n > K_x$. But if such drastic action must be taken, there is no point in performing a numerical simulation of the dispersion process, since the essential physical process is suppressed. A more reasonable solution is suggested by Chevereau and Preissmann (1971), who recommend the following measures:

(1) use Δx as small as possible within the time and cost limits of the study;

(2) use Δt as large as possible without losing resolution in the description of the dispersion process;

(3) choose Δt and Δx such that $\Delta x \approx \dfrac{U\Delta t}{n}$ where n is a positive integer.

There exist other numerical schemes for the solution of Equation (8.10), all of which are more or less plagued by the numerical diffusion problem. Examples are the methods described by Land (1978); Bowles, Fread and Grenny (1977), and Martin (1975). A method which introduces no artificial diffusion is the two-step half-implicit, half-explicit scheme described by Leendertse (1970) and applied to river transport problems by Holly and Cunge (1975). Unfortunately the method's attractive zero-diffusion property is somewhat tainted by its numerical *dispersion*. By this we refer to that fact that individual Fourier components which comprise any concentration distribution propagate at different speeds (*see* Section 3.2). In Fig. 8.5 we show the results of the Leendertse scheme applied to

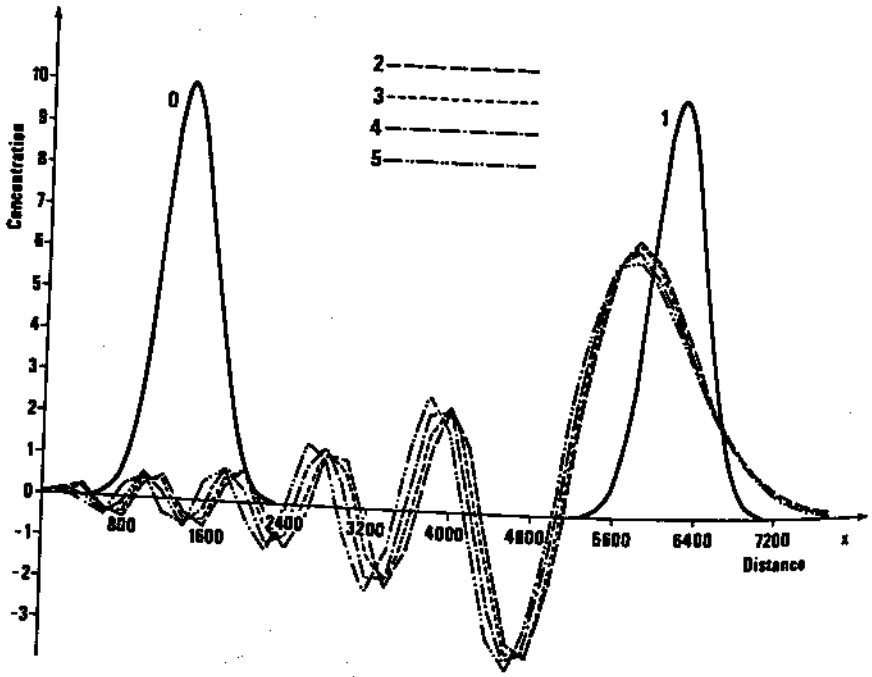

Fig. 8.5. Numerical dispersion in the Leendertse (1970) scheme. 0, initial concentration distribution, $t = 0$; 1, concentration distribution at $t = 9600$ s, exact solution; 2, concentration distribution at $t = 9600$ s, $Cr = 0.25$; 3, concentration distribution at $t = 9600$ s, $Cr = 0.50$; 4, concentration distribution at $t = 9600$ s, $Cr = 0.75$; 5, concentration distribution at $t = 9600$ s, $Cr = 1.00$

the idealized channel described above; we see that this propagation speed error gives rise to an oscillation-like behaviour as well as an error in peak concentrations which can be just as troublesome as artificial diffusion. Moreover, the negative concentrations pose a problem: they are physically meaningless, yet to suppress them means falsifying conservation of mass in the numerical solution.

These problems of numerical diffusion and dispersion have led researchers to try to develop more accurate methods. Most of the developments in this respect have come from outside the river hydraulics field (*see*, for example, Boris and Book, 1973). Nonetheless one accurate scheme was developed specifically for use in river and ocean pollution problems (Holly and Preissmann, 1977), and we shall briefly describe it here.

The basis of the scheme, which we call the 'two-point fourth-order method', is similar to that of Equation (8.15) in that we follow the trajectory leading to point $(i+1, n+1)$ back to point ξ where it intersects the x-axis as in Fig. 8.3b. But instead of interpolating linearly between $C_a(i-1, n)$ and $C_a(i, n)$ to find $C_a(\xi, n)$, we interpolate using a *cubic* polynomial constructed between $(i-1, n)$

and (i, n) based on the assumption that not only $C_a(i-1, n)$ and $C_a(i, n)$, but also their derivatives $\frac{\partial C_a}{\partial x}(i-1, n)$ and $\frac{\partial C_a}{\partial x}(i, n)$ are known. The details of this procedure are developed by Holly and Preissmann (1977); the result is

$$C_a(i+1, n+1) = C_a(\xi, n) = a_1 C_a(i-1, n) + a_2 C_a(i, n) + a_3 \frac{\partial C_a}{\partial x}(i-1, n) + a_4 \frac{\partial C_a}{\partial x}(i, n) \qquad (8.22)$$

in which

$$\begin{aligned} a_1 &= Cr^2 (3 - 2Cr) \\ a_2 &= 1 - a_1 \\ a_3 &= Cr^2 (1 - Cr)(x_i - x_{i-1}) \\ a_4 &= -Cr (1 - Cr)^2 (x_i - x_{i-1}) \end{aligned} \qquad (8.23)$$

The derivatives themselves are then convected forward by a similar process. Denoting $\frac{\partial C_a}{\partial x}$ by C_a', we take the derivative of Equation (8.10) with respect to x, which yields

$$\frac{\partial C_a'}{\partial t} + U \frac{\partial C_a'}{\partial x} = 0$$

for the case U = constant. By a procedure similar to that leading to Equation (8.22), we obtain

$$C_a'(i+1, n+1) = C_a'(\xi, n) = b_1 C_a(i-1, n) + b_2 C_a(i, n) + b_3 C_a'(i-1, n) + b_4 C_a'(i, n) \qquad (8.24)$$

in which

$$\begin{aligned} b_1 &= 6Cr (Cr - 1)/(x_i - x_{i+1}) \\ b_2 &= -b_1 \\ b_3 &= Cr (3Cr - 2) \\ b_4 &= (Cr - 1)(3Cr - 1) \end{aligned} \qquad (8.25)$$

This scheme introduces very little numerical diffusion and dispersion as shown in its application to our ideal channel (Fig. 8.6). It is not possible to derive an overall numerical diffusion coefficient as we did previously, because the scheme's numerical diffusion, while extremely small, depends on the size of the concentration distribution compared to Δx as well as the Courant number Cr (*see* Holly and Preissmann, 1977). The cost of the method's favourable accuracy compared to a more simple scheme such as Equation (8.15) is two-fold:

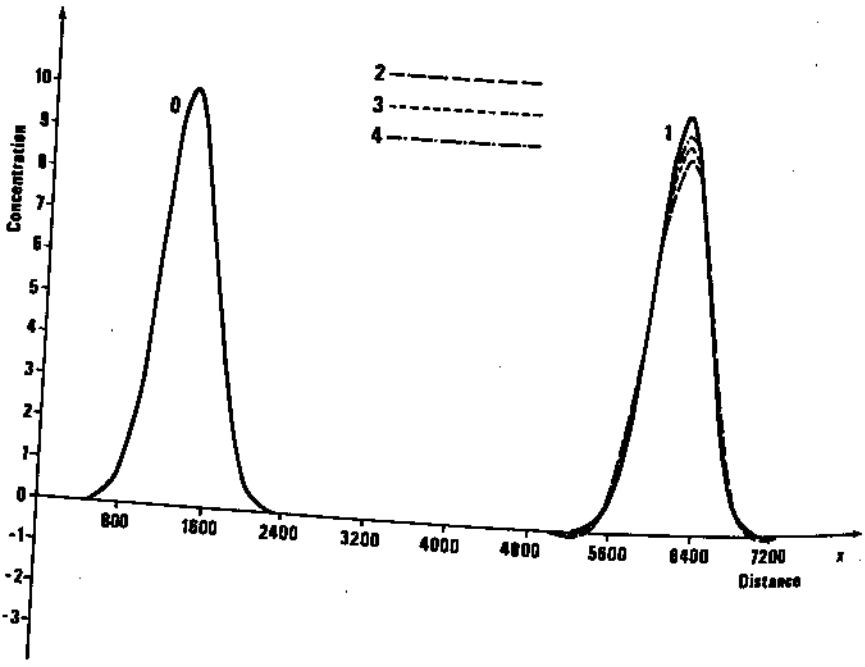

Fig. 8.6. Numerical dispersion in the Holly and Preissmann (1977) scheme. 0, initial concentration distribution, $t = 0$; 1, concentration distribution at $t = 9600$ s, $Cr = 1.0$ and exact solution; 2, concentration distribution at $t = 9600$ s, $Cr = 0.25$; 3, concentration distribution at $t = 9600$ s, $Cr = 0.50$; 4, concentration distribution at $t = 9600$ s, $Cr = 0.75$

additional computer time needed for the calculation of coefficients a_1, b_1, etc., and additional storage for the derivatives C'_a. These are, however, insignificant factors on most modern computing equipment, and there is no reason not to use schemes which virtually eliminate numerical diffusion from consideration, and thus permit us to model physical convection and physical diffusion without having to compensate for numerical inadequacy.

In schemes such as the two-point fourth-order method the artificial diffusion decreases as the size of the concentration distribution increases compared to Δx. Thus the presence of *physical* diffusion tends to improve the accuracy, simply because physical diffusion tends to spread the concentration distribution over a larger and larger spatial extent as time increases. An important consequence of this is that when both the convection and diffusion portions of Equation (8.7) are simulated in a model (we consider the diffusion portion below) the presence of strong diffusion tends to mask inadequacies of the convection calculation which may become important if the concentration distribution passes into a zone of weak diffusion, such as a reservoir pool. Figure 8.7 demonstrates this in comparing the two-point fourth-order scheme and Martin's (1975) fourth-order

scheme in our idealized channel with weak and strong diffusion, i.e. with $K_x = 1\ m^2\ s^{-1}$ and $K_x = 10\ m^2\ s^{-1}$.

It is clearly evident that strong physical diffusion tends to hide errors in the convection which may nonetheless hurt the simulation in zones of weak physical diffusion.

Whatever the scheme chosen for the calculation of pure convection, Equation (8.10) requires that an initial condition and one upstream boundary condition be furnished. This upstream condition is simply the known or assumed variation of concentration as a function of time. In addition, for implicit schemes such as those of Leendertse (1967), Stone and Brian (1963), and Land (1978), a supplementary downstream boundary condition is required. This physically-redundant condition is usually taken as $\frac{\partial C_a}{\partial x} = 0$ at the downstream model limit. We will see in Section 8.8 that this artificial condition can lead to problems in the case of a continuous release of tracer.

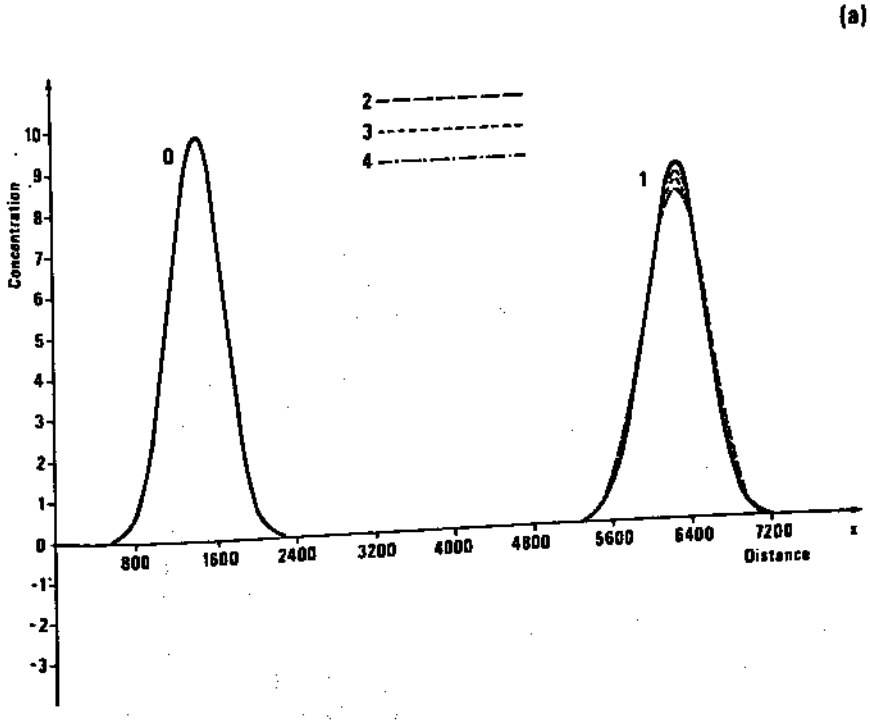

Fig. 8.7 *see page 331*

(b)

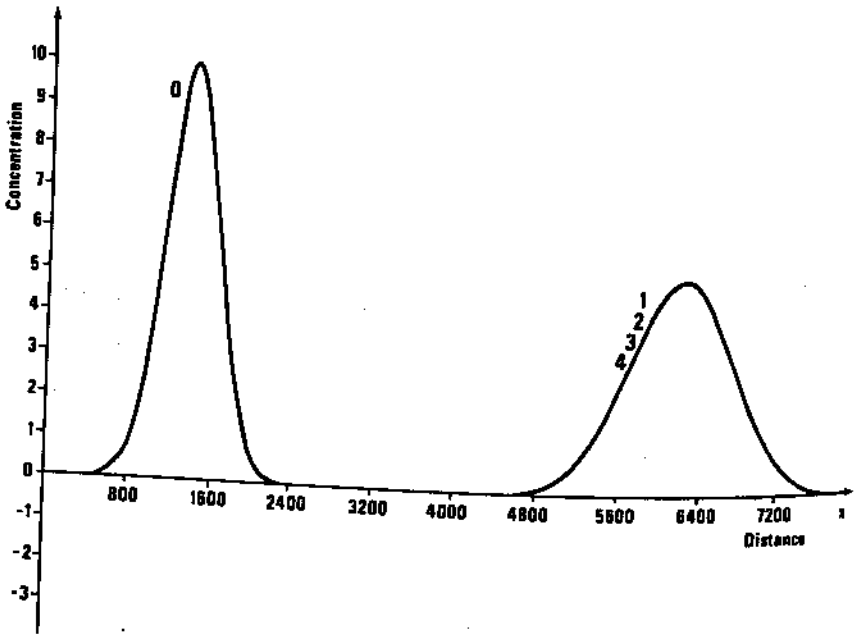

(c)

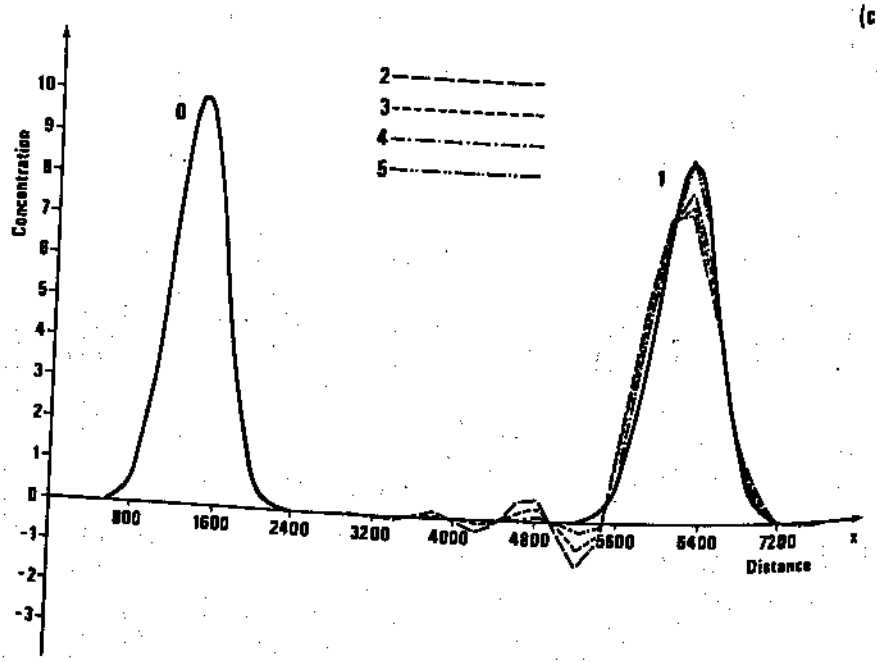

Fig. 8.7 *see page 331*

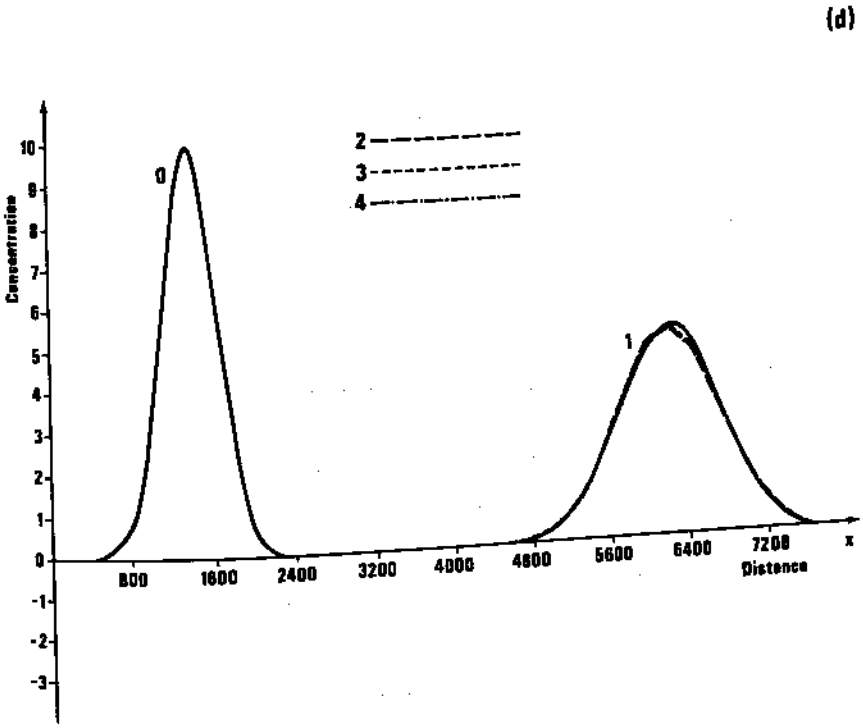

Fig. 8.7. Tendency of strong physical diffusion to hide numerical diffusion. 0, initial concentration distribution, $t = 0$; 1,5, concentration distribution at $t = 9600$ s, $Cr = 1.0$ and exact solution; 2, concentration distribution at $t = 9600$ s, $Cr = 0.50$; 3, concentration distribution at $t = 9600$ s, $Cr = 0.25$; 4, concentration distribution at $t = 9600$ s, $Cr = 0.75$. (a) Method of Holly and Preissmann (1977), $K_x = 1$ m^2 s^{-1}; (b) method of Holly and Preissmann (1977), $K_x = 10$ m^2 s^{-1}; (c) method of Martin (1975), $K_x = 1$ m^2 s^{-1}; (d) method of Martin (1975), $K_x = 10$ m^2 s^{-1}

8.6 NUMERICAL SOLUTION OF THE ONE-DIMENSIONAL DIFFUSION EQUATION

In most one-dimensional dispersion models the convection and diffusion are calculated in separate steps. In a given time step, the solution of Equation (8.10) is followed immediately by the solution of

$$A \frac{\partial C_a}{\partial t} = \frac{\partial}{\partial x} \left(A K_x \frac{\partial C_a}{\partial x} \right) \tag{8.26}$$

A commonly used finite difference method for the solution of Equation (8.26) is an explicit centred scheme as described by Chevereau and Preissmann (1971). We want to express conservation of mass in the volume limited by points $i-1/2$ and $i+1/2$ in Fig. 8.8. The rate of mass diffusion into the volume at $i-1/2$ is

$$AK_x \left.\frac{\partial C_a}{\partial x}\right|_{i-1/2} \approx A_{i-1/2}\, K_{x_{i-1/2}} \frac{C_a(i,n) - C_a(i-1,n)}{x_i - x_{i-1}} \tag{8.27}$$

and the rate of diffusion out at $i+1/2$ is

$$AK_x \left.\frac{\partial C_a}{\partial x}\right|_{i+1/2} \approx A_{i+1/2}\, K_{x_{i+1/2}} \frac{C_a(i+1,n) - C_a(i,n)}{x_{i+1} - x_i} \tag{8.28}$$

The rate of accumulation of mass in the volume is written

$$A \left.\frac{\partial C_a}{\partial t}\right|_i \approx A_i \frac{C_a(i,n+1) - C_a(i,n)}{\Delta t} \tag{8.29}$$

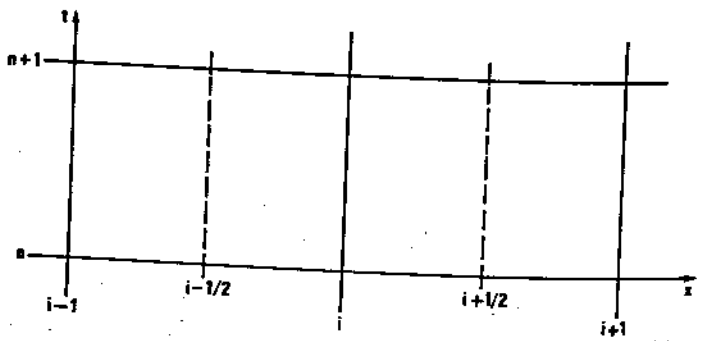

Fig. 8.8. Computational grid for diffusion calculation

By equating the rate of accumulation to the net inflow, we obtain the working relationship,

$$C_a(i,n+1) - C_a(i,n) = \frac{\Delta t}{A_i(x_{i+1/2} - x_{i-1/2})} \left[A_{i-1/2}\, K_{xi-1/2} \times \frac{C_a(i,n) - C_a(i-1,n)}{x_i - x_{i-1}} - A_{i+1/2}\, K_{xi+1/2} \frac{C_a(i+1,n) - C_a(i,n)}{x_{i+1} - x_i} \right] \tag{8.30}$$

The scheme is stable as long as

$$\frac{K_x \Delta t}{(x_{i+1} - x_i)(x_i - x_{i-1})} \leqslant 0.5 \tag{8.31}$$

Equation (8.26) being parabolic, we need to supply both upstream and downstream boundary conditions. The upstream value is once again the known variation of concentration as a function of time, while the downstream condition is generally an assumption of no diffusion,

$$\frac{\partial^2 C_a}{\partial x^2} = 0$$

The initial condition for a given time step is the result of the convection calculation as described earlier, the simulation proceeding by calculating an alternating series of convection and diffusion steps.

The stability limit as expressed by Equation (8.31) can be removed by using an implicit version of Equation (8.30) in which the space derivatives are evaluated at the future time $n + 1$ (Holly, 1975). This scheme requires, however, a matrix inversion or double-sweep procedure (*see* Chapter 3), and thus is more difficult to program than the explicit version. Whenever the time step is limited in the convection calculation (for example by the fact that a particular method is programmed under the assumption that the trajectory falls between $i - 1$ and i or i and $i + 1$, etc.) then the explicit scheme for diffusion may be perfectly adequate.

8.7 EXAMPLE OF ONE-DIMENSIONAL DISPERSION MODELLING – THE VIENNE RIVER†

In 1971 a comprehensive study of pollution simulation in the Vienne River (France) was conducted for the French government by SOGREAH and IRCHA (Brebion *et al.*, 1971). The 27 km reach of the Vienne, situated between Pilas and Confolens, is crossed by seven bridges and contains 12 weirs as shown in Fig. 8.9. It was recognized that oxygen depletion in the river could be correctly modelled only if a correct simulation of convection and diffusion was included.

A one-dimensional unsteady flow model was first applied to furnish water surface elevations and velocities for the range of essentially steady-flow discharges to be studied. Since paper mill wastes are dumped into the river in such a way as to be rather fully mixed over the entire cross section, a one-dimensional dispersion model was judged to be adequate. The longitudinal dispersion coefficient K_x was evaluated experimentally using an injection of Rhodamine dye at Pilas and observing the cross-sectional average concentration at Chabanais, then assuming that the Gaussian law of Equation (8.8) approximately holds in order to estimate K_x, which was found to be about 2 $m^2\ s^{-1}$, corresponding to $K_x = 20\ U_* h$.

The dispersion model was based on the convection calculation scheme of Equation (8.15), and the diffusion scheme of Equation (8.30). Computational points 50 m apart were interpolated between the sections used for the flow

†Courtesy IRCHA and SOGREAH.

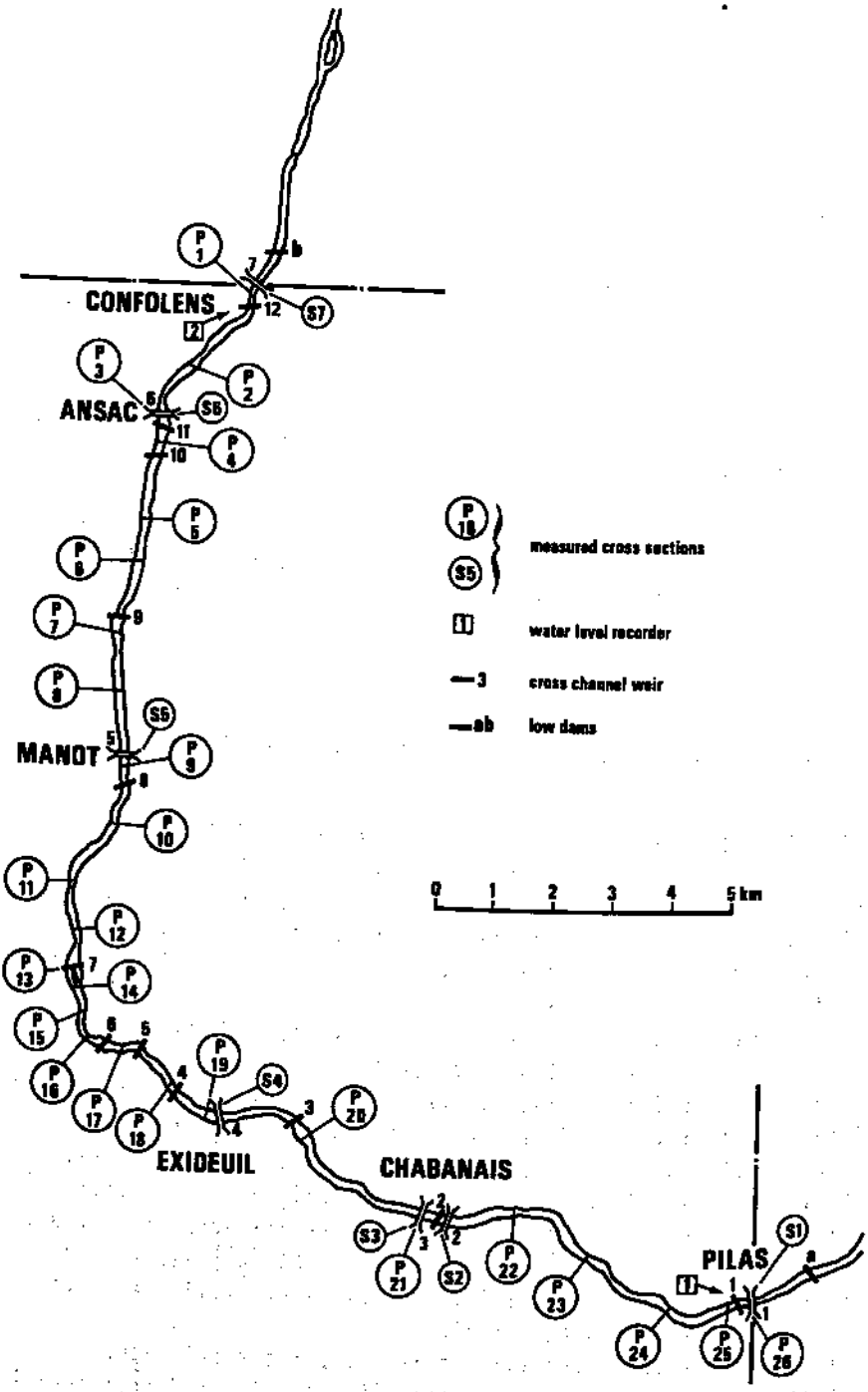

Fig. 8.9. Site of Vienne river dispersion study

model, spaced at roughly 1 km intervals; the same time step of 15 min was used in both the flow and dispersion models. With these values the diffusion calculation stability limit Equation (8.31), was approximately satisfied and the artificial diffusion K_n was about 25% as large as K_x. Figure 8.10 shows the

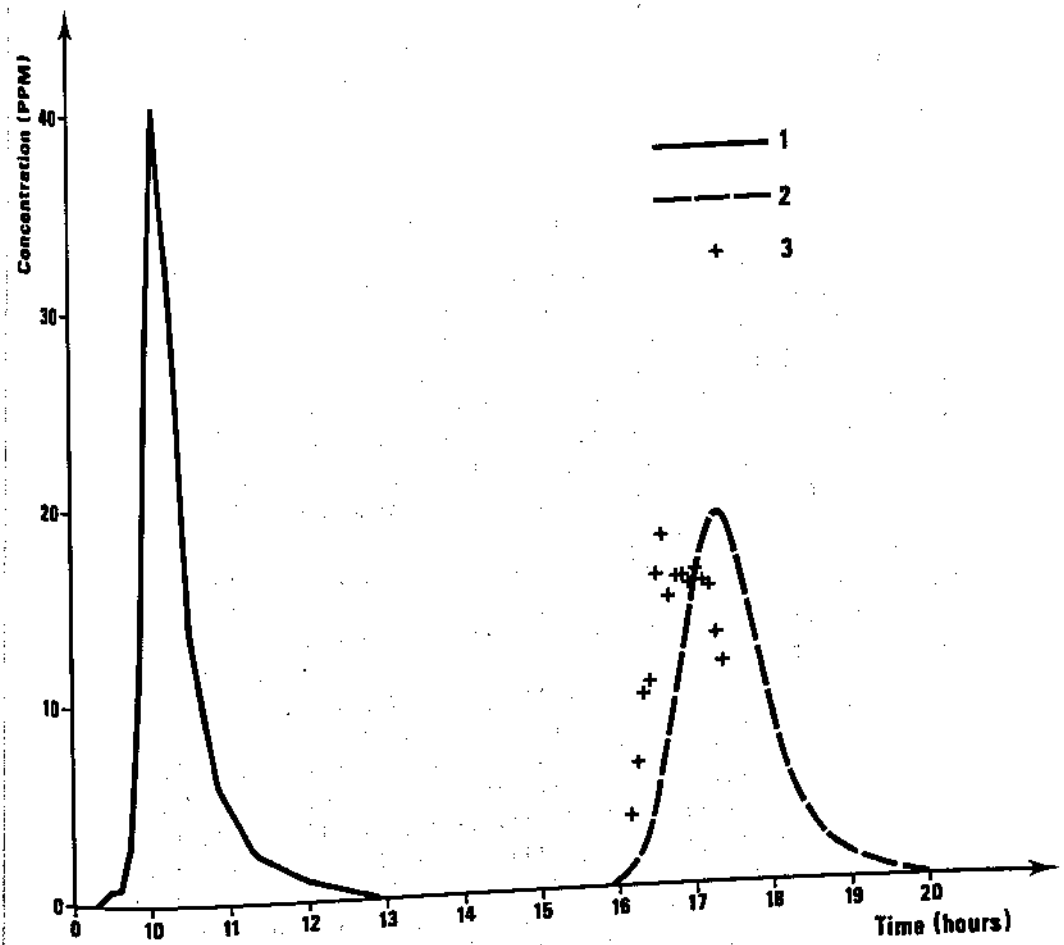

Fig. 8.10. Results of Vienne river dispersion study. 1, Initial concentration distribution at Pilas; 2, calculated concentration distribution at Chabanais; 3, measured concentration distribution at Chabanais

observed and simulated concentration distributions resulting from the Rhodamine injection at Pilas, using $K_x = 2\ m^2\ s^{-1}$ for the calculation. The peak concentration at Chabanais is reproduced within 5%, though the observed distribution appears to arrive about 30 min sooner than the calculated one and to rise somewhat more steeply. During the exploitation phase of the study, the

dispersion model was incorporated into an overall water quality simulation procedure based on the Streeter–Phelps equation.

One of the most important conclusions of the study, which underlines the close relationship between water quality modelling and flow modelling, was that '. . . it is necessary to have a good understanding of the flow details. If hydraulic parameters are treated in too approximate a manner . . . the development of pollution models can only be hindered. On the other hand, the information brought in by a mathematical model of flow eliminates a major cause of imprecision in the pollution model itself'.

8.8 TWO-DIMENSIONAL DISPERSION MODELLING

The one-dimensional analogy as described in Section 8.3 can be useful if one is interested only in the mixing far from the source (i.e. distances greater than L from the injection point) of a tracer which is more or less suddenly dumped into the river. In addition, the mixing coefficient K_x must be known for the flow situation being modelled. But if one needs to predict the mixing relatively close to a source which is concentrated at one bank, or distributed over only part of the cross section, it may be necessary to employ a two-dimensional model to obtain useful results. By two-dimensional, we mean capable of predicting the depth-averaged concentration anywhere in the cross section, i.e. through the solution of Equation (8.6). For example, Eheart, Joeres and Hoopes (1978) describe the role of two-dimensional models in the 'clear lane' water quality concept, in which quality standards apply to certain portions of the cross section. There is no way to study such situations with a one-dimensional model.

Our interest in two-dimensional modelling, however, goes beyond the need for more detailed predictions in certain engineering situations. We developed in Chapter 4 the notion that a model's *predictive* capacity depends on the degree to which true physical phenomena are taken into account. For example, a flood propagation model based on the Muskingum method cannot be used to predict events for which it is not specifically calibrated, since the routing coefficients are not uniquely related to physical river properties. Similarly, the one-dimensional mixing coefficient K_x is not a fixed property of the river, but rather a catch-all parameter which depends on the shape of the cross section and flow distribution within it, and on the turbulent mixing coefficient ϵ_z. Thus K_x is a property of a particular flow condition, and its value changes if the discharge, channel shape, or channel roughness are changed. On the other hand, the mixing coefficients ϵ_x and ϵ_z, while not purely physical properties such as ϵ_m and $\tilde{\epsilon}_x$, $\tilde{\epsilon}_y$ and $\tilde{\epsilon}_z$, can be directly related to the depth and shear velocity as we described in Section 8.2. Thus a two-dimensional model based on Equation (8.6), which requires as data only ϵ_x and ϵ_z in addition to the velocity field, has no *a priori* limitation as far as predictions are concerned. (We describe in Section 8.11 the problem of velocity field estimation.) Even if the engineer is studying a truly one-dimensional physical mixing situation (in the sense that the tracer

occupies all of the cross section), he may find it worthwhile to use a two-dimensional model to simulate the mixing process if he needs to predict the mixing in situations for which he cannot obtain a calibrated K_x (unusually high or low discharges, future channel modification through dredging, dam construction, etc.).

A two-dimensional model based on Equation (8.6) could be developed by writing a finite difference algorithm to solve for convection and diffusion in the longitudinal x and transverse z directions. A simpler and more economic approach makes use of the fact that the transverse velocity w is small compared to the longitudinal velocity u. We imagine that the river is divided into a series of adjacent stream tubes (*see* Fig. 8.11) in each of which the discharge is constant, as we assume steady river flow conditions. (The stream tube method was first introduced by Fischer (1966).) Once the dimensions and discharges of each tube are fixed at the upstream flow section, their depths, widths, and velocities vary longitudinally so as to maintain the same discharge in each tube through the changing cross-sectional shapes and velocity distributions encountered at different points along the river. As we shall see below, the lateral shifting of each tube's position with respect to the banks takes into account the depth-averaged transverse velocity w. Based on this schematization, an algorithm can be developed which simulates two-dimensional mixing as the simultaneous occurrence of three mechanisms:

(1) longitudinal convection in each stream tube
(2) longitudinal diffusion in each stream tube
(3) transverse diffusion between adjacent stream tubes

We now describe in more detail this procedure, whose complete development is available in Holly (1975), and in Holly and Cunge (1975).

Equation (8.6), which describes tracer mass conservation at a point, must be integrated over the width of a stream tube, since the quasi-two-dimensional model we propose recognizes only an average concentration in each stream tube.

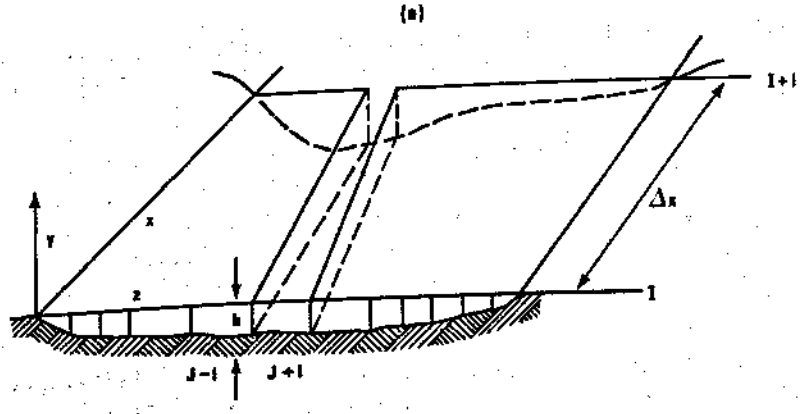

Fig. 8.11 *see page 338*

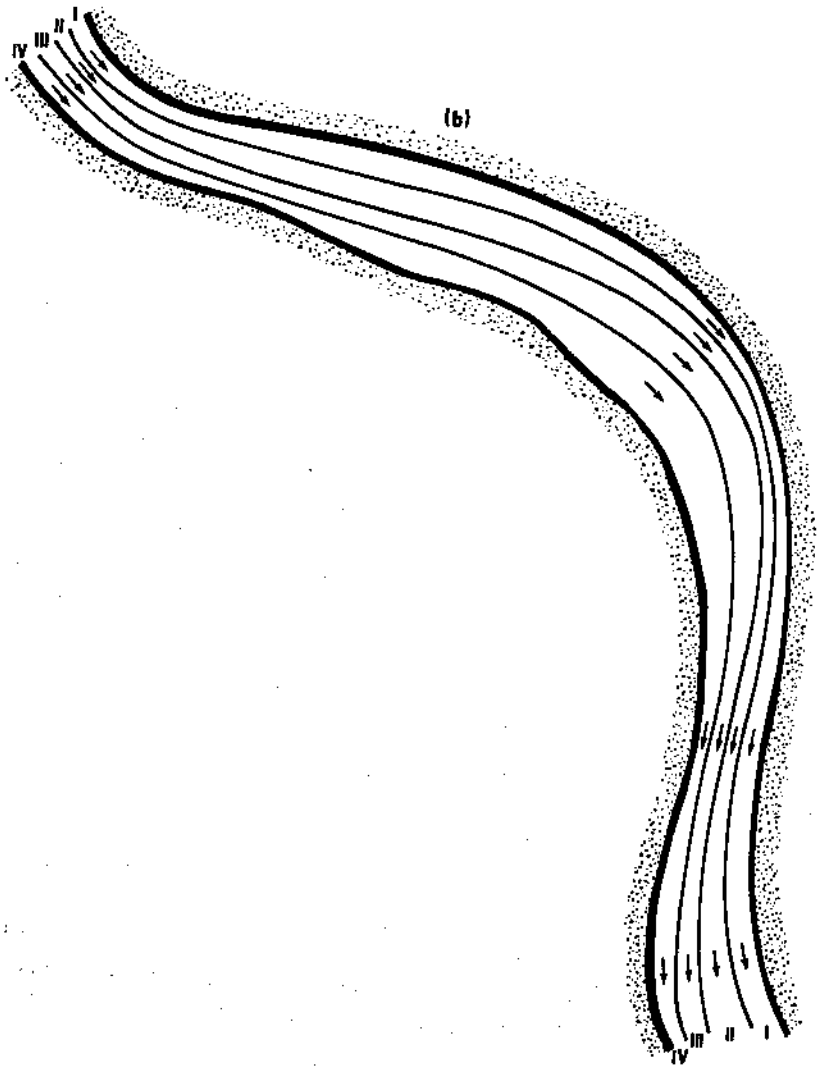

Fig. 8.11. Discretization of river into stream tubes. (a) Stream tube variation between two cross sections. (b) Stream tube widths reflect flow distribution in the river

The resulting expression is the following:

$$A\frac{\partial C}{\partial t} + \frac{\partial}{\partial x}(AuC) = \frac{\partial}{\partial x}\left(A\,\epsilon_x\,\frac{\partial C}{\partial x}\right) + \left(h\,\epsilon_z\,\frac{\partial C}{\partial z}\right)_l - \left(h\,\epsilon_z\,\frac{\partial C}{\partial z}\right)_r \tag{8.32}$$

in which A is the area of the stream tube perpendicular to the flow direction, C, U and ϵ_x are understood to be stream-tube average values, and the subscripts l

and r refer to the left and right boundaries of the stream tube, facing downstream. We note that the transverse velocity w no longer appears in Equation (8.32), but this does not mean that it has been assumed to be zero. The longitudinal variation of stream tube widths, which is required to satisfy continuity, results in a longitudinal variation of the transverse coordinates of stream tube centroids. An observer moving with the flow in a particular stream tube would see this as a gradual movement across the channel, i.e. as the effect of depth-averaged transverse velocity. The stream tube averaging process has removed w as an explicit parameter, but w implicitly governs the dimensioning of stream tubes.

The finite difference solution of Equation (8.32) is accomplished by dividing the river into a series of computational reaches separated by computational points. The solution then proceeds in three distinct steps during each time increment:

(1) *Longitudinal convection* is calculated in each stream tube from its upstream limit to its downstream limit. For pure convection, Equation (8.32) is written:

$$A \frac{\partial C}{\partial t} + \frac{\partial}{\partial x} (AuC) = 0 \tag{8.33}$$

Thus we have once again the one-dimensional convection equation (8.10) (*see* footnote p. 320) which can be solved using the methods described in Section 8.5. The artificial diffusion problem becomes particularly important here; Δt and Δx will be the same for all the tubes, but the velocity in each one is different. Thus the Courant number cannot in general be given an integer value in all the tubes, and it is especially important to use a convection scheme which guarantees that K_n is small for a broad range of Courant numbers.

(2) *Longitudinal diffusion* in each stream tube proceeds also from the upstream to the downstream boundary; Equation (8.32) is written:

$$A \frac{\partial C}{\partial t} = \frac{\partial}{\partial x} \left(A \epsilon_x \frac{\partial C}{\partial x} \right) \tag{8.34}$$

in which the 'old' concentrations have already been convected by Equation (8.33). Equation (8.34) is identical to Equation (8.26) with K_x replaced by ϵ_x, and consequently the scheme presented in Section 8.6 is perfectly applicable to this case. Many authors have noted the insignificance of longitudinal diffusion compared to longitudinal dispersion. Indeed, the inclusion of Equation (8.34) in an overall model can be considered optional, necessary only when extremely strong concentration gradients near the source must be modelled.

(3) *Transverse diffusion* between stream tubes and along their entire length is calculated using

$$A \frac{\partial C}{\partial t} = \left(h \epsilon_z \frac{\partial C}{\partial z} \right)_1 - \left(h \epsilon_z \frac{\partial C}{\partial z} \right)_r \tag{8.35}$$

Equation (8.35) is analogous to Equation (8.34); but it is solved from bank to bank at each computational point, the boundary conditions being zero transport at the banks. The numerical scheme described in Section 8.6 can be applied, for example, if we consider 'r' to represent $i + 1/2$, 'l' to represent $i - 1/2$; and the indices $i - 1$, i and $i + 1$ to represent adjacent stream tubes.

The repetition of these three stages for each time step simulates the two-dimensional dispersion process in a natural channel. It is of course implicitly understood that if transverse mixing between stream tubes is due principally to helicoidal currents in bends, and not simple diffusion, the two-dimensional approach must be abandoned in favour of fully three-dimensional models, which as of this writing are not yet in industrial use. Only field experiments or undistorted physical model tests can yield useful predictions of mixing in sharp bends.

8.9 EXAMPLE: SIMULATION OF TWO-DIMENSIONAL DISPERSION IN THE MISSOURI RIVER FROM A CONTINUOUS SOURCE

Figure 8.12 shows the 10 km stretch of the Missouri River (U.S.A.) in which Yotsukura, Fischer and Sayre (1970) measured the transverse diffusion of Rhodamine dye being injected continuously from a bridge at the upstream limit of the reach. The dye quickly mixed over the flow depth, and spread laterally so as to begin touching the banks in the downstream portions of the reach. A model of this experiment was constructed using a program which incorporated the two-point fourth-order scheme for convection (Equations (8.22)–(8.25)), and an implicit version of the centred scheme for longitudinal and transverse diffusion (Equation (8.30)).

The model used 11 stream tubes, computational points spaced at about 200 m intervals, and a time step of 1 min. A steady state distribution corresponding to the field experiment was obtained by simulating a time period corresponding to the transit time through the reach of the slowest velocities in the section, about 4 h real time. Longitudinal mixing was left out of the calculation, since it has little effect on steady state distributions. The transverse coefficient was taken as $\epsilon_z = 0.67 U_* h$ as suggested by Yotsukura, Fischer and Sayre. Figure 8.13 shows the results of the simulation along with corresponding measured values. The results agree closely with those computed by Yotsukura *et al.*, who used a different set of stream tubes and a steady state dispersion equation.

The same simulation was performed by Holly (1975) but using Leendertse's (1970) stable method for the convection. The results agree quite closely, but the fact that they are not identical (even though the stream tubes and the diffusion calculation were identical) brings out an interesting point. As we discussed in

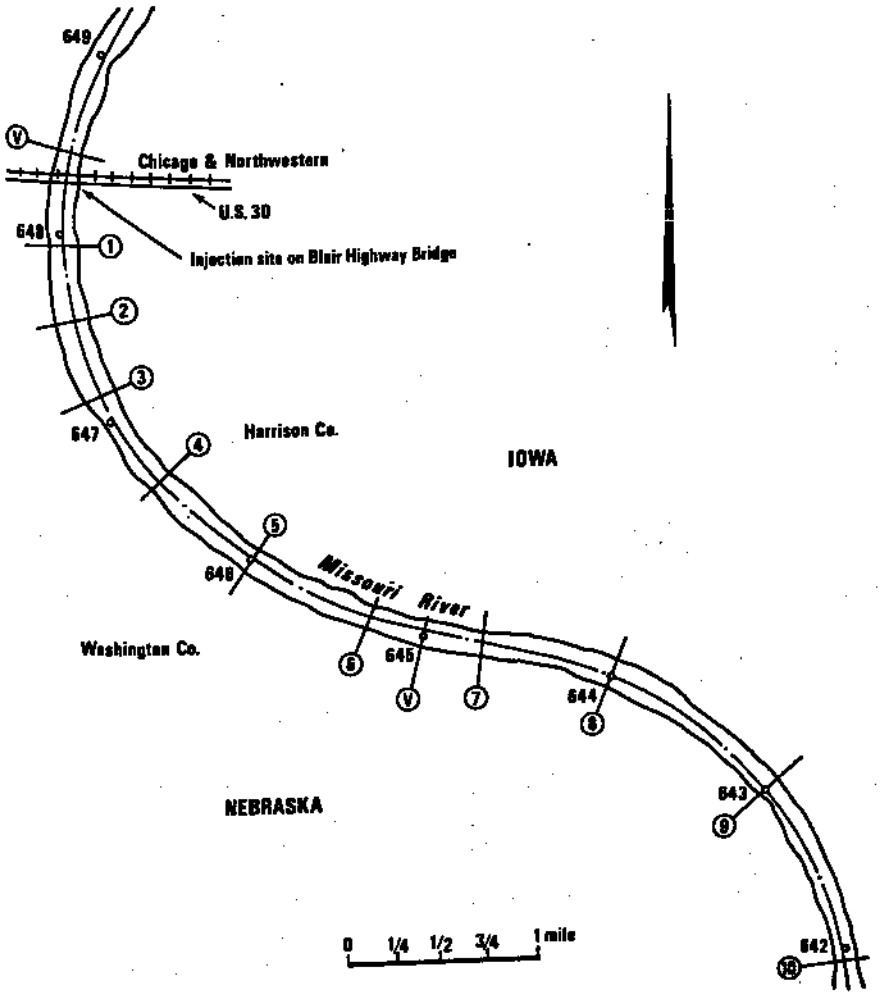

Fig. 8.12. Site of Missouri river dispersion study (after Yotsukura *et al.*, (1970) ②, Cross section for dye sampling; Ⓥ, cross section for velocity measurement; 648, river mileage

Section 8.5, the Leendertse method introduces no numerical diffusion. Moreover, for continuous injection of tracer at steady state both Leendertse's artificial dispersion and the two-point fourth-order method's artificial diffusion and dispersion are virtually non-existent, since the tracer is spread out over a long distance compared to Δx. But it was observed that whereas the two-point fourth-order method settled down into a true steady state after 4 h, the Leendertse method produced slightly oscillating concentrations throughout the flow field, even after 12 h of real time simulation. These oscillations appeared

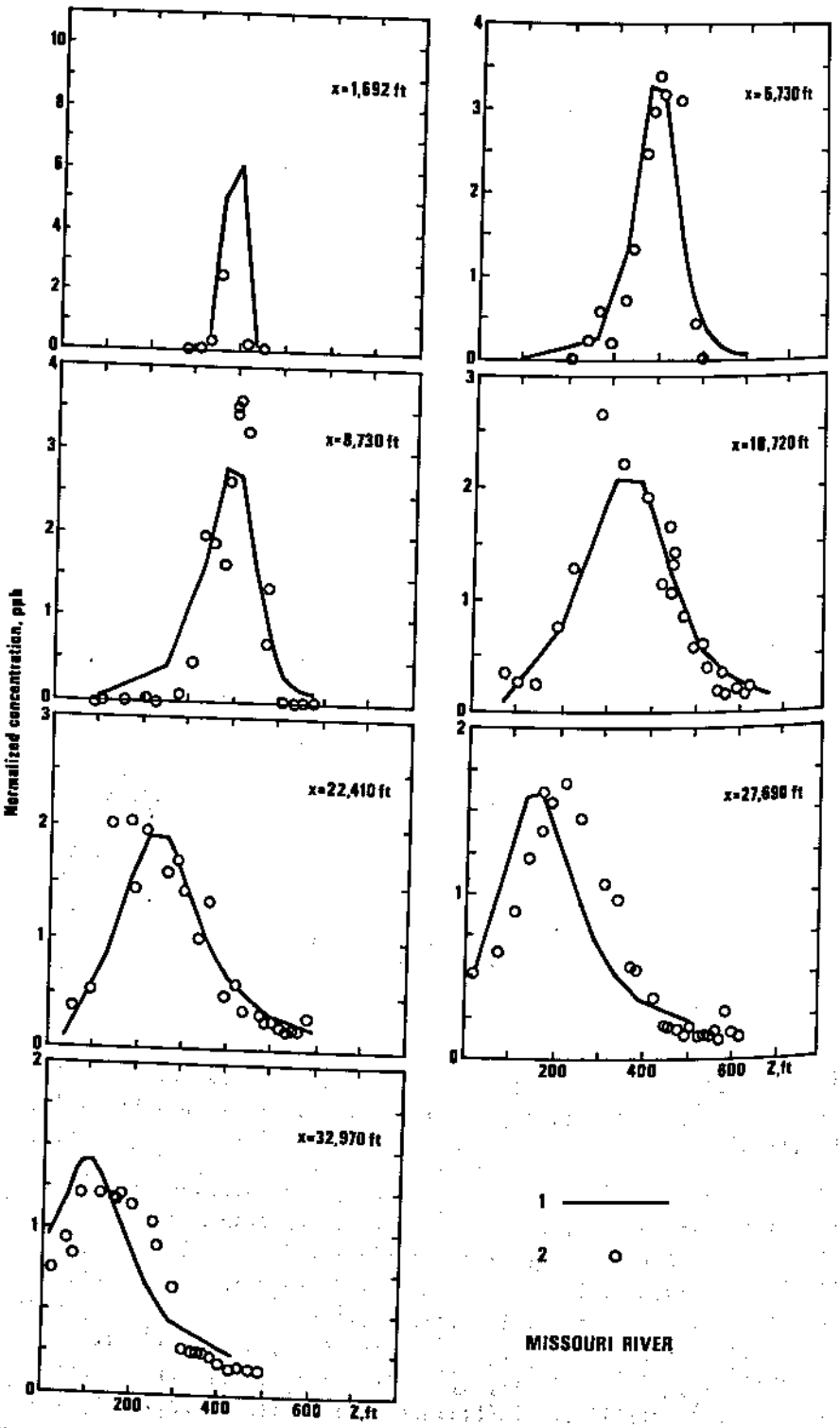

Fig. 8.13. Results of Missouri river dispersion study. 1, Simulation, $\epsilon_z = 0.63\, U_* h$; 2, measured concentrations, normalized

to be due to the downstream boundary condition for the convection. We noted in Section 8.5 that whereas Equation (8.10) as well as its solution by an explicit method require no downstream boundary conditions, the implicit method requires that we impose an artificial condition, which in this case was $\frac{\partial C}{\partial x} = 0$. In the Missouri River simulation, this represents a discontinuous derivative at the downstream limit (since $\frac{\partial C}{\partial x} \neq 0$ normally) which in the Fourier series representation of the solution creates wave components which are short compared to Δx. As shown in Holly (1975) it is these short wavelength components which undergo the most severe numerical dispersion, causing oscillations in the supposed steady state solution.

8.10 EXAMPLE: SIMULATION OF ONE-DIMENSIONAL DISPERSION IN CLINCH RIVER

The Clinch River mixing experiment as reported by Godfrey and Frederick (1970) consisted in the sudden injection of radioactive tracer over the entire cross section, and the measurement of its dispersion over a 7 km reach. The authors' program used for the Missouri River simulation was used to construct and operate a model capable of reproducing the experiment. The river was divided into 11 stream tubes of equal discharge; longitudinal computational points were placed at roughly 350 m intervals, interpolated between the six measured cross sections at which the channel shape and transverse velocity distribution were known. The observed concentration distribution at $x = 2260$ ft, assumed to be fully mixed over the cross section, was taken as the upstream boundary condition for the model. Since no particular transverse mixing data were available, Elder's mixing coefficients were adopted,

$$\epsilon_z = 0.23\, U_* h$$
$$\epsilon_x = 5.93\, U_* h$$

Figure 8.14 shows the maximum centreline concentrations observed during the passage of the tracer cloud at each of six measuring stations. The upper solid line represents the corresponding model results (the observed concentration distribution at station 1 was used as the upstream boundary condition in the model). By comparison, the dashed line represents exactly the same calculation, but using Leendertse's scheme for convection. The rather large difference in computed concentrations between the two methods, which is greatest near the source and diminishes with downstream distance, is due essentially to Leendertse's numerical dispersion, since the two-point fourth-order method introduces very little error. This points out the importance of interpreting calculated results in view of the scheme's known error characteristics; from the Leendertse calculation we would conclude that $\epsilon_z = 0.23 U_* h$ is the appropriate

value, when in fact the Holly and Preissmann result suggests that this value of ϵ_z is too small.

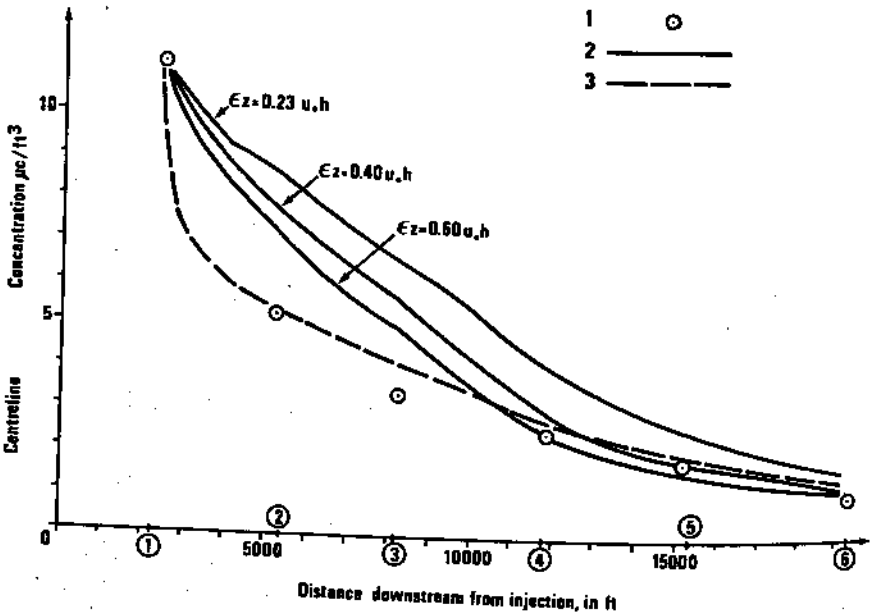

Fig. 8.14. Clinch river dispersion experiment. 1, Measured concentrations; 2, method of Holly and Preissmann (1977) for various values of ϵ_z; 3, method of Leendertse (1970) for $\epsilon_z = 0.23\ U_*h$

The two lower solid lines in Fig. 8.14 show the results of the Preissmann method with $\epsilon_z = 0.40U_*h$ and $0.60U_*h$, which accentuate the dispersion and yield predictions which are somewhat closer to the measured values. Even with such relatively large values of ϵ_z, the simulation is obviously unable to reproduce the rapid drop in concentration from $x = 2260$ ft to $x = 5170$ ft. The reason for this is probably that the measured *centreline* concentration at $x = 2260$ ft was assumed in the model to apply to the entire cross section as if it were the injection point, when in fact the centreline concentrations were already leading the rest of the cloud, and diffusing transversely into clear water. (Paradoxically, Leendertse's strong initial artificial dispersion seems to compensate for this behaviour quite well but, being physically wrong, would have led to false results in predictive use of the model.)

It is also instructive to compare the observed and calculated time-histories of centreline concentration at $x = 8170$ ft, as shown in Fig. 8.15. We note first of all that the Preissmann and Leendertse predictions peak at 21 and 15 min, respectively, before the observed distribution, indicating that the measured velocities assumed to apply to the reach 2260–8170 ft were not truly representative of conditions throughout the reach; additional model calibration would normally be necessary to correct this error (*see* Chapter 5). The oscillations in the Leendertse method are the manifestation of its numerical

dispersion; we see that even though the maximum concentration is predicted reasonably well, the shape of the predicted distribution is quite distorted compared to the observed one. The Preissmann method overpredicts the peak concentration by a similar amount, but the shape of its predicted distribution resembles quite closely that of the observed curve.

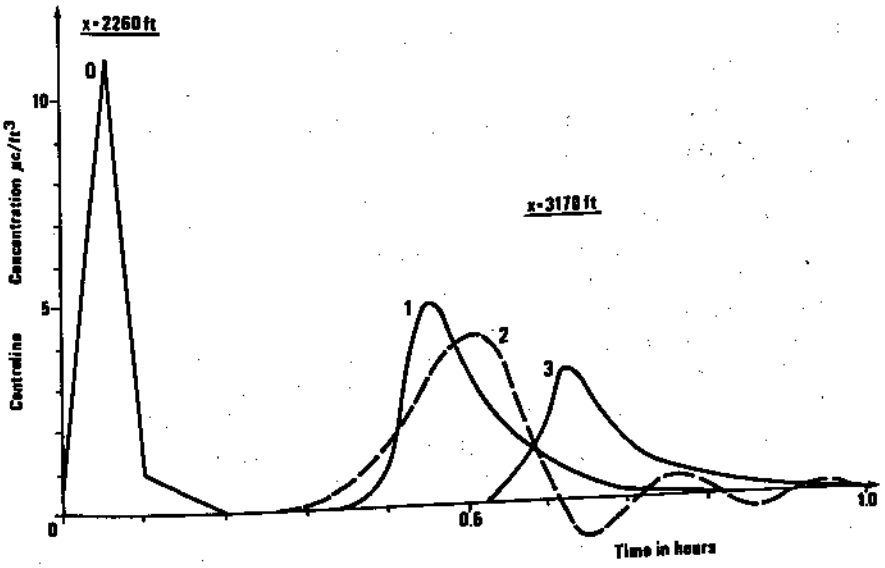

Fig. 8.15. Clinch river dispersion experiment. 0, Upstream concentration distribution; 1, method of Holly and Preissmann (1977), $\epsilon_z = 0.60U_*h$; 2, method of Leendertse (1970), $\epsilon_z = 0.23U_*h$; 3, measured distribution

Considerable attention has been devoted recently to the so-called 'tails' of one-dimensional concentration distributions – in Fig. 8.15, the measured distribution's 'tail' is the portion from, say, $t = 0.75$ h onward, where the concentration does not drop back to zero immediately after the passage of the main cloud, but remains relatively high for some time. Various so-called 'dead zone' models have been proposed to explain these tails as the result of tracer being trapped in the boundary layer and later released back into the main flow (*see*, for example, Petersen (1977) or Valentine and Wood (1977). While the dead zone theory undoubtedly represents a real physical process, it is interesting to note that the Holly and Preissmann prediction of Fig. 8.15 displays a tail which is qualitatively similar to the observed one. In the model there is neither dead zone accounting nor appreciable numerical error to explain the computed tail. We conclude that such tails can be at least partly explained by the fact that once the main tracer cloud has passed a point at the centre of the river,there is re-diffusion of tracer from the slower waters near the banks back towards the

centre. If convection in each tube is well computed, then it is possible to reproduce this re-diffusion process which feeds the observed tails. Only a two-dimensional model can reproduce this essentially two-dimensional phenomenon; it should not be forgotten that the dead zone accounting of a one-dimensional model can only partially explain the observed tails.

8.11 ESTIMATING THE TRANSVERSE DISTRIBUTION OF LONGITUDINAL VELOCITY

We have seen in this chapter that dispersion of a tracer which is fully mixed over the flow depth is essentially a two-dimensional phenomenon. The one-dimensional simplification of the process as described in Section 8.3 is based on an overall longitudinal mixing coefficient K_x whose value depends on the transverse distribution of velocity, $u(z)$, as seen in Equation (8.9). Two-dimensional models, described in Section 8.8, also require that the transverse distribution of velocity be taken into account in the dimensioning of stream tubes. On occasion measurements of the distribution of $u(z)$ are available for particular flow conditions, but in general we must construct a transport model based only on the results of a one-dimensional flow model. The problem, then, is how to generate the distribution $u(z)$ when only gross flow parameters are available.

A one-dimensional flow model, as described in Chapter 4, is constructed using known channel sections, that is to say, the transverse variation of bed elevation $y_b(z)$ is known at each computational point. The flow model results furnish the discharge Q, the water surface elevation y, and the energy slope $S_f = \frac{Q^2}{K^2}$ for each computational point, K being the overall section conveyance which is a predetermined function of y if the cross section shape and roughness distribution within it are known.

If we assume that the energy slope is the same for all points in the cross section, and we apply the Strickler equation locally to different points within the cross section, we can calculate an estimated $u(z)$ distribution. If $h(z)$ is the local flow depth, that is to say

$$h(z) = y(z) - y_b(z) \tag{8.36}$$

then we write the Strickler equation as

$$u(z) = k_{str}(z)\, h(z)^{2/3}\, S_f^{1/2} \tag{8.37}$$

$k_{str}(z)$ being the transverse distribution of bed roughness. The application of this procedure to each known cross section yields a rough estimate of the velocity distribution needed for Equation (8.9) or for stream tube dimensioning. It is however important to recognize the approximate nature of this calculation; the rate of energy loss per unit length of channel is probably never really constant all across the cross section, and moreover the transverse distribution of roughness

can only be roughly estimated. Nevertheless this assumption is compatible with one-dimensional propagation models.

Figure 8.16 compares the measured $u(z)$ distribution at one of the known

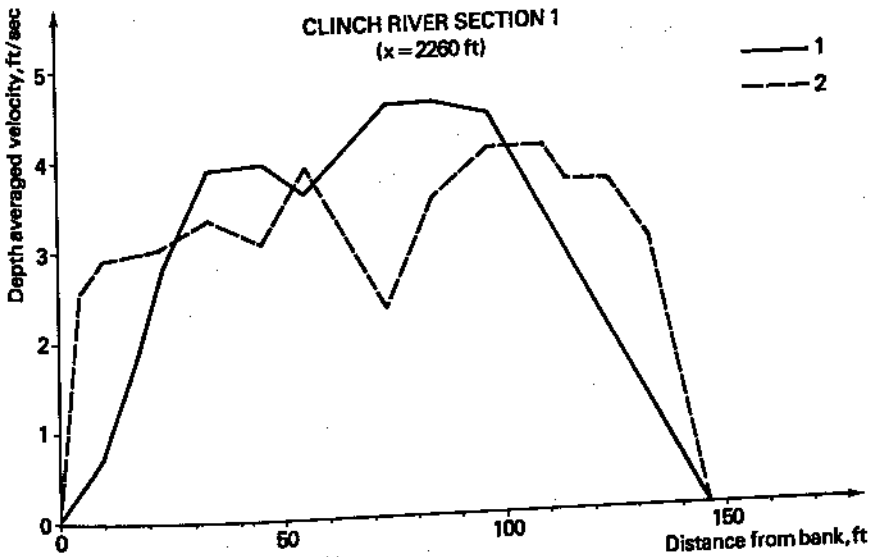

Fig. 8.16. Transverse velocity distributions in Clinch river at section 1, $x =$ 2260 ft. 1, Measured velocity distribution; 2, calculated velocity distribution, Equation (8.32)

cross sections of Clinch River with a distribution computed using Equation (8.37), assuming that the bed roughness was the same throughout the section. We note that the computed $u(z)$ distribution is more uniform than the measured one, in that it gives larger velocities near the banks. Figure 8.17 compares the results of a full dispersion calculation of Section 8.10 using the computed and real distributions, both for $\epsilon_z = 0.23U_*h$. As we might have anticipated, the computed velocity distribution's relative uniformity results in less dispersion; this is entirely consistent with the notion of dispersion being the interaction between turbulent diffusion and *differential* convection. The simplified procedure in Equation (8.37), especially if applied using $k_{str}(z) =$ constant, tends to reduce differential convection by producing a more uniform velocity distribution.

Another example is the reproduction of the Vienne River experiment using computed $u(z)$ distributions, since no measurements of $u(z)$ were available. (The original study used a one-dimensional model with a calibrated K_x coefficient, *see* Section 8.7).

A two-dimensional model was constructed by assuming that the measured cross section at Pilas was representative of the upstream half of the reach, and that the measured section at Chabanais was representative of the down-

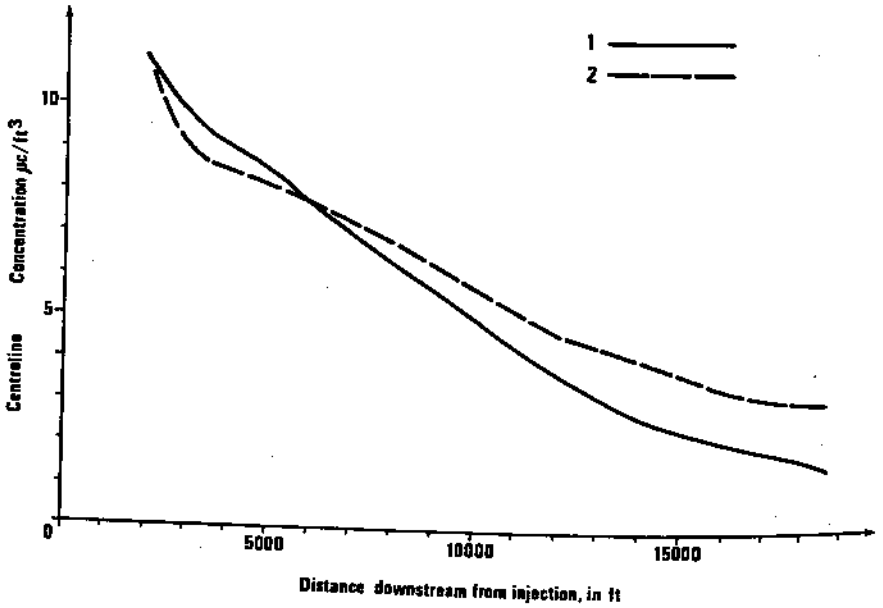

Fig. 8.17. Effect of using measured and computed velocities in Clinch river dispersion simulation. 1, Measured velocities, $\epsilon_z = 0.23U_*h$; 2, computed velocities, $\epsilon_z = 0.23U_*h$

stream half. The known discharge and downstream water level were used along with the Strickler coefficient of 25 determined by the authors (Chevereau and Preissmann, 1971) to perform a backwater calculation through the reach. Equation (8.37) was used to estimate the transverse velocity distributions throughout the reach.

The Vienne experiment is a particularly interesting one to model because the concentration distributions at Pilas and Chabanais were measured at several points within each cross section. The Rhodamine dye was injected several kilometres upstream of Pilas, but the cloud was far from being fully mixed over the cross section even at Chabanais. The observed non-uniform distributions were put into the two-dimensional model as the upstream boundary condition at Pilas. Transverse and longitudinal mixing coefficients of $\epsilon_z = 0.23U_*h$ and $\epsilon_z = 5.9U_*h$ were used for lack of any other detailed information on the reach.

Figure 8.18 shows the results obtained using the Holly and Preissmann method and the same two-dimensional program as applied to the Missouri and Clinch River experiments. Also shown for comparison are the 1-D simulation results of Fig. 8.10. All concentrations shown are cross-sectional averages, even though the two-dimensional model actually furnished a different curve for each stream tube. We see that even with estimated velocities, the two-dimensional model predicts the peak concentration at Chabanais within 15% of the observed value, although this peak arrives about 35 min before the observed one. The one-dimensional model peak concentration is within 5% of the observed value, and

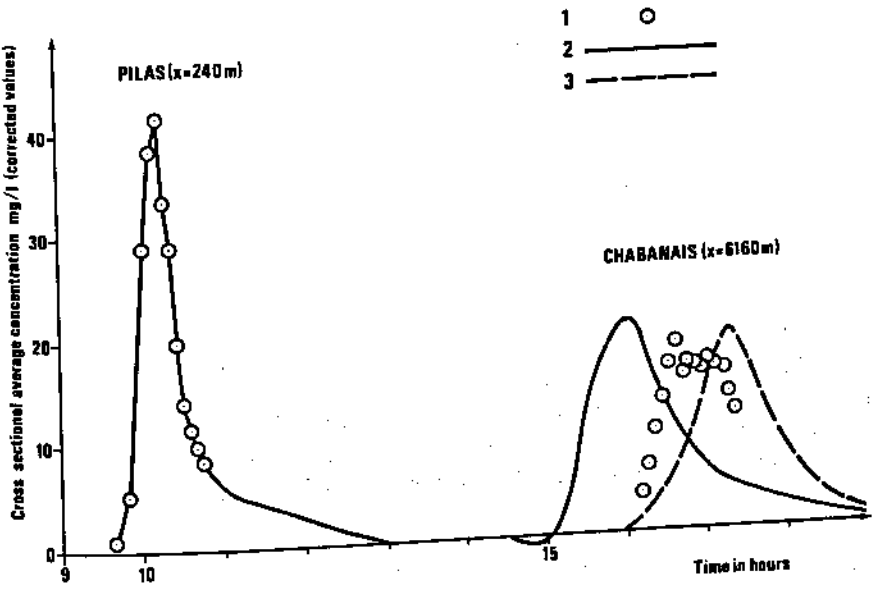

Fig. 8.18. Simulation of Vienne river dispersion experiment using a two-dimensional model. 1, Measured concentrations; 2, two-dimensional model ($\epsilon_z = 0.23U_*h$, $\epsilon_x = 5.9U_*h$, computed velocities); 3, one-dimensional model ($K_x = 20U_*h$, measured velocities)

arrives about 40 min later. It is important to remember, however, that the one-dimensional model's $K_x = 20U_*h$ is a *calibrated value based on the experiment itself*, whereas the two-dimensional model required only hydraulic data.

8.12 CONCLUSIONS

If there is one central conclusion to be drawn from the various examples we have presented, it is this: one must never lose sight of the fact that in 'calibrating' mixing coefficients so as to better reproduce observed concentrations, he may only be compensating for numerical simulations errors and/or incomplete hydraulic data. The more accurate the numerical method used and the more faithful the schematization of the physical flow field, the better the chance that one can find mixing coefficients which are representative of real physical phenomena.

9 Special applications

The purpose of this chapter is to describe briefly several fields of application which, by virtue of their unique problems, can be considered as special applications of the modelling techniques we have been describing. Each of these applications could easily be the subject of an entire book; our intention here is just to show how they relate to ordinary river network modelling. These fields are:

- Flood forecasting and prediction
- Simulation of dam break waves
- Unsteady flow modelling in storm drain networks

9.1 FLOOD FORECASTING AND PREDICTION

River flow modelling for flood prediction and flood forecasting purposes is subject to some special requirements compared to ordinary flood simulation models. As we described in Chapter 4, flood simulation models, built in order to study flood wave propagation through a hydrographic network, are mainly used for flood protection and control studies, estimation of maximum discharges and stages and their times of arrival at different points of the network, determination of the extent of flooded zones, duration of submersion, flood damages, effectiveness of dyke protection, dams, floodways, etc. As a simulation model is a tool of analysis, it may be as complex as needed; its accuracy may be as high as allowed by the quality of calibration data, and it is never run on a real time basis. It is exploited in the consultant's office, where a highly qualified staff and powerful computer are available.

Now we come back to flood forecasting and prediction models, which are based on an essentially different concept. The state of flow in the hydrographic system (watershed plus propagation channels) is known at some updating time tu_1; nothing is known beyond that time, and yet it is necessary to predict the evolution of flood variables (water stages and/or discharges) at certain points of the hydrographic system until some time $tu_1 + T_f$, where T_f is called the fore-

casting interval. Moreover, at some time after tu_1 a forecast concerning this evolution is to be issued. The purpose of the forecasting model is to give a warning with adequate lead time, and to do so during the entire duration of the flood at specified intervals of time. The model must be run during the flood, since it uses real time indications, and therefore it is subject to constraints such as:

- communication with on-line measuring and data transmission equipment;
- constant availability, best guaranteed by implementation of the computer (or appropriate terminal) and software at the forecasting centre;
- capability of giving reasonable estimates of data which are missing but necessary for the prediction;
- necessity of rapid computation methods to give enough lead time;
- high reliability of both the computer and the software.

The reader is of course aware that a complete prediction model for a river basin would usually include a hydrologic model of the watershed, furnishing a simulation of rainfall-runoff mechanisms and thus providing inflows for the hydraulic simulation. In fact, when the hydrographic network of a basin is extensive enough, the prediction consists of two steps:

(i) estimation of the discharges entering the different propagation channels from the watershed using a hydrologic model;

(ii) computation of the evolution of the resulting flood waves as they propagate along the channel network using a hydrodynamic model.

For small basins the first step is sufficient and the only one which matters. For large river basins such as the Mekong or Niger, along which the flood, rising in the upstream mountainous basin, propagates during several months, the first step may be irrelevant for the prediction concerning the stations located 1000 km downstream. In what follows we shall discuss only the second step, concerning modelling of flood wave propagation.

Let us consider a river basin such as shown in Fig. 9.1. Point A is a gauging station at which water stage is continuously recorded and transmitted to the

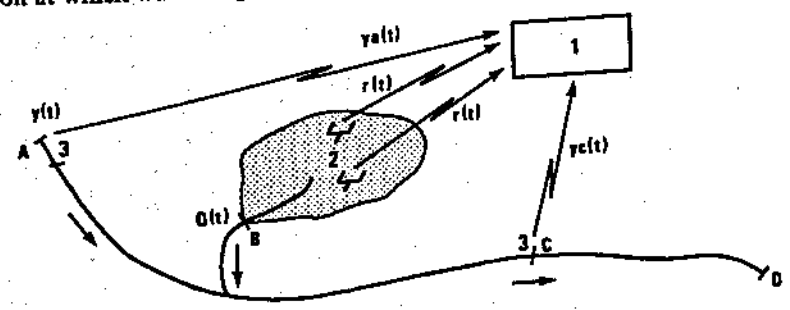

Fig. 9.1. Flood forecasting network in a river basin. 1, Forecasting centre; 2, transmitting rain gauge; 3, transmitting stage recorder

forecasting centre. Point B is the outlet of the shaded smaller basin, a tributary which flows into the main river. Rainfall recorders within the basin transmit rainfall amounts to the forecasting centre, which has a hydrologic model of the basin at its disposal and uses it to transform the rainfall into the tributary discharge at point B. For all practical purposes, as far as the river itself is concerned, the discharge hydrograph $Q(t)$ is given at location B and the measured stage hydrograph $y(t)$ is furnished at A.

The model purpose is to forecast flood conditions at location C on the basis of these two upstream inputs. In what follows, we assume that the flow simulation system is a well-calibrated hydrodynamic model of the watercourse with upstream boundary conditions at A and with an outflow boundary condition at D, sufficiently far downstream so as not to significantly influence flow conditions at section C, for which the forecast is to be made. Suppose that the forecasting operations begin at some time tu_0 where tu_i represents updating times, $i = 0, 1, 2, \ldots$ Based on estimated upstream inputs at A and B for the period tu_0 to tu_1, the propagation model predicts the evolution of the flow variables at C for the same period. At time tu_1, therefore, forecasting personnel have two hydrographs at C available; the computed one, and the observed one as shown in Fig. 9.2c. If the propagation model is well calibrated, the difference between the two hydrographs is essentially due to errors in originally estimated inputs for A and B for the period tu_0 to tu_1. The updating process consists in first correcting the state of the entire model at time tu_1 to account for known (by now) inputs at A and B up to tu_1, then simulating the period tu_1 to t_4 so that the calculated hydrograph at C up to t_4 can be issued as a forecast. Now let's consider these two operations in more detail.

The transmission of recorded flow data at A, B, and C for the period tu_0 to tu_1 begins at tu_1 and is completed at t_1, at which time the model operator can begin his updating operation. First, he repeats the propagation calculation for the period tu_0 to tu_1 using the *known* values at A and B as input. If the model is well calibrated, this calculation will reproduce the known hydrograph at C with very little error, and moreover, the computed water levels and discharges in the entire model will be close to real (though unmeasured) values at time tu_1. This computed state, which will serve as the initial condition for the upcoming forecast calculation, could of course be obtained by measurements of stages and discharges all along the river at tu_1, but this is obviously unrealistic – a well calibrated model supplies these data with high reliability and lower cost. Nonetheless, the influence of an ungauged tributary upstream of C may make it difficult to obtain a correct computed initial state; successive trial runs may have to be performed using different assumed tributary inflows until the hydrograph accuracy at C is satisfactory.

In parallel with the initial state calculation for time tu_1, forecast personnel use their meteorological data and possibly a hydrologic model to estimate the probable evolution of input data at A and B from tu_1 to t_4. As soon as these estimates are ready, the new forecast calculation is run, i.e. flow in the model is simulated from tu_1 to t_4 using the updated initial state at tu_1 and estimated

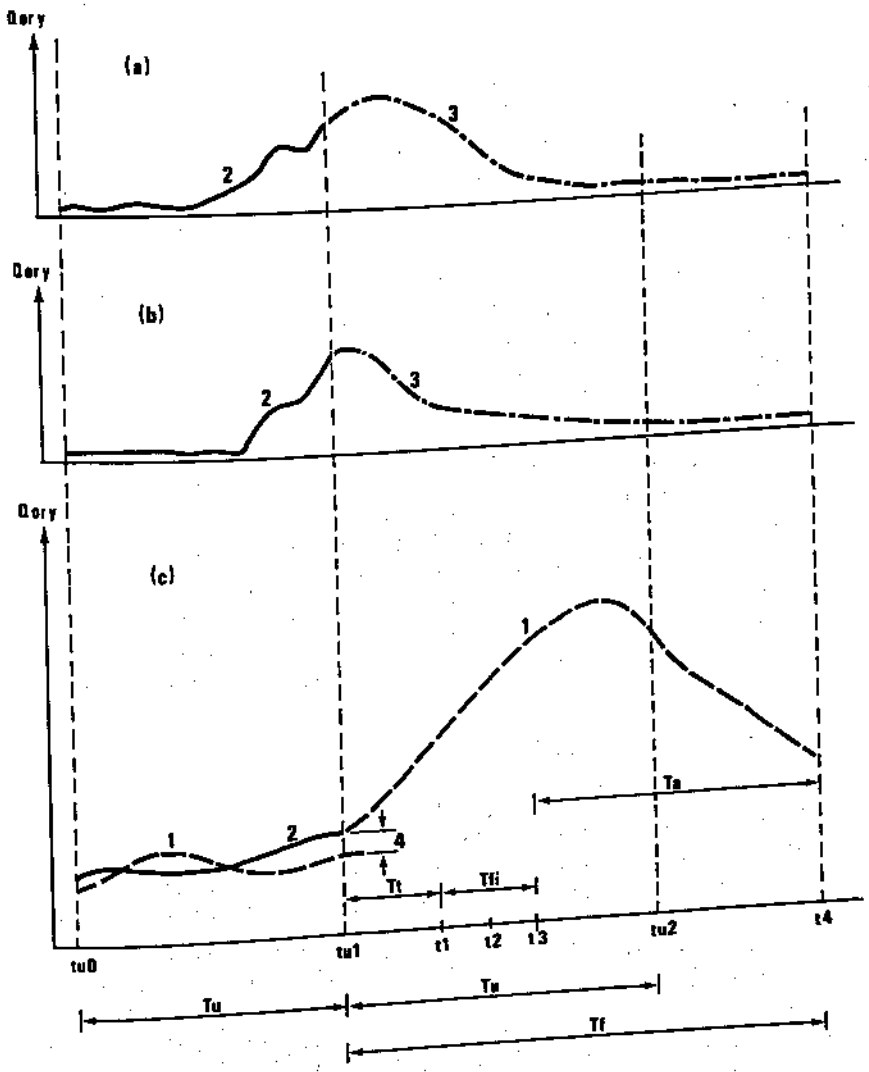

Fig. 9.2. Example of flood forecasting in the river basin of Fig. 9.1. (a) Discharge or level hydrograph at station A. (b) Discharge or level hydrograph at station B. (c) Discharge or level hydrograph at station C. 1, Computed by model based on forecast input data; 2, recorded and transmitted to forecasting centre; 3, forecast input data; 4, forecast error (*Tu* = updating interval; *Tf* = forecasting interval; *Tt* = transmission interval; *Tfi* = forecast issuing interval; *Ta* = time advantage)

inflows at A and B. The calculation is completed at time t_2 and the forecast is issued at time t_3, the delay from t_2 to t_3 being needed to prepare the forecast for C from the computed results and transmit it.

The forecasting interval T_f is usually many times longer than the updating interval T_u. Indeed, the situation shown in Fig. 9.2 would be unacceptable in real life since the interval T_u is so large that all accuracy is lost. The length of T_u depends upon the rapidity of fluctuation of variables and on the forecasting centre's capabilities. A typical updating interval for most large European rivers would be from 6 to 24 h with a forecast interval of 12–72 h. For rapidly rising floods the desired T_u interval may be of the order of 30 min, but if the time necessary to update the model, to compute and to prepare the forecast (forecast issuing interval $T_{fi} = t_3 - t_1$) is of the same order of magnitude or longer, such an updating frequency makes no sense.

Before going further, we would like to stress the fact that the forecasted variable at C may be either $Q_c(t)$ or $y_c(t)$. Since forecasting techniques have their origins in hydrology (for example, many of the above concepts and terminology are those used by the World Meteorological Organization) and because hydrologists usually work with discharges, it is often implicitly assumed that the forecast variables should be discharges. But as has already been said in previous chapters, most often we are much more interested in water stages, and if the $Q(y)$ rating curve is not single valued, the two variables may not be equivalent at all as far as forecasts are concerned. This must be kept in mind not only when choosing the forecast variable, but also when selecting a modelling technique to be used for the prediction operation as we shall see further on.

Strategy for implementation of forecasting models

The need for real-time model operation and initial state updating usually precludes the use of large computers and highly specialized personnel for flood forecasting. The possibility of easy access to powerful computers exists nowadays in more industrialized countries, but even there, forecasting centres prefer generally to have their own more modest equipment. Decreases in the cost of computer core memory may make it theoretically possible to have powerful computers and sophisticated models at forecasting centres in the near future, but even then it is doubtful, barring some exceptions, that forecasting centres would want or be able to employ technicians fully capable of dealing with very sophisticated models. And even if this were the case, such technicians would of course occasionally be on holiday, out of town, or in bed the night of a catastrophic flood. Therefore the prediction tools must be as simple as possible, and the shorter the time advantage T_a (*see* Fig. 9.2c) the simpler must be the tool. One may use a very complex prediction tool for rivers such as the Mekong, Niger, or Mississippi for which the forecasting interval T_f would be of the order of 10 days. Such a solution is unacceptable when T_f is of the order of only several hours, in which case the rapidity of the process of recording basic information → transmission → computation → forecast is more important than the accuracy. Consequently engineering practice relies heavily upon simplified models and small computers, typically desk computers with 8K to 16K word core memory (1979) and a small printer. Such models are most often based

upon the Muskingum method or one of its variants such as SSARR or the Kalinin–Miljukov method (*see* Miller and Cunge, 1975) or upon level gauge correlation. However, the use of models based on simplified equations may lead to difficulties in practice, most often because of one of two factors: developments in the river basin and the limited range of applicability of simplified methods.

As we described in Chapters 2, 3 and 4, simplified methods are predictive only as long as the inputs stay within the range for which the model has been calibrated, and as long as the system itself does not change. Suppose, for example, that a forecasting system using the Muskingum method was built for a river basin, and then a series of hydraulic works (dams, dykes, etc.) changed the river's flow characteristics. The forecasting system might well become useless and, in order to have enough new calibration data for a simplified approach, it might be necessary to wait 20 years. As for a simplified model's range of applicability, we pointed out in Chapters 2 and 4 that simplified equations can describe the flood propagation along steep rivers reasonably well, but cannot be used when the longitudinal free surface slope is small. It is not at all clear where the borderline should be located between complete and simplified methods, but it is next to impossible to estimate the error introduced by using a simplified method for a river having an intermediate slope (say about 0.1 m km^{-1}). Clearly, models based on the full de St Venant equations are free of such applicability limits since they are valid for the entire range of riverine slopes and have the capability of representing any future development in the basin (dykes, dams, etc.).

The above difficulties in application of simplified models have led engineers to use a three-step strategy in their development and implementation of important forecasting systems.

(i) First a detailed model based on the full de St Venant equations is built, and is calibrated with all available data just as is a usual flood simulation model. Being based on the full equations and sound physical hypotheses, the model allows not only for the simulation of exceptional, unrecorded events beyond the range of calibration, but also for the inclusion of river system modifications such as dams, dykes, etc., without the loss of its essential predictive capacity.

(ii) A simplified model is conceived for use in the forecasting itself. To that end several possible methods are studied (such as Muskingum, SSARR, gauge correlation); each of them is tested using the complete calibrated model in (i) to simulate flood events, and their respective applicabilities and forecasting capabilities are assessed. Once the simplified method to be used is chosen, its coefficients are calibrated by repeated use of the full model. Then the real-life system (flood forecasting on a small computer using a simplified method, recording of input data, transmission, lack of data at some input stations, random transmission incidents, etc.) is simulated in order to check its applicability and improve its efficiency.

(iii) The simplified model is implemented on the smaller computer at the forecast centre.

When such a strategy is used, one benefits from the efforts of the specialized and qualified staff who built and operated the full model using a powerful computer. This model is then maintained in operating condition – an action which allows for quick revision of the simplified model. The revision is either periodic, based upon every year's forecasting experience, or exceptional, when the river is modified in a significant way. With such a strategy, the forecasting system is a durable investment which is useful for studies of future developments and their consequences thanks to its foundation in a full-equation model.

Particular calibration and sensitivity study problems

A flood forecast is usually made for only a few points, and not all of the flood's characteristics are of interest to the forecasters; for example, maximal water stage, or the time when it occurs, may be of interest, but the sequence of events which occur before the water stage attains some fixed alert elevation is of no direct interest to the forecaster. Nevertheless, the calibration phase of the full-equation model must treat the full range of flow events. Thus it is most important to establish the propagation times of discharge coming from different tributaries and watersheds of the basin, as well as their respective weights in the formation of the flood wave. The simulation of a large number of elementary, fictitious floods coming from different parts of the basin and propagating upon different states of the system (different ways of filling up of the storage volume of the river network) is necessary for the evaluation of the significant lumped parameters of the simplified model. Such simulations also make it possible to group together some parts of the basin (thus limiting the number of reaches) and to define the physically significant time step for the simplified model. Such computations allow also for the definition of the maximum forecast interval T_f beyond which forecasting of the concerned flood variable is useless, and thus to remove from the simplified model all the upstream part of it which does not influence the forecast variable within this T_f interval. Of great help in the calibration of the simplified model are propagation times, which may be roughly estimated from steady state backwater curves. Indeed, when inertia terms are neglected in the flow equations, the propagation time along any reach can be expressed by

$$\frac{dV}{dQ} = T(Q) \tag{9.1}$$

where V = volume stored in a reach; Q = steady state discharge. The curves $T(Q)$ are readily constructed from the steady state water surface lines computed with the full de St Venant model.

The simplified model calibration should also include the definition of the network of input data stations. The network should be as limited as possible, but it must be able to give a complete picture of flood development. The simulation runs may well also lead to elimination of some existing stations or to the implementation of other new stations. The network must then be tested by

simulation as to the loss of information: the forecast should not be jeopardized because one or two stations are out of order during a flood. Expressed differently, one must know which stations must be kept operational at any price. This information is obtained by simulating floods with the full model and with a variable number of input data stations. Once the sensitivity of the system is determined, the simplified model is calibrated using minimal configurations. In an analogous manner, the updating interval T_u to be used during the forecast operations themselves is defined.

9.2 SIMULATION OF DAM BREAK WAVES

It is the extreme rapidity of variation of water stages and velocities that makes simulation of unsteady flow due to dam failure a special case of river flow modelling. In spite of scores of published papers and studies on the subject, numerical methods for simulation of the problem remain controversial and the results are, if not suspect, at best only roughly accurate. To the authors' best knowledge, the problem of simulation of dam break wave propagation has not been solved for the general case; every particular situation must be examined separately before a modelling method can be chosen.

The purpose of this section is to point out some difficulties in numerical modelling of the phenomenon and especially to underline the differences between modelling of flood waves and dam break waves. In many practical cases these differences are negligible. For example, when one considers the failure of a dam on a very wide river where there is no possibility of total and instantaneous obliteration of the dam, the wave resulting from a catastrophe such as a partial breach is much more like a rapid flood wave than anything else. In such circumstances we can compute its propagation with a modelling system appropriate for the solution of the de St Venant equations, such as one used for the simulation of rapidly varying flow in power canals (*see* Chapter 6). Such techniques are used whenever the hypotheses of partial breaching or not too rapidly varying flow (or topography) are acceptable. Indeed there have been studies of two-dimensional dam break wave propagation made with tidal wave propagation models, taking into account the variable limits of the modelled domain. We leave all such applications aside here since they follow the general rules of modelling explained in Chapters 4, 5 and 6. We will limit ourselves to the case of instantaneous and complete failure of a dam built on a natural and rather narrow (mountain) river. Such a situation (complete obliteration of the dam) is not purely hypothetical: the Malpasset and Teton dam failures are two only too real examples. At any rate, such cases are considered to be the most dangerous.

Physical description of the phenomenon and governing equations

When a dam collapses, the water retained behind it begins to move; the wall of water 'rotates' at the dam section, as shown in Fig. 9.3. After the initial phase of

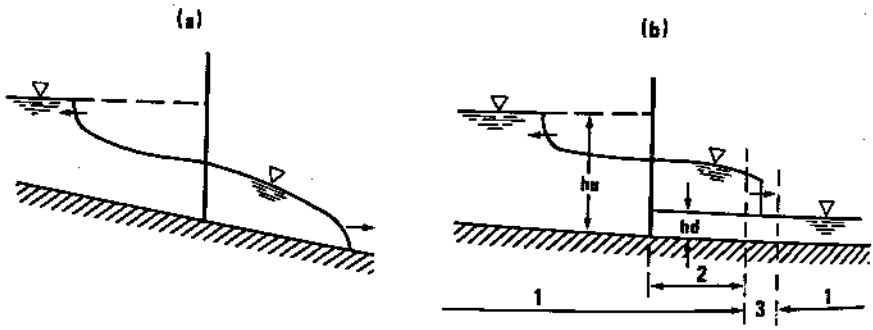

Fig. 9.3. Two types of dam break waves. (a) Propagation on a dry bed. (b) Propagation on an initial depth. 1, One-dimensional flow described by the de St Venant equations; 2, possibly supercritical flow, if $hd/hu < 0.14$; 3, wave front region, treated as a discontinuous bore advancing on a finite depth or as a tip wave advancing on a dry bed

acceleration, a negative wave is created upstream of the dam and propagates along the reservoir with a celerity depending upon the topography. The negative wave corresponds to the volume evacuated as a positive wave propagating downstream, advancing either on a dry bed, or on a water depth corresponding to the downstream flow before the failure. The downstream initial conditions are of decisive importance as to the character and behaviour of the positive wave. If the wave propagates on a dry bed, its front has very strong curvature near its tip as shown in Fig. 9.3a. The celerity of the front is equal to the velocity of the water particles situated immediately behind it. If the wave propagates on some initial depth of water, its front is much more like a mobile hydraulic jump (bore) which may be most conveniently schematized as a sharp discontinuity with two different water stages and two different discharges at the same longitudinal point, as seen in Fig. 9.3b.

Generally the flow in the reservoir is subcritical, at least until the negative wave reaches the upstream limit of the reservoir. After that time, it all depends upon the reservoir's topography (longitudinal slope) and upon the discharge entering it through the upstream section. As for the flow downstream, its character depends upon the topography of the valley and also upon the initial depth of water downstream of the dam. For a rectangular frictionless cross section, if the ratio of the initial downstream depth to the initial upstream (reservoir) depth is less than about 14% (the exact solution of the analytical case being 0.1384), the flow downstream of the dam after its failure will be supercritical (Stoker, 1957). Otherwise it will be subcritical. An analogous criterion may be derived for a valley of arbitrary shape (by using the average depths, $h = A/b$, rather than local depths). The character of the flow may of course change farther downstream as a function of the topography; variations in cross-sectional shape may well create, in addition to singular head losses, abrupt changes in water stage, from which reflected waves may transform themselves

into discontinuous shock waves (bores) propagating upstream, etc.

In general, in a natural valley, the flow will be three-dimensional and, strictly speaking, should be computed as such. During the first stage of the flow development, any two-dimensional schematization is inaccurate since vertical accelerations and velocities predominate over horizontal ones. Realistic simulation of this first stage of the phenomenon is always too difficult or too costly; moreover, engineers are more interested in what happens several minutes after the break than in what is going on during the first seconds. Therefore this initial phase is neglected in all existing models. Computations begin with an initial situation, which, for most cases is defined according to the one-dimensional concept depicted in Fig. 9.3b and discussed below. Clearly, if such a simplified concept is acceptable for most valleys because of the dominance of horizontal velocities, it is not really applicable when the valley is composed of a series of narrows and enlargements. Nor is it valid for the computation of the front itself, in the neighbourhood of which vertical accelerations cannot be neglected and often an undular jump is observed.

In the light of the above discussion, one is tempted to ask, why bother with a computational concept which is so far from reality? Indeed, whenever three-dimensional (and even two-dimensional) phenomena prevail, and if one is interested in their consequences, a hydraulic scale model will give a more faithful simulation than a computation. However the dam break wave may propagate along distances of tens and sometimes even hundreds of kilometres; no physical model may be built to simulate such long distances unless it is distorted so severely that its results are even more suspect than those of a computation.

As shown in Fig. 9.3b, the de St Venant equations are assumed to be valid for the zones upstream and downstream of the front. Clearly the inertia terms in these equations cannot be neglected – the extreme rapidity of water stage and discharge variations in time and space (*see* for example Fig. 9.4 where the stage

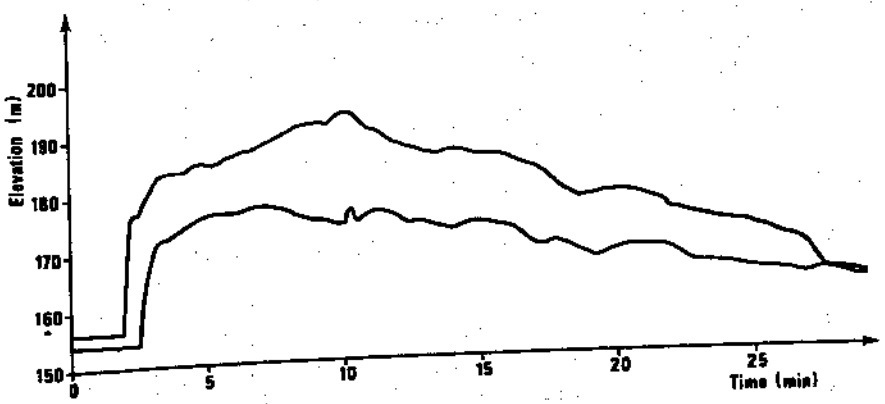

Fig. 9.4. Stage hydrographs at two points in a natural valley downstream of a dam break (time in minutes)

hydrographs in a natural valley are shown) requires that the derivatives $\partial u/\partial t$ and $\frac{\partial}{\partial x}(u^2/2g)$ be taken into account. Consequently any method based upon simplified equations would be inapplicable. Moreover, the divergent form of the flow equations should theoretically be used because of the important role played by momentum in the phenomenon (*see* Chapter 2).

As for the front itself, the Rankine–Hugoniot equations properly describe the transition between unsteady gradually varied flow on both sides of the discontinuity if it propagates upon some non-zero depth of water. When the front propagates on a dry bed, special equations describing the phenomenon should be used (expressing equality of the celerity of the front and the water velocity behind it).

Because of the strongly non-linear character of the equations and of the variation of cross-sectional shape along the valley, secondary shocks and discontinuities appear between the main front and the upstream boundary of the model. As was shown in Chapter 2, the de St Venant equations lead to such discontinuities but cannot describe their evolution. Therefore techniques analogous to those used for the principal front should be applied; secondary shocks are in fact quite well described by the Rankine–Hugoniot conditions. The standard method of approach of this type is a one-dimensional mathematical model based on a numerical integration method which allows either for a discontinuous or a weak solution (*see* Chapters 2 and 3) at the front. The flow behind the front is then computed on a strictly one-dimensional basis. This hypothesis, although generally used, is of course simplistic. Natural valleys are very irregular and most often present a series of contractions and abrupt widenings. They often meander and the associated curvature invalidates the hypothesis of a horizontal free surface at a given section. Phenomena such as undular mobile jumps, oblique shocks, extensive dead water zones and horizontal vortices which must form are not taken into account. Chervet and Dallèves (1970) made the following pertinent observation after analysing the results of a survey of the valley downstream of Malpasset dam: at some points, because of the cross-sectional shape variations, the highest water level was that of the energy line elevation. In clearer terms, all the kinetic energy $u^2/2g$ was transformed locally into potential energy!

Computational problems

The typical approach to one-dimensional modelling of dam break waves is based on two steps:

(i) Given a known state of the system (water stages y and discharges Q) at time t, one computes first the new position of the front at time $t + \Delta t$. This is done using the method of characteristics jointly with the Rankine–Hugoniot relationships (Equations (2.68), (2.69)) or with appropriate equations for a front propagating on dry bed. New values of the flow variables Q and y at time

$t + \Delta t$ are then computed on both sides (or upstream only for dry bed) of the shock.

(ii) The new computed values upstream and downstream of the front, together with the boundary conditions at the model limits, are then used to compute the discharges Q and water stages y along the model for time $t + \Delta t$ by numerical integration of the de St Venant equations.

Although this general concept is simple, its practical execution is subject to considerable difficulties. The front computation itself, as described in Chapter 2, is clear, although its programming may be complex. Let us recall the relationships which are valid across a shock propagating on a finite water depth:

$$v = \frac{A_1(u_1 - u_2)}{A_1 - A_2} + u_2 \tag{2.68}$$

$$u_1 - u_2 = \pm \left(g \frac{A_1 - A_2}{A_1 A_2} (A_1 \eta_1 - A_2 \eta_2) \right)^{\frac{1}{2}} \tag{2.69}$$

$$\eta = \frac{I}{A}$$

where subscripts 1, 2 concern the variables behind and in front of the shock respectively, $Q = Au$ = discharge, A = cross-sectional area, η = distance from the centroid of the cross-sectional area to the free surface, v = celerity of the shock. The above formulation assumes that the shock is a vertical wall of water and that at the same location there are two values of discharge (Q_1, Q_2) and two water stages (y_1, y_2).

The new position of the shock at time $t + \Delta t$ usually does not coincide with the points for which data are known; hence it is necessary to interpolate geometrical features $A(x, y)$ and $I(x, y)$ of the valley between known cross sections along the x-axis. The modelling system must provide for this interpolation and for the introduction or computation of functions A and I.

The method of numerical integration of the flow equations along the gradually varied flow reaches must be chosen with care. Indeed, it must be able to deal with zones of supercritical flow which may subsequently become subcritical, and with discontinuities (secondary shocks) which are created and propagate between the main wave front and the upstream limit of the model. The following numerical methods are used:

- pure method of characteristics with an arbitrary network of computational points in the (x, t) plane;
- method of characteristics on specified intervals;
- explicit finite difference schemes such as 'local characteristics', Lax, Lax–Wendroff;
- two step predictor (implicit) – corrector (explicit) finite difference method.

In theory the pure method of characteristics is the best one because of the clear and theoretically justified way it deals with supercritical flow and shocks. However, whenever several shocks are present, the programming of the method becomes extremely complex. In addition, it requires constant interpolation of geometric data in the (x, y) plane. Consequently we know of only one published case of its application, by Chervet and Dallèves (1970). The description of applications of other methods may be found in published references such as: Cunge (1970); Vasiliev (1970); Rajar (1972); Benoist *et al.* (1973); Colin and Pochat (1976). It must be said, however, that none of these methods may be considered as having given full satisfaction. The introduction of numerical dissipation (either implicitly, or explicitly through interpolation, pseudo-viscosity or 'dissipative operators') has the effect of smoothing the computed variables. If properly applied to the divergent form of the equations, this allows the simulation of secondary discontinuities by steep but continuous weak solutions (Chapters 2 and 3). Although the computation of supercritical flow with these methods is not really justified in theory, their practical application seems to lead to acceptable results. Finally, when used to compute schematic test cases (dam-break waves in a prismatic channel of constant slope and cross section), they furnish nearly exactly the same results in that the wave front celerity, water stage variations, and discharges are, within reasonable limits, the same for all methods. One exception is the Lax scheme which introduces an unacceptable amount of numerical damping.

If the same methods are used to simulate wave propagation in a real valley, the results may become completely different from one method to another. Schemes such as the specified interval characteristics of the Lax–Wendroff method, with a supplement of numerical pseudoviscosity, introduce enough damping to keep the computation running, but the continuity equation is not satisfied (we shall come back to this question later on). The predictor–corrector method, applied to raw geometrical data (i.e. without smoothing of natural slopes and cross sections), creates energy in the computational system: the energy line rises wildly along the valley, and most often numerical instability appears. It is interesting to note that the higher order schemes (predictor–corrector, Lax–Wendroff, etc.) not only conserve momentum and mass of water, but also maintain discontinuities which are not due to the non-linearity of the equations, but rather to the data. Whenever discontinuities in parameters such as longitudinal slope, width, cross-sectional area, etc., are encountered, they will be maintained and propagated by non-dissipative (higher order) schemes. The flow picture becomes unrealistic and moreover, instability may eventually develop. To avoid such situations a 'diffusive operator' is often imposed upon the results (Vasiliev, 1970; Colin and Pochat, 1976). An important question is how much arbitrary smoothing one is ready to accept and what confidence one may put in the results thus obtained. Another question may be asked as well: is it better to use raw data and smooth the results every second time step or to smooth the data first?

Still another important consideration is water volume conservation during

computations. Consider a dam break wave propagating along a natural valley on a finite depth of water. The shock celerity v may be as high as 20 m s^{-1}. The shock height is usually of the order of 1 or 2 m, but the rate of rise of the water stage behind the shock may be as high as 0.5–1.0 m s^{-1} in narrow valleys. Thus during one computational time step Δt of say 10 s, the argument y of the tabulated functions such as A, b or I may vary by as much as several metres. For irregular cross sections, the errors due to such interpolation are usually quite important. Another source of error is the variation of cross-sectional characteristics along the river valley; in 10 s the front may travel some 100–200 m, and the values of geometrical functions used to compute its evolution during that time are averaged between the two cross sections separated by that distance. Thus, for natural cross sections, the process is inherently inaccurate and mass conservation is not satisfied in the shock computation. The same comments are valid for the computation behind the shock. However, if a conservative finite difference scheme is applied to the divergent form of the differential equations, volume is of course conserved. That does not mean, however, that the results are better, since the interpolation still will yield fictitious variation of geometric features. If the method is not conservative in volume, continuity will not be satisfied. For example, Table 9.1, taken from Benoist *et al.* (1973) shows the volume loss phenomenon clearly. Analogous behaviour was observed by SOGREAH (private communication, 1979) using the specified intervals characteristic method.

Table 9.1 Variation of initial volume in %

Trapezoidal canal of 45 m length			Natural valley	
Method of local characteristics (explicit finite differences)		Lax–Wendroff method	Local characteristics 60 km	Lax–Wendroff 100 km
$\Delta x = 0.5$ m	$\Delta x = 0.10$ m	$\Delta x = 0.5$ m	$\Delta x = 100$ m	$\Delta x = 100$ m
−20%	−5%	−2%	up to −70%	−10% to +10%

In order to avoid such volume discrepancies, modellers have adopted various strategies in practical applications. One consists in piece-wise smooth representation of the geometrical data, which at least eliminates errors with respect to this representation (the conformity of the representation to reality is still another question). Such is the method adopted by Chervet and Dallèves (1970) and, probably, by Vasiliev (1970). Sakkas and Strelkoff (1976) developed a rational computational technique based on the method of characteristics applied to prismatic channels of general parabolic section. On that basis dimensionless graphs were prepared by Sakkas (1974) which permit

the estimation of the time of arrival of the flood-wave front, the maximum flood level, and the time at which the maximum flood level occurs after dam failure. It is possible to use the graphs if the natural valley may be schematized as a prismatic one; this procedure is used by the U.S. Army Corps of Engineers. The Laboratoire National d'Hydraulique (LNH), Electricité de France, has probably the world's most extensive experience in this domain, having computed more than 60 dam break cases, often with a cascade of dams, sometimes collapsing one after another (Benoist *et al.*, 1973). Geometrical features are however simulated at discrete computational points, so that when the valley widens or narrows abruptly, some smoothing of the geometry is inevitable. In Fig. 9.5 are shown the results of a dam break in a natural valley simulated by SOGREAH, where an approach similar to that of the LNH is used.

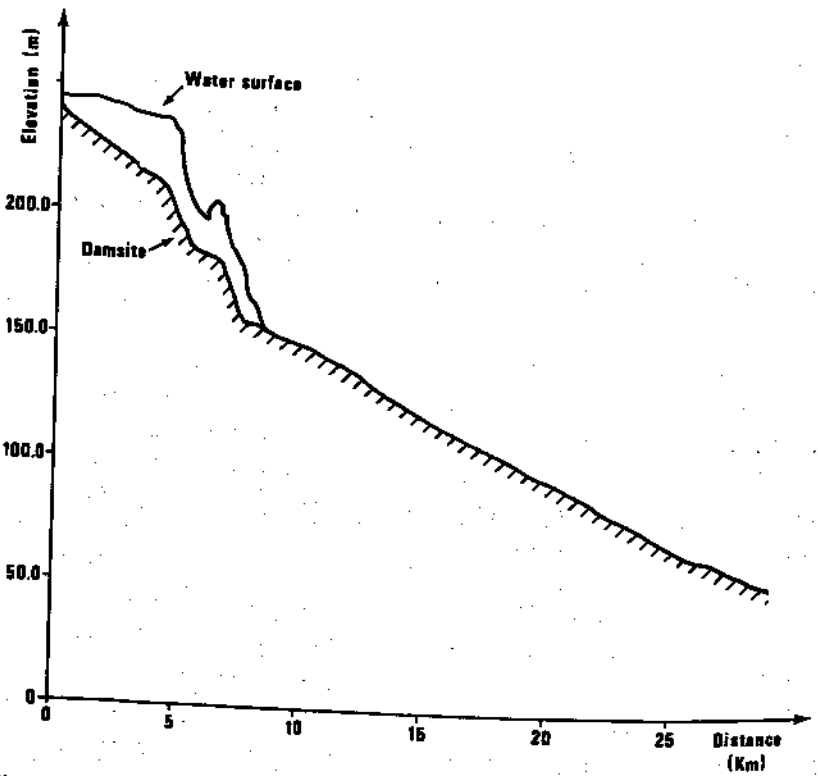

Fig. 9.5. Water surface profile downstream of a dam break (dam at kilometre 5.0; lower line represents bed)

The cost of dam break wave simulation is very high, in terms of computer time as well as manpower. Benoist *et al.* (1973) used 2 to 10 h of CDC 6600 computer CPU time to simulate wave propagation along natural valleys of 100–250 km length (presumably using the Lax–Wendroff method). Chervet and Dallèves (1970) used 5 h of CDC 6500 computer CPU time to simulate wave propagation along 9 km downstream of Malpasset dam (using the pure method of characteristics). SOGREAH's experience has shown that it takes about 5 h of

IBM 360-65 computer CPU time for a 50 km valley using a mixed specified interval characteristics/implicit predictor–corrector method. The operation of existing modelling systems is not always smooth. The modellers often have to reinitialize the computations after runs which, for one reason or another are prematurely aborted. The complexity of the topography and the cost of the study may even lead to the use of one method during the first stage of propagation (in the upper valley) and then a switch to a different algorithm when the wave attains the lower and flatter downstream valley.

In conclusion, dam break wave simulation has yet to undergo considerable developments before it will become a really reliable engineering tool like flood propagation modelling. Meanwhile, dam break modelling requires considerable effort during both the simulation itself and the interpretation of results. As for the future, efficient two-dimensional models are needed, and some first developments in that direction have been made – *see* for example Katopodes and Strelkoff (1978).

9.3 UNSTEADY FLOW MODELLING IN STORM DRAIN NETWORKS

Storm drain network modelling is in many ways closely related to river network modelling. The same basic hydraulic equations govern the flow, and the same general class of numerical methods is used. But there are nonetheless several particular and very important features of drainage network modelling which set it apart from river flow modelling – in fact, river flood propagation programs are seldom used for drainage network modelling, these differences being important enough to merit the development of special programs. The purpose of this section is to alert the reader to the special needs of drainage network modelling, and to review some of the modelling techniques used.

The role of unsteady flow modelling in drainage networks is one of simulation and verification of existing and/or proposed conditions. We make a distinction between this simulation role of unsteady flow models and the essentially design role of simplified methods, which automatically select collector pipe sizes using assumptions such as steady flow at peak inflow discharges, predetermined flow distribution in looped networks, and absence of backwater effects. While these design tools are capable of furnishing economic and generally correct guidance for pipe sizing in new networks, only an unsteady flow simulation model can verify the safety and economy of the design, and pinpoint critical flow situations needing further design attention. In the case of old, existing networks which are to be improved, expanded, or automated, the use of simulation models is an essential part of the planning and design process. In both cases, the engineer uses the model to simulate one or several storm events by furnishing input hydrographs (storm runoff) at a number of network inflow points, and observing the evolution of free surface (and piezometric) levels and discharges throughout the system.

A frequently-voiced objection to the use of drainage network simulation

models is the following one: 'Since I have such an imprecise knowledge of the urban hydrology processes which feed storm waters into the network, why should I construct an accurate network model which is itself subject to relatively little error?' This question was addressed by Chevereau, Holly and Preissmann (1978), whose conclusions can be summarized in two principal points:

(1) If the volume of runoff entering a drainage network can be accurately predicted, the simulation of flow in the pipe network is relatively insensitive to errors in the shape or time lag of input hydrographs.
(2) The value of a simulation model for comparing alternative development schemes does not depend on precise hydrological input data. The performance of the competing proposals can be compared for a range of assumed hydrological events which, though imprecise, reflect the general trends of past observed events.

In this section we limit our attention to truly unsteady flow models, and especially those which are capable of representing the effects of downstream influences in causing backflow, pressurization, etc. Yevjevich (1975) discusses the importance of taking such effects into account; we will come back to this point later on.

What, then, are some of the particular features of drainage network flow which impose special requirements on modelling techniques?

- Flow in pipes can pass alternatively from free surface to pressurized conditions and back again.
- The flow in and out of junctions, or nodes, does not follow predetermined directions. Reverse flow may occur in one branch due to the early arrival of storm flows in another branch adjacent to it.
- Backwater effects must be taken into account, especially for networks in flat regions having very little slope where downstream conditions can be felt throughout the system.
- Small depth situations, which must be treated carefully in river flow models (*see* Chapter 4), occur constantly in drainage system models. In fact, the initial condition of many simulations is an almost dry network.
- Drainage networks, especially old ones, are often looped (multiply connected) in the topological sense, thus requiring special solution algorithms (*see* Chapter 3).
- Special hydraulic features such as weirs, gates, pumping stations, singular head losses, storage basins, etc., abound in drainage networks, and industrial modelling systems must be able to simulate such situations easily.

We shall now briefly consider each of these points.

Pressurized flow

Insofar as modelling is concerned, the essential feature of pressurized flow is that

it has an extremely high wave celerity, c; c is infinite, in fact, in an inelastic system. In practical terms, this means simply that since there is no further storage volume available once a pipe is completely full, any change in discharge at the upstream end is immediately transmitted to the downstream end. This implies that explicit finite difference schemes, which are subject to the Courant condition for stability,

$$c\Delta t \leqslant \Delta x; \quad c = \left(g\frac{A}{b}\right)^{\frac{1}{2}} \tag{9.2}$$

cannot be used. As the width b approaches zero as a pipe approaches full flow, c gets larger and larger, and even before pressure flow occurs Δt must be kept very small to avoid instability.

By using an implicit finite difference scheme, one can avoid both the high cost of calculation associated with small Δt values and the programming gymnastics required to isolate pressurized sections and treat them separately. Since the implicit method is unconditionally stable, a time step can be chosen which is appropriate for the average flow conditions in the network, the large Courant numbers occurring for nearly pipeful and pressurized flow causing no stability problems. But once again, if a change of equations between pressurized and free surface flow is to be avoided, we must be able to simulate pressurized conditions using the *free surface* de St. Venant flow equations. The key to the problem was first described by Cunge and Wegner (1964), who, following Preissmann's (1961) suggestion, added a vertical slot over each pipe as shown in Fig. 9.6. As long as normal free surface flow conditions prevail, the slot

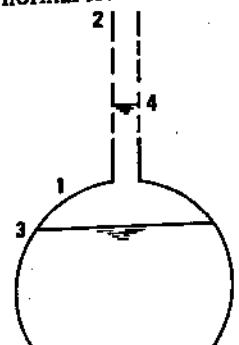

Fig. 9.6. Use of fictitious slot to simulate pressurized flow. 1, Physical pipe; 2, fictitious slot (width is exaggerated here); 3, water level in free surface flow; 4, water level in pressurized flow

has no effect and the de St Venant equations apply as usual. In pressurized flow, the free surface level is in the slot as shown; in fact, it is the piezometric level. Since the slot is extremely narrow (of the order of 1 cm) the volume of water it contains is negligible compared to the pipe volume, so the continuity equation is still satisfied. We see from Equation (9.2) that the small slot width, b, produces a

large celerity, and this is the essential object of adding the slot. Thus the nearly infinite wave propagation speed of pressurized flow is simulated using the free surface flow equations, no special treatment being needed. In the construction of the model, pipe sections are defined with slots extending indefinitely upwards; but the section conveyance never exceeds its maximum value, which corresponds to a depth of about 94% of the pipe diameter.

Backflow from junctions

The backflow phenomenon is one which must be modelled if the simulation is to reproduce the attenuation of peak flows due to the filling up of available volume in the pipe network. As long as the numerical method chosen permits flow reversal and divergent branching, backflow can be modelled with no special treatment. Centred implicit methods, such as the Preissmann scheme, handle reverse flow as a normal situation.

Backwater effects

The need to model backwater effects eliminates the use of simplified methods such as the Muskingum and kinematic wave approaches from all but very steep networks. Downstream controls such as gates, weirs, and pressurized flow can have backwater effects which are felt throughout the network if it is flat. Whether or not upstream overflow occurs may depend critically on whether downstream flow capacity is adequate at a given crucial moment. Thus a simulation system that does not take such downstream effects into account loses all its value as a design verification tool.

Small depths

The small depth problem, which is exceptional in one-dimensional river systems, is commonplace in drainage network models. There are two aspects to the problem. The first is described in Chapter 4, and concerns the fact that as the water level decreases at the downstream end of a computational reach, the water surface slope increases, and so does the discharge. But for small depths, the effect of the slope increase may be dominated by the decrease in flow area, which has the effect of decreasing the discharge. Computationally this situation, which can lead to oscillations, is avoided by taking the conveyance at the upstream section as representative of the entire reach, so that the discharge increases monotonically as the downstream level decreases, (i.e. as the slope increases).

A second aspect of the small depth problem is related to an advancing wave in a conduit containing very little water. Figure 9.7 shows a reach which at time t carries a small discharge at uniform flow depth, curve 1. At time $t + \Delta t$ the advancing wave causes a large depth increase at point j. But the discharge at point j may not appreciably increase even though the water level rises

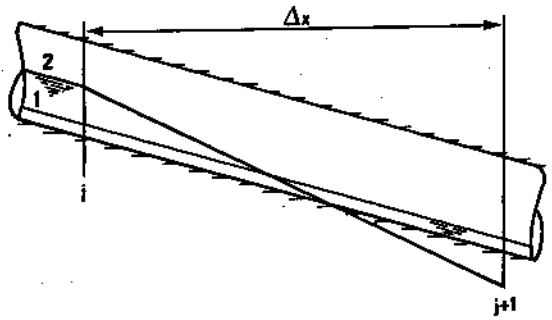

Fig. 9.7. Small depth problem when Δx is too large. 1, Low flow water level; 2, advancing wave front

substantially. Thus since there is virtually no inflow into the reach, the only way for the continuity equation, written between j and $j + 1$, to be satisfied is for the level at point $j + 1$ to drop *below* the conduit invert, as shown in curve 2. The problem is essentially one of too long a distance between j and $j + 1$. Since flood waves generally arrive quickly in storm drain networks, the distance step Δx must usually be kept small, of the order of 100 m. Even if an iterative method is used which allows the discharge at j to increase during the same time step as the depth, Δx must be kept relatively small so that the advancing wave can be properly represented.

Looped networks

By cross-connecting different portions of drainage networks, engineers can optimize drainage capacity in taking into account the non-uniformity of rainfall. These cross links make it possible to route storm flows from areas of high rainfall intensity toward areas of low intensity, thus reducing the outflow capacity needed from any particular area. Of course this advantage disappears under uniform rainfall conditions, but cross links also make it possible to isolate certain portions of a network for maintenance, and to manage low flows so as to avoid deposition of material in pipes. In modelling terms, these cross links render a network topologically looped (*see* Chapter 4), thus requiring a looped solution algorithm as described in Chapter 3. The same looped solution algorithm can be used in river and drainage network models; but in drainage networks where the number of nodes can be relatively large, it is especially important to use a computationally efficient algorithm which limits matrix inversion time.

Hydraulic works

In river models, hydraulic elements such as weirs, singular head losses, drop structures, etc., are rather infrequent, which is why we usually call them 'special' points. In drainage networks, on the other hand, such points can be more numerous than 'normal' ones. Thus a drainage network modelling system should have no built-in limitations as to the correct representation of hydraulic works. For example, recalling our discussions in Chapter 3, a modelling method which computes levels and discharges at the same points lends itself much more easily to the integration of hydraulic works than a method which computes y and Q at different points.

One feature of drainage models which makes life easier for the programmer is the limited number of cross-sectional shapes. A typical model contains a preponderance of a certain shape – circular, square, ovoid, etc. It is necessary to calculate tables of cross-sectional areas and conveyances only once for each section-type in the model. These basic tables are then used for the entire model, local conduit scale factors and roughness values being applied only at the time of calculation. The result is a considerable saving in core storage and/or auxiliary file requirements compared to a river model, in which each cross section is unique and must be stored somewhere.

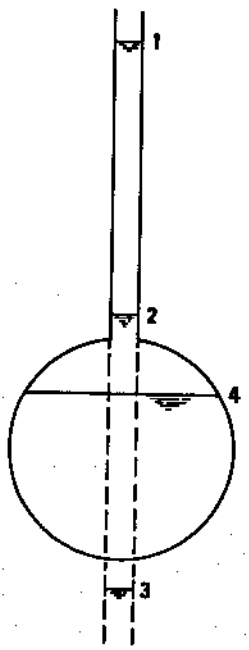

Fig. 9.8. Illustration of computational problems when pressurized flow passes into free surface conditions. 1, Time t, highly pressurized flow; 2, time $t + \Delta t$, slightly pressurized flow; 3, time $t + 2\Delta t$, negative depth calculated without iterations; 4, time $t + 2\Delta t$, correct depth calculated with iterations

Remark

Modelling systems which are based on, or have the possibility of, iterations within each time step (*see* Chapter 3) can make better use of the pressurized-flow slot system described above than those which do not iterate. As illustrated in Fig. 9.8, once the peak flow has passed, water levels within the slot begin to descend. But since the volume in the slot is small, the water levels tend to drop rather quickly. In a system without iterations, the change in water level during a time step is calculated using the width at the previous water level. Thus if the previous water level was only slightly into the slot, as shown in Fig. 9.8, the calculated drop in the next time step will be too large, since being based upon the slot width it cannot take into account the true volume of the pipe just below the slot. At best, the result will be a loss of water volume in the system. At worst, the water level will drop below the level of the pipe invert and destroy the calculation, as shown. The interest in being able to iterate within a time step is that the water levels which drop from the slot into the pipe itself (or below its invert) can be corrected, thus maintaining the integrity of the calculation.

10 Costs, benefits and quality

In the study and design of large engineering projects, investors, development agencies, and consultants often deal with the concepts of cost/benefit and cost/quality ratios. In fact, the decision to go ahead with a large project is often based to a large extent on its quantitatively-estimated cost/benefit ratio. Since mathematical models are so often used in the study and design phases of hydraulic works, it is legitimate to ask if they, too, should not be subject to some sort of cost/benefit or cost/quality analysis. The purpose of this chapter is to analyse the factors affecting the costs, benefits, and quality of mathematical models, and to try to determine whether the use of and choice among various models can be based on such quantitative ratios.

10.1 COST/BENEFIT AND COST/QUALITY RATIOS

As far as the relationship between costs and benefits is concerned, Ivicsics (1975) includes in his book a chapter dealing with cost/benefit analysis in which he investigates in detail the factors which influence the economic (and social) efficiency of flow simulation using reduced scale hydraulic models. A parallel analysis can be made for mathematical modelling, and we refer the reader to Ivicsic's book for the details. Unfortunately, such an analysis cannot furnish precise, quantitative guidelines for the assessment of the cost/benefit ratio of a given model.

The only way to pin down the true cost/benefit ratio of a model would be to finance several different studies of the same project using several mathematical models, and to compare the respective savings with a study which uses no model at all. Obviously no one is willing to go to such extreme lengths, and as a consequence the serious quantitative cost/benefit analysis of models would appear to be out of the question.

There are two situations in which the cost of *not* using a model can be all too precisely appreciated: when a new structure or channel development scheme proves to be worthless in view of the goal for which it was designed, or when a catastrophic event, which could have been predicted by a model, causes loss of

life and extensive property damage. In both cases it is too late to do the model study.

At times the decision to use a mathematical model is a political one, when a government or an international agency requires that a mathematical model study be included as part of the project without requiring that the model justify itself by a favourable cost/benefit ratio. Another possibility is that an expert consultant, based on his experience and intuition, calls for a mathematical model. In both cases the model will be built because of an *a priori*, non-economic decision and not because all parties have studied and accepted the model's favourable cost/benefit ratio. The decision as to whether or not to use a mathematical model stems rarely from a rational analysis of its social and economic effects.

Thus, even though we cannot define a proposed cost/benefit ratio for mathematical models, we can try to develop an equally important concept: the problem of model *quality* and its relation to cost. What is model quality? We find it difficult to give a precise definition, just as it is difficult to define the quality of an engineering design or an economic study before it is submitted to the test of time. Of course the essential quality of a mathematical model is its ability to faithfully simulate physical flow phenomena. But a model's quality is also related to other circumstances surrounding its use – its dependability, its insensitivity to minor physical modifications, the accessibility of its internal procedures in case of malfunctions, etc. The notion of model quality thus applies both to the model construction itself and to the software on which it is based.

It would seem impossible to establish a general quantitative relationship between the cost and the quality of mathematical modelling. One can determine something like a cost/quality relationship for a particular model after having defined the criteria of quality for that model and for the specific study for which it is used. For example, during the calibration phase of a model it is possible, after several trials, to get an idea of the possible increase in accuracy at different computational points (stations) as a function of labour and computer costs. Then one has to consider the importance of each station in the context of the overall problem studied, the representativity of the calibrated stations with respect to the river as a whole, and other factors which make up for what could be defined as calibration quality criteria (*see* Chapter 5).

Instead of trying to quantify a general cost/quality relationship which seems to us too elusive to be pursued, we prefer to investigate the principal factors which have an effect upon cost and which are related to the quality of models. We shall investigate first of all the cost items of a mathematical model, and then various aspects of what can be considered to make up its quality. In a way, these two points can be considered as 'objective' factors. We shall also mention other 'subjective' factors: the market situation, relationships between the modeller and the client, etc. Their importance cannot be appreciated until the objective factors are thoroughly analysed.

10.2 FACTORS AFFECTING THE COST OF A MATHEMATICAL MODEL

The overall cost of a mathematical model of river or channel flow may be broken down into the following items, each of which will be considered in some detail: development of the numerical method and associated software with which the model is constructed; preliminary study and the determination of the type of model to be used; adaptation of the existing software to the project's particular features; construction of the model; supplementary surveys and measurements; model calibration; model exploitation (operational runs) and interpretation of results; and possible transfer of the model and its implementation on the client's equipment. Of course a typical project does not necessarily include all these items. The cost of the basic surveying and field measurement campaign is not considered here since it depends too much upon particular local conditions, but it must not be forgotten that this campaign can represent an important part of the overall model cost.

Algorithm and software development

In all but exceptional cases, a modelling organization maintains an arsenal of on-the-shelf properly developed algorithms and their corresponding software. These tools represent a considerable initial investment whose amortization must be reflected in the cost of particular models. Experience has shown that this rather obvious fact is only seldom acknowledged by clients and most often investment cost recovery is not specified in contracts. Quite obviously this means that modelling system amortization is hidden somewhere else, for example, in the profit margin, or in artificial inflation of other items. In some situations the client may commission a model based on a program whose investment cost is next to nothing because it is unresearched, undeveloped and inapplicable to real life problems. The lack of acknowledgement of the need to recover program investment costs and its consecutive hiding elsewhere in the contract makes it impossible to estimate its relative importance as compared to overall model cost. Thus one cannot always detect, in formal bids, the depth of development behind the models proposed by various modelling organizations. It is of utmost importance to analyse not only the apparent price of a model, but also the depth of experience behind it, whether or not the modeller is still trying to amortize his investment, the model's position compared to present-day state of the art, etc.

It is often tacitly assumed that the cost of industrial program development and model exploitation is directly related to the 'completeness' of the system of equations used – that the Muskingum method is less expensive than the full de St Venant equations, etc. In order to see why this assumption is incorrect we must consider both program development and operational costs. It has been the authors' experience that, once the solution algorithm has been developed and tested, the bulk of the programming effort necessary to develop a modelling system is in input–output management, error detection, topological ordering

and verification, initial state loading, calculation control, graphical output, etc. These tasks, which can become complex in generalized systems, must be programmed whether the basic solution method is simplified or complete. It is true that implicit methods (*see* Chapter 3) require by definition considerably more programming effort than explicit ones, especially in looped networks; but even then development cost is dominated by tasks unrelated to the solution method. As an example consider the CARIMA system developed by SOGREAH, which is designed to be as automatic and as user-oriented as possible. The looped network algorithm, using the Preissmann method applied to the full equations for channel flow, and non-inertial equations for flood-plain flow, had been already programmed and run before the CARIMA development was begun. The programming of the method itself represented only about 25% of the total development costs; had an explicit method been used, this figure would have been around 15%.

As for operational costs, the possible savings per time step which can be realized by using a simplified method are generally insignificant compared to other costs. Again using CARIMA as an example, the CPU time which corresponds to the actual flow equation solution (calculation of coefficients, matrix inversion, etc.) is less than 20% of the total CPU time. Therefore an economy of no more than 20% could be effected by using a simpler method, even if the same large time steps could be maintained.

These conclusions do not apply to a program which is non-automatic, that is to say one which does no more than execute the solution algorithm for a model manually prepared by the user. But in such case, model exploitation cost is dominated by the manpower needed to carry out the often tedious and delicate task of model preparation. In summary, then, as long as the software is efficiently programmed, the cost of program development and model exploitation depends much less on the solution method used than on the generality and ease of application of the basic software.

Preliminary study

The purpose of this stage in the project is to define the type of model to be used for the particular project (Correlative or deterministic? One- or two-dimensional? Fixed or movable bed? etc.). It should comprise a field investigation and the assessment of all existing data, including the collection of additional data if necessary. Although this stage can be a decisive one as far as overall cost and quality of model results are concerned, it is all too often considered unimportant or ignored. To be useful, the preliminary study should take place before proposals are submitted to the client. But for an important model the cost of the preliminary study may be as high as 10 000–50 000 U.S. dollars (1978 value), and no bidding organization is willing to invest this amount of money unless it has a pretty good chance of winning the overall modelling contract itself. In one case known to the authors, an international body launched an open bid for the mathematical model of a river basin in a developing country and asked 18

bidders to submit proposals. In the absence of a short list, the chances of winning were 1:18; the bidding organizations had no choice but to play a high risk game. It is to be expected that under such circumstances some of them would gamble (in making hopeful assumptions about the type of model needed); others would do substandard work during the preliminary study stage and thus, if chosen, might fail to perform the study itself correctly and in so doing would distort the client's perception of the usefulness of mathematical models in general.

The authors are familiar with several cases in which the client, understanding the importance of the preliminary study to overall cost reduction and model quality, has divided the contract into two parts: first the preliminary study, second the modelling itself. Of course for routine engineering problems, the preliminary study has less importance. But when the overall contract is of the order of a million dollars and when the physical problem is difficult, a well conceived preliminary study may easily save as much as 20% of computer cost and possibly shorten the study duration by several months.

Adaptation of existing software to the project's particular features

There are some software systems which can handle a wide range of physical situations and require no particular adaptation, especially when the project presents no unusual problems. Nevertheless, experience shows that it is seldom possible to perform a model study without introducing some modification of the standard software system for particular man-made structures, automatic regulating devices, special graphical output, etc. Such modifications may be inexpensive and quickly carried out or, in some cases, may be very costly indeed if the software system is not designed for easy modification. For example, a long lateral weir is not generally a standard structure in programs which simulate surge propagation along power canals. If such a weir is one of the features to be studied, it must first be incorporated into the software system, bringing in supplementary cost. This cost will depend not only upon the inherent hydraulic complexity of the structure, but especially upon the software system's ability to accept new subroutines and particular features. This cost will include labour as well as computer time, the latter being generally small as compared to the former.

Quite clearly the cost of software adaptation is closely related to the quality of the algorithm and software. If the initial programming is efficient and if structured programming techniques have been incorporated (Baker, 1972), the adaptation costs can be nil or very small. If the program used is not an industrial system designed for convenient modification, but rather a quasi-experimental undeveloped product, the adaptation costs may rival those of the initial investment.

Construction of the model

The cost of this item can be very well defined once the type of model is determined (as it should be during a preliminary study) and the characteristics of the software which is to be used during data processing are known. Model construction consists in the schematization of the studied area (definition of reaches, cells, computational points, links between them, etc.), the preparation of the corresponding topographic and hydraulic data (cross-sectional areas, stage-storage curves, Manning–Strickler coefficients, boundary conditions, etc.) and the processing of the data in order to put it into the form required by the software to be used.

At this stage of the study, ultimate model quality can be assured only if the modelling team tries to understand the detailed physical features of the domain to be simulated; the cost of this effort depends upon the complexity of the natural situation and the data available. This understanding, together with the preliminary study choices, will also determine the cost and quality of model exploitation and interpretation of results. For example when a complex flow pattern is evident, one may wish to represent the modelled area by a looped network of storage cells and channels, and the schematization and data preparation cost of such a solution might be relatively high. Another possibility is the replacement of such a complex flow pattern by a one-dimensional branched model, as described in Chapter 4. If the modelling organization is able to accomplish such a schematization in an intelligent manner, the model construction may be less expensive in terms of computer cost, even though the process of analysing, understanding, and schematizing may be much more costly than for a looped channel-cell model. If the modelling team is not capable of correctly exploiting the one-dimensional assumption, the cost may be low but so will be the quality of the final product.

Consider some typical model construction situations and their cost implications.

- Model construction of a cascade of trapezoidal hydropower canals with well defined standard structures (hydropower plant, contractions, weirs, etc.) can be accomplished in several days by trained personnel having efficient software at their disposal. The corresponding computer cost would be negligible.
- The typical time necessary for model construction of an average river with flooded plains and complicated flow patterns is of the order of 1–2 months and requires a team of 2 men, who are faced with the continuous task of deciding where to place computational points, where to use one-dimensional and two-dimensional modelling, what roughnesses to use, etc.; *see* Chapter 4 for some examples of these kinds of model schematization choices.
- More manpower is needed for important models which cover a large part of the entire river basin. Examples of such models are the new Mekong Delta model run by the Mekong Committee in Bangkok (UNESCO, 1969; Zanobetti *et al.*, 1970); the Senegal River model run in Dakar by the OMVS (*see* Chapter 5); and the Niger River model, in which cases the purpose was to have a tool which is

always available, continuously updatable and improvable in order to study the consequences of future structures upon water management policy. Such models can have as many as 1000–3000 interconnected computational points and cells. Simulation of complex flow patterns must be rendered possible and the model discretization should be defined in view of all possible future uses of the model, from flood forecasting to water quality studies in order to get as much benefit as possible from the model investment. The construction cost may correspond to a period of several (say, for example 6–18) months work of a team of 2–4 engineers.

Computational costs corresponding to model construction, in terms of central processing unit time, are negligible as compared to labour costs (between 5 and 15%). However the cost of graphical output, which is used to verify cross-section data for example, may equal that of the computer time itself and is roughly proportional to the duration of the model construction phase. The cost of using graphical aids should never deter the model constructor from using them; the correction of a false calibration due to mistakes in input data will be much more expensive, especially if one is into the model exploitation phase before the mistakes are discovered.

Supplementary surveys and measurements

The topographic and hydraulic data available are not always sufficient for the construction and calibration of a model of high quality. Thus new complementary survey measurements and data collection campaigns may well be considered, and these may be very costly. The need for such action is sometimes not realized until during the model construction phase or even later, during its calibration. Such situations are encountered not only in regions lacking systematic recording of data but also in those areas where such records are not collected in the homogeneous way required for mathematical modelling (*see* Chapter 5).

A classic example is the Mekong River model whose calibration was described by Cunge (1975c). The complementary 1965 measuring campaign cost represented about 20% of the total measurements cost in the detailed breakdown given further on in this chapter. We would like to stress that it is not always easy to convince commissioning bodies of the necessity of such complementary expenses (which may become very important) when one has already spent a lot of money for data collection; it is psychologically hard to admit that the data are not exactly what was needed. The fear of losing face leads sometimes to a model of poor quality which does not meet its design objectives.

Model calibration

This phase of modelling is usually the longest and often the most expensive. The cost varies considerably with the purpose of the model, the definition of

accuracy, the accuracy required, the skill and experience of the modelling team, and data availability. In the Senegal River project (*see* Chapter 5), the contract specified the required accuracy as 10 cm difference between computed and observed water stages at 16 stations along 1000 km of the river. The accuracy problem is discussed in Chapter 5 and here we note only that differences of 15 cm maximum were obtained rather quickly; but it took a couple of months and about ten complete runs (simulating the entire flood lasting 3 months) to convince the client that:

(i) it was impossible to satisfy the 10 cm criterion without adopting physically absurd coefficients; only a new surveying campaign and possibly a new schematization of some areas could improve the situation;

(ii) the observed differences were perfectly acceptable in view of the model purpose.

Such incidents may double the cost of the calibration phase and bear heavily upon the overall study cost. We may incidentally note that if the Senegal modelling team had introduced absurd coefficients it would have quickly obtained the required coincidence between calculated and observed levels, saving money but completely destroying the model's predictive reliability and thus its quality. As is shown further on in the examples, the calibration phase can involve considerable labour (counted in months if not years of work for a team of 2–4 persons) and computer resources (sometimes CPU time costing the equivalent of several months of engineers' time).

There are two applications of mathematical modelling which do not require any calibration phase at all: planned man-made canals whose roughness coefficients cannot be measured but can be fairly well estimated, and dam-break wave propagation for which prototype measurements are, most fortunately, non-existent (*see* Chapter 9).

Model exploitation (operational runs) and interpretation of results

Each operational run of a model consists of three main stages: preparation of the data (most often the boundary conditions) for the run, the run itself, and interpretation of the results. Except for dam-break wave simulation or for very large models of thousands of computational points, computer cost is not very important even if a large number of computations are required.

Often the most expensive part of the exploitation phase is the time lost due to poor planning of the simulations and to inefficient software which is not designed to give the user convenient access to computed results, preferably in graphical form. A good example of the benefits of having a well conceived and thoroughly tested program is the study of the Rio Parana project between Corpus and Itaipu, where it was possible to execute 132 runs in 15 days (Courtesy of SOGREAH, private communication, 1977). The project managers' preoccupations were identified in advance, and modellers took the initiative of running a few cases which were not specifically requested rather than risking

problems in meeting the study deadline. Very efficient graphical output software grouped the most important results of each run, permitting subsequent global interpretation once all exploitation runs were finished. Such a streamlined operation is not always possible, but it can significantly reduce the cost of model exploitation.

The order of magnitude of the computer CPU time needed (of the class, say, IBM 360-155 computer) to execute one run of an average river model is from 1 to 3 min, though very complex models may take as much as 20 min. One must multiply that by an 'error factor' and add input–output cost. All things considered, the cost does not generally go beyond 1000 U.S. dollars (1978) per run, and is usually nearer 200 dollars. If a mathematical modelling specialist (say a junior engineer) waits around for a day because hydraulic specialists wonder what the next run should be, it would cost the client 200–300 dollars.

An exception to these general rules is the dam-break simulation problem, in which computer CPU/time (still corresponding to the same type of machine) may well run into hours for one run.

Transfer of models

This item is not typical of all contracts but it is becoming more and more often requested by model commissioning organizations. Model transfer is considered in detail in Chapter 11 and here we give only a list of points which must be taken into account when the cost is considered:

- training of the client's personnel which brings in the need to remunerate teaching personnel furnished by the modelling organization;
- program adaptation to the client's computer, which might be quite different from that of the modelling organization;
- possible acceptance tests;
- implementation of the model on the client's facilities;
- selling price asked for the software itself.

For all but the last point one should not forget the computer time in cost estimates.

10.3 QUALITY OF A MODEL

The quality of a mathematical model is related to the same factors as is its cost. What is troublesome, however, is the practical difficulty of defining objective, universally applicable quality norms. We can only try to define what constitutes model quality by considering a few specific situations, bearing in mind that a model's overall purpose is to provide faithful simulation of physical flow processes.

As we have seen, a two-dimensional situation may sometimes be well simulated by a one-dimensional model and the results, especially if they are

interpreted by the same team who defined the schematization in an intelligent manner, can be quite reliable. On the other hand such one-dimensional simulation of two-dimensional or three-dimensional phenomena may be made by personnel lacking the necessary practical experience and knowledge; the result can then be disastrous in terms of predictive capability. Thus one aspect of model quality is the modelling team's ability to interpret results in a manner consistent with the assumptions on which the model is based.

It is useless to pursue model calibration very far if physically absurd coefficients are needed to obtain better coincidence between observed and computed values (*see* Chapter 5). The predictive quality of the model will actually be decreased by such efforts, even though computed and observed water levels coincide quite well. Thus another aspect of quality is the modelling team's constant awareness of the physical implications of calibrated empirical coefficients.

These two examples of quality considerations are linked to schematization and calibrating difficulties. There are others, such as the software problem; well developed and well researched software is certainly a key factor in model quality. But the software problem has several components: the basic equations and their discretization, the solution algorithm, data input, and processing of results. For some projects only very advanced software can bring about a solution; there is no hope of simulating situations such as those described for the Mekong, Senegal or Niger Rivers without having two-dimensional techniques available. But for others, less sophisticated programs can supply results of good quality, provided there is necessary backup and interpretation furnished by experienced specialists.

The quality of models is also a function of the commissioning body's attitude. In a case known to the authors, a modelling organization was recently consulted by an administration to study the propagation of a dam-break wave. The proposal was prepared and sent to the client who objected to the price (it was of the order of 40 000 U.S. dollars, 1978) saying that, 'since it is only a preliminary study, can't you take a uniform trapezoidal cross section and constant bed slope downstream of the dam in order to diminish the cost?'. The modeller agreed that this would indeed divide the cost by a factor of five, but warned the user that he would not even be able to estimate the error introduced by such a schematization. That did not stop the user from commissioning the model and its exploitation; but who can assess the quality of the results obtained?

When considering the quality of mathematical models of river and channel flow, a distinction must be made between a *model* of a given physical situation and a *modelling system* (i.e. ensemble of software) which may be used for a large number of different studies.

The quality of a mathematical *model* built for some specific project may be formulated very simply as the model's concordance with the existing prototype flows, and its predictive capability. If the model is able to reproduce observed past events and furnish its user with a physically reasonable interpretation of those events, the concordance is satisfactory to a certain degeee (this degree

depends on the user's needs). The predictive capability of the model should enable its user to extrapolate existing physical situations and to simulate with acceptable accuracy events which have never been observed, such as exceptional floods, or the influence of new system characteristics, such as dams, weirs, canals and other man-made structures or natural modifications.

The quality of a *modelling system* is related to its applicability to as wide a range of physical situations to be simulated as possible. Moreover, these applications should be easy to execute, should not require any basic modifications of the software, furnish reliable results, free the hydraulic specialist from programming and algorithmic 'bugs' and stay within reasonable cost limits.

It is quite possible to obtain reasonable simulation results while using a very inefficient program which cannot possibly simulate more than a few very particular problems. Thus the quality of the particular model may be considered satisfactory while the quality of the program as a modelling system is very poor. If a different model is built using the same software, its quality may be poor and the results unusable. On the other hand, an experienced modelling team which understands a particular physical phenomenon well can schematize the real life situation and interpret the results in such a way that even the limited modelling system may be used with a certain success. Although such situations are not typical, they do exist and this is why quality criteria are hard to define.

The reader might object to our assertion that a modelling system is of poor quality because it is not capable of simulating a wide range of situations. Indeed, certain systems which model, for example, one-dimensional branched river flow, can be considered to be of high quality in the sense that they reliably, efficiently, and economically solve the unsteady flow equations in network types for which they were designed. But modelling is the art of simulating three-dimensional, continuous natural phenomena using one, two, or perhaps one day three-dimensional discrete techniques. The wider the range of applicability of a modelling system, the less the chance that the modeller will have to force-fit parts of the natural flow situation to his necessarily limited simulation system, and the higher the quality of the final results.

In the following paragraphs we review some other factors which relate to model quality.

Differential equations

The choice of differential equations on which a simulation system is based, is made by the modelling organization and usually accepted without much investigation by its clients. As was shown in Chapter 2, there are several forms of the one-dimensional flow equations and some elementary questions must be asked about the system used, for example:

- Are the equations written in the form of conservation laws for volume and momentum? If not, they should not be used for studies on which steep wave front propagation is important and loss of water volume cannot be tolerated.

- Is the longitudinal change of momentum due to the non-prismaticity of the river channel and bed taken into account in the dynamic equation? If not, the simulation of wave propagation through non-prismatic channels will be subject to considerable error.

The detailed discussion presented in Chapter 2 may be used to judge the quality of a particular differential equation system.

Finite difference operator

Here again the modelling organization has made its choice which may be evaluated using criteria developed in Chapter 3. Such an evaluation is not always easy because the details of finite difference discretization are sometimes kept secret by modelling organizations. This is a delicate question from a commercial point of view, but it should be said that it is impossible to assess the value of the discretizing operator without knowing in detail how it is conceived. Usually the error characteristics of the operator are given as applied to the linearized form of the flow equations, but its quality also depends upon the way it represents the non-linear terms and boundary conditions occurring in real life. These problems were discussed in Chapter 3.

Solution algorithm and treatment of special features

Evaluation of solution techniques is the subject of Chapter 3, and some of the more important algorithms are described there. The careful reader will of course realize that these algorithms are in a way incomplete. They cannot be applied to problems which include such special features as man-made structures, sills, sudden change of cross section, reaches which dry up, etc. As a rule these details are not available in scientific publications since they are considered by modelling organizations as their main trump cards in the game of international bid competition. In our discussions of flow in natural rivers and flow regulation problems (Chapters 4 and 6) we describe some aspects of such details and conclude that they fall more often within the competence of the craftsman than the scientist. Sometimes the quality of the algorithm consists in not interrupting the computation and of locally accepting poor representation of the flow for a certain period, for example, simulating a dry reach by assuming it carries a very small discharge at a small depth.

Most often the quality of an algorithm (or at least its sale price) is considered high if it accepts all sorts of man-made structures, which implies, in addition to craftsmanship in simulation and an excellent knowledge of hydraulics, a very high quality of programming. Since such craftsmanship does not represent any scientific innovation, it is hard to reproach the modelling organizations for their desire to keep the details secret. But the quality of their software should be and can be evaluated on test examples, in order to check whether or not the modeller's craftsmanship respects real flow laws.

Data input and output

This point concerns the software itself and is readily assessed. It is a question of the ease and rapidity with which one may change such data as cross-sectional shape, roughness, conveyances, number of computational points and their topological relationships (links between the points), boundary conditions, dam operating rules, etc. It is quite dangerous to use a model which one will hesitate to modify, during calibration or exploitation phases, only because of the material difficulty of such interventions. The more versatile the software in this regard, the higher the quality of the system.

Simulation of observed situations

Chapter 5 deals in detail with the calibration problem. The quality of a model in this respect may be assessed by a comparison of observed and computed stage hydrographs. If the quality of the differential equations used, their finite difference discretization, and solution algorithm is satisfactory, a given modelling system should make it possible to obtain a good calibration. If a good calibration is difficult to obtain (and it has been verified that the problem is not due to incorrect field data), the quality of the model itself must be questioned. Thus the quality components here will be proper schematization, density of computational points, correspondence between real cross sections and stage/storage relationships compared to those introduced into the model, etc.

10.4 MODELLER–USER RELATIONSHIP

The key to decreasing the cost and increasing the quality of a model lies in the relationship between the developer of a model or a modelling system and its user, if indeed they are not one and the same person. Whether we are talking about the relationship between two engineers employed by the same consulting firm, one of them working in a mathematical modelling group and another in the river hydraulics department, or of that between a consultant and his client, the problems are nearly the same.

If the user can properly evaluate the model proposed by its builder, there is a good chance that a mutual trust relationship will be established and the cost/quality ratio minimized. This mutual confidence atmosphere is very difficult to create. One of the reasons is that the modeller is not always able to give a quantitative answer to the user's questions. Or, to be more precise, it is often impossible to assess the exact value of the inaccuracies. Thus, if the modeller is honest, the user gets the impression that he has paid for more than he has received. If the modeller is not explicit in his reports, the user may be overconfident as far as the accuracy of results is concerned.

An ideal situation consists in the participation of the user in the model construction process, from the preliminary study through the calibration to the

exploitation runs. If the user is not prepared to enter into such a co-operation, he has to accept that he has not obtained the highest value for his money. Nonetheless, he ought always to have at his disposal some means of evaluating the model he is buying.

The prospective model commissioner who has no means of evaluating the quality of proposed models can only choose by using cost criterion, while believing everything he is told by the modeller. It is true that there are still some users who regard the model as an unnecessary item of the proposal, included only in order to satisfy technical specifications and serving no practical purpose. For them the model quality does not matter; the cheaper the model the better. But, on the other hand, there are still 'too many models constructed and sold that are ill-conceived, inaccurate and inefficient, that lack basic understanding, data interpretation, numerics, analysis and even simply common sense. The decisions based on these models are correspondingly ill founded, giving rise on the one hand to a waste of resources and on the other, to unsafe and even downright dangerous situations' (Abbott, 1977). And thus the lack of a proper model evaluation, which may result in some savings at the beginning of the project, may also lead to costs out of all proportion arising from model-based project decisions which turn out to be wrong.

10.5 EXAMPLES OF COST OF MATHEMATICAL MODELS

As was mentioned earlier, it is extremely difficult to obtain model cost data, and even more difficult to publish them because of commercial discretion or organizational sensitivity. We shall try to illustrate what we have said in the preceding paragraphs by using two examples for which some cost data are available: the Upper Nile Basin and the Mekong River.

Upper Nile Basin

The mathematical model of the Upper Nile Basin simulates the hydraulics of the River Nile, its lakes, and its tributaries from the headwaters in Rwanda and Burundi to a point about 20 km north of the outlet of Lake Mobutu. The model, as described by Nemec and Kite (1978), consists of 3 main components:

(a) a catchment component determining the runoff fed into the rivers which flow into the lakes and subsequently into the Nile.

(b) A lake component which balances the inputs to the lakes with their outflows.

(c) A channel component which simulates the water flow through river channels.

Actually only component (c), which is a mathematical model of river flow based upon Preissmann's four point implicit finite difference scheme, corresponds to

the subject of the present book, components (a) and (b) being hydrologic models. The model construction was commissioned by the UNDP and WMO after the first phase of the HYDROMET project, consisting of systematic collection of data during a five year period (1967–1972). The objectives of the model included the investigation of various schemes of regulation of lake outflows and training of the local staff. The model construction was put out to open bid in 1974 and 10 (!) companies submitted proposals for the study. The proposed prices varied by a factor of three with the lowest being 50% below average, the highest 160% above average. A panel of six experts analysed the proposals according to several criteria, some of which are given below in anonymous form (WMO, private communication, 1975). The rating scale was very good, good, fair, poor. The following points were considered in detail:

(a) data handling (displayed awareness of problems, experience with handling large data systems, method of data handling);
(b) computer facilities (hardware, software, model language, contractor's capability);
(c) model (type proposed, model capability, contractor's experience with the model, cost);
(d) model synthesis, i.e. putting three models together in one system (clarity of concept, emphasis, contractor's capability, cost);
(e) demonstration and documentation for the client (time spent in Nairobi by contractor's staff);
(f) training (time versus number of persons, emphasis on training, type of training, contractor's capabilities);
(g) general (contractor's resources, contractor's structure: loose, fragmented or compact; contractor's bias; i.e. type of models best known and most often built; overall cost).

The overall cost of bids varied from 195 000 to 612 000 U.S. dollars in 1974. The cost structure changed considerably from one bidder to another as follows:

Lake model	3–17% of the total
Channel model	4–25%
Catchment model	7–45%
Model synthesis	0–10%
Training	7–44%

The method of analysis is noteworthy because of its generality – the cost is only one of the factors – and thoroughness. It is also the only example known to the authors wherein the client informed the bidders, after the decision had been taken, of the method of analysis applied to assess and rate the bids.

Mekong River Delta

It is not possible here to relate all the details of the Mekong Delta project. The interested reader may find a summary and references in the UNESCO (1969)

synthesis report. We shall limit ourselves to certain information which concerns the present chapter, namely the detailed budget of the modelling project and comments on the quality of the model.

Budget

The total cost of the project was nearly 1.3 million U.S. dollars. Its consolidated plan of expenditure, given in Table 10.1, can be compared with the work time chart as shown in Fig. 10.1. It is important to consider the dollar value of the expenditures in terms of the inflation occurring since the period 1962–1965, when the bulk of the work was done. Table 10.2 gives another breakdown of the budget, this time along the lines exposed in the present chapter. Information concerning the project is exceptionally rich as compared to other similar ventures, but even under these conditions it is next to impossible to pin down the cost breakdown according to the list of items given in Section 10.2.

Quality control

The Mekong project is a good example of special concern for the quality of the results, the credit for which must go to UNESCO, the executive agency for the project. The technical specifications for the model were evolved by a group of international experts as the result of a preliminary mission in Viet-Nam and Cambodia. Then a short list of three consultant firms was established and, after thorough negotiation, the contract was awarded.

The contract had two features specifically designed to assure high model quality:

(i) All work done by the contractor was submitted every three months to a panel of five experts: three hydraulic specialists (one of them having spent half of his professional life in Indochina), an applied mathematician and a data processing and high level computer specialist. One of these experts came from a firm which unsuccessfully bid for the contract. These experts, representing four different countries, acted as an advising body to the client; within budget limits, their decisions were final. After the first few working meetings, each of them lasting from 1 to 5 days, a relationship of mutual trust and professional respect developed among the experts and the contractor's engineers.

(ii) The contract provided for a preliminary study under the experts' control. During that decisive phase, the modeller and the client were in close communication.

Thanks to the above situation, when it was necessary to decide if the calibration effort was sufficient or if further trials were necessary, the decisions taken by the experts were accepted by the modeller as well as by the client. The model was calibrated first on the basis of the 1963 flood which was rather below average, and thus this calibration did not meet the contract requirements. Since the contract provided for two calibration floods, it was decided to carry out a second measurement and calibration campaign in 1964. This flood turned out to be just average, but with features clearly different from those of the 1963 flood.

Table 10.1 Mekong Delta Model Plan of Expenditure. Source: UNESCO/UN (1969)

	Item	Man-months	U.S. dollars (spent between 1962 and 1968)
Services and facilities provided by the UNDP special Fund	1. Experts – consultants	19	46 393
	2. Fellowships in organization of model utilization, hydraulic engineering, computational hydraulics	74	27 154
	3. Equipment and supplies: Computers, instruments, equipment, transport, final report translating and editing		376 232
	4. Subcontracts: Main contract: analysis of available data, preliminary computations, measurement campaign, final calibration and exploitation, interpretation (exclusive of computer cost).		588 301
	Transfer of model: adaptation of programs and user's manual (*see* Chapter 11 for detailed description).		30 612
	Acceptance tests before implementation (in France, on computer facilities analogous to those in Bangkok).		3000
	Implementation of the model in Bangkok (expenses and travelling costs excluded)		2750
	5. Miscellaneous		4411
	Total gross project cost		1 078 853
	6. Executing Agency overhead cost		57 500
	Total		1 136 353
Services and facilities provided by the Governments of riparian countries	Main contract (mainly for measurement campaign)		
	Government of Cambodia		97 271
	Government of Viet-Nam		42 629
	Total		139 900
Total cost of the project			1 276 253

Fig. 10.1 Work chronogram of the Mekong Delta Project. Source: UNESCO/UNDP (1969)

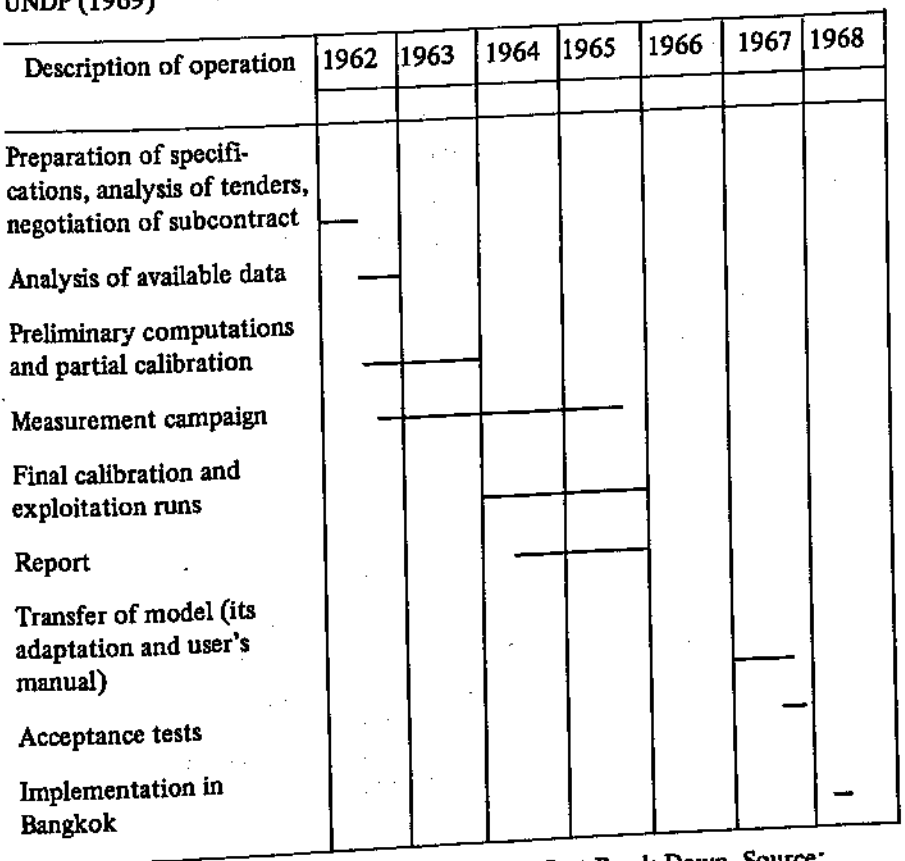

Table 10.2 Mekong Delta Mathematical Model Cost Break Down. Source: Zanobetti *et al.* (1968)

Items	U.S. dollars
1. Reconnaissance, preliminary missions, data analysis (preliminary study in the sense of the present chapter)	30 258
2. Adaptation of the existing software, construction of the 'preliminary' model	52 585
3. Measurement campaigns	103 598
cost of equipment	549 248
cost of personnel and maintenance	
4. Model calibration and exploitation	228 844
Total	964 533

The fact that measurement campaigns were carried out while the model was being calibrated made it possible to improve the quality of observed data by changing the observation network density and the location of some recording stations. The experts decided to carry out a third campaign of measurements in 1965; this flood was below average, thus not used for calibration.

The quality of the calibration phase can be measured to some extent by the differences between the observed and computed levels as shown in Table 10.3.

Table 10.3 Mekong model calibration results. Percentage of Total number of 29 Computational Cells calibrated. Source: Zanobetti *et al.* (1968)

Maximum error of calibration	Flood 1963	1964
less than 10 cm	60	53
less than 20 cm	84	89

Given the way in which 'observed' hydrographs were established (it was of course impossible to have a gauge in the middle of each cell) and the security problem in Indochina, the above results may be considered as quite satisfactory. The discharge check measurements (1228 measurements made in main rivers, tributaries, and canals, the range being from 2.8 $m^3 s^{-1}$ to 34 640 $m^3 s^{-1}$) were reproduced by the model with an average accuracy of 6.8%.

11 Transfer of mathematical models

11.1 INTRODUCTION

Most mathematical models are constructed by consulting engineering organizations who use them to study particular aspects of their client's problem. In such cases the client is interested in the conclusions of the study and sometimes in the details of the procedures used to arrive at these conclusions; but he is generally not interested in having an operating model at his disposal at the end of the study. In some cases, on the other hand, the client desires to have a working model of all or part of his river system permanently available at his headquarters, so that he may use it as an integral part of his water resource management activities. In this case the client either develops his own in-house modelling capabilities or, as is more often the case, he retains a consulting engineering organization to construct, calibrate, and install the model at the client's headquarters. We refer to this process as the *transfer* of a mathematical model; we use the word transfer firstly because the construction and calibration phases are usually carried out on the consultant's facilities, as we shall see further on, and secondly because the consultant must not only install the model at the client's headquarters, but also communicate his model operation know-how to the client's staff.

A distinctly different type of transfer problem is that of the installation of a general modelling program or system of programs at the headquarters of a client who wishes to establish or expand his modelling capabilities. This type of transfer being rather unusual, we shall not devote too much discussion to it. We are especially interested in transfers of software related to a *specific model*.

The transfer of a mathematical model from the organization which has built it to the user may be desired for various reasons, some examples of which are as follows:

(i) model exploitation may be efficient only when it is carried out by the user, such as in the case of short-term flood forecasting where results are needed immediately;

(ii) model exploitation would be less costly if performed by the user since he owns a computer and the cost of model operation is marginal;

(iii) the authority which commissioned the model construction decides that for political reasons, the exploitation and maintenance of the model should be its own future responsibility. Such a case arises most often when a river basin authority acquires a model built and calibrated and wants to use it for years to come as a planning tool, with no need of further intervention by the modeller;

(iv) the client wants not only to use the transferred model for its primary purpose, that is to say the study of a given river system, perhaps over a long period of time, but also in order to build its own potential in the field of mathematical modelling and/or river hydraulics, using the software system on which the particular model is based. Indeed, such software may become a centre of activity in itself and an excellent tool for educational purposes, permitting a major step forward in hydraulic training within the client's organization.

The purpose of a particular transfer operation is, most often, a combination of the above motivations, some of which are seldom explicitly stated by the user. When examining any transfer deal, one has to keep in mind that the modeller is generally more experienced and better equipped than is the user in terms of computer hardware and modelling expertise. This does not necessarily mean, however, that the modeller's product can be easily transferred and used by somebody else. His software may be poorly documented, to the extent that it is unusable by any outsider; and there is a pretty good chance that he has taken all possible advantage of his computer and operating system features, some of which are non-standard and thus untransferable.

It is important to realize that, except in some particular cases, any model transfer is a complex operation. The difficulties which may arise fall into one of three general categories:

- relationship between the modeller and the user;
- differences between computers and operating systems;
- availability of trained computer system personnel and numerical hydraulics specialists.

Let us consider these three topics in more detail while keeping in mind the purpose of the model transfer.

11.2 MODELLER–USER RELATIONSHIP

The success of a model transfer operation depends on a precise definition of user–modeller reciprocal obligations and of the transfer purposes. A user who desires to implement at his headquarters a mathematical model built and calibrated elsewhere should remember that a mathematical modelling system, especially an industrialized one which is designed to handle many different kinds of problems, will be based on very complex programming, and experience has shown that there is no such thing as foolproof software. Even when a modelling system has been used for years, it can happen that a particular configuration

or a particular loop which has never been tested brings about a breakdown of the computer run, which thus yields no results and the mathematical model can only be considered inoperable. In addition there are myriad possibilities of errors in the definition of topographic and hydraulic data, discharge coefficients, man-made structures, etc. Any modelling system has its own rules of model construction which may not have been violated by the modeller but which will be violated by the user, and so on.

There are two levels of possible incidents with a transferred model: formal incidents, due to the fact that the modelling system rules were not followed, and more subtle incidents caused by deficient software or poor numerical representation of hydraulic laws. It is highly unlikely that a model could be used for an extended period of time without the occurrence of both types of incidents. To achieve the transfer objectives, the user will have to deal with the organization who built the model (the modeller), who may be a university, a governmental institution or a commercial organization. In each case the user must define reciprocal obligations in such a way as to insure himself to as great an extent as possible against incidents such as those described above. In view of this objective, each of the above three types of organizations has certain advantages and certain disadvantages.

A university modelling system might be a good teaching tool and its theoretical foundations are usually easily ascertained. Most often, however, a detailed operating manual either cannot be furnished or may be of poor quality. It is doubtful that a great deal of tedious and unglamorous testing of the software has been carried out. It is possible that due to the continuous turnover of graduate students, the modeller will in a few years have no one available who knows the details of the program. All these deficiencies stem from the fact that university modelling systems are generally put together by graduate students whose primary goal, and quite legitimately so, is the completion of their theses and/or research rather than the less exciting task of programming a general, incident-proof modelling system. The graduate students are supervised by a professor who is responsible for several projects of this kind, plus his own research, plus administrative work, and thus quite rightfully considers program debugging to be outside of the domain of his scientific activity.

There is only one way the user can hope to make effective use of a model based on a university software system: he must learn as much about it as its authors know themselves. This is in fact quite possible, since the user will usually be welcome at the university and the modelling staff will be eager to explain every detail. However, is it worth it to have such a model transferred? Most likely it would be better to learn the modelling system's principles and program it from scratch oneself.

An example of the kind of effort needed to transform a research-oriented software system into an industrialized product is that of SOGREAH's POLDER program (Pollution Des Rivières = river pollution). This program, which simulates time-dependent two-dimensional pollutant dispersion in natural rivers, began life as a graduate student tool used to investigate various numerical techniques

and to analyse the results of laboratory experiments (Holly, 1975; Holly and Cunge, 1975; Holly and Simons, 1975). While the documentation of the numerical techniques used was fairly complete; the same could not be said of the input–output procedures and interpretation of results. Moreover, the program had very little error detection capability, only rudimentary graphical output routines, and required that the user perform manually the tedious task of stream tube discretization (*see* Chapter 8). Thus although the program was based on sound numerical techniques and was efficiently written, it could by no means have been considered a transferrable product in its university version.

The remainder of this example departs somewhat from the university-to-client transfer scenario, because in this case it was the program's author who transferred himself to another organization, where he was assigned the task of developing an industrialized version of the program. Nevertheless it proved difficult to try simply to generalize the university code, so it was necessary to start from scratch as suggested above. The re-programming process, including automatic stream tube preparation, complete graphical output of results, and effective error detections required about four man-months of effort and about 5 h of computer time (IBM 370-155). It should not be forgotten that this effort was devoted not to the development and testing of a new numerical technique, but simply to the transition of the program from a university version to an industrialized (transferrable) version.

A governmental institution modelling system may well have some of the same deficiencies as the university product described above. Experience has shown that some governmental agencies in some countries can develop program systems and construct models based on excellent theoretical bases and can acquire considerable experience. Their systems however may lack good documentation (such as operating manuals containing efficient exploitation rules, etc.). In addition it is sometimes impossible to obtain documentation from these agencies which is written for transfer purposes. Agency personnel are more or less willing to explain how their software functions and the theoretical foundation of their method, but to furnish detailed documentation implies the acceptance of responsibility for future operations. The agencies are usually reluctant to do this since they know that modelling systems are not foolproof. Mishandling of such a model by the user would discredit the agency which, consequently, does not like the transfer idea.

Notable exceptions to these general observations are governmental agencies specifically charged with the development and public dissemination of modelling programs, such as the U.S. Army Corps of Engineers, the U.S. Geological Survey, the U.S. Environmental Protection Agency, U.S. Soil Conservation Service, etc. Such organizations willingly transfer modelling systems to consulting engineering firms, local public authorities, etc., and with reasonable documentation. But this kind of transfer, lacking a commercial motivation to supply a product which is self-contained and meets the transfer contract specifications, depends for its success on the never-ending follow-up communication between the supplier and the user for the resolution of program and model problems.

A commercial organization may always be required to furnish a detailed documentation, and moreover it will do everything possible to make its model foolproof in the interest of preserving its reputation and protecting its profit margins. Indeed, the people who work in such organizations are paid for the necessary but unglamorous work of quality control through checking, testing, debugging and writing error messages and operation manuals. A commercial organization will also always agree to sign a transfer contract if it is linked to a main contract of model construction and calibration.

There is, however, another problem when commercial organizations are concerned: they are not eager to create their own competitors. Thus the purpose of the model transfer intervenes quite explicitly. Commercial firms will gladly supply the model and the software under some usable form, as well as operating manuals and aftersale assistance, but not all of them will explain the details of the software. Or, if they do, it might mean that the particular software transferred is not their latest, most efficient version. Or again they may ask a price which covers the software development costs. It all depends upon the model purpose: any organization will agree to transfer its software in the form of binary decks which do not reveal any software secrets, but by the same token cannot be modified to meet evolving model needs.

Some organizations will agree to properly train their clients' engineers if the client agrees to limit model applications to one river basin or to one country. But a very high price indeed must be paid if one wants to obtain from a modeller the tools with the aid of which one would like to become the modeller's competitor.

We would like to stress that the policies adopted by various commercial firms are not all the same. Their attitudes depend upon many factors, but their fears of loss of market competitiveness because of 'leaks' of modelling secrets are usually baseless. Indeed, the development of a commercially sound capacity in mathematical modelling of river and channel flow demands several years of time, a team of several people who are very competent in hydraulics, numerical methods, and data processing, proper management of this group, and access to a rather large computer. The software is only one element of the whole set of conditions and, while being important, it is not decisive when the human support is not there.

On the other hand, the commercial organization who transfers a model does run another kind of risk; that of a damaged reputation. This risk may be attenuated only by thorough documentation and training of the user. If the user's expectations are not satisfied, or if the transferred model does not work or works poorly, the modeller's reputation will be tarnished, sometimes irreversibly. Whatever the situation, a transfer cannot be properly made unless the partners trust one another in the deal and recognize each other's fears and motivations.

11.3 COMPUTER AND OPERATING SYSTEM PROBLEMS

Transfer difficulties due to differences between computers and computer operating systems are of another kind, since they are objective in nature, and as such, nearly independent of transfer purposes.

Let us consider the simplest of all situations, when the user's and modeller's computers are both of the same type, built by the same manufacturer and both having the required core storage capacity. Even in such a case the implementation of the program may run into trouble since the manufacturer may not have implemented the same version of his operating system on both machines. Indeed, the manufacturer's software has usually several options, or versions, and data processing centres are free to choose between them as they please. These kinds of differences do not intervene at the programming level, but rather at the level of program exploitation. Operating problems due to such differences can be worked out in a few hours, but only if the modeller's personnel charged with implementing the model have a rather good knowledge of the computer job control language and if the system analysts and operators on the user's side are sufficiently qualified. In the example of the Senegal model transfer given at the end of this chapter, some difficulties of this type are described. We would like to stress the fact that the main problems in this respect are computer-related and not program-related. It seems that often the two aspects, i.e. computer versus program, are confused when the technical specifications for bids and contracts are drawn up by the users or their advisers.

The above difficulties as well as others exist when another, more complicated case is considered: the user's computer is of the same type as the modeller's but its capacity or computational speed is inferior, or it is of a completely different type. In that case it is possible that some reprogramming is necessary and, in order to minimize costs, the testing of the program should take place before the transfer on a computer of the same type as that of the user.

Let us consider the following recommendations concerning transfers and given by Nemec and Kite (1978):

(a) 'What must always be required is that the model be developed by the subcontractor (modeller) on the same type of computer that will eventually be used and that the model developer, from the beginning, tailor his model to the exact machine, operating system, library routines and facilities of the user.'

(b) 'It is desirable to design the system so that the capabilities of the users are taken into account.'

Such recommendations may be pertinent if the client commissions a software manufacturer to write a particular program from scratch for his particular purpose and for his particular computational centre. If the model purpose is educational, as stated in point (iv) of Section 11.1, both recommendations will be relevant. However, in situations most often encountered, the transfer is the last stage of the project. Except for very particular cases the bulk of the project consists of constructing, calibrating and exploiting the mathematical model.

To satisfy Nemec and Kite's requirements, the client who desires to use the model beyond the project duration and to have it implemented at his headquarters has only two choices:

- either to find a modeller who, by chance, uses the same equipment as he does;
- or to require that the model be built, calibrated and run by the modeller at the user's computational centre.

The former solution might well eliminate all existing modellers or, at very best, lead to a rather arbitrary choice as to who is going to build the model. The latter solution would burden the project with high costs which can be otherwise avoided. The construction and calibration of the model at the user's office implies setting up in residence a team of the modeller's specialists during several months, possibly multiplying the time needed for the job by an important factor. When the model is built, calibrated and run at the modeller's office, it benefits from an environment which cannot possibly exist elsewhere: an experienced staff, a powerful computer, consultancy backup, etc. Even for educational purposes it is better to bring the user's personnel to the modeller's headquarters than vice versa. Thus there is a good chance that if the modeller uses 'tailored to the user's machine' software during the building and calibrating phases, the user will either pay a very high price for his model or be obliged to accept the services of a modeller who may not be the most qualified for the job.

The fear that a program which runs on one computer cannot be run on another is not justified if one is ready to insure himself adequately by bringing qualified computer system personnel and programmers onto the job. Unless the original software is in complete disorder, it can be translated into a different computer language with no technical problem, though it may take some time. Past bad experiences in this respect come most often from the fact that the job was not entrusted to qualified system personnel guided by numerical hydraulics specialists, but to hydraulic engineers who had only limited experience in programming.

In conclusion, if the computers are really different and the software must be rewritten, it is the original modeller who most likely would do the best job.

11.4 TRAINED PERSONNEL PROBLEMS

From what was written above, the reader has probably already concluded that the user who wishes to operate a model must have at his disposal not only an adequate computer, but also trained computer system personnel capable of running the machine and exploiting the manufacturer's operation systems. Such is usually the case for any medium size computer installation, but it is important to ensure the availability of its personnel for model intervention when necessary.

The purpose of the transfer and possibly the distance between the modeller's and user's headquarters will define the needs in trained numerical hydraulics

personnel. For the purpose of running the model without introducing any major modifications, a very modest amount of training is needed provided that the user's manual is very comprehensive. There are examples (Senegal–see below) when two weeks were enough. If some modifications are needed or if exploitation problems arise, the modeller's specialists may be called in for a few days. Such a use of the model requires on the user's side only a general knowledge of the principles on which the model is based and of its associated software. It implies, in return, that there is a special maintenance contract with the modeller and that the modeller's engineers are available for such interventions.

If the user wants to have full control of the model and/or to use the modelling system for cases other than the original study, then he must accept the responsibility of imposing on the modeller the full training of his specialists. That means that they must learn the theory, the method of solution, all details of solution algorithms, and the program itself. As is shown below in the Mekong model transfer example, the user must be prepared to pay for this training and allow for such training time as is necessary for his specialists, who need to know the meaning of every statement in the software used. The price includes also the willingness to let these people stay in their job for a sufficient time to train others. The last remark is especially important for developing countries. Indeed, it is well known to international organizations such as UN, WMO, etc. (see for example Askew, 1978) that there is a considerable mobility of professional staff in these countries, with unexpected transfers of personnel from one department to another or their rapid promotion from technical to administrative posts.

It is obvious that the user's personnel should have sufficient qualifications to be able to profit from such training. If such is not the case, the independence which the user hoped to obtain will never exist and he is actually wasting his money. What then are the qualifications required in order that the user's numerical hydraulics specialists be able to take full responsibility for the operation and modification of a transferred model and modelling system? The following list is certainly not exhaustive, but at least establishes certain minimum qualifications.

(1) A thorough background in river hydraulics, including the unsteady flow equations, channel resistance properties, and hydraulic structures.

(2) A working knowledge of numerical hydraulics, including the more common finite difference methods, stability and convergence properties, matrix operations, and the solution of large systems of equations.

(3) Detailed knowledge of the program language being used, practical experience in this domain being especially valuable.

(4) An appreciation of the functioning of the computer's operating system; especially the definition of auxiliary files and management of input-output operations.

11.5 EXAMPLES OF TRANSFER OPERATIONS

The transfer of the Mekong Delta mathematical model from Grenoble (France) to Bangkok (Thailand)

The Mekong Delta mathematical model was built, calibrated and run in Grenoble (France) by SOGREAH between 1962 and 1966, as described by Zanobetti *et al.* (1970), UNESCO (1969), and also Cunge (1975c). The client was the UNDP with the UNESCO acting as its executing agency. The Mekong Committee, established by the riparian countries of the Lower Mekong River Basin, wished to use the model as a tool to study development projects of its own and for that purpose asked the UNDP to finance the model transfer from Grenoble to Bangkok.

Difficulties arose from the fact that the Bangkok computer was a different model from the Grenoble one. The original Mekong model, as run at the end of the project, was implemented in Grenoble on the IBM 7044 machine having a core memory of 256 K bytes; the original model used 128 K of that storage. The Bangkok computer was the IBM 360-40 model with a core memory of 64 K bytes. The differences between the two computers were not limited to speed and core storage, but also concerned the number of peripheral units and the type of operating system. Thus, in order to transfer the model onto the Bangkok computer it was necessary to completely rewrite the existing program. Moreover, given the purpose of the transfer and the distance separating the modeller's and user's offices, the transfer operation had to be made in such a way as to give the client full autonomy in operating and modifying the model. This result was ensured by the contract, whose most important articles are quoted below – they give an excellent definition of the transfer operation. The contract called for

'. . . the reanalysis of the existing work, particularly as to the programme and its pertinent data in order to reduce the computer memory requirement and to eliminate operative errors. This provision is foreseen to be necessary because of the reduction of available computer memory capacity from 128K to 64K.

Adaptation of the existing mathematical model for use in the new computer, which will be model IBM 360-40, is further defined by Annex I, which lists all items of equipment. The mathematical model shall faithfully reflect the hydraulic characteristics of the Mekong Delta.

The adapted mathematical models shall include all the programming, directions, mathematical theory, punch cards, tapes and other pertinent documents, material and data which are used in the computer calculations of the problems set forth herein. The accuracy of the adapted models shall be equal to that of the original model. All of the approximately 300 computational points of the original model shall be included in the adapted models.

A descriptive and operating manual shall be prepared which will provide detailed instructions for the operation of the adapted models. The instructions will be sufficiently clear and concise so that any person with a reasonable preparation in training and experience with the IBM 360-40 model computer

will be able to operate the adapted models without need for additional consultation and/or training. The writing of the manual shall include, among others, the following items:

(a) a description of the mathematical philosophy of the models;
(b) the programming of the models in the Fortran language;
(c) a description of the general organisation of the programme;
(d) the manner of entering data into the computer;
(e) a description of all probable malfunctions and their rectification;
(f) a careful analysis of operations to ensure a smooth operation of the models;
(g) a careful and detailed description of the limitations of the adapted models as to their accuracy, and the boundaries of the area within which they can be assumed to be effective.

All matters relative to the effective, accurate and trouble-free operation of the models shall be included.

The adapted models can be used for the study of physical conditions other than those defined under the previous contract. In order to be able to do this, the adapted models must be further modified by changing parameters, programming, etc. Although these changes and modifications to the adapted models are not part of the work which is the subject of this contract, a special chapter of the descriptive and operating manual shall describe, in a general way, a certain number of these possibilities for modifications, such as:

(a) the construction and operation of a barrage on the Tonle Sap (already in the existing models);
(b) construction of a canal to bring water from a higher elevation into the Grand Lac;
(c) construction of pumping facilities in both directions through the Tonle Sap barrage;
(d) construction of new dykes and/or canals within the Delta area;
(e) construction of a barrage downstream from Phnom Penh.

The intention is to provide general explanations, adequate to permit an experienced and trained analyst, with the consultation of a competent hydraulic expert, to make adjustments and changes in the models to meet new physical conditions. It is not the intention of the above paragraph to require detailed programmes or specific changes.

The operating manual shall also include a section which shall describe in a general way the manner in which the adapted models can be refined by the inclusion of new flood observations and new values of rain and/or evaporation.

The submission of the adapted models shall include the following items:

(a) a listing of the programmes in the Fortran language shall be submitted in three copies in standard readily usable format;
(b) the programme in the Fortran language shall be submitted ready for use in magnetic tapes and punched cards, in three copies;

(c) the 'sequence' file which defines topological and hydraulical data shall be submitted in magnetic tape and punched cards in three copies accompanied by three copies of complete tables of coefficients in decimal form;

(d) the data file shall be submitted in magnetic tape and punched cards accompanied by a 'listing' of the tables used to generate the data tape. The three flood periods of four months each for 1961, 1963 and 1964 shall be submitted on one magnetic tape and one punched-card file in three copies each;

(e) the descriptive and operating manual shall be written in the French and English languages and submitted in four copies for correction and acceptance. Following the conclusion of the model work upon successful acceptance trials, both language versions shall be submitted in 25 copies. With the approval of UNESCO, the English text may be submitted at a later date for final corrections and approval prior to final printing. Both language versions shall be written in a style and with a vocabulary readily understandable in all respects by machine operators who are trained to work with IBM 360-40 equipment and whose mother tongues are French and English respectively.

At the request of UNESCO, not later than 30 days following the receipt of the preliminary submission of all documents, an acceptance test may be undertaken at a laboratory acceptable to UNESCO and to the Contractor, using a computer and peripheral equipment which for all practical purposes is identical in function to that which will be available in the Thai Government's Statistical Office in Bangkok. All arrangements for the laboratory services shall be made by the Contractor. The Contractor shall submit proposals for a suitable laboratory, and for dates for the tests, not later than three months following the authorization for starting this Contract. The programme for the tests shall be agreeable to both UNESCO and the Contractor. UNESCO shall advise the Contractor of its acceptance or rejection not later than two months following this submittal.

At the request of UNESCO, the Contractor shall hold himself ready to assist and to instruct the Bangkok personnel regarding the use of the adapted models and all pertinent documents for a period of one year following the completion and acceptance of the work. During this period and upon notice of three months, he shall be ready to send to Bangkok an engineer skilled in the operation of the adapted models. The engineer shall devote three weeks' time in Bangkok, to demonstrations of the uses of the models, to assist the Mekong Committee in the efficient, accurate and useful exploitation of the models and documents, and to assist the Mekong Committee to make modifications of the programme which fall within the terms of reference of the first contract, if necessary . . .'

The transfer project consisted of three phases. During phase I, which began in June 1967, new software was written in Fortran basic language to be acceptable for the Bangkok operation system (the original program was written partly in Fortran IV, a more advanced language, and partly in Assembler). The new software permitted model operation on the smaller computer by using transfers

between its core storage and peripheral units. The computational time increased considerably but the implementation was made possible. A detailed user's manual was drafted and tested during phase I. It comprised not only usual indications of how to feed the data into the computer but also three supplementary parts:

(i) the description of all possible control messages provoked by errors or inconsistencies in the data;
(ii) the detailed documentation necessary for one to proceed from the formulation of flow equations to the programming;
(iii) the list of all routines in Fortran accompanied by detailed flow charts.

The user's manual was then submitted to the committee of experts supervising the contract execution. The committee was composed of a hydraulics specialist, a data processing expert and a representative of the Mekong Committee who was a hydrometeorologist with a good knowledge of computers. All three of them knew the original project well and two of them were well acquainted with the original program. The committee approval ended phase I of the project.

During phase II the committee of experts prepared a set of modifications and special runs of the program using only the user's manual. The modeller was completely unaware of the contents of the set of data prepared by the experts. The software (recorded on magnetic tapes) was implemented by the modeller on the computer of an independent computational centre whose geographic location was different from that of the modeller but within reasonable distance. The computer configuration was cut down to exactly the same size as the Bangkok centre and the same brand of computer was used. Then the experts operated the model during three days solely with the aid of the user's manual, in the presence of the modeller's staff but without its intervention. The experts' satisfaction as to the possibility of the model running without the modeller's intervention ended phase II.

In phase III, the software was sent to Bangkok and implemented by the user on his computer. Some basic tests as to the compatibility of the Fortran language were run by the user. Then a modeller's engineer went to Bangkok where he spent 3 weeks. During that period all routine operations and the repetition of the flood simulations were performed. A major modification of the model was made by introducing a dyke which completely isolated the Bassac River (*see* Fig. 4.10a) from the region on its right bank. One of the largest floods was selected and simulated with and without the above modification. This test was made jointly by the Mekong Committee engineers and the modeller's representative. Then a series of dyking alternatives in Vietnam was considered and introduced into the model, but this time entirely by the local staff, with no participation of the modeller's engineer. The last operation was successful and it served as a final proof that the Mekong committee staff was fully knowledgeable in model operation. This ended the project in April 1968.

During the implementation phase, the modeller's representative ran into two kinds of problems. First, access to the computer was limited since the machine

belonged to the Thai administration and not to the client. Second, there were several particularities of the IBM operating system which required minor modifications of the system control programs. The latter difficulties were overcome only because the modeller had some knowledge of the system.

The Mekong model remained in continuous use by the local staff without need of the modeller's intervention between April 1968 and 1976. At that time the Mekong Committee obtained access to a more powerful computer. Also new modelling needs appeared – namely the need to study low flow periods for which the original model was not calibrated. Thus it was necessary to modify the software in order to decrease the computational time, then to recalibrate the model. It was decided to entrust the original modeller, SOGREAH, with the job. The Committee could probably have done it as well but the original modeller had the benefit of his established team, greater experience, and a better environment. The work was accomplished within a few months and the client's engineers' previous knowledge of the program obviated the need for a complete new transfer operation. It was sufficient for two of the user's engineers to spend a few weeks at the modeller's headquarters where they themselves wrote the modifications to the operating manual.

The measure of the success of the Mekong model transfer is the fact that the model was run for 8 years by the user, during which period the modeller received neither complaints nor requests for assistance. However, the price of this success was not small. It included training of the user's engineers (during the building and calibrating of the original model), the release by the modeller of all details of the algorithms and software used, reprogramming, writing of a detailed user's manual, acceptance tests and the implementation of the software by the modeller. The last four operations took 8 months and cost nearly 40 000 dollars in 1967/68.

The transfer of the Senegal River model from Grenoble (France) to Dakar (Senegal)

The mathematical model of the Senegal River was built, calibrated and run by SOGREAH in 1969 and 1970. The client was FAO and the work was supervised by a committee of experts, very much as the Mekong model project was. During the project SOGREAH developed a user's manual for the model but the client did not ask for the model to be transferred to his headquarters.

In 1978 it was decided to transfer the model to Dakar where an American consulting firm (Gannet Fleming) was in charge of environmental studies. The studies were made for the OMVS (organization of the riparian states) and financed by the USAID.

The user wanted to run the model frequently while modifying some simulated topographical or structural features, but he was seeking neither the possibility of using the software in order to build another model nor the capability of modifying the programs themselves. Hence it was possible, after a short preparation in Grenoble, to implement the model directly on the com-

puters in Dakar. The user's computers being of the same type as the modeller's, the operating manual could be used without modification. The software was written partly in Fortran IV language, partly in IBM 360 Assembler.

The transferred software consisted of the programs themselves, two River Senegal models (one of the natural valley and one comprising the projected dams, dykes, and irrigation perimeters), several floods and initial states. All these elements were stored on magnetic tape and brought to Dakar by a modeller's engineer having a complete knowledge of the above software *and* a good knowledge of the operating systems of the IBM 370-155 computers. The engineer spent two weeks in Dakar, after which period the user was able to run the model with no trouble.

The fortnight spent in Dakar, however, was not a restful one. There were two IBM 370-155 computers in Dakar run by two different administrative departments, and the mathematical model was only a marginal occupation for them. The computational centre authorities had had bad experience with some water quality mathematical models which had been run on its computer before: each run had taken 4–5 h. This was obviously due to inefficient software, but the result was the same: a blocked computer. Upon hearing about the mathematical model of the Senegal, the authorities were reluctant to have it implemented on their computers, fearing once again excessive run time. This obstacle was not removed until the 11th day after the arrival of the SOGREAH engineer!

The two computers were run with two different versions of the operating system and with very different peripheral unit configurations. One had only magnetic tapes as peripheral units available; another, only disk packs with no possibility of permanent storage. Since it was not possible to limit the implementation of the software to one of the two computers, the modeller's engineer had to prepare auxiliary data management routines for both systems permitting the shift of data and files from one support to the other. That took him only a few hours because he was well acquainted with the operating system. Had this not been the case, the whole transfer operation would have taken several days or even weeks.

During the first ten days the modeller explained the operating manual to the users. The users themselves prepared the set of tests and modifications and when the software was finally implemented on both computers, the users ran the model with their test packages. The implementation and the tests were made during the last five days of the modeller's engineer's stay in Dakar. Since then the user has run the model there with only one or two minor difficulties smoothed out by telex. The whole operation took less than two months and its cost was, travel expenses excluded, less than 25 000 U.S. dollars (1978).

The reader should keep in mind that the Senegal model run in Dakar is, in a way, a black box as far as the user is concerned. The latter has the Fortran listing at his disposal, but he has no real possibility of modifying it or of resolving possible problems by himself. These transfer conditions are acceptable only if the model purpose is limited and only if the client can rely upon the future assistance of the modeller if something goes wrong.

The cost of and the time needed for the transfer of the Senegal model may surprise the reader as being low, especially as compared to those of the Mekong. This is due to the fact that the model development and user's manual were both paid for by the first FAO project which explicitly specified that the transfer of the software might be required in the future. Also the 'black box' character of the model use obviated the need for extensive personnel training.

References

Abbott, M. B. (1966). *An Introduction to the Method of Characteristics*, Thames and Hudson, London, and American Elsevier, New York.

Abbott, M. B. (1975a). Method of characteristics, Chapter 3 of *Unsteady Flow in Open Channels*, Water Resources Publications, Fort Collins, Colorado.

Abbott, M. B. (1975b). Weak solutions of the equations of open channel flow, Chapter 7 of *Unsteady Flow in Open Channels*, Water Resources Publications, Fort Collins, Colorado.

Abbott, M. B. (1977). Commercial and scientific aspects of mathematical modelling, *Int. Conf. on Appl. Num. Modelling*, University of Southampton, England, July.

Abbott, M. B. (1979). *Computational Hydraulics*; *Elements of the Theory of Free Surface Flows*, Pitman Publishing Limited, London.

Abbott, M. B. and Cunge, J. A. (1975). Two-dimensional modelling of tidal deltas and estuaries, Chapter 18 of *Unsteady Flow in Open Channels*, Water Resources Publications, Fort Collins, Colorado.

Abbott, M. B. and Ionescu, F. (1967). On the numerical computation of nearly-horizontal flows, *J. Hyd. Res.*, **5**, No.2, pp. 97–117.

Abbott, M. B., Marshall, G. and Ohno, T. (1969). *On Weak Solutions of the Equations of Nearly Horizontal Flow*, Report Series 3, International Institute for Hydraulic and Environmental Engineering, Delft.

Abbott, M. B. and Rodenhuis, G. S. (1972). A numerical simulation of the undular hydraulic jump, *J. Hyd. Res.*, **10**, No. 10, pp. 239–257.

Abramov, A. A. (1961). On the translation of boundary conditions for systems of linear ordinary differential equations (a variant of the sweep method), *URSS Comput. Math. and Math. Phys.*, No.1 (in Russian).

Abramov, A. A. and Andrieyev, V. B. (1963). Application of the double-sweep method, *J. Applied Math. and Math. Phys.*, **3**, No. 2 (in Russian).

Alalykin, G. B., Godunov, S. K., Kirieeva, I. L. and Pliner, L. A. (1970). Solution of one-dimensional problems of gas dynamics on moving grids.

Amein, M. M. and Fang, C. S. (1970). Implicit flood routing in natural channel, *JHYD*, ASCE, **96**, No. HY12, December.

ASCE (1968). *Automation of Irrigation and Drainage Systems*, National Irrigation and Drainage Specialty Conference, Phoenix, November.

ASCE (1975). *Sedimentation Engineering*, Manual and Reports on Engineering Practice, No. 54.

Askew, A. J. (1978). Use of catchment models for flood forecasting in Central America, *Int. Symp. on Logistics and Benefits of using Mathematical Models of Hydrologic and Water Resource Systems*, IIASA, Laxenburg.

Bagnérès, J. (1972). Comparaison économique des différents systèmes de régulation dans les canaux, *Congrès de l'Association Internat pour l'Etude des Irrigations et Drainage*, Varna, Bulgarie.

Baker, F. T. (1972). Chief programmer team management of production programming, *IBM Syst. J.*, **11**, No. 1.

Balloffet, A., Cole, E. and Balloffet, A. F. (1974). Dam collapse wave in a river, *JHYD*, ASCE, **100**, No. HY5.

Benet, F. and Cunge, J. (1971). Analyse d'expériences sur les ondulations secondaires dues aux intumescences dans les canaux trapézoidaux, *J. Hyd. Res.*, **9**, No. 1, pp. 11–13.

Benoist, G., Daubert, A., Fabre, L., Miquel, H. and Pugnet, L. (1973). Calcul des ondes de submersion à l'aval des barrages d'Electricité de France, *Proceedings XVth Congress IAHR, Istanbul*, Vol. 5, pp. 5–9.

Blanchet, Ch. (1971). Rapport général du sujet C thème 3, *14th Congress of the IAHR, Paris*.

Bodley, W. E. and Wylie, E. B. (1978). Control of transients in series channel with gates *J. Hyd. Div., ASCE*, **104**, No. HY10, October.

Boris, J. P. and Book, D. L. (1973). Flux-corrected transport. I. SHASTA, a fluid transport algorithm that works, *J. Comput. Phys.*, **11**, pp. 38–69.

Bouvard, M., Chollet, J-P. and Cunge, J. A. (1977). Progrès récents et difficultés de simulation mathématique de rivières alluvionnaires, *17th Congress of the IAHR, Baden-Baden*.

Bowles, D. S., Fread, D. L. and Grenny, W. J. (1977). Coupled dynamic stream flow-temperature models, *JHYD*, ASCE, **103**, No. HY5, May.

Brebion, S., Lebrun, B., Chevereau, G. and Preissmann, A. (1971). Modèles mathématiques de la pollution, *IRCHA*, Centre de Recherche, 91 Vert-le-Petit, France, November.

Carrère, J. (1977). *Etude Préliminaire en Vue de l'Etablissement d'un Modèle Mathématique du fleuve Niger. Etude de Données Cartographiques et Topographiques*, Institut Géographique National, Paris.

Chang, H. H. and Hill, J. C. (1977). Minimum stream power for rivers and deltas, *JHYD*, ASCE, **103**, No. HY12, December.

Chen, Y. H. (1973). Mathematical modelling of water and sediment routing in natural channels, *Ph. D. Thesis*, Colorado State University, Fort Collins.

Chen, Y. H. and Simons, D. B. (1975). Mathematical modelling of alluvial channels, *ASCE Symposium on Modelling Techniques 'Modelling 75'*, Vol. 1, San Francisco, Sept. 3–5.

Chervet, A. and Dallèves, P. (1970). Calcul de l'onde de submersion consécutive à la rupture d'un barrage, *Schweizerische Bauzeitung* 88, No. 19, May.

Chevereau, G. and Gauthier, M. (1976). Use of mathematical models as an approach to flow control problems, *Proceedings of the Int. Symp. on Unsteady Flow in Open Channels,* BHRA Fluid Engineering, Newcastle-upon-Tyne.

Chevereau, G., Holly, F. and Preissmann, A. (1978). Can detailed hydraulic modelling be worthwhile when hydrologic data is incomplete?, *Int. Conf. on Urban Storm Drainage*, University of Southampton, April.

Chevereau, G. and Preissmann, A. (1971). Etude mathématique, programme de calcul, Appendix 3 of Brebion *et al.* (1971).

Chollet, J. P. (1977). *Ecoulement non-permanent sur fond mobile de rugosité instationnaire. Modèle mathématique.* Thesis submitted to l'Université Scientifique et Médicale and l'Institut National Polytechnique de Grenoble, February.

Chollet, J. P. and Cunge, J. A. (1979). New interpretation of some head loss–flow velocity relationships for deformable beds, submitted to *J. Hyd. Res.*, **17**, No. 1, pp. 1–13.

Chollet, J. P. and Cunge, J. A. (1980). Head loss–flow velocity relationships for deformable movable beds, *Appl. Math. Modelling*.

Chow, V. T. (1959). *Open Channel Hydraulics*, McGraw-Hill, New York.

Cleary, R. W. and Adrian, D. D. (1973). New analytical solutions for dye diffusion equations, *JEED*, ASCE, **99**, No. EE3, June, pp. 213–227.

Clément, R. (1966). Calcul des débits dans les réseaux d'irrigation fonctionnant 'à la demande'. Première et deuxième formules de la demande et évolution de la demande dans le temps. Théorie et introduction aux applications pratiques, *La Houille Blanche*, No. 5, pp. 553–576.

Colin, E. and Pochat, R. (1976). One dimension open channel flow (dissipative operator), *Proceedings Int. Symp. Unsteady Flow in Open Channels.* BHRA Fluid Engineering, Newcastle-Upon-Tyne.

Combes, G. (1968). Quelques réflexions sur l'évolution des systèmes de régulation de débits et de niveaux dans les canaux, *La Houille Blanche*, No. 1, pp. 45–49.

Corps of Engineers (1976). *HEC-2 Water Surface Profiles, Users Manual with Supplement*, Hydrologic Engineering Center, Corps of Engineers, U.S. Army, Davis, California, November.

Courant, R., Friedrichs, K. O. and Lewy, H. (1928). On the partial difference equations of mathematical physics. *Math. Ann.*, **100**, p. 32 (in German).

Courant, R. and Hilbert, D. (1953). *Methods of Mathematical Physics*, Vol. 1, Interscience Publishers, New York.

Craya, A. (1946). Calcul graphique des régimes variables dans les canaux, *La Houille Blanche*, new ser. no. 1, Nov. 1945–Jan 1946, pp. 79–38, and no. 2, Mar. 1946, pp. 117–130.

Cunge, J. A. (1966a). *Etude d'un schéma de différences finies appliqué à l'intégration numérique d'un certain type d'équation hyperbolique d'écoulement*, Thesis presented to the Faculty of Science of Grenoble University, 27 May.

Cunge, J. A. (1966b). Comparaison des résultats des essais d'intumescences effectués sur le modèle réduit et sur le modèle mathématique du canal Oraison-Manosque, *La Houille Blanche*, No. 1, pp. 55–70.

Cunge, J. A. (1969). On the subject of a flood propagation computation method (Muskingum method), *J. Hyd. Res.*, 7, No. 2, pp. 205–230.

Cunge, J. A. (1970). Calcul de propagation des ondes de rupture de barrage, *La Houille Blanche*, No. 1, pp. 15–23.

Cunge, J. A. (1972). Deposition of sediment in transient flow, Discussion of Proc. Paper 8191 by Chang and Richards, *JHYD*, ASCE, 98, No. HY2.

Cunge, J. A. (1975a). Applied mathematical modelling of open channel flow, Chapter 10 of *Unsteady Flow in Open Channels*, Water Resources Publications, Fort Collins, Colorado.

Cunge, J. A. (1975b). Rapidly varying flow in power and pumping canals, Chapter 14 of *Unsteady Flow in Open Channels*, Water Resources Publications, Fort Collins, Colorado.

Cunge, J. A. (1975c). Two-dimensional modelling of flood plains, Chapter 17 of *Unsteady Flow in Open Channels*, Water Resources Publications, Fort Collins, Colorado.

Cunge, J. A. and Perdreau, N. (1973). Mobile Bed Fluvial Mathematical Models, *La Houille Blanche*, no. 7.

Cunge, J. A. and Simons, D. B. (1975). Mathematical model of unsteady flow in movable bed rivers with alluvial channel resistance, *Proceedings of the XVIth Congress, IAHR*, Sao Paulo.

Cunge, J. A. and Wegner, M. (1964). Intégration numérique des équations d'écoulement de Barré de St. Venant par un schéma implicite de différences finies. Application au cas d'une galerie tantôt en charge tantôt à surface libre, *La Houille Blanche*, No. 1, p. 33–39.

De Saint Venant B. (1871). Théorie du mouvement non-permanent des eaux avec application aux crues des rivières et à l'introduction des marées dans leur lit, *Acad. Sci. Comptes rendus*, 73, pp. 148–154, 237–240.

De Vries, M. (1973a). *River Bed Variations – Aggradation and Degradation*, Delft Hydraulic Lab., Publ. No. 107, Delft, The Netherlands.

De Vries, M. (1973b). *Application of Physical and Mathematical Models for River Problems*, Publication No. 112, Delft Hydraulics Laboratory, Delft, The Netherlands, April.

Dobbins, W. E. and Bella, D. A. (1968). Difference modelling of stream pollution, *JSED*, ASCE, 94, No. SA5, October.

Dracos, Th. (1970). Computation of instantaneous flows in open channels of any geometry, *Schweizerische Bauzeitung*, 88, No. 19, May, pp. 21/1–21/8 (in German).

Eheart, J. W., Joeres, E. F. and Hoopes, J. A. (1978). Optimization of waste removal for wide shallow rivers, *JEED*, ASCE, 104, No. EE4, August, pp. 593–600.

Einstein, H. A. (1950). The bed load function for sediment transportation in open channel flows, *U.S. Dept. of Agriculture, Tech. Bull. 1026.*

Elder, J. W. (1959). The dispersion of marked fluid in turbulent shear flow, *J. Fluid Mech.*, **5**, No. 4, pp. 544–560.

Engelund, F. and Hansen, E. (1967). A monograph on sediment transport in alluvial streams, Technical University of Denmark.

Favre, H. (1935). *Etude Théorique et Expérimentale des Ondes de Translation dans les Canaux Découverts*, Dunod, 92, rue Bonaparte, Paris.

Fischer, H. B. (1966). *Longitudinal Dispersion in Laboratory and Natural Streams*, Report No. KH-R-12, W.M. Keck Laboratory of Hydraulics and Water Resources, California Institute of Technology, Pasadena.

Fischer, H. B. (1973). Longitudinal dispersion and turbulent mixing in open-channel flow, *Ann. Rev. Fluid Mech.*, pp. 59–78.

Flood Studies Report (1975) *Volume III, Flood Routing Studies*, Natural Environment Research Council, 27 Charing Cross Road, London.

Friazinov, I. D. (1970). Solution algorithm for finite difference problems on directed graphs, *J. Math. and Math. Phys.*, **10**, No. 2 (in Russian).

Gelfand, I. M. and Lokutsievski, O. V. (1964). The double sweep method for solution of difference equations, Appendix II to Godunov and Ryabenki (1964).

Godfrey, R. C. and Frederick, B. J. (1970). *Stream Dispersion at Selected Sites*, U.S. Geological Survey Professional Paper 433-K.

Godunov, S. K. and Ryabenki, V. S. (1964). *Theory of Difference Schemes*, North-Holland, Amsterdam.

Gunaratnam, D. and Perkins, F. E. (1970). *Numerical Solutions of Unsteady Flow in Open Channels*, Hydrodynamics Laboratory T.R. No. 127, Dept. of Civil Engineering, MIT, Cambridge, Massachusetts.

Harder, J. A., Shand, M. J. and Buyalski, C. P. (1972). Automatic downstream control of canal check gates by the hydraulic filter offset (HYFLO) method, *8th Congress, Int. Commission on Irrigation and Drainage, Varna.*

Henderson, F. M. (1966). *Open Channel Flow*, McMillan Company, New York.

Holley, E. R. (1971). *Transverse Mixing in Rivers*, Report No. S 132, Delft Hydraulics Laboratory, Delft.

Holly, F. M. (1975). *Two-dimensional Mass Dispersion in Rivers*, Hydrology Paper No. 78, Colorado State University, Fort Collins.

Holly, F. M. and Cunge, J. A. (1975). Prediction of time-dependent mass dispersion in natural streams, *Proceedings of Modelling 75*, ASCE Hydraulics Division, September.

Holly, F. M. and Preissmann, A. (1977). Accurate calculation of transport in two dimensions, *JHYD* ASCE, **103**, No. HY11, November.

Holly, F. M. and Simons, D. B. (1975). Transverse mixing of neutrally-buoyant tracers in non-rectangular channels, *Proceedings of the XVIth Congress, IAHR*, Sao Paulo, July.

IAHR (1976). *Symposium: Fluid motion stability in hydraulic systems with automatic regulators, Bucharest*, September.

Isaacson, E., Stoker, J. J. and Troesch, B. A. (1954). *Numerical Solution of Flood Prediction and River Regulation Problems (Ohio–Mississippi floods)*, Report II, New York University, Inst. Math. Sci. Rept. IMM-NYU-205.

Ivanova, A. A. (1966). Variations of stage/discharge relationship with distance for a prismatic channel during the propagation of release waves (numerical experiments), *GGI Trudy*, No. 136, pp. 18–24 (in Russian).

Ivanova, A. A. (1967), Analysis of stage discharge relation in the propagation of release waves in prismatic channels (a numerical experiment), *GGI Trudy*, No. 140, pp. 44–63 (in Russian).

Ivicsics, L. C. (1975). *Hydraulic Models*, Res. Inst. for Water Resources Development, Budapest.

Jain, S. C. (1976). Longitudinal dispersion coefficients for streams, *JEED*, ASCE, **102**, No. EE2, April.

Jobson, H. E. and Keefer, T. N. (1976). Use of depth profiles for flow-model calibration, *Symposium on Inland Waters for Navigation, Flood control, and Water Diversions*, ASCE, pp. 641–649, August.

Jobson, H. E. and Keefer, T. N. (1979). Modeling highly transient flow, mass, and heat transport in the Chattahoochee River near Atlanta, Georgia, *USGS Open File Report* 79-270, NSTL Station, Mississippi 39529.

Jolly, J. P. and Yevjevich, V. (1971). *Amplification Criterion of Gradually Varied Single Peak Waves*, Hydrology Paper No. 51, Colorado State University, Fort Collins, Colorado.

Kalinin, G. P. and Miljukov, P. I. (1958). On the computation of unsteady water flow along channels by the use of reach-travel curves, *Meteorologiya i Gidrologiya*, No. 7, pp. 18–25 (in Russian).

Katopodes, N. and Strelkoff, T. (1978). Computing two-dimensional dam break waves, *JHYD*, ASCE, **104**, No. HY9, September.

Kiselev, P. G. (1957). *Handbook of Hydraulic Computations* (in Russian), Moscow.

Kyozo Suga (1969). On the simulation of river-bed variations by characteristics, *13th Congress of the IAHR*, Kyoto.

Land, L. F. (1978). Unsteady solute-transport simulation in streamflow using a finite-difference model, *USGS Water Resource Investigations 78-18*, NSTL Station, Mississippi 39529.

Lax, P. D. (1954). Weak solutions of non-linear hyperbolic equations and their numerical applications, *Comm. Pure Appl. Math.*, 7, pp. 159–193.

Lax, P. D. and Wendroff, B. (1960). Systems of conservation laws, *Comm. Pure Appl. Math.*, **13**, pp. 217–237.

Leendertse, J. J. (1970). *A Water-Quality Simulation Model for Well-Mixed Estuaries and Coastal Seas: Vol. I*, Principles of Computation, Rand Corporation Memorandum, RM-6230-RC, February.

Lemoine, R. (1948). Sur les ondes positives de translation dans les canaux et sur le ressaut ondulé de faible amplitude, *La Houille Blanche*, No. 2, pp. 183–185.

Liggett, J. A. (1975). Basic equations of unsteady flow, Chapter 2 of *Unsteady Flow in Open Channels*, Water Resources Publications, Fort Collins, Colorado.

Liggett, J. A. and Cunge, J. A. (1975). Numerical methods of solution of the unsteady flow equations, Chapter 4 of *Unsteady Flow in Open Channels*, Water Resources Publications, Fort Collins, Colorado.

Liu, H. (1977). Predicting dispersion coefficient of streams, *JEED*, ASCE, Proc. Paper 12724, February.

Lugiez, F. (1976) (group leader). Problèmes de sédimentation dans les retenues, *International Commission on Large Dams, 12th Congress*, Mexico.

Martin, B. (1975). Numerical representations which model properties of the solution to the diffusion equation, *J. Comput. Phys.*, 17, pp. 358–383.

Massau, J. (1889). L'intégration graphique, and Appendice au mémoire sur l'intégration graphique, *Assoc. des Ingénieurs sortis des Ecoles Spéciales de Gand, Belgium, Annales*, 12, pp. 185–444.

McQuivey, R. S. and Keefer, T. N. (1976). Convective model of longitudinal dispersion, *JHYD*, ASCE, **102**, No. HY10, October.

Meijer, Th. J. F. P., Vreugdenhil, C. B. and de Vries, M. (1965). A method of computation for non-stationary flow in open-channel networks, *Proceedings, 11th Congress IAHR*, Leningrad, Paper 3.28.

Miller, W. A. and Cunge, J. A. (1975). Simplified equations of unsteady flow, Chapter 5 of *Unsteady Flow in Open Channels*, Water Resources Publications, Fort Collins, Colorado.

Myers, W. R. C. (1978). Momentum transfer in a compound channel. *J. Hyd. Res., IAHR*, **16**, No. 2.

Nemec, J. and Kite, G. W. (1978). Mathematical model of the upper Nile basin, *Int. Symp. on Logistics and Benefits of using Mathematical Models of Hydrologic and Water Resource Systems*, IIASA, Laxenburg.

Nordin, C. F. and Sabol, G. V. (1974). *Empirical Data on Longitudinal Dispersion in Rivers*, U.S. Geological Survey Water Resource Investigation 20–24, August.

Perdreau, N. and Cunge, J. A. (1971). Sedimentation dans les estuaires et les embouchures, bouchon marin et bouchon fluvial, *14th Congress of the IAHR*, Paris.

Petersen, F. B. (1977). *Prediction of Longitudinal Dispersion in Natural Streams*, Series Paper 14, Institute of Hydrodynamics and Hydraulic Engineering, Technical University of Denmark, Lyngby.

Ponsy, J. and Carbonnell, M. (1972). Etude photogrammétrique d'intumescences dans le canal d'amenée de l'usine d'Oraison, Centre d'Actualisation Scientifique et Technique, *INSA*, Lyon, France, pp. 161–171.

Preissmann, A., (1961). Propagation des intumescences dans les canaux et rivières, *First Congress of the French Association for Computation, Grenoble, September.*

Preissmann, A. (1965). Difficultés rencontrées dans le calcul des ondes de translation à front raide, *Proceedings, 11th Congress IAHR*, Leningrad, paper 3.52.

Preissmann, A. and Chevereau, G. (1976). Remarques sur le choix des méthodes d'appréciation de la qualité des divers systèmes de régulation de canaux à surface libre, *Symposium: Fluid Motion Stability in Hydraulic Systems with Automatic Regulators, Bucharest.*

Preissmann, A. and Cunge, J. A. (1961a). Calcul des intumescences sur machines électroniques, *IX meeting of the IAHRE*, Dubrovnik.

Preissmann, A. and Cunge, J. A. (1961b). Calcul du mascaret sur machine électronique, *La Houille Blanche*, No. 5, pp. 588–596.

Preissmann, A. and Cunge, J. A. (1967). Le ressaut ondulé de faible amplitude dans les canaux trapézoidaux, *J. Hyd. Res.*, **5**, No. 4, pp. 263–279.

Preissmann, A. and Cunge, J. A. (1968). Included in Zanobetti *et al.* 1968.

Rajar, R. (1972). Recherche théorique et expérimentale sur la propagation des ondes de rupture de barrage dans une vallée naturelle, *Thesis* submitted to l'Université Paul Sabatier, Toulouse, June.

Richtmyer, R. D. (1957). *Difference Methods for Boundary Value Problems*, Interscience, New York.

Rozenberg, L. I. and Rusinov, M. I. (1967). Some singularities of schematization of channels with flood plains in unsteady flow computations, *GGI Trudy*, No. 140, pp. 83–90 (in Russian).

Rusinov, M. I. (1967). Influence of some parameters of prismatic channels with flood plains on the velocity of release wave crests, *GGI Trudy*, No. 140, pp. 64–82 (in Russian).

Sakkas, J. G. (1974). *Dimensionless Graphs of Floods from Ruptured Dams*, Report to Hydrologic Engineering Center, Contract DAC W05-74-C-0029, US Army Corps of Engineers, Davis, California.

Sakkas, J. G. and Strelkoff, T. (1976). Dimensionless solutions of dam-break flood waves, *JHYD*, ASCE, **102**, No. HY2, February.

Sayre, W. W. (1968). *Dispersion of Mass in Open Channel Flow*, Hydraulic Paper No. 3, Colorado State University, Fort Collins, Colorado, February.

Schaffranek, R. W. and Baltzer, R. A. (1978). Fulfilling model time-dependent data requirements, *Symposium on Technical, Environmental, Socio-economical and Regulatory Aspects of Coastal Zone Management*, Waterways and Harbors Division, ASCE, March.

Schönfeld, J. C. (1951), Propagation of tides and similar waves, *Thesis*, Technical University, Delft, The Netherlands.

Shen, H. T. (1978). Transient mixing in river channels, *JEED*, ASCE, **104**, No. EE3, June, pp. 445–459.

SOGREAH (1961). *Comparison of the de St. Venant Equations and Muskingum Method on the Rhône River*, internal report.

Stevens, M. A. and Simons, D. B. (1973). Manning's roughness coefficients for the Padma River, *15th Congress of the IAHR*, Vol. 1, Istanbul.

Stoker, J. J. (1957). *Water Waves*, Interscience, New York.

Stone, H. L. and Brian, P. T. (1963). Numerical Solution of convective transport problems, *Am. Inst. Chem. Engng. J.*, No. 9, pp. 681–688.

Taylor, G. I. (1954). The Dispersion of Matter in Turbulent Flow Through a Pipe, *Proc. R. Soc. London*, 233A, pp. 446–468.

UNESCO/SOGREAH (1964). *Mekong Delta mathematical model, Vol. II*, Preliminary Investigation, Sept.

UNESCO (1969). *Mekong River Delta Model Study*, Report Series 9, Paris.

Valentine, E. M. and Wood, I. R. (1977). Longitudinal dispersion with dead zones, *JHYD*, ASCE, **103**, No. HY9, September.

Vasiliev, O. F. (1970). Numerical solution of the non-linear problems of unsteady flow in open channels, *Proceedings of the 2nd International Conference on Numerical Methods in Fluid Dynamics, Berkeley*, pp. 410–421 (also in *Lecture Notes in Physics*, Vol. 8, Springer-Verlag, Bonn–New York, 1971).

Vasiliev, O. F. and Godunov, S. K. (1963). Numerical method of computation of wave propagation in open channels; application to the problem of floods, *Dokl. Akad. Nauk SSSR*, **151**, No. 3 (in Russian).

Vasiliev, O. F., Temnoeva, T. A. and Shugrin, S. M. (1965). Numerical method for the calculation of unsteady flows in open channels, *Izv. Akad. Nauk SSSR, Mechanics*, No. 2 (in Russian).

Verdet, G. (1975). Mathematical model of movable bed applied to Isère upstream from Grenoble (France) and movable bed model of the River Durance at Saint Auban Plant (France), *Unsteady Flow in Open Channels*, Water Resources Publications, Fort Collins, Colorado, pp. 861–864.

Verwey, A. (1971). Mathematical model for flow in rivers with realistic bed configuration, Report series No. 12, *International Courses in Hydraulic and Sanitary Engineering*, Delft.

Von Neumann, J. and Richtmyer, R. D. (1950). A method for the numerical calculations of Hydrodynamic shocks, *J. Appl. Phys.*, 21 pp. 232.

Vreugdenhil, C. B. (1973). *Computational Methods for Channel Flow*, Publication No. 100, Delft Hydraulics Laboratory, Delft.

Vreugdenhil, C. B. and de Vries, M. (1967). *Computations of Non-steady Bed-load Transport by a Pseudo Viscosity Method*, Delft Hydr. Lab. Publ. No. 45, Delft, The Netherlands.

Wood, E., Harley, B. M. and Perkins, F. G. (1975). *Transient Flow Routing in Channel Networks*, Report RR-75-1, IIASA, Laxenburg.

Yevjevich, V. (1975). Storm-drain networks, Chapter 16 of *Unsteady Flow in Open Channels*, Water Resources Publications, Fort Collins, Colorado.

Yotsukura, N., Fischer, H. B. and Sayre, W. W. (1970). *Measurement of Mixing Characteristics of the Missouri River between Sioux City, Iowa and Plattsmouth, Nebraska*, U. S. Geological Survey Water Supply Paper 1899-G.

Zanobetti, D., Lorgeré, H., Preissmann, A. and Cunge, J. A. (1968). Le modèle mathématique du delta du Mékong, *La Houille Blanche*, No. 1, 4 and 5.

Zanobetti, D., Lorgeré, H., Preissmann, A. and Cunge, J. A. (1970). Mekong Delta mathematical model program construction, *J. Waterways and Harbors Division*, ASCE, **96**, No. WW2, May.

Index

Abbott-Ionescu type scheme, 69, 86, 89, 97, 104
Adour River, 139, 147, 172
Algorithm,
  Abbott-Ionescu scheme, 106, 109, 120
  inundated plain model, 113
  multi-connected (looped) networks, 117
  Preissmann scheme, 108, 111, 117
  simply-connected (branched) networks, 109
Amplification factor, 83, 87–9
Amplitude portraits, 86, 88
Approximation error, 77

BIVAL regulator, 238
Bore, hydraulic *see* Surge
Boundary conditions,
  characteristics theory viewpoint, 29
  convection-diffusion problem, 329, 343
  data needs, 230
  discretization, 72
  downstream, choice of, 36
  exterior, 167
  formal requirements, 31
  interior, 50, 167
  model calibration, 198
  model exploitation, 230
  movable bed models, 278
  non reflective, 36
  rating curve, 36

Calibration,
  accuracy of, 222
  boundary conditions, 198
  cost of, 378
  quality of, 384
  steady flow situations, 186
  two-dimensional zones, 206, 212, 219
  unsteady flow situations, 193–207, 212, 219
CAREDAS modelling system, 5, 104
CARIMA modelling system, 5, 104, 109, 172, 221, 375
Celerity,
  flood peaks, 198–206
  shocks, 42
  small waves, 29
CFL condition *see* Courant–Friedrichs–Lewy
Channel flow, 7
  equations, 14, 44, 48, 49
  integral relationships, 11, 13
Characteristics, 24 *et seq.*, 26, 29, 281
  numerical integration method, 54, 260
  specified interval (Hartree) method, 58
  variable grid method, 57
Chèzy formula, 22
Clinch River, 343
Compatibility conditions *see* Boundary conditions, interior
Computational hydraulics, 2
Conservation equations,
  differential form of, 13, 40, 43
  energy, 8, 128
  integral form of, 9, 40, 43
  mass, 8, 11, 14, 16–18
  momentum, 8, 13, 15–17
Consistency, 79
Convection,
  of polluted material, 320
  one-dimensional equation, 320
Conveyance,
  calibration of, 187
  coefficients of, 87
  computation in compound sections, 21
  definition, 20
  representation in models, 163
Convergence, 77, 163
Convergence coefficients, 88

Cost of mathematical models, 372 *et seq.*
Courant–Friedrichs–Lewy (CFL) condition, 53, 85
Courant number, 85, 323
Critical flow, 26, 32, 177

Dam-break wave simulation, 357
  computational problems, 360
  equations, 359
Damping, numerical *see* Amplitude portraits
Data needs, 225
  hydraulic, 230
  movable bed models, 280
  topographic, 228
Data, representation in models, 128
Delft Hydraulics Laboratory scheme, 68, 86, 105
Dependent variables, 8, 16, 17
Difference methods *see* Finite difference methods
Diffusion,
  apparent, 316
  artificial (numerical), 321–5
  of pollutants *see* Transport of pollutants
Diffusion analogy, 46
Discontinuities *see* Discontinuous flow variables
Discontinuous flow variables, 8, 18, 26, 31, 56
Discontinuous solutions, 37, 127, 243, 250, 260
  examples of simulation, 250
  modelling considerations, 260–63
  numerical methods, 37
Discretization, 53
  hydraulic, 159
  nonlinear terms and coefficients, 92
  one-dimensional equations, 63–75
  one- or two-dimensional, 138
  quasi-two-dimensional, 75–7
  topological, 143
Dispersion,
  numerical, 326, 328
    see also Phase portraits
  physical process of, 313
Dissipative interface, 89, 126
Divergent form of flow equations *see* Conservation equations
Domain of dependence, 25
Double sweep methods, 106
  multiconnected (looped) networks, 117
  simple-connected (branched) networks, 109
  single channel, 106
Double sweep methods (*contd*)
  two-dimensional inundated plain networks, 113

Explicit schemes *see* Finite difference methods

Favre waves *see* Undular bore
Finite difference methods
  discretization of boundary conditions, 72
  discretization of coefficients, 92
  discretization of quasi-two-dimensional relations, 75
  explicit schemes, 66
  general description, 59
  implicit schemes, 66, 86
  order of approximation, 61
  representation of derivatives, 60
  representation of functions, 61
  schemes for differential equations, 68
  schemes for integral relationships, 63
Flood forecasting and prediction, 350
  calibration and sensitivity of models, 356
  methodology, 351
  model implementation strategy, 354
Flood plain flow, 7, 24, 50, 147, 155
Flow,
  critical, 27
  one-dimensional, 7
  quasi-two-dimensional, 50
  subcritical, 27
  supercritical, 27
Flow equations,
  one-dimensional
    differential, 14–17
    integral relationships, 11–13
    simplified, 44
    steady, 48, 181
  quasi-two-dimensional, 52
Flow regulation,
  irrigation canals, 233
  low head power plants, 253

Growth factor *see* Amplification factor
Gunaratnam–Perkins scheme, 72

Holly–Preissmann scheme, 326 *et seq.*

Implicit schemes *see* Finite difference methods
Independent variables, 8, 16, 17
Inertia terms of equations, 45, 135

Initial conditions,
definition, 32
influence, 33–6
requirements, 29–33
Integral flow relations, 9
Inverse computation, 31, 242
Irreversibility, 31
Irrigation regulating systems *see* Flow regulation
Iterative solution methods,
for solving systems of equations, 105
for updating coefficients, 104, 172

Kinematic wave, 46
Kirkuk–Adhaim irrigation project, 240

Lateral inflow, 18, 23
Lax scheme, 67, 81, 88
Lax theorem, 79
Leap-frog scheme, 67
Linearization of coefficients, 103
Linearized flow equations, 80
Live cross-section, 24
Looped networks, 141, 147, 369

Manning,
formula, 20
'global' coefficient, 190
Mekong Delta model, 113, 138, 140, 147, 150, 386, 399
Mississippi river, 2, 295
Missouri river, 340
Modelling systems, 2, 5, 374, 381

Niger river model, 133
Nile river, 23, 385
Numerical damping *see* Amplitude portraits
damping *see* Amplitude portraits
diffusion *see* Diffusion
dispersion *see* Dispersion; Phase portraits
solution of equations, 54–9
stability, 79–86

Ohio River, 2
One-dimensional flow hypotheses, 7, 22, 138, 146
Oraison–Manosque canal, 33, 244
Order of approximation, 60–62
Orifice flow, 76

Parana river model, 137
Phase portraits, 86, 88, 89
Physical models, 1, 7
Power cascades, 253
Preissmann scheme, 65, 86, 89, 92
Pseudo-viscosity method, 124

Quality of mathematical models, 372, 380 *et seq.*

Range of influence, 25
Rankine–Hugoniot relationships, 38
Rating curve, 36, 186
boundary condition, 198
loop due to unsteadiness of flow, 195
loop due to roughness variations, 199
Resistance laws, 20, 295
Rhône River models, 45, 135, 216, 253, 255–9
Riemann invariants, 29

Saint Venant, de,
equations, 8
hypotheses, 7, 8
Schemes of finite differences,
Abbott–Ionescu type, 69
based on differential equations, 66–72
based on integral relationships, 63–6
boundary conditions, 72–5
Delft Hydraulic Laboratory, 68
explicit, 66
Gunaratnam–Perkins, 72
Holly–Preissmann, 326
implicit, 66
lax, 67
leap-frog, 67
Preissmann, 65–6
Vasiliev, 71
Sediment transport,
analysis of equations, 281
classification of models, 277
numerical solution of equations, 287
resistance formulas, 295
Senegal river model, 208, 403
Setit river, 299
Sewage network modelling, 365
Shock fitting, 122, 260
Simplified flow equations, 44–6, 137
Sisteron canal model, 248
SIVA modelling system, 5, 70, 97, 104
Slope,
energy or friction, 13, 20, 22, 129, 162, 298
neglected terms in simplified equations, 45, 135
Small depth problem, 175, 368
Stability,
canal regulation, 235

Stability (*contd*)
numerical, 79–80
Steady flow, 48, 181
Steep front, 120–28, 248–52
Storage,
area, 18
width, 18, 23, 146
Storm drains *see* Sewage network modelling
Strickler formula, 20
Surge,
celerity, 26, 38, 43
computational methods, 121, 246, 260
formation of, 37, 243
relation to differential flow equations, 39, 42
relation to integral flow relationships, 40
simulation examples, 240
undular *see* Undular bore

Through methods, 126, 260
Tidal effects, 35
Topological discretization, 143
Training of personnel, 397
Transfer of models, 391
cost, 380, 388
Mekong model, 399
Senegal model, 403
Transition and control structures modelling 263–70
Transport of pollutants, 312
dispersion equation, 316
estimating transverse velocity distribution, 346
numerical solution, convection equation, 320
numerical solution, diffusion equation, 331
one-dimensional modelling, 318
two-dimensional modelling, 336
Two-dimensional,
discretization, 170
hypotheses, 50, 138, 146
methods of solution, 75, 113

Undular bore, 244, 245–8

Vasiliev scheme, 71, 86
Velocity distribution in cross-section, 22, 346
Vienne River model, 333

Weak solutions, 42, 127
Weir flow simulation, 76, 168, 178, 180